John F. Miller
Chief, Water Management Information
    Division
Office of Hydrology, NWS

NOAA Technical Report NWS 23

Meteorological Criteria for Standard Project Hurricane and Probable Maximum Hurricane Windfields, Gulf and East Coasts of the United States

Washington, D.C.
September 1979

U.S. DEPARTMENT OF COMMERCE
National Oceanic and Atmospheric Administration
National Weather Service

NOAA TECHNICAL REPORTS

National Weather Service Series

The National Weather Service (NWS) observes and measures atmospheric phenomena; develops and distributes forecasts of weather conditions and warnings of adverse weather; collects and disseminates weather information to meet the needs of the public and specialized users. The NWS develops the national meteorological service system and improves procedures, techniques, and dissemination for weather and hydrologic measurements, and forecasts.

NWS series of NOAA Technical Reports is a continuation of the former series, ESSA Technical Report Weather Bureau (WB).

Reports listed below are available from the National Technical Information Service, U.S. Department of Commerce, Sills Bldg., 5285 Port Royal Road, Springfield, Va. 22161. Prices vary. Order by accession number (given in parentheses).

ESSA Technical Reports

WB   1   Monthly Mean 100-, 50-, 30-, and 10-Millibar Charts January 1964 through December 1965 of the IQSY Period. Staff, Upper Air Branch, National Meteorological Center, February 1967, 7 p, 96 charts. (AD 651 101)

WB   2   Weekly Synoptic Analyses, 5-, 2-, and 0.4-Mb Surfaces for 1964 (based on observations of the Meteorological Rocket Network during the IQSY). Staff, Upper Air Branch, National Meteorological Center, April 1967, 16 p, 160 charts. (AD 652 696)

WB   3   Weekly Synoptic Analyses, 5-, 2-, and 0.4-Mb Surfaces for 1965 (based on observations of the Meteorological Rocket Network during the IQSY). Staff, Upper Air Branch, National Meteorological Center, August 1967, 173 p. (AD 662 053)

WB   4   The March-May 1965 Floods in the Upper Mississippi, Missouri, and Red River of the North Basins. J. L. H. Paulhus and E. R. Nelson, Office of Hydrology, August 1967, 100 p.

WB   5   Climatological Probabilities of Precipitation for the Conterminous United States. Donald L. Jorgensen, Techniques Development Laboratory, December 1967, 60 p.

WB   6   Climatology of Atlantic Tropical Storms and Hurricanes. M. A. Alaka, Techniques Development Laboratory, May 1968, 18 p.

WB   7   Frequency and Areal Distributions of Tropical Storm Rainfall in the United States Coastal Region on the Gulf of Mexico. Hugo V. Goodyear, Office of Hydrology, July 1968, 33 p.

WB   8   Critical Fire Weather Patterns in the Conterminous United States. Mark J. Schroeder, Weather Bureau, January 1969, 31 p.

WB   9   Weekly Synoptic Analyses, 5-, 2-, and 0.4-Mb Surfaces for 1966 (based on meteorological rocket-sonde and high-level rawinsonde observations). Staff, Upper Air Branch, National Meteorological Center, January 1969, 169 p.

WB 10   Hemispheric Teleconnections of Mean Circulation Anomalies at 700 Millibars. James F. O'Connor, National Meteorological Center, February 1969, 103 p.

WB 11   Monthly Mean 100-, 50-, 30-, and 10-Millibar Charts and Standard Deviation Maps, 1966-1967. Staff, Upper Air Branch, National Meteorological Center, April 1969, 124 p.

WB 12   Weekly Synoptic Analyses, 5-, 2-, and 0.4-Millibar Surfaces for 1967. Staff, Upper Air Branch, National Meteorological Center, January 1970, 169 p.
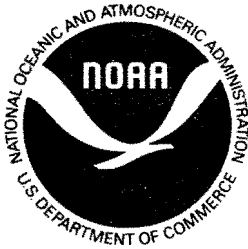
NOAA Technical Reports

NWS 13   The March-April 1969 Snowmelt Floods in the Red River of the North, Upper Mississippi, and Missouri Basins. Joseph L. H. Paulhus, Office of Hydrology, October 1970, 92 p. (COM-71-50269)

NWS 14   Weekly Synoptic Analyses, 5-, 2-, and 0.4-Millibar Surfaces for 1968. Staff, Upper Air Branch, National Meteorological Center, May 1971, 169 p. (COM-71-50383)

NWS 15   Some Climatological Characteristics of Hurricanes and Tropical Storms, Gulf and East Coasts of the United States. Francis P. Ho, Richard W. Schwerdt, and Hugo V. Goodyear, May 1975, 87 p. (COM-75-11088)

John F. Miller
Chief, Water Management Information
    Division
Office of Hydrology, NWS

NOAA Technical Report NWS 23

Meteorological Criteria for Standard Project Hurricane and Probable Maximum Hurricane Windfields, Gulf and East Coasts of the United States

Washington, D.C.
September 1979

CONTENTS

FIGURES

ABBREVIATIONS

by	:	bypassing
°C	:	degrees Celsius
CoE	:	Corps of Engineers
ex	:	exiting
ft	:	feet
°F	:	degrees Fahrenheit
GMT	:	Greenwich Mean Time
gpm	:	geopotential meter(s)
HMR	:	Hydrometeorological Report
hr	:	hour(s)
Hydromet	:	Hydrometeorological
in.	:	inch(es)
°K	:	degrees Kelvin
km	:	kilometer(s)
kPa	:	kilopascal(s)
kt	:	knot(s)
Lat.	:	Latitude
Long.	:	Longitude
m	:	meter(s)
mb	:	millibar(s)
mi	:	mile(s)
min	:	minute(s)
n.mi.	:	nautical mile(s)
N/A	:	Not Applicable
NHC	:	National Hurricane Center
NHEML	:	National Hurricane and Experimental Meteorology Laboratory
NHRP	:	National Hurricane Research Project
NOAA	:	National Oceanic and Atmospheric Administration
NRC	:	Nuclear Regulatory Commission
NWS	:	National Weather Service
PMH	:	Probable Maximum Hurricane
sec	:	second(s)
sig	:	significant

SPH	:	Standard Project Hurricane
U.S.	:	United States
WMID	:	Water Management Information Division

SYMBOLS

A   :   category of central pressure (6.4.2)*

         :   category of forward speed (PMH – 11.5.2.1; SPH – 11.6.2.1)

         :   asymmetry factor (12.2.3.1)

         :   geographical region along gulf coast (15.3.4)

A_{i+n} :   discrete value used in obtaining smoothed frequency value F_i (8.2.4)

B   :   category of central pressure (6.4.2)

         :   category of forward speed (PMH – 11.5.2.1; SPH – 11.6.2.1)

         :   geographical region along south Florida coast (15.3.4)

C   :   constant of proportionality for pressure profile formulas I and II (6.4.1)

         :   category of forward speed (PMH – 11.5.2.1; SPH – 11.6.2.1)

         :   geographical region along east coast (15.3.4)

D_W :   average distance from the pressure center to the points where p_w is calculated (15.3.7.2)

e   :   base of Naperian logarithms $\cong 2.71828$ (6.2)

f   :   coriolis parameter (9.4.1)

F   :   factor for reducing gradient wind speed to 10-m, 10-min wind speed (12.2.1)

F_i :   smoothed frequency value (8.2.4)

ff   :   filling adjustment factor (15.3.4)

g   :   acceleration of gravity (8.3.3.1)

H   :   Hydromet pressure profile formula (6.2)

Hg   :   mercury (table 6.3)

i   :   exponent; i.e., $k = k_1 R^i$ (6.2)

         :   undefined parameter in HMR 31 (6.3)

I   :   pressure profile formula I (6.3)

II   :   pressure profile formula II (6.3)

j   :   undefined parameter in HMR 31 (6.3)

k   : $= r \left[\ln \left| \frac{p_w - p_o}{p - p_o} \right| \right] = k_1 R^i$ (6.2)

         :   surface friction coefficient (15.2.4.3)

---

*Section where the symbol is defined or first referenced.

K	:	density coefficient $= \left(\dfrac{1}{\rho e}\right)^{1/2}$ (12.1.1)
k_c	:	onshore to overwater wind speed ratio at the coast (15.2.4.1)
	:	k_i at the coast for onshore winds (15.2.4.3)
k_e	:	offshore to overwater wind speed ratio (15.2.4.2) [equilibrium surface friction coefficient (15.2.4.3)]
k_i	:	previous surface friction coefficient at the last upwind boundary between surface friction categories (15.2.4.3)
	:	k_c at the coast for onshore winds (15.2.4.3)
k_1	:	$= \dfrac{k}{R^i}$ (6.2)
LR	:	lower limit of R (tables 2.3 to 2.6)
LT	:	lower limit of T (tables 2.3 to 2.6)
	:	point where T first falls below T_L (16.5.3.3)
M	:	a radial through V_x (12.2.3.3.1)
MSG	:	missing (tables 4.1 to 4.6)
n	:	undefined parameter in HMR 31 (table 6.1)
	:	a number (8.2.4)
N	:	sample size (tables 5.1 and 5.2)
p	:	pressure (6.2)
P	:	pressure (8.2.3)
p_c	:	mean sea-level pressure for typhoons (12.4)
p_{H40}	:	pressure computed at 40 n.mi. (74 km) from a hurricane center using H (6.4.2)
p_{H80}	:	pressure computed at 80 n.mi. (148 km) from a hurricane center using H (6.4.2)
p_{I40}	:	pressure computed at 40 n.mi. (74 km) from a hurricane center using Formula I (6.4.2)
p_{I80}	:	pressure computed at 80 n.mi. (148 km) from a hurricane center using Formula I (6.4.2)
p_{II40}	:	pressure computed at 40 n.mi. (74 km) from a hurricane center using Formula II (6.4.2)
p_{II80}	:	pressure computed at 80 n.mi. (148 km) from a hurricane center using Formula II (6.4.2)
p_L	:	pressure at lower surface of a layer (8.3.3.1)
p_n	:	asymptotic peripheral pressure (7.1)
p_{nx}	:	hurricane peripheral pressure from table 3-1 of NHRP Report No. 5 (7.1)

P_o : central pressure (5.2)

P_{s40} : hurricane pressure observed or estimated at 40 n.mi. (74 km) from center (6.4.2)

P_{s80} : hurricane pressure observed or estimated at 80 n.mi. (148 km) from hurricane center(6.4.2)

P_U : pressure at upper surface of a layer (8.3.3.1)

P_w : peripheral pressure from weather maps (5.2)

P_{wi} : peripheral pressure from last closed isobar (7.2)

Q : interpolation coefficient used in computing the surface friction coefficient, k (15.2.4.3)

r : zero-order correlation coefficient (5.3.1)

    : distance from storm center (6.2)

    : distance to the coast from a circle representing the PMH (11.5.2.1)

R : radius of maximum winds (5.2)

r' : multiple correlation coefficient (5.4)

r'^2 : reduction of variance (5.4)

r_o : outer radius from which inflow air originates with negligible momentum relative to the earth (9.4.1)

R_{lim} : limiting radius of maximum winds (9.4.1)

$\overline{R.H.}$: mean relative humidity (tables 8.5 to 8.7)

s : distance from a surface friction category boundary (15.2.4.3)

S : surge (8.2.3)

$s_{y \cdot x}$: standard error of estimate (5.4)

sf : stalling adjustment factor (16.4.1.4)

t : landfall time (15.3.4)

    : some specified time (15.3.6)

T : forward speed (5.2)

t_c : temperature in °Celsius (see conversion table)

t_f : temperature in °Fahrenheit (see conversion table)

t_k : temperature in °Kelvin (see conversion table)

$\overline{T}$: mean temperature (8.3.3.2.2)

T_d : dew-point temperature (8.3.3.2.3)

T_L : minimum forward speed permissible for maintaining PMH intensity (16.5.3.2)

T_o : forward speed unit parameter (12.2.3.1.1)

T_s : sea-surface temperature (8.3.3.2.2)

$\overline{T}_v$: mean adjusted virtual temperature (8.3.3.1)

UR : upper limit of R (tables 2.3 to 2.6)

UT : upper limit of T (tables 2.3 to 2.6)

V : hurricane (typhoon) wind speed (12.1.3.1)

  : 10-m, 10-min overwater wind speed at a point (12.2.3.3)

V_c : cyclostrophic wind speed (12.1.2)

V_{cx} : maximum cyclostrophic wind speed (12.1.2)

V_g : gradient wind speed (12.1.2)

V_{gx} : maximum gradient wind speed (12.1.1)

V_k : 10-m, 10-min wind speed adjusted for underlying terrain (15.2.4.3)

V_m : maximum sustained surface wind speed for typhoons (12.4)

V_{max} : maximum wind at R_{lim} (9.4.1)

  : maximum wind corresponding to Δp_{max} (16.4.1.4)

V_s : overwater wind speed in a stationary hurricane at radius r (12.2.3.3)

V_x : maximum 10-m, 10-min overwater wind speed (12.2.3.2)

V_{xs} : V_x for a stationary hurricane (12.2.2)

VGL : V_{gx} for the lower limit of R (2.3)

VGU : V_{gx} for the upper limit of R (2.3)

VLL : V_x for the lower limit of R and the lower limit of T (2.3)

VLU : V_x for the lower limit of R and the upper limit of T (2.3)

VUL : V_x for the upper limit of R and the lower limit of T (2.3)

VUU : V_x for the upper limit of R and the upper limit of T (2.3)

W_C : overwater wind speed at landfall (15.3.6)

W_I : overland wind speed at some specified time after landfall (15.3.6)

W_n : weighting function (8.2.4)

x	:	one of the variables in a normal distribution (5.3.1)
	:	empirical constant (12.2.3.1.1)
X-X	:	a wind path (3.3.4.1)
y	:	one of the variables in a normal distribution (5.3.1)
	:	empirical constant (12.2.3.1.1)
	:	ordinate (16.5.4.2)
Y	:	regression function of a random variable (5.4)
Y-Y	:	a wind path (3.3.4.2)
z	:	height (8.3.3.1)
α	:	coefficient employed in fitting mathematical expression to filling adjustment curves (15.3.6)
β	:	fraction of tangential component of momentum generated in the inflow layer, between r_o and R_{lim}, that is dissipated by surface stress (9.4.1)
	:	angle between track direction and surface wind direction (12.2.3.1.2)
	:	coefficient employed in fitting mathematical expression to filling adjustment curves (15.3.6)
β_M	:	angle between track direction and surface wind direction computed along radial M (12.2.3.3.2)
β^1	:	coefficient for expressing stress opposition to coriolis force (9.4.1)
Σ	:	summation (6.4.3)
θ	:	track direction (5.2)
θ_a	:	surface wind direction (12.2.3.1)
θ_e	:	equivalent potential temperature (8.2.4)
θ_t	:	tangential wind direction (12.2.3.3.1)
λ	:	longitude (tables 5.1 and 5.2)
ρ	:	population correlation coefficient (5.3.1)
	:	air density (8.3.3.1)
σ	:	standard deviation (5.4)
ϕ	:	wind inflow angle (5.2)
	:	geopotential (8.3.3.1)
ϕ_r	:	wind inflow angle at r (12.2.3.3.1)
ϕ_R	:	wind inflow angle at r = R (12.2.3.3.1)
ψ	:	latitude (tables 5.1 and 5.2)

Ω	:	angular velocity of rotation of earth (12.1.1)
Δp	:	pressure drop, or peripheral pressure (p_w) minus central pressure (p_o) (8.4)
	:	pressure at upper surface of a layer minus pressure at lower surface of same layer (tables 8.5 to 8.7)
Δp_{max}	:	greatest pressure drop for a given storm (16.4.1)
Δp_o	:	change in central pressure with changes in other parameters (table 8.10)
Δp_t	:	pressure drop at hurricane landfall (15.3.4)
$\Delta p/D_W$	:	average pressure gradient (15.3.7.2)
*	:	significant correlation between variables (tables 5.1 and 5.2)
§	:	duplicate hurricanes (tables 4.1 to 4.4)
∫	:	hurricane symbol (fig. 12.5)
+	:	storms for which analyzed wind fields were not available (13.2.1)

METEOROLOGICAL CRITERIA FOR STANDARD PROJECT HURRICANE AND PROBABLE MAXIMUM HURRICANE WIND FIELDS, GULF AND EAST COASTS OF THE UNITED STATES

RICHARD W. SCHWERDT, FRANCIS P. HO, AND ROGER R. WATKINS
WATER MANAGEMENT INFORMATION DIVISION
OFFICE OF HYDROLOGY, NATIONAL WEATHER SERVICE
NATIONAL OCEANIC AND ATMOSPHERIC ADMINISTRATION
U.S. DEPARTMENT OF COMMERCE

ABSTRACT. Criteria for determining wind fields along the Gulf and East coasts of the United States for the most severe hurricane reasonably characteristic of a region, Standard Project Hurricane (SPH), and for the hurricane that will produce the highest sustained wind that can probably occur at a specified coastal location, Probable Maximum Hurricane (PMH), are presented. A single limiting value for the meteorological parameters of peripheral pressure (p_w) and central pressure (p_o), was determined. Upper and lower limits were determined for the radius of maximum winds (R), forward speed (T), track direction (θ), and inflow angle (ϕ). Interrelations between the several parameters p_o, R, T, θ, latitude (ψ) or longitude (λ) were investigated.

1. INTRODUCTION

1.1 AUTHORIZATION AND FUNDING

Concentrated effort to determine revised values of meteorological parameters for wind fields prescribed by the Standard Project Hurricane (SPH) and Probable Maximum Hurricane (PMH) started in early 1975. Funding for the studies was provided jointly by the U.S. Nuclear Regulatory Commission (NRC) Contract No. AT (49-24)-120, and the Corps of Engineers (CoE), Department of the Army.

1.2. DEFINITIONS

1.2.1. SPH

The SPH is a steady state* hurricane having a severe combination of values of meteorological parameters that will give high sustained wind speeds reasonably characteristic of a specified coastal location. By reasonably characteristic is meant that only a few hurricanes of record over a large region have had more extreme values of the meteorological parameters. The "SPH wind field" is specified from the parameters. One of several uses of the wind field is to compute critical storm surge at coastal points. The SPH wind field is also a factor in calculating wind load.

A frequency can be determined for any combination of values of meteorological parameters that define an SPH wind field. This combined frequency for the total wind field will generally have a recurrence interval of several hundred years.

1.2.2. PMH

The PMH is a hypothetical steady state* hurricane having a combination of values of meteorological parameters that will give the highest sustained wind speed that can probably occur at a specified coastal location. From values of the parameters, a wind field is specified which is termed the "PMH wind field." One of several possible uses of the values of meteorological parameters is to compute maximum storm surge at coastal points when the hurricane approaches along the most critical track. The PMH wind field is also a factor to be considered for calculating wind load.

The PMH is a rare event. As with the SPH, frequency could be determined for a combination of meteorological parameters used to develop any specific PMH wind field and then combined to determine the recurrence interval for that total event. Other combinations of parameters would give different PMH wind fields, and frequencies could be determined for each. These frequencies would have such a large uncertainty as to make the effort meaningless.

---

*See par. 1.2.3.

1.2.3. STEADY STATE

By steady state in this report we mean there is no change in the values of p_w, p_o, R, T, θ, ϕ, wind speed, and limits of rotation of wind fields during at least the last several hours before an SPH or PMH makes landfall. The SPH is a steady state hurricane. The PMH is a steady state hurricane except for the coast between mileposts 900 and 1300 (fig. 1.1). Here it is not steady state because it is defined as a recurving, weakening hurricane, i.e., p_o is increasing with time. If the user wishes to consider the PMH steady state in this area, he must use the p_o at the coast.

We consider the SPH and PMH to be steady state because there is not enough tropical cyclone data to define the time variation of the pertinent parameters.

1.3 PURPOSE

Abnormally high winds, pounding waves, and storm surge from hurricanes produce severe damage and a threat to life. The CoE is responsible for assessing the potential for damage resulting from hurricanes along coasts, proposing and designing structures to alleviate this damage, and consulting with State and local communites on these matters. Local records of hurricane behavior are inadequate for these purposes, not only because of often incomplete water-level observations but also these and other records may be available for only a few years. In addition, hurricanes may cross a particular section of coast infrequently. Communities that have been spared a severe storm for decades or may never have experienced a severe hurricane in recorded history are not immune to this danger in the future. In order to bring to bear the entire body of knowledge of hurricane behavior in a consistent manner, the concept of the SPH has been developed for the gulf and east coasts as a bench mark against which to judge the hazards for particular communities.

In addition to the SPH, there is a need for defining the wind fields associated with the PMH. Such a storm may be used by the CoE in planning and design of barriers near the coast to protect life. Guidance by

4
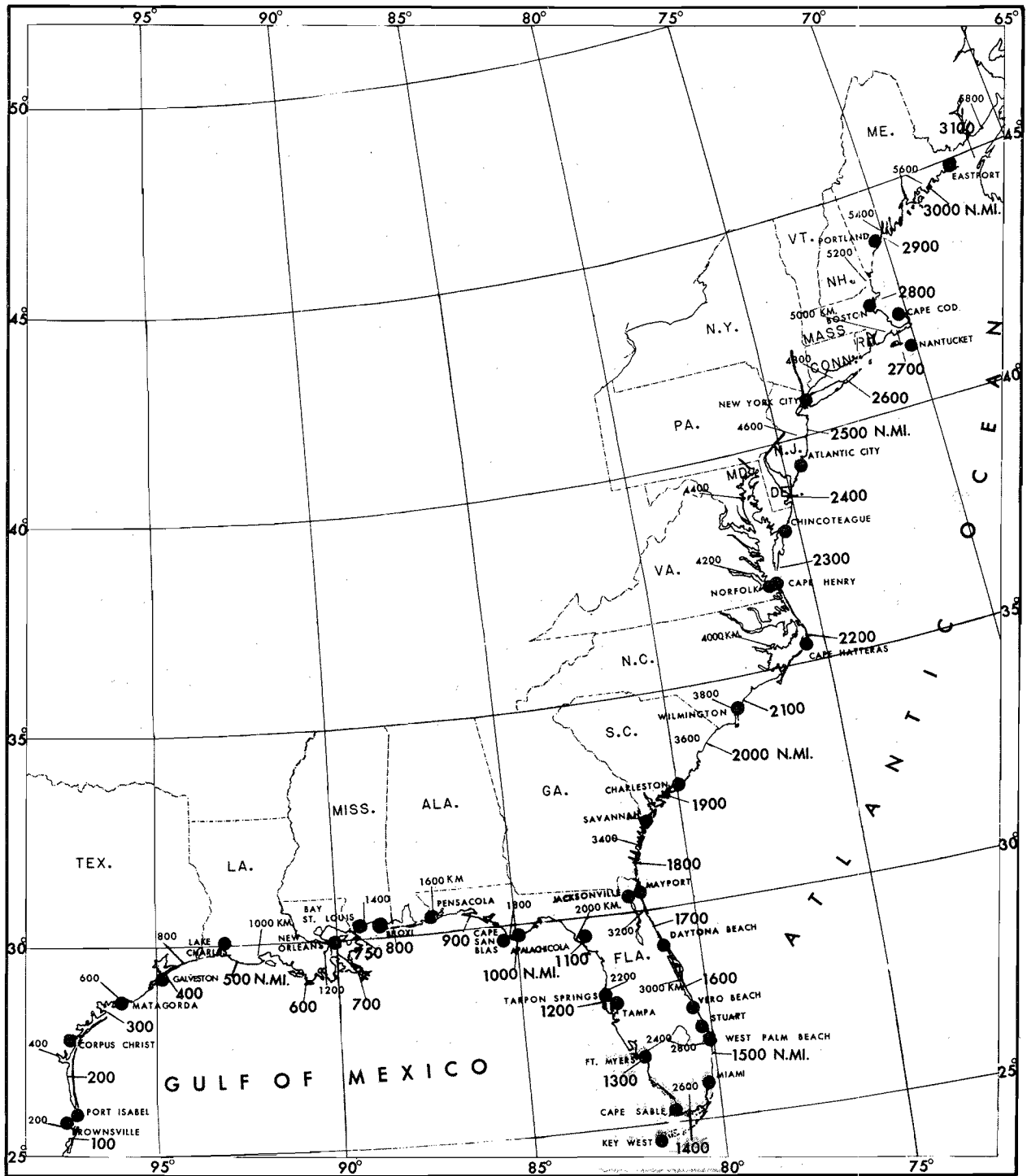
Figure 1.1.--Locator map with coastal distance intervals marked in nautical miles and kilometers.

the NRC for planning and design of nuclear power plants suggests the use of
PMH in locations where high winds, waves and storm surge could pose a threat
to the public health and safety from a hurricane-induced accident at a
nuclear power plant.

Consistency is needed in developing values of various parameters for
both the SPH and PMH. For example, the interrelations between central
pressure and other parameters, while not necessarily the same for both the
SPH and PMH, should be consistent and must be evaluated.

1.4 SCOPE

The geographical region covered by this report is the U.S. Gulf of Mexico
and east coasts from Texas to Maine. Hurricane (through 1975) and typhoon
(through 1974) data were used. An understanding of hurricane behavior
through 1977 was used for studying and evaluating values of parameters for
the SPH and PMH.

The meteorological parameters evaluated are:

> central pressure (p_o)
> peripheral pressure (p_w)
> radius of maximum winds (R)
> forward speed (T)
> track direction (θ)
> inflow angle (ϕ)

Other necessary considerations for defining wind fields are covered in this
report. These include the wind speed distribution and limits of rotation
of wind fields.

The study develops a meteorologically consistent set of criteria. We
describe in chapters 2 and 3 how these parameters can be used to develop SPH
and PMH wind fields. The application of these wind fields to surge genera-
tion, erosion of beaches, wind load, etc., is a task for oceanographers,
engineers, and others, and is left to them.

We assumed that p_o (relative to p_w) is the most important meteorological parameter. We developed our procedure by first establishing values of $\Delta p = p_w - p_o$ at all coastal points for the SPH and the PMH. For the PMH, a primary maximization is in the determination of Δp. The other meteorological parameters are not assigned a single value, but *ranges* of allowable values are given to be used in conjunction with Δp to produce a variety of possible wind fields. The user must select the combination that is most critical for a given problem.

The criteria developed in this report are for hurricanes making landfall (entering hurricanes) along the U.S. gulf and east coasts. Criteria have not been developed for exiting hurricanes except for small peninsulas or the tips of capes, e.g., Cape Cod, the Mississippi Delta, etc., where the SPH or PMH is allowed to exit after crossing a small land area. Generalized criteria for exiting storms is beyond the scope of this report.

Analysis of the few extreme coastal data required smoothing. Large variations over short distances were avoided unless supported by data or theoretical considerations. The study is to be used along relatively smooth unbroken sections of coastline. Application to bays and other places where the coastline undergoes sharp changes in orientation would require modifications to the criteria in this study.

Criteria are given for the SPH and the PMH only. *No attempt should be made to simply interpolate between SPH and PMH to establish criteria for a hurricane stronger than SPH but weaker than PMH. Another study would be needed for this purpose.*

Hurricanes are a threat to life and property not only from high winds, waves, and storm surge but from rain-induced floods. This latter problem is not considered in the present study. The frequency and areal distribution of tropical storm rainfalls in a form suitable for use in engineering design along the gulf coast is the subject of a report by Goodyear (1968). Extreme limits of rainfall (Probable Maximum Precipitation) are the subject of National Weather Service Hydrometeorological Reports.

1.5 PREVIOUS STUDIES

1.5.1 SPH

Generalized meteorological specifications for the SPH for the gulf and east coasts were first given in a study, "Meteorological Considerations Pertinent to Standard Project Hurricane, Atlantic and Gulf Coasts of the United States," by Howard E. Graham of the Hydrometeorological Section, Hydrologic Services Division, U.S. Weather Bureau, and Dwight E. Nunn of the Office of Chief of Engineers, CoE. This was published as *National Hurricane Research Project* (NHRP) Report No. 33 (Graham and Nunn 1959). Hereafter this report will be referred to as NHRP 33. This work brought together and generalized numerous earlier specifications for the SPH developed by the Hydrometeorological Branch for several locations along the gulf and east coasts. These earlier studies were conducted for and funded by the CoE.

The specifications in NHRP 33 were partially revised in an unpublished study (National Weather Service 1972). The revision incorporated data from storms since 1956, which indicated the wind fields should be stronger than shown in NHRP 33 for selected coastal regions.

1.5.2 PMH

The first PMH studies were requested by the CoE for the Narragansett Bay and New Orleans regions (U.S. Weather Bureau 1959a and b). The central pressures were determined as a ratio to the central pressure for the SPH. The remaining factors for the PMH were essentially the same as for the SPH. An unpublished PMH study (U.S. Weather Bureau 1968) generalized criteria for the PMH along both coasts. The central pressure and peripheral pressure differed from that of the SPH; values of the other parameters remained unchanged even though the list of hurricanes of record was updated.

1.5.3 HURRICANE CLIMATOLOGY

NOAA Technical Report NWS 15 (Ho et al. 1975) presented a climatology of hurricane factors important to storm surge for the gulf and east coasts. This climatology was an analysis of all available hurricane data beginning with the storm tracks of 1871. Data for most other factors were available subsequent to 1900. Discussions were presented to provide possible

8

explanations of the alongshore variations of the parameters, but the analyses were not extensively modified on the basis of subjective reasoning. In the SPH, and particularly the PMH, considerably more smoothing beyond what has occurred is necessary for an estimate of what *can* happen.

1.5.4 COMPARISONS BETWEEN PREVIOUS SPH AND PMH STUDIES AND THIS REPORT

Previous SPH and PMH studies defined values of meteorological parameters that could occur within broad coastal zones (seven zones covered the coast from Texas to Maine). Data points representing each zone were joined by smooth curves to permit interpolation along the coast. This technique is a more generous smoothing than used in the present study. Here, alongshore variations were determined by developing estimates within each of more than 60 overlapping zones and smoothing between designated points.

1.6 ORGANIZATION

Figure 1.1 shows the coastline and distances from an initial starting point south of the United States – Mexico border. Geographical names are shown to aid identification. Figure 1.2 is a chart showing distance as the abscissa. Along the top, locations are given for easy identification of coastal points. This figure will be used throughout the report for presenting various types of data analyses.

Chapter 2 presents a summary of the major results of this report.

Chapter 3 gives procedures for constructing SPH and PMH wind fields and an example.

Chapter 4 describes the data used in the report. Limitations of the observed data are given.

Chapter 5 defines each of the pertinent meteorological parameters and gives their interrelations.

Chapter 6 develops the pressure profile equation. This equation is basic to defining the wind field.
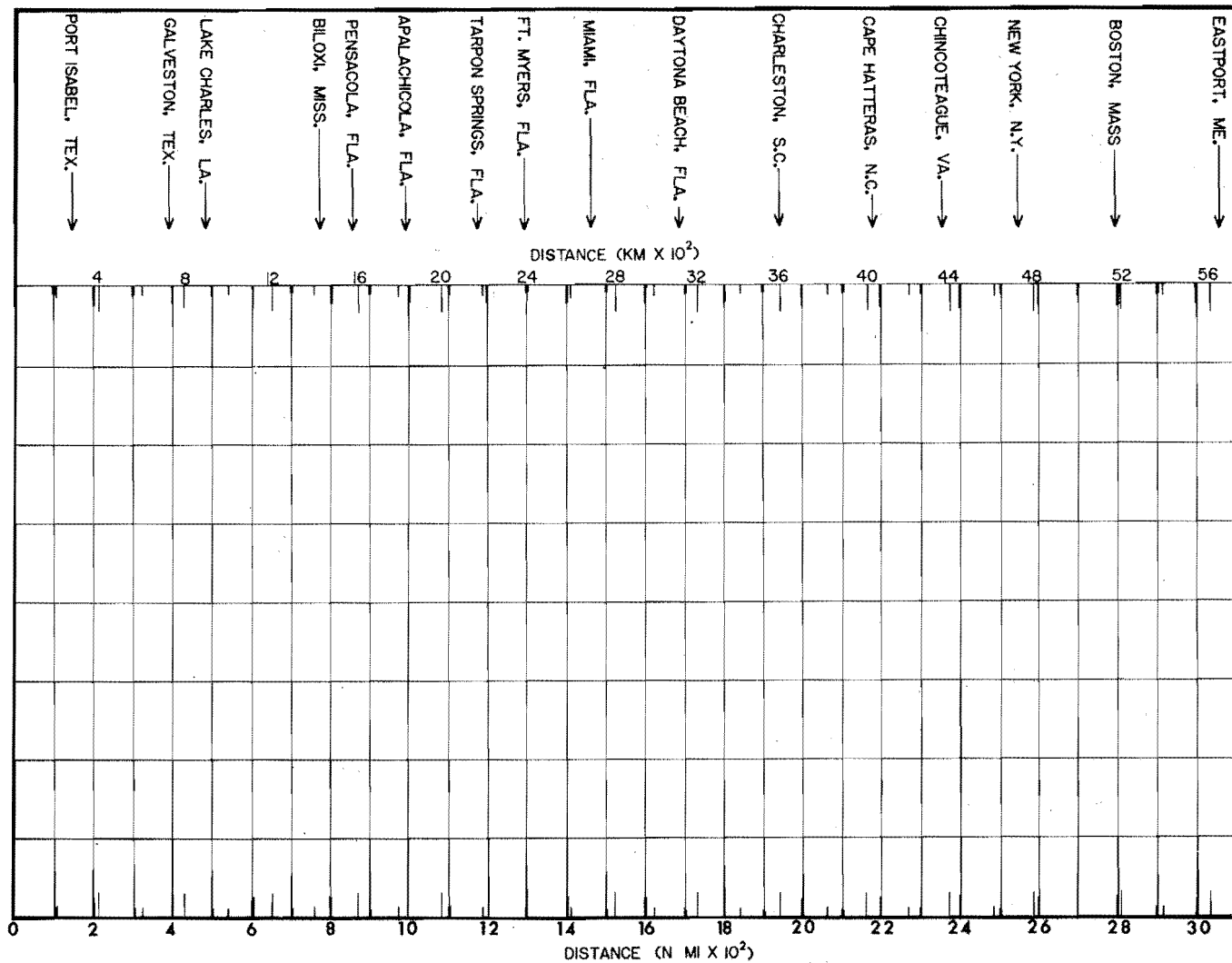
Figure 1.2.--Chart used for presenting various types of alongshore data analyses.

Chapters 7 through 11 consider separately five of the six meteorological parameters (all but ϕ) and describe the methods used to determine our estimates of values for the SPH and PMH. Magnitudes of the parameters are shown as profiles along the coasts except for p_w which is constant.

Chapter 12 is concerned with computation of maximum overwater winds. Gradient winds are calculated first. These are then reduced to 10-m (32.8-ft) 10-min overwater winds (V_x). Tables 2.3 to 2.6 give some values of meteorological factors and parameters for the SPH and PMH at 100-n.mi. (185.3-km) mileposts to provide a general overview of the magnitude of possible wind speeds. The user should compute wind speeds for many values of parameters at specific coastal locations to determine the one most critical for his use. This chapter also discusses 10-m, 10-min overwater winds other than at V_x.

Chapter 13 develops relative wind profiles from the radius of maximum winds (R) to 300 n.mi. (556 km) from the eye of the SPH and the PMH. Relative wind profiles are also determined for inside R to the hurricane center. Limits of rotation [the range of angles within which the maximum winds can be placed relative to track direction (θ)] are also given in this chapter.

Chapter 14 describes the method of determining inflow angle (ϕ).

Chapter 15 discusses 1) the adjustment to wind fields when the hurricane approaches the coast, and 2) the adjustment to wind fields after the center crosses the coast.

Chapter 16 looks at problems associated with a stalling PMH.

2. EXECUTIVE SUMMARY

2.1 INTRODUCTION

This chapter presents a summary of the results of chapters 6 to 16 (sec. 2.2) and a comparison of computed maximum SPH and PMH winds with computed winds for hurricanes of record using observed or estimated values of meteorological parameters or factors for each hurricane (sec. 2.3). All wind computations are based on equations 2.2, 2.6, and 2.7.

Information is often given in figures and tables with brief definitions and explanations. Ranges of permissible values are given for several parameters. The user should determine for his particular application the most critical values within these ranges. Complete documentation of the logic and data supporting the results can be found in the chapter listed next to each subsection.

The basic data on Gulf of Mexico and North Atlantic hurricanes (within 150 n.mi. of the U.S. coast) and on western north Pacific typhoons used in this study are listed in chapter 4. A more complete definition of the parameters used in this study and their interrelations are given in chapter 5.

Chapter 3 describes how to compute wind fields. It refers only to this summary chapter for needed information.

2.2 RESULTS OF THE STUDY

2.2.1 PRESSURE PROFILE FORMULA (CHAPTER 6)

The pressure profile formula used to develop the maximum gradient wind speed equation for the SPH and the PMH is:

$$\frac{p - p_o}{p_w - p_o} = e^{-R/r} \tag{2.1}$$

where p is the sea-level pressure at distance r from the hurricane center and p_o, p_w, and R are as defined in the following three subsections.

2.2.2 PERIPHERAL PRESSURE (CHAPTER 7)

Peripheral pressure (p_w), the sea-level pressure at the outer limits of the hurricane circulation, is the average pressure around the hurricane where the isobars change from cyclonic to anticyclonic curvature. In this study, p_w was determined at four equally spaced points around the storm center (north, east, south, and west).

We adopted 29.77 in. (100.8 kPa) as the p_w for the SPH and 30.12 in. (102.0 kPa) as the p_w for the PMH.

2.2.3 CENTRAL PRESSURE (CHAPTER 8)

Central pressure (p_o) is simply the lowest sea-level pressure at the hurricane center. Figures 2.1 and 2.2, respectively, show the adopted coastal variation of p_o for the SPH and for the PMH.

In general, p_o increases with latitude for both the SPH and the PMH. Coastal orientation relative to possible hurricane tracks results in the sharp rise in p_o between the southern New England coast and the Boston area.

Figure 2.3 shows Δp or $p_w - p_o$ for the SPH and the PMH. It compares the relative magnitude of the most important parameter used in computing hurricane wind speeds.

2.2.4 RADIUS OF MAXIMUM WINDS (CHAPTER 9)

The radius of maximum winds (R) is the radial distance from the hurricane center to the band of strongest winds within the hurricane wall cloud, just outside the hurricane eye. Figures 2.4 and 2.5 show the adopted coastal variation of the permissible range in R for the SPH and the PMH, respectively.

R generally increases with latitude for both the SPH and the PMH. R is also somewhat dependent on p_o. The PMH is envisioned as a fully developed, tightly wound hurricane whose R for any particular coastal point is less than the R of the SPH at that location.
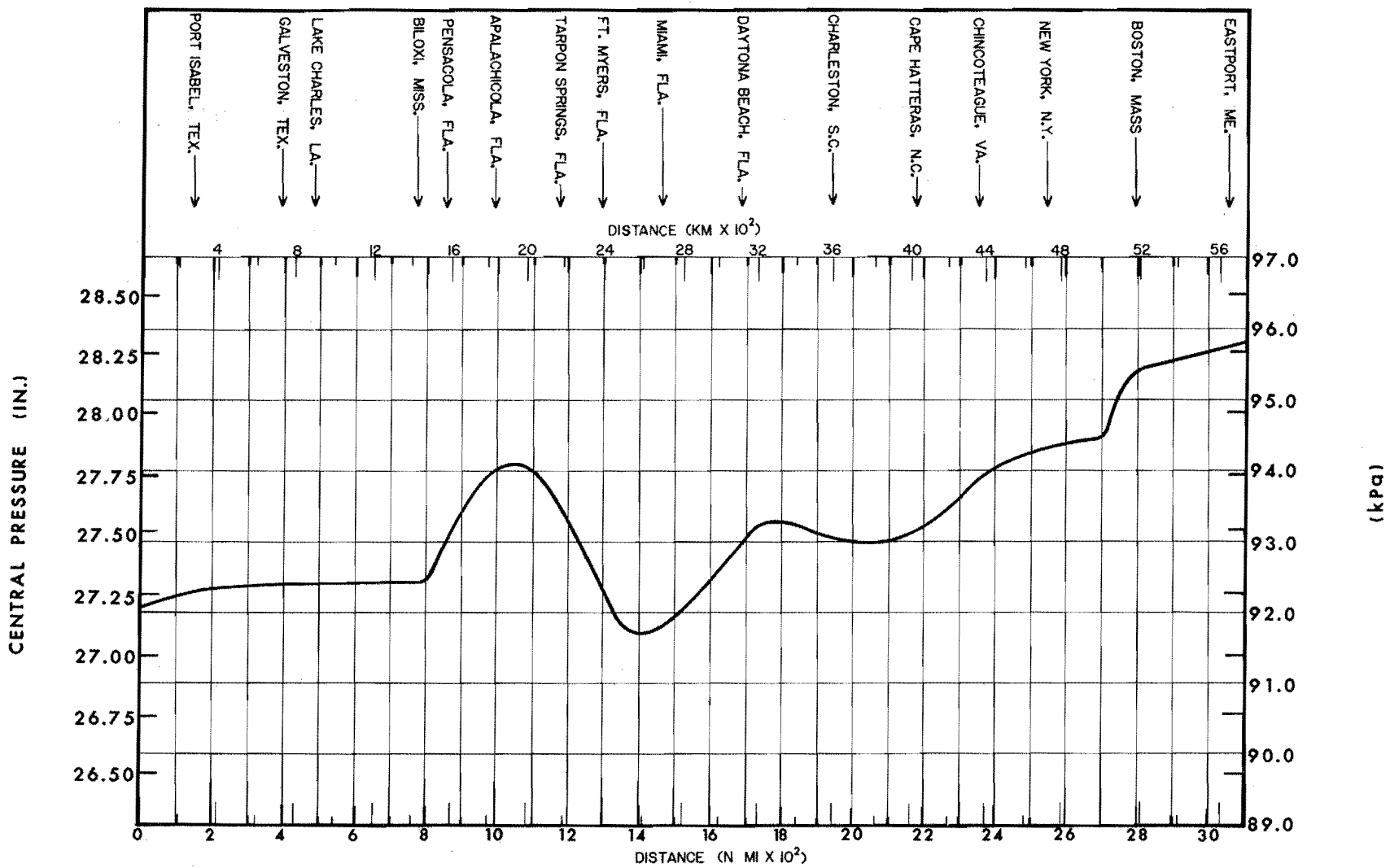
Figure 2.1.--Plot showing the adopted SPH p_o.
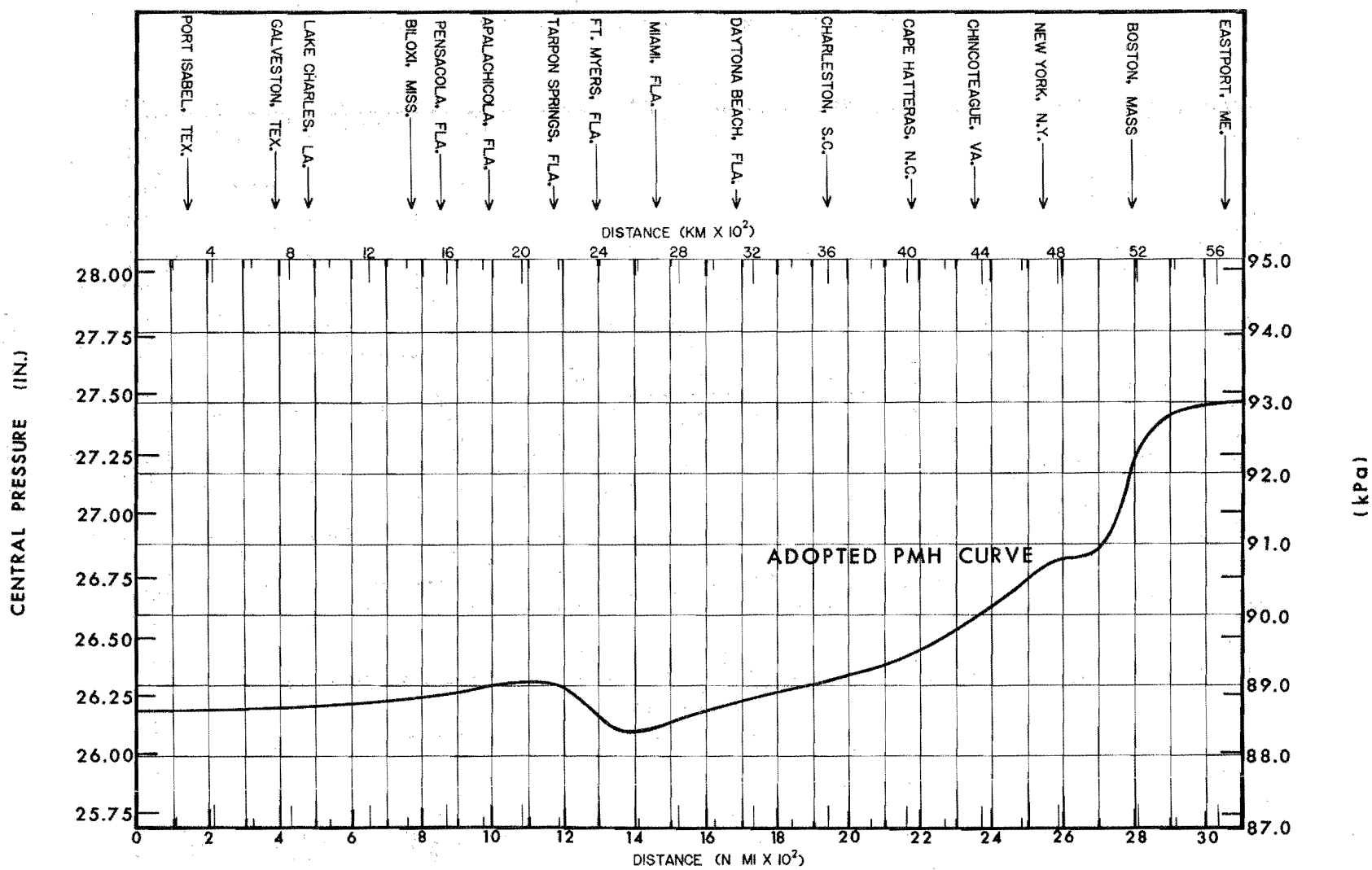
Figure 2.2.--Plot showing the adopted PMH p_o.
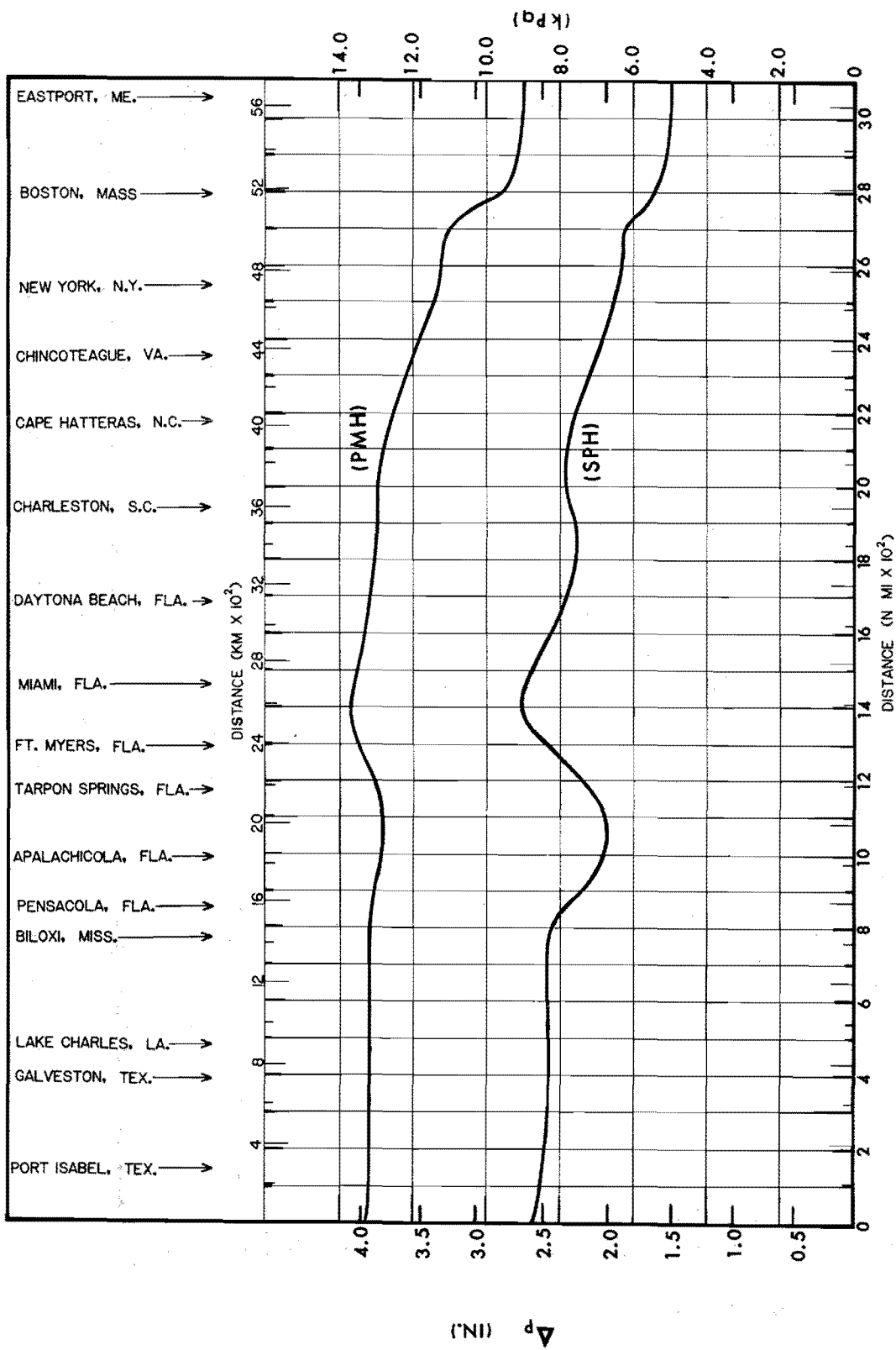
Figure 2.3.—Comparison of pressure drop (Δp) for the PMH and SPH
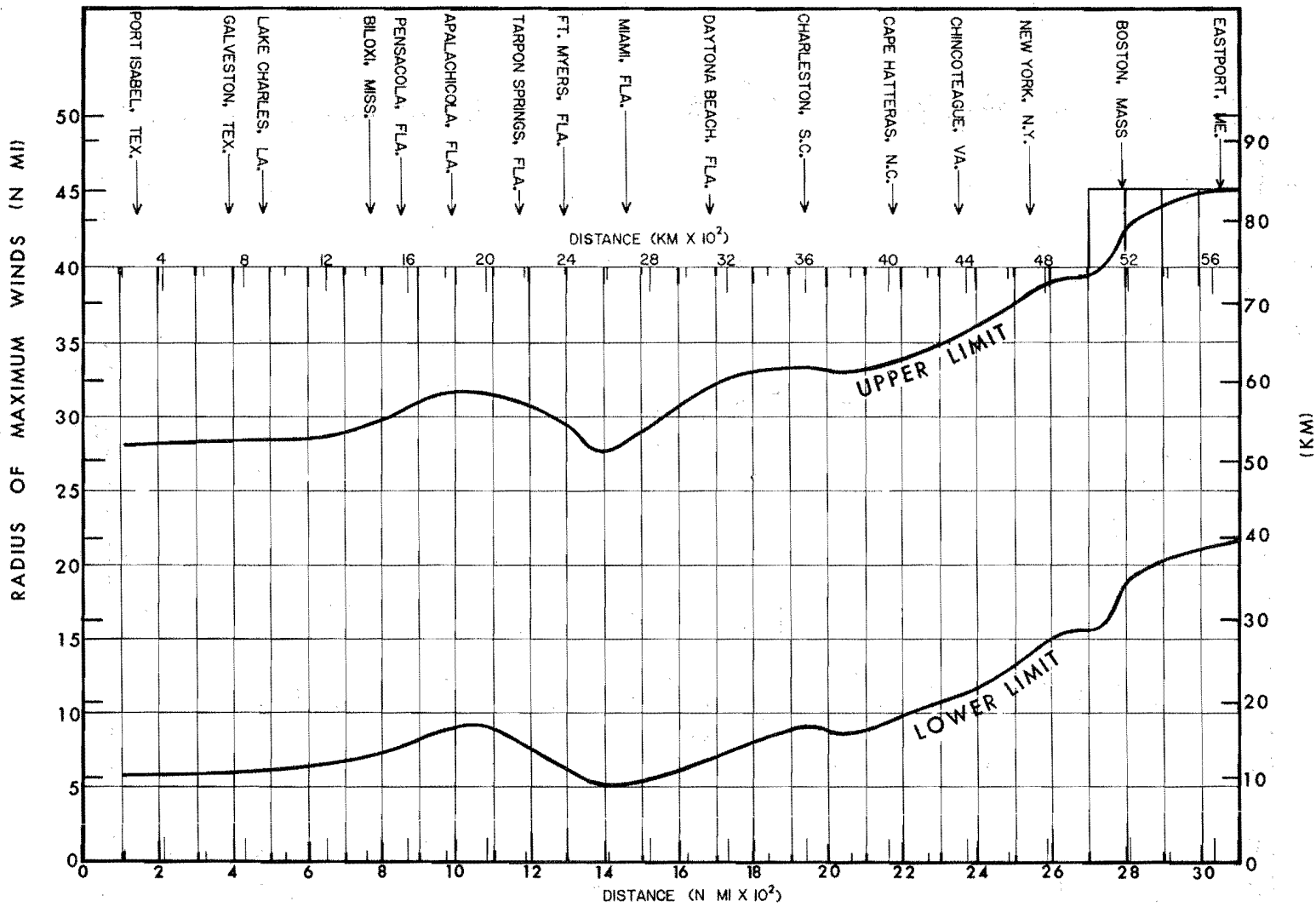
Figure 2.4.—Adopted upper and lower limits of radius of maximum winds for the SPH.
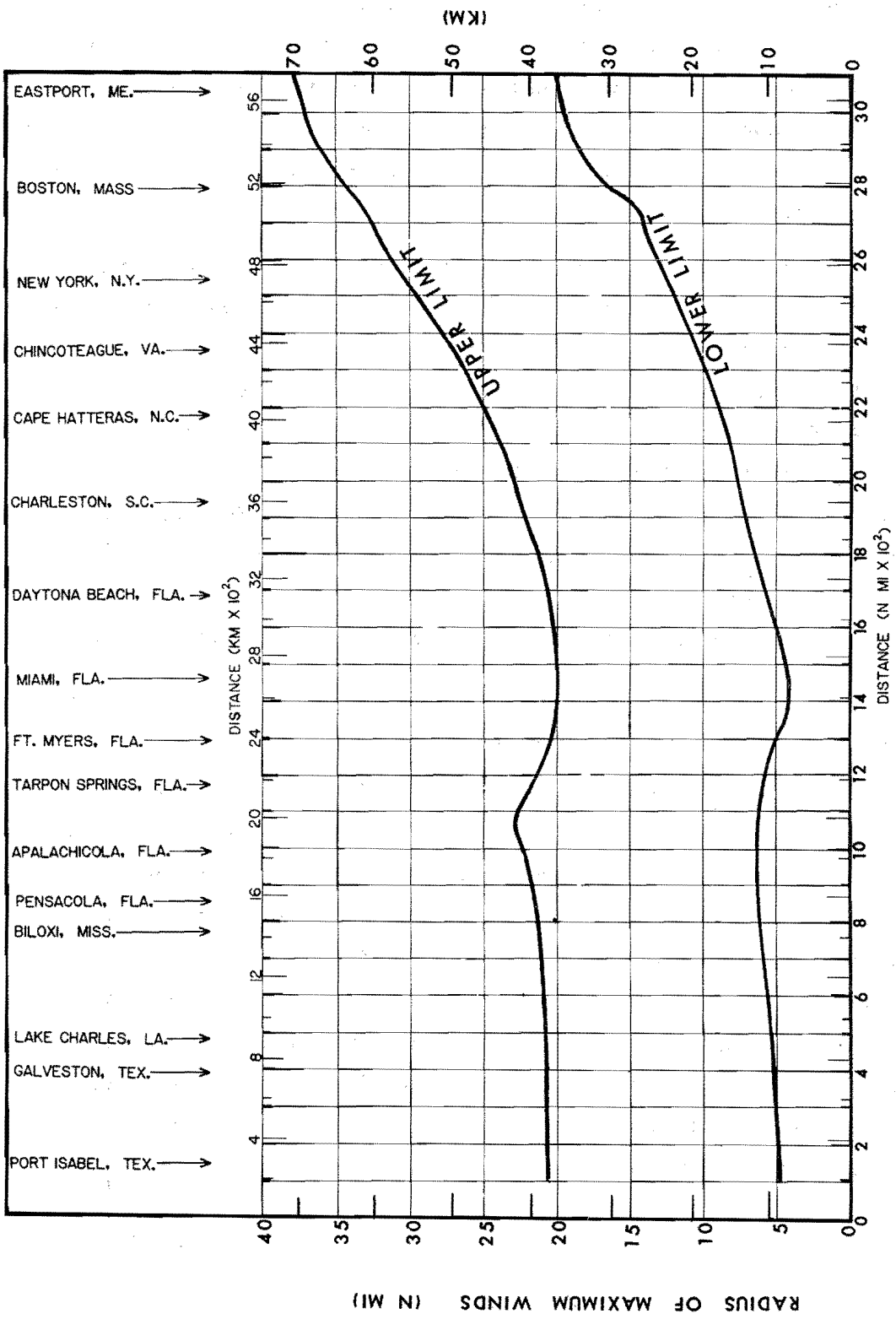
Figure 2.5.—Adopted upper and lower limits of radius of maximum winds for the PMH.

2.2.5 FORWARD SPEED (CHAPTER 10)

Forward speed (T) refers to the rate of translation of the hurricane center from one geographical point to another. It is one component of the wind field of a moving storm and results in higher winds on the right side of the storm and lower on the left. Figure 2.6 shows the adopted coastal variation of the permissible range in T for the SPH and figure 2.7 shows this variation for the PMH.

Available data indicate that the upper limit of T for severe storms should be held constant with latitude to about milepost 1800. Similarly, the lower limit is constant for the PMH except for the northeastern Gulf, where the PMH is defined as a recurving, faster-moving hurricane. The lower limit for the SPH is constant to Cape Hatteras. North of Cape Hatteras, the lower and upper limits of both the PMH and SPH increase with latitude, although the increase is only slight north of Cape Cod. The range of PMH forward speeds is less than that for the SPH. Very slow speeds weaken a hurricane (see chapters 10 and 16). Very fast speeds result in a very asymmetrical wind field which is considered more possible with an SPH than a PMH.

2.2.6 TRACK DIRECTION (CHAPTER 11)

The track direction (θ), or the path of forward movement along which the hurricane is coming (measured clockwise from north), is considered to be noninstantaneous in this report, i.e., the SPH and the PMH are not allowed to change course during the last several hours before striking the coast. Figures 2.8 and 2.9 show the permissible range of θ for the SPH and the PMH, respectively. Limiting θ's are based on possible directions over the open ocean, further constrained by sea-surface temperatures and other meteorological features. The permissible range is also a function of forward speed (T). As the angle between the coastal orientation and θ decreases, the slower hurricane weakens more than the faster-moving hurricane. Table 2.1 gives the T, by category, required for using figures 2.8 and 2.9.
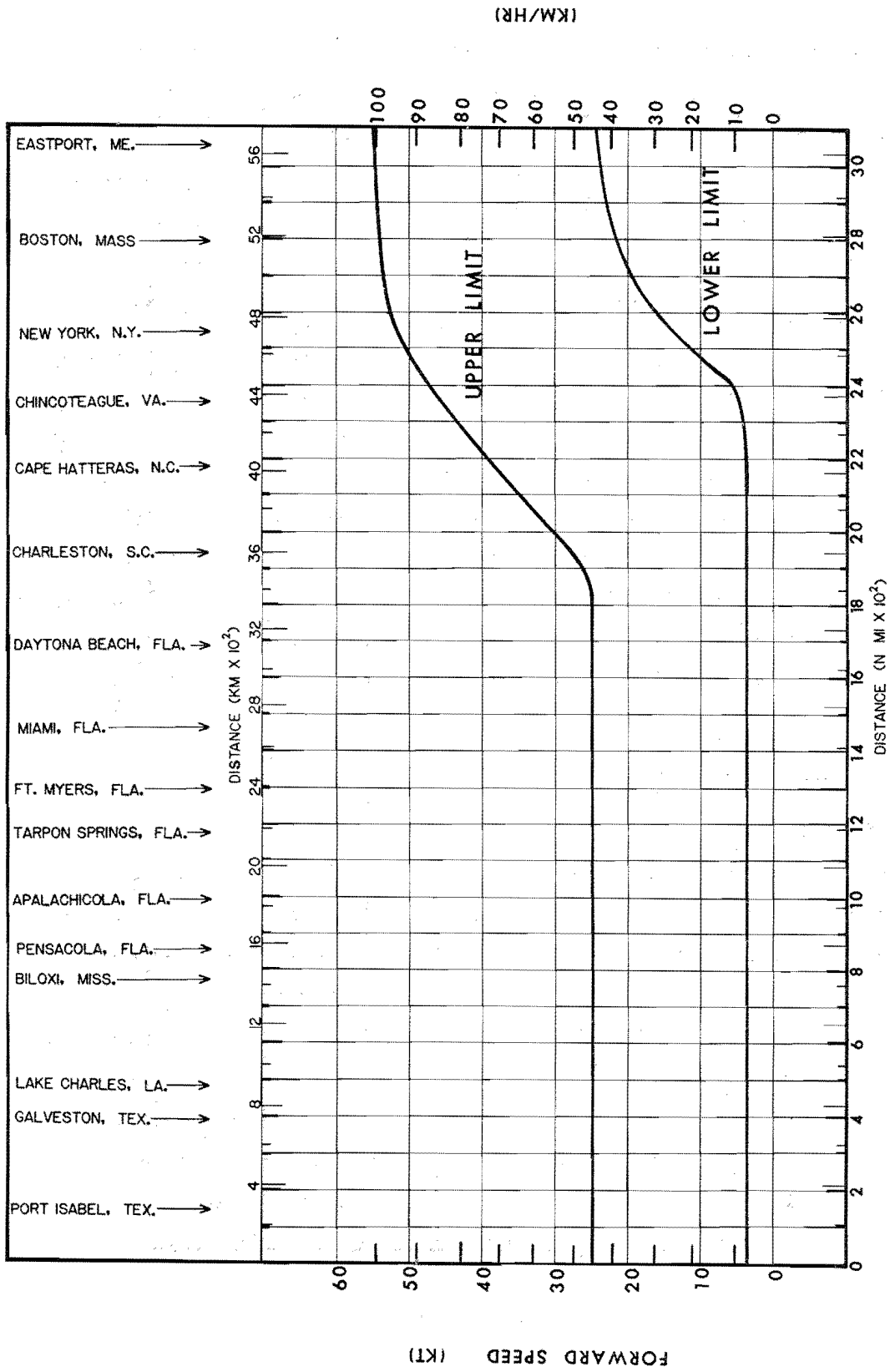
Figure 2.6.--Adopted SPH upper and lower limits of T.

20
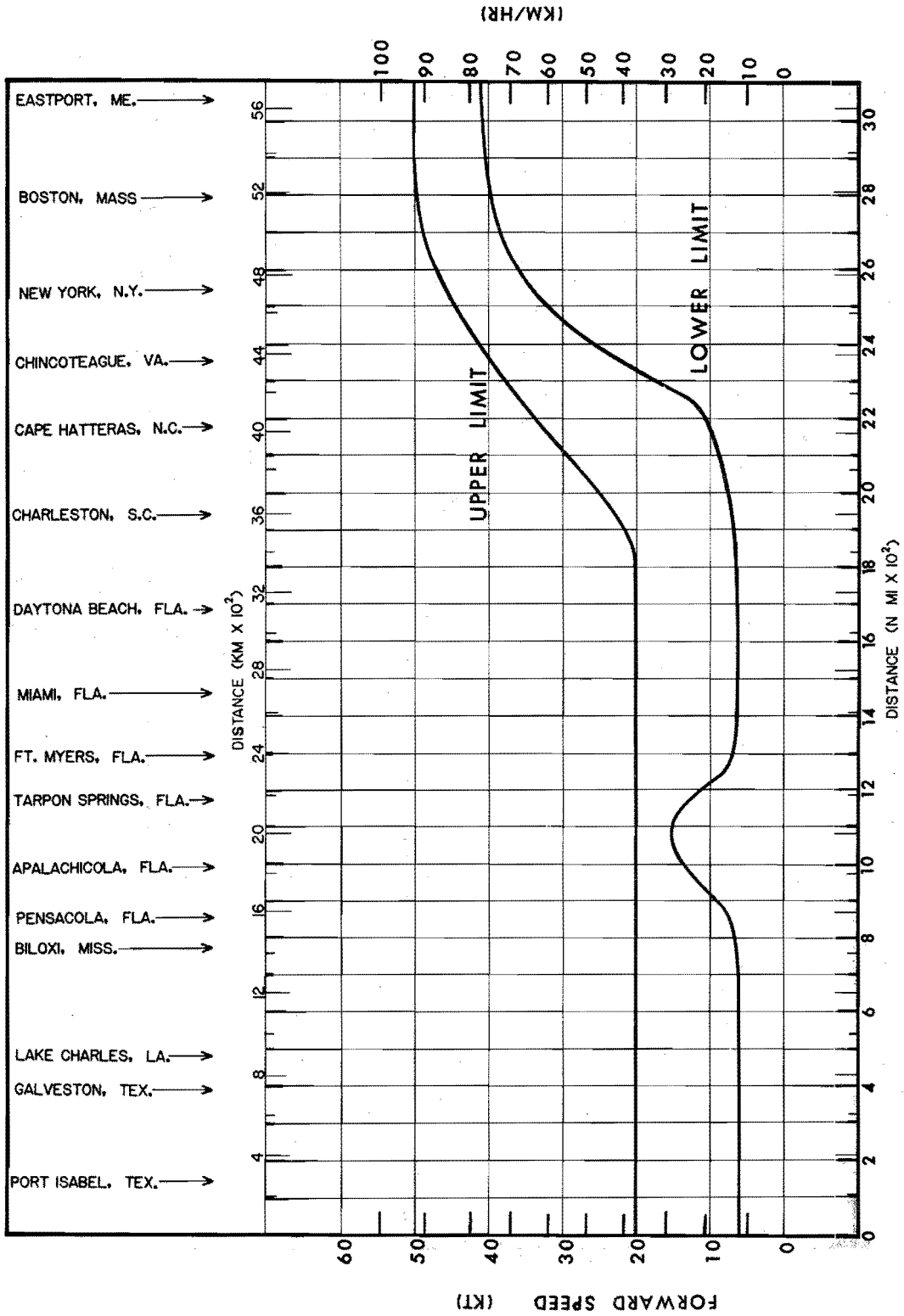
Figure 2.7.--Adopted PMH upper and lower limits of T.
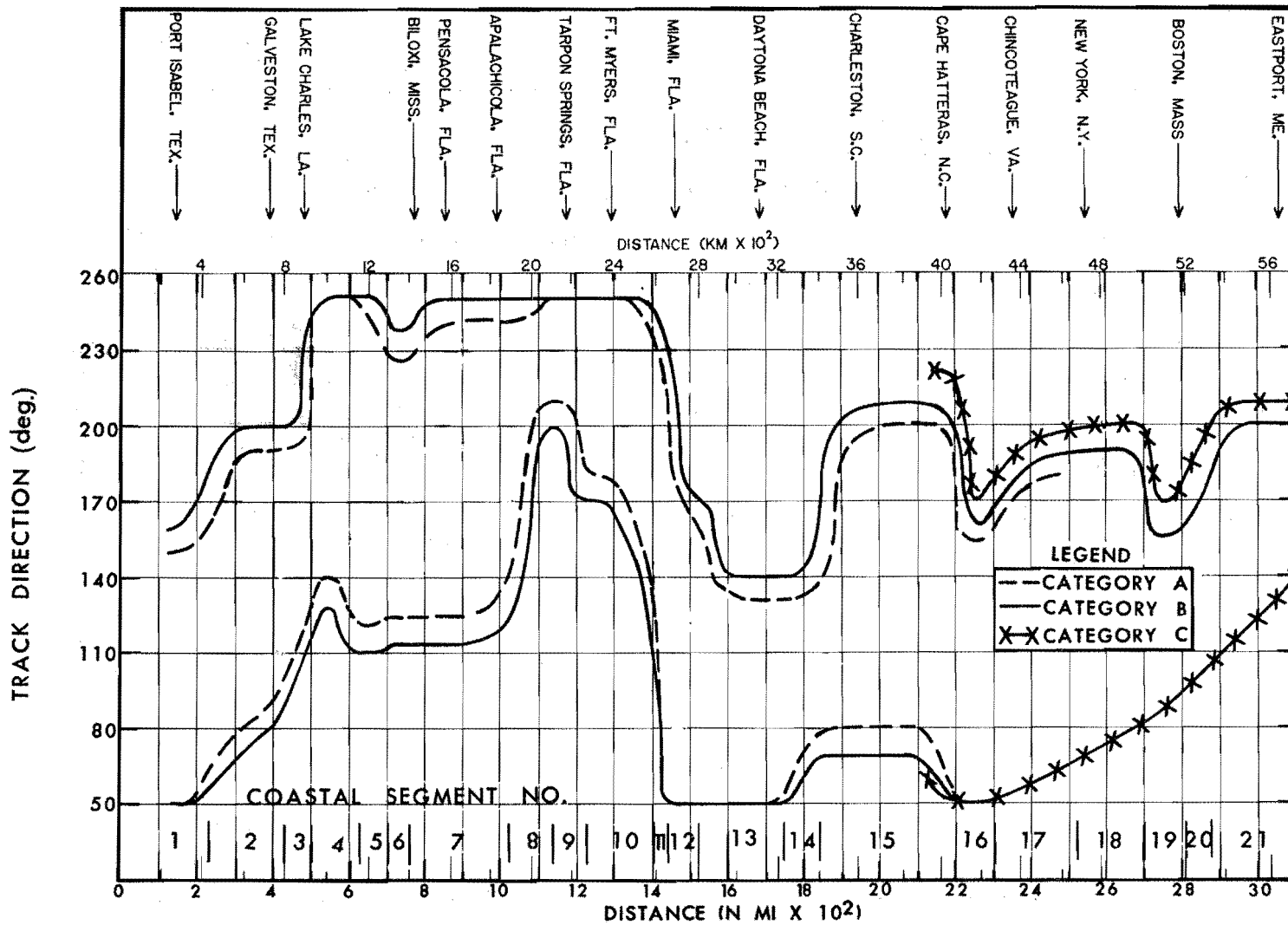
Figure 2.8.--Maximum allowable range of SPH θ after smoothing is represented by the area between the outermost curves.
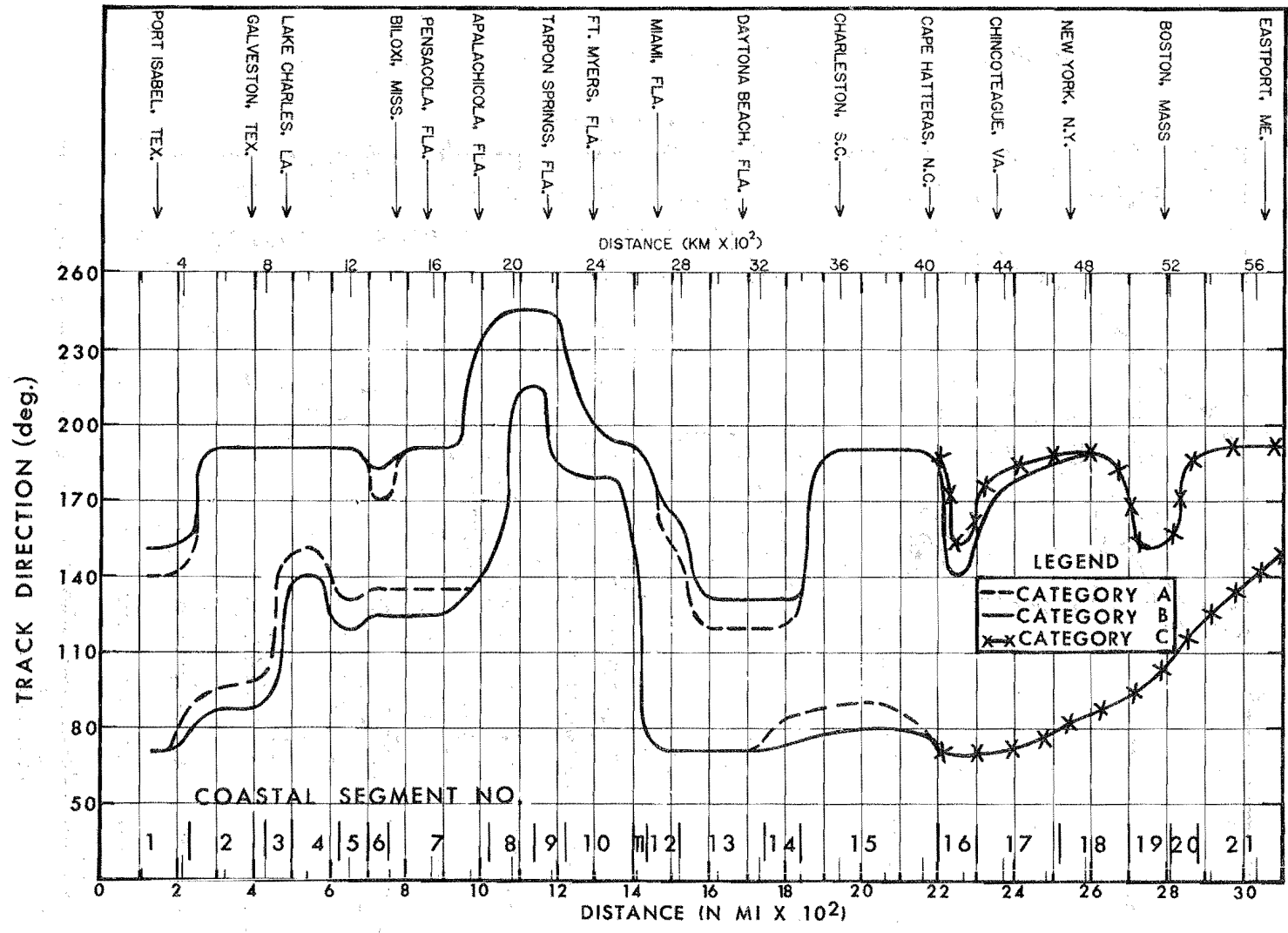
Figure 2.9.--Maximum allowable range of PMH θ after smoothing is represented by the area between the outermost curves.

Table 2.1.--Relation between forward speed (T) and track direction (θ)

a. For the PMH	
Speed category	Forward speeds (T)
A	$6 \text{ kt} \leq T \leq 10 \text{ kt}$ $(11 \text{ km/hr} \leq T \leq 19 \text{ km/hr})$
B	$10 \text{ kt} < T \leq 36 \text{ kt}$ $(19 \text{ km/hr} < T \leq 67 \text{ km/hr})$
C	$T > 36 \text{ kt}$ $(T > 67 \text{ km/hr})$
b. For the SPH	
Speed category	Forward speeds (T)
A	$4 \text{ kt} \leq T \leq 10 \text{ kt}$ $(7 \text{ km/hr} \leq T \leq 19 \text{ km/hr})$
B	$10 \text{ kt} < T \leq 36 \text{ kt}$ $(19 \text{ km/hr} < T \leq 67 \text{ km/hr})$
C	$T > 36 \text{ kt}$ $(T > 67 \text{ km/hr})$

2.2.7 OVERWATER WINDS (CHAPTER 12)

2.2.7.1 MAXIMUM GRADIENT WINDS (V_{GX}). Gradient wind is defined as a wind blowing under conditions of circular motion, parallel to the isobars, in which the centripetal and coriolis accelerations together exactly balance the horizontal pressure-gradient force per unit mass. The gradient wind, independent of duration, is computed by solving the equation:

$$V_{gx} = K \ (p_w - p_o)^{1/2} - \frac{Rf}{2} \tag{2.2}$$

where p_w, p_o, and R are as previously defined and

f = coriolis parameter, dependent on latitude

$K = \left(\frac{1}{\rho e}\right)^{1/2}$ = density of the air (ρ) computed from sea-surface temperatures; $e \cong 2.71828$

Values of K along both coasts are graphed in figures 2.10 and 2.11 for the SPH and PMH, respectively. These are based on the variation of sea-surface temperatures. For the PMH, the 0.99 probability level was used. For the SPH we used the 0.75 level.
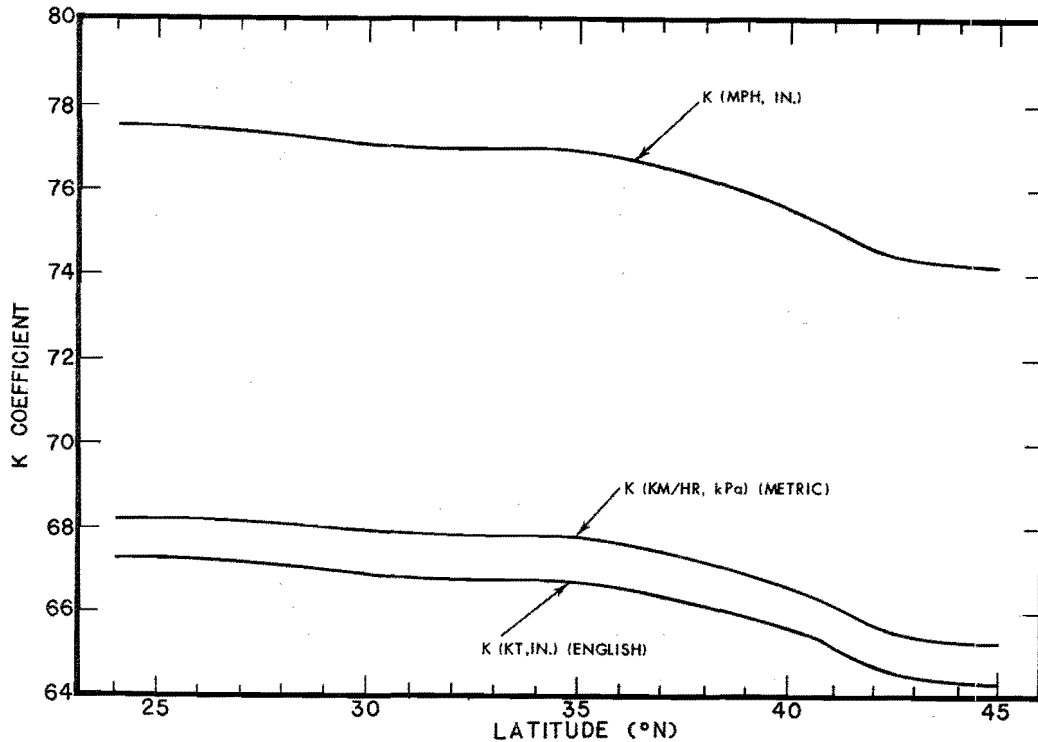
Figure 2.10.-- Values of latitude-dependent K coefficient for three units of measurement for the SPH.

2.2.7.2 TEN-METER 10-MINUTE OVERWATER WINDS

2.2.7.2.1 WINDS IN A STATIONARY HURRICANE. Observed maximum 10-m (32.8-ft), 10-min winds (V_x) over open water in hurricanes of above average intensity have been found to vary from about 75 to slightly over 100% of V_{gx}. We have adopted two empirical equations for estimating V_x in a stationary hurricane.

$$V_x = 0.9 \ V_{gx}, \text{ for the SPH} \tag{2.3}$$

$$V_x = 0.95 \ V_{gx}, \text{ for the PMH} \tag{2.4}$$

The 0.95 for the PMH was selected on the grounds of representing a more extreme condition.

V_x for a stationary hurricane, we shall call V_{xs}. Knowing V_{xs}, we can use the information on relative wind profiles (sec. 2.2.8) to determine 10-m, 10-min overwater winds at any distance from the hurricane center.
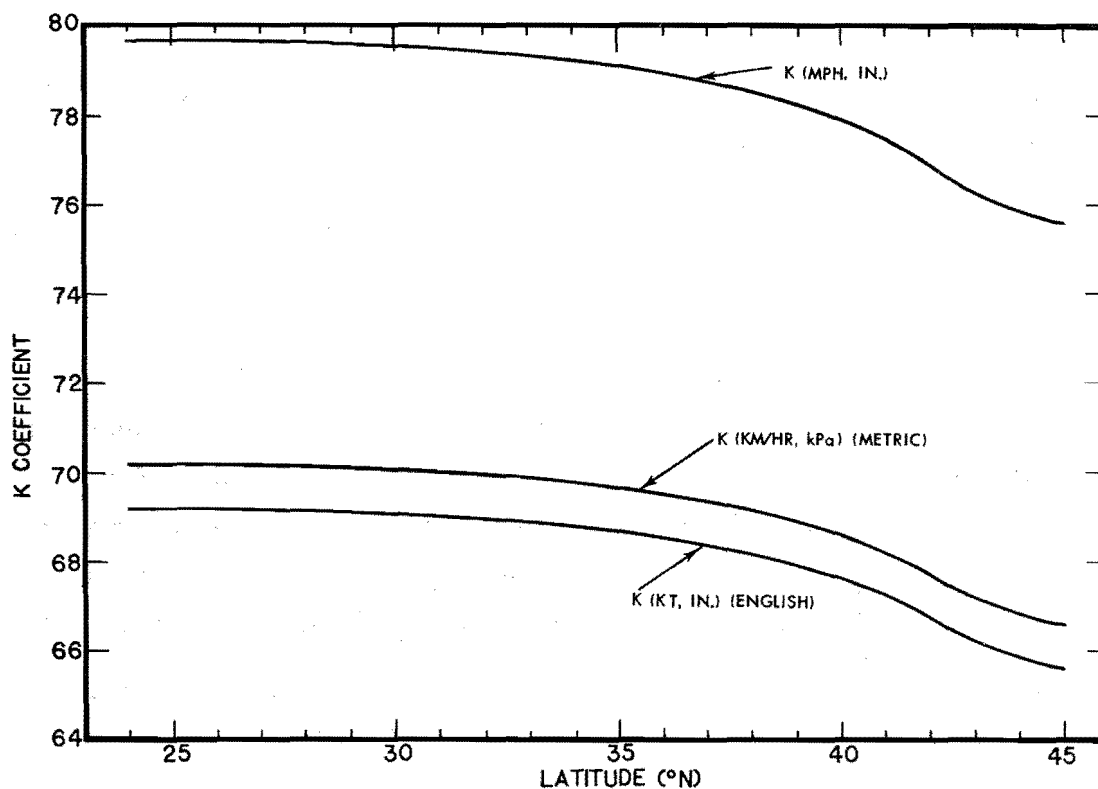
Figure 2.11.--Values of the latitude-dependent K
coefficient for three units of measurement for the
PMH.

2.2.7.2.2 WINDS IN A MOVING HURRICANE. Equations 2.3 and 2.4 are simplified forms of a general equation for V_x that includes an asymmetry factor, A. This factor is

$$A = 1.5 \ (T^{0.63}) \ (T_o^{0.37}) \ \cos \beta \qquad (2.5)$$

where

T = forward speed

T_o = 1 when units are in kt, 0.514791 when units are in ms^{-1}, 1.853248 when units are in km hr^{-1}, and 1.151556 when units are in mi hr^{-1}.

β = the angle between track direction (θ) and the surface wind direc-
tion. β varies around the hurricane at any constant radial (r)
and along a radial with varying distances from the hurricane center.
A is added to the winds on the right of a storm track and subtracted from
those on the left.

When we add A to equations 2.3 and 2.4, we arrive at our adopted SPH and
PMH V_x for a moving hurricane. For the SPH

$$V_x = 0.9 \, V_{gx} + 1.5 \, (T^{0.63}) \, (T_o^{0.37}) \cos \beta \qquad (2.6)$$

For the PMH

$$V_x = 0.95 \, V_{gx} + 1.5 \, (T^{0.63}) \, (T_o^{0.37}) \cos \beta \qquad (2.7)$$

V_x occurs at the point along the circumference of maximum winds where the
surface wind direction is parallel to track direction (θ). Here β = 0 and
cos β = 1. The inherent relation between β and inflow angle (φ) requires
the point at which V_x occurs to fall in the right-rear quadrant of a hurri-
cane. Section 2.2.9 will set allowable limits of rotation for this point.

The general equation for 10-m, 10-min overwater winds at any point other
than where V_x occurs is:

$$V = V_s + 1.5 \, (T^{0.63}) \, (T_o^{0.37}) \cos \beta \qquad (2.8)$$

where V is the wind speed at radius r and V_s is the wind speed in a station-
ary hurricane at radius r. Relative wind profiles for computing V_s are
discussed in sec. 2.2.8. The example in chapter 3 shows how β is computed
along any radial out from the center of a hurricane.

2.2.8 RELATIVE WIND PROFILES (CHAPTER 13)

The adopted variation of wind speed outward from R for a stationary storm
is given in figure 2.12. These profiles (based on actual storms of record)
are R dependent and are expressed in terms of relative winds (V_s/V_{xs}) and
distance outward from R. Figure 2.13 shows the variation of relative wind
speed (V_s/V_{xs}) with relative distance (r/R) inward from R for a stationary
hurricane. This profile is not R dependent and is based on wind profiles of
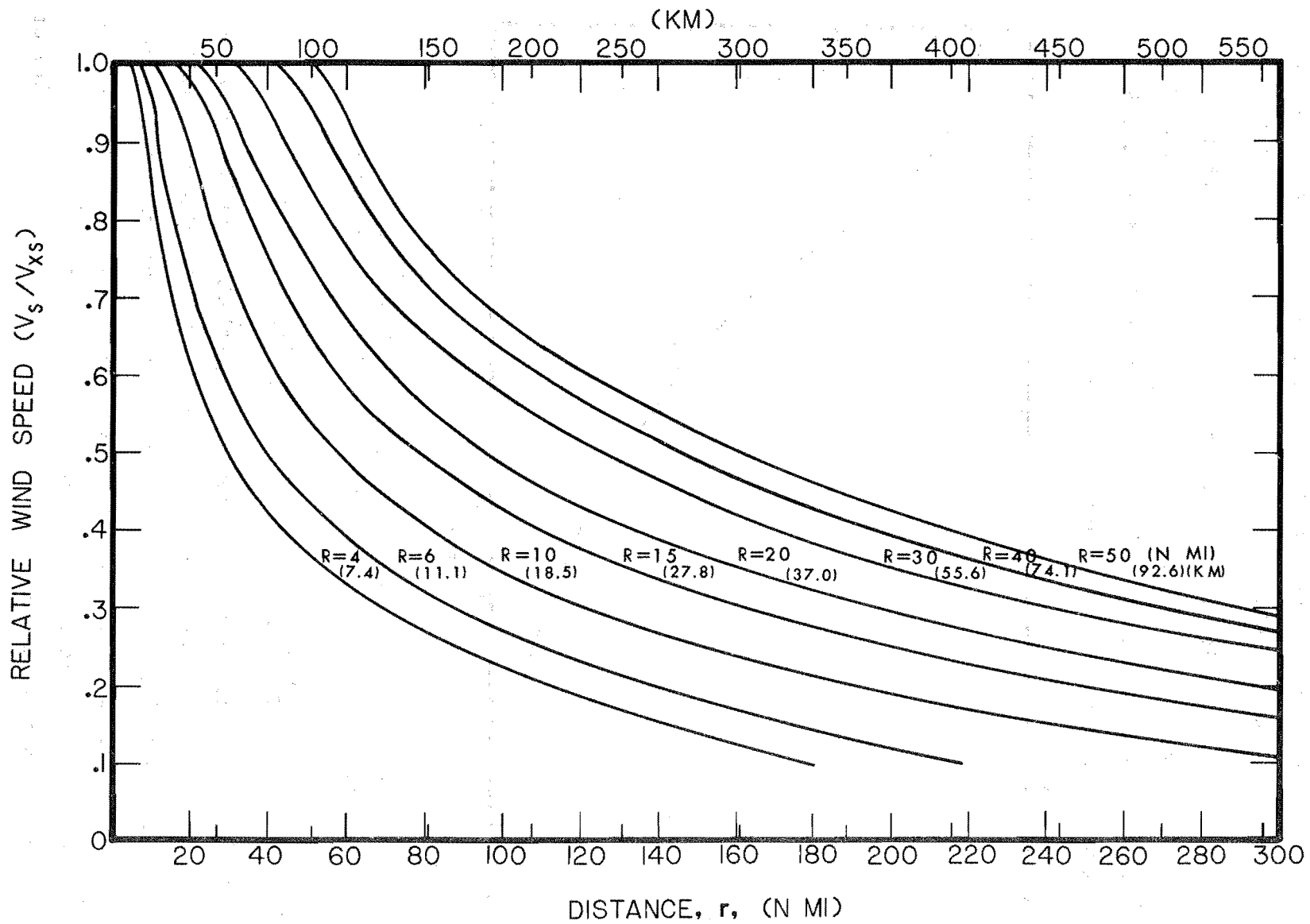
Figure 2.12.--Adopted standardized wind profiles outward from R for the stationary SPH and PMH.

28

intense hurricanes. The relative wind profiles (figs. 2.12 and 2.13) are
identical for the SPH and PMH.

The relative wind profiles shown in figures 2.12 and 2.13 enable us to
determine values of V_s at various r's given V_{xs}. Once we have determined V_s,
we can compute actual winds (V) in a moving hurricane by using eq. 2.8.
The example in chapter 3 shows how we do this.
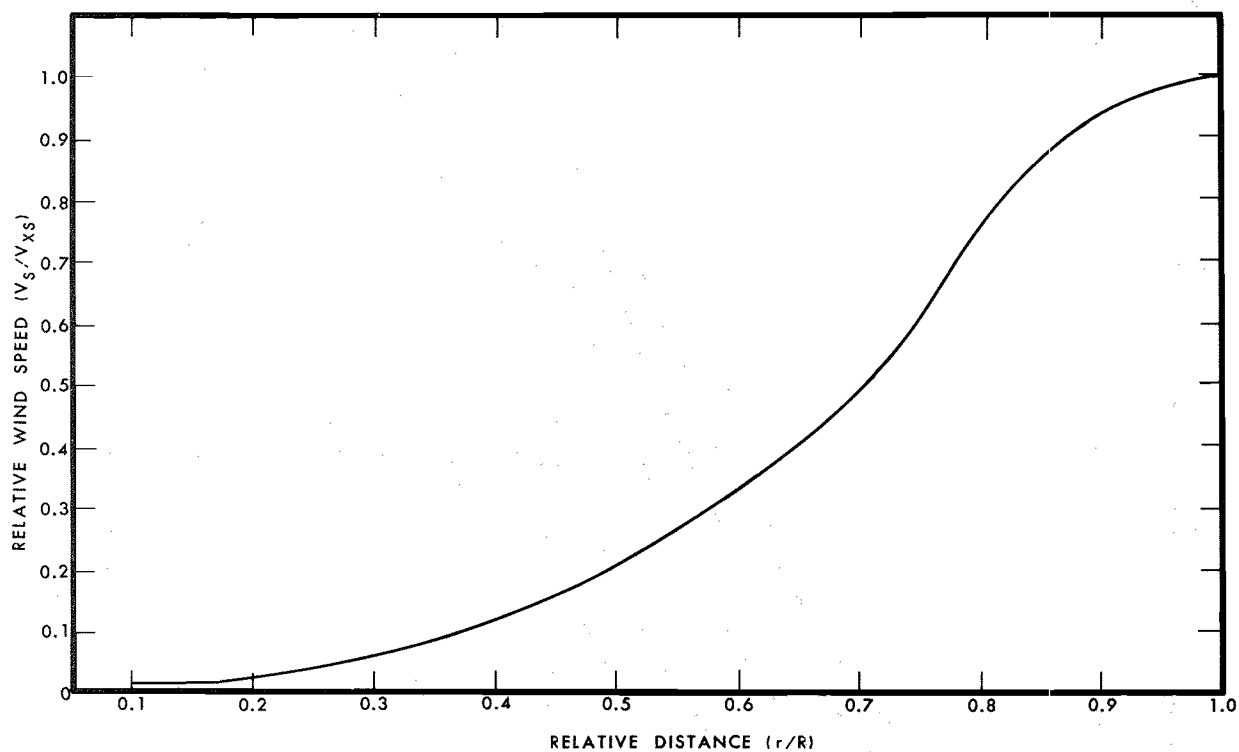
Figure 2.13.--*Variation of relative wind speed with relative distance
within the radius of maximum winds for the stationary SPH and PMH.*

2.2.9 LIMITS OF ROTATION OF WIND FIELDS (CHAPTER 13)

The SPH and PMH 10-m, 10-min overwater wind equations developed in section
2.2.7.2.2 require the region of maximum winds in these hurricanes to fall in
the right rear quadrant. Observational data indicate that this constraint
is too restrictive. We will allow the isotach maximum of the SPH or PMH to
occur at any position between 0° and 180° clockwise from the track
direction as defined in sec. 2.2.6.

2.2.10   Wind Inflow Angle (Chapter 14)

Hurricane winds blow spirally inward and not along a circle concentric with the hurricane center.   The angle between the true wind direction and a tangent to one of these circles is known as the inflow angle (ϕ).   Figures 2.14 and 2.15 show the adopted inflow angle criteria for the SPH and the PMH, respectively.   These criteria are for selected values of R for a continuum of distances from the hurricane center out to 130 n.mi. (241 km)
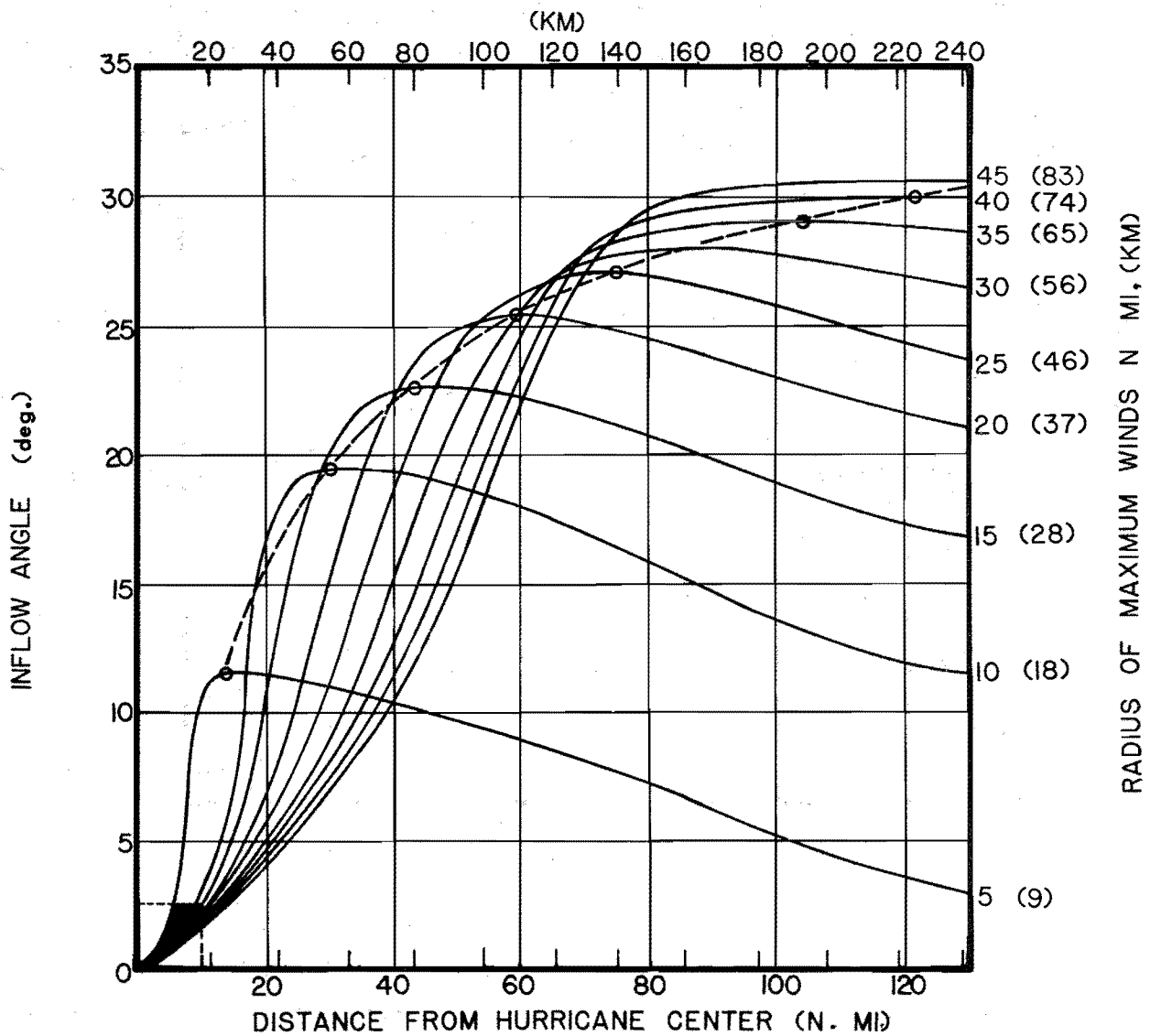
Figure 2.14.--Adopted SPH inflow angles vs. distance from the hurricane center at selected R values.   Open circles denote maximum inflow angle at each R.

and are based on a number of assumptions and constraints. The dashed line
on each figure delineates a line of maximum φ which is helpful when inter-
polating for intermediate R values.
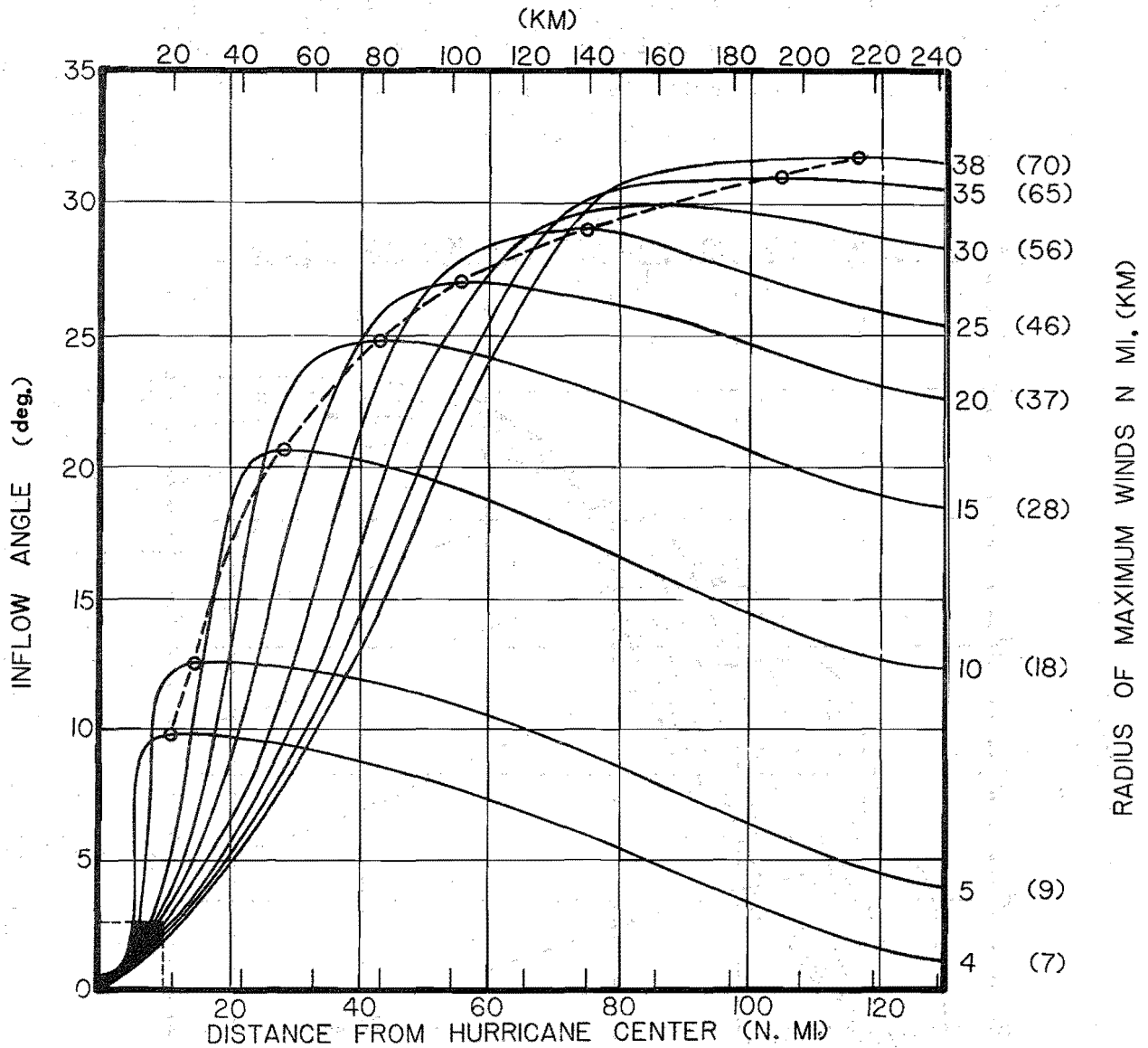
Figure 2.15.--Same as figure 2.14 except for the PMH.

The inflow angle profiles of figures 2.14 and 2.15 indicate no inflow at
the center of the SPH or PMH. The range of φ for a small value of R is less
than the range in φ for storms with a larger value of R. For example, for
the SPH (fig. 2.14), a storm with an R of 10 n.mi. (19 km) has a range in
φ from 0 to 19° and a storm with an R of 20 n.mi. (37 km) has a range in φ
from 0 to 26°.

2.2.11 ADJUSTMENT OF WIND SPEED FOR FRICTIONAL EFFECTS (CHAPTER 15)

At the coast, onshore winds will abruptly decrease as a result of a change in surface friction characteristics. We developed adjustment ratios to account for this effect. These ratios are given in table 2.2. As the wind path continues around the storm, further reductions in wind speed occur until an equilibrium is reached or the wind path again crosses the coast to an open water area. After crossing the coast this second time, the wind will regain its full strength. We developed ratios between offshore and overwater winds (fig. 2.16) for the other friction categories: awash, land, and rough terrain. We applied these same ratios to the onshore winds after the immediate reduction for the coastal effect.

Table 2.2.--Onshore to Overwater Winds Ratio (k_c)

Water to land	: 0.89
Water to awash	: 0.95
Water to rough terrain	: 0.83

Definitions of the four categories are: Water--open water with no significant obstructions to surface winds, e.g., oceans (including all tidewater to the indicated coastline) and large inland water bodies. Awash--normally dry ground with tree or shrub growth, hills or dunes, which are noninundated during a storm surge. Land--relatively flat noninundated terrain or buildings. Rough terrain--major urban areas, dense forests, and mountains with abrupt changes in elevation over short distances.

The adopted ratios of offshore to overwater winds vary with wind speed. Use of the surface friction coefficient increases these ratios to unity 10 n.mi. (19 km) offshore. The awash curve lies halfway between the land curve and 1.0. The dashed curve for rough terrain is based on the 0.4 factor from winds at Brookhaven National Laboratory, N.Y., considered a "rough" location.

These ratios were developed to permit the construction of a wind field as a hurricane approached and crossed the coast. They should only be applied within a reasonable distance of the open coast. They do not take

into consideration the effects of significant mountain ranges such as the Blue Ridge Mountains in Virginia.
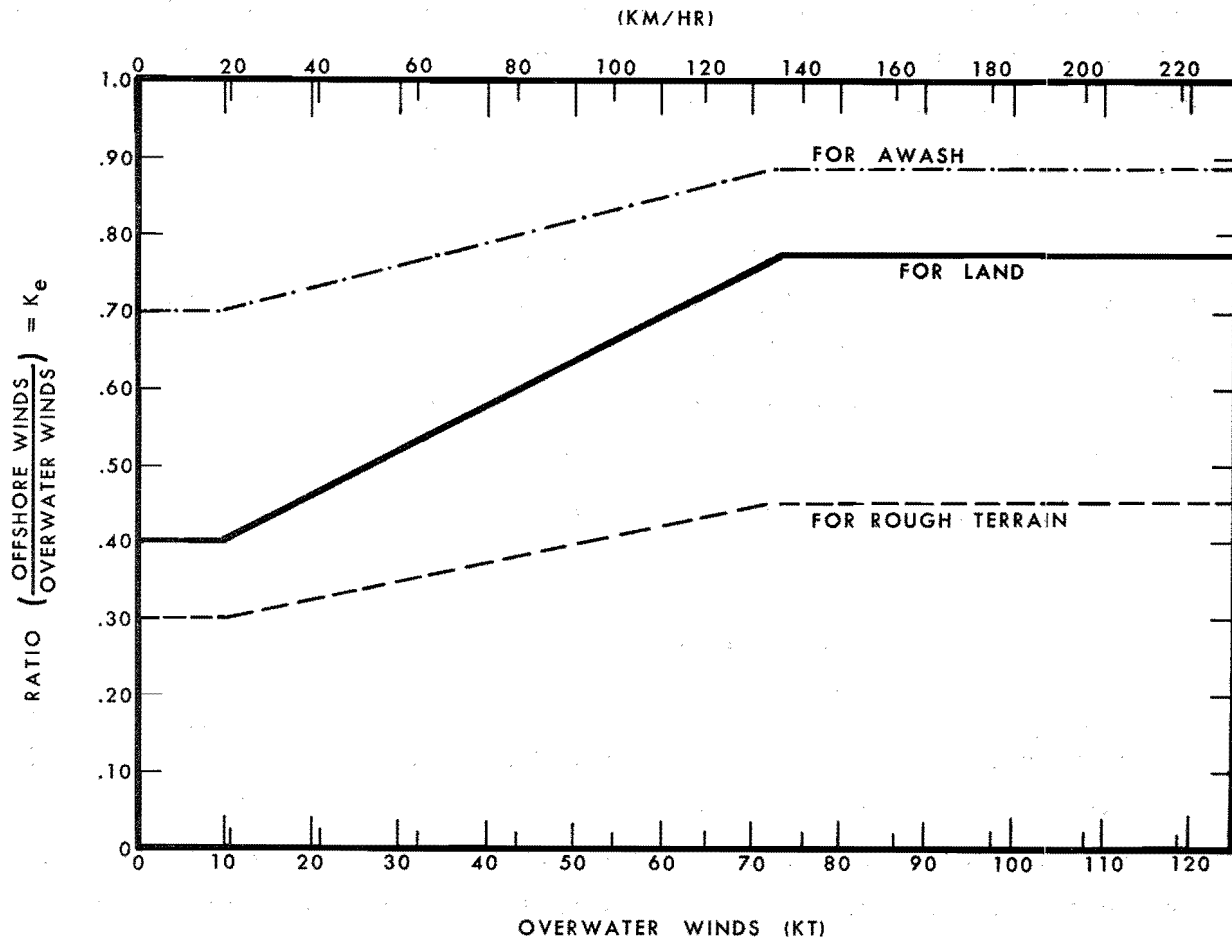
Figure 2.16.--Offshore to overwater winds ratio (k_e).

In general, the 10-m, 10-min frictionally reduced wind speed near shore can be determined from

$$V_k = k\,V \qquad (2.9)$$

where

V = the 10-m, 10-min overwater wind speed for a given location.

V_k = the 10-m, 10-min wind speed adjusted for underlying terrain.

The onshore and offshore winds are assumed to reach equilibrium after being over any underlying friction surface a distance of 10 n.mi. (19 km). The change in the surface friction coefficient after crossing to a new friction category is determined from:

$$k = k_e + Q (k_i - k_e) \qquad (2.10)$$

where

k_e = the equilibrium surface friction coefficient at a point (fig. 2.16).

k_i = the previous surface friction coefficient at the last upwind boundary between surface friction categories; $k_i = k_c$ at the boundary between water and other surfaces for onshore winds.

Q = an interpolation coefficient ranging in value from 1.0 to 0. The value of Q is determined from

$$Q = 1 - 0.195s + 0.0095s^2, \qquad (2.11)$$

where

s = distance from surface friction category boundaries. Q is defined as 0 when s$\geq$ 10 n.mi. (19 km). At the initial boundary of any surface friction category, Q = 1.0. Figure 2.17 shows the graphical form of equation 2.11.

Figure 2.18 is a schematic picture of the frictional adjustments which may be helpful to the user. The k_e values shown are for overwater wind speeds $\geq$ 73 kt (135 km/hr).
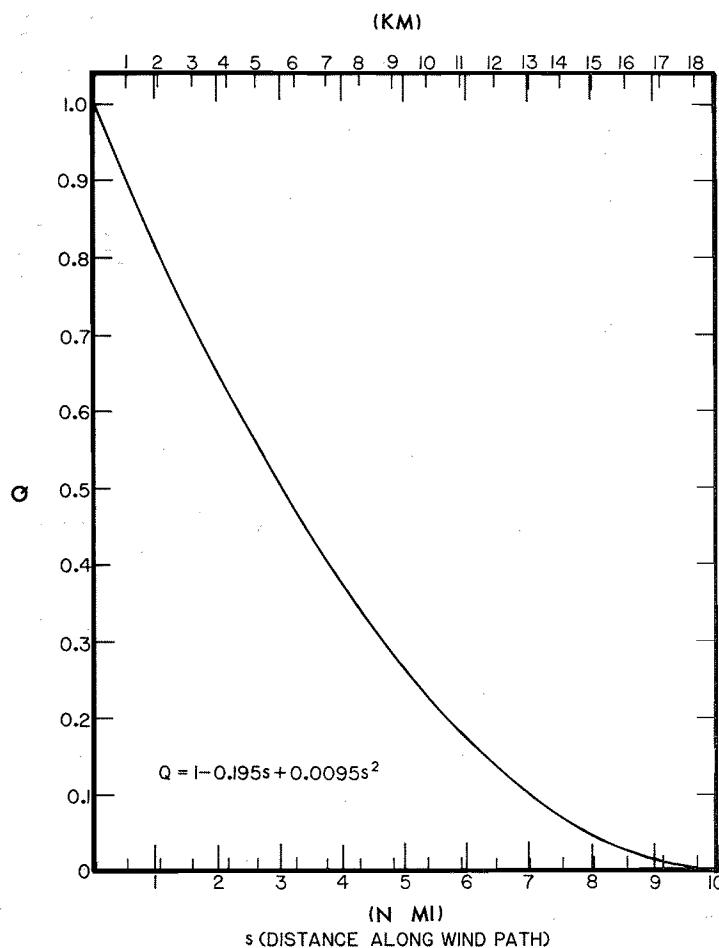
Figure 2.17.--Graphical solution for Q (eq. 2.11).

(KM)
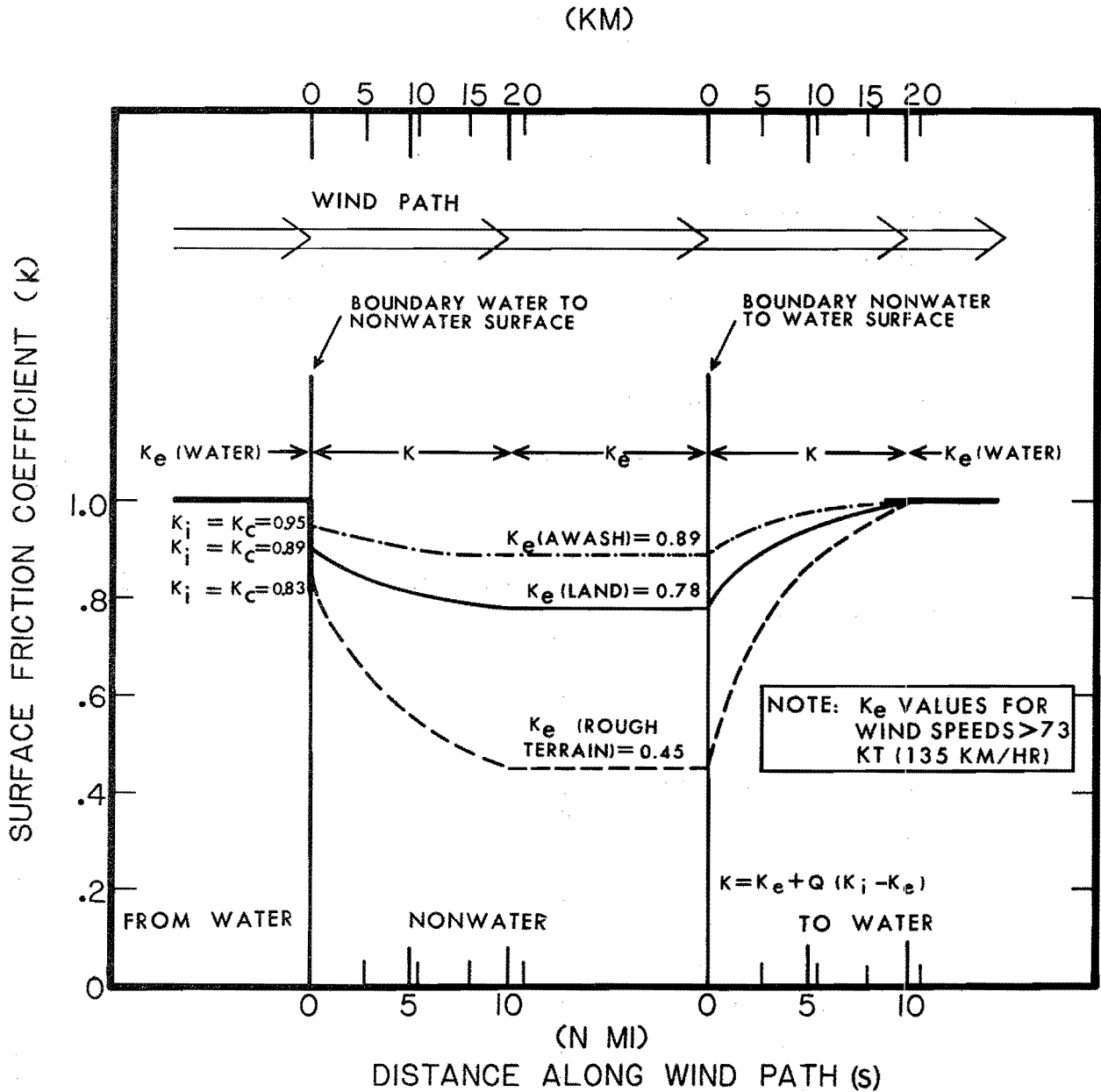
Figure 2.18.--Schematic of near shore frictional adjustments.

2.2.12 ADJUSTMENT OF WIND SPEED BECAUSE OF FILLING OVERLAND (CHAPTER 15)

After the center of a hurricane crosses from sea to land, central pressure rises faster than any change in peripheral pressure [the pressure drop $(p_w - p_o)$ decreases] and winds begin to decrease. Adjustment factors were determined for the reduction of SPH and PMH wind speeds anywhere in the hurricane after landfall. This reduction can then be coupled with the

adjustment of wind speed near shore (sec. 2.2.11) to yield a total wind field adjustment after landfall. It is a percentage adjustment applied to the computed wind field adjusted for surface friction effects.

Figure 2.19 shows three curves of smoothed adjustment factors vs. time after landfall for three geographic regions for the SPH and PMH. Figure 2.20 shows the three regions A, B, and C and also dashed lines between the lettered curves, where linear interpolation should be used in figure 2.19.

2.2.13 THE STALLED PMH (CHAPTER 16)

Scouring and erosion at the beach may result from hurricanes. These conditions are augmented when the storm is slow moving. It is greatest with a stalled hurricane since storm winds and waves will continue to cause scouring and erosion at the same location as long as the storm remains stationary. We define a stalled hurricane as one which maintains a T $\leq$ 5 kt (9 km/hr) for a period of 24 hours or longer. We have not considered stalls of lesser duration. A stalled hurricane may also loop but not all looping hurricanes stall.

The percentage decrease in PMH winds with time after stall is shown by the curve in figure 2.21. This curve may be used along the gulf and east coasts south of the Virginia-North Carolina border (milepost 2260). Stalls are limited to a maximum of 120 hours (5 days). The solid portion of the curve is based on data from two or more hurricanes or typhoons. The dashed portion beyond 60 hours is an extrapolation beyond this data.

Forward speed (T) for a stalled former PMH is given by definition, i.e., $\leq$ 5 kt (9 km/hr). Since looping and other erratic storm motions may accompany a stalled former PMH, no limiting values are assigned to track direction (θ) for a stalled PMH. For radius of maximum winds (R) and inflow angle (ϕ), the user should continue to refer to figures 2.5 and 2.15, respectively. After stalling, a former PMH south of the Virginia-North Carolina border may reintensify to its maximum intensity before stalling after moving at T > 5 kt (9 km/hr) for a period approximately 60 percent as long as the length of the stall.
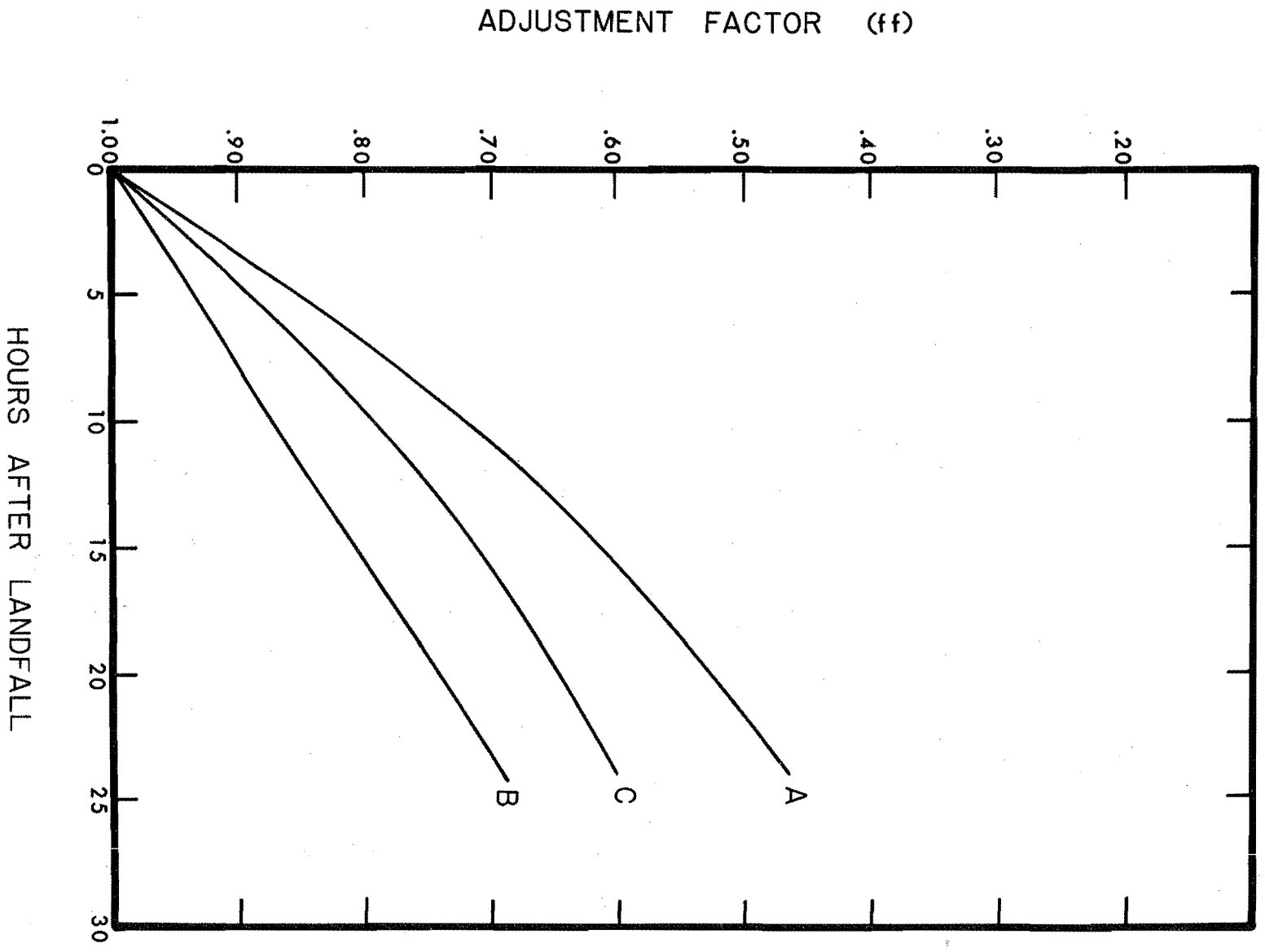
Figure 2.19.--Smoothed adjustment factor curves for reducing hurricane wind speeds when center is overland for the three geographic regions defined in figure 2.20.
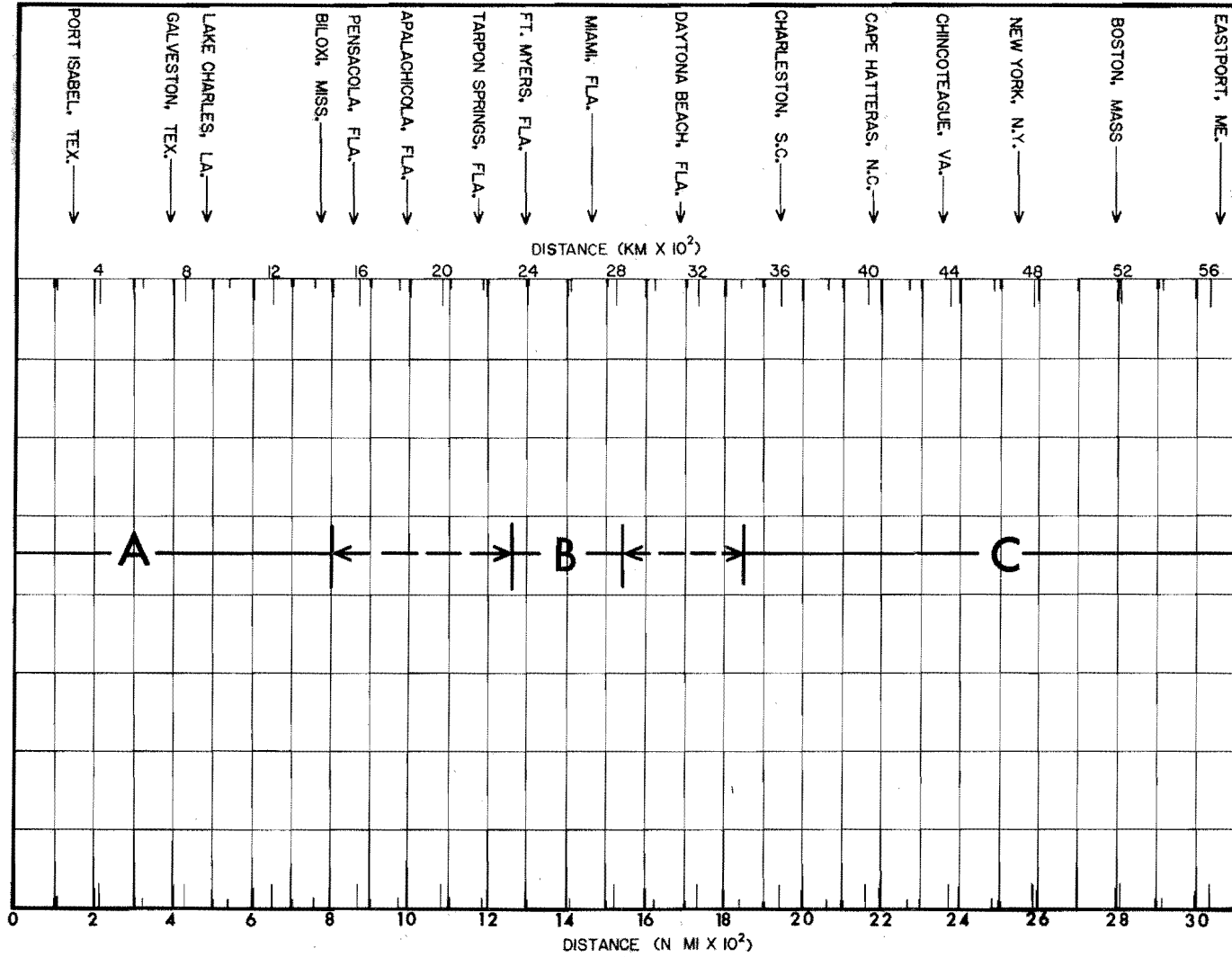
Figure 2.20.--Limits of three geographic regions (A, B, and C). The dashed lines delineate where linear interpolation should be used to develop intermediate curves in figure 2.19.
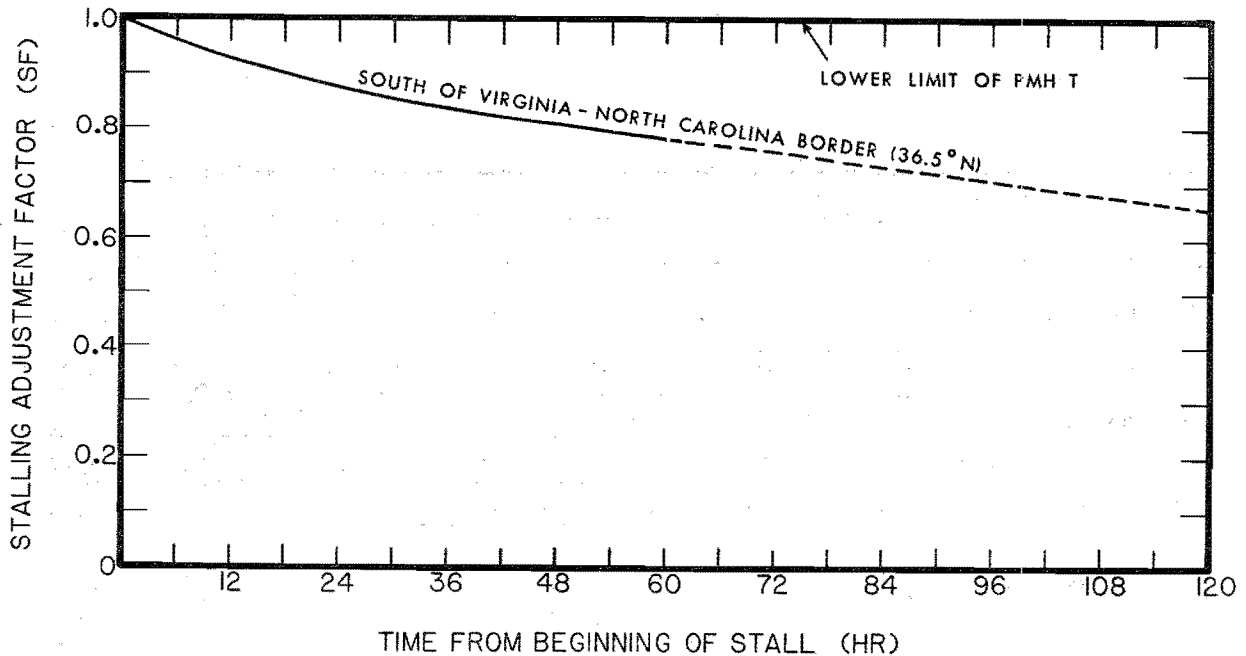
Figure 2.21.--*Stalling adjustment factor (sf) curve for the PMH to be used south of the Virginia - North Carolina border (36.5° N).*

Figure 2.21 is to be applied to the former PMH south of milepost 2260. From there northward, the lower limit of T increases rapidly and criteria for a stalled hurricane may not be valid until we first consider the weakening that would occur when a PMH travels at speeds less than the lower limit of T but greater than the stall speed. We have not studied this problem but have nevertheless developed an empirical procedure based on judgment. It is a reasoned extension of the procedures for more southerly latitudes. This procedure is given in section 16.11.

2.3 COMPARISON OF SPH AND PMH WITH RECORD HURRICANES

Tables 2.3 to 2.6 list computed values of V_{gx} and V_x for both the SPH and PMH at 100-n.mi. (185-km) intervals in both metric and English units for the following six categories:

VGL = V_{gx} for the lower limit of R.

VLL = V_x for the lower limit of R and lower limit of T.

VLU = V_x for the lower limit of R and upper limit of T.

VGU = V_{gx} for the upper limit of R.

VUL = V_x for the upper limit of R and lower limit of T.

VUU = V_x for the upper limit of R and upper limit of T.

These values were computed using equations 2.2 and 2.6 for the SPH and equations 2.2 and 2.7 for the PMH. Values of K in the tables were taken from figure 2.10 (SPH) or figure 2.11 (PMH). A peripheral pressure of 29.77 in. (100.8 kPa) was used for the SPH and 30.12 in. (102.0 kPa) for the PMH (see sec. 2.2.2). The central pressure for the SPH comes from figure 2.1 and for the PMH from figure 2.2. The upper and lower limiting values of R come from figure 2.4 for the SPH and figure 2.5 for the PMH. The upper and lower limiting values of T are from figure 2.6 (SPH) and figure 2.7 (PMH). Table notes appear on the page preceding the tables. The computed wind speeds for the six categories are also shown in figures 2.22 to 2.24 for the SPH and 2.25 to 2.27 for the PMH. Two curves are plotted on each graph. The data

NOTES FOR TABLES 2.3 TO 2.6

MPOST = milepost (n.mi. or km)

LAT = latitude

PW = peripheral pressure

PO = central pressure

$K = \left(\dfrac{1}{\rho e}\right)^{1/2}$; see section 2.27

LR = lower limit of radius of maximum winds

UR = upper limit of radius of maximum winds

LT = lower limit of forward speed

UT = upper limit of forward speed

VGL = maximum gradient wind speed (V_{gx}) for LR – hurricane stationary

VGU = maximum gradient wind speed (V_{gx}) for UR – hurricane stationary

VLL = maximum 10-m, 10-min overwater wind speed (V_x) for LR and LT

VUL = maximum 10-m, 10-min overwater wind speed (V_x) for UR and LT

VLU = maximum 10-m, 10-min overwater wind speed (V_x) for LR and UT

VUU = maximum 10-m, 10-min overwater wind speed (V_x) for UR and UT

KM/H = km/hr

Table 2.3.--Ranges of maximum gradient and 10-m, 10-min overwater winds at 100-n.mi. intervals for the SPH (English units).

MPOST N MI	LAT DEG	PW IN.	PO IN.	K KT-IN.	LR NMI	UR NMI	LT KT	UT KT	VGL KT	VLL KT	VLU KT	VGU KT	VUL KT	VUU KT
100.	25.5	29.77	27.23	67.3	6.	28.	4.	25.	106.6	99.5	107.3	104.1	97.3	105.1
200.	26.9	29.77	27.26	67.2	6.	28.	4.	25.	105.8	98.8	106.6	103.1	96.4	104.2
300.	28.5	29.77	27.29	67.1	6.	28.	4.	25.	104.9	98.0	105.8	102.2	95.5	103.4
400.	29.3	29.77	27.29	67.0	6.	28.	4.	25.	104.8	97.9	105.7	101.9	95.3	103.1
500.	29.6	29.77	27.29	66.9	6.	28.	4.	25.	104.6	97.7	105.5	101.7	95.2	103.0
600.	29.1	29.77	27.29	67.0	7.	28.	4.	25.	104.6	97.8	105.6	101.9	95.3	103.2
700.	29.2	29.77	27.29	67.0	7.	29.	4.	25.	104.6	97.8	105.6	101.8	95.2	103.0
800.	30.2	29.77	27.29	66.8	7.	30.	4.	25.	104.3	97.4	105.3	101.2	94.7	102.5
900.	30.4	29.77	27.55	66.8	8.	31.	4.	25.	98.3	92.1	99.9	95.3	89.4	97.2
1000.	29.8	29.77	27.76	66.9	9.	32.	4.	25.	93.6	87.9	95.7	90.6	85.2	93.0
1100.	29.5	29.77	27.79	67.0	9.	32.	4.	25.	93.1	87.4	95.2	90.1	84.7	92.5
1200.	28.0	29.77	27.55	67.1	8.	31.	4.	25.	98.9	92.6	100.4	96.0	90.0	97.8
1300.	26.5	29.77	27.29	67.2	6.	30.	4.	25.	105.1	98.2	106.0	102.3	95.7	103.5
1400.	25.2	29.77	27.08	67.3	5.	28.	4.	25.	109.8	102.4	110.2	107.2	100.1	107.9
1500.	26.5	29.77	27.17	67.2	5.	29.	4.	25.	107.7	100.6	108.4	104.9	98.0	105.8
1600.	28.2	29.77	27.32	67.1	6.	31.	4.	25.	104.3	97.5	105.3	101.2	94.7	102.5
1700.	29.6	29.77	27.46	66.9	7.	32.	4.	25.	100.6	94.2	102.0	97.4	91.2	99.0
1800.	31.1	29.77	27.55	66.8	8.	33.	4.	25.	98.3	92.1	99.9	94.9	89.0	96.8
1900.	32.5	29.77	27.52	66.7	9.	33.	4.	26.	98.7	92.4	100.5	95.3	89.3	97.4
2000.	33.5	29.77	27.46	66.7	9.	33.	4.	30.	99.9	93.5	102.7	96.4	90.4	99.6
2100.	34.5	29.77	27.46	66.7	9.	33.	4.	35.	99.9	93.5	104.0	96.3	90.3	100.8
2200.	35.6	29.77	27.52	66.7	10.	34.	4.	39.	98.4	92.1	103.6	94.7	88.8	100.3
2300.	37.3	29.77	27.64	66.3	11.	35.	4.	43.	94.9	89.0	101.5	91.1	85.6	98.0
2400.	38.8	29.77	27.73	65.9	12.	36.	6.	47.	92.1	87.5	99.8	88.1	84.0	96.3
2500.	40.1	29.77	27.82	65.6	14.	38.	12.	50.	89.2	87.5	97.9	85.2	83.8	94.3
2600.	41.0	29.77	27.88	65.1	15.	39.	16.	53.	86.9	86.8	96.5	82.8	83.1	92.8
2700.	41.7	29.77	27.91	64.9	16.	40.	19.	54.	85.7	86.7	95.7	81.5	83.0	91.9
2800.	42.5	29.77	28.17	64.6	19.	43.	22.	54.	78.2	80.9	88.9	73.9	77.1	85.1
2900.	43.9	29.77	28.23	64.4	20.	44.	23.	54.	76.2	79.4	87.1	71.8	75.4	83.1
3000.	44.5	29.77	28.26	64.3	21.	45.	24.	55.	75.0	78.6	86.3	70.6	74.7	82.3
3100.	45.3	29.77	28.29	64.2	22.	45.	24.	55.	73.9	77.6	85.2	69.6	73.8	81.4

Table 2.4.--Ranges of maximum gradient and 10-m, 10-min overwater winds at selected intervals for the SPH (metric units).

MPOST KM	LAT DEG	PW KPA	PO KPA	K $\frac{KM}{H}$-KPA	LR KM	UR KM	LT KM/H	UT KM/H	VGL KM/H	VLL KM/H	VLU KM/H	VGU KM/H	VUL KM/H	VUU KM/H
185.	25.5	100.8	92.2	68.2	11.	52.	7.	46.	197.5	184.4	198.9	192.9	180.3	194.7
371.	26.9	100.8	92.3	68.1	11.	52.	7.	46.	196.0	183.0	197.5	191.1	178.7	193.2
556.	28.5	100.8	92.4	68.0	11.	52.	7.	46.	194.5	181.7	196.1	189.4	177.1	191.5
741.	29.3	100.8	92.4	67.9	11.	52.	7.	46.	194.1	181.4	195.8	188.9	176.7	191.1
927.	29.6	100.8	92.4	67.8	11.	52.	7.	46.	193.8	181.1	195.6	188.5	176.3	190.8
1112.	29.1	100.8	92.4	67.9	13.	52.	7.	46.	193.9	181.2	195.6	188.9	176.7	191.2
1297.	29.2	100.8	92.4	67.9	13.	54.	7.	46.	193.9	181.2	195.6	188.7	176.5	190.9
1483.	30.2	100.8	92.4	67.7	13.	56.	7.	46.	193.3	180.6	195.1	187.6	175.5	190.0
1668.	30.4	100.8	93.3	67.7	15.	57.	7.	46.	182.3	170.7	185.2	176.6	165.6	180.1
1853.	29.8	100.8	94.0	67.8	17.	59.	7.	46.	173.5	162.8	177.3	168.0	157.8	172.3
2039.	29.5	100.8	94.1	67.9	17.	59.	7.	46.	172.5	161.9	176.4	167.0	156.9	171.4
2224.	28.0	100.8	93.3	68.0	15.	57.	7.	46.	183.2	171.6	186.0	178.0	166.8	181.3
2409.	26.5	100.8	92.4	68.1	11.	56.	7.	46.	194.8	182.0	196.5	189.6	177.3	191.8
2595.	25.2	100.8	91.7	68.2	9.	52.	7.	46.	203.4	189.7	204.2	198.7	185.4	199.9
2780.	26.5	100.8	92.0	68.1	9.	54.	7.	46.	199.7	186.4	200.8	194.5	181.7	196.1
2965.	28.2	100.8	92.5	68.0	11.	57.	7.	46.	193.3	180.6	195.1	187.6	175.5	189.9
3151.	29.6	100.8	93.0	67.8	13.	59.	7.	46.	186.5	174.5	189.0	180.5	169.1	183.5
3336.	31.1	100.8	93.3	67.7	15.	61.	7.	46.	182.2	170.7	185.1	175.9	165.0	179.5
3521.	32.5	100.8	93.2	67.6	17.	61.	7.	48.	182.8	171.2	186.2	176.6	165.6	180.5
3706.	33.5	100.8	93.0	67.6	17.	61.	7.	56.	185.2	173.3	190.4	178.7	167.5	184.6
3892.	34.5	100.8	93.0	67.6	17.	61.	7.	65.	185.1	173.3	192.7	178.5	167.3	186.8
4077.	35.6	100.8	93.2	67.6	19.	63.	7.	72.	182.3	170.8	192.1	175.6	164.7	185.9
4262.	37.3	100.8	93.6	67.2	20.	65.	7.	80.	175.9	165.0	188.1	168.8	158.6	181.7
4448.	38.8	100.8	93.9	66.8	22.	67.	11.	87.	170.7	162.2	185.0	163.4	155.6	178.5
4633.	40.1	100.8	94.2	66.5	26.	70.	22.	93.	165.3	162.1	181.5	157.8	155.3	174.7
4818.	41.0	100.8	94.4	66.0	28.	72.	30.	98.	161.1	160.9	178.9	153.4	154.0	172.0
5004.	41.7	100.8	94.5	65.8	30.	74.	35.	100.	158.9	160.8	177.3	151.1	153.8	170.3
5189.	42.5	100.8	95.4	65.5	35.	80.	41.	100.	144.9	149.9	164.8	137.0	142.8	157.7
5374.	43.9	100.8	95.6	65.3	37.	82.	43.	100.	141.1	147.1	161.3	133.1	139.8	154.1
5560.	44.5	100.8	95.7	65.2	39.	83.	44.	102.	139.1	145.8	159.9	130.9	138.4	152.5
5745.	45.3	100.8	95.8	65.1	41.	83.	44.	102.	137.0	143.9	158.0	129.0	136.7	150.8

42

Table 2.5.--Ranges of maximum gradient and 10-m, 10-min overwater winds at 100-n.mi. intervals for the PMH (English units).

MPOST N MI	LAT DEG	PW IN.	PO IN.	K KT-IN.	LR NMI	UR NMI	LT KT	UT KT	VGL KT	VLL KT	VLU KT	VGU KT	VUL KT	VUU KT
100.	25.5	30.12	26.16	69.2	5.	21.	6.	20.	137.1	134.9	140.1	135.3	133.2	138.4
200.	26.9	30.12	26.19	69.2	5.	21.	6.	20.	136.5	134.4	139.6	134.6	132.6	137.8
300.	28.5	30.12	26.19	69.1	5.	21.	6.	20.	136.3	134.1	139.4	134.3	132.2	137.5
400.	29.3	30.12	26.19	69.1	5.	21.	6.	20.	136.3	134.1	139.4	134.2	132.2	137.4
500.	29.6	30.12	26.19	69.1	5.	21.	6.	20.	136.3	134.1	139.4	134.2	132.1	137.4
600.	29.1	30.12	26.22	69.1	6.	21.	6.	20.	135.7	133.5	138.8	133.7	131.7	137.0
700.	29.2	30.12	26.22	69.1	6.	21.	6.	20.	135.7	133.5	138.8	133.7	131.7	137.0
800.	30.2	30.12	26.22	69.0	6.	22.	7.	20.	135.4	133.8	138.6	133.3	131.8	136.6
900.	30.4	30.12	26.25	69.0	6.	22.	9.	20.	134.9	134.2	138.1	132.8	132.1	136.1
1000.	29.8	30.12	26.28	69.1	6.	22.	13.	20.	134.6	135.4	137.8	132.5	133.4	135.8
1100.	29.5	30.12	26.31	69.1	7.	23.	15.	20.	134.0	135.5	137.2	131.9	133.6	135.2
1200.	28.0	30.12	26.25	69.1	6.	22.	12.	20.	135.2	135.6	138.3	133.2	133.7	136.4
1300.	26.5	30.12	26.16	69.2	5.	20.	7.	20.	137.1	135.3	140.1	135.3	133.7	138.4
1400.	25.2	30.12	26.11	69.2	4.	20.	6.	20.	138.2	135.9	141.2	136.4	134.2	139.5
1500.	26.5	30.12	26.13	69.2	4.	20.	6.	20.	137.7	135.5	140.7	135.8	133.7	138.9
1600.	28.2	30.12	26.19	69.1	5.	20.	6.	20.	136.3	134.1	139.4	134.5	132.4	137.6
1700.	29.6	30.12	26.22	69.1	6.	21.	6.	20.	135.6	133.5	138.8	133.7	131.7	136.9
1800.	31.1	30.12	26.25	69.0	6.	21.	6.	20.	134.9	132.8	138.1	132.9	130.9	136.1
1900.	32.5	30.12	26.28	68.9	7.	22.	7.	22.	134.0	132.4	137.8	131.9	130.4	135.8
2000.	33.5	30.12	26.31	68.8	8.	23.	8.	26.	133.1	132.0	138.1	130.9	130.0	136.1
2100.	34.5	30.12	26.37	68.7	8.	24.	9.	29.	131.9	131.2	137.8	129.5	129.0	135.5
2200.	35.6	30.12	26.40	68.7	9.	25.	10.	34.	131.1	131.0	138.4	128.7	128.7	136.1
2300.	37.3	30.12	26.49	68.3	10.	26.	17.	38.	128.6	131.1	137.0	126.0	128.7	134.6
2400.	38.8	30.12	26.61	68.0	11.	28.	26.	41.	125.7	131.1	134.9	122.9	128.4	132.3
2500.	40.1	30.12	26.75	67.6	12.	29.	32.	44.	122.0	129.2	132.2	119.1	126.5	129.4
2600.	41.0	30.12	26.81	67.3	13.	31.	36.	47.	120.2	128.5	131.1	117.1	125.5	128.2
2700.	41.7	30.12	26.84	66.9	14.	33.	39.	49.	118.7	127.8	130.2	115.4	124.7	127.0
2800.	42.5	30.12	27.23	66.4	17.	34.	40.	50.	109.9	119.8	122.1	106.9	116.9	119.2
2900.	43.9	30.12	27.40	65.9	18.	36.	40.	50.	105.3	115.4	117.7	102.1	112.3	114.6
3000.	44.5	30.12	27.43	65.8	19.	37.	41.	50.	104.4	114.7	116.8	101.1	111.6	113.6
3100.	45.3	30.12	27.46	65.6	20.	38.	41.	50.	103.2	113.6	115.7	99.9	110.4	112.5

Table 2.6.--Ranges of maximum gradient and 10-m, 10-min overwater winds at selected intervals for the PMH (metric units).

MPOST KM	LAT DEG	PW KPA	PO KPA	K KM/H-KPA	LR KM	UR KM	LT KM/H	UT KM/H	VGL KM/H	VLL KM/H	VLU KM/H	VGU KM/H	VUL KM/H	VUU KM/H
185.	25.5	102.0	88.6	70.2	9.	39.	11.	37.	254.1	250.0	259.7	250.7	246.8	256.5
371.	26.9	102.0	88.7	70.2	9.	39.	11.	37.	253.1	249.0	258.8	249.5	245.7	255.4
556.	28.5	102.0	88.7	70.1	9.	39.	11.	37.	252.6	248.6	258.3	248.9	245.1	254.8
741.	29.3	102.0	88.7	70.1	9.	39.	11.	37.	252.6	248.6	258.3	248.8	244.9	254.7
927.	29.6	102.0	88.7	70.1	9.	39.	11.	37.	252.6	248.6	258.3	248.7	244.9	254.7
1112.	29.1	102.0	88.8	70.1	11.	39.	11.	37.	251.4	247.4	257.2	247.9	244.1	253.8
1297.	29.2	102.0	88.8	70.1	11.	39.	11.	37.	251.4	247.4	257.2	247.8	244.0	253.8
1483.	30.2	102.0	88.8	70.0	11.	41.	13.	37.	251.0	247.9	256.8	247.1	244.2	253.1
1668.	30.4	102.0	88.9	70.0	11.	41.	17.	37.	250.0	248.6	255.9	246.1	244.9	252.1
1853.	29.8	102.0	89.0	70.1	11.	41.	24.	37.	249.5	251.0	255.3	245.6	247.3	251.7
2039.	29.5	102.0	89.1	70.1	13.	43.	28.	37.	248.3	251.2	254.2	244.4	247.5	250.6
2224.	28.0	102.0	88.9	70.1	11.	41.	22.	37.	250.5	251.3	256.3	246.8	247.8	252.9
2409.	26.5	102.0	88.6	70.2	9.	37.	13.	37.	254.0	250.8	259.7	250.8	247.7	256.6
2595.	25.2	102.0	88.4	70.2	7.	37.	11.	37.	256.1	251.9	261.6	252.8	248.7	258.5
2780.	26.5	102.0	88.5	70.2	7.	37.	11.	37.	255.2	251.0	260.8	251.7	247.7	257.5
2965.	28.2	102.0	88.7	70.1	9.	37.	11.	37.	252.6	248.6	258.4	249.2	245.3	255.1
3151.	29.6	102.0	88.8	70.1	11.	39.	11.	37.	251.4	247.4	257.2	247.8	244.0	253.7
3336.	31.1	102.0	88.9	70.0	11.	39.	11.	37.	250.0	246.1	255.9	246.2	242.5	252.3
3521.	32.5	102.0	89.0	69.9	13.	41.	13.	41.	248.4	245.4	255.4	244.4	241.7	251.7
3706.	33.5	102.0	89.1	69.8	15.	43.	15.	48.	246.7	244.7	256.0	242.7	240.8	252.2
3892.	34.5	102.0	89.3	69.7	15.	44.	17.	54.	244.4	243.2	255.3	239.9	239.0	251.1
4077.	35.6	102.0	89.4	69.7	17.	46.	19.	63.	243.0	242.7	256.5	238.5	238.4	252.2
4262.	37.3	102.0	89.7	69.3	19.	48.	32.	70.	238.3	242.9	253.9	233.6	238.5	249.4
4448.	38.8	102.0	90.1	68.9	20.	52.	48.	76.	232.9	242.9	250.1	227.7	238.0	245.2
4633.	40.1	102.0	90.6	68.5	22.	54.	59.	82.	226.1	239.5	245.0	220.8	234.4	239.9
4818.	41.0	102.0	90.8	68.2	24.	57.	67.	87.	222.7	238.1	243.0	216.9	232.7	237.5
5004.	41.7	102.0	90.9	67.8	26.	61.	72.	91.	219.9	236.9	241.2	213.8	231.0	235.4
5189.	42.5	102.0	92.2	67.3	32.	63.	74.	93.	203.7	222.0	226.2	198.2	216.7	220.9
5374.	43.9	102.0	92.8	66.8	33.	67.	74.	93.	195.2	213.9	218.2	189.2	208.1	212.4
5560.	44.5	102.0	92.9	66.7	35.	69.	76.	93.	193.4	212.6	216.4	187.3	206.8	210.6
5745.	45.3	102.0	93.0	66.5	37.	70.	76.	93.	191.3	210.6	214.4	185.1	204.6	208.5
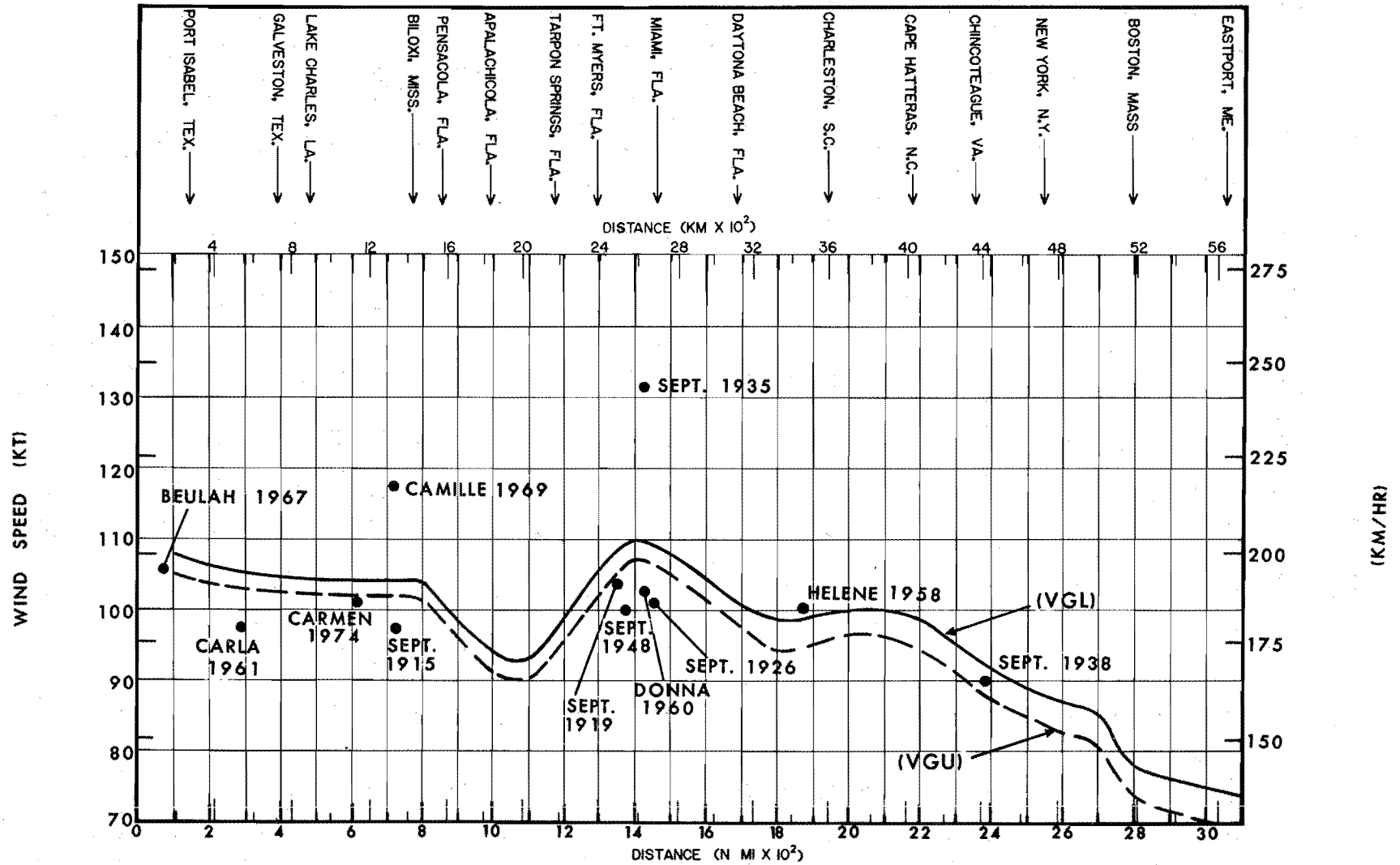
Figure 2.22.—Maximum gradient wind speed for lower (VGL) and upper (VGU) limits of R for the stationary SPH. V_{gx} data from tables 4.1 to 4.4 are plotted for some intense hurricanes.
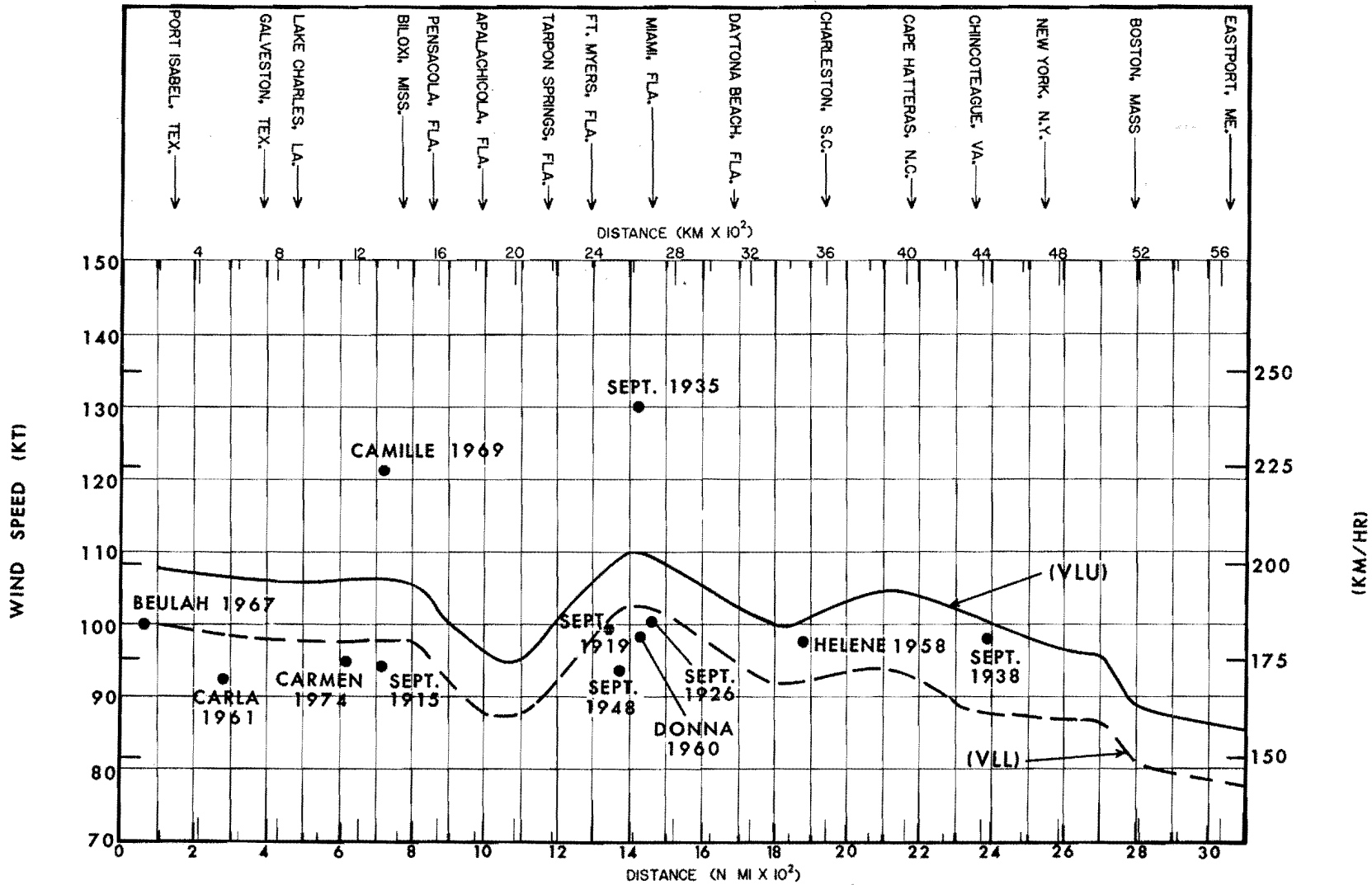
Figure 2.23.—Maximum 10-m, 10-min overwater wind speed for the SPH for the lower limit of R and upper limit of T (VLU) and lower limit of R and lower limit of T (VLL). V_x data from tables 4.1 to 4.4 are plotted for some intense hurricanes.

46

DISTANCE (KM X 10²)

PORT ISABEL, TEX.→
GALVESTON, TEX.→
LAKE CHARLES, LA.→
BILOXI, MISS.→
PENSACOLA, FLA.→
APALACHICOLA, FLA.→
TARPON SPRINGS, FLA.→
FT. MYERS, FLA.→
MIAMI, FLA.→
DAYTONA BEACH, FLA.→
CHARLESTON, S.C.→
CAPE HATTERAS, N.C.→
CHINCOTEAGUE, VA.→
NEW YORK, N.Y.→
BOSTON, MASS→
EASTPORT, ME.→

150
140
130
120
110
100
90
80
70

WIND SPEED (KT)

(KM/HR)
250
225
200
175
150

4 8 12 16 20 24 28 32 36 40 44 48 52 56

SEPT. 1935
CAMILLE 1969
(VUU)
SEPT. 1919
SEPT. 1926
BEULAH 1967
SEPT. 1915
HELENE 1958
SEPT. 1938
CARLA 1961
CARMEN 1974
DONNA 1960
SEPT. 1948
(VUL)

0 2 4 6 8 10 12 14 16 18 20 22 24 26 28 30
DISTANCE (N MI X 10²)

Figure 2.24.—Same as figure 2.23 except for the upper limit of R and upper limit of T (VUU) and upper limit of R and lower limit of T (VUL).
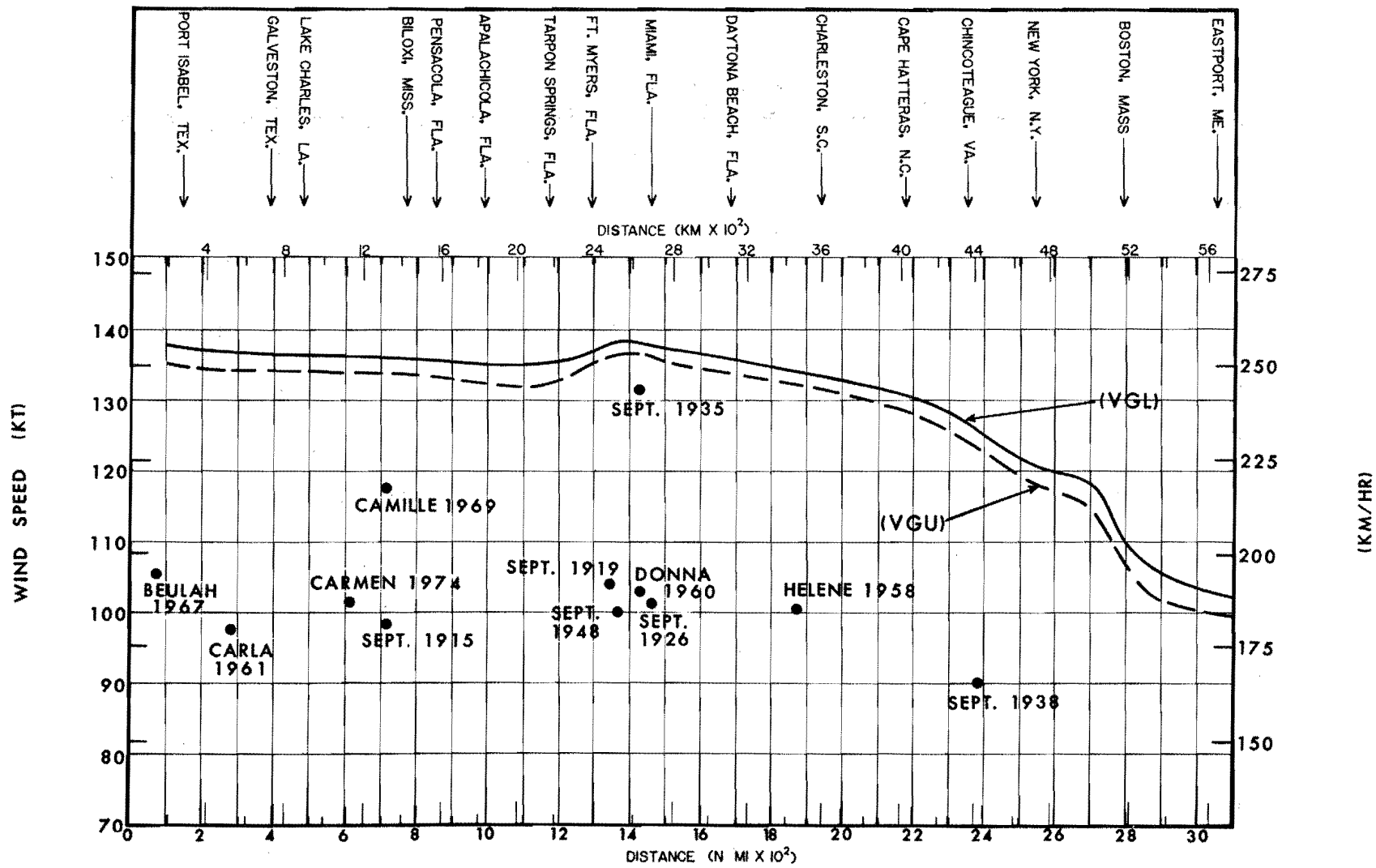
Figure 2.25.--Same as figure 2.22 except for the stationary PMH.
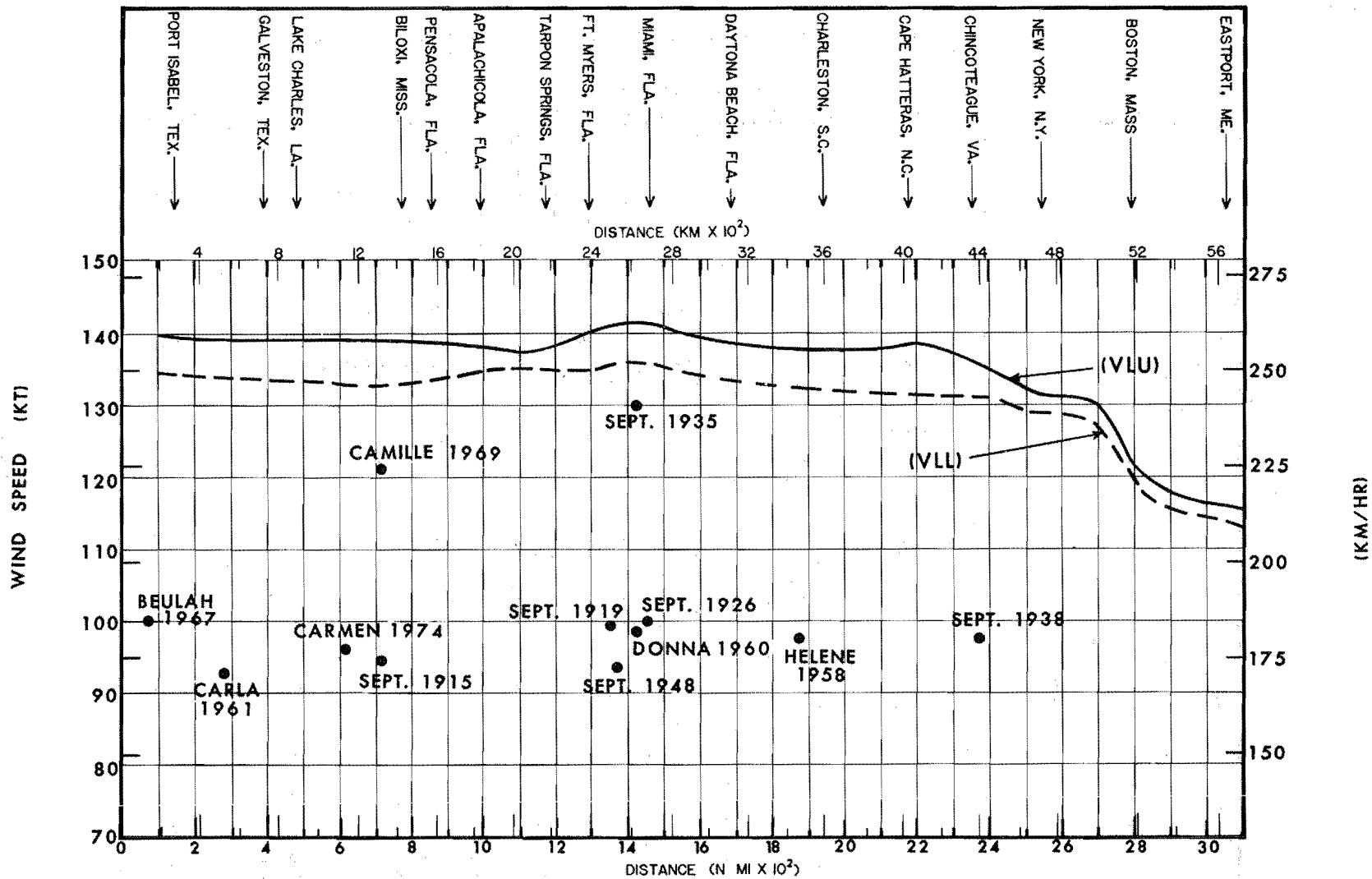
Figure 2.26.--Same as figure 2.23 except for the PMH.
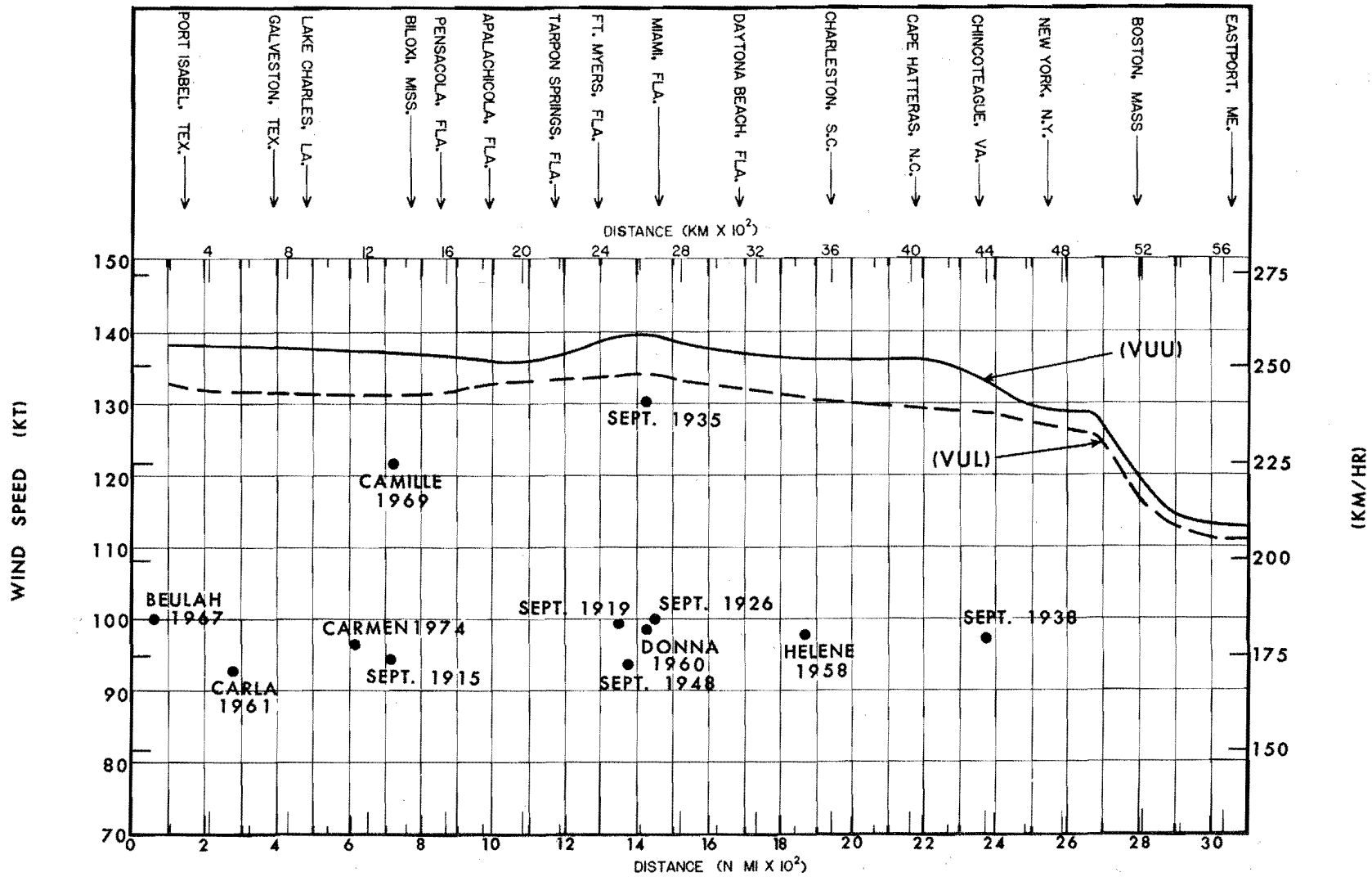
Figure 2.27.—Same as figure 2.24 except for the PMH.

on the figures are computed V_{gx} and V_x winds for hurricanes of record using observed or estimated values of meteorological parameters and factors for each hurricane. SPH criteria and equations 2.2 and 2.6 were used for all storms except Camille and the Labor Day hurricane of 1935. For these latter storms, PMH criteria and equations 2.2 and 2.7 were used.

Coastal values of VGL and VGU are shown in figure 2.22 for the SPH. Wind speeds generally decrease with increasing latitude. The gulf coast minimum near milepost 1100 is in agreement with the central pressure (p_o) maximum in that area.

Forward speed is a factor present in figures 2.23 (VLU and VLL) and 2.24 (VUU and VUL) for the SPH. Wind speeds decrease with increasing latitude but a noticeable maximum appears along the North Carolina coast. This maximum is a result of somewhat lower p_o's in this area, and in the case of VLU higher forward speeds may also be important.

The V_{gx} winds of the Labor Day hurricane of 1935, Camille, and Helene exceed the SPH VGL and SPH VGU winds in figure 2.22. The V_x winds of the Labor Day hurricane and Camille exceed the winds represented by the four curves in figures 2.23 and 2.24. Helene and the New England hurricane of 1938 exceed all but the VLU curve.

Coastal values of VGL and VGU are shown in figure 2.25 for the PMH. Wind speeds generally decrease with increasing latitude. The gulf coast minimum is near milepost 1100 but is not as pronounced as the SPH minimum (fig. 2.22). The nonstationary storm is considered in figures 2.26 (VLU and VLL) and 2.27 (VUU and VUL) for the PMH. The two upper limit of T curves record their maxima along the southern Texas coast and the Florida Keys. A tertiary maximum appears near Cape Hatteras, where higher forward speed more than compensates for the latitudinal increase in p_o. This effect diminishes north of Cape Hatteras where p_o increases much more rapidly. This maximum is not evident in the VLL and VUL curves. These latter curves have their gulf coast minima near milepost 700. Recurving relatively fast moving storms near milepost 1100 contribute to these minima near milepost 700. The VLU and VLL curves and the VUU and VUL curves converge near

milepost 1100. This convergence is a result of rapidly increasing lower limit PMH forward speed in this area while the upper forward speed remains constant.

The PMH V_{gx} and V_x winds exceed all the hurricane V_{gx} and V_x winds shown in figures 2.25 to 2.27. The Labor Day hurricane of 1935 and Camille (the two storms with the lowest central pressure near the east and gulf coasts of the United States) are exceeded by a lesser margin.

3. APPLICATION OF CRITERIA

3.1 INTRODUCTION

This chapter illustrates procedures for computing SPH and PMH overwater wind fields resulting from the interaction of these hurricanes with land. Coastal values of V_{gx} and V_x for 100-n.mi. (185-km) intervals along the coast for upper and lower limits of R and T, where appropriate, are given in tables 2.3 to 2.6. Smoothed alongshore graphs of these wind values are shown in figures 2.22 to 2.27.

Determination of SPH or PMH overwater wind fields can be done with a computation form, table 3.1. Part I of this table lists the information needed for these computations and where it is given. Part II covers the maximum wind speeds for a stationary hurricane; Part III, the profile of wind speed for a stationary hurricane; and Part IV covers adjustments for asymmetry due to forward speed (T). Necessary notes or instructions for using table 3.1 are given in section 3.2. Table 3.2 is an example of the use of table 3.1 for a selected PMH. The example was selected to illustrate one of many possible combinations of meteorological parameters and some terrain situations that could be encountered.

We then cover:

Adjustment of overwater wind field for frictional effects (sec. 3.3).

Adjustment of wind field when hurricane center moves overland (sec. 3.4).

Adjustment of wind field for a stalled PMH (sec. 3.5).

3.2 OVERWATER WIND FIELDS (REFER TO TABLE 3.1)

Part I. Designated hurricane location and values of meteorological parameters.

Fill in blank spaces by making reference to the designated figures for the required SPH or PMH.

Part II. Maximum wind speeds (V_{gx} and V_{xs}) for a stationary hurricane.

a. Substitute appropriate values from *Part I* into equation 2.2.

b. Multiply value in a. by 0.9 (0.95) for the SPH (PMH) to obtain V_{xs}: the maximum 10-m (32.8 ft), 10-min overwater wind speed for a stationary hurricane.

Part III. Profile of wind speed for a stationary hurricane.

a. Outward from R to 130 n.mi. (241 km) [R $\leq$ r $\leq$ 130 n.mi.]

1. Enter figure 2.12 with designated R to obtain V_s/V_{xs} at numerous distances from R. Tabulate distance and ratios in columns 1 and 2 of table, respectively.

2. Multiply ratios of column 2 by V_{xs} of *Part IIb* to obtain V_s values. Tabulate in column 3 of table.

b. Hurricane center to R *(r $\leq$ R)*

1. Using designated R, compute r. Tabulate in column 3 of table.

2. Compute V_s values using V_{xs} of *Part IIb*. Tabulate in column 4 of table.

c. Plot the wind speeds, V_s, of the tables against distance, r.

Part IV. Adjustment for asymmetry due to storm forward speed (T).

$$V = V_s + 1.5 \ (T^{0.63}) \ (T_o^{0.37}) \cos \beta \qquad (3.1)$$

$$A, \text{ the assymetry factor, } = 1.5 \ (T^{0.63}) \ (T_o^{0.37}) \cos \beta \qquad (3.2)$$

Note:

$T_o = 1$ when T, V and V_s are in kt.

$T_o = 0.514791$ when T, V, and V_s are in m s^{-1}.

$T_o = 1.151556$ when T, V, and V_s are in mi hr^{-1}

$T_o = 1.853248$ when T, V, and V_s are in km hr^{-1}.

a. *For a radial through the point of maximum wind (radial M):*

at r $\neq$ R: $\beta = \phi_r - \phi_R$ $\qquad\qquad$ (3.3)

at r = R: $\beta = \phi_R - \phi_R = 0$ $\qquad\qquad$ (3.4)

1. For the SPH, enter figure 2.14 (use fig. 2.15 for the PMH) with the designated R to obtain ϕ for any distance (r) of *Part III*. Tabulate r's and corresponding ϕ's in columns 1 and 2 of table.

2. Using β (eq. 3.3 and 3.4), compute β_M's (β's for radial M). List in column 3. List cos β_M in column 4.

3. With cos β_M, $T^{0.63}$, and $T_o^{0.37}$, compute A's (eq. 3.2). Tabulate in column 5.

4. Add A's to V_s values of *Part III* to obtain values of V. Tabulate in column 6.

5. Plot these V values vs. r. This is the asymmetry adjusted radial M.

b. For other radials:

1. Copy values of r and β_M from columns 1 and 3 of *Part IVa* to columns 1 and 2.

2. Determine the degree of rotation (counterclockwise) between radial M and another radial.

3. Add number of degrees (item 2) to the β_M values (col. 2) for corresponding distances r (col. 1). This gives β values for the desired radial. Tabulate in column 3. List cos β in column 4.

4. Compute A values using equation 3.2 and tabulate in column 5.

5. Add these A values to V_s values of *Part III* to obtain values of V. Tabulate in column 6.

6. Plot these V values vs. r. This is the asymmetry adjusted radial.

7. Repeat steps 1 through 6 for as many radials as required to adequately define the isotachs over all portions of the hurricane.

c. Plot resulting winds on a map and analyze.

Part V. Miscellaneous

a. Spot ϕ values (from fig. 2.14 for the SPH or 2.15 for the PMH) on map of *Part IV* for the degree of detail needed.

b. If desired, rotate isotachs of *Part IV*, keeping point of maximum wind
0° to 180° clockwise from θ.

Table 3.2 shows application of table 3.1 to a specific PMH. The resulting
wind field determined from many radials is shown in figure 3.1.

3.3 ADJUSTMENT OF OVERWATER WIND FIELD FOR FRICTIONAL EFFECTS

3.3.1 INTRODUCTION

This section gives a procedure for evaluating the effects of surface fric-
tion on overwater wind speed as an SPH or PMH approaches shore. Application
would be best accomplished with a high-speed computer. For instance, with
computer application we could make computations of the frictionally adjusted
wind speed at very close intervals allowing for better resolution of the
analysis near shore.

We first summarize the procedure and then provide some examples of
frictionally reduced winds for different terrain situations.

3.3.2 WIND PATHS

Steps to determine wind paths are as follows:

a. Go to figure 2.14 (for the SPH) or figure 2.15 (for the PMH) and extract
inflow angles at various distances from the hurricane center for an R of
interest.

b. Plot these on a polar coordinate diagram of the same scale as the
determined overwater wind field.

c. Sketch lines of wind paths. Such a wind path diagram is shown in
figure 3.2. This is for a PMH with an R of 15 n.mi. (28 km) (table 3.2,
fig. 3.1).

d. Center the wind path diagram over the overwater wind field.

e. Outline the coast and pertinent terrain features (as described in
sec. 2.2.11) drawn to the same scale and placed in position relative to
the overwater wind field.

56

Table 3.1.--Overwater wind field computation form

Part I. Designated hurricane location and values of meteorological parameters:

SPH ☐ and PMH ☐ (check one)

a. Milepost (fig. 1.1): _____

b. Latitude in degrees (ψ) (fig. 1.1): _____

c. Coriolis parameter (f) = 2 Ω sin ψ (sec^{-1}) = 14.584 X 10^{-5} sin ψ (sec^{-1})

$$\sin \psi = \sin \underline{\quad}° = \underline{\qquad}$$
$$14.584 \text{ X } 10^{-5} \sin \psi \text{ (sec}^{-1}) = \underline{\qquad}$$

		SPH	PMH
d.	Peripheral pressure (p_w)*:	_____	_____
e.	Central pressure (p_o), fig. 2.1	_____ fig. 2.2	_____
f.	Radius of max. winds (R), fig. 2.4	_____ fig. 2.5	_____
g.	Forward speed (T), fig. 2.6	_____ fig. 2.7	_____
h.	Track direction (θ), fig. 2.8	_____ fig. 2.9	_____
i.	Density coefficient (K), fig. 2.10	_____ fig. 2.11	_____

---

*SPH: p_w = 29.77 in. (Hg); p_w = 100.8 kPa; p_w = 1008 mb

*PMH: p_w = 30.12 in. (Hg); p_w = 102.0 kPa; p_w = 1020 mb

Part II. Maximum wind speeds (V_{gx} and V_{xs}) for a stationary hurricane:

a. Maximum gradient wind speed (V_{gx}) = K $(p_w - p_o)^{1/2} - \dfrac{Rf}{2}$ (2.2)

b. V_{gx} adjusted to maximum 10-m, 10-min value (V_{xs}) for a stationary hurricane.

SPH: 0.9 V_{gx} = 0.9 (_____) = _____ = V_{xs}

PMH: 0.95 V_{gx} = 0.95 (_____) = _____ = V_{xs}

Table 3.1 (continued)

Part III. Profile of wind speed for a stationary hurricane

  a. *Outward from R to 130 n.mi. (241 km)* [R $\leq$ r $\leq$ 130 n.mi.]:

(1)	(2)	(3)
Distance from center, r ( )	$\dfrac{V_s}{V_{xs}}$ (fig. 2.12)	V_s ( )

58

Table 3.1 (continued)

b. *Hurricane center to R (r ≤ R):*

(1) $\frac{r}{R}$	(2) $\frac{V_s}{V_{xs}}$ (fig. 2.13)	(3) r ( )	(4) V_s ( )
1.0	1.000		
0.9	0.937		
0.8	0.771		
0.7	0.491		
0.6	0.330		
0.5	0.206		
0.4	0.118		
0.3	0.060		
0.2	0.020		
0.1	0.010		

Table 3.1 (continued)

Part IV. Adjustment for asymmetry due to storm forward speed (T).

a. For a radial through point of maximum wind (radial M):

$$T = \underline{\hspace{2cm}} \qquad T^{0.63} = \underline{\hspace{2cm}} \qquad T_o^{\,0.37} = \underline{\hspace{2cm}}$$

	(1) r ( )	(2) $\phi*$ (deg.)	(3) β_M (deg.)	(4) $\cos \beta_M$	(5) A ( )	(6) V ( )
0.1R=						
0.2R=						
0.3R=						
0.4R=						
0.5R=						
0.6R=						
0.7R=						
0.8R=						
0.9R=						
R=						

Inside R / Outside R

*From figure 2.14 or 2.15.

Table 3.1 (continued)

b. *For other radials:*

Degree of counterclockwise rotation from M _____°

$T =$ _____ $T^{0.63} =$ _____ $T_o^{0.37} =$ _____

(1)*	(2)Δ	(3)	(4)	(5)	(6)
r ( )	β_M (deg.)	$\beta = \beta_M +$ angle between M and other radial (deg.)	cos β	A ( )	V ( )
0.1R=					
0.2R=					
0.3R=					
0.4R=					
0.5R=					
0.6R=					
0.7R=					
0.8R=					
0.9R=					
R=					

(Inside R — arrow; Outside R — arrow labels along left side)

ΔCopy from column 3, *Part IVa.*
*Copy from column 1, *Part IVa.*

Table 3.2.--Example of application of table 3.1

Part I. Designated hurricane location and values of meteorological parameters

       SPH ☐   and PMH ☑   (check one)

a. Milepost (fig. 1.1): <u>2000</u>

b. Latitude in degrees (ψ) (fig. 1.1): <u>33.5</u>

c. Coriolis parameter (f) = 2 Ω sin ψ (sec^{-1}) = 14.584 X 10^{-5} sin ψ (sec^{-1})

$$\sin \psi = \sin \underline{33.5°} = \underline{0.552}$$

$$14.584 \text{ X } 10^{-5} \sin \psi \text{ (sec}^{-1}) = \underline{8.049 \times 10^{-5} sec^{-1} = 0.290 hr^{-1}}$$

		SPH	PMH
d.	Peripheral pressure (p_w)*:	_____	<u>30.12 in. (Hg)</u>
e.	Central pressure (p_o), fig. 2.1	_____	fig. 2.2 <u>26.31 in.</u>
f.	Radius of max. winds (R), fig. 2.4	_____	fig. 2.5 <u>15 n.mi.</u>
g.	Forward speed (T), fig. 2.6	_____	fig. 2.7 <u>10 kt</u>
h.	Track direction (θ), fig. 2.8	_____	fig. 2.9 <u>180°</u>
i.	Density coefficient (K), fig. 2.10	_____	fig. 2.11 <u>68.8</u>

---

*SPH: p_w = 29.77 in. (Hg); p_w = 100.8 kPa; p_w = 1008 mb

*PMH: p_w = 30.12 in. (Hg); p_w = 102.0 kPa; p_w = 1020 mb

Part II. Maximum wind speeds (V_{gx} and V_{xs}) for a stationary hurricane:

a. maximum gradient wind speed (V_{gx}) = K $(p_w - p_o)^{1/2} - \dfrac{Rf}{2}$ (2.2)

$$= 68.8 (30.12 - 26.31)^{1/2} - \frac{15(0.290)}{2}$$

$$= 134.3 - 2.2$$

$$= 132.1 \text{ kt}$$

62

Table 3.2 (continued)

b. V_{gx} adjusted to maximum 10-m, 10-min value (V_{xs}) for a stationary hurricane.

SPH: 0.9 V_{gx} = 0.9 (_____) = _____ = V_{xs}

PMH: 0.95 V_{gx} = 0.95 (*132.1 kt*) = *125.5 kt* = V_{xs}

Table 3.2 (continued)

Part III. *Profile of wind speed for a stationary hurricane*

a. *Outward from R to 130 n.mi. (241 km)* [R ≤ r ≤ 130 n.mi.]:

(1) Distance from center, r (*n. mi.*)	(2) $\frac{V_s}{V_{xs}}$ (fig. 2.12)	(3) V_s (*kt*)
15	1.000	125.5
30	.870	109.2
60	.590	74.0
100	.428	53.7
200	.250	31.4
300	.158	19.8

Table 3.2 (continued)

b.   *Hurricane center to R (r ≤ R):*

(1) $\dfrac{r}{R}$	(2) $\dfrac{V_s}{V_{xs}}$ (fig. 2.13)	(3) r (n. mi.)	(4) V_s (kt)
1.0	1.000	15.0	125.5
0.9	0.937	13.5	117.6
0.8	0.771	12.0	96.8
0.7	0.491	10.5	61.6
0.6	0.330	9.0	41.4
0.5	0.206	7.5	25.8
0.4	0.118	6.0	14.8
0.3	0.060	4.5	7.5
0.2	0.020	3.0	2.5
0.1	0.010	1.5	1.3

Table 3.2 (continued)

Part IV. Adjustment for asymmetry due to storm forward speed (T).

a. For radial through point of maximum wind (radial M):

$$T = \underline{\quad 10 \, Kt \quad} \qquad T^{0.63} = \underline{\quad 4.266 \, Kt \quad} \qquad T_o^{0.37} = \underline{\qquad\qquad}$$

	(1) r (n.mi.)	(2) ϕ^* (deg.)	(3) β_M (deg.)	(4) $\cos \beta_M$	(5) A (Kt)	(6) V (Kt)
0.1R=	1.5	0.3	353.1	.99276	6.4	7.7
0.2R=						
0.3R=						
0.4R=						
0.5R=						
0.6R=						
0.7R=	10.5	4.0	356.8	.99844	6.4	68.0
0.8R=						
0.9R=						
R=	15	7.2	0.0	1.0000	6.4	131.9
	30	23.6	16.4	.95931	6.2	115.4
	60	24.5	17.3	.95476	6.1	80.1
	100	20.9	13.7	.97155	6.2	54.9
	200	15.9	8.7	.98849	6.3	37.7
	300	14.2	7.0	.99255	6.4	26.2

Inside R (rows 0.1R–0.9R); Outside R (rows 30–300).

*From figure 2.14 or 2.15.

Table 3.2 (continued)

b. *For other radials:*

Degree of counterclockwise rotation from M __30__ °

$$T = \underline{\text{/0 } Kt} \qquad T^{0.63} = \underline{4.266 \, Kt} \qquad T_o{}^{0.37} = \underline{\qquad\qquad}$$

	(1)* r (n. mi.)	(2)Δ β_M (deg.)	(3) $\beta = \beta_M$ + angle between M and other radial (deg.)	(4) cos β	(5) A (Kt)	(6) V (Kt)
Inside R ↕	0.1R= 1.5	353.1	23.1	.99276	5.9	7.2
	0.2R=					
	0.3R=					
	0.4R=					
	0.5R=					
	0.6R=					
	0.7R= 10.5	356.8	26.8	.99844	5.7	67.3
	0.8R=					
	0.9R=					
	R= 15	0.0	30.0	1.0000	5.5	131.0
Outside R ↕	30	16.4	46.4	.95931	4.4	113.6
	60	17.3	47.3	.95476	4.3	78.3
	100	13.7	43.7	.97155	4.6	58.3
	200	8.7	38.7	.98849	5.0	36.4
	300	7.0	37.0	.99255	5.1	24.9

Δ Copy from column 3, *Part IVa.*

* Copy from column 1, *Part IVa.*
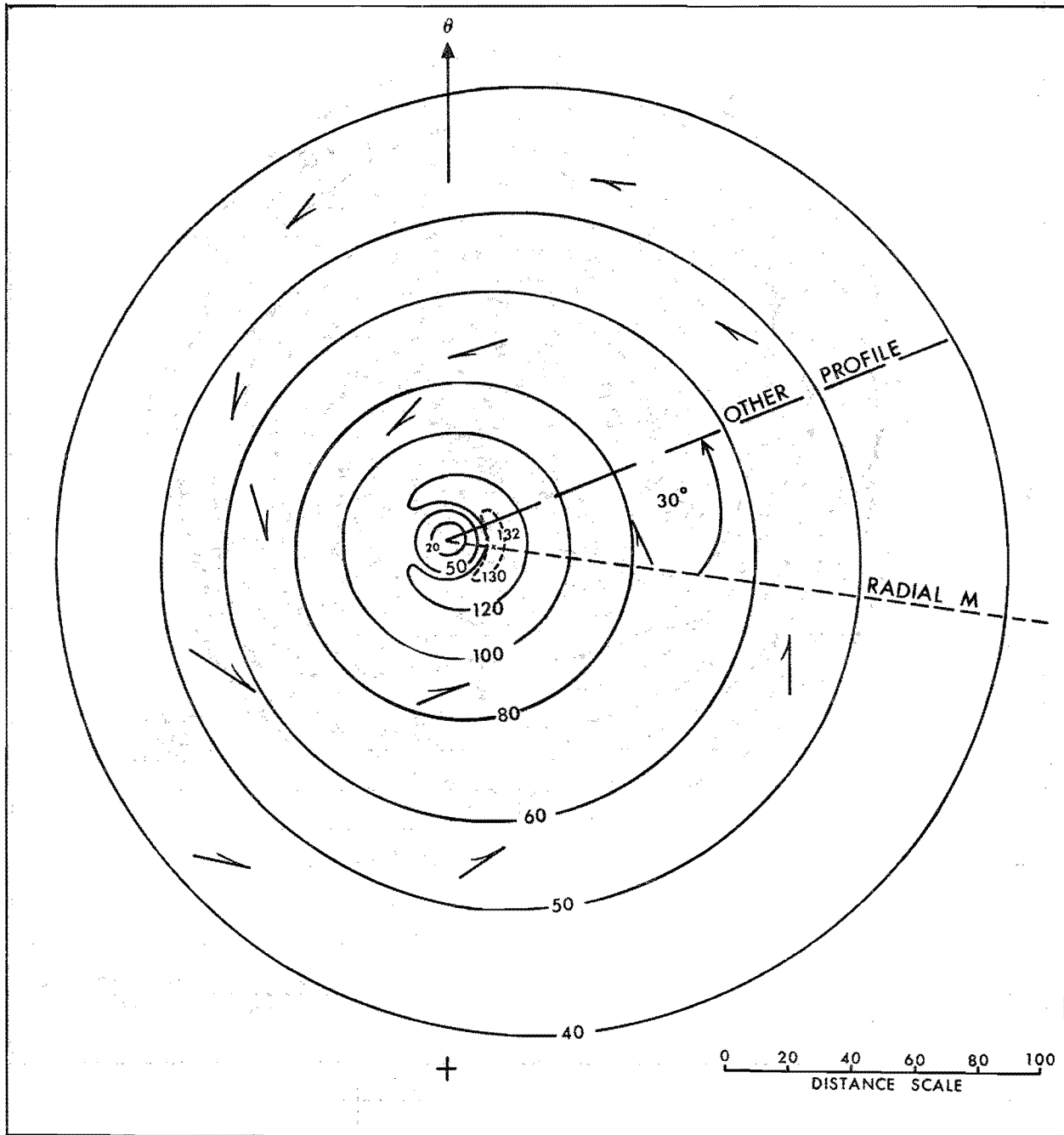
Figure 3.1.--Overwater PMH (R = 15 n.mi.) wind field computed for the example (sec. 3.2). If desired, this wind field may be rotated keeping the point of maximum wind within 0° to 180° clockwise from θ.
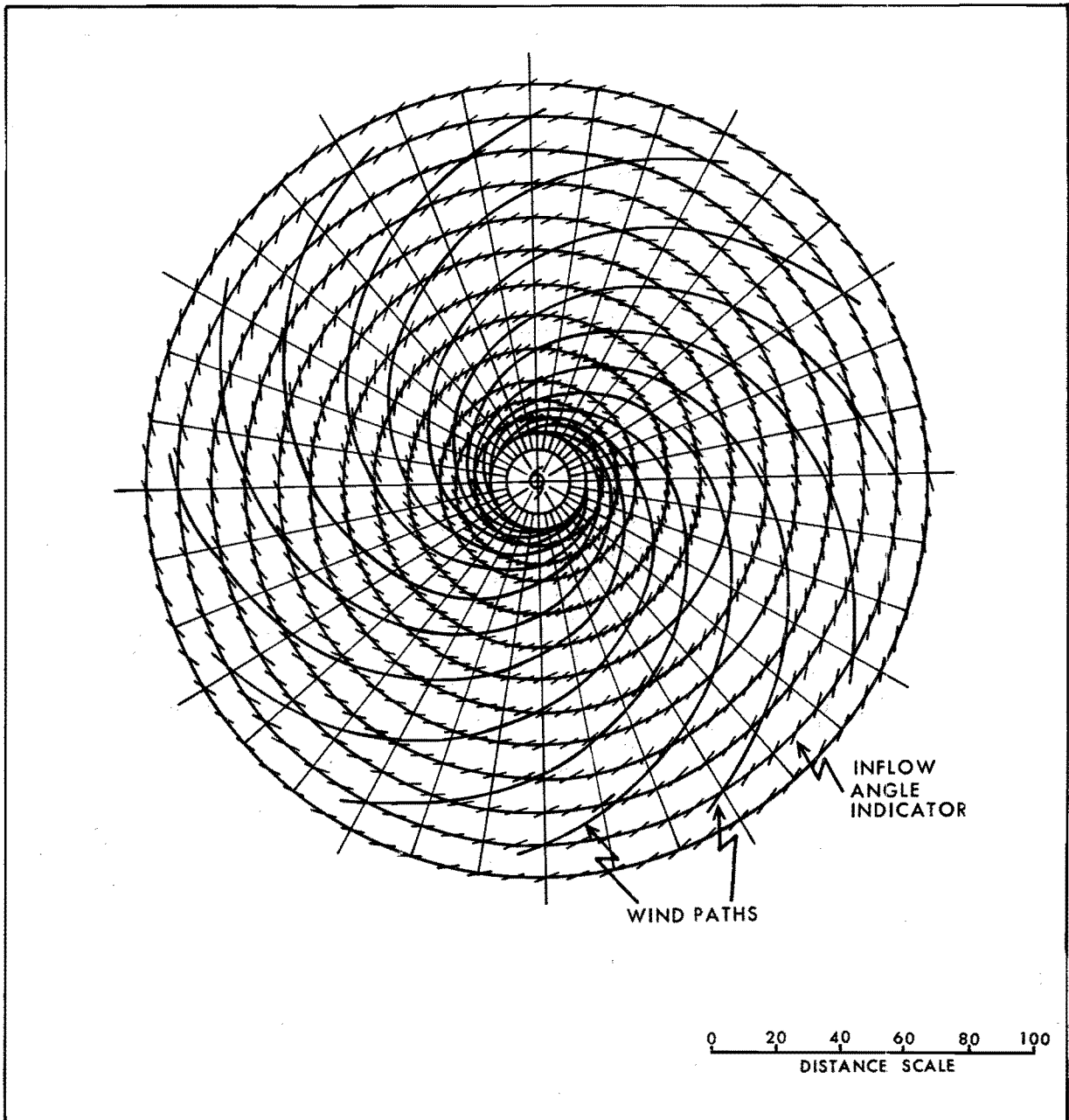
Figure 3.2.--Example of wind directions and sketched wind paths for PMH with R = 15 n.mi. (see sec. 3.3.2).

f. Trace wind paths over the portion of the wind field that is overland. (The wind path chart can be rotated to obtain additional paths, if required.)

3.3.3 FRICTION COEFFICIENTS

Summarizing from chapter 2:

$$V_k = kV \qquad (3.5)$$

$$k = k_e + Q(k_i - k_e) \qquad (3.6)$$

k is the friction coefficient at a point along a wind path (definition of k_e and k_i are given in sec. 2.2.11). The interpolation device Q (sec. 2.2.11), is:

$$Q = 1 - 0.195s + 0.0095s^2 \qquad (3.7)$$

where s = distance downstream from a change in surface friction category.

3.3.4 EXAMPLES OF COMPUTATION OF SURFACE FRICTIONALLY ADJUSTED WIND SPEED NEAR SHORE

The following computations of surface frictionally adjusted winds are for the previously determined PMH overwater wind field with an R of 15 n.mi.(28 km) in figure 3.1. Points along two wind paths that intercept the coast at a certain time for which computations are made are shown in figure 3.3. Wind paths X - X and Y - Y were traced onto this figure from figure 3.2.

3.3.4.1 WIND PATH X - X

Computational procedure for V_k (eq. 3.5)   Remarks

Point A

  V = 51 kt (overwater wind speed at A)   Computation of V_k at coast:

  s = 0 n.mi. (initial boundary point)   water-rough terrain boundary point.

  Q = 1.0 (from fig. 2.17 or eq. 3.7)

  $k_i = k_c = 0.83$; from table 2.2
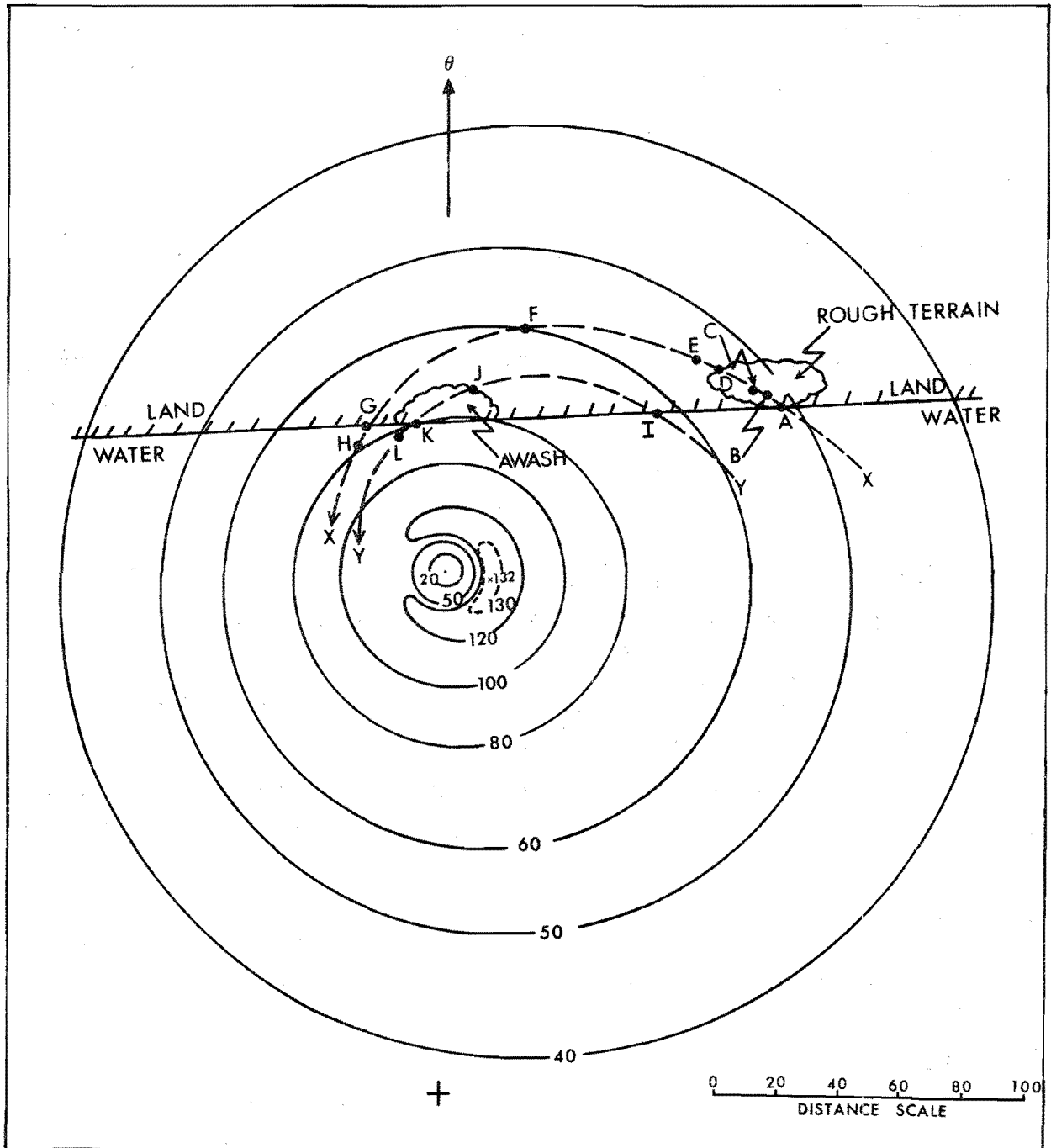
Figure 3.3.--Overwater PMH (R = 15 n.mi.) wind field and locations of points A to L for which adjustments are given (sec. 3.3).

Computational procedure for V_k (eq. 3.5)   Remarks

Point A – Continued

  $k = k_e + Q (k_i - k_e)$ from eq. 3.6

  $k = k_i = 0.83$

$V_k = k V = 0.83 (51) = 42$ kt

Point B

  V = 52 kt (overwater wind speed at B)   Computation of V_k at a point

  s = 6 n.mi. (distance from A to B) ≤ 10 n.mi. downstream from

  Q = 0.17 (from fig. 2.17 or eq. 3.7)   coastal boundary point.

  k_i = 0.83 (k of point A)

  k_e = 0.40 (rough terrain curve from fig. 2.16
            for V = 52 kt)

  $k = k_e + Q (k_i - k_e)$ from eq. 3.6

  $k = 0.40 + 0.17 (0.83 - 0.40) = 0.47$

$V_k = k V = 0.47 (52) = 24$ kt

Point C

  V = 53 kt (overwater wind speed at C)   Shows that friction coef-

  s = 10 n.mi. (distance from A to C)   ficient $k = k_e$ at s = 10 n.mi.

  Q = 0 (by definition)   (Q = 0)

  k_i = 0.83 (k of point A)

  k_e = 0.41 (rough terrain curve
          from fig. 2.16 for V = 53 kt)

  $k = k_e + Q (k_i - k_e)$ from eq. 3.6

  $k = k_e$

$V_k = k V = 0.41 (53) = 22$ kt

Computational procedure for V_k (eq. 3.5)	Remarks

Point D

V = 54 kt (overwater wind speed at D)

s = >10 n.mi. (distance from A to D);

Q = 0 (by definition)

k_i = 0.83 (k of point A)

k_e = 0.41 (rough terrain curve
      from fig. 2.16 for V = 54 kt)

$k = k_e = Q (k_i - k_e)$ from eq. 3.6

$k = k_e$

$V_k = k V = 0.41 (54) = 22$ kt

Shows procedure for computing V_k at s >10 n.mi. downstream from onshore boundary point. Also shows that at D (a boundary point itself) we still measure s from A.

Point E

V = 55 kt (overwater wind speed at E)

s = 8 n.mi. (distance from D to E)

Q = 0.05 (from eq. 3.7 or fig. 2.17)

k_i = 0.41 (k of point D)

k_e = 0.67 (land curve from fig. 2.16 for
      V = 55 kt)

$k = k_e + Q (k_i - k_e)$ from eq. 3.6

$k = 0.67 + 0.05 (0.41 - 0.67) = 0.66$

$V_k = k V = 0.66 (55) = 36$ kt

Computation of V_k after passing from one inland terrain surface to another.

Point F

V = 60 kt (overwater wind speed at F)

s = >10 n.mi. (distance from D to F)

Q = 0 (by definition)

k_i = 0.41 (k of point D)

Shows that Q = 0 after 10 n.mi. and k = k_e no matter what kind of terrain surface we are passing over. Computation the same as point D though this is not

Computational procedure for V_k (eq. 3.5)   <u>Remarks</u>

<u>Point F</u> - Continued

k_e = 0.70 (land curve from fig. 2.16   a boundary point.
            for V = 60 kt)

$k = k_e + Q (k_i - k_e)$ from eq. 3.6

$k = k_e$

$V_k = k \ V = 0.70 \ (60) = 42$ kt

<u>Point G</u>

V = 75 kt (overwater wind speed at G)   Procedure follows that given

s = > 10 n.mi. (distance from D to G)   for points D and F except

Q = 0 (by definition)   now we are computing V_k at

k_i = 0.41 (k of point D)   the offshore boundary point

                                               between land and water.
k = 0.78 (land curve from fig. 2.16
            for V = 75 kt)

$k = k_e + Q (k_i - k_e)$ from eq. 3.6

$k = k_e$

$V_k = k \ V = 0.78 \ (75) = 58$ kt

<u>Point H</u>

V = 78 kt (overwater wind speed at H)   Shows how to compute over-

s = 7 n.mi. (distance from G to H)   water V_k for offshore wind.

Q = 0.10 (from eq. 3.7 or fig. 2.17)

k_i = 0.78 (k from point G)

k_e = 1.00 (equilibrium k for water)

$k = k_e + Q (k_i - k_e)$ from eq. 3.6

$k = 1.00 + 0.10 \ (0.78 - 1.00) = 0.98$

$V_k = k \ V = 0.98 \ (78) = 76$ kt

Computational procedure for V_k (eq. 3.5)   <u>Remarks</u>
_____

3.3.4.2 WIND PATH Y - Y

<u>Point I</u>

  V = 64 kt (overwater wind speed at I)

  s = 0 n.mi. (initial boundary point)

  Q = 1.0 (from fig. 2.17 or eq. 3.7)

$k_i = k_c = 0.89$ (from table 2.2)

  $k = k_e + Q (k_i - k_e)$ from eq. 3.6)

  $k = k_i = 0.89$

$V_k = k V = 0.89 (64) = 57$ kt

Procedure follows that given for point A but for land rather than rough terrain.

<u>Point J</u>

  V = 73 kt (overwater wind speed at J)

  s = > 10 n.mi. (distance from I to J)

  Q = 0 (by definition)

  $k_i = 0.89$ (k of point I)

  $k_e = 0.78$ (land curve from fig. 2.16
        for V = 73 kt)

  $k = k_e + Q (k_i - k_e)$ from eq. 3.6

  $k = k_e$

$V_k = k V = 0.78 (73) = 57$ kt

Procedure follows that given for point D but now we are at boundary point between land and an awash area.

<u>Point K</u>

  V = 80 kt (overwater wind speed at K)

  s = > 10 n.mi. (distance from J to K)

  Q = 0 (by definition)

  $k_i = 0.78$ (K of point J)

Shows how to use awash curve in fig. 2.16.

Computational procedure for V_k (eq. 3.5)   <u>Remarks</u>

<u>Point K - Continued</u>

k_e = 0.89 (awash curve from fig. 2.16
 at V = 80 kt)

$k = k_e + Q (k_i - k_e)$ from eq. 3.6

$k = k_e$

$V_k = k V = 0.89 (80) = 71$ kt

<u>Point L</u>

V = 83 kt (overwater wind speed at L)

s = 8 n.mi. (distance from K to L)

Q = 0.05 (from eq. 3.7 or fig. 2.17)

k_i = 0.89 (k of point K)

k_e = 1.00 (equilibrium k for water)

$k = k_e + Q (k_i - k_e)$ from eq. 3.6

$k = 1.00 + 0.05 (0.89 - 1.00) = 0.99$

$V_k = k V = 0.99 (83) = 82$ kt

Shows that the procedure
followed when computing off-
shore overwater winds after
leaving an awash area is
the same as that followed
at point H after leaving
land. Of course, the k_i's
are different.

3.4 ADJUSTMENT OF WIND FIELD WHEN HURRICANE CENTER MOVES OVERLAND

When the center of a hurricane crosses the coast, overwater wind speeds
are reduced because of filling by a factor which decreases with time after
landfall. (The adjustments for near shore friction given in sec. 3.3 would
have to be accomplished first.) Determination of the filling factor and its
application to a wind field are as follows:

a. Enter figure 2.20 at the specified project location or milepost and
determine which filling adjustment factor curve (A, B, C, or an interpolation
between these curves) to use.

b. Use figure 2.19 to determine the filling adjustment factor for the specific time after landfall of interest.

c. Multiply all wind field isotach values by the filling adjustment factor for the indicated time after landfall.

d. Interpolate for desired isotach interval.

3.5 ADJUSTMENT OF WIND FIELD FOR A STALLED PMH

When a PMH stalls offshore south of the Virginia-North Carolina border, overwater wind speeds are reduced (because of upwelling and mixing) by a factor which decreases with time after landfall. (Unlike sec. 3.4, adjustments for frictional effects given in sec. 3.3 should be completed after the wind field has been reduced.) Determination of the stalling factor and its application to a wind field follows:

a. South of the Virginia-North Carolina border, immediately use the curve in figure 2.21 to determine the stalling adjustment factor for the specific time of interest after stalling begins. [From Virginia northward, the lower limit of T (T_L) is too fast (fig. 2.7) for a PMH to reach a stall speed in a period of a few hours or less. The PMH will weaken before it reaches its stall speed; it will weaken at a lesser rate than during a stalled condition. An empirical procedure was developed to compute this lesser rate of weakening. It is given in sec. 16.11.]

b. Multiply all wind field isotach values by the stalling adjustment factor for the indicated time after stalling begins.

c. Interpolate for desired isotach interval.

4. DATA

4.1 INTRODUCTION

Observations from hurricanes occurring near the United States Gulf of
Mexico and east coasts and from western North Pacific typhoons are used
throughout most of this study to determine SPH and PMH criteria. Definitions
of the several meteorological parameters used are given in chapter 5.

Data presented in this chapter are used in later chapters of the report.
If additional data are required for a specific purpose, it is given in the
chapter where required. Such data may be found in chapters 7, 8, 10 and 16.

4.2 SOURCES OF DATA

4.2.1 HURRICANES

Original sources of hurricane data are barograph traces from land stations
and ships, wind records from National Weather Service and military stations,
aircraft reconnaissance flight data, radar data, miscellaneous pressure and
wind reports, and textual descriptions in scientific literature. The descrip-
tions have appeared in the periodicals *Monthly Weather Review* (published
since June 1872) and *Climatological Data National Summary* (since 1950),
National Hurricane Research Project Report No. 39 (Graham and Hudson 1960),
NOAA Technical Memorandum NWS SR-56 (Sugg et al. 1971), the book *Tropical
Cyclones* (Cline 1926), and other sources.

Tables 4.1 to 4.4 list gulf coast and east coast hurricanes during the years
1900-78 with central pressure $(p_o) \leq 29.00$ in. (98.2 kPa). Values of
meteorological parameters used in this report are given for these hurricanes.
The storms occurred within 150 n.mi. (278 km) of the coast. Hurricanes whose
centers passed through the Florida Keys are listed in the gulf *and* east coast
tables for the convenience of the user. Tables 4.1 and 4.2 provide informa-
tion in metric units (kilometers, kilometers/hr, and kilopascals*) and tables
4.3 and 4.4 give the English values (nautical miles, knots, and inches.)
Both measurement systems are provided because the report is being issued at
the time of transition from one system to another. These tables are an update
and extension of tables 1 and 2 in *NOAA Technical Report* NWS 15 (Ho et al.

---

*A kilopascal is equal to 10 millibars.

1975). There are two changes in the previously published data. On the basis of additional data discovered since the 1975 study, we revised the radius of maximum winds for Carla to 30 n.mi. (56 km) from 20 n.mi. (37 km) and the central pressure for Donna (near the Florida Keys) to 27.45 in. (93.0 kPa) from 27.55 in. (93.3 kPa.)

4.2.1.1 HURRICANE PRESSURE DATA. The criterion for tables 4.1 to 4.4 (p_0 $\leq$29.00 in., 98.2 kPa) was based on the consideration that the maximum cyclostrophic wind speed, computed from the Hydrometeorological Branch model (Myers 1954, eq. 6), with a p_0 of 29.00 in. (98.2 kPa) and a p_w of 30.00 in. (101.6 kPa) is 63 kt (117 km/hr), or about the wind speed required for classification as a hurricane. In tables 4.1 to 4.4, if a hurricane crossed the coast on one side of the Florida peninsula with a p_0 $\leq$29.00 in. (98.2 kPa) and decreased in intensity to p_0 >29.00 in. when it was >50 n.mi. (93 km) from the opposite coast, it was listed for only the initial coastline it crossed.

The specific p_0 values given for hurricanes in tables 4.1 to 4.4 are the lowest p_0 either measured by barometer or a dropsonde from reconnaissance aircraft. If the measurement was not very close to the hurricane center, p_0 was estimated from observations. The Hydrometeorological Branch pressure profile formula (chapter 6) was used to estimate p_0, particularly for earlier hurricanes.

For some hurricanes prior to 1942, p_0's were adjusted back to the coast where the storm entered land. This was done for those p_0's for which the lowest observed pressure was from a station well inland or at a coastal station when the storm was emerging from land to sea. These adjustments were made for 13 hurricanes and were carried over from Ho et al. (1975) and earlier reports including Graham and Nunn (1959). They were based on the average rate of filling developed in chapter 5 of Myers (1954). We did not recompute these p_0's using information contained in our chapter 15 because the 13 hurricanes were all relatively weak (p_0 $\geq$ 28.17 in., 95.4 kPa) and, thus, would not affect our determination of SPH or PMH p_0. In addition, recomputed p_0's employing knowledge gained since 1954 would still be close to Myers' results.

A virtual absence of pressure data made it necessary to omit one storm altogether--the Louisiana hurricane of August 6, 1918, in which the closest recorded pressure was some 90 n.mi. (167 km) from the path of the storm center. An estimate of p_o from such a distance would be so unreliable as to be useless. Two hurricanes appearing in NHRP 33 are not presented in tables 4.1 to 4.4. They are the storms of September 11, 1903 (gulf coast) and October 20, 1924 (east coast). Both storms crossed the Florida peninsula. Upon reanalysis of the data, it was determined that both had weakened to tropical storm strength before they reached a point 50 n.mi. (93 km) from where they exited the coast.

4.2.1.2 HURRICANE RADIUS OF MAXIMUM WINDS (R) DATA. The values of R for hurricanes were derived from several sources listed in decreasing order of preference:

a. wind speed records from land stations

b. approximation from hurricane "eye" radii gathered by aircraft or radar

c. wind reports from aerial reconnaissance

d. computed from the Hydromet Pressure Profile Formula

e. narrative or tabular data in the *Monthly Weather Review* or other publications.

A detailed description of these procedures are found in *NOAA Technical Report* NWS 15 (Ho et al. 1975, pp 41-46).

4.2.1.3 HURRICANE FORWARD SPEED (T) AND TRACK DIRECTION (Θ). In tables 4.1 to 4.4, T and Θ (measured clockwise from north) of landfalling, alongshore and exiting hurricanes were extracted from storm track charts. Hurricane tracks from Cry (1965) and the *Monthly Weather Review* (National Oceanic and Atmospheric Administration 1965-73, American Meteorological Society, 1974-78) were used. These charts give 12-or 24-hr positions that sometimes indicate lower or higher T or different Θ than more detailed tracks showing hourly positions. Detailed track charts (e.g., Myers 1954, Graham and Hudson 1960) depicting hourly or two-hourly positions in the vicinity of the coast exist for many hurricanes, and these were used

if available. The listed T and θ pertain to the time of landfall, exit or closest approach to the coast.

4.2.2 TYPHOONS

Records show there have been numerous western North Pacific typhoons with central pressures considerably lower than hurricanes of the Atlantic Ocean, including the Caribbean Sea and Gulf of Mexico. We made use of meteorological parameters observed or estimated for these typhoons as guidance for certain determinations in this study.

Typhoons were selected from lists given in the *Annual Typhoon Report* (U.S. Department of Defense 1960–74) if their central pressures were $\leq$ 29.10 in. (98.5 kPa) when near the coasts of Japan, Taiwan and the Philippine Islands. Table 4.5 lists data from these typhoons in metric units and table 4.6 provides the same items in English units. Values of parameters were determined from reconnaissance flight data taken every 6 hours on the average. T is a 6-hr average forward speed closest to the time when p_o was selected. This definition differs from the definition of T for North Atlantic hurricanes where T pertains to the time of landfall or closest approach to the coast. θ is the track direction from which the typhoon moves(measured clockwise from north)and is also at or near the time of p_o. For the time of p_o, R was approximated by adding 25% to the reported radius of the typhoon eye. The 25% is an estimate we made from data given by Shea and Gray (1972).

4.3 LIMITATIONS ON USE OF TYPHOON DATA

There are indications that the typhoons from the western North Pacific may not fit into the same family as U.S. coastal hurricanes. In general, storms of the western North Pacific draw moisture from a much larger water surface than those of the North Atlantic. The typhoon data also span a larger range in latitude. Nonetheless, we believe the added storm data are helpful in making judgments and drawing conclusions. Data from tropical cyclone regions other than the North Atlantic and western North Pacific were not used in this study.

V_{gx} : Gradient wind speed (see chapter 12).

V_x : Maximum 10-m, 10-min sustained wind speed. To convert to 1-min sustained winds divide by 0.863^1 (see chapter 12).

P_w : Peripheral pressure estimated at or near time of p_o (see chapter 7).

p_o : Central pressure (see chapter 8).

R : Radius of maximum winds observed or computed at or near time of p_o. Computed values are used where a station or specific location is not given (see chapter 9).

T : Forward speed pertaining to the time of landfall or closest approach to the coast (see chapter 10).

θ : Track directon from which the hurricane moves measured clockwise from north and pertaining to the time of landfall or closest approach to the coast (see chapter 11).

$\sim$: Data not used in determining values of most meteorological parameters for the SPH or PMH. It is included here to update tables through 1978 (no hurricanes qualified in 1978.)

§ : Same hurricane as previous line.

by : Bypassing hurricane.

ex : Exiting hurricane.

MSG : Missing.

* : Date applies to the time hurricane was at or closest to the approximate coastal reference point.

‡ : Refers to the lowest p_o within 150 n.mi. (278 km) seaward of the coast or 50 n.mi. (93 km) landward. Lower p_o beyond these limits were not considered.

† : Point at which hurricane entered, exited, or came closest to the coast (fig. 1.1). These points are generally different from Ho et al. (1975), who read the points in terms of rounded latitudinal and longitudinal values and then converted these to reference distances. In this study we read the reference distances directly.

∞ : Latitude or longitude of coastal reference point or point at which hurricane was closest to the coastal reference point.

---

[1]Thom, H.C.S., "Distributions of Extreme Winds Over Oceans," Proceedings of the ASCE, Waterways, Harbors and Coastal Engineering Division, February 1973.

Table 4.1.--U.S. gulf coast hurricanes (1900-78) with central pressure ≤ 29.00 in. (98.2 kPa) listed chronologically (metric units).

Approximate coastal ref. point (km)†	Date (GMT)*	Name	Lat.	Long.∞	Track direction (θ)	P_o‡ (kPa)	Location at p_o Lat.	Long.	P_w (kPa)	R (km)	Station(s) where R was observed	T (km/hr)	V_{gx} (km/hr)	V_x (km/hr)
723	Sept 9,1900		29.2	95.1	130	93.6	29.2	95.1	101.2	26		19	184	178
1269	Aug 15,1901		29.3	89.7	195	97.3	29.3	89.7	101.3	61		26	128	130
2585	June 17,1906		25.1	81.1	185	97.9	25.1	81.1	101.3	48		19	120	120
1445	Sept 27,1906		30.4	88.5	160	96.5	30.4	88.5	101.3	80	Mobile, AL	30	138	141
2585	Oct 18,1906		25.2	80.9	230	97.7	25.0	81.0	101.0	65		11	116	113
704	July 21,1909		29.0	95.2	115	95.9	29.0	95.2	101.5	35		22	156	154
1205	Sept 20,1909		29.2	90.2	150	98.0	29.2	90.2	101.2	MSG		20	MSG	MSG
2595	Oct 11,1909 by		24.7	81.1	235	95.7	24.7	81.1	100.9	41	Key West, FL	19	151	147
2465	Oct 18,1910		26.0	81.8	200	94.1	24.5	82.9	100.8	30		20	173	168
704	Aug 17,1915		29.1	95.2	130	94.9	29.1	95.2	101.2	54	Galveston & Houston, TX	20	164	160
1223	Sept 29,1915		29.1	90.2	170	93.2	27.0	89.3	100.9	48	New Orleans, LA & other stations	19	182	176
1427	July 5,1916		30.4	89.0	160	96.1	30.4	89.0	101.1	83	Mobile, AL	46	141	148
343	Aug 18,1916		27.0	97.5	115	94.8	27.0	97.5	101.4	46		20	169	165
1593	Oct 18,1916		30.4	87.2	200	97.4	30.4	87.2	101.2	35	Pensacola, FL	39	128	134
1668	Sept 29,1917		30.4	86.6	230	96.4	30.4	86.6	101.5	61	Pensacola, FL	24	145	145
2502	Sept 10,1919 by		24.7	82.9	110	92.9	24.7	82.9	101.2	28		15	193	184
408	§Sept 14,1919		27.3	97.5	105	94.8	27.3	97.5	101.2	MSG		37	MSG	MSG
1130	Sept 21,1920		29.2	90.9	155	98.0	29.2	90.9	101.3	52		52	117	128
593	June 22,1921		28.6	96.4	175	95.4	28.6	96.4	101.4	32		20	163	159
2224	Oct 25,1921		28.1	82.8	235	95.2	28.1	82.8	101.0	33		19	160	156
2505	Oct 21,1924		25.9	81.6	250	97.2	24.7	82.9	101.2	35		15	132	129
1112	Aug 26,1926		29.3	91.3	180	95.9	29.3	91.3	101.5	50		19	154	151
1566	Sept 20,1926		30.3	87.5	120	95.5	30.3	87.5	101.4	32	Pensacola, FL	13	161	154
2650	Oct 21,1926 by		25.1	80.1	220	93.2	23.6	81.8	100.8	39		30	183	181

See notes preceding table 4.1.

Table 4.1.--U.S. gulf coast hurricanes (metric units), continued

Approximate coastal ref. point (km)†	Date (GMT)*	Name	Lat.	Long.∞	Track direction (θ)	p_o† (kPa)	Location at p_o Lat.	Long.	P_W (kPa)	R (km)	Station(s) where R was observed	T (km/hr)	V_{gx} (km/hr)	V_x (km/hr)
2261	Sept 17,1928		27.7	81.7	120	95.8	27.7	81.7	101.2	MSG		22	MSG	MSG
556	June 28,1929		28.5	96.5	130	96.9	28.5	96.5	100.9	24		28	133	135
1798	Sept 30,1929		29.7	85.4	160	97.5	29.7	85.4	101.3	102	Pensacola, FL	11	119	116
723	Aug 14,1932		29.1	95.0	135	94.2	29.1	95.0	101.3	22		28	178	176
241	Aug 5,1933		25.7	97.1	70	97.5	25.7	97.1	101.3	46	Brownsville, TX	19	127	126
2252	Sept 4,1933		27.8	81.1	120	96.4	27.8	81.6	101.2	54	Tampa,FL	20	142	141
259	Sept 5,1933		26.2	97.1	90	94.9	26.2	97.1	101.2	37	Brownsville, TX	15	166	160
1093	June 16,1934		29.3	91.2	180	96.6	29.3	91.2	100.6	69		30	127	130
2613	Sept 3,1935		24.8	80.9	130	89.2	24.8	80.9	101.4	11		17	242	241
2585	Nov 5,1935 ex		25.2	81.1	65	97.3	25.6	80.4	101.6	19	Miami, FL	28	139	140
1668	July 31,1936		30.4	86.5	150	96.4	30.4	86.5	101.6	35		17	150	146
834	Aug 8,1940		29.9	93.9	140	97.0	29.9	93.9	101.4	20		15	137	133
686	Sept 23,1941		28.9	95.4	180	95.9	28.9	95.4	101.1	39		24	150	149
1881	Oct 7,1941		29.9	84.7	170	98.1	29.9	84.7	101.6	33		20	123	123
612	Aug 30,1942		28.5	96.2	135	95.1	28.5	96.2	101.0	33		26	161	159
788	July 27,1943		29.5	94.5	110	97.5	29.5	94.5	101.4	30	Houston, TX	15	130	128
2335	Oct 19,1944		27.0	82.5	195	94.9	24.7	82.9	101.2	50		24	165	163
612	Aug 27,1945		28.6	96.2	200	96.7	28.6	96.2	101.0	33		7	135	128
2669	Sept 15,1945		25.5	80.3	130	95.1	25.5	80.3	101.4	44	Miami, FL	19	166	161
2492	Sept 18,1947 ex		26.2	81.8	85	94.9	26.3	81.3	101.6	63		13	169	161
1371	§Sept 19,1947		29.7	89.5	115	96.6	29.8	90.3	101.4	43	New Orleans, LA	30	142	144
2557	Sept 21,1948		24.5	81.5	210	93.5	24.5	81.5	101.0	13		15	185	177
2567	Oct 5,1948		24.7	81.3	230	97.7	24.7	81.3	101.0	57	Miami, FL	24	117	119
2317	Aug 27,1949		27.2	81.2	130	96.1	27.2	81.2	101.5	43	W.Palm Beach, FL	26	153	152
667	Oct 4,1949		28.8	95.6	190	96.3	28.8	95.6	101.2	37	Composite of many TX stations	20	146	144
1520	Aug 31,1950	Baker	30.2	88.0	190	97.9	30.2	88.0	100.4	39		20	102	112

See notes preceding table 4.1.

Table 4.1.--U.S. gulf coast hurricanes (metric units), continued.

Approximate coastal ref point (km)†	Date (GMT)*	Name	Lat.	Long.∞	Track direction (θ)	p_o‡ (kPa)	Location at p_o Lat. Long.		p_w (kPa)	R (km)	Station(s) where R was observed	T (km/hr)	V_{gx} (km/hr)	V_x (km/hr)
2131	Sept 5,1950	Easy	28.6	82.8	230	95.8	29.1	83.1	100.9	28		6	150	141
2224	Oct 18,1950	King	28.0	81.6	150	97.8	28.0	81.6	101.4	MSG		32	MSG	MSG
1677	Sept 24,1956	Flossy	29.2	89.6	235	97.4	30.3	86.5	101.3	41	Burrwood, LA	19	129	128
852	June 27,1957	Audrey	29.8	93.6	200	94.6	29.8	93.6	100.7	35		26	162	160
2595	Sept 10,1960	Donna	24.7	80.9	140	93.0	24.3	80.5	101.2	37	Near Conch Key, FL	17	191	183
1381	Sept 15,1960	Ethel	30.4	86.1	175	97.2	26.6	89.3	101.5	33	Keesler AFB, MS	19	137	135
547	Sept 11,1961	Carla	28.4	96.4	170	93.1	28.4	96.4	100.8	56		11	182	172
1103	Oct 3,1964	Hilda	29.5	91.4	175	95.9	29.5	91.4	101.5	39	Near 26°N, 92°W	13	156	150
2502	Oct 14,1964	Isbell	25.8	81.3	220	96.4	24.3	82.7	101.3	19	Near 24°N, 83°W	28	149	149
2548	Sept 8,1965	Betsy	25.2	82.1	90	94.8	25.2	82.1	101.3	35	W. of Cape Sable, FL	28	169	168
1186	§Sept 10,1965	Betsy	29.2	90.3	135	94.1	28.2	89.2	101.1	59	Port Sulpher, LA	32	173	172
1909	June 9,1966	Alma	30.1	84.3	200	97.1	29.1	84.3	101.5	43	Near 30°N, 84°W	17	139	136
2632	Oct 4,1966 by	Inez	24.9	80.6	65	97.7	24.1	84.2	101.3	35	Key West, FL	13	125	122
278	Sept 20,1967	Beulah	26.1	97.2	155	92.3	24.8	96.3	100.9	46	Brownsville, TX	16	194	185
2113	Oct 19,1968	Gladys	28.8	82.9	235	97.7	28.8	82.9	101.1	39		19	120	120
1390	Aug 18,1969	Camille	30.3	89.5	160	90.8	28.2	88.8	100.8	15	Near 28°N, 89°W	30	219	224
482	Aug 3, 1970	Celia	27.9	97.2	115	94.4	27.9	97.2	101.0	17	Corpus Christi, TX	26	171	169
19	Sept 12,1970	Ella	23.9	97.7	100	96.7	23.9	97.7	100.8	39		13	133	130
630	Sept 10,1971	Fern	28.5	95.6	50	97.9	28.5	95.6	100.8	48	Palacios & Port Comfort, TX	9	110	106
871	Sept 16,1971	Edith	29.4	93.2	230	97.8	29.4	93.2	100.9	50	Lake Charles, LA	28	113	117
1742	June 19,1972	Agnes	30.1	85.6	195	97.8	28.5	85.7	101.0	37	Near 28°N, 86°W	20	117	118
1093	Sept 8,1974	Carmen	29.2	91.1	155	93.6	28.0	90.7	101.3	19	Near 28°N, 91°W	17	186	179
74	Aug 31, 1975	Caroline	24.3	97.7	110	96.3	24.3	97.7	101.2	19	Near 24°N, 97°W	9	149	141
1668	Sept 23,1975	Eloise	30.4	86.5	195	95.5	30.4	86.5	101.5	33	Near 30°N, 86.5°W	41	162	165
19	∿Sept 2,1977	Anita	23.9	97.8	60	92.6	24.2	97.1	101.2	22	Near 24°N, 97°W	19	196	189

See notes preceding table 4.1.

Table 4.2.--U.S. east coast hurricanes (1900-78) with central pressure $\leq$ 29.00 in. (98.2 kPa) listed chronologically (metric units).

Approximate coastal ref. point (km)†	Date (GMT)*	Name	Lat.	Long.∞	Track direction (θ)	p_o‡ (kPa)	Location at p_o Lat.	Long.	p_w (kPa)	R (km)	Station(s) where R was observed	T (km/hr)	V_{gx} (km/hr)	V_x (km/hr)
2780	Sept 12,1903		26.5	80.0	120	97.7	26.5	80.0	101.6	80		15	125	123
2863	June 17,1906 ex		27.3	80.2	220	97.9	25.1	81.1	101.3	48		22	120	121
3707	Sept 17,1906		33.6	78.9	105	98.1	33.6	78.9	101.8	82	Charleston, SC	30	118	122
2733	Oct 18,1906 ex		26.0	80.1	220	97.7	25.0	80.6	101.0	65		11	116	113
2595	Oct 11,1909 by		24.7	81.1	230	95.7	24.7	81.1	100.9	41	Key West, FL	19	151	147
3466	Aug 28 1911		32.1	81.0	100	97.9	32.1	81.0	101.6	50	Savannah, GA	15	123	121
3920	Sept.3,1913		34.7	76.4	115	97.6	34.7	76.4	102.0	70	Hatteras, NC	30	131	134
2502	Sept.10,1919 by		24.7	82.9	110	92.9	24.7	82.9	101.2	28		15	193	184
3104	Oct 26,1921 ex		29.0	81.0	260	97.9	28.6	81.8	101.2	MSG		19	MSG	MSG
4040	Aug 26,1924 by		35.0	75.0	210	97.2	35.0	75.2	101.4	63	Hatteras, NC	41	129	135
5022	§Aug 26,1924 by		41.1	69.8	220	97.2	41.1	69.8	101.4	122	Nantucket, MA	54	115	126
3920	Dec 2,1925		34.7	76.6	220	98.0	34.7	76.6	101.9	100	Wilmington, NC	26	118	121
2974	July 28,1926		28.2	80.4	150	96.0	28.2	80.4	101.6	26		15	158	152
2706	Sept 18,1926		25.8	80.1	110	93.4	25.8	80.1	101.4	44		32	187	186
2650	Oct 21,1926 by		25.1	80.1	220	93.2	23.6	81.8	100.8	39		30	183	181
2789	Sept 17,1928		26.7	80.0	120	93.5	26.7	80.0	101.2	52		24	182	178
2641	Sept 28,1929		25.1	80.4	90	94.8	25.1	80.4	100.9	52		19	162	158
4179	Aug 23,1933		36.8	75.9	145	97.0	36.8	75.9	101.4	67	Hatteras, NC	33	131	135
2836	Sept 4,1933		26.9	80.1	120	94.8	26.9	80.1	101.4	MSG		20	MSG	MSG
4003	Sept 16,1933		35.0	76.2	180	95.7	35.0	76.2	101.7	74	Hatteras,NC	17	154	150
2613	Sept 3,1935		24.8	80.9	130	89.2	24.8	80.9	101.4	11		17	242	241
2706	Nov 4,1935		25.8	80.1	60	97.3	25.8	80.1	101.5	19	Miami, FL	22	138	137
4133	Sept 18,1936 by		36.1	75.4	160	96.6	35.2	74.6	102.0	63		30	147	148
4809	Sept 21,1938		40.7	72.7	180	94.0	38.7	72.5	101.5	93		87	168	182
3493	Aug 11,1940		32.4	80.9	100	97.5	32.4	80.9	101.8	50	Savannah, GA	17	135	131
4040	Sept 14,1944		35.2	75.5	195	94.4	35.2	75.5	101.1	32	Hatteras, NC	43	170	173
4874	§Sept 15,1944		40.9	72.2	220	95.9	40.9	72.2	101.3	67	Providence, RI	56	142	152
2669	Sept 15,1945		25.5	80.3	130	95.1	25.5	80.3	101.4	44	Miami, FL	19	166	161

See notes preceding table 4.1

Table 4.2.--U.S. east coast hurricanes (metric units), continued.

Approximate coastal Ref. Point (km)†	Date (GMT)*	Name	Lat.	Long.∞	Track direction (θ)	P_o† (kPa)	Location at p_o Lat.	Long.	P_w (kPa)	R (km)	Station(s) where R was observed	T (km/hr)	V_{gx} (km/hr)	V_x (km/hr)
2733	Sept 17,1947		26.3	80.1	80	94.0	26.3	80.1	101.5	63	Miami, FL	19	179	173
3410	Oct 15,1947		31.8	81.1	80	96.8	31.8	81.1	101.3	24		32	140	142
2845	Sept 22,1948 ex		27.3	80.1	230	96.2	26.6	81.0	100.7	30		20	141	139
2659	Oct 5,1948 ex		25.2	80.3	230	97.7	25.2	80.3	101.0	57	Miami, FL	24	117	119
4040	Aug 24,1949 by		35.0	75.1	220	97.7	35.1	75.3	101.8	44		41	130	136
2789	Aug 27,1949		26.7	80.0	130	95.4	26.7	80.0	101.5	43	W.Palm Beach, FL	26	163	161
2706	Oct 18,1950	King	25.8	80.2	150	95.5	25.8	80.2	101.4	11	Miami, FL	11	164	156
4059	Aug 31,1954	Carol	35.4	75.4	210	96.0	33.4	76.8	101.1	MSG		19	MSG	MSG
4818	§Aug 31,1954	Carol	40.8	72.5	200	96.1	40.8	72.5	101.8	41	Many coastal stns.	61	151	161
4059	Sept 10,1954 by	Edna	35.0	75.0	210	94.3	34.0	75.6	101.1	MSG		37	MSG	MSG
5059	§Sept 11,1954	Edna	41.6	70.2	210	94.7	39.7	71.3	101.0	33	Nantucket, MA	74	161	173
3818	Oct 15,1954	Hazel	33.9	78.5	190	93.7	33.9	78.5	101.1	39	Myrtle Beach, SC	48	178	182
3920	Aug 12,1955	Connie	34.7	76.1	200	96.2	34.7	76.1	101.1	83		13	137	132
3920	Sept 19,1955	Ione	34.7	76.7	175	96.0	34.7	76.7	101.6	78		17	148	144
4021	Aug 28,1958 by	Daisy	35.2	74.2	180	95.7	35.2	74.2	101.5	46	Near 35°N, 74°W	32	155	156
5041	§Aug 29,1958 by	Daisy	40.6	69.1	240	97.9	40.6	69.1	101.4	93	Near 40.5°N, 69°W	39	109	116
3966	Sept 27,1958 by	Helene	34.8	75.9	240	93.2	32.4	78.5	101.2	39		26	185	181
3521	Sept 29,1959	Gracie	32.6	80.4	150	95.1	32.2	80.2	101.6	19	Near 30°N, 78°W	22	169	166
2595	Sept 10,1960	Donna	24.7	80.9	140	93.0	24.3	80.5	101.2	37	Near Conch Key,FL	17	191	183
3910	§Sept 12,1960	Donna	34.6	77.3	215	95.8	33.9	77.9	101.2	63	Wilmington, NC	48	147	154
4818	§Sept 12,1960	Donna	40.7	72.6	205	96.1	40.7	72.6	101.0	89	Suffolk Co. AFB, NY	59	131	143
2696	Aug 27,1964	Cleo	25.7	80.1	160	96.7	25.7	80.1	101.2	13	Miami, FL	17	141	138
3178	Sept 10,1964	Dora	29.9	81.4	100	96.6	29.9	81.4	101.3	37	Near 30°N, 80°W	13	143	138
2632	Sept 8,1965	Betsy	25.0	80.6	90	95.2	25.0	80.6	101.3	41	Plantation Key, FL	20	164	160
4188	Sept 17,1967	Doria	36.5	75.9	20	98.1	38.0	71.9	101.8	37	Near 38°N, 74°W	17	123	121
5680	Sept 10,1969	Gerda	44.7	67.3	195	97.9	40.6	69.6	101.1	MSG		74	MSG	MSG
4021	∿Aug 9, 1976	Belle	35.2	74.4	190	95.9	32.5	75.2	101.5	15	Near 32.5°N. 75°W	39	157	161
4624	∿Aug 10,1976	Belle	40.6	73.3	200	97.5	38.2	73.9	101.9	56		39	130	135

See notes preceding table 4.1.

Table 4.3.--U.S. gulf coast hurricanes (1900-78) with central pressure $\leq$ 29.00 in. (98.2 kPa) listed chronologically (English units).

Approximate coastal reference point† (n.mi.)	Date (GMT)*	Name	p_o(in.)‡	p_w(in.)	R(n.mi.)	T(kt)	V_{gx} (kt)	V_x (kt)
390	Sept 9, 1900		27.64	29.88	14	10	99	96
685	Aug 15, 1901		28.72	29.91	33	14	69	70
1395	June 17, 1906		28.91	29.91	26	10	65	65
780	Sept 27, 1906		28.50	29.91	43	16	75	76
1395	Oct 18, 1906		28.84	28.83	35	6	63	61
380	July 21, 1909		28.31	29.97	19	12	84	83
650	Sept 20, 1909		28.94	29.88	MSG	11	MSG	MSG
1400	Oct 11, 1909 by		28.26	29.80	22	10	81	79
1330	Oct 18, 1910		27.80	29.77	16	11	93	91
380	Aug 17, 1915		28.01	29.88	29	11	88	86
660	Sept 29, 1915		27.53	29.80	26	10	98	95
770	July 5, 1916		28.38	29.86	45	25	76	80
185	Aug. 18, 1916		28.00	29.94	25	11	91	89
860	Oct 18, 1916		28.76	29.88	19	21	69	72
900	Sept 29, 1917		28.48	29.97	33	13	79	78
1350	Sept 10, 1919 by		27.44	29.88	15	8	104	99
220	§Sept 14, 1919		27.99	29.88	MSG	20	MSG	MSG
610	Sept 21, 1920		28.93	29.91	28	28	63	69
320	June 22, 1921		28.17	29.94	17	11	88	86
1200	Oct 25, 1921		28.12	29.83	18	10	86	89
1350	Oct 21, 1924		28.70	29.88	19	8	71	70
600	Aug 26, 1926		28.31	29.97	27	10	83	81
845	Sept 20, 1926		28.20	29.94	17	7	87	83
1430	Oct 21, 1926 by		27.52	29.77	21	16	99	98
1220	Sept 17, 1928		28.30	29.88	MSG	12	MSG	MSG

See notes preceding table 4.1.

Table 4.3.--U.S. gulf coast hurricanes   (English units), continued.

Approximate coastal reference point† (n.mi.)	Date (GMT)*	Name	p_o(in.)‡	p_w(in.)	R(n.mi.)	T(kt)	V_{gx} (kt)	V_x (kt)
300	June 28, 1929		28.62	29.80	13	15	72	73
970	Sept 30, 1929		28.80	29.91	55	6	64	62
390	Aug 14, 1932		27.83	29.91	12	15	96	95
130	Aug 5, 1933		28.80	29.91	25	10	69	68
1215	Sept 4, 1933		28.48	29.88	29	11	77	76
140	Sept 5, 1933		28.02	29.88	20	8	90	86
590	June 16, 1934		28.52	29.71	37	16	69	70
1410	Sept 3, 1935		26.35	29.94	6	9	131	130
1395	Nov 5, 1935 ex		28.73	30.00	10	15	75	76
900	July 31, 1936		28.46	30.00	19	9	81	79
450	Aug 8, 1940		28.70	29.94	11	8	74	72
370	Sept 23, 1941		28.31	29.86	21	13	81	80
1015	Oct 7, 1941		28.98	30.00	18	11	66	66
330	Aug 30, 1942		28.07	29.83	18	14	87	86
425	July 27, 1943		28.78	29.94	16	8	70	69
1260	Oct 19, 1944		28.02	29.88	27	13	89	88
300	Aug 27, 1945		28.57	29.83	18	4	73	69
1440	Sept 15, 1945		28.09	29.94	24	10	89	87
1345	Sept 18, 1947 ex		28.03	30.00	34	7	91	87
740	§Sept 19, 1947		28.54	29.94	23	16	77	77
1380	Sept 21, 1948		27.62	29.83	7	8	100	95
1385	Oct 5, 1948		28.85	29.83	31	13	63	64
1250	Aug 27, 1949		28.37	29.97	23	14	83	82
360	Oct 4, 1949		28.45	29.88	20	11	79	78
820	Aug 31, 1950	Baker	28.92	29.65	21	23	55	61

See notes preceding table 4.1.

Table 4.3.--U.S. gulf coast hurricanes (English units), continued

Approximate coastal reference point† (n.mi.)	Date (GMT)*	Name	p_o(in.)‡	p_w(in.)	R(n.mi.)	T(kt)	V_{gx} (kt)	V_x (kt)
1150	Sept 5, 1950	Easy	28.30	29.80	15	3	81	76
1200	Oct 18, 1950	King	28.88	29.94	MSG	17	MSG	MSG
905	Sept 24, 1956	Flossy	28.76	29.91	22	10	70	69
460	June 27, 1957	Audrey	27.95	29.74	19	14	87	87
1400	Sept 10, 1960	Donna	27.45	29.88	20	9	103	99
745	Sept 15, 1960	Ethel	28.70	29.97	18	10	74	73
295	Sept 11, 1961	Carla	27.49	29.77	30	6	98	93
595	Oct 3, 1964	Hilda	28.33	29.97	21	7	84	81
1350	Oct 14, 1964	Isbell	28.47	29.91	10	15	80	80
1375	Sept 8, 1965	Betsy	27.99	29.91	19	15	91	91
640	§Sept 10, 1965	Betsy	27.79	29.86	32	17	93	93
1030	June 9, 1966	Alma	28.65	29.97	23	9	75	73
1420	Oct 4, 1966 by	Inez	28.85	29.91	19	7	68	66
150	Sept 20, 1967	Beulah	27.26	29.80	25	8	105	100
1140	Oct 19, 1968	Gladys	28.85	29.86	21	10	65	65
750	Aug 18, 1969	Camille	26.81	29.77	8	16	118	121
260	Aug 3, 1970	Celia	27.89	29.83	9	14	92	91
10	Sept 12, 1970	Ella	28.55	29.77	21	7	72	70
340	Sept 10, 1971	Fern	28.91	29.77	26	5	59	57
470	Sept 16, 1971	Edith	28.88	29.80	27	15	61	63
940	June 19, 1972	Agnes	28.88	29.83	20	11	63	64
590	Sept 8, 1974	Carmen	27.64	29.91	10	9	101	96
40	Aug 31, 1975	Caroline	28.44	29.88	10	5	80	76
900	Sept 23, 1975	Eloise	28.20	29.97	18	22	87	89
10	∿Sept 2, 1977	Anita	27.35	29.88	12	10	106	102

See notes preceding table 4.1.

Table 4.4.--U.S. east coast hurricanes (1900-78) with central pressure $\leq$ 29.00 in. (98.2 kPa) listed chronologically (English units).

Approximate coastal reference point† (n.mi.)	Date (GMT)*	Name	P_o(in.)‡	P_w(n.mi)	R(n.mi.)	T(kt)	V_{gx} (kt)	V_x (kt)
1500	Sept 12, 1903		28.84	30.00	43	8	67	66
1545	June 17, 1906 ex		28.91	29.91	26	12	65	65
2000	Sept 17, 1906		28.98	30.06	44	16	63	66
1475	Oct 18, 1906 ex		28.84	29.83	35	6	63	61
1400	Oct 11, 1909 by		28.26	29.80	22	10	81	79
1870	Aug 28, 1911		28.92	30.00	27	8	66	65
2115	Sept 3, 1913		28.81	30.12	38	16	71	72
1350	Sept 10, 1919 by		27.44	29.88	15	8	104	99
1675	Oct 26, 1921 ex		28.91	29.88	MSG	10	MSG	MSG
2180	Aug 26, 1924 by		28.70	29.94	34	22	69	73
2710	§Aug 26, 1924 by		28.70	29.94	66	29	62	68
2115	Dec 2, 1925		28.95	30.09	54	14	64	65
1605	July 28, 1926		28.34	30.00	14	8	85	82
1460	Sept 18, 1926		27.59	29.94	24	17	101	100
1430	Oct 21, 1926 by		27.52	29.77	21	16	99	98
1505	Sept 17, 1928		27.62	29.88	28	13	98	96
1425	Sept 28, 1929		28.00	29.80	28	10	87	85
2255	Aug 23, 1933		28.63	29.94	36	18	71	73
1530	Sept 4, 1933		27.98	29.94	MSG	11	MSG	MSG
2160	Sept 16, 1933		28.25	30.03	40	9	83	81
1410	Sept 3, 1935		26.35	29.94	6	9	131	130
1460	Nov 4, 1935		28.73	29.97	10	12	74	74
2230	Sept 18, 1936 by		28.52	30.12	34	16	79	80
2595	Sept 21, 1938		27.75	29.97	50	47	90	98
1885	Aug 11, 1940		28.78	30.06	27	9	72	70
2180	Sept 14, 1944		27.88	29.86	17	23	92	93
2630	§Sept 15, 1944		28.31	29.91	36	30	77	82

See notes preceding table 4.1.

Table 4.4.--U.S. east coast hurricanes (English units), continued.

Approximate coastal reference point† (n.mi.)	Date (GMT)*	Name	p_o(in.)‡	p_w(in.)	R(n.mi.)	T(kt)	V_{gx} (kt)	V_x (kt)
1440	Sept 15, 1945		28.09	29.94	24	10	89	87
1475	Sept 17, 1947		27.76	29.97	34	10	97	93
1840	Oct 15, 1947		28.59	29.91	13	17	75	77
1535	Sept 22, 1948 ex		28.41	29.74	16	11	76	75
1435	Oct 5, 1948 ex		28.85	29.83	31	13	63	64
2180	Aug 24, 1949 by		28.86	30.06	24	22	70	74
1505	Aug 27, 1949		28.16	29.97	23	14	88	87
1460	Oct 18, 1950	King	28.20	29.94	6	6	88	84
2190	Aug 31, 1954	Carol	28.35	29.86	MSG	10	MSG	MSG
2600	§Aug 31, 1954	Carol	28.38	30.06	22	33	82	87
2190	Sept 10, 1954 by	Edna	27.85	29.86	MSG	20	MSG	MSG
2730	§Sept 11, 1954	Edna	27.97	29.83	18	40	87	93
2030	Oct 15, 1954	Hazel	27.66	29.86	21	26	96	98
2115	Aug 12, 1955	Connie	28.40	29.86	45	7	74	71
2115	Sept 19, 1955	Ione	28.35	30.00	42	9	80	78
2170	Aug 28, 1958 by	Daisy	28.26	29.97	25	17	84	84
2720	§Aug 29, 1958 by	Daisy	28.91	29.94	50	21	58	63
2140	Sept 27, 1958 by	Helene	27.52	29.88	21	14	100	98
1900	Sept 29, 1959	Gracie	28.08	30.00	10	12	91	89
1400	Sept 10, 1960	Donna	27.45	29.88	20	9	103	99
2110	§Sept 12, 1960	Donna	28.29	29.88	34	26	80	83
2600	§Sept 12, 1960	Donna	28.38	29.83	48	32	71	77
1455	Aug 27, 1964	Cleo	28.57	29.88	7	9	76	74
1715	Sept 10, 1964	Dora	28.52	29.91	20	7	77	74
1420	Sept 8, 1965	Betsy	28.11	29.91	22	11	88	86
2260	Sept 17, 1967	Doria	28.97	30.06	20	9	66	65
3065	Sept 10, 1969	Gerda	28.91	29.86	MSG	40	MSG	MSG
2170	⌐Aug 9, 1976	Belle	28.32	29.97	8	21	85	87
2550	⌐Aug 10, 1976	Belle	28.79	30.09	30	21	70	73
See notes preceding table 4.1.								

NOTES FOR TABLES 4.5 AND 4.6

p_o : central pressure

R : radius of maximum winds estimated at or near time of p_o

T : forward speed based on a 6-hr average encompassing the time of p_o

θ : track direction from which the hurricane moves measured clockwise from north at or near the time of p_o

MSG : missing

Table 4.5.--Western North Pacific typhoons (1960-74) with central pressure ≤ 29.10 in. (98.5 kPa) listed chronologically (metric units).

Name	Month	Date	Year	Time (GMT)	Lat. (°N)	Long. (°E)	Track direction (θ)	P₀ (kPa)	R (km)	T (km/hr)
Mary	June	8	1960	1800	22.5	114.0	200°	97.5	MSG	9
Olive	June	25	1960	0019	13.3	127.8	105°	95.0	6	22
Polly	July	22	1960	0926	23.7	127.2	155°	95.0	20	6
Trix	Aug.	6	1960	2050	23.4	129.8	125°	91.8	11	33
Virginia	Aug.	10	1960	0800	31.4	136.3	140°	97.1	41	37
Bess	Aug.	19	1960	2155	32.4	139.1	185°	98.0	17	15
Carmen	Aug.	18	1960	2215	23.9	127.8	290°	97.0	93	9
Della	Aug.	28	1960	0330	29.1	133.3	155°	96.8	46	13
Elaine	Aug.	22	1960	0515	21.7	121.3	215°	97.6	11	19
Faye	Aug.	30	1960	0825	31.8	141.0	195°	97.9	24	35
Kit	Oct.	6	1960	0400	12.8	124.6	095°	96.6	20	13
Nina	Oct.	26	1960	2300	32.9	142.7	220°	96.0	57	63
Lola	Oct.	12	1960	0030	15.4	125.2	080°	97.8	35	7
Phyllis	Dec.	18	1960	0330	17.2	124.3	180°	96.2	57	6
Alice	May	17	1961	2230	17.2	114.0	150°	92.5	35	13
Betty	May	25	1961	0315	17.8	124.0	135°	94.6	35	22
Elsie	July	13	1961	0330	21.5	122.1	110°	97.4	41	7
Helen	July	29	1961	0900	25.3	131.0	160°	97.1	24	15
June	Aug.	6	1961	0845	22.0	121.8	115°	96.1	30	11
Kathy	Aug.	16	1961	2130	30.8	133.8	140°	98.0	24	20
Lorna	Aug.	23	1961	2215	19.4	124.2	130°	94.7	41	17
Nancy	Sept.	13	1961	2200	22.7	129.4	160°	90.2	46	26
Pamela	Sept.	11	1961	0700	23.7	125.7	090°	91.4	7	32
Tilda	Oct.	1	1961	2210	25.3	130.7	100°	93.5	24	22
Violet	Oct.	8	1961	2145	27.2	136.7	180°	93.0	11	28
Ellen	Dec.	9	1961	0300	14.2	124.2	140°	94.5	43	11
Hope	May	20	1962	1006	20.7	127.6	230°	97.9	9	30
Kate	July	22	1962	0333	21.1	120.6	220°	96.4	15	20
Louise	July	26	1962	0340	31.0	136.5	140°	97.0	35	13
Nora	July	30	1962	2200	23.3	127.8	140°	96.8	30	19
Opel	Aug.	5	1962	0340	22.0	123.1	145°	91.0	20	26
Patsy	Aug.	8	1962	2220	14.1	117.4	110°	98.0	17	30
Ruth	Aug.	19	1962	0315	32.4	130.7	185°	95.4	17	6
Sarah	Aug.	20	1962	1000	30.1	127.3	240°	97.8	30	13
Thelma	Aug.	25	1962	0790	31.4	136.6	180°	94.7	19	20
Wanda	Aug.	31	1962	0930	20.9	117.4	110°	94.9	6	22
Amy	Sept.	3	1962	2150	20.6	125.5	135°	94.1	26	19
Dinah	Oct.	1	1962	2221	20.7	126.1	095°	95.3	46	28
Gilda	Oct.	27	1962	0040	18.0	125.6	180°	95.6	43	9
Jean	Nov.	10	1962	0515	15.4	111.1	095°	96.0	24	4
Karen	Nov.	15	1962	2225	27.0	132.0	230°	94.8	46	45
Lucy	Nov.	28	1962	2200	10.3	114.8	080°	97.4	35	24
Shirley	June	17	1963	0945	22.4	127.0	150°	96.2	35	20
Trix	June	30	1963	0444	21.5	116.7	180°	98.1	17	17
Wendy	July	15	1963	0400	20.9	125.7	125°	92.8	11	22
Bess	July	7	1963	2202	28.7	133.2	165°	95.7	57	9
Carmen	Aug.	12	1963	2145	13.4	124.7	130°	89.8	30	19
Della	Aug.	26	1963	2200	30.4	132.1	210°	96.9	15	30
Faye	Sept.	4	1963	0347	19.0	125.7	115°	97.6	30	30
Gloria	Sept.	9	1963	2206	22.7	125.8	125°	91.2	43	13
Winnie	June	29	1964	1020	14.5	122.6	085°	96.8	41	26
Betty	July	5	1964	0400	26.8	123.7	150°	95.8	24	13
Flossie	July	28	1964	2200	34.8	123.1	195°	97.4	24	24
Helen	Aug.	1	1964	0400	29.6	131.6	125°	96.7	35	24
Ida	Aug.	6	1964	0352	16.4	125.5	110°	92.7	46	24
Kathy	Aug.	20	1964	2225	27.4	130.3	160°	94.5	15	4
Marie	Aug.	17	1964	1000	24.7	134.3	160°	98.1	39	13
Ruby	Sept.	4	1964	1000	20.7	117.8	125°	96.3	20	22
Sally	Sept.	8	1964	1030	18.2	124.1	100°	89.4	15	24
Tilda	Sept	20	1964	1015	18.6	112.4	060°	95.2	15	11
Wilda	Sept	23	1964	0355	26.5	131.2	140°	93.5	44	15
Clara	Oct	6	1964	0930	17.3	114.3	095°	97.9	24	22
Dot	Oct.	12	1964	0300	20.2	115.2	155°	97.6	93	11

See notes preceding table 4.5.

Table 4.5.--Western North Pacific typhoons (metric units), continued.

Name	Month	Date	Year	Time (GMT)	Lat. (°N)	Long. (°E)	Track direction (θ)	P_o (kPa)	R (km)	T (km/hr)
Louise	Nov.	18	1964	0300	8.6	129.8	090°	91.4	15	22
Opal	Dec.	11	1964	2200	9.1	134.1	130°	90.3	9	26
Amy	May	26	1965	0900	25.7	132.1	220°	97.6	24	54
Dinah	June	17	1965	0300	17.5	123.8	130°	93.2	9	19
Freda	July	12	1965	2120	16.3	124.4	120°	92.2	11	32
Harriet	July	25	1965	0910	21.5	125.2	110°	97.3	24	32
Jean	Aug.	4	1965	0300	25.7	126.8	175°	94.0	35	13
Lucy	Aug.	21	1965	0230	31.3	137.6	125°	95.3	41	11
Mary	Aug.	17	1965	0310	21.2	129.0	125°	93.6	24	20
Rose	Sept.	4	1965	1012	20.2	114.5	090°	96.8	20	20
Shirley	Sept.	8	1965	2100	26.3	131.7	165°	93.6	17	17
Trix	Sept.	15	1965	0200	22.9	128.7	165°	93.0	70	6
Faye	Nov.	23	1965	2142	17.9	127.1	170°	92.5	24	22
Irma	May	17	1966	0300	12.4	122.2	120°	97.1	11	13
Judy	May	29	1966	0914	20.9	117.1	245°	97.0	24	11
Kit	June	26	1966	2110	24.3	132.3	205°	91.2	9	30
Tess	Aug.	16	1966	0230	26.7	122.9	090°	97.4	11	32
Viola	Aug.	21	1966	0325	29.1	146.2	140°	97.8	24	30
Alice	Sept.	2	1966	0205	26.1	125.9	100°	93.8	24	20
Cora	Sept.	4	1966	2200	24.6	125.2	175°	91.7	24	6
Elsie	Sept.	15	1966	0330	21.4	117.8	225°	94.3	20	9
Ida	Sept.	24	1966	0207	27.5	138.1	170°	96.1	57	56
Pamela	Dec.	26	1966	0830	11	126	110°	96.7	17	19
Violet	April	7	1967	0900	16.1	125.8	110°	94.7	24	19
Anita	June	28	1967	1600	19.2	121.8	120°	96.7	24	19
Clara	July	10	1967	2103	23.5	123.2	110°	96.0	17	15
Marge	Aug.	27	1967	0400	18.0	124.5	055°	93.7	17	24
Nora	Aug.	28	1967	2035	22.9	125.6	110°	98.1	24	26
Opal	Sept.	13	1967	1530	31.6	140.0	215°	96.3	6	19
Carla	Oct.	16	1967	0400	16.3	125.6	120°	93.5	24	24
Dinah	Oct.	24	1967	0257	22.9	129.1	085°	95.0	30	7
Emma	Nov.	2	1967	2200	12.0	127.7	110°	90.8	17	26
Freda	Nov.	9	1967	0940	11.8	117.7	105°	97.1	24	24
Gilda	Nov.	15	1967	0300	17.0	131.8	110°	91.9	46	28
Lucy	June	30	1968	1430	20.7	129.4	150°	96.8	17	13
Mary	June	27	1968	2059	31.0	135.2	155°	96.9	11	15
Shirley	Aug.	21	1968	0558	21.6	114.7	145°	96.3	57	17
Wendy	Sept.	2	1968	0234	22.7	133.3	095°	93.5	35	35
Della	Sept.	21	1968	2359	22.8	125.5	160°	93.0	46	17
Carmen	Sept.	22	1968	2100	34.8	144.9	200°	97.2	57	19
Elaine	Sept.	27	1968	0300	16.8	124.7	120°	90.8	6	15
Mamie	Nov.	20	1968	0300	9.6	119.4	090°	97.2	11	22
Nina	Nov.	26	1968	0820	9.3	112.8	110°	95.9	30	24
Ora	Nov.	28	1968	0815	15.2	126.4	085°	94.9	24	24
Susan	April	21	1969	2130	8.2	129.0	115°	94.3	11	11
Tess	July	10	1969	0000	14.5	113.8	095°	96.9	24	28
Viola	July	26	1969	2100	19.7	122.4	100°	89.1	30	24
Betty	Aug.	8	1969	0200	25.4	122.0	130°	96.2	17	22
Cora	Aug.	19	1969	1135	25.4	127.4	175°	93.4	17	15
Elsie	Sept.	24	1969	2150	22.1	132.4	110°	91.8	33	26
Nancy	Feb.	24	1970	0900	11.2	128.6	115°	94.9	30	30
Olga	July	2	1970	0015	21.0	125.6	150°	91.5	7	17
Wilda	Aug.	13	1970	0300	27.5	129.0	185°	94.1	17	15
Anita	Aug.	20	1970	0300	28.0	135.6	160°	92.4	24	28
Billie	Aug.	27	1970	2100	27.8	129.9	125°	94.6	41	16
Clara	Aug.	28	1970	2100	35.6	142.2	220°	97.3	41	9
Georgia	Sept.	10	1970	0600	15.2	125.2	115°	92.0	15	19
Iris	Oct.	6	1970	0902	19.9	113.9	220°	94.4	26	6
Joan	Oct.	12	1970	2100	12.9	125.2	120°	90.1	30	20
Kate	Oct.	17	1970	0300	4.4	130.3	090°	93.8	11	15
Patsy	Nov.	18	1970	0957	14.2	126.6	090°	91.6	20	28

See notes preceding table 4.5.

Table 4.5.--Western North Pacific typhoons (metric units), continued.

Name	Month	Date	Year	Time (GMT)	Lat. (°N)	Long. (°E)	Track direction (θ)	P$_o$ (kPa)	R (km)	T (km/hr)
Wanda	May	2	1971	0404	15.8	108.8	170°	97.6	44	15
Dinah	May	25	1971	2200	12.4	125.5	100°	92.0	7	26
Freda	June	15	1971	1603	17.6	121.3	110°	97.3	11	19
Gilda	June	27	1971	0100	17.6	113.1	120°	97.5	24	24
Harriet	July	5	1971	1310	16.2	110.8	100°	92.1	9	24
Jean	July	16	1971	1900	16.6	111.8	130°	97.5	9	20
Lucy	July	19	1971	1000	18.6	125.0	115°	92.0	11	15
Nadine	July	24	1971	2215	20.9	124.9	120°	91.9	30	22
Olive	Aug.	4	1971	2130	31.7	130.1	180°	93.5	15	26
Rose	Aug.	15	1971	1500	19.3	114.8	135°	95.9	30	11
Trix	Aug.	29	1971	0002	29.5	130.1	180°	91.4	11	11
Virginia	Sept.	7	1971	0715	32.9	138.6	210°	97.6	30	30
Agnes	Sept.	18	1971	0355	23.6	123.1	120°	97.4	46	17
Bess	Sept.	21	1971	0955	22.8	127.6	105°	92.1	24	20
Della	Sept.	28	1971	1810	19.1	113.3	090°	98.1	30	22
Elaine	Oct.	6	1971	2330	16.4	115.6	160°	95.7	24	13
Faye	Oct.	11	1971	0200	15.3	118.4	320°	98.4	30	13
Hester	Oct.	22	1971	1900	14.3	110.2	115°	96.7	30	24
Irma	Nov.	13	1971	1200	21.7	127.0	175°	93.8	6	15
Kit	Jan.	7	1972	0300	11.8	127.6	095°	93.3	6	22
Ora	June	24	1972	0350	11.4	126.5	110°	98.1	17	24
Phyllis	July	14	1972	1030	29.4	138.6	135°	98.0	30	22
Rita	July	24	1972	0345	25.9	127.1	215°	95.4	57	13
Susan	July	8	1972	0927	18.8	118.0	180°	98.5	9	17
Tess	July	23	1972	0000	31.1	134.3	125°	97.0	46	30
Alice	Aug.	6	1972	1705	32.8	140.9	160°	97.8	57	20
Betty	Aug.	16	1972	1630	25.7	122.3	125°	93.7	15	19
Cora	Aug.	27	1972	0632	18.5	114.0	115°	97.6	24	7
Elsie	Sept.	3	1972	0600	15.5	109.9	085°	97.4	32	7
Flossie	Sept.	14	1972	1026	15.1	112.0	085°	97.5	24	13
Helen	Sept.	16	1972	0449	31.4	134.5	205°	95.9	46	54
Ida	Sept.	24	1972	0030	32.3	142.7	215°	94.9	24	45
Pamela	Nov.	7	1972	0645	16.0	112.5	125°	94.2	26	24
Therese	Dec.	7	1972	1200	13.3	115.9	110°	94.4	35	11
Anita	July	8	1973	1010	18.5	106.2	105°	98.0	35	15
Billie	July	16	1973	1600	26.4	125.6	180°	92.9	15	15
Georgia	Aug.	10	1973	0645	19.5	113.3	085°	97.6	17	11
Iris	Aug.	15	1973	2112	30.0	126.6	130°	97.2	57	17
Louise	Sept	5	1973	1000	19.9	114.7	095°	97.4	15	17
Marge	Sept.	13	1973	0900	18.9	113.1	095°	96.4	15	22
Nora	Oct.	6	1973	1020	14.9	125.9	090°	89.4	15	17
Opal	Oct.	5	1973	2340	13.1	112.0	175°	96.8	17	7
Ruth	Oct.	15	1973	0947	15.1	122.9	120°	96.1	30	22
Dinah	June	10	1974	0235	15.6	122.2	115°	97.4	24	20
Gilda	July	5	1974	0840	28.9	126.6	185°	95.5	35	17
Ivy	July	19	1974	2032	15.3	123.0	105°	94.6	9	28
Mary	Aug.	24	1974	2141	26.6	132.1	240°	96.4	30	26
Polly	Aug.	31	1974	2055	31.4	133.9	150°	95.6	35	13
Shirley	Sept.	7	1974	0856	28.6	127.6	180°	97.2	46	7
Bess	Oct.	10	1974	0907	17.2	125.2	100°	98.0	24	20
Della	Oct.	25	1974	0456	18.2	114.4	100°	95.8	17	26
Elaine	Oct.	27	1974	1430	17.3	123.7	095°	95.3	41	26
Gloria	Nov.	6	1974	0916	17.0	126.2	105°	93.1	24	26

See notes preceding table 4.5.

Table 4.6.--Western North Pacific typhoons (1960-74) with central pressure ≤ 29.10 in. (98.5 kPa) listed chronologically (English units).

Name	Month	Date	Year	Time (GMT)	Lat. (°N)	Long. (°E)	Track direction (θ)	P₀ (in.)	R (n.mi.)	T (kt)
Mary	June	8	1960	1800	22.5	114.0	200°	28.79	MSG	5
Olive	June	25	1960	0015	13.3	127.8	105°	28.05	3	12
Polly	July	22	1960	0926	23.7	127.2	155°	28.05	11	3
Trix	Aug.	6	1960	2050	23.4	129.8	125°	27.11	6	18
Virginia	Aug.	10	1960	0800	31.4	133.6	140°	28.67	22	20
Bess	Aug.	19	1960	2155	32.4	139.1	185°	28.94	9	8
Carmen	Aug.	18	1960	2215	23.9	127.8	290°	28.64	50	5
Della	Aug.	28	1960	0330	29.1	133.3	155°	28.59	25	7
Elaine	Aug.	22	1960	0515	21.7	121.3	215°	28.82	6	10
Faye	Aug.	30	1960	0825	31.8	141.0	195°	28.91	13	19
Kit	Oct.	6	1960	0400	12.8	124.6	095°	28.52	11	7
Nina	Oct.	26	1960	2300	32.9	142.7	220°	28.35	31	34
Lola	Oct.	12	1960	0030	15.4	129.2	080°	28.89	19	4
Phyllis	Dec.	18	1960	0330	17.2	124.3	180°	28.41	31	3
Alice	May	17	1961	2230	17.2	114.0	150°	27.32	19	7
Betty	May	25	1961	0315	17.8	124.0	135°	27.94	19	12
Elsie	July	13	1961	0330	21.5	122.1	110°	28.76	22	4
Helen	July	29	1961	0900	25.0	131.0	160°	28.67	13	8
June	Aug.	6	1961	0845	22.0	121.8	115°	28.38	16	10
Katy	Aug.	16	1961	2130	30.8	133.8	140°	28.94	13	11
Lorna	Aug.	23	1961	2215	19.4	124.2	130°	27.97	22	9
Nancy	Sept.	13	1961	2200	22.7	129.4	160°	26.64	25	14
Pamela	Sept.	11	1961	0700	23.7	125.7	090°	26.99	4	17
Tilda	Oct.	2	1961	2210	25.3	130.7	100°	27.61	13	12
Violet	Oct.	7	1961	2145	27.2	136.7	180°	27.46	6	15
Ellen	Dec.	9	1961	0300	14.2	124.2	140°	27.91	23	6
Hope	May	20	1962	1006	20.7	127.6	230°	28.91	5	16
Kate	July	22	1962	0333	21.1	120.6	220°	28.47	8	11
Louise	July	26	1962	0340	31.0	136.5	140°	28.64	19	7
Nora	July	30	1962	2200	23.3	127.8	140°	28.59	16	10
Opel	Aug.	5	1962	0340	22.0	123.1	145°	26.87	11	14
Patsy	Aug.	8	1962	2220	14.1	117.4	110°	28.94	9	16
Ruth	Aug.	19	1962	0314	32.4	140.7	185°	28.17	9	3
Sarah	Aug.	20	1962	1000	30.1	127.3	240°	28.88	16	7
Thelma	Aug.	25	1962	0700	31.4	136.6	180°	28.97	10	11
Wanda	Aug.	21	1962	0930	20.9	117.4	110°	28.02	3	12
Amy	Sept.	3	1962	2150	20.6	125.5	135°	27.79	14	10
Dinah	Oct.	1	1962	2221	20.7	126.1	095°	28.14	25	15
Gilda	Oct.	27	1962	0040	18.0	125.6	180°	28.23	23	5
Jean	Nov.	10	1962	0515	15.4	111.1	095°	28.35	13	2
Karen	Nov.	15	1962	2225	27.0	132.0	230°	27.99	25	24
Lucy	Nov.	28	1962	2200	10.3	114.8	080°	28.76	19	13
Shirley	June	17	1963	0945	22.4	127.0	150°	28.41	19	11
Trix	June	30	1963	0444	21.5	116.7	180°	28.97	9	9
Wendy	July	15	1963	0400	20.9	125.7	125°	27.40	6	12
Bess	July	7	1963	2202	28.7	133.2	165°	28.26	31	5
Carmen	Aug.	12	1963	2145	13.4	124.7	130°	26.52	16	10
Della	Aug.	26	1963	2200	30.4	132.1	210°	28.62	8	7
Faye	Sept.	4	1963	0347	19.0	125.7	115°	28.82	16	16
Gloria	Sept.	9	1963	2206	22.7	125.8	125°	26.93	23	7
Winnie	June	29	1964	1020	14.5	122.6	085°	28.59	22	14
Betty	July	5	1964	0400	26.8	123.7	150°	28.29	13	7
Flossie	July	28	1964	2200	34.8	123.1	195°	28.76	13	13
Helen	Aug.	1	1964	0400	29.6	131.6	125°	28.56	19	13
Ida	Aug.	6	1964	0352	16.4	125.5	110°	27.37	25	13
Kathy	Aug.	20	1964	2225	27.4	130.3	160°	27.91	8	2
Marie	Aug.	17	1964	1000	24.7	134.3	160°	28.97	21	7
Ruby	Sept.	4	1964	1000	20.7	117.8	125°	28.44	11	12
Sally	Sept.	8	1964	1030	18.2	124.1	100°	26.40	8	13
Tilda	Sept.	20	1964	1015	18.6	112.4	060°	28.11	8	6
Wilda	Sept.	23	1964	0355	26.5	131.2	140°	27.61	24	8
Clara	Oct.	6	1964	0930	17.3	114.3	095°	28.91	13	12
Dot	Oct.	12	1964	0300	20.2	115.2	155°	28.82	50	6

See notes preceding table 4.5

Table 4.6.--Western North Pacific typhoons (English Units), continued.

Name	Month	Date	Year	Time (GMT)	Lat. (°N)	Long. (°E)	Track Direction (θ)	P₀ (in.)	R (n.mi.)	T (kt)
Louise	Nov.	18	1964	0300	8.6	129.8	090°	26.99	8	12
Opal	Dec.	11	1964	2200	9.1	134.1	130°	26.67	5	14
Amy	May	26	1965	0900	25.7	132.1	220°	28.82	13	29
Dinah	June	17	1965	0300	17.5	123.8	130°	27.52	5	10
Freda	July	12	1965	2120	16.3	124.4	120°	27.23	6	17
Harriet	July	25	1965	0910	21.5	125.2	110°	28.73	13	17
Jean	Aug.	4	1965	0330	25.7	126.8	175°	27.76	19	7
Lucy	Aug.	21	1965	0230	31.3	137.6	125°	28.14	22	6
Mary	Aug.	17	1965	0310	21.2	129.0	125°	27.64	13	11
Rose	Sept.	4	1965	1012	20.2	114.5	090°	28.59	11	11
Shirley	Sept.	8	1965	2100	26.3	131.7	165°	27.64	9	9
Trix	Sept.	15	1965	0200	22.9	128.7	165°	27.46	38	3
Faye	Nov.	23	1965	2142	17.9	127.1	170°	27.32	13	12
Irma	May	17	1966	0300	12.4	122.2	120°	28.67	6	7
Judy	May	29	1966	0915	20.9	117.1	245°	28.64	13	6
Kit	June	26	1966	2110	24.3	132.3	205°	26.93	5	16
Tess	Aug.	16	1966	0230	26.7	122.9	090°	28.76	6	17
Viola	Aug.	21	1966	0325	29.1	146.2	140°	28.88	13	16
Alice	Sept.	2	1966	0205	26.1	125.9	100°	27.70	13	11
Cora	Sept.	4	1966	2200	24.6	125.2	175°	27.08	13	3
Elsie	Sept.	15	1966	0330	21.4	117.8	225°	27.85	11	5
Ida	Sept.	24	1966	0207	27.5	138.1	170°	28.38	31	30
Pamela	Dec.	26	1966	0830	11.6	126.6	110°	28.56	9	10
Violet	April	7	1967	0900	16.1	125.8	110°	27.97	13	10
Anita	June	28	1967	1600	19.2	121.8	120°	28.56	13	10
Clara	July	10	1967	2103	23.5	123.2	110°	28.35	9	8
Marge	Aug.	27	1967	0400	18.0	124.5	055°	27.67	9	13
Nora	Aug.	28	1967	2035	22.9	125.6	110°	28.97	13	14
Opal	Sept.	13	1967	1530	31.6	140.0	215°	28.44	3	10
Carla	Oct.	16	1967	0400	16.3	125.6	120°	27.61	13	13
Dinah	Oct.	24	1967	0257	22.9	129.1	085°	28.05	16	4
Emma	Nov.	2	1967	2200	12.0	127.7	110°	26.81	9	14
Freda	Nov.	9	1967	0940	11.8	111.7	105°	28.67	13	13
Gilda	Nov.	15	1967	0300	17.0	131.8	110°	27.14	25	15
Lucy	June	30	1968	1430	20.7	129.4	150°	28.59	9	7
Mary	June	27	1968	2059	31.0	135.2	155°	28.62	6	8
Shirley	Aug.	21	1968	0558	21.6	114.7	145°	28.44	31	9
Wendy	Sept.	2	1968	0234	22.7	133.3	095°	27.61	19	19
Della	Sept.	21	1968	2359	22.8	125.5	160°	27.46	25	9
Carmen	Sept.	22	1968	2100	34.8	144.9	200°	28.70	31	10
Elaine	Sept.	27	1968	0300	16.8	124.7	120°	26.81	3	8
Mamie	Nov.	20	1968	0300	9.6	119.4	090°	28.70	6	12
Nina	Nov.	26	1968	0820	9.3	112.8	110°	28.32	16	13
Ora	Nov.	28	1968	0815	15.2	126.4	085°	28.02	13	13
Susan	April	21	1969	2130	8.2	129.0	115°	27.85	6	6
Tess	July	10	1969	0000	14.5	113.8	095°	28.62	13	15
Viola	July	26	1969	2100	19.7	122.4	100°	26.31	16	13
Betty	Aug.	8	1969	0200	25.4	122.0	130°	28.41	9	12
Cora	Aug.	19	1969	1135	25.4	127.4	175°	27.58	9	8
Elsie	Sept.	24	1969	2150	22.1	132.4	110°	27.11	18	14
Nancy	Feb.	24	1970	0900	11.2	128.6	115°	28.02	16	16
Olga	July	2	1970	0015	21.0	125.6	150°	27.02	4	9
Wilda	Aug.	13	1970	0300	27.5	129.0	185°	27.79	9	8
Anita	Aug.	20	1970	0300	28.0	135.6	160°	27.29	13	15
Billie	Aug.	27	1970	2100	27.8	129.9	125°	27.94	22	8
Clara	Aug.	28	1970	2100	35.6	142.2	220°	28.73	22	5
Georgia	Sept.	10	1970	0600	15.2	125.2	115°	27.17	8	10
Iris	Oct.	6	1970	0902	19.9	113.9	220°	27.88	14	3
Joan	Oct.	12	1970	2100	12.9	129.2	120°	26.61	16	11
Kate	Oct.	17	1970	0300	4.4	130.3	090°	27.70	6	8
Patsy	Nov.	18	1970	0957	14.2	126.6	090°	27.05	11	15
Wanda	May	2	1971	0404	15.8	108.8	170°	28.82	24	8
Dina	May	25	1971	2200	12.4	125.5	100°	27.17	4	14

See notes preceeding table 4.5

Table 4.6.--Western North Pacific typhoons (English units), continued.

Name	Month	Date	Year	Time (GMT)	Lat. (°N)	Long. (°E)	Track direction (θ)	P_o (in.)	R (n.mi.)	T (kt)
Freda	June	15	1971	1603	17.6	121.3	110°	28.73	6	10
Gilda	June	27	1971	0100	17.6	113.1	120°	28.79	13	13
Harriet	July	5	1971	1310	16.2	110.8	100°	27.20	5	13
Jean	July	16	1971	1900	16.6	111.8	130°	28.79	5	11
Lucy	July	19	1971	1000	18.6	125.0	115°	27.17	6	8
Nadine	July	24	1971	2215	20.9	124.9	120°	27.14	16	12
Olive	Aug.	4	1971	2130	31.7	130.1	180°	27.61	8	14
Rose	Aug.	15	1971	1500	19.3	114.8	135°	28.32	16	6
Trix	Aug.	29	1971	0002	29.5	130.1	180°	26.99	6	6
Virginia	Sept.	7	1971	0715	32.9	138.6	210°	28.82	16	16
Agnes	Sept.	18	1971	0355	23.6	123.1	120°	28.76	25	9
Bess	Sept.	21	1971	0955	22.8	127.6	105°	27.20	13	11
Della	Sept.	28	1971	1810	19.1	113.3	090°	28.97	16	12
Elaine	Oct.	6	1971	2330	16.4	115.6	160°	28.26	13	7
Faye	Oct.	11	1971	0200	15.0	118.4	320°	29.06	16	7
Hester	Oct.	22	1971	1900	14.3	110.2	115°	28.56	16	13
Irma	Nov.	13	1971	1200	21.7	127.0	175°	27.70	3	8
Kit	Jan.	7	1972	0300	11.8	127.6	095°	27.55	3	12
Ora	June	24	1972	0350	11.4	126.5	110°	28.97	9	13
Phyllis	July	14	1972	1030	29.4	138.6	135°	28.94	16	12
Rita	July	24	1972	0345	25.9	127.1	215°	28.17	31	7
Susan	July	8	1972	0927	18.8	118.0	180°	29.09	5	9
Tess	July	23	1972	0000	31.1	134.3	125°	28.64	25	15
Alice	Aug.	6	1972	1705	32.8	140.9	160°	28.88	31	11
Betty	Aug.	16	1972	1630	25.7	122.3	125°	27.67	8	10
Cora	Aug.	27	1972	0632	18.6	114.0	115°	28.82	13	4
Elsie	Sept.	3	1972	0600	15.5	109.9	085°	28.76	17	4
Flossie	Sept.	14	1972	1026	15.1	112.0	085°	28.79	13	7
Helen	Sept.	16	1972	0449	31.4	134.5	205°	28.32	25	29
Ida	Sept.	24	1972	0030	32.3	142.7	215°	28.02	13	24
Pamela	Nov.	7	1972	0645	16.0	112.5	125°	27.82	14	13
Therese	Dec.	7	1972	1200	13.3	115.9	110°	27.88	19	6
Anita	July	8	1973	1010	18.5	106.2	105°	28.94	19	8
Billie	July	16	1973	1600	26.4	125.6	180°	27.43	8	8
Georgia	Aug.	10	1973	0645	19.5	113.3	085°	28.82	9	6
Iris	Aug.	15	1973	2112	30.0	126.6	130°	28.70	31	9
Louise	Sept.	5	1973	1000	19.9	114.7	095°	28.76	8	9
Marge	Sept.	13	1973	0900	18.9	113.1	095°	28.47	8	12
Nora	Oct.	6	1973	1020	14.9	125.9	090°	26.40	8	9
Opal	Oct.	5	1973	2340	13.1	112.0	175°	28.59	9	4
Ruth	Oct.	15	1973	0947	15.1	122.9	120°	28.38	16	12
Dinah	June	10	1974	0235	15.6	122.2	115°	28.76	13	11
Gilda	July	5	1974	0840	28.9	126.6	185°	28.20	19	9
Ivy	July	19	1974	2032	15.3	123.0	105°	27.94	5	15
Mary	Aug.	24	1974	2141	26.3	132.1	240°	28.47	16	14
Polly	Aug.	31	1974	2055	31.4	133.9	150°	28.23	19	7
Shirley	Sept.	7	1974	0856	28.6	127.6	180°	28.70	25	4
Bess	Oct.	10	1974	0907	17.2	125.2	100°	28.94	13	11
Della	Oct.	25	1974	0456	18.2	114.4	100°	28.29	9	14
Elaine	Oct.	27	1974	1430	17.3	123.7	095°	28.85	22	14
Gloria	Nov.	6	1974	0916	17.0	125.2	105°	27.49	13	14
Irma	Nov.	27	1974	0245	15.7	126.2	090°	27.76	19	11

See notes preceding table 4.5

5. METEOROLOGICAL AND OTHER PARAMETERS AND THEIR INTERRELATIONS

5.1 INTRODUCTION

This chapter focuses on the interrelations of parameters which influence the strength and regional variation of hurricane wind fields. This is preceded by brief definitions of the meteorological parameters used in this study: peripheral pressure (p_w), central pressure (p_o), radius of maximum winds (R), forward speed (T), track direction (θ), and wind inflow angle (ϕ). Two other parameters, latitude (ψ) and longitude (λ), were also considered.

To what extent parameters important to extreme hurricane wind fields are interrelated is of interest from two standpoints. One is from a broad aspect, in that a detailed study should show interrelations, even though they may not be sufficient to use in the SPH/PMH criteria. The other is to make use in this study of clear-cut relations shown in the tropical cyclone data.

5.2 DEFINITION OF METEOROLOGICAL PARAMETERS

Peripheral pressure (p_w) - the sea-level pressure at the outer limits of the hurricane circulation. p_w in this study is the average pressure for the first anticyclonically turning isobar outward from the storm center. We averaged the pressure north, east, south, and west of the hurricane center.

Central pressure (p_o) - the lowest sea-level pressure in a hurricane.

Radius of maximum winds (R) - the radial distance from the hurricane center to the band of strongest winds within the hurricane wall cloud.

Forward speed (T) - the rate of translation of the hurricane center from one geographical point to another.

Track direction (θ) - the path of forward movement along which the hurricane is coming measured in degrees clockwise from the north.

Wind inflow angle (ϕ) - the angle between true wind direction and a tangent to a circle concentric with the hurricane center.

5.3   INTERRELATIONS BETWEEN PAIRS OF PARAMETERS

Interrelations between pairs of parameters were examined using linear correlation analyses. In most cases, these relations are curvilinear. However, from plots of the data we determined that these curvilinear relations closely approximated linear relations. Differences between curvilinear and linear relations are *least* for more intense cyclones, our primary area of interest. In addition, statistical relations between pairs of parameters cannot be used to estimate SPH and PMH wind fields directly (we would be extrapolating beyond the data). Also, more than two parameters are involved in the development of wind fields. The developed linear relations and graphical plots were considered adequate for general guidance.

Interrelations with p_w and ϕ were not considered. p_w varies slowly with time. ϕ (a function of the other parameters) is difficult to measure with any precision.

5.3.1   ZERO-ORDER LINEAR CORRELATION COEFFICIENTS

Linear correlation studies are based upon the assumption that the distribution of values (x, y) is a two-variable normal distribution. If the assumption of normality is satisfied, it is possible to use the observed value of the sample zero-order linear correlation coefficient (r) to test for independence. If the two variables are independent, regression curves take the form of horizontal or vertical straight lines. This implies that the population correlation coefficient (ρ) is equal to zero. If r (which is an estimate of ρ) is near zero, we shall say that we do not have sufficient reason to doubt the independence between x and y. However, if r is far from zero as determined by tests of significance, we shall reject the hypothesis that the two variables are independent (Dixon and Massey, Jr. 1957). Independence signifies that there is no relation between the variables, meaning that any conclusions drawn regarding one parameter in this report do not necessarily affect another parameter.

Table 5.1 summarizes the r's and standard errors of estimate $(s_{y \cdot x})$*
between pairs of the five parameters $(p_o$, R, T, θ and ψ, λ) for tropical
cyclone data from each of three regions (east coast, gulf coast, and western
North Pacific) and for three combinations of these regions (east and gulf
coast, east coast and western North Pacific, and east and gulf coast and
Western North Pacific). A storm is included for each region only when
values were available for all parameters. Thus, some storms were not used,
e.g., the gulf coast storm of September 20, 1909 for which R could not be
determined; (see table 4.1). The table also indicates if the r is signi-
ficant at the 1% or 5% level. The 5% level gives the values that would
occur on the average once in 20 times in random sampling from uncorrelated
material. The 1 % level is a more severe test.

Four of the r's between the pairs of parameters shown in table 5.1 are
>0.50. (The table shows eight but half of these are mirror images of the
other half.) These four are significant at the 1% level. All have latitude
as one of the pair. The highest r (0.68) is T for east coast hurricanes.
The next highest (0.52) is the θ for typhoons and with R for east coast
hurricanes. The last (0.51) is with R for the combined set of east coast
hurricanes and typhoons. These interrelations are guidance for establishing
SPH and PMH criteria along the east coast (see chapters 9 to 11).

5.3.2 PLOTS OF DATA

Trend lines are drawn on all seven figures discussed in this subsection.
These lines are drawn through the data by eye and are shown for illustrative
purposes. The linear regression lines are not shown because most of the
interrelations shown in the seven figures are somewhat curvilinear. r and
$s_{y \cdot x}$† from table 5.1 are indicated in figures 5.1 to 5.7 for convenience.

---

*For both r and $s_{y \cdot x}$ we are assuming in a gross sense that all relations are
linear. For a loose definition of $s_{y \cdot x}$ see section 5.4.

†Here again we are assuming in a gross sense that all relations are linear.

Notes for Tables 5.1 and 5.2

P_o : central pressure

R : radius of maximum winds

θ : track direction

T : forward speed

ψ : latitude (east coast hurricanes and typhoons)

λ : longitude (gulf coast hurricanes)

r : linear correlation coefficient

r' : multiple correlation coefficient

r'^2 : reduction of variance (square of the multiple correlation coefficient)

$s_{y \cdot x}$: standard error of estimate

r sig, r' sig : r, r' is significant at the 5 % level /*
: r, r' is significant at the 1 % level */*
: r, r' is neither significant at the 1% nor 5 % levels /

N : sample size

vs. : versus

N/A : not applicable

Table 5.1.--Linear correlation coefficients between pairs of meteorological and other parameters.

Dependent Variable (y)	p_o r	$s_{y \cdot x}$	r sig	R r	$s_{y \cdot x}$	r sig	θ r	$s_{y \cdot x}$	r sig	T r	$s_{y \cdot x}$	r sig	ψ, λ r	$s_{y \cdot x}$	r sig
EAST COAST HURRICANES N = 49															
p_o in. (kPa)	-	-	-	.39	.49(1.7)	*/*	.02	.53(1.8)	/	-.10	.53(1.8)	/	.27	.51(1.8)	/
R n.mi. (km)	.39	12.2(22.6)	*/*	-	-	-	.30	12.6(23.4)	/*	.32	12.5(23.2)	/*	.52	11.3(20.9)	*/*
θ deg.	.02	55.3	/	.30	52.9	/*	-	-	-	.35	51.8	/*	.35	51.9	/*
T kt (km/hr)	-.10	9.2(17.0)	/	.32	8.7(16.1)	/*	.35	8.6(15.9)	/*	-	-	-	.68	6.7(12.4)	*/*
ψ deg.	.27	5.4	/	.52	4.8	*/*	.35	5.3	/*	.68	4.1	*/*	-	-	-
GULF COAST HURRICANES N = 67															
p_o in. (kPa)	-	-	-	.33	.51(1.7)	*/*	.14	.53(1.8)	/	.09	.53(1.8)	/	-.02	.54(1.8)	/
R n.mi. (km)	.33	8.3(15.4)	*/*	-	-	-	.19	8.7(16.1)	/	.15	8.7(16.1)	/	-.06	8.8(16.3)	/
θ deg.	.14	50.2	/	.19	49.8	/	-	-	-	.02	50.7	/	-.32	48.0	/
T kt(km/hr)	.09	4.6(8.5)	/	.15	4.6(8.5)	/	.02	4.6(8.5)	/	-	-	-	.02	4.6(8.5)	/
λ deg.	-.02	6.1	/	-.06	6.1	/	-.32	5.8	/	.02	6.1	/	-	-	-
WESTERN NORTH PACIFIC TYPHOONS N = 178															
p_o in. (kPa)	-	-	-	.20	.68(2.3)	*/*	.18	.68(2.3)	/*	-.07	.69(2.3)	/	.18	.68(2.3)	/*
R n.mi. (km)	.20	8.2(15.2)	*/*	-	-	-	.22	8.1(15.0)	*/*	-.02	15.4(8.3)	/	.26	8.0(14.8)	*/*
θ deg.	.18	44.5	/*	.22	44.1	*/*	-	-	-	± 0	N/A	/	.52		*/*
T kt (km/hr)	-.07	5.0(9.3)	/	-.02	5.0(9.3)	/	± 0	N/A	/	-	-	-	.10	5.0(9.3)	-
ψ deg.	.18	6.4	/*	.26	6.3	*/*	.52	5.5	*/*	.10	6.5	/	-	-	-

Table 5.1.--*Linear correlation coefficients between pairs of meteorological and other parameters, continued.*

Dependent Variable (y) \ Independent Variable (x)	p_o			R			θ			T			ψ, λ		
	r	$s_{y \cdot x}$	r sig	r	$s_{y \cdot x}$	r sig	r	$s_{y \cdot x}$	r sig	r	$s_{y \cdot x}$	r sig	r	$s_{y \cdot x}$	r sig
EAST AND GULF COAST HURRICANES N = 116															
p_o in. (kPa)	-	-	-	.34	.50(1.7)	*/*	.09	.53(1.8)	/	-.02	.53(1.8)	/			
R n.mi. (km)	.34	10.6(19.6)	*/*	-	-	-	.23	11.0(20.4)	/*	.32	10.7(19.8)	*/*			
θ deg.	.09	52.5	/	.23	51.3	/*	-	-	-	.20	51.6	/*			
T kt (km/hr)	-.02	7.3(13.5)	/	.32	6.9(12.8)	*/*	.20	7.1(13.2)	/*	-	-	-			
EAST COAST HURRICANES AND WESTERN NORTH PACIFIC TYPHOONS N = 227															
p_o in. (kPa)	-	-	-	.26	.64(2.2)	*/*	.16	.66(2.2)	/*	-.03	.66(2.2)	/	.22	.65(2.2)	*/*
R n.mi. (km)	.26	10.7(19.8)	*/*	-	-	-	.30	10.5(19.5)	*/*	.27	10.6(19.6)	*/*	.51	9.5(17.6)	*/*
θ deg.	.16	47.9	/*	.30	46.2	*/*	-	-	-	.19	47.6	*/*	.50	42.1	*/*
T kt (km/hr)	-.03	6.6(12.2)	/	.27	6.3(11.7)	*/*	.19	6.4(11.9)	*/*	-	-	-	.39	6.0(11.1)	*/*
ψ deg.	.22	7.4	*/*	.51	6.6	*/*	.50	6.6	*/*	.39	7.1	*/*	-	-	-
EAST AND GULF COAST HURRICANES AND WESTERN NORTH PACIFIC TYPHOONS N = 294															
p_o in. (kPa)	-	-	-	.28	.61(2.1)	*/*	.17	.63(2.1)	*/*	-.02	.64(2.2)	/			
R n.mi. (km)	.28	10.3(19.1)	*/*	-	-	-	.30	10.3(19.1)	*/*	.24	10.4(19.3)	*/*			
θ deg.	.17	49.0	*/*	.30	47.4	*/*	-	-	-	.15	49.1	/*			
T kt (km/hr)	-.02	6.2(11.5)	/	.24	6.0(11.1)	*/*	.15	6.1(11.3)	/*	-	-	-			

Table 5.2.--Multiple correlation coefficients involving meteorological and other parameters†

	r'	r'sig	r'^{2}	$s_{y \cdot x}$
EAST COAST HURRICANES N = 49				
p_o vs. R	.39	*/*	.15	0.49 in. (1.7 kPa)
p_o vs. R, T	.45	*/*	.20	0.48 in. (1.6 kPa)
p_o vs. R, T, ψ	.54	*/*	.30	0.45 in. (1.5 kPa)
R vs. ψ	.52	*/*	.27	11.3 n.mi. (20.4 km)
R vs. ψ, p_o	.58	*/*	.33	10.8 n.mi. (20.0 km)
θ vs. T	.35	/*	.12	51.8°
T vs. ψ	.68	*/*	.46	6.8 kt (12.5 km/hr)
T vs. ψ, p_o	.74	*/*	.55	6.2 kt (11.5 km/hr)
ψ vs. T	.68	*/*	.46	4.1°
ψ vs. T, p_o	.76	*/*	.58	3.6°
WESTERN NORTH PACIFIC TYPHOONS N = 178				
p_o vs. R	.20	*/*	.04	0.68 in. (2.3 kPa)
p_o vs. R, θ	.24	*/*	.06	0.67 in. (2.3 kPa)
R vs. ψ	.26	*/*	.07	8.0 n.mi. (14.9 km)
R vs. ψ, p_o	.30	*/*	.09	7.9 n.mi. (14.7 km)
θ vs. ψ	.52	*/*	.27	38.5°
T vs. ψ	.10	/	.01	5.0 kt (9.3 km/hr)
T vs. ψ, p_o	.13	/	.02	5.0 kt (9.3 km/hr)
ψ vs. θ	.52	*/*	.27	5.6°

†Only ordinary zero-order correlation coefficients are listed where additional combinations of parameters did not yield significant increases in r'.

5.3.2.1 INTERRELATIONS WITH CENTRAL PRESSURE (P_O). Figure 5.1 is a composite plot of p_O and R data for all hurricanes (tables 4.1-4.4) and typhoons (tables 4.5-4.6). The three data regions (east coast, gulf coast and western North Pacific) are distinguished by different plotting symbols. The conclusion from this plot is that R tends to be smaller and has a smaller range for lower p_O. This conclusion is supported by Myers (1954), Colon (1963), Sheets (1967), Shea and Gray (1972) and others. We also observe that the typhoon sample has nearly all R's ≤ 31 n.mi. (58 km) whereas quite a few hurricanes have R > 31 n.mi. Part of this may be explained by the hurricane sample extending into more northerly latitudes, where R's are generally larger, than the typhoon sample selected (see sec. 5.3.2.2).

A plot of p_O vs θ for all three regions (fig. 5.2) indicates that for the
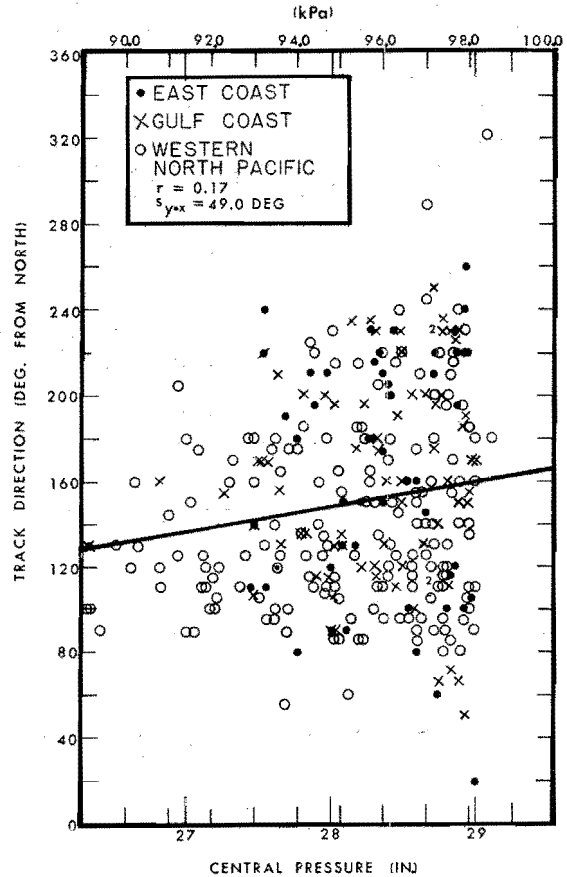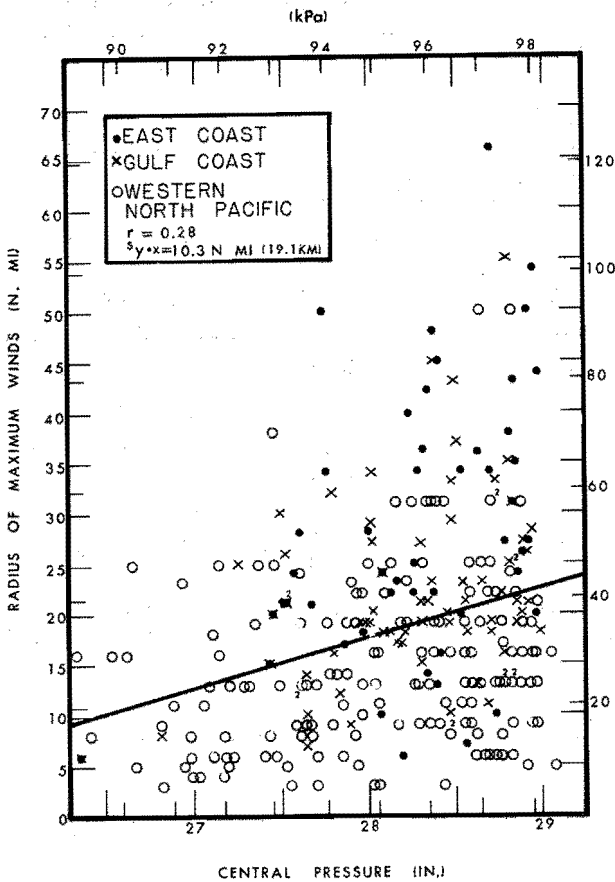

Figure 5.1.--Central pressure (p_O) vs. radius of maximum winds (R).

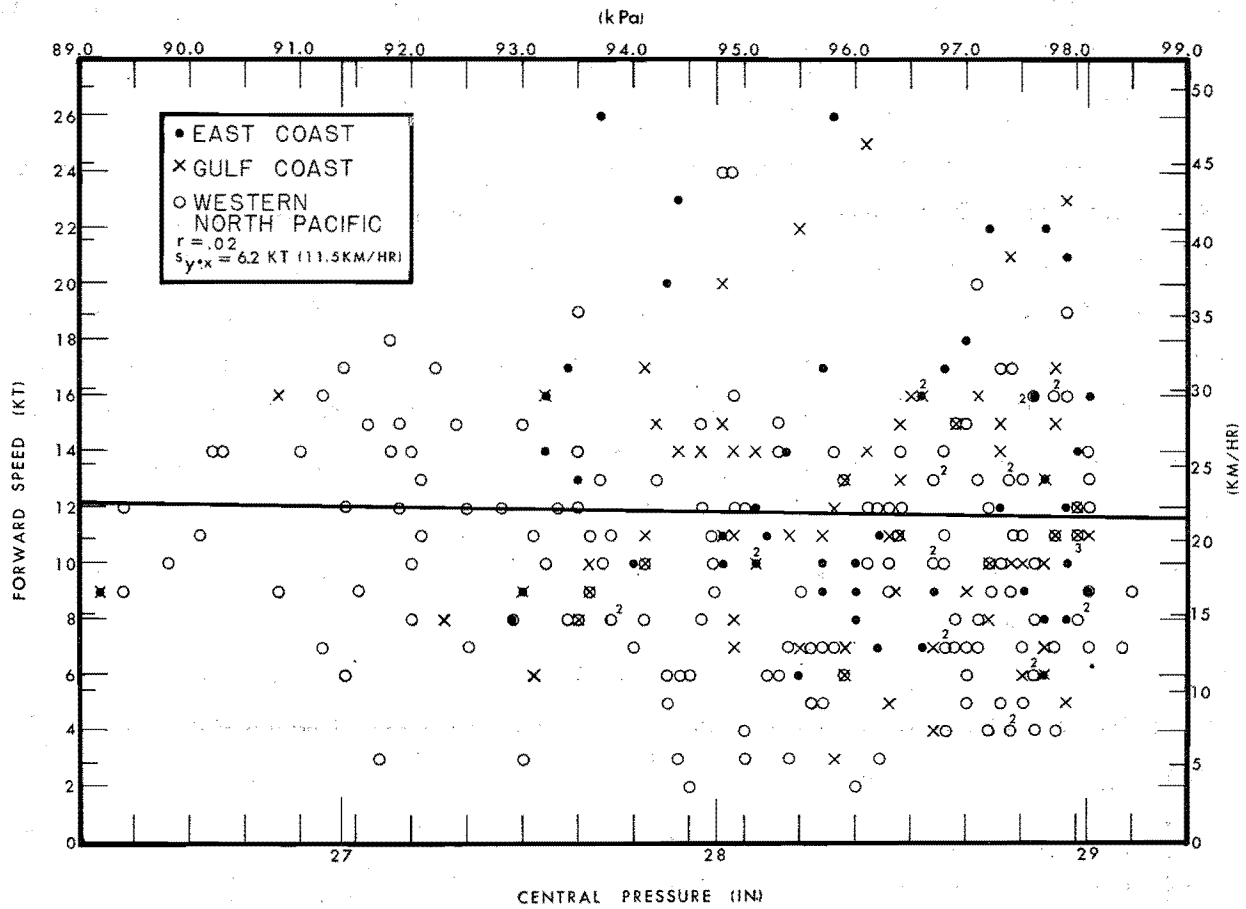Figure 5.2.--Central pressure (p_O) vs. track direction (θ).
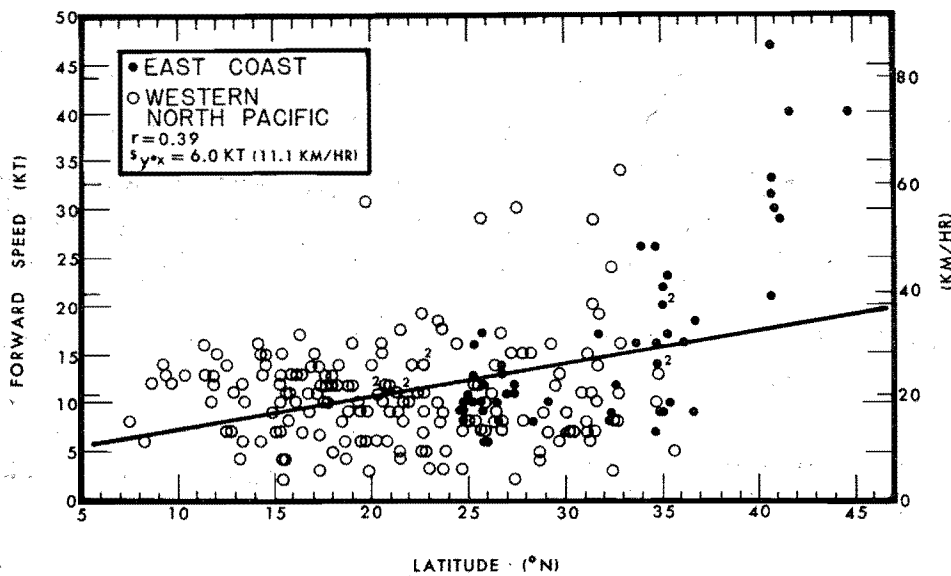
Figure 5.3.—Central pressure (p_o) vs. forward speed (T).

Figure 5.4.—Latitude (ψ) vs. forward speed (T).

more extreme tropical cyclones [$\leq$27.46 in. (93.0 kPa)] the range of θ is more restricted than it is for weaker storms. This indication supports restrictions on the entry direction of extreme storms at the coast.

Investigation of the interrelation between p_o and T (fig. 5.3) shows that storms with lower p_o move at slower speeds. Higher T's occur outside of tropical latitudes. Along the gulf coast, the most extreme storms ($p_o \leq$ 27.46 in., 93.0 kPa) have moved between 8 and 16 kt (15 and 30 km/hr). Along the east coast, storms with p_o <27.75 in. (94.0 kPa) have traveled at T between 8 and 26 kt (15 and 48 km/hr). Western North Pacific typhoons have T between 3 and 18 kt (6 and 33 km/hr) for $p_o \leq$ 27.46 in. (93.0 kPa). Weaker hurricanes and typhoons have a larger range of T.

5.3.2.2   INTERRELATIONS WITH LATITUDE (ψ).   A composite plot of ψ vs. T data is shown in figure 5.4 for east coast hurricanes and typhoons of the western North Pacific. The general conclusion from this plot is that T tends to be lower and has a smaller range with lower ψ. The storms with higher T's north of 25°N have recurved and have consequently accelerated.

p_o is higher at temperate latitudes than at tropical latitudes, partly because of warmer sea-surface temperatures to the south. Higher p_o at temperature latitudes is shown by a plot of ψ vs. p_o data (fig. 5.5), a trend line, and the enveloping minimum p_o curve for east coast hurricanes and western North Pacific typhoons.

A plot of ψ vs. θ is shown in figure 5.6 for east coast hurricanes and western North Pacific typhoons. r has a relatively high value of 0.50. This plot shows the well-known pattern of tropical cyclones moving from the east at lower ψ and changing to directions from the south and southwest as they move clockwise around the outer edge of the subtropical high.

Figure 5.7 is a plot of ψ vs. R for east coast hurricanes and western North Pacific typhoons. r is again relatively high at 0.51. This plot supports what many meteorologists have observed as a characteristic of hurricanes and typhoons, i.e., storms expand in size as they move northward out of the tropics.
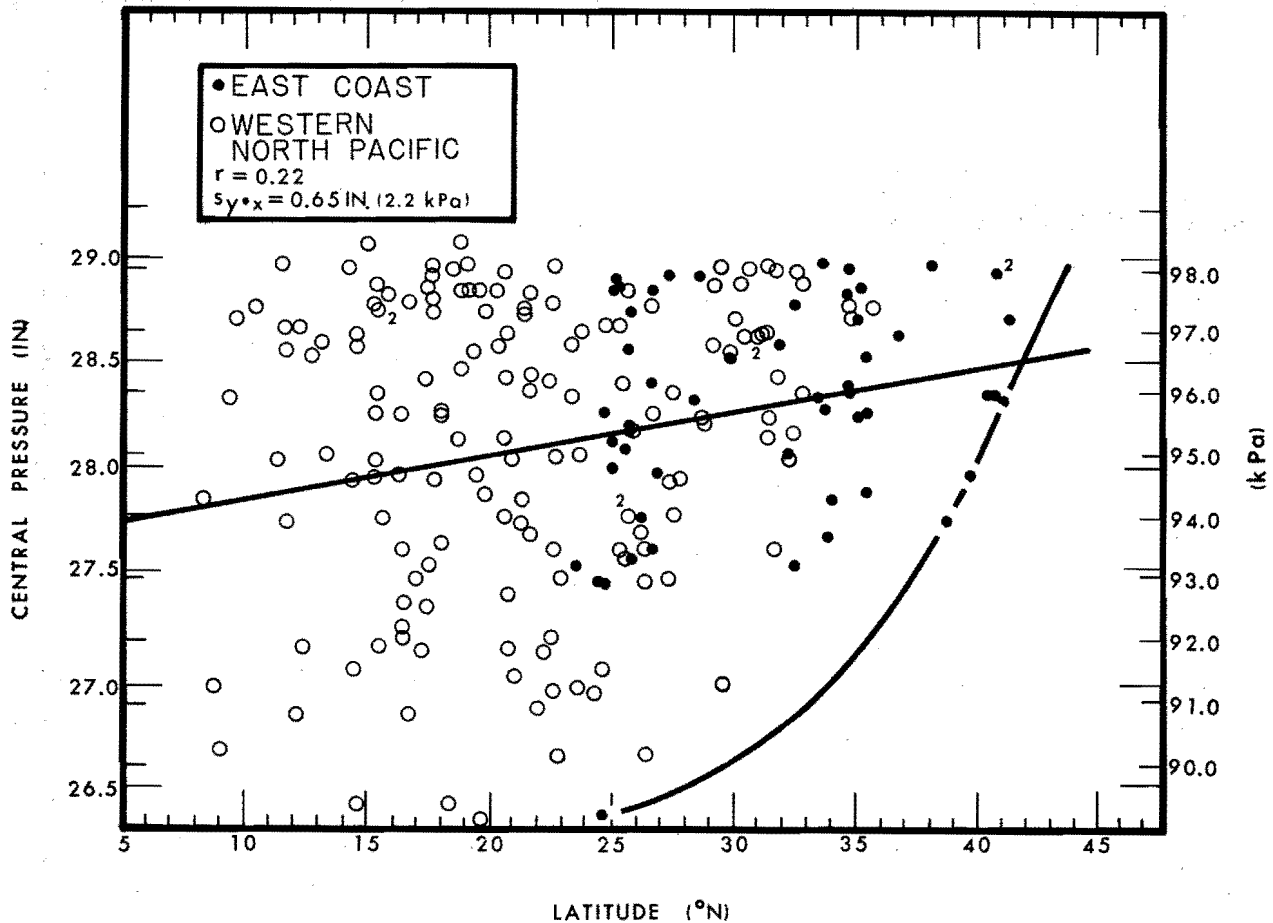
Figure 5.5.--Latitude (ψ) vs. central pressure (p_O)

5.4 MULTIPLE INTERRELATIONS BETWEEN SETS OF PARAMETERS

Multiple correlation coefficients (r'), using the same parameters as in table 5.1, were calculated for east and gulf coast hurricanes, and for typhoon data (table 5.2). In cases where only an ordinary zero-order correlation coefficient is listed for a pair of parameters, e.g., θ vs. T (east coast), additional combinations of parameters did not yield significant increases in r'. For gulf coast hurricanes, the addition of a second parameter failed to yield significant increases in r' for all cases studied. Table VII of Mills (1955) was used to estimate significance. A screening technique selects the second, third, and fourth parameters which give the greatest increase in r' as each is added. A discussion of r' follows.

If Y denotes the regression function of a random variable y with respect to certain other variables x_1, x_2, ..., x_n, then the coefficient of multiple
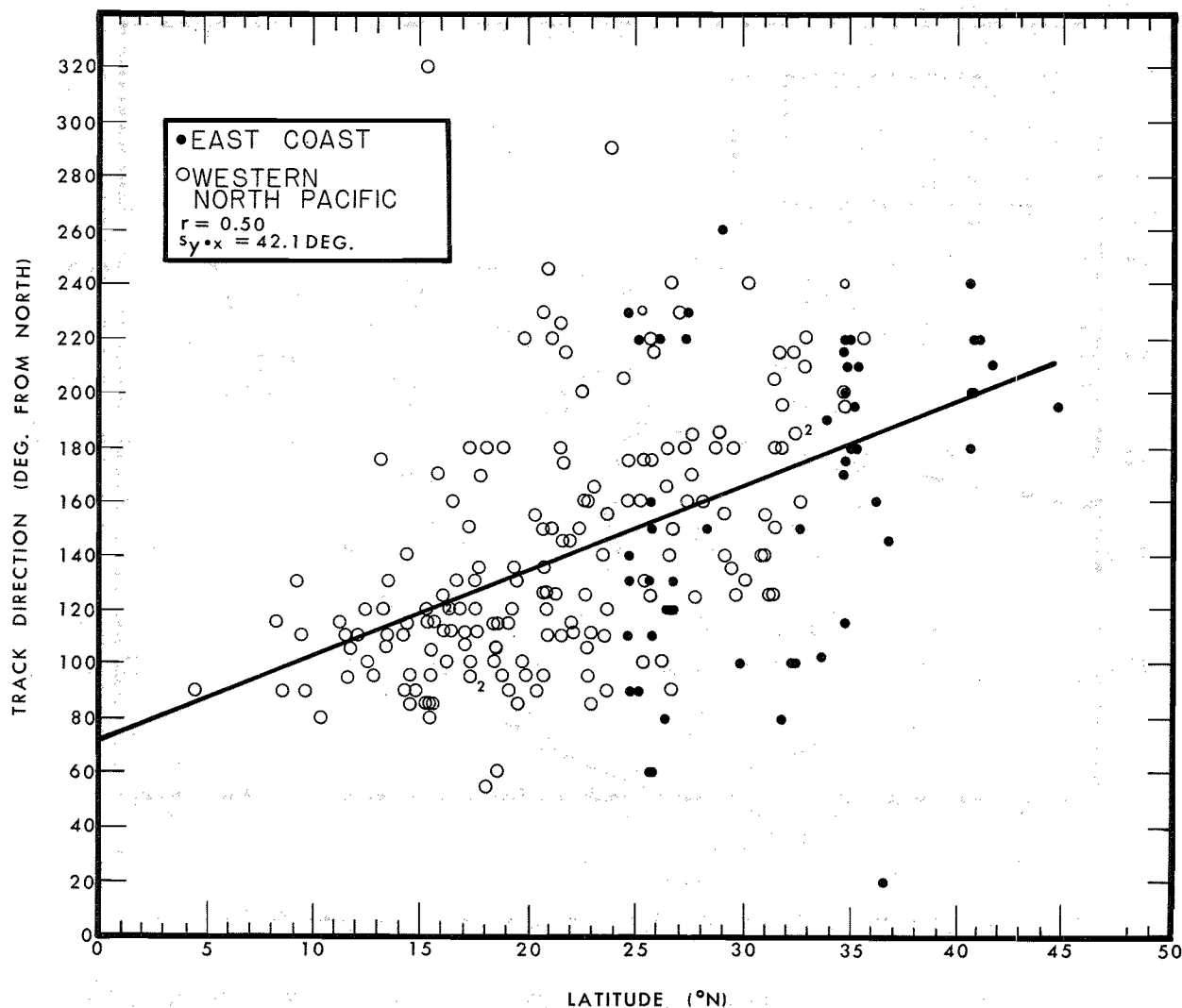
Figure 5.6.--Latitude (ψ) vs. track direction (θ).

correlation (r') between y and the x's is defined as the coefficient of
simple linear correlation (r) between y and Y. However, the constants of the
regression function automatically adjust the algebraic sign, with the result
that the coefficient of correlation (r') between y and Y cannot be negative;
in fact, its value is precisely equal to the ratio of their two standard
deviations, i.e; σ(Y)/σ(y). Therefore, r' ranges from 0 to 1, and the
square of r' is equal to the relative reduction, i.e., the ratio of explained
variance to total variance (Huschke 1959). Table 5.2 lists the coefficient
of multiple correlation (r'), significance tests on r' at the 5 and 1 percent
levels (Mills 1955), the reduction of variance (r'^2) and the standard error of
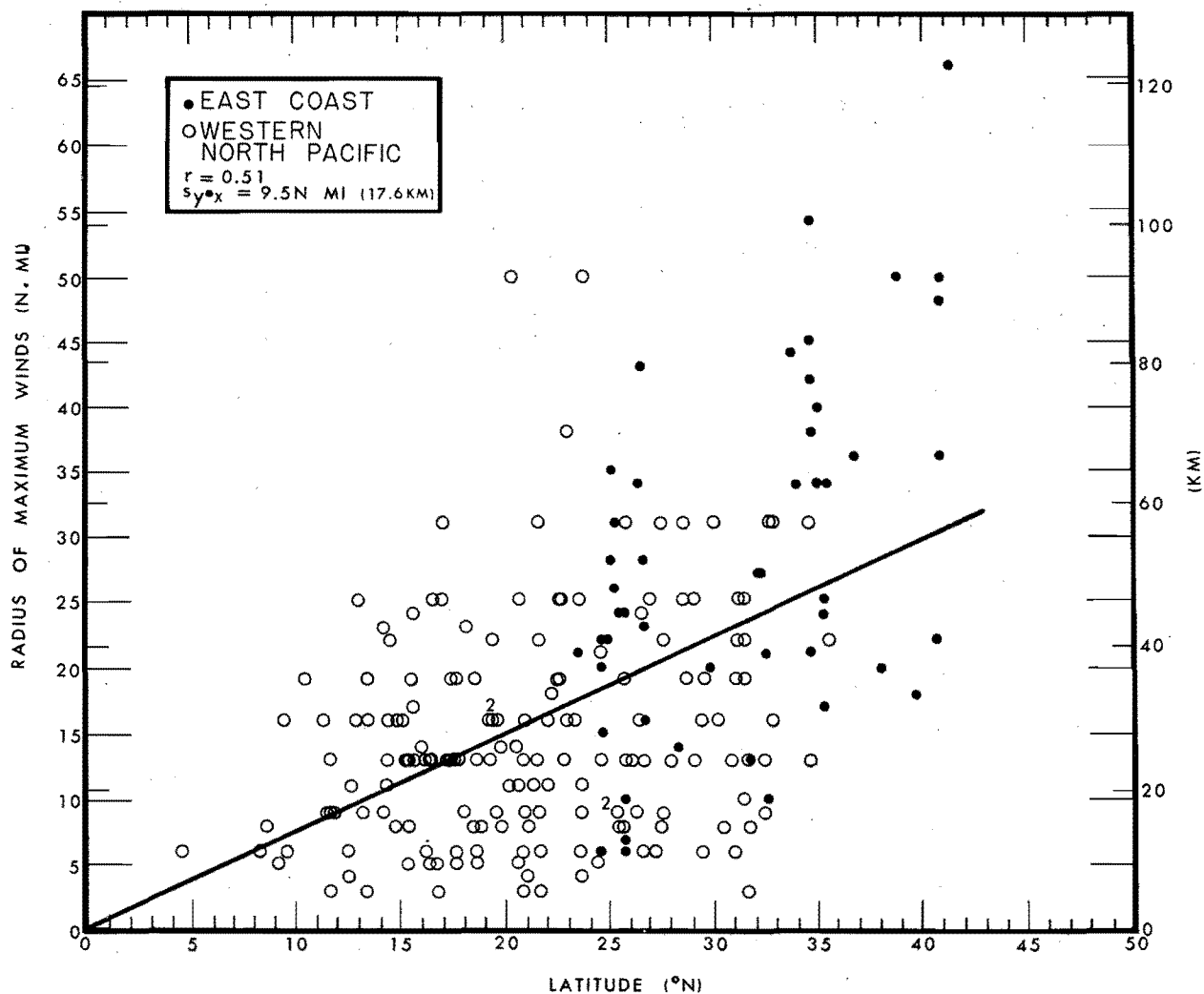estimate $(s_{y.x})$.

Figure 5.7.--Latitude (ψ) vs. radius of maximum winds (R).

The relation between reduction of variance (r'^2), standard deviation (σ), and standard error of estimate $(s_{y \cdot x})$ is given by:

$$r'^2 = 1 - s_{y \cdot x}^2/\sigma^2 = (\sigma^2 - s_{y \cdot x}^2)/\sigma^2 \qquad (5.1)$$

where

r'^2 = reduction in variance

σ = standard deviation, or the positive square root of the variance about the mean of the data.

$s_{y \cdot x}$ = standard deviation about the regression line.

Multiple correlations for the east coast hurricanes are higher than for the other two regions except for those involving θ. The highest $r' = 0.76$ [between ψ and T, p_o] occurs with east coast data.

5.5 SUMMARY

The zero-order linear and multiple correlation coefficients, although often significant at the 1 % level, could not be used directly in developing criteria throughout this report. There are two reasons for this. First, the coefficients are derived from data for all hurricanes and typhoons from our period of record--not just the most extreme ones, which are too few in number to develop meaningful interrelations. Second, though the results are significant they explain only about one quarter of the variance and the standard error of estimates are large in relation to the magnitude of the individual variables.

The interrelations, however, were important guides in setting the along-coast variation of values for the SPH and PMH. Extrapolation beyond the data (especially for the PMH) was based primarily on theory and experience, taking into account trends shown in extrapolation of the data.

Meteorological parameters for western North Pacific typhoons blend in well with those of the east and gulf coast hurricanes for the common latitude span ($25°$ to $35°N$) in many of the interrelations shown (figs. 5.5, 5.6, and 5.7, for example). Some typhoon data fall out of the general limits of the hurricane data (fig. 5.1, for example). This is due to latitudinal and possibly other effects. Values of the typhoon parameters are less reliable than those of the hurricanes because of approximations, less detailed analyses, and fewer observations, particularly in earlier years. In general, however, the typhoon data support trends shown by the hurricane data; it is most helpful in supplementing data sparse areas on the plotted diagrams (for example, lower p_o and smaller R on fig. 5.1).

6. Pressure Profile Formula

6.1 Introduction

We are interested in determining SPH and PMH wind field criteria along the coast from Texas to the Canadian border. In our approach, the hurricane wind field is related to the variations in the pressure field. Therefore, the profile of pressure through the storm must be a very good approximation to observed hurricane pressure profiles. A sea-level pressure profile was derived in Hydrometeorological Report No. 31 (Schloemer 1954), hereafter referred to as HMR 31. This formula has been used extensively in many hurricane studies. Henceforth, we will refer to it as the Hydromet formula or H. Our objective is to test H and other formulas against data from recent hurricanes.

6.2 Development and Early Use of the Hydromet Formula

The Hydromet formula (H) is: $\dfrac{p - p_o}{p_w - p_o} = e^{-R/r}$, (6.1)

where p is the sea-level pressure at distance r from the hurricane center. In the development of H, $\dfrac{p - p_o}{p_w - p_o}$ was plotted against distance from the hurricane center using observed pressure values from each of nine Florida hurricanes. When the data were replotted on a semilog scale with the origin at $\dfrac{p - p_o}{p_w - p_o} = 1$, the curves (fig. 6.1) suggested a family of rectangular hyperbolas which have the general formula, $xy = k$. Substituting directly, Schloemer

obtained $r \ln \dfrac{p_w - p_o}{p - p_o} = k$, where $y = r =$ distance from the center of the hurricane and $x = \ln \dfrac{p_w - p_o}{p - p_o}$.

The distance from the hurricane center to the maximum winds (R) is important to the determination of these maximum winds. Schloemer assumed k would be some function of R. He examined the general relation $k = k_1 R^i$.
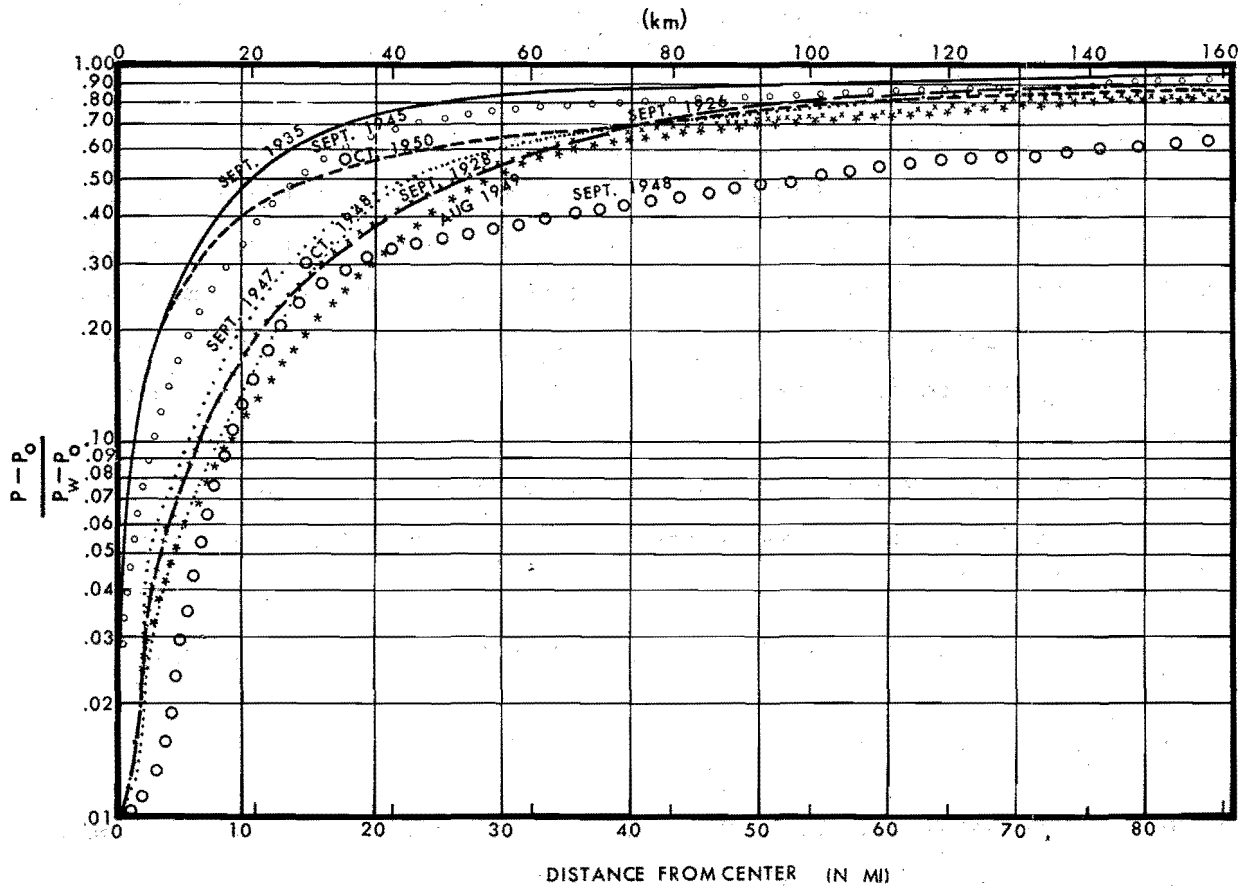
Figure 6.1.--Smoothed pressure profiles of Florida hurricanes using observed pressure values (after Schloemer 1954).

Here, the restricted hurricane sample became a severe limitation. Examination of the data indicated no consistent value for k_1 and i. The values from his storm sample did not differ greatly from unity. The use of unity did not introduce appreciable error in hurricane wind computations. Replacing k by R and taking antilogarithms results in H (eq. 6.1). Schloemer believed that H was a reasonable representation of the sea-level pressure profile of a hurricane out to a distance of about 87 n.mi. (161 km).

Myers (1954) used H to obtain sea-level pressure profiles for east and gulf coast hurricanes that occurred between 1900-50. At the time of that study R, p_o, and p_w for most of the hurricanes were not known. Myers did not check the validity of H.

6.3 Pressure Profile Formulas Tested and Data Sample

HMR 31 gives a list of general formulas for replicating storm sea-level pressure profiles. The first seven formulas in table 6.1 are identical to those in HMR 31 if the values of i and j of that report are set equal to one. The last two formulas (I and II) in table 6.1 were developed for this study.

We selected 19* of the more intense hurricanes during the period 1950-74 for testing against sea-level pressure profiles computed from the formulas in table 6.1. Some major hurricanes, such as Betsy (1965), were not tested since complete data were not available. We tested only hurricanes whose p_o's and R's could be determined from observations by reliable meteorological instruments. Table 6.2 chronologically lists by coast these hurricanes and their pertinent data. No attempt should be made to compare the revised data for King (1950) in table 6.2 to the pressure profile for the October 1950 hurricane in figure 6.1. The storms are one and the same, but the eye-fitted visual profile for King in this report was analyzed using information unavailable to Schloemer (1954). Figure 6.2 shows a data plot for Camille (1969) and an eye-fitted visual profile to the data. Also shown are computed profiles using H, formula I and formula II.

6.4 Comparison of Eye-Fitted Hurricane Pressure Profiles with Pressure Profiles from Formulas

6.4.1 In General

A comparison of computations using the first seven formulas of table 6.1 (from HMR 31) with storm profiles showed they do not replicate observed events as well as H. The computed profiles would either shoot up too rapidly toward $\frac{p - p_o}{p_w - p_o} = 1$ with distance away from the storm center or flatten out much too rapidly toward $\frac{p - p_o}{p_w - p_o} = 0$ with short distances near the storm center. Initial computations with formulas I and II showed they gave more realistic sea-level pressure profiles than the other seven formulas tested.

---

*Although 19 hurricanes were selected, there were 22 profiles because Daisy (1958) was tested off North Carolina and Massachusetts and Donna (1960) was tested off Florida, North Carolina, and New York.

Table 6.1.--Pressure profile formulas tested in addition to the Hydromet formula

$$\frac{p - p_o}{p_w - p_o} = 1 - e^{-Rr}$$

$$\frac{p - p_o}{p_w - p_o} = \frac{1}{1 + \frac{1}{Rr}}$$

$$\frac{p - p_o}{p_w - p_o} = \frac{2}{\pi} \left(\arctan \frac{1}{Rr} \right)$$

$$\frac{p - p_o}{p_w - p_o} = \frac{2}{\pi} \left(\operatorname{arccot} \frac{-1}{Rr} \right)$$

$$\frac{p - p_o}{p_w - p_o} = \frac{2}{\pi} \left[\operatorname{arcsec} (1 + Rr) \right]$$

$$\frac{p - p_o}{p_w - p_o} = \frac{2}{\pi} \left[\operatorname{arccsc} \left(1 + \frac{1}{Rr} \right) \right]$$

$$\frac{p - p_o}{p_w - p_o} = \tanh Rr$$

I: $\dfrac{p - p_o}{p_w - p_o} = C \, (\arctan r/R)$, C is a constant

II: $\dfrac{p - p_o}{p_w - p_o} = C \left[\operatorname{arccsc} \left(1 + \frac{R}{r} \right) \right]$, C is a constant

Note: $p_w \overset{\sim}{=} p_n$ (see chapter 7)

R = n from HMR 31, table 2 (Schloemer 1954)

Numerous computations were made using different values of the constant of proportionality, C, in formulas I and II (table 6.1). Of course, in "fitting" a particular storm, a certain C value is best. Suitable values of C range from 0.50 to 0.65. The rounded average (0.6) from the above fittings was used in I and II for the pressure profile comparison in this study.

Table 6.2--Comparison of storm and three pressure profile formulas

Storm	Year	P_w (in)	P_o* (in.)	R (n.mi.)	Storm profile P_{40} (in.)	P_{80} (in.)	Hydromet Formula(eq. 6.1) P_{40} (in.)	P_{80} (in.)	Formula I** P_{40} (in.)	P_{80} (in.)	Formula II*** P_{40} (in.)	P_{80} (in.)	#	P_{s40} $-P_{H40}$ (in.)	P_{s40} $-P_{I40}$ (in.)	P_{s40} $-P_{II40}$ (in.)	P_{s80} $-P_{H80}$ (in.)	P_{s80} $-P_{I80}$ (in.)	P_{s80} $-P_{II80}$ (in.)
East Coast																			
King	1950	29.94	28.20	6	29.42	29.57	29.70	29.81	29.68	29.76	29.30	29.44	A	-.28	-.26	+.12	-.24	-.19	+.13
Daisy (NC)	1958	29.97	28.26	25	--	29.59	--	29.51	--	29.56	--	29.15	A	--	--	--	+.08	+.03	+.44
Daisy (NE)	1958	29.94	28.91	50	--	29.67	--	29.46	--	29.54	--	29.32	B	--	--	--	+.21	+.13	+.35
Gracie	1959	30.00	28.08	10	29.24	29.55	29.57	29.77	29.61	29.75	29.15	29.34	A	-.33	-.37	+.09	-.22	-.20	+.21
Donna (FL)	1960	29.88	27.55	20	28.99	29.47	28.96	29.37	29.10	29.40	28.57	28.85	A	+.03	-.11	+.42	+.10	+.07	+.62
Donna (NC)	1960	29.88	28.29	34	28.91	29.25	28.97	29.33	29.12	29.41	28.83	29.03	A	-.06	-.21	+.08	-.08	-.16	+.22
Donna (NE)	1960	29.83	28.38	48	28.66	28.99	28.82	29.18	28.99	29.28	28.80	28.97	B	-.16	-.33	-.14	-.19	-.29	+.02
Cleo	1964	29.88	28.57	7	29.64	29.77	29.71	29.77	29.67	29.74	29.37	29.49	B	-.03	-.03	+.27	0	+.03	+.28
Dora	1964	29.91	28.52	20	29.10	29.47	29.38	29.60	29.44	29.63	29.13	29.29	B	-.26	-.34	-.03	-.13	-.16	+.18
Gulf coast																			
Easy	1950	29.80	28.30	15	29.40	29.56	29.33	29.54	29.39	29.55	29.03	29.20	A	+.07	+.01	+.37	+.02	+.01	+.36
Flossy	1956	29.91	28.80	22	--	29.61	--	29.64	--	29.67	--	29.40	B	--	--	--	-.03	-.06	+.21
Ethel	1960	29.97	28.98	18	29.62	29.81	29.61	29.77	29.66	29.78	29.43	29.55	B	+.01	-.04	+.19	+.04	+.03	+.26
Carla	1961	29.77	27.49	30	28.59	29.08	28.57	29.06	28.76	29.15	28.32	28.60	A	+.02	-.17	+.27	+.02	-.07	+.48
Isbell	1964	29.91	28.47	10	29.59	29.71	29.59	29.74	29.62	29.72	29.27	29.42	B	0	-.03	+.32	-.03	-.01	+.29
Alma	1966	29.97	28.65	23	29.34	29.59	29.39	29.64	29.48	29.67	29.19	29.35	B	-.05	-.14	+.15	-.05	-.08	+.24
Beulah	1967	29.80	27.85	25	28.82	29.33	28.89	29.28	29.03	29.33	28.63	28.86	A	-.07	-.21	+.19	+.05	0	+.47
Camille	1969	29.77	26.81	8	29.15	29.48	29.23	29.49	29.25	29.42	28.56	28.84	A	-.08	-.10	+.59	-.01	+ 06	+.64
Celia	1970	29.83	27.89	9	29.50	29.74	29.44	29.62	29.46	29.59	29.00	29.19	A	+.06	+.04	+.50	+.12	+.15	+.55
Fern	1971	29.77	28.91	26	29.41	29.58	29.36	29.53	29.42	29.56	29.25	29.35	B	+.05	-.01	+.16	+.05	+.02	+.23
Edith	1971	29.80	28.88	27	29.50	29.70	29.35	29.54	29.42	29.57	29.23	29.35	B	+.15	+.08	+.27	+.16	+.13	+.35
Agnes	1972	29.83	28.88	20	29.26	29.41	29.46	29.62	29.51	29.64	29.30	29.41	B	-.20	-.25	-.04	-.21	-.23	0
Carmen	1974	29.91	28.11	10	29.39	29.59	29.51	29.70	29.55	29.68	29.11	29.29	A	-.12	-.16	+.28	-.11	-.09	+.30

*Pressure obtained at the coast - used in developing pressure profiles. In some cases it differs from p_o in tables 4.1 - 4.4.

**Formula I: $\dfrac{p-p_o}{p_w-p_o} = .6 \left(\arctan \dfrac{r}{R}\right)$

***Formula II: $\dfrac{p-p_o}{p_w-p_o} = .6 \left[\text{arccsc} \left(1 + \dfrac{R}{r}\right)\right]$

#A: $p_o \leq 28.30$ in. (95.8 kPa) [see table 6.3]

#B: $p_o > 28.30$ in. (95.8 kPa) [see table 6.3]

1 standard inch of Hg = 3.386 kPa

p_s40: storm pressure at a distance of 40 n.mi. (74 km) from the hurricane center; p_{H40}: storm pressure computed from the Hydromet formula at a distance of 40 n.mi. (74 km) from the hurricane center.
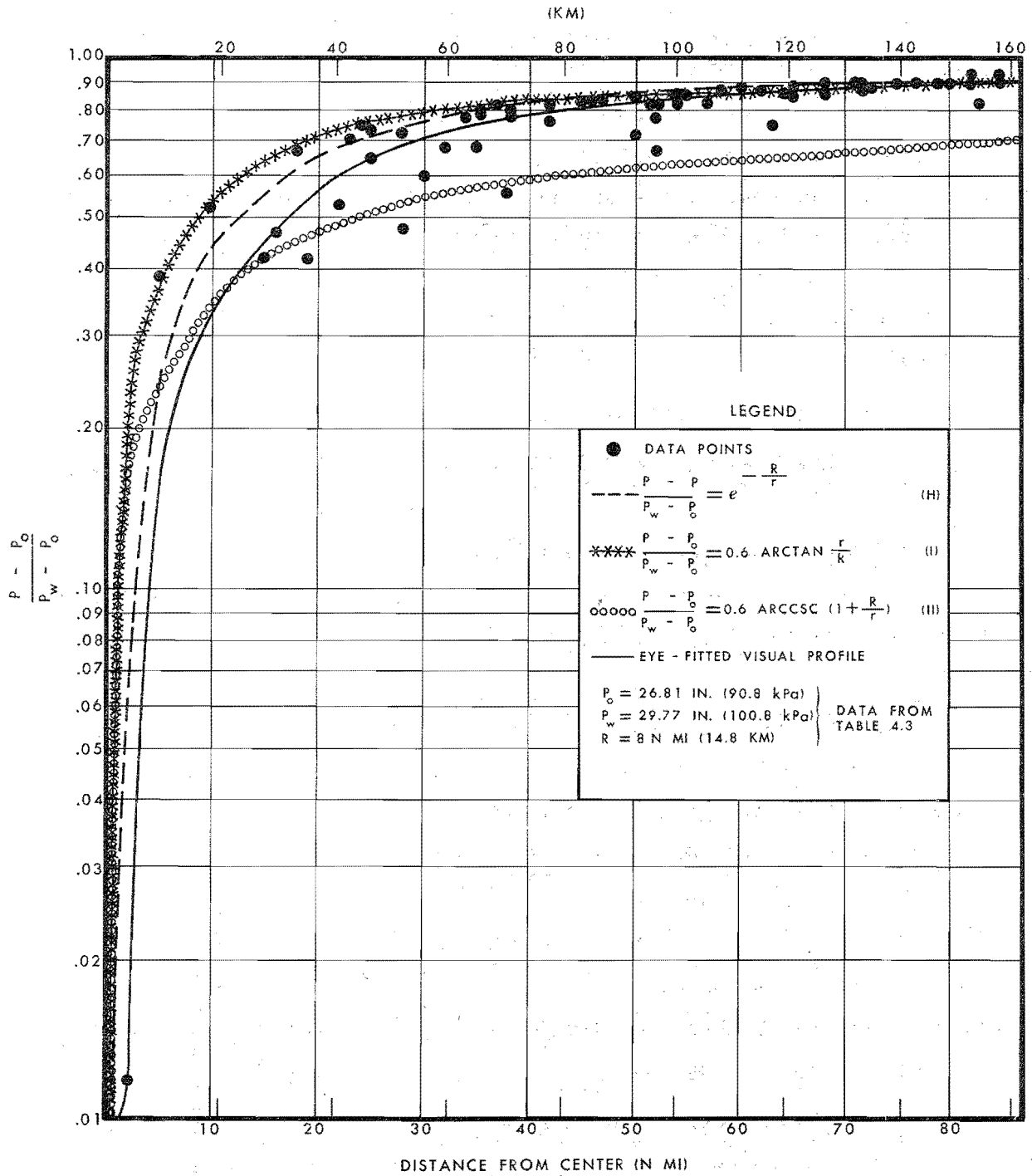
Figure 6.2.--Eye-fitted and computed pressure profiles, Camille 1969.

Figure 6.2 shows that H is a closer fit to the visual profile than I or II for hurricane Camille (1969). A different constant of proportionality in I would result in a better fit to the visual profile for Camille. However, C = 0.6, proved to be about the best overall fit for all the tested storms and was used in the comparisons of the three pressure profiles (table 6.2).

A close study of figure 6.2 tells us the formula I curve rises more rapidly than the Hydromet formula, formula II, or the visual profile. This is a characteristic of the formula I pressure profile evident in all hurricanes studied.

6.4.2 AT 40 AND 80 NAUTICAL MILES (74 AND 148 KILOMETERS)

Pressures for distances of 40 and 80 n.mi. (74 and 148 km) from the storm center were taken from the "eye fit" hurricane sea-level pressure profiles and from computed formula pressure profiles. Farther out, the profiles tend to converge toward 1. Closer than 40 n.mi. (74 km) to the storm center, the storm data tend to become sparse for some storms, leading to less reliable comparisons.

Table 6.2 shows these sea-level pressures for the eye-fitted storm profiles and the profiles for H, I, and II, in that order. We then give the differences in pressure $(p_{s40} - p_{H40})$, etc. p_{s40} is the storm pressure at a distance of 40 n.mi. (74 km). p_{H40} is the pressure computed from H at the same distance. p_{I40}, p_{II40}, p_{s80}, p_{H80}, p_{I80}, and p_{II80} are similarly defined. A plus difference means the storm profile pressure is greater.

Table 6.3 summarizes the differences in sea-level pressures at the two distances. Hurricanes have been divided into two categories; those with central pressure $(p_o \leq 28.30$ in. (95.8 kPa), Category A; those with p_o >28.30 in. (95.8 kPa), Category B. Beneath the sum of positive and negative differences are the number of profiles. There are only 19 profiles for the 40 n.mi. distance since data this close to the eye were not sufficient to define profiles for three hurricanes.

Formula II is definitely biased toward giving lower pressures at both 40 and 80 n.mi. (74 and 148 km) for both storm categories. Therefore, it is not suitable for use as the pressure profile formula for this report.

Table 6.3.—Summary of differences in pressure for formulas H, I and II for two categories of central pressure.

	Pressure from storm profiles minus pressure from computed pressure profiles (in.)		
At a distance of 40 n.mi. (74 km) (19 profiles)	H*	I**	II***
Category A			
$P_o \leq$ 28.30 in. (95.8 kPa) (10 profiles)			
Sum of positive diff.	.18	.05	2.91
No. of profiles	4	2	10
Sum of negative diff.	.94	1.59	0
No. of profiles	6	8	0
No. of profiles with no diff.	0	0	0
Category B			
$P_o >$ 28.30 in. (95.8 kPa) (9 profiles)			
Sum of positive diff.	.21	.08	1.36
No. of profiles	3	1	6
Sum of negative diff.	.70	1.17	.21
No. of profiles	5	8	3
No. of profiles with no diff.	1	0	0
At a distance of 80 n.mi. (148 km) (22 profiles)			
Category A			
$P_o \leq$ 28.30 in. (95.8 kPa) (11 profiles)			
Sum of positive diff.	.39	.32	4.42
No. of profiles	6	5	11
Sum of negative diff.	.66	.71	0
No. of profiles	5	5	0
No. of profiles with no diff.	0	1	0
Category B			
$P_o >$ 28.30 in. (95.8 kPa) (11 profiles)			
Sum of positive diff.	.46	.34	2.41
No. of profiles	4	5	10
Sum of negative diff.	.64	.83	0
No. of profiles	6	6	0
No. of profiles with no diff.	1	0	1

* Hydromet pressure profile formula (eq. 6.1)

** $\dfrac{p - P_o}{p_w - P_o} = .6 \arctan \dfrac{r}{R}$ 1 standard inch of Hg = 3.386 kPa

*** $\dfrac{p - P_o}{p_w - P_o} = .6 \; \text{arccsc} \left(1 + \dfrac{R}{r}\right)$

Differences between formulas H and I are very small. H is a slightly better overall fit at 40 and 80 n.mi. (74 and 148 km), particularly for the stronger category A hurricanes.

6.4.3 FOR FIVE INTENSE HURRICANES

We selected the most intense hurricanes from table 6.2 [p_o <27.90 in. (94.5 kPa)] for special attention. Data from table 6.2 for these five hurricanes [Donna (Fla.), 1960; Carla, 1961; Beulah, 1967; Camille, 1969; and Celia, 1970] are summarized in table 6.4.

Table 6.4.--Summary of pressure differences from table 6.2 for formulas H and I for five intense hurricanes (p_o <27.90 in., 94.5 kPa)

	40 n.mi. (74 km) Storm pressure minus computed pressure		80 n.mi. (148 km) Storm pressure minus computed pressure	
	H	I	H	I
Σ + diff. in. (kPa)	0.11 (0.4)	0.04 (0.1)	0.29 (1.0)	0.28 (0.9)
No. of storms	3	1	4	3
Σ - diff. in. (kPa)	-0.15 (-0.5)	-0.59 (-2.0)	-0.01 (-0.0)	-0.07 (-0.2)
No. of storms	2	4	1	1
No difference	0	0	0	1

Results using the five most intense hurricanes (p_o <27.90 in., 94.5 kPa) in table 6.2 again show only slight differences between formulas H and I with H being a better overall fit at 40 and 80 n.mi. (74 and 148 km).

6.4.4 HURRICANE CAMILLE

Data from table 6.2 indicates that the Hydromet formula provides a better fit to the storm profile than formula I for extremely intense hurricane Camille (1969).

6.5 CONCLUSIONS

Based upon comparisons in section 6.4, we conclude that the Hydromet formula gives a reasonably representative sea-level pressure profile of a hurricane and is therefore the best means of determining the maximum gradient wind speed (see chapter 12) for the SPH and PMH. The reasons supporting this argument are as follows:

a) Only formula I from table 6.1 replicates observed hurricane events with any degree of precision.

b) For east and gulf coast hurricanes (1950-74) the Hydromet formula is a better overall fit than formula I for the entire storm sample of table 6.2, the five most intense hurricanes considered together, and hurricane Camille (1969).

c) The formula I pressure profile, when fitted to p_o, rises too rapidly within a few miles of the pressure centers of hurricanes we studied. The Hydromet formula shows a more realistic gradual change in pressure in this short distance from p_o.

d) The Hydromet formula has been used extensively in earlier studies. To justify a change, we would need to show significant improvement. We have not been able to do this.

Can H be improved upon? As indicated by Schloemer in HMR 31, there may be a constant multiplier and an exponent of R other than unity. The problem is a reliable determination of other values for identifying these constants.* The results would be only as good as the pressure data and the tracks of the hurricanes. A refinement of the formula by employing two other constants might make it a better fit for the hurricane sample, but less applicable to the hurricane population. More than one set of constants varying with hurricane intensity or some other parameter might be the ultimate solution. We believe that such refinements would not improve the reliability of H at this time because of the rather large scatter of pressure data around most hurricane profiles (fig. 6.2).

*See the work of Graham and Hudson (1960, pp. 89-90) for a discussion of fitting an exponential constant to develop a modified exponential equation for hurricane Hazel (1954).

7. PERIPHERAL PRESSURE

7.1 INTRODUCTION

Peripheral pressure (p_w) is the sea-level pressure at the outer limits of the hurricane circulation. It is used to compute pressure drop (peripheral pressure minus central pressure), which is related to wind speed; see chapter 12.

Prior to this report, the most complete listing of hurricane peripheral pressure (p_{nx}) data was in *National Hurricane Research Project* Report No. 5 (NHRP 5), table 3-1(U.S. Weather Bureau 1957). p_{nx} data are mostly values of asymptotic pressure (p_n) and a few values read from weather maps (p_w). p_n is that value to which an exponential pressure profile defined by the Hydromet pressure profile formula is asymptotic.

In NHRP 33 (Graham and Nunn 1959), a fixed peripheral pressure of 29.92 in. (101.3 kPa) was used to compute SPH winds. This is standard sea-level pressure and also an average of peripheral pressure for storms listed in NHRP 5.

In HUR 7-97 (U.S. Weather Bureau 1968), peripheral pressure criteria are related to latitude by a curve that envelops the peripheral pressure (given in NHRP 5) of hurricanes within gulf and east coast zones. The highest peripheral pressure, used at 25°N, is that required to produce the maximum cyclostrophic wind for a central pressure of 26.00 in. (88.0 kPa) [see fig. 22, of NHRP 33]. The variation with latitude is based mainly on the p_n's of record hurricanes.

In HUR 7-120 (National Weather Service 1972), peripheral pressure is also related to latitude by an eye-fitted, least-error average curve through peripheral pressures for record hurricanes of table 3-1 of NHRP 5.

These studies have used several techniques for evaluating peripheral pressure. In this chapter we will describe what we believe is the best approach.

7.2 METHODS OF DETERMINING PERIPHERAL PRESSURE

p_w is frequently considered as the average pressure around the hurricane where the isobars change from cyclonic to anticyclonic curvature. This pressure occurs at a distance from the storm center near where storm inflow

begins and, therefore, has physical meaning. In this study, p_w was determined at four equally spaced points around the storm center (north, east, south, and west). Values of p_w were rounded off to the nearest 0.03 in. (0.1 kPa).

Another method of obtaining weather map peripheral pressure uses the value of the last closed isobar. This value is designated by p_{wi}. p_{wi}'s were also determined to the nearest 0.03 in. (0.01 kPa).

Table 7.1 lists values of p_w and p_{wi} for gulf and east coast hurricanes. These values of p_w are the same as those listed in tables 4.1-4.4. All the values are at or near the time of lowest p_o within 150 n.mi. (278 km) of the coast. Also shown in table 7.1 are values of p_{nx} given in NHRP 5, which are mostly p_n's except for a few p_w's where the p_n was not available.

7.3 COMPARISON OF P_W AND P_{WI} WITH P_{NX}

We wish to use either p_w or p_{wi} and not p_{nx} because peripheral pressure from weather maps is not based on how well the Hydromet pressure profile formula fits an individual storm profile of record. Before eliminating p_{nx}, however, we would like to compare p_w and p_{wi} to p_{nx}. We stated earlier that the average of peripheral pressures (p_{nx}) for storms listed in NHRP 5 is 29.92 in. (101.3 kPa). The average of p_w for all hurricanes in table 7.1 is 29.90 in. (101.3 kPa) and the average of p_{wi} for all hurricanes is 29.79 in. (100.9 kPa). p_w is comparable to p_{nx} while p_{wi} is somewhat lower.

7.4 INTERRELATIONS AMONG P_W, P_{WI}, LATITUDE AND P_O

We have chosen to determine which peripheral pressure is best suited for this study by evaluating the interrelations, if any, between the peripheral pressure, latitude, and central pressure.

7.4.1 PLOTS CONTAINING P_W

A plot of ψ vs p_w for east coast hurricanes is shown in figure 7.1. p_w is plotted at the latitude for the location of p_o (tables 4.1-4.2). The storms have been stratified into three groups. The 19 with central pressure (p_o) ≤ 28.17 in. (95.4 kPa) are circled. The 17 with $p_o \geq 28.64$ in. (97.0 kPa) are boxed. There are 18 remaining storms with p_o between 28.18 and 28.63 in. (95.4 and 97.0 kPa).

Table 7.1.--Comparison of three peripheral pressures for gulf and east coast hurricanes, 1900-75.

G U L F   C O A S T   H U R R I C A N E S

Month	Date	Year	Name	P_w (in.)	P_{wi} (in.)	P_w-P_{wi} (in.)	P_{nx} (in.)	P_w (kPa)	P_{wi} (kPa)	P_w-P_{wi} (kPa)	P_{nx} (kPa)
Sept.	9	1900		29.88	29.74	0.14	29.78	101.2	100.7	0.5	100.8
Aug.	15	1901		29.91	29.83	0.08	30.16	101.3	101.0	0.3	102.1
June	17	1906		29.91	29.83	0.08	29.98	101.3	101.0	0.3	101.5
Sept.	27	1906		29.91	29.77	0.14	30.07	101.3	100.8	0.5	101.8
Oct.	18	1906		29.83	29.74	0.09	29.80	101.0	100.7	0.3	100.9
July	21	1909		29.97	29.85	0.12	30.27	101.5	101.1	0.4	102.5
Sept.	20	1909		29.88	29.85	0.03	30.30	101.2	101.1	0.1	102.6
Oct.	11	1909 by		29.80	29.77	0.03	30.07	100.9	100.8	0.1	101.8
Oct.	18	1910		29.77	29.71	0.06	29.77	100.8	100.6	0.2	100.8
Aug.	17	1915		29.88	29.77	0.11	29.57	101.2	100.8	0.4	100.1
Sept.	29	1915		29.80	29.74	0.06	30.14	100.9	100.7	0.2	102.1
July	5	1916		29.86	29.74	0.12	30.03	101.1	100.7	0.4	101.7
Aug.	18	1916		29.94	29.83	0.11	30.77	101.4	101.0	0.4	104.2
Oct.	18	1916		29.88	29.85	0.03	30.20	101.2	101.1	0.1	102.3
Sept.	29	1917		29.97	29.88	0.09	29.88	101.5	101.2	0.3	101.2
Sept.	10	1919 by		29.88	29.77	0.11	29.73	101.2	100.8	0.4	100.7
§Sept.	14	1919		29.88	29.74	0.14		101.2	100.7	0.5	
Sept.	21	1920		29.91	29.85	0.06	29.90	101.3	101.1	0.2	101.3
June	22	1921		29.94	29.83	0.11	30.03	101.4	101.0	0.4	101.7
Oct.	25	1921		29.83	29.71	0.12	29.59	101.0	100.6	0.4	100.2
Oct.	21	1924		29.88	29.77	0.11	29.62	101.2	100.8	0.4	100.3
Aug.	26	1926		29.97	29.88	0.09	30.35	101.5	101.2	0.3	102.8
Sept.	20	1926		29.94	29.77	0.17	30.13	101.4	100.8	0.6	102.0
Oct.	21	1926 by		29.77	29.68	0.09	29.97	100.8	100.5	0.3	101.5
Sept.	17	1928		29.88	29.74	0.14	30.38	101.2	100.7	0.5	102.9
June	28	1929		29.80	29.71	0.09	29.97	100.9	100.6	0.3	101.5
Sept.	30	1929		29.91	29.83	0.08	29.96	101.3	101.0	0.3	101.5
Aug.	14	1932		29.91	29.83	0.08	30.11	101.3	101.0	0.3	102.0
Aug.	5	1933		29.91	29.80	0.11	29.96	101.3	100.9	0.4	101.5
Sept.	4	1933		29.88	29.74	0.14	29.98	101.2	100.7	0.5	101.5
Sept.	5	1933		29.88	29.71	0.17	30.24	101.2	100.6	0.6	102.4
June	16	1934		29.71	29.59	0.12	29.94	100.6	100.2	0.4	101.4
Sept.	3	1935		29.94	29.83	0.11	29.92	101.4	101.0	0.4	101.3
Nov.	5	1935 ex		30.00	29.83	0.17		101.6	101.0	0.6	
July	31	1936		30.00	29.85	0.15	30.00	101.6	101.1	0.5	101.6
Aug.	8	1940		29.94	29.85	0.09	29.75	101.4	101.1	0.3	100.7
Sept.	23	1941		29.86	29.71	0.15	29.66	101.1	100.6	0.5	100.4
Oct.	7	1941		30.00	29.97	0.03	30.19	101.6	101.5	0.1	102.2
Aug.	30	1942		29.83	29.71	0.12	29.64	101.0	100.6	0.4.	100.4
July	27	1943		29.94	29.85	0.09	30.02	101.4	101.1	0.3	101.7
Oct.	19	1944		29.88	29.77	0.11	29.67	101.2	100.8	0.4	100.5
Aug.	27	1945		29.83	29.68	0.15	30.13	101.0	100.5	0.5	102.0
Sept.	15	1945		29.94	29.80	0.14	30.00	101.4	100.9	0.5	101.6
Sept.	18	1947 ex		30.00	29.88	0.12	29.83	101.6	101.2	0.4	101.0
§Sept.	19	1947		29.94	29.83	0.11	29.70	101.4	101.0	0.4	100.6
Sept.	21	1948		29.83	29.74	0.09	29.61	101.0	100.7	0.3	100.3
Oct.	5	1948		29.83	29.77	0.06	29.77	101.0	100.8	0.2	100.8
Aug.	27	1949		29.97	29.85	0.12	30.12	101.5	101.1	0.4	102.0
Oct.	4	1949		29.88	29.74	0.14	30.13	101.2	100.7	0.5	102.0
Aug.	31	1950	Baker	29.65	29.53	0.12	29.71	100.4	100.0	0.4	100.6
Sept.	5	1950	Easy	29.80	29.71	0.09		100.9	100.6	0.3	
Oct.	18	1950	King	29.94	29.77	0.17		101.4	100.8	0.6	
Sept.	24	1956	Flossy	29.91	29.77	0.14		101.3	100.8	0.5	
June	27	1957	Audrey	29.74	29.62	0.12		100.7	100.3	0.4	
Sept.	10	1960	Donna	29.88	29.77	0.11		101.2	100.8	0.4	
Sept.	15	1960	Ethel	29.97	29.88	0.09		101.5	101.2	0.3	

Table 7.1.--Comparison of three peripheral pressures for gulf and east coast hurricanes, 1900-75, continued.

GULF COAST HURRICANES

Month	Date	Year	Name	P_w (in.)	P_{wi} (in.)	P_w-P_{wi} (in.)	P_{nx} (in.)	P_w (kPa)	P_{wi} (kPa)	P_w-P_{wi} (kPa)	P_{nx} (kPa)
Sept.	11	1961	Carla	29.77	29.65	0.12		100.8	100.4	0.4	
Oct.	4	1964	Hilda	29.97	29.83	0.14		101.5	101.0	0.5	
Oct.	14	1964	Isbell	29.91	29.77	0.14		101.3	100.8	0.5	
Sept.	8	1965	Betsy	29.91	29.80	0.11		101.3	100.9	0.4	
§Sept.	10	1965	Betsy	29.86	29.77	0.09		101.1	100.8	0.3	
June	9	1966	Alma	29.97	29.88	0.09		101.5	101.2	0.3	
Oct.	4	1966 by	Inez	29.91	29.80	0.11		101.3	100.9	0.4	
Sept.	20	1967	Beulah	29.80	29.65	0.15		100.9	100.4	0.5	
Oct.	19	1968	Gladys	29.86	29.77	0.09		101.1	100.8	0.3	
Aug.	18	1969	Camille	29.77	29.65	0.12		100.8	100.4	0.4	
Aug.	3	1970	Celia	29.83	29.77	0.08		101.0	100.8	0.2	
Sept.	12	1970	Ella	29.77	29.65	0.12		100.8	100.4	0.4	
Sept.	10	1971	Fern	29.77	29.68	0.09		100.8	100.5	0.3	
Sept.	16	1971	Edith	29.80	29.71	0.09		100.9	100.6	0.3	
June	19	1972	Agnes	29.83	29.68	0.15		101.0	100.5	0.5	
Sept.	8	1974	Carmen	29.91	29.80	0.11		101.3	100.9	0.4	
Aug.	31	1975	Caroline	29.88	29.80	0.08		101.2	100.9	0.3	
Sept.	23	1975	Eloise	29.97	29.80	0.17		101.5	100.9	0.6	

EAST COAST HURRICANES

Month	Date	Year	Name	P_w (in.)	P_{wi} (in.)	P_w-P_{wi} (in.)	P_{nx} (in.)	P_w (kPa)	P_{wi} (kPa)	P_w-P_{wi} (kPa)	P_{nx} (kPa)
Sept.	12	1903		30.00	29.85	0.15	30.12	101.6	101.1	0.5	102.0
June	17	1906 ex		29.91	29.83	0.08	29.98	101.3	101.0	0.3	101.5
Sept.	17	1906		30.06	29.91	0.15	30.38	101.8	101.3	0.5	102.9
Oct.	18	1906 ex		29.83	29.74	0.09	29.80	101.0	100.7	0.3	100.9
Oct.	11	1909 by		29.80	29.77	0.03	30.07	100.9	100.8	0.1	101.8
Aug.	28	1911		30.00	29.85	0.15	30.10	101.6	101.1	0.5	101.9
Sept.	3	1913		30.12	30.00	0.12	29.98	102.0	101.6	0.4	101.5
Sept.	10	1919 by		29.88	29.77	0.11	29.73	101.2	100.8	0.4	100.7
Oct.	26	1921 ex		29.88	29.74	0.14	29.59	101.2	100.7	0.5	100.2
Aug.	26	1924 by		29.94	29.71	0.23	30.33	101.4	100.6	0.8	102.7
§Aug.	26	1924 by		29.94	29.71	0.23	29.62	101.4	100.6	0.8	100.3
Dec.	2	1925		30.09	29.88	0.21	29.90	101.9	101.2	0.7	101.3
July	28	1926		30.00	29.83	0.17	29.91	101.6	101.0	0.6	101.3
Sept.	18	1926		29.94	29.71	0.23	29.99	101.4	100.6	0.8	101.6
Oct.	21	1926 by		29.77	29.68	0.09	29.97	100.8	100.5	0.3	101.5
Sept.	17	1928		29.88	29.74	0.14	30.38	101.2	100.7	0.5	102.9
Sept.	28	1929		29.80	29.71	0.09	30.08	100.9	100.6	0.3	101.9
Aug.	23	1933		29.94	29.71	0.23	29.48	101.4	100.6	0.8	99.8
Sept.	4	1933		29.94	29.83	0.11	29.98	101.4	101.0	0.4	101.5
Sept.	16	1933		30.03	29.88	0.15	29.82	101.7	101.2	0.5	101.0
Sept.	3	1935		29.94	29.83	0.11	29.92	101.4	101.0	0.4	101.3
Nov.	4	1935		29.97	29.85	0.12		101.5	101.1	0.4	
Sept.	18	1936 by		30.12	29.97	0.15	29.42	102.0	101.5	0.5	99.6
Sept.	21	1938		29.97	29.80	0.14	29.52	101.5	101.0	0.5	100.0
Aug.	11	1940		30.06	29.83	0.23	30.02	101.8	101.0	0.8	101.7
Sept.	14	1944		29.86	29.80	0.06	30.66	101.1	100.9	0.2	103.8
§Sept.	15	1944		29.91	29.85	0.06	29.39	101.3	101.1	0.2	99.5

Table 7.1.--Comparison of three peripheral pressures for gulf and east coast hurricanes, 1900-75, continued.

E A S T   C O A S T   H U R R I C A N E S

Month	Date	Year		Name	p_w (in.)	p_{wi} (in.)	p_w-p_{wi} (in.)	p_{nx} (in.)	p_w (kPa)	p_{wi} (kPa)	p_w-p_{wi} (kPa)	p_{nx} (kPa)
Sept.	15	1945			29.94	29.80	0.14	30.00	101.4	100.9	0.5	101.6
Sept.	17	1947			29.97	29.80	0.17	29.83	101.5	100.9	0.6	101.0
Oct.	15	1947			29.91	29.80	0.11	29.65	101.3	100.9	0.4	100.4
Sept.	22	1948	ex		29.74	29.68	0.06	29.83	100.7	100.5	0.2	101.0
Oct.	5	1948	ex		29.83	29.77	0.06	29.77	101.0	100.8	0.2	100.8
Aug.	24	1949	by		30.06	29.94	0.12	30.20	101.8	101.4	0.4	102.3
Aug.	27	1949			29.97	29.85	0.12	30.12	101.5	101.1	0.4	102.0
Oct.	18	1950		King	29.94	29.77	0.17		101.4	100.8	0.6	
Aug.	31	1954		Carol	29.86	29.77	0.09		101.1	100.8	0.3	
§Aug	31	1954		Carol	30.06	29.97	0.09		101.8	101.5	0.3	
Sept.	10	1954	by	Edna	29.86	29.83	0.03		101.1	101.0	0.1	
§Sept.	11	1954		Edna	29.83	29.68	0.15	29.26	101.0	100.5	0.5	99.1
Oct.	15	1954		Hazel	29.86	29.77	0.09	29.32	101.1	100.8	0.3	99.3
Aug.	12	1955		Connie	29.86	29.80	0.06	29.77	101.1	100.9	0.2	100.8
Sept.	19	1955		Ione	30.00	29.88	0.12	29.87	101.6	101.2	0.4	101.2
Aug.	28	1958	by	Daisy	29.97	29.77	0.20		101.5	100.8	0.7	
§Aug.	29	1958	by	Daisy	29.94	29.77	0.17		101.4	100.8	0.6	
Sept.	27	1958	by	Helene	29.88	29.83	0.05		101.2	101.0	0.2	
Sept.	29	1959		Gracie	30.00	29.88	0.12		101.6	101.2	0.4	
Sept.	10	1960		Donna	29.88	29.77	0.11		101.2	100.8	0.4	
§Sept.	12	1960		Donna	29.88	29.77	0.11		101.2	100.8	0.4	
§Sept.	12	1960		Donna	29.83	29.77	0.06		101.0	100.8	0.2	
Aug.	27	1964		Cleo	29.88	29.77	0.11		101.2	100.8	0.4	
Sept.	10	1964		Dora	29.91	29.88	0.03		101.3	101.2	0.1	
Sept.	8	1965		Betsy	29.91	29.80	0.11		101.3	100.9	0.4	
Sept.	17	1967		Doria	30.06	30.00	0.06		101.8	101.6	0.2	
Sept.	10	1969		Gerda	29.86	29.68	0.18		101.1	100.5	0.6	

§, ex, by: Defined in the notes preceeding tables 4.1 to 4.4.

p_w: Peripheral pressure-defined as the sea level pressure at the outer limits of the hurricane circulation determined by moving outward from the storm center to the first anticyclonically turning isobar in four equally spaced directions and averaging the four pressures thus obtained.

p_{wi}: Peripheral pressure-defined as the sea level pressure at the outer limits of the hurricane circulation determined by moving outward from the storm center to the last closed isobar in four equally spaced directions and averaging the four pressures thus obtained.

p_{nx}: A mixture of peripheral pressure defined as that value to which an exponential pressure profile employing the Hydromet Pressure Profile formula becomes asymptotic and peripheral pressure defined by p_w. These values were published in NHRP 5, table 3-1 under p_n (in.) Some of the conversions to millibars were in error in table 3-1. These have been corrected in converting to kilopascals.
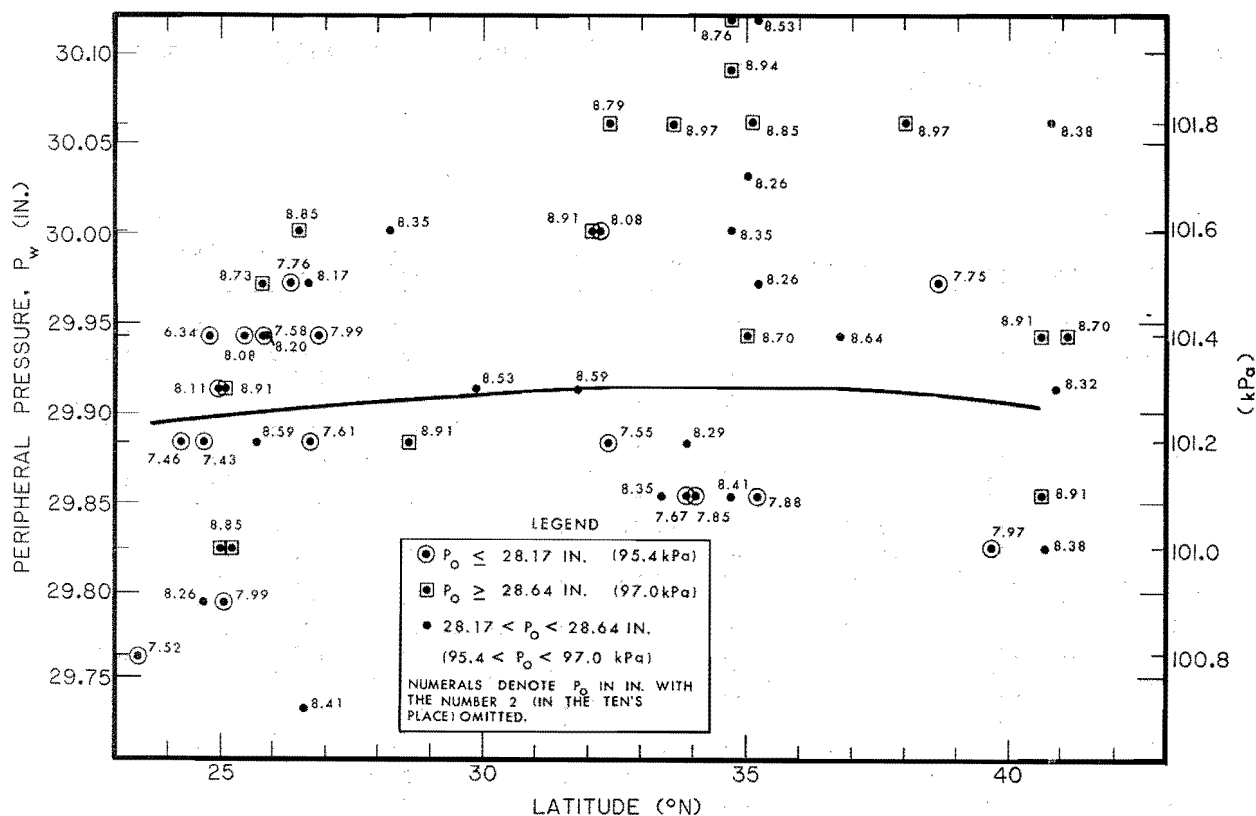
Figure 7.1.--Latitude (ψ) vs. peripheral pressure (p_w) for east coast hurricanes stratified into three intensity groupings.

An envelope of all the data (fig. 7.1) shows highest p_w near latitude 35°N, near the average position of the subtropical high. North and south of 35°N, enveloping p_w is less. The envelope, however, is made up of the weakest two groups of storms. An eye-fitted mean line through data for the strongest group ($p_o \leq 28.17$ in. or 95.4 kPa) shows a less pronounced latitudinal trend in p_w. Figure 7.2 is a plot of ψ vs. p_w for gulf coast hurricanes. The data do not show a latitudinal trend.

Figure 7.3 is a plot of p_o vs. p_w for all hurricanes. The envelope indicates a higher p_w for storms with higher p_o with one outstanding exception. This is the extreme Labor Day hurricane of 1935, which struck the Florida Keys with a p_o of 26.35 in. (89.2 kPa). This exception warns us against overly restricting p_w for storms with low p_o.

7.4.2 PLOTS CONTAINING P_{WI}

Figure 7.4 is a plot of ψ vs p_{wi} for all hurricanes. p_{wi} is plotted at the latitude for the location of p_o (tables 4.1-4.2). If the data points were

labeled with values of p_o, they would show essentially the same pattern as that indicated in figure 7.1. Figure 7.5, a plot of p_o vs. p_{wi} for all hurricanes, shows essentially the same enveloping trend as figure 7.3.

7.4.3 PLOTS OF LATITUDE VS. P_W AND P_{WI} FOR WESTERN NORTH PACIFIC TYPHOONS

p_w was plotted against latitude (fig. 7.6) for typhoons with $p_o \leq 27.46$ in. (93.0 kPa) at the location given in tables 4.5-4.6. p_w and p_{wi} for these typhoons are listed in table 7.2. Data for all these typhoons were selected between 8° and 30°N. Little if any

Figure 7.2--Latitude (ψ) vs. peripheral pressure (p_w) for gulf coast hurricanes.

trend of latitude with p_w is apparent. p_{wi} was also plotted against latitude (not shown) for the same sample of intense typhoons and no obvious trend was present. The average difference between p_w and p_{wi} was about 0.11 in. (0.4 kPa).

7.5 CONCLUSIONS

a. We decided to use p_w rather than p_{wi} for both the SPH and PMH criteria. p_w can be understood in a physical sense as being near the region of a hurricane where storm inflow begins. p_{wi} would lie inward from this region. Trends shown by plots (sec. 7.4) are similar for p_w and p_{wi}. Also, p_w is the more accepted definition of peripheral pressure.

b. We also decided not to vary the p_w with ψ for either the SPH or PMH. While an envelopment of the data (fig. 7.1) would give the highest p_w near 35°N, with lower values to the north and south, the more intense storms

Figure 7.3.--Central pressure (p_o) vs. peripheral pressure (p_w) for all hurricanes. The dashed line envelops all data except the Labor Day hurricane of 1935.

$[p_o \leq 28.17$ in. (95.4 kPa)] indicate less of a trend. We may infer that this trend would be dampened out completely for SPH and PMH intensity storms. Typhoon data (fig. 7.6) do not show any significant latitudinal variation.

c. The larger the Δp, the more intense the hurricane. We do not know of a theoretical approach for determining the upper bound of p_w for the PMH. Earlier studies have solved for p_n (using the Hydromet formula) which sometimes resulted in unrealistically high values.

For the SPH, we adopted a value of p_w = 29.77 in. (100.8 kPa) which is reasonably characteristic of extreme hurricanes, e.g., the October 21, 1926 Florida Keys hurricane with a p_o of 27.52 in. (93.2 kPa). The p_w for
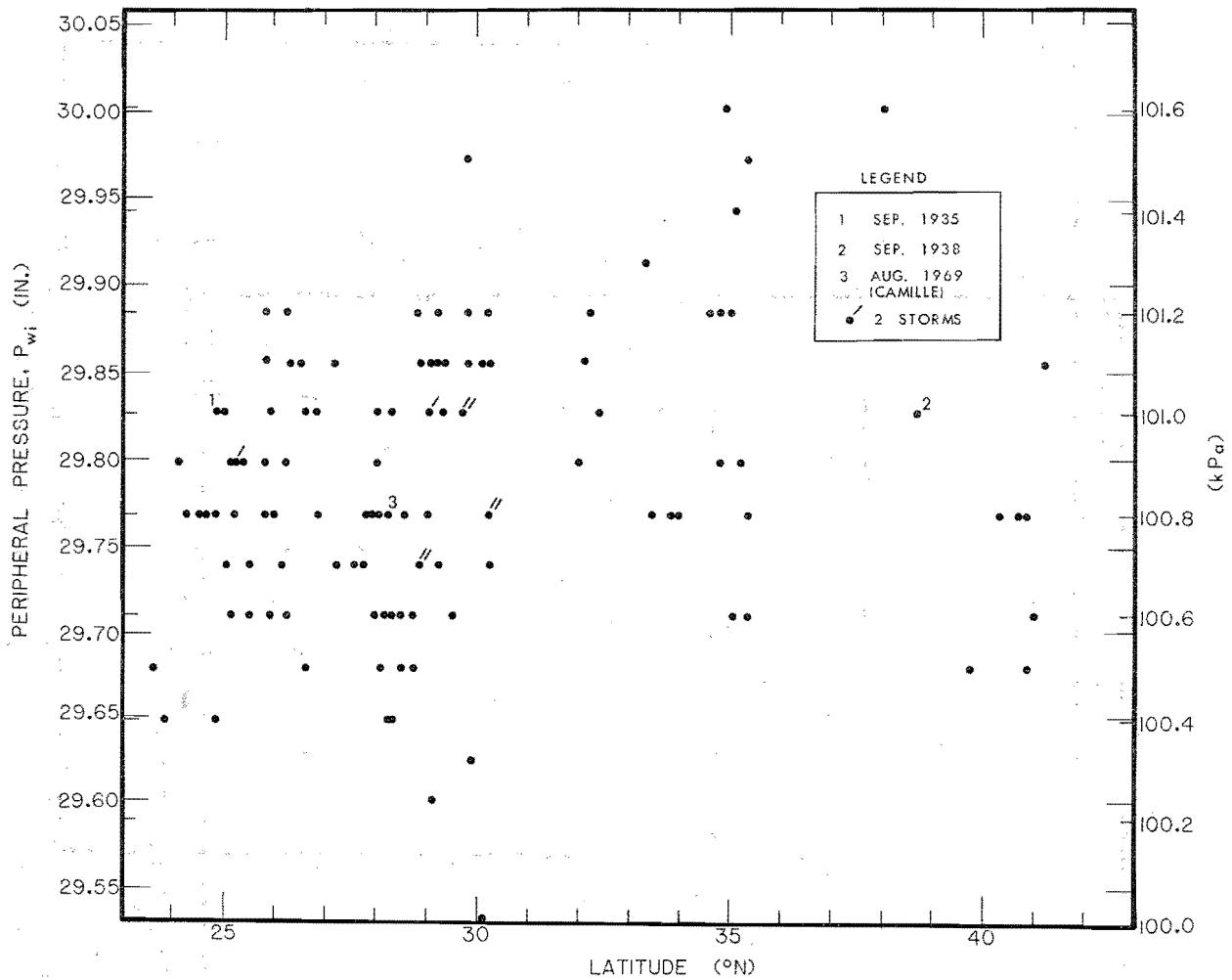
Figure 7.4 Latitude (ψ) vs. peripheral pressure (p_{wi}) for all hurricanes.

the most extreme hurricane on record (Labor Day hurricane of 1935) was 29.94 in. (101.4 kPa). This suggests that p_w for the PMH should be not less than 29.94 in. (101.4 kPa). We adopted 30.12 in. (102.0 kPa) for p_w. This is an upper bound for the data shown in figures 7.1 and 7.4.
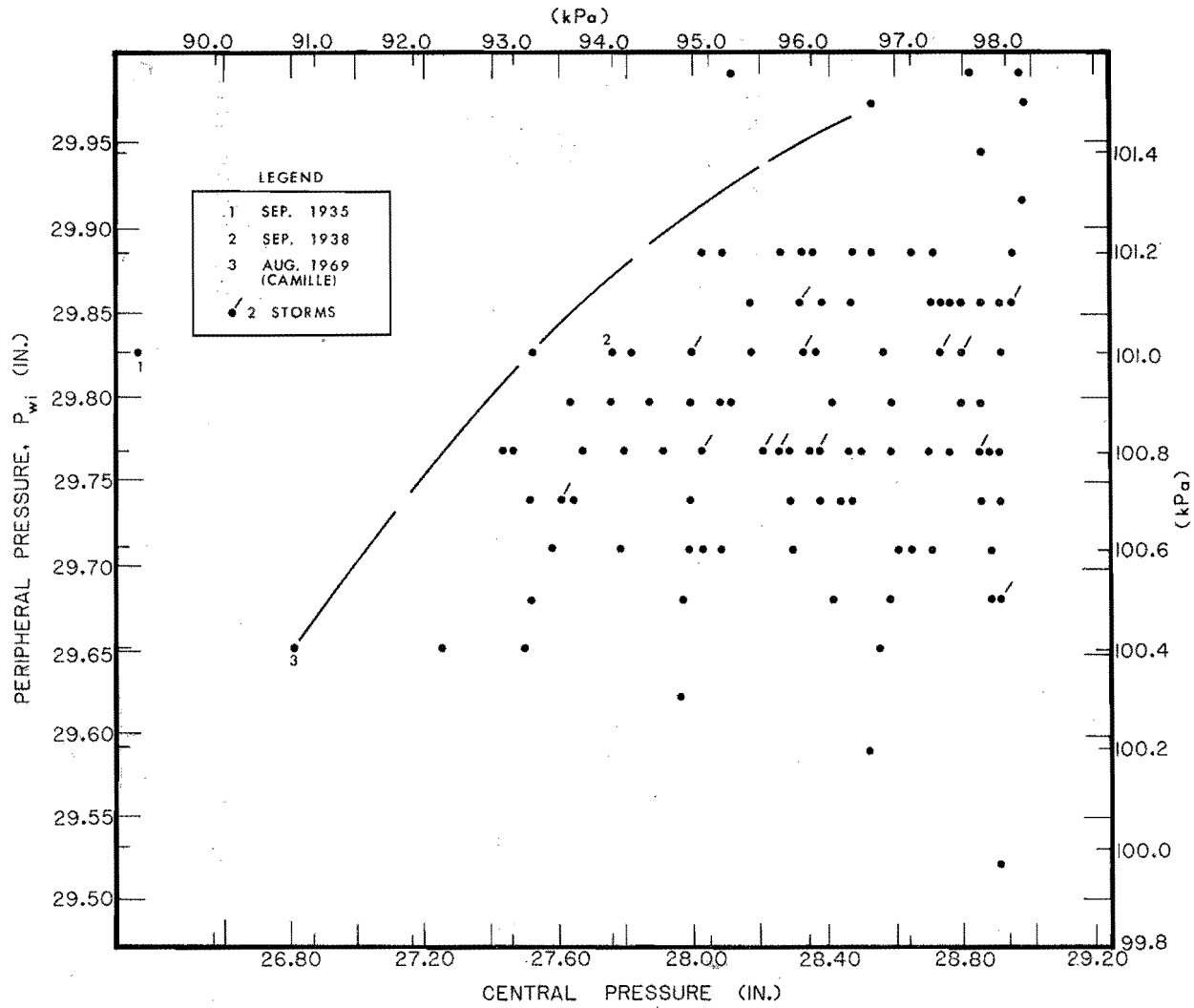
Figure 7.5.--Central pressure (p_o) vs. peripheral pressure (p_wi) for all hurricanes. The dashed line envelops all data except the Labor Day hurricane of 1935.
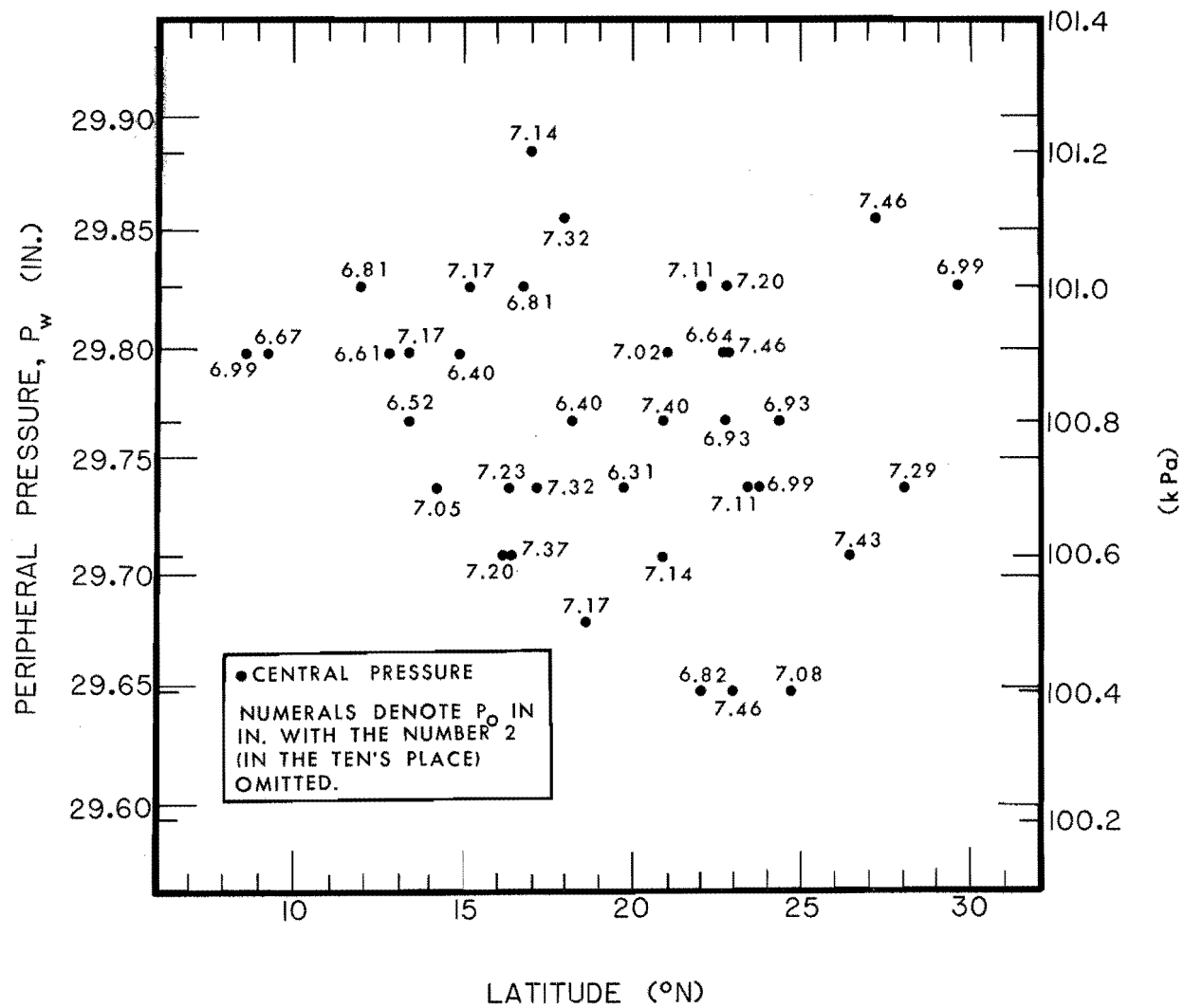
Figure 7.6.--Latitude (ψ) vs. peripheral pressure (p_w) for intense typhoons (p_o ≤ 27.46 in. or 93.0 kPa), 1960-74

Table 7.2.—Comparison of two peripheral pressures for typhoons with p_o ≤ 27.46 in. (93.0 kPa), 1960-74

Month	Date	Year	Name	p_w (in.)	p_{wi} (in.)	$p_w - p_{wi}$ (in.)	p_w (kPa)	p_{wi} (kPa)	$p_w - p_{wi}$ (kPa)
Aug.	6	1960	Trix	29.74	29.53	0.21	100.7	100.0	0.7
May	17	1961	Alice	29.74	29.62	0.12	100.7	100.3	0.4
Sept.	13	1961	Nancy	29.80	29.68	0.12	100.9	100.5	0.4
Sept.	11	1961	Pamela	29.74	29.62	0.12	100.7	100.3	0.4
Oct.	8	1961	Violet	29.86	29.71	0.15	101.1	100.6	0.5
Aug.	5	1962	Opel	29.65	29.56	0.09	100.4	100.1	0.3
July	15	1963	Wendy	29.77	29.68	0.09	100.8	100.5	0.3
Aug.	12	1963	Carmen	29.77	29.71	0.06	100.8	100.6	0.2
Sept.	9	1963	Clara	29.77	29.71	0.06	100.8	100.6	0.2
Aug.	6	1964	Ida	29.71	29.53	0.18	100.6	100.0	0.6
Sept.	8	1964	Sally	29.77	29.68	0.09	100.8	100.5	0.3
Nov.	18	1964	Louise	29.80	29.74	0.06	100.9	100.7	0.2
Dec.	11	1964	Opal	29.80	29.71	0.09	100.9	100.6	0.3
July	12	1965	Freda	29.74	29.56	0.18	100.7	100.1	0.6
Sept.	15	1965	Trix	29.65	29.56	0.09	100.4	100.1	0.3
Nov.	23	1965	Faye	29.86	29.80	0.06	101.1	100.9	0.2
June	26	1966	Kit	29.77	29.56	0.21	100.8	100.1	0.7
Sept.	4	1966	Cora	29.65	29.56	0.09	100.4	100.1	0.3
Nov.	2	1967	Emma	29.83	29.68	0.15	101.0	100.5	0.5
Nov.	15	1967	Gilda	29.88	29.80	0.08	101.2	100.9	0.3
Sept.	21	1968	Della	29.80	29.68	0.12	100.9	100.5	0.4
Sept.	27	1968	Elaine	29.83	29.77	0.06	101.0	100.8	0.2
July	26	1969	Viola	29.74	29.56	0.18	100.7	100.1	0.6
Sept.	24	1969	Elsie	29.83	29.68	0.15	101.0	100.5	0.5
July	2	1970	Olga	29.80	29.65	0.15	100.9	100.4	0.5
Aug.	20	1970	Anita	29.74	29.62	0.12	100.7	100.3	0.4
Sept.	10	1970	Georgia	29.83	29.77	0.06	101.0	100.8	0.2
Oct.	12	1970	Joan	29.80	29.68	0.12	100.9	100.5	0.4
Nov.	18	1970	Patsy	29.74	29.68	0.06	100.7	100.5	0.2
May	25	1971	Dinah	29.80	29.68	0.12	100.9	100.5	0.4
July	5	1971	Harriet	29.71	29.59	0.12	100.6	100.2	0.4
July	19	1971	Lucy	29.68	29.56	0.12	100.5	100.1	0.4
July	24	1971	Nadine	29.71	29.65	0.06	100.6	100.4	0.2
Aug.	29	1971	Trix	29.83	29.77	0.06	101.0	100.8	0.2
Sept.	21	1971	Bess	29.83	29.77	0.06	101.0	100.8	0.2
July	16	1973	Billie	29.71	29.56	0.15	100.6	100.1	0.5
Oct.	6	1973	Nora	29.80	29.71	0.09	100.9	100.6	0.3

p_w: Peripheral pressure—defined as the sea-level pressure at the outer limits of the typhoon circulation determined by moving outward from the storm center to the first anticyclonically turning isobar in four equally spaced directions and averaging the four pressures thus obtained.

p_{wi}: Peripheral pressure – defined as the sea-level pressure at the outer limits of the typhoon circulation determined by moving outward from the storm center to the last closed isobar in four equally spaced directions and averaging the four pressures thus obtained.

8. CENTRAL PRESSURE

8.1 INTRODUCTION

Central pressure (p_o) is a universally used index of hurricane intensity.
Everything else being equal, the square of the wind speed varies directly
with Δp ($\Delta p = p_w - p_o$). p_o is fundamental to the whole hurricane wind field.
Reid and Wilson (1954), Harris (1959) and Jelesnianski (1972) demonstrated
that storm surge height is approximately proportional to Δp, holding all
other parameters constant.

8.2 CENTRAL PRESSURE FOR THE SPH

8.2.1 INTRODUCTION

This study uses a less statistically bound approach than previous studies
in setting the level of the SPH p_o along the east and gulf coasts. Statisti-
cal results when using limited data are subject to considerable uncertainty,
particularly when developing values for rare recurrence intervals. Reliable
observations have been taken for only about 80 years and there has been an
average of less than one hurricane per year for the period of record for
either coast. This data sample (tables 4.1 to 4.4) must, therefore, be
considered a limited sample. Since the criteria must stand the test of time,
meteorological judgment was applied to the few extreme events rather than
relying heavily on statistical analysis. Guides to this judgment were
obtained by averaging several lowest p_o's of record (for several lengths of
coastline and various overlapping intervals). These averages emphasized two
extreme p_o's, that of Camille (1969) and the Labor Day hurricane of 1935.

8.2.2 BASIC DATA

Tables 8.1 and 8.2 listed hurricanes by date, latitude and longitude, p_o,
and milepost (the distance from a point on the Mexican coast at about 24°N,
see fig. 1.1). These tables differ from tables 4.1 to 4.4 in that the
milepost is for the lowest p_o. In the Gulf of Mexico, the milepost is the
shortest distance to the coast. In the North Atlantic, it is the latitude
of p_o. This procedure for the Atlantic easily relates p_o to the sea-surface
temperature (T_s) at that latitude. Such a relation is useful when determin-
ing PMH p_o in section 8.3.

8.2.3 HISTORICAL STORMS

In order to supplement our limited sample of extreme hurricanes, we reviewed historical accounts of hurricanes occurring prior to the turn of this century. Table 8.3 lists dates and locations of some extreme hurricanes prior to 1900. For five of these storm reports (noted with an "S"), comparisons with recent high surges in these locations allowed an appraisal of the p_o's in the hurricanes. For two cases (noted with a "P"), the p_o was estimated from pressure readings given by Ludlum (1963). Because of the difficulty in determining p_o from surge observations, and uncertainty in pressure readings prior to the establishment of standardized instruments and observational procedures, these data are used only in qualitative evaluations.

8.2.4 PROCEDURE

Our general method for determining p_o for the SPH was to let the observed data be the control on the level of p_o. The data were grouped within overlapping lengths. At the outset, we needed to decide on the best coastal zone length to use. We started with coastal zones 200, 400, 500 and 800 n.mi. (371, 741, 927 and 1483 km) in length covering both coasts. We averaged the three, five, seven, and ten lowest p_o's of record within each zone length and compared the averages with the lowest, or most extreme, of record. This was done a) for the original data set in tables 8.1 and 8.2; b) for the original data set plus the historical storm data (table 8.3); and c) for the original data set minus Camille (1969) and the Labor Day hurricane of 1935. These last two storms were given special treatment because their p_o's are considerably lower than all other east and gulf coast hurricanes. Coastal lengths were overlapped by 50, 100 and 200 n.mi. (93, 185, and 371 km). One additional set was run with no overlapping. We thus prepared 192 plots (4 zone lengths x 4 averages x 3 data sets x 4 overlappings) of p_o averages and minimums.

From a comparison of results we discarded those based on 200- and 800-n.mi. (371- and 1483-km) zone lengths; those with averages based on the three and ten lowest p_o's; those based on the original data set plus historical values; and those based on no overlapping and 100- and 200-n.mi. (185- and 371-km) overlapping. The remaining sets were the only ones considered to give

Table 8.1.--Hurricane central pressure (p_o)-U.S. gulf coast.

Date	lat. (°N)	long. (°W)	p_o (in.)	p_o (kPa)	milepost (n.mi.)	milepost (km)
9-12-70	23.9	97.7	28.55	96.7	10	(19)
8-31-75	24.3	97.7	28.44	96.3	40	(74)
9-20-67	24.8	96.3	27.26	92.3	60	(111)
8-05-33	25.7	97.1	28.80	97.5	130	(241)
9-05-33	26.2	97.1	28.02	94.9	140	(259)
8-18-16	27.0	97.5	28.00	94.8	185	(343)
9-14-19	27.3	97.5	27.99	94.8	220	(408)
8-03-70	27.9	97.2	27.89	94.5	260	(482)
9-11-61	28.4	96.4	27.49	93.1	295	(547)
6-28-29	28.5	96.5	28.62	96.9	300	(556)
6-22-21	28.6	96.4	28.17	95.4	320	(593)
8-30-42	28.5	96.2	28.07	95.1	330	(612)
8-27-45	28.6	96.2	28.57	96.8	330	(612)
9-10-71	28.5	95.6	28.91	97.9	340	(630)
10-04-49	28.8	95.6	28.45	96.3	360	(667)
9-23-41	28.9	95.4	28.31	95.9	370	(686)
7-21-09	29.0	95.2	28.31	95.9	380	(704)
8-17-15	29.1	95.2	28.01	94.9	380	(704)
8-14-32	29.1	95.0	27.83	94.2	390	(723)
9-09-00	29.2	95.1	27.64	93.6	390	(723)
7-27-43	29.5	94.5	28.78	97.5	425	(788)
8-08-40	29.9	93.9	28.70	97.2	450	(834)
6-27-57	29.8	93.6	27.95	94.7	460	(852)
9-16-71	29.4	93.2	28.88	97.8	470	(871)
6-16-34	29.3	91.2	28.52	96.6	590	(1093)
10-03-64	29.5	91.4	28.33	95.9	595	(1103)
8-26-26	29.3	91.3	28.31	95.9	600	(1112)
9-08-74	28.0	90.7	27.64	93.6	605	(1121)
9-21-20	29.2	90.9	28.93	98.0	610	(1130)
9-20-09	29.2	90.2	28.94	98.0	650	(1205)
9-19-47	29.8	90.3	28.54	96.7	670	(1242)
8-15-01	29.3	89.7	28.72	97.3	685	(1269)
9-29-15	27.0	89.3	27.53	93.2	705	(1307)
9-15-60	26.6	89.3	28.70	97.2	705	(1307)
8-18-69	28.2	88.8	26.81	90.8	705	(1307)
9-10-65	28.2	89.2	27.79	94.1	710	(1316)
7-05-16	30.4	89.0	28.38	96.1	770	(1427)
9-27-06	30.4	88.5	28.50	96.5	780	(1445)
8-31-50	30.2	88.0	28.92	97.9	820	(1520)
9-20-26	30.3	87.5	28.20	95.5	845	(1566)
10-18-16	30.4	87.2	28.76	97.4	960	(1593)
9-24-56	30.3	86.5	28.76	97.4	890	(1649)
9-29-17	30.4	86.6	28.48	96.4	900	(1668)
7-31-36	30.4	86.5	28.46	96.4	900	(1668)
9-23-75	30.4	86.5	28.20	95.5	900	(1668)

Table 8.1.--*Hurricane central pressure* (p_o) - *U.S. gulf coast -*
continued.

Date	lat. (°N)	long. (°W)	p_o (in.)	(kPa)	milepost (n.mi.)	(km)
9-30-29	29.7	85.4	28.80	97.5	970	(1798)
6-19-72	28.5	85.7	28.88	97.8	990	(1835)
10-07-41	29.9	84.7	28.98	98.1	1015	(1881)
6-09-66	29.1	84.3	28.65	97.0	1030	(1909)
9-05-50	29.1	83.1	28.30	95.8	1120	(2076)
10-19-68	28.8	82.9	28.85	97.7	1140	(2224)
10-25-21	28.1	82.8	28.12	95.2	1200	(2224)
10-18-50	28.0	81.6	28.88	97.8	1200	(2252)
9-04-33	27.8	81.6	28.48	96.4	1215	(2261)
9-17-28	27.7	81.7	28.30	95.8	1220	(2317)
8-27-49	27.2	81.2	28.37	96.1	1250	(2317)
9-18-47	26.3	81.3	28.03	94.9	1320	(2446)
9-08-65	25.2	82.1	27.99	94.8	1375	(2548)
10-05-48	24.7	81.3	28.85	97.7	1380	(2557)
6-17-06	25.1	81.1	28.91	97.9	1395	(2585)
10-18-06	25.0	81.0	28.84	97.7	1395	(2585)
10-11-09	24.7	81.1	28.26	95.7	1400	(2595)
9-03-35	24.8	80.9	26.35	89.2	1410	(2613)
9-10-60	24.3	80.5	27.45	93.0	1410	(2613)
11-05-35	25.6	80.4	28.73	97.3	1440	(2669)
9-15-45	25.5	80.3	28.09	95.1	1440	(2669)
9-21-48	24.5	81.5	27.62	93.5	1380	(2557)
10-21-26	23.6	81.8	27.52	93.2	1380	(2557)
10-14-64	24.3	82.7	28.47	96.4	1360	(2521)
10-17-10	24.5	82.9	27.80	94.1	1355	(2511)
9-10-19	24.7	82.9	27.44	92.9	1350	(2502)
10-20-24	24.7	82.9	28.70	97.2	1350	(2502)
10-19-44	24.7	82.9	28.02	94.9	1350	(2502)
10-04-66	24.1	84.2	28.85	97.7	1330	(2465)

Table 8.2.--*Hurricane central pressure* (p_o) - *U.S. east coast*

Date	lat. (°N)	long. (°W)	p_o (in.)	p_o (kPa)	milepost (n.mi.)	milepost (km)
9-10-19	24.7	82.9	27.44	92.9	1350	(2502)
10-21-26	23.6	81.8	27.52	93.2	1380	(2557)
6-17-06	25.1	81.1	28.91	97.9	1395	(2585)
10-18-06	25.0	80.6	28.84	97.7	1395	(2585)
10-11-09	24.7	81.1	28.26	95.7	1400	(2595)
9-10-60	24.3	80.5	27.45	93.0	1410	(2613)
9-03-35	24.8	80.9	26.35	89.2	1410	(2613)
9-08-65	25.0	80.6	28.11	95.2	1420	(2632)
9-28-29	25.1	80.4	28.00	94.8	1425	(2641)
10-05-48	25.2	80.3	28.85	97.7	1435	(2659)
9-15-45	25.5	80.3	28.09	95.1	1440	(2669)
8-27-64	25.7	80.1	28.57	96.8	1455	(2695)
9-18-26	25.8	80.1	27.59	93.4	1460	(2706)
11-04-35	25.8	80.1	28.73	97.3	1460	(2706)
10-18-50	25.8	80.2	28.20	95.5	1460	(2706)
9-17-47	26.3	80.1	27.76	94.0	1475	(2733)
9-12-03	26.5	80.0	28.84	97.7	1500	(2780)
9-22-48	26.6	81.0	28.41	96.2	1500	(2780)
9-17-28	26.7	80.0	27.62	93.5	1505	(2789)
8-27-49	26.7	80.0	28.16	95.4	1505	(2789)
9-04-33	26.9	80.1	27.98	94.8	1530	(2836)
7-28-26	28.2	80.4	28.34	96.0	1605	(2974)
10-26-21	28.6	81.8	28.91	97.9	1630	(3021)
9-10-64	29.9	81.4	28.52	96.6	1715	(3178)
10-15-47	31.8	81.1	28.59	96.8	1840	(3410)
8-28-11	32.1	81.0	28.92	97.9	1870	(3466)
9-29-59	32.2	80.2	28.08	95.1	1875	(3475)
8-11-40	32.4	80.9	28.78	97.5	1885	(3493)
9-27-58	32.4	78.5	27.52	93.2	1885	(3493)
8-31-54	33.4	76.8	28.35	96.0	1980	(3669)
9-17-06	33.6	78.9	28.98	98.1	2000	(3707)
10-15-54	33.9	78.5	27.66	93.7	2030	(3762)
9-12-60	33.9	77.9	28.29	95.8	2030	(3762)
9-10-54	34.0	75.6	27.85	94.3	2035	(3771)
9-03-13	34.7	76.4	28.81	97.6	2115	(3920)
12-02-25	34.7	76.6	28.95	98.0	2115	(3920)
8-12-55	34.7	76.1	28.40	96.2	2115	(3920)
9-19-55	34.7	76.7	28.35	96.0	2115	(3920)
8-26-24	35.0	75.2	28.70	97.2	2160	(4003)
9-16-33	35.0	76.2	28.25	95.7	2160	(4003)
8-24-49	35.1	75.3	28.86	97.7	2165	(4012)
9-18-36	35.2	74.6	28.52	96.6	2170	(4021)
9-14-44	35.2	75.5	27.88	94.4	2170	(4021)
8-28-58	35.2	74.2	28.26	95.7	2170	(4021)
8-23-33	36.8	75.9	28.63	97.0	2255	(4179)

Table 8.2.--Hurricane central pressure (p_o) - U.S. east coast - continued.

Date	lat. (°N)	long. (°W)	p_o (in.)	(kPa)	milepost (n.mi.)	(km)
9-17-67	38.0	71.9	28.97	98.1	2340	(4337)
9-21-38	38.7	72.5	27.75	94.0	2395	(4439)
9-11-54	39.7	71.3	27.97	94.7	2465	(4667)
9-09-69	40.6	69.6	28.91	97.9	2540	(4707)
8-29-58	40.6	69.1	28.91	97.9	2540	(4707)
9-12-60	40.7	72.6	28.38	96.1	2560	(4745)
8-31-54	40.8	72.5	28.38	96.1	2575	(4772)
9-15-44	40.9	72.2	28.31	95.9	2590	(4799)
8-26-24	41.1	69.8	28.70	97.2	2615	(4846)

Table 8.3.--Selected extreme hurricanes prior to 1900

Date	Location	Estimated p_o (in.)	(kPa)	Origin
Aug. 31, 1837	nr. Apalachicola	27.46	93.0	S
Oct. 5, 1842	nr. Cedar Key	28.26	95.7	S
Sept. 25, 1848	nr. Tampa	28.05	95.0	P
Oct. 11, 1846	Florida Keys	26.81	90.8	P
Sept. 7-8, 1846	nr. Nags Head	27.96	94.7	S
Sept. 23, 1815 } Aug. 25, 1635 }	from central Conn. coast to coast between Narragansett and Buzzards Bays	27.76	94,0	S

S : surge reports

P : pressure observations

realistic answers to the problem at hand, i.e., coastal zone lengths of 400
and 500 n.mi. (741 and 927 km); averages of the lowest five and seven p_o's;
original data sets with and without Camille (1969) and the Labor Day hurri-
cane of 1935; and within the 400- and 500.-n.mi. zones overlapping by
centering them at 50-n.mi. intervals along the coast.

Figure 8.1 is an example of the plots. This one is for averages of the five
lowest p_o's and the minimum p_o within 500-n.mi. (927 km) lengths centered at
50 - n.mi. (93 km) intervals and including Camille and the Labor Day hurricane
of 1935.

The next step was to introduce a method of smoothing. The procedure used
by Ho et al. (1975) section 2.2.1.1, was adopted. The data for the two zone
lengths were smoothed by weighted averaging of each successive 11 data
points. These discrete values (A) may be considered as a continuous input
series. The smoothed frequency value (F_i) for a point is obtained from the
equation:

$$F_i = \frac{\sum\limits_{n=-5}^{n=5} W_n A_{i+n}}{\sum\limits_{n=-5}^{n=5} W_n} \tag{8.1}$$

We used assigned weights for W_n, as in low pass filtering in time series
analysis (after Craddock 1969) as follows*:

W_n = 0.300, 0.252, 0.140, 0.028, -0.040, -0.030; for

n = 0, $\pm$ 1, $\pm$2, $\pm$3, $\pm$4, $\pm$5, respectively.

The weighting function adopted here is designed to maintain the frequency
and phase angle of the original input series. These weights were applied to
all successive discrete values from Texas to Maine, yielding a weighted mean
storm p_o at each 50-n.mi. (93 km) milepost of the smoothed coastline.
These values were connected to give a continuous smoothed curve. The two

---

*An alternate smoothing procedure often applied in climatological analyses
uses a running mean approach (W_n = 1). The results thus obtained may have
distortions in phase angle variation (shifting of maximum or minimum posi-
tions) and in the total area under the curve.
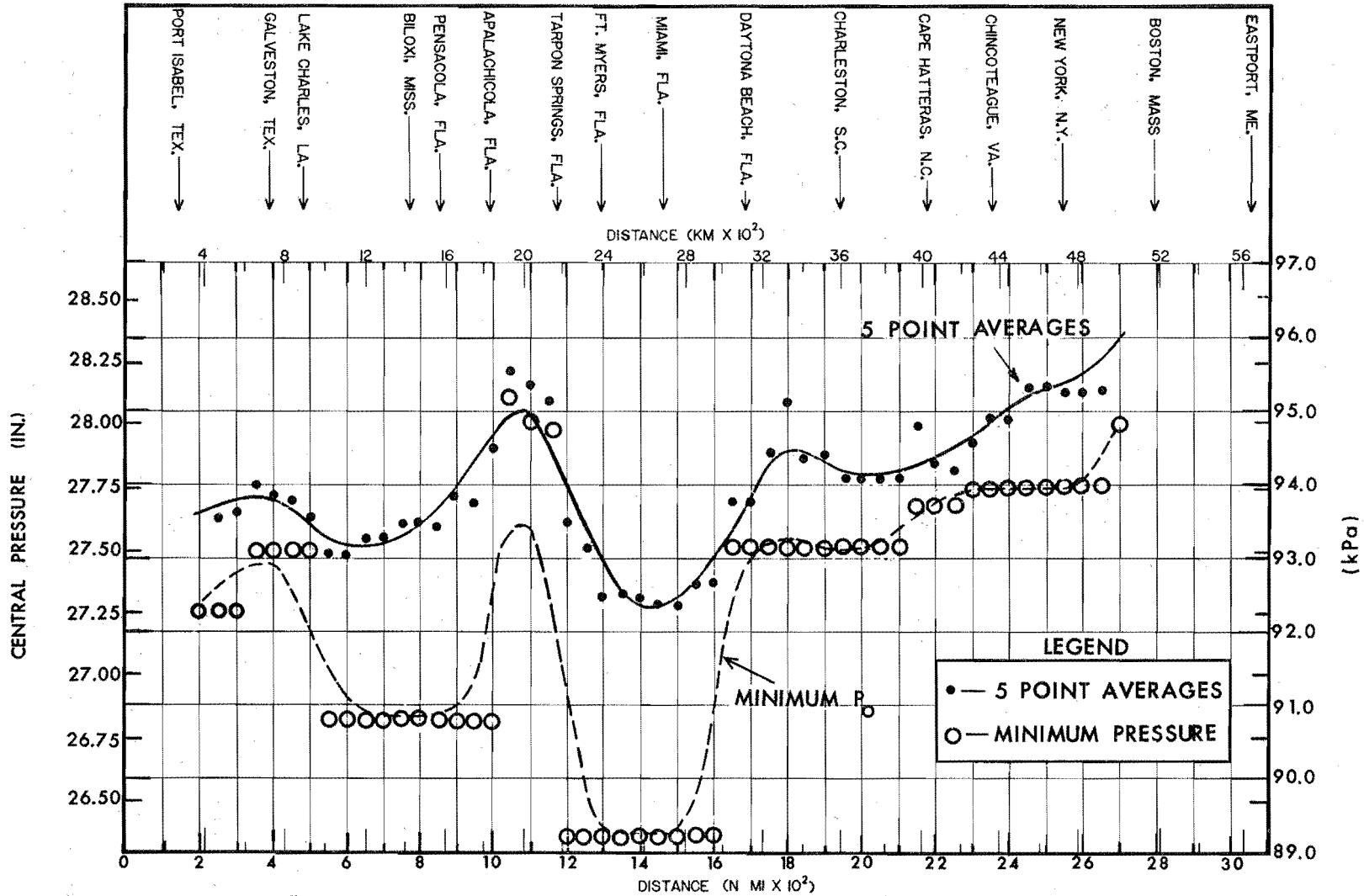
Figure 8.1.--Plot showing averages of the five lowest p_o's (black dots) within 500-n.mi. (927 km) lengths overlapping by 50 n.mi. (93 km) for all hurricanes. Also shown are minimum p_o's (open circles) within 500-n.mi. lengths overlapping by 50 n.mi. The two curves were drawn using the smoothing technique described in section 8.2.4.

curves in the example of figure 8.1 are the results of this smoothing technique. We raised the solid curve near milepost 2600 to reflect the observed trend of increasing p_o with latitude along the east coast.

We compared the averages based on 400- and 500-n.mi. (741- and 927-km) zone lengths and concluded the averages for the 500-n.mi. (927-km) lengths were best. We also decided to use the averages of the seven lowest p_o's rather than the averages of the five lowest p_o's. Figure 8.2 shows a smoothed curve based on the 7-point averages with and without Camille (1969) and the Labor Day hurricane of 1935. Also shown for comparison are data for all hurricanes with $p_o \leq 28.41$ in. (96.2 kPa). These data come from tables 4.1 to 4.4. The data are plotted along the gulf coast at the coastal location closest to the point where p_o was observed and along the east coast at the latitude where p_o was observed. We selected these two curves as the pair that give the better relative variation of p_o along both coasts.

At this stage we decided the curve not considering Camille (1969) and the Keys (1935) storms should be used. Our decision was based on the idea that these two hurricanes contained extremely low p_o's resulting in sustained wind speeds that were not reasonably characteristic of the northern gulf coast and the Florida Keys.

The next question is, where should the relative variation be anchored? The decision was made to tie into the observed pressures in the 1938 New England hurricane and hurricane Helene (1958). Reasons for this decision are:

a. So anchored (fig. 8.3) the level of p_o is less than for the two most extreme hurricanes along the gulf coast (Camille and Labor Day hurricane of 1935) while enveloping the rest of the data. These two hurricanes are much more severe than any other in the gulf and are therefore not "reasonably characteristic."

b. The curve passes relatively close to p_o for Edna (1954) at milepost 2465 --the second most intense hurricane since 1900 north of the Chesapeake Bay area--and Hazel (1954) at milepost 2030.
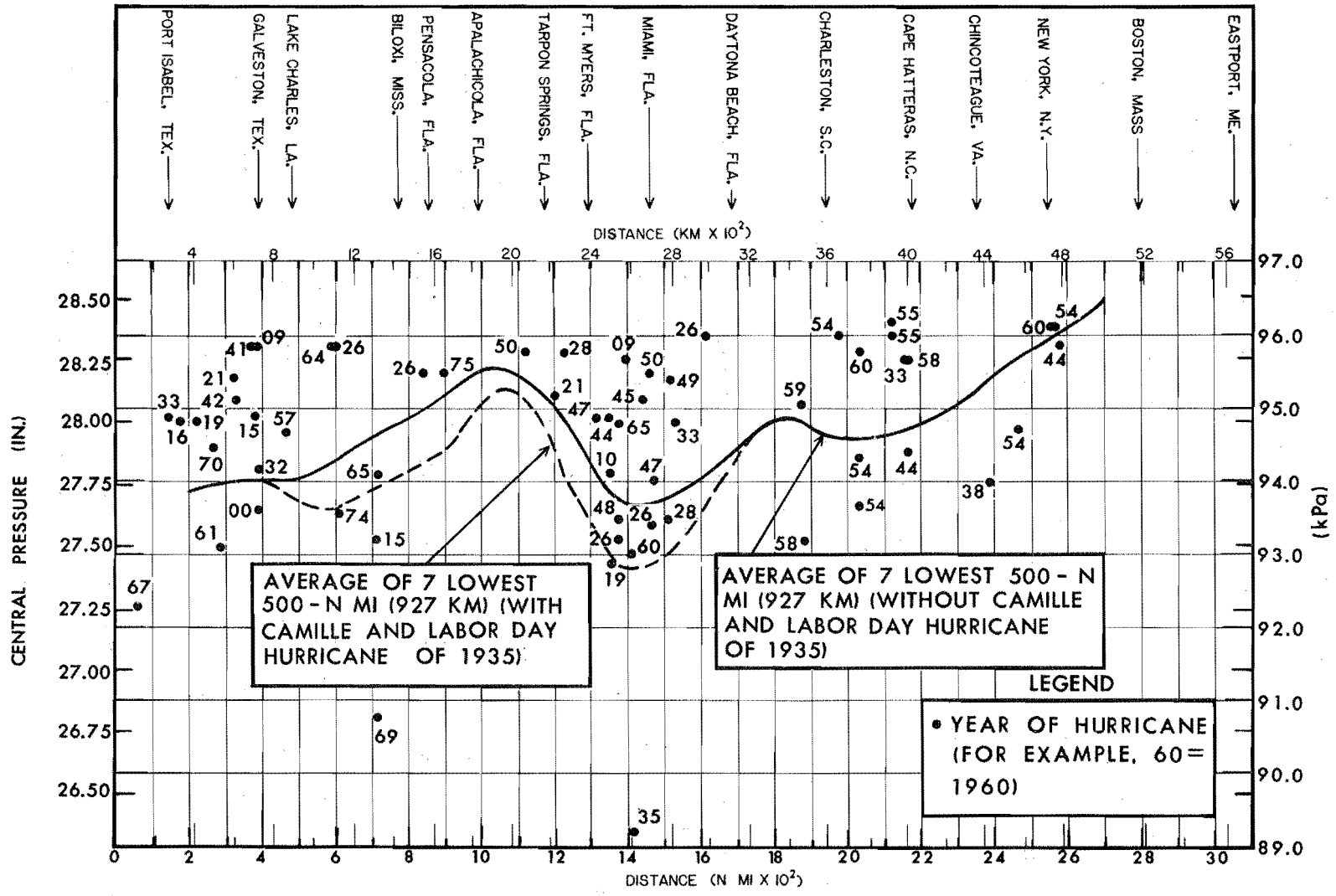
Figure 8.2.--Plot showing smoothed curves through averages of the seven lowest p_o's within 500-n.mi. (927 km) lengths overlapping by 50 n.mi. (93 km). The broken curve includes Camille and the Labor Day hurricane of 1935. The unbroken curve omits these storms. Data points are hurricanes of record with $p_o \leq 28.41$ in. (96.2 kPa).
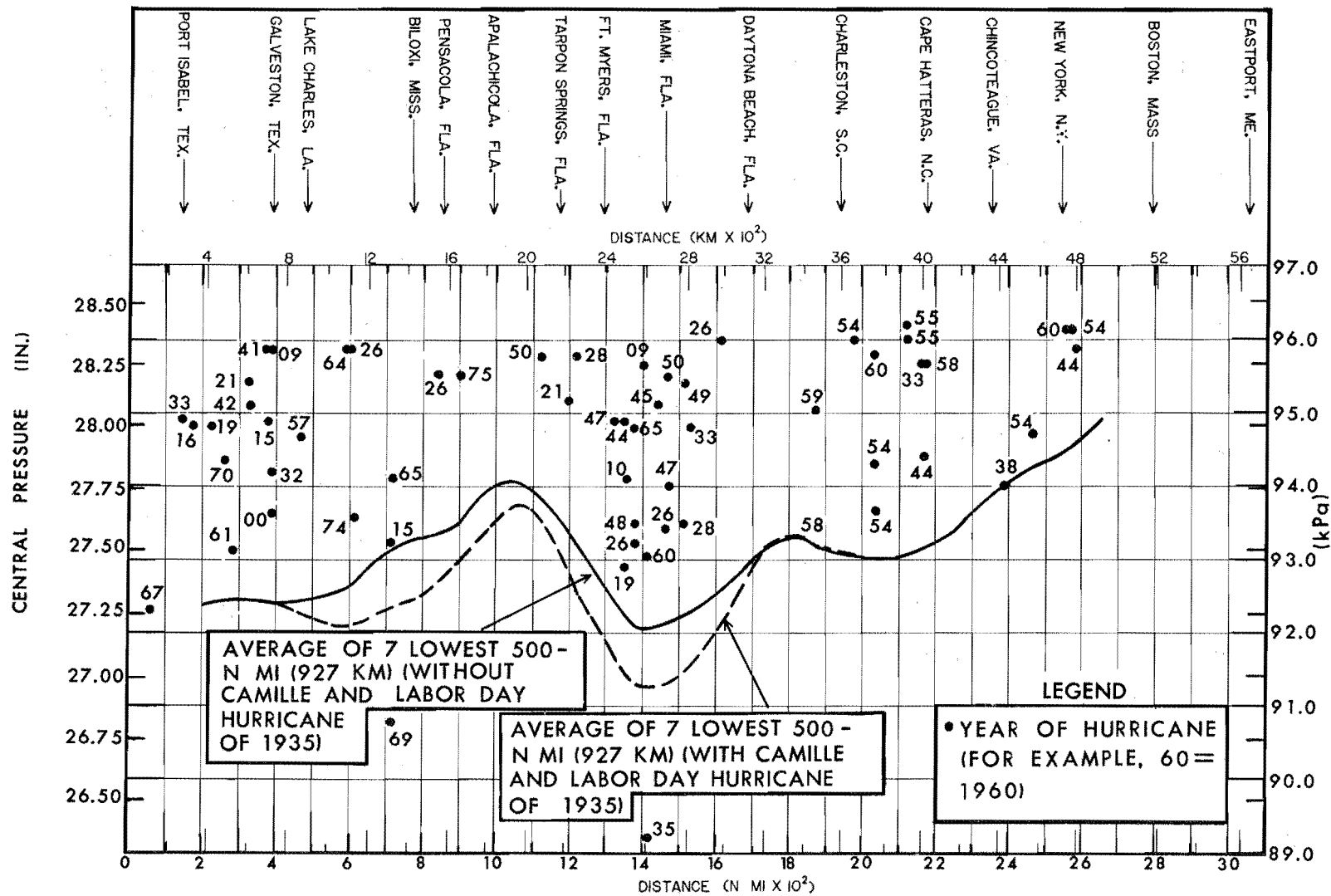
Figure 8.3.--Plot showing smoothed curves through averages of the seven lowest p_Q's within 500-n.mi. (927 km) lengths overlapping by 50 n.mi.(93 km) after anchoring the relative variation into the 1938 hurricane and Helene (1958). The broken curve includes Camille and the Labor Day hurricane of 1935. The unbroken curve omits these storms. Data points are hurricanes of record with $p_o \leq 28.41$ in. (96.2 kPa).

c. If the curve were extended, it would come close to hitting Beulah (1967)--the hurricane with the third lowest p_o in tables 4.1 to 4.4--near milepost 60.

d. From extreme storm surges observed along the New England coast prior to 1900 (table 8.3) we estimated that there have been two storms of about the same intensity as the 1938 hurricane.

From about milepost 500 to milepost 1050, we then made an adjustment in our selected curve. We know of no valid meteorological reason for the SPH p_o in the Biloxi-Pensacola area (about milepost 800) to be higher than at Lake Charles, La. (about milepost 500). Camille entered the coast near Biloxi although it could have just as well entered 50 to 100 n.mi. (93 to 185 km) farther west with little, if any, loss of intensity. East of the Pensacola area, however, the Florida peninsula keeps an SPH from attaining the strength of an SPH farther west. Along this stretch of coast, a major portion of the eastern semicircle of an alongshore west Florida hurricane is overland. Therefore, a quantity of the storm's latent and sensible heat (cooling effect of falling rain) sources are reduced, the equivalent potential temperature (θ_e) of the surface air is lowered, and the radial gradient of θ_e at the surface is weakened.

We also adjusted the curve downward near milepost 1400. The Florida Keys south of 25°N are more than a degree of latitude farther south than Port Isabel and should be represented by somewhat lower SPH p_o.

We adjusted the curve downward to lower p_o along a portion of the nearly eastward oriented southern New England coast where SPH p_o should not rise rapidly. We then raised the curve sharply between mileposts 2700 and 2800 where the coast resumes a basically north-south orientation.

Figure 8.4 shows a) the adopted SPH p_o; b) the data for storms with p_o $\leq$ 28.41 in.(96.2 kPa), plotted in the same fashion as figures 8.2 and 8.3; c) the estimated pressure readings from historical data prior to the turn of this century (table 8.3); d) p_o's from three previous studies. Tabular data from the adopted SPH p_o's are presented in chapter 2.
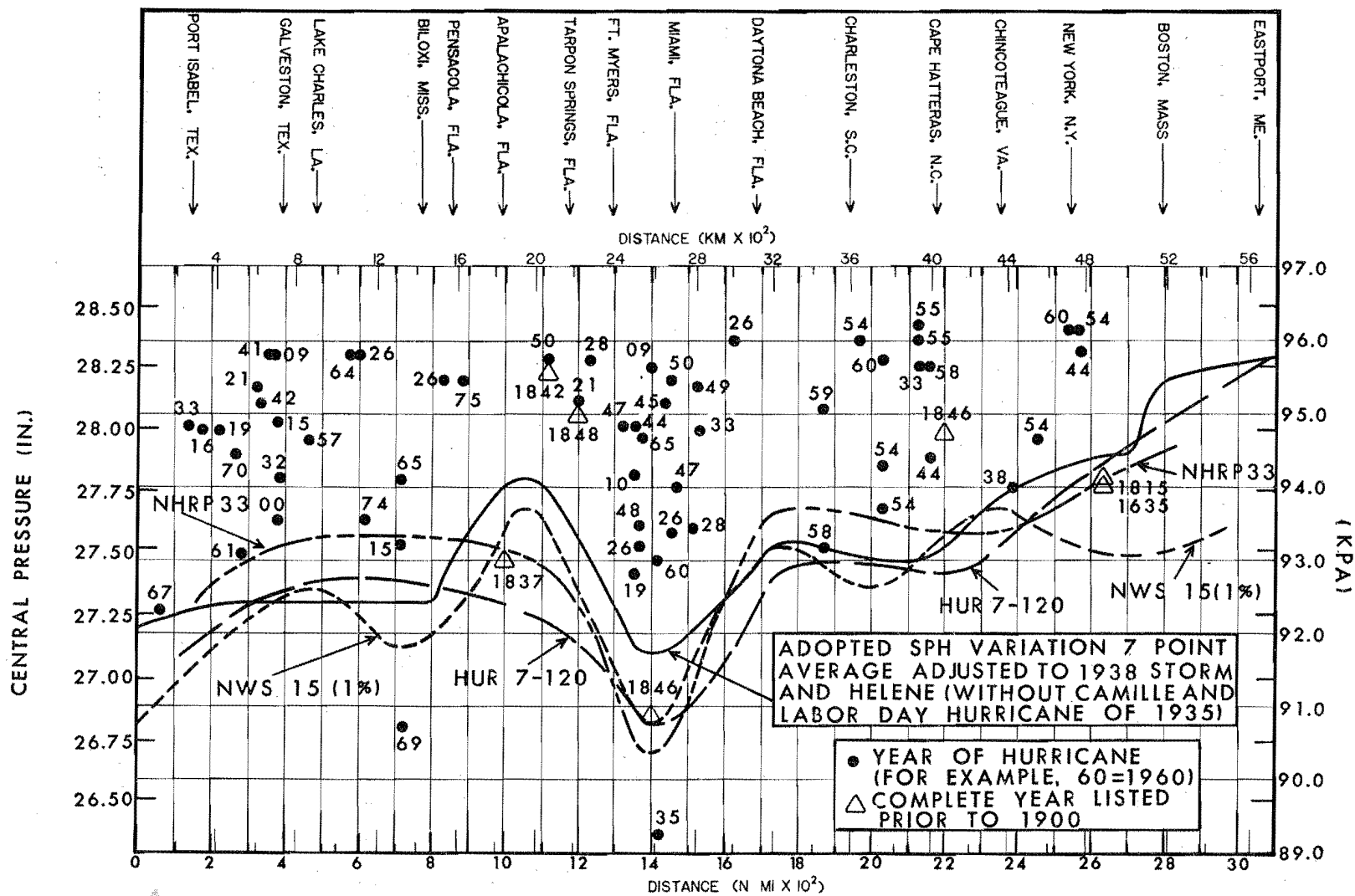
Figure 8.4.--Plot showing the adopted SPH p_o and p_o's from three previous studies. The adopted SPH p_o is a modified version of the unbroken curve in figure 8.3. The basic data set (1900-75) and observed and estimated historical p_o's prior to the 20th century are shown.

147

8.3   Central Pressure for the PMH

8.3.1   Introduction

We first summarize the lowest observed central pressure in the North
Atlantic and western North Pacific Oceans.   Then we determine a tropical
PMH sounding which is used in conjunction with equation 8.4 (one form of the
hydrostatic equation) to determine PMH p_o.

8.3.2   Lowest Observed P_o's

Over the North Atlantic, the lowest reported p_o, 26.35 in. (89.2 kPa), was
in the Florida Keys from the Labor Day hurricane of 1935.   The second lowest,
26.72 in. (90.5 kPa) occurred over the Gulf of Mexico more than 150 n.mi.
(278 km) south of the Mississippi coast near 25°N, 87°W, during hurricane
Camille (1969).

Over the North Pacific, the lowest reported p_o is 25.87 in. (87.6 kPa),
within the eye of typhoon June, in November 1975.   The second lowest is
25.90 in. (87.7 kPa) reported in both typhoon Ida, September 1958, and in
typhoon Nora, October 1973.   During the last 17 years (1961-77), seven other
typhoons have had p_o's lower than 26.35 in. (the lowest of record for North
Atlantic hurricanes).   These 10 typhoons occurred between late July and
mid-November.   All were south of the Florida Keys.

8.3.3   PMH P_o South of 25° N

8.3.3.1   Hydrostatic Approximation.   One way to estimate the lowest
probable p_o is to use the hydrostatic approximation to compute the surface
pressure in the eye of a hurricane which has certain physical characteristics
that can be optimized realistically.   The hydrostatic equation between the
vertical pressure force and the force of gravity is:

$$\frac{dp}{dz} = -\rho g,$$
(8.2)

where

  dp = incremental pressure

  dz = incremental height

  ρ = density of air

  g = acceleration of gravity

Another form of the hydrostatic equation:

$$\Delta\phi = 29.289 \ \overline{T}_v \ln \frac{P_L}{P_U} \qquad (8.3)$$

[adapted from Smithsonian Meteorological Tables (List 1951), p.203, using natural logarithms, instead of common logarithms].

where

$\Delta\phi$ = difference in geopotential (in geopotential meters) between p_L and p_U

$\overline{T}_v$ = mean adjusted virtual temperature (°K) [273°K = 32°F = 0°C]

p_L and p_U = pressures. p_L is the pressure at the lower surface of a layer and p_U is the pressure at the upper surface.

Computations of surface pressure in the eye of hurricanes are possible because we know that the eye is a vertical warm core. In his classical work, Haurwitz (1935) showed that subsidence of upper tropospheric air of high potential temperature is necessary to achieve the extremely low hydrostatic surface pressure inside the eye. The existence of this central core of subsidence and associated dry adiabatic warming is supported by high temperatures and an absence of significant clouds in the eye. Unusually warm dry eyes of hurricanes are almost always associated with intense or intensifying storms.

Malkus (1958) and Kuo (1959) have proposed that subsidence inside the eye may be explained by the presence of supergradient winds in the vicinity of the eye wall within R. Supergradient winds within the inner region of hurricanes have also been studied by Shea and Gray (1972). The outward acceleration that results from the supergradient winds produces a mean outward radial acceleration and a compensating sinking of air in the eye.

8.3.3.2 CONSTRUCTION OF TROPICAL PMH SOUNDING

The physical characteristics needed (not listed in order of importance) to compute the lowest p_o by using the hydrostatic approximation for the tropical North Atlantic are:

a. the lowest *reasonable* height of the 10 kPa (2.95 in.) level, which is the assumed height of the tropopause.

b. a distribution of temperature between 70 kPa (20.67 in.) and the tropopause somewhere between the dry adiabatic and the moist adiabatic but nearer to the latter, and an isothermal layer from 70 kPa to near the sea surface. The temperature near 70 kPa should be at least 86°F (30°C).

c. reasonably high moisture content in the column. Details now follow:

8.3.3.2.1 HEIGHT OF TROPOPAUSE. A hurricane is a system of inflow at low levels and outflow at high levels. In the inflow levels the pressure gradient must be directed inward and in the outflow levels mildly outward. Somewhere in transitioning from inward to outward there must be an approximately horizontal constant pressure surface. Various analyses, e.g., Willett (1955) indicate that the outflow region of a typical hurricane lies near 10 kPa (2.95 in.). This approximately horizontal constant pressure surface could also be deduced from the location of the tropopause. In the PMH, by deduction, the outflow level might be forced a little higher than in the average hurricane but would still be near 10 kPa because this layer cannot extend far into the stratosphere. The hydrostatic computation is not unduly sensitive to the exact pressure given the height chosen for the level surface and 10 kPa appears to be representative.

U.S. Weather Bureau Technical Paper No. 32 (Ratner 1957) lists average and extreme heights and temperatures at pressure levels from the surface to 1.5 kPa (0.44 in.) for the period 1946-55. Stations south of 26°N for which monthly data are published include Brownsville, Tex.; Havana, Cuba; Miami, Fla.; San Juan, Puerto Rico; and Isla del Cisne (Swan Island), Honduras (table 8.4).

We chose August as the month of greatest potential for the PMH because the Labor Day hurricane of 1935 and hurricane Camille (1969) both developed during August. We believe that a PMH could occur anytime between July and early October.

The lower the tropopause height, the lower the p_o when the hydrostatic approximation is used. To avoid compounding probabilities excessively, we decided to use an average height of the tropopause for the PMH p_o. The

Table 8.4.--August 10-kPa (2.95 in.) average heights (after Ratner 1957) during the period 1946-55

Station	Latitude (nearest degree)	Mean August 10-kPa height (gpm)	Max. August 10-kPa height (gpm)	Min. August 10-kPa height (gpm)	σ* (gpm)
Gulf coast					
Brownsville, Tex.	26°N	16632	16852	16472	54
Lake Charles, La.	30°N	16633	16761	16487	58
Burrwood, La.	29°N	16642	16880	16522	52
Tampa, Fla.	28°N	16629	16825	16418	57
East coast					
Miami, Fla.	26°N	16613	16776	16474	56
Charleston, S.C.	33°N	16644	16802	16520	49
Hatteras, N.C	35°N	16643	16832	16495	62
Interior southeastern United States					
Atlanta, Ga.	34°N	16637	16781	16474	48
Caribbean					
Havana, Cuba	23°N	16634	16761	16485	55
Isla del Cisne (Swan Island)	18°N	16586	16736	16416	49
San Juan, P. R.	18°N	16595	16764	16471	54

*σ = standard deviation of heights.

mean August 10 kPa (2.95 in.) Isla del Cisne height of 16,586 gpm* was used because it was the lowest mean of the five southernmost radiosonde stations listed by Ratner (1957).

8.3.3.2.2 DISTRIBUTION OF TEMPERATURE. Since we used the mean August 10 kPa (2.95 in.) Isla del Cisne height, we also used the corresponding 10 kPa mean August temperature ($\overline{T}$) of -74°C (-101.2°F). We did this because temperatures in the upper troposphere decrease with decreasing p_o [Gentry (1967) and Sheets (1969)], although via hydrostatic methods warmer temperatures yield lower p_o's.

The air temperature should be very warm and nearly isothermal from about 70 kPa (20.67 in.) down to near the sea surface. This is a pattern observed in extreme hurricanes and typhoons. We chose a temperature of 33°C (91.4°F). This is about 3°C (5.4°F) warmer than the warmest observed eye soundings at 70 kPa, e.g., typhoons Wilda (1964) and Nora (1973), and corresponds to a temperature ~ 1°C (1.9°F) warmer than the 99th percentile of the sea-surface temperature for the Florida Keys (U.S. Navy 1975). To obtain a temperature of 33°C (91.4°F), at 70 kPa, we warmed the air approximately dry adiabatically between 10 kPa (2.95 in.) where $\overline{T}$ = -74°C (-101.2°F) and 50 kPa (14.76 in.). We then warmed the air nearly moist adiabatically from 50 kPa where the temperature was set at 23°C (73.4°F) to 70 kPa. Warming near the moist adiabatic rate would result from lateral mixing of the descending air with cooler moist air originating in the convective eye wall. The evaporation of liquid water reduces the compressional warming and increases the humidity of subsiding air (Malkus 1958).

The sea-surface temperature (T_s) bounding the lower end of the tropical PMH sounding was chosen in the following way. Ninety-nine percent frequency levels of T_s (U.S. Navy 1975) were plotted along the gulf coast from southern Texas to the southern Florida coast. This consistently yielded

---

*A geopotential meter (gpm) results from a hydrostatic computation in which gravity is assigned a value of 9.8 m (32.2 ft) s^{-2} throughout the world at all elevations rather than its true value which varies slightly with location and elevation. The gpm is the international standard for computing heights from radiosonde observations.

temperatures between 89.0° and 89.5°F (31.7° and 31.9°C). We chose to use 89.5°F (~32°C) as the T_s, which allows the $\overline{T}$ to be 91.4°F (33.0°C), or about 2°F (~1°C) warmer than T_s.

8.3.3.2.3 MOISTURE CONTENT. Maximum persisting 12-hr dew points (T_d) used by the Hydrometeorological Branch of 78°F (25.6°C) to compute upper limits of rainfall rates reach 78°F (25.6°C) for much of the southeastern United States during the warmest months of the year. The 78°F T_d is set by higher T_s some distance offshore. Logic would lead us to believe that persisting 12-hr T_d close to the sea surface around the center of a PMH in the tropics cannot be less than 78°F. In addition, at any instant T_d values can be substantially higher than persisting 12-hr T_d's.

We are not assuming saturation at the eye center so the dew-point temperature at the eye center would have to be less than our assumed temperature of 91.4°F (33.0°C). We have decided to let the T_d = 82°F (27.8°C) between 85 kPa (25.10 in.) and the sea surface. This yields a mean relative humidity of about 75%. This is decreased slowly to 70% between 85 kPa and the top of the isothermal column or 70 kPa (20.67 in.). Further aloft relative humidity is decreased to 50% between 70 kPa and 50 kPa (14.76 in.), to 40% between 50 kPa and 40 kPa (11.81 in.) and to 5% between 20 kPa (5.91 in.) and 10 kPa (2.95 in.). Hawkins and Imbembo (1976) noted relative humidities falling under 50% at 65 kPa (19.19 in.) within the eye of hurricane Inez (1966). The mean relative humidities for the PMH in the Tropics are listed in table 8.5 along with $\overline{T}$ for seven layers of the troposphere. The mean relative humidities and $\overline{T}$ in table 8.5 were converted to $\overline{T}_v$ (List 1951).

We used the preceding criteria to construct our adopted Tropical PMH sounding shown on a pseudoadiabatic chart in figure 8.5. An actual hurricane sounding for Inez (1966) at maximum intensity (27.37 in., 92.7 kPa) south of Puerto Rico is shown for comparison. The Inez sounding is the most complete sounding obtained from a hurricane of such great intensity. A partial typhoon sounding to about 50 kPa (14.76 in.) is presented for typhoon Marge on August 15, 1951, at 0155 GMT (Simpson 1952). This sounding

Table 8.5.--Computation of p_0 for the tropical North Atlantic

10 kPa height of 16,586 gpm

[Isla del Cisne (Swan Island) - August mean]

Δp ($P_U - P_L$) (kPa)	$\overline{T}_v$ (°C)	$\overline{T}$ (°C)	$\overline{R.H.}$ (%)	$\Delta\phi$ (gpm)	Remarks
10 - 20	-56.5	-56.5	5	4399	20 kPa height 12187 gpm
20 - 30	-28	-28	20	2912	30 kPa height 9275 gpm
30 - 40	- 5.7	- 6	30	2253	40 kPa height 7022 gpm
40 - 50	+15.6	+14	40	1887	50 kPa height 5135 gpm
50 - 70	+31.7	+28	50	3004	70 kPa height 2131 gpm
70 - 85	+38.4	+33	70	1770	85 kPa height 361 gpm
> 85	+38.1	+33	75		

P_U = pressure at a specified upper level

P_L = pressure at a specified lower level

$\overline{T}_v$ = mean virtual temperature

$\overline{T}$ = mean temperature

$\overline{R.H.}$ = mean relative humidity

$\Delta\phi$ = difference between p_U and p_L (gpm)

°K = °C + 273.2°

$\Sigma = 16225$

$$\ln \frac{P_L}{P_U} = \frac{\Delta\phi}{29.289 \ (\overline{T}_v)}$$

$$\ln \frac{P_L}{85} = \frac{361 \ \text{gpm}}{29.289 \ (311.3 \ °K)}$$

$$\ln \frac{P_L}{85} = \frac{361}{9117.666} = .03959$$

$$\ln P_L = .03959 + \ln 85$$

$$\ln P_L = .03959 + 4.44265$$

$$\ln P_L = 4.48224$$

$$P_L = P_0 = 26.11 \text{ in.}$$
$$(88.4 \text{ kPa})$$
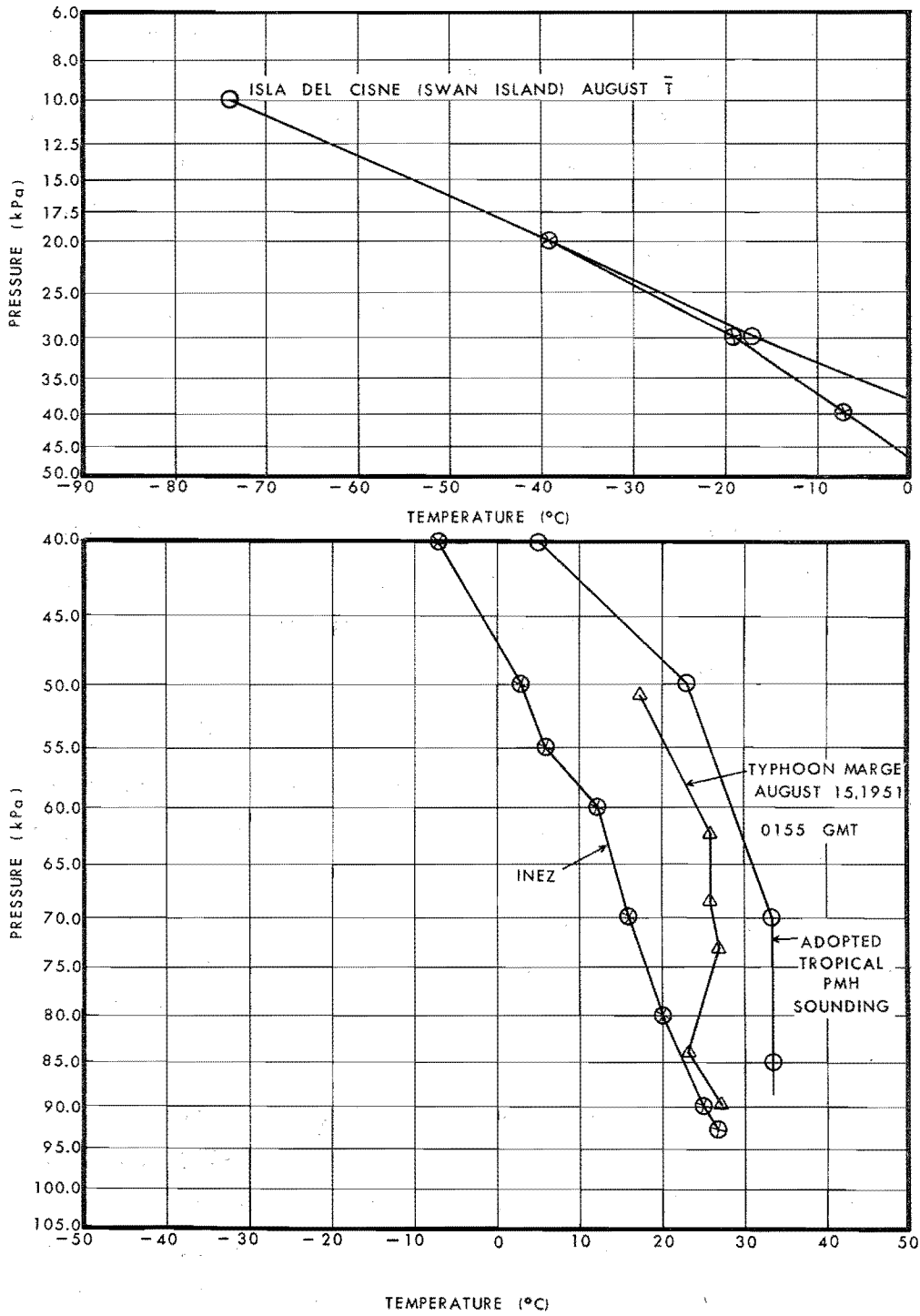
Figure 8.5.--Adopted tropical PMH sounding. Also shown are soundings for hurricane Inez (1966) and typhoon Marge (1951).

is considerably warmer than the Inez sounding and is one of the warmest
typhoon soundings on record. Marge's p_o was 26.43 in. (89.5 kPa).

8.3.3.3 CALCULATION OF P_o. Values of $\Delta\phi$ calculated from equation 8.3
for the upper six pressure layers are listed in table 8.5. Subtracting the
accumulating sum of the $\Delta\phi$'s from 16,586 gpm (assumed height of tropopause)
gives the height at the respective p_L's. Thus, in our computation, the
accumulated sum of $\Delta\phi$'s is 16,225 gpm at the 85-kPa (25.10-in.) level; the
85-kPa height is 361 gpm (16,586-16,225).

Now, if we wish to find the pressure at the surface of the sea, p_L, we
can rewrite equation 8.3 in the form:

$$\ln p_L = \frac{\Delta\phi}{29.289 \ \overline{T}_v} + \ln p_U \qquad (8.4)$$

The 85-kPa level becomes p_U, $\Delta\phi$ = 361 gpm, and $\overline{T}_v$ = 38.1°C (311.3°K).
Then $\ln p_L$ = 4.48224; p_L = 26.11 in. (88.4 kPa). Sensitivity of computed
p_o from soundings to changes in values of meteorological parameters is
covered in section 8.3.6.

8.3.3.4 COMPARISON OF COMPUTED PMH P_o WITH OTHER ESTIMATES

The Hydrometeorological Branch (U.S. Weather Bureau 1968) decided on a
value of 25.94 in. (87.8 kPa) for the PMH p_o based on a frequency approach
to the problem. Prior to this, the Hydrometeorological Branch (U.S.
Weather Bureau 1959b) made p_o computations using $\overline{T}_v$ from a saturated
moist adiabatic ascent around the eye from the surface to the 10-kPa
(2.95 in.) level with a corresponding dry adiabatic descent inside the eye.
Their computation gave a value near 26.00 in. (88.0 kPa).

We may also estimate a PMH p_o for the North Atlantic by looking at data
from the western North Pacific. Atkinson and Holliday (1977) have stated
that peripherial pressure (p_w) is normally about 0.295 in. (1 kPa) lower
over the western North Pacific than over the corresponding region of maxi-
mum tropical cyclone activity over the tropical North Atlantic. For the
tropical North Atlantic, if we used the PMH p_w of 30.12 in. (102.0 kPa) with
the lowest observed p_o of 26.35 in. (89.2 kPa), we have a pressure reduction
of 12.5%. Lowering the p_w 0.295 in. (1 kPa) to 29.82 in. (101.0 kPa) over

the western North Pacific and using the lowest observed p_o of 25.87 in. (87.6 kPa) gives a reduction of 13.3%. If we increase the pressure reduction of the North Atlantic from 12.5 to 13.3% our PMH p_o would equal 26.11 in. (88.4 kPa).

We believe that a hurricane in an optimum tropical environment for at least 36 hours could in that time equal the explosive deepening of typhoon Irma (1971) even though the tropical North Atlantic is smaller in size than the tropical western North Pacific. Irma deepened from 28.97 in. (98.1 kPa) to 26.10 in. (88.4 kPa) in 24.5 hours.

These considerations lend support to our estimate of PMH p_o, 26.11 in. (88.4 kPa), for the Florida Keys south of 25°N. North of 25°N, we will increase PMH p_o as described later in this chapter.

8.3.4 PMH P_o AT CAPE HATTERAS

Cape Hatteras was another location chosen for computing PMH p_o. This location is still far enough south to be in a subtropical environment *during a PMH situation*. We followed a procedure similar to that given for the tropical sounding (secs. 8.3.3.1 to 8.3.3.3). Table 8.6 lists the values of parameters used and figure 8.6 shows the PMH sounding (solid line) on a pseudoadiabatic chart. We calculate the PMH p_o at Cape Hatteras at 26.40 in. (89.4 kPa).

8.3.5 PMH P_o NEAR 45°N

8.3.5.1 FROM A SOUNDING. Since sea-surface temperatures (T_s's) at 45°N are too cool to nurture a PMH p_o the only recourse is to move a hurricane from south of Cape Hatteras at a fast forward speed, thereby avoiding excessive decay.

We computed a p_o at 45°N from a sounding in much the same way as we did for the Cape Hatteras sounding. The major difference in the sounding (fig. 8.6) is that we must make modifications for a nontropical environment. Such modifications lead to less confidence because they do not consider weakening effects caused by entrainment of ambient air into the eye, strong T_s gradients, and other factors. We therefore consider our computed p_o (table 8.7) as a lower limit for 45°N.

Table 8.6.—Computation of p_o for Cape Hatteras

10 kPa height of 16,643 gpm (August mean)

Δp ($p_U - p_L$) (kPa)	$\overline{T}_v$ (°C)	$\overline{T}$ (°C)	$\overline{R.\,H.}$ (%)	$\Delta\phi$ (gpm)	Remarks
10 - 20	−53	−53	5	4470	20 kPa height / 12173 gpm
20 - 30	−29.5	−29.5	20	2893	30 kPa height / 9280 gpm
30 - 40	− 8.2	− 8.5	30	2232	40 kPa height / 7048 gpm
40 - 50	+12.3	+11	40	1864	50 kPa height / 5184 gpm
50 - 71	+28.6	+25.5	50	3097	71 kPa height / 2087 gpm
71 - 85	+36.1	+31	75	1630	85 kPa height / 457 gpm
> 85	+35.8	+31	80		

p_U = pressure at a specified upper level

p_L = pressure at a specified lower level

$\overline{T}_v$ = mean virtual temperature

$\overline{T}$ = mean temperature

$\overline{R.H.}$ = mean relative humidity

$\Delta\phi$ = difference between p_U and p_L (gpm)

°K = °C + 273.2°

$\Sigma = 16186$

$$\ln \frac{p_L}{p_U} = \frac{\Delta\phi}{29.289\,(\overline{T}_v)}$$

$$\ln \frac{p_L}{85} = \frac{457}{29.289\,(309)}$$

$$\ln \frac{p_L}{85} = \frac{457}{9050.301} = .05050$$

$$\ln p_L = .05050 + \ln 85$$

$$\ln p_L = .05050 + 4.44265$$

$$\ln p_L = 4.49315$$

$$p_L = p_o = 26.40 \text{ in.} = (89.4 \text{ kPa})$$
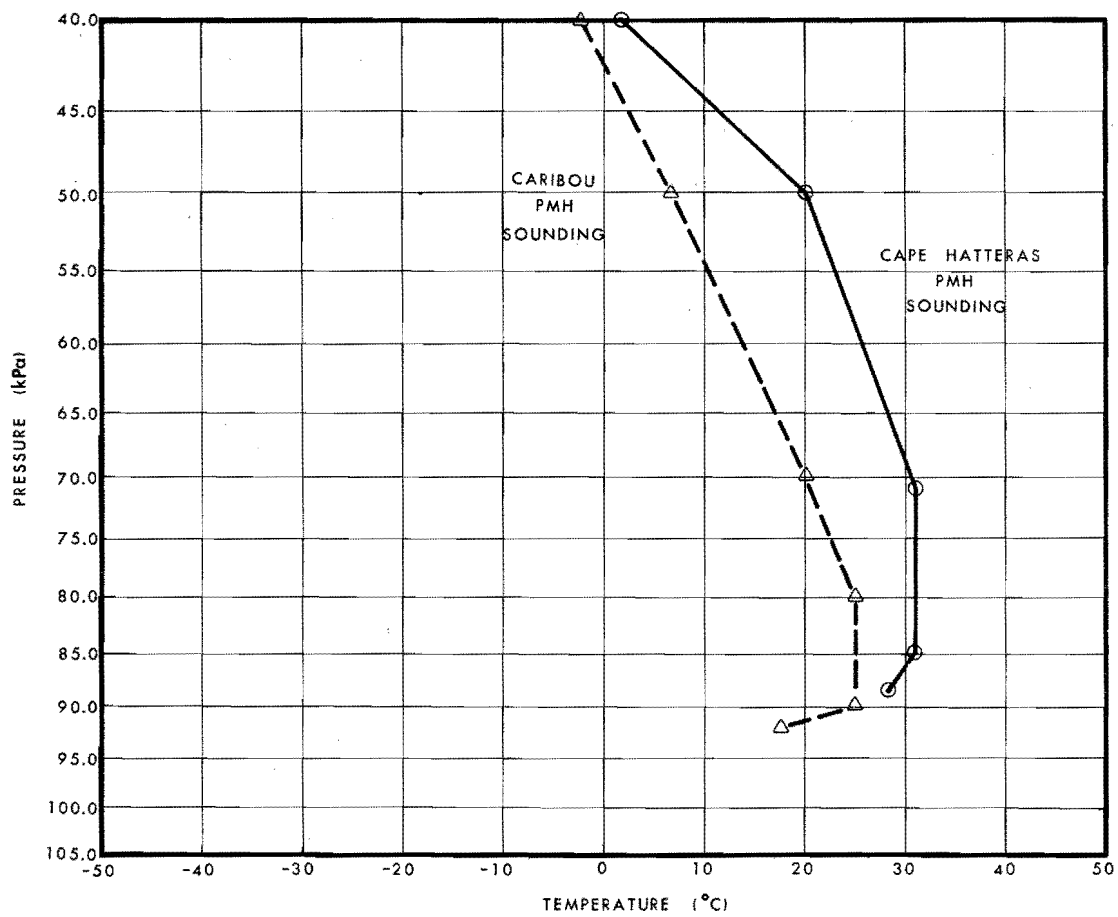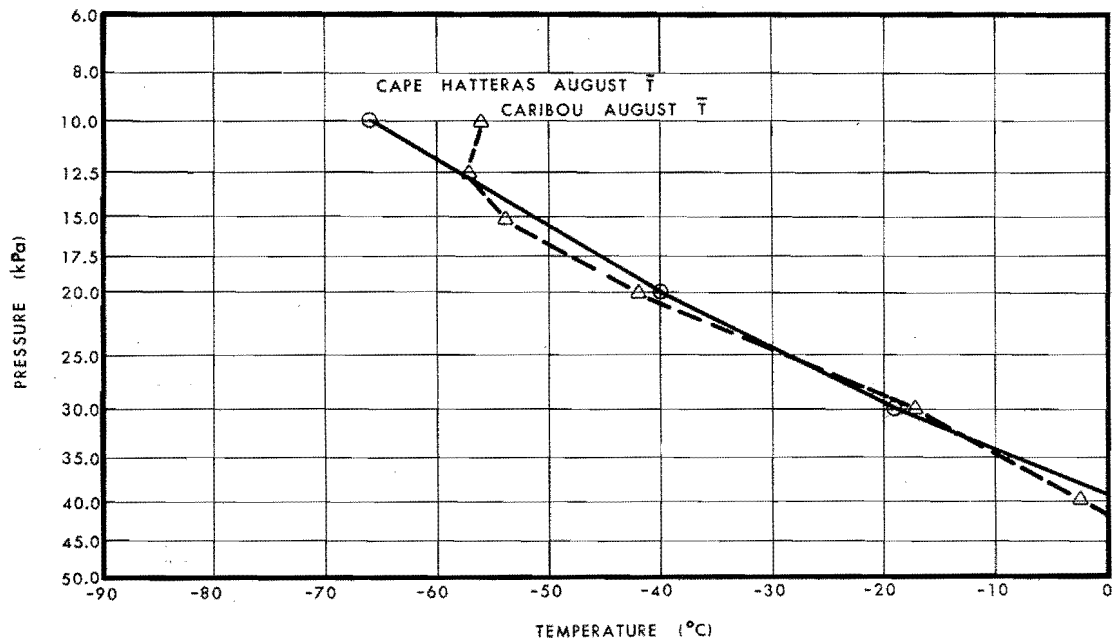
Figure 8.6.--Adopted PMH soundings for Cape Hatteras, N.C., and Caribou, Maine.

Table 8.7.--Computation of p_o for Caribou, Maine (applied to 45°N)

12.5 kPa height of 15,110 gpm (August mean)

Δp $(p_U - p_L)$ (kPa)	$\overline{T}_v$ (°C)	$\overline{T}$ (°C)	$\overline{R.\ H.}$ (%)	$\Delta\phi$ (gpm)	Remarks
12.5 - 15	-55.5	-55.5	0	1162	15 kPa height 13948 gpm
15 - 20	-48	-48	5	1883	20 kPa height 12065 gpm
20 - 30	-29.5	-29.5	25	2895	30 kPa height 9170 gpm
30 - 40	- 9.2	- 9.5	30	2207	40 kPa height 6963 gpm
40 - 50	+ 3.2	+ 2.5	40	1806	50 kPa height 5157 gpm
50 - 70	+14.9	+13.5	50	2838	70 kPa height 2319 gpm
70 - 80	+25.6	+22.5	75	1147	80 kPa height 1172 gpm
80 - 90	+28.6	+25	85	1041	90 kPa height 131 gpm
> 90	+24.4	+21.4	95		

$\Sigma = 14979$

p_U = pressure at a specified upper level

p_L = pressure at a specified lower level

$\overline{T}_v$ = mean virtual temperature

$\overline{T}$ = mean temperature

$\overline{R.H.}$ = mean relative humidity

$\Delta\phi$ = difference between p_U and p_L (gpm)

°K = °C + 273.2°

$$\ln \frac{p_L}{p_U} = \frac{\Delta\phi}{29.289\ (\overline{T}_v)}$$

$$\ln \frac{p_L}{90} = \frac{131}{29.289\ (297.6)}$$

$$\ln \frac{p_L}{90} = \frac{131}{8716.406} = .01503$$

$$\ln p_L = .01503 + \ln 90$$

$$\ln p_L = .01503 + 4.49981$$

$$\ln p_L = 4.51484$$

$$p_L = p_o = 26.98 \text{ in. } (91.4 \text{ kPa})$$

In constructing the sounding, we used data from Caribou (47°N) rather than two other New England radiosonde stations (Nantucket, 41°N and Portland, 43.5°N) because for the months of August and September, Caribou had the lowest tropopause heights and warmest temperatures (yielding lower p_o). We elected to use the August height rather than September because T_s's are highest off the Maine coast during this month. This height is near 12.5 kPa (3.69 in.), 15,110 gpm, rather than 10 kPa (2.95 in.) used for the other two soundings.

The values of parameters selected are given in table 8.7. The computed p_o is 26.98 in. (91.4 kPa).

8.3.5.2 FROM HISTORICAL STORMS. We studied storms north of 40°N along the Atlantic coast and those near Japan.

8.3.5.2.1 AFFECTING NEW ENGLAND, NOVA SCOTIA, AND NEWFOUNDLAND.

The two lowest p_o's along the New England coast since 1900 are listed in table 8.8. Record low p_o's from hurricanes affecting Sydney and Halifax (Nova Scotia) and Gander (Newfoundland) are also indicated. The p_o at Gander from Ione approximates the lowest p_o in that hurricane on the given date. The lowest p_o over Nova Scotia is undoubtedly lower than 28.63 in. (97.0 kPa) because the centers of Helene and the 1927 storm did not pass directly over Sydney nor Halifax.

The 27.86 in. (94.3 kPa) p_o along the Connecticut coast during the New England hurricane of 1938 is a record low p_o for New England from either a hurricane or winter-type storm. For Nova Scotia and Newfoundland, however, winter storms have had lower p_o's. Newfoundland has reported an all-time low p_o of 27.94 in. (94.6 kPa) and Nova Scotia 28.06 in. (95.0 kPa).

8.3.5.2.2 AFFECTING JAPAN. It is of interest to examine the lowest recorded p_o's from other midlatitude land areas other than the North American east coast. We used *Climatic Table of Japan, Part 3* (Japan Meteorological Agency 1972) to study p_o's over the western North Pacific. Table 8.9 lists these lowest p_o's from Japan occurring within designated 5° latitude bands. Comparing this table with table 4.1, we see that the Labor Day hurricane of 1935 (24.8°N) with a p_o of 26.35 in. (89.2 kPa) and

Table 8.8.--Lowest observed p_o's from New England, Nova Scotia and New-
foundland during hurricane passages.

Hurricane	Date	Lati-tude	p_o (in.)	p_o (kPa)	Place p_o recorded or estimated
		New England			
New England	Sept. 21, 1938	41.3°N	27.86	94.3	Just west of New Haven, CT
Edna	Sept. 11, 1954	41.7°N	28.05	95.0	Chatham, MA
		Nova Scotia			
Helene	Sept. 29, 1958	46.1°N	28.63	97.0	Sydney
---	Aug. 25, 1927	44.6°N	28.69	97.2	Halifax
		Newfoundland			
Ione	Sept. 22, 1955	49.0°N	28.26	95.7	Gander

Table 8.9.--Lowest observed p_o for selected latitude bands (Japan)

Latitude Band (°N)	p_o (in.)	p_o (kPa)	Date	Location and latitude
<25	26.82	(90.8)	Sept. 15, 1959	Miyakojima (24°47')
25-30	27.11	(91.8)	Sept. 15, 1961*	Naze (28°23')
30-35	26.92	(91.2)	Sept. 21, 1934	Murotchisaki (33°15')
35-40	27.68	(93.7)	Sept. 16, 1961*	Kyoto (35°01')
40-45	28.24	(95.6)	Mar. 18, 1912**	Nemuro (43°20')
>45	28.37	(96.1)	Sept. 17, 1961*	Wakkanai (45°25')

*Typhoon Nancy

**Extratropical cyclone

hurricane Camille while offshore (28.2°N) with a p_o of 26.81 (90.8 kPa) were
more intense than the typhoons of 1959 and 1961, respectively. Ho et al.
(1975) gave a p_o of 26.85 in. (90.9 kPa) for Camille north of 30°N, which is
lower than the typhoon of 1934. Tables 8.8 and 8.9 indicate that the New
England hurricane of 1938 (41.3°N) and hurricane Ione (49.0°N) were stronger
than any typhoons affecting Japan north of 40°N. Only between 35° and 40°N
has a p_o been recorded that was lower on land in Japan than along the U.S.
east coast.

8.3.5.3 FROM PREVIOUS ESTIMATES. The only earlier estimate of PMH p_o along the east coast near 45°N is 27.66 in. (93.7 kPa) (U.S. Weather Bureau 1968) based on an estimated 1000-yr return period p_o developed from extrapolation of observational data north of 38°N.

8.3.5.4 RECOMMENDED VALUE OF PMH p_o NEAR 45° N. The computed p_o for the PMH from a sounding based on the hydrostatic approximation is highly dependent on the assumptions that go into setting the sounding. For example, if the height of the 12.5 kPa (3.69 in.) level were raised 1 σ away from the mean height for Caribou (Ratner 1957) to 15,202 gpm, the computed p_o would increase from 26.98 in. (91.4 kPa) to 27.25 in. (92.3 kPa). It would not be too hard to raise the computed p_o to 27.46 in. (93.0 kPa) by revising the values of other input factors.

A p_o of 27.86 in. (94.3 kPa) has occurred near 41°N only once in this century and possibly twice before that (see sec. 8.2.4). We shall assume that a p_o lower than 27.86 in. could occur at 45°N.

We have decided to adopt 27.46 in. (93.0 kPa) as the PMH p_o at 45°N. This is a rounded metric value about halfway between the values from the sounding and the 1938 hurricane in New England.

8.3.6 SENSITIVITY OF ADOPTED PMH p_o COMPUTATIONS TO CHANGES IN INPUT FACTORS

Important to any computation of p_o from an assumed sounding is the sensitivity of the results to variations in the input factors. Such sensitivity tests were made for the adopted tropical and Cape Hatteras soundings. Results are shown in table 8.10.

The most important factor in table 8.10 is the temperature of the column in the layer between about 70 and 40 kPa (20.67 in. and 11.81 in.). In the lower portion of this layer, the lapse rate of temperature was assumed to be approximately equal to the moist adiabatic rate, and in the upper portion, the dry adiabatic rate was approximated. For the tropical sounding, we chose to reduce the $\overline{T}_v$ in this layer by 4.9°F (2.7°C) from 74.7°F (23.7°C) to 69.8°F (21.0°C). This is the $\overline{T}_v$ if we connect the temperatures near 70 and 40 kPa with a straight line, thereby bypassing the temperature shown at 50 kPa (14.76 in.) in figure 8.5. The lower $\overline{T}_v$ raises our tropical PMH p_o

Table 8.10.--*Sensitivity of computed PMH* p_o *to changes in input factors*

| Input factor | Tropical sounding p_o = 26.11 in. (88.4 kPa) | | Cape Hatteras sounding p_o = 26.40 in. (89.4 kPa) | |
	Change in value	Δp_o	Change in value	Δp_o
1. Height of tropopause	$\pm \sigma$ = 49 gpm	$\pm$ 0.15 in. ($\pm$ 0.48 kPa)	$\pm \sigma$ = 62 gpm	$\pm$ 0.19 in. ($\pm$ 0.62 kPa)
2. Temperature at tropopause	$\pm \sigma$ = 4.5°F (2.5°C)	$\pm$ 0.08 in. ($\pm$0.28 kPa)	$\pm \sigma$ = 5.0°F (2.8°C)	$\pm$ 0.09 in. ($\pm$ 0.30 kPa)
3. Height and temperature at tropopause	+ σ (item 1) - σ (item 2)	+ 0.22 in. (+ 0.75 kPa)	+ σ (item 1) - σ (item 2)	+ 0.27 in. (+ 0.91 kPa)
	- σ (item 1) + σ (item 2)	- 0.22 in. (-0.75 kPa)	- σ (item 1) + σ (item 2	- 0.27 in. (- 0.91 kPa)
4. Cooling the column between 40 and about 70 kPa	$\overline{T}_v$ for column from 74.7°F (23.7°C) to 69.8°F (21.0°C)	+ 0.21 in. (+ 0.70 kPa)	$\overline{T}_v$ for column from 68.9°F (20.5°C) to 64.8°F (18.2°C)	+ 0.19 in. (+ 0.62 kPa)
5. Relative humidity	Lowered 10% below 50 kPa and 20% above 50 kPa	+ 0.11 in. (+ 0.36 kPa)	Lowered 10% below 50 kPa and 20% above 50 kPa	+ 0.09 in. (+ 0.29 kPa)

from 26.11 in. (88.4 kPa) to 26.32 (89.1 kPa). The reduced $\overline{T}_v$ results in only about a 1% change in p_o.

In our computations we used a mean August height for the tropopause. If the values are normally distributed, approximately 2/3 of them will be within $\pm \sigma$ of the mean value. A variation of the tropopause height by this amount results in a less than 1% change in p_o.

The sensitivity tests shown in table 8.10 indicate that by using $\pm \sigma$ from the mean August tropopause heights and temperatures our estimate of PMH p_o could be too high or too low by as much as 0.22 in. (0.75 kPa). The indicated changes in items 4 and 5 would increase not lower PMH p_o.

We did not add changes in item 4 to those of item 3 to raise p_o even more. Although meteorologically realistic, such an approach would raise the p_o of the tropical sounding to a level higher than what was observed at Long Key, Florida Keys, in September 1935. For the Cape Hatteras sounding, which used the same technique of construction, we believe the effect of adding changes in items 3 and 4 together would also underestimate the PMH p_o. Adding changes of items 3 and 5 or 4 and 5 would also underestimate PMH p_o for both locations.

8.3.7 GENERALIZED ALONGSHORE VARIATION OF P_o FOR THE PMH

8.3.7.1 EAST COAST. The tropical PMH p_o of 26.11 in. (88.4 kPa) is applied south of 25°N (milepost 1400) and the p_o of 26.40 in. (89.4 kPa) at Cape Hatteras, near milepost 2180. Between these two points we increased the p_o in proportion to the decrease in sea-surface temperatures (T_s) at the 99% level along the east coast (fig. 8.7). We are not implying a dynamical relation between the T_s and minimum p_o, but are using observational data which have shown that the lower the T_s the higher the p_o, everything else being equal. Between Cape Hatteras and 45°N (near Eastport, Maine), a first approximation to the coastal variation of p_o was obtained by increasing p_o in proportion to the decrease in T_s at the 99% level.

A modification to this general procedure was made between mileposts 2550 (near New York City) and milepost 2700 (near Martha's Vineyard). Here T_s indicated p_o should rise faster than the adopted variation shown in
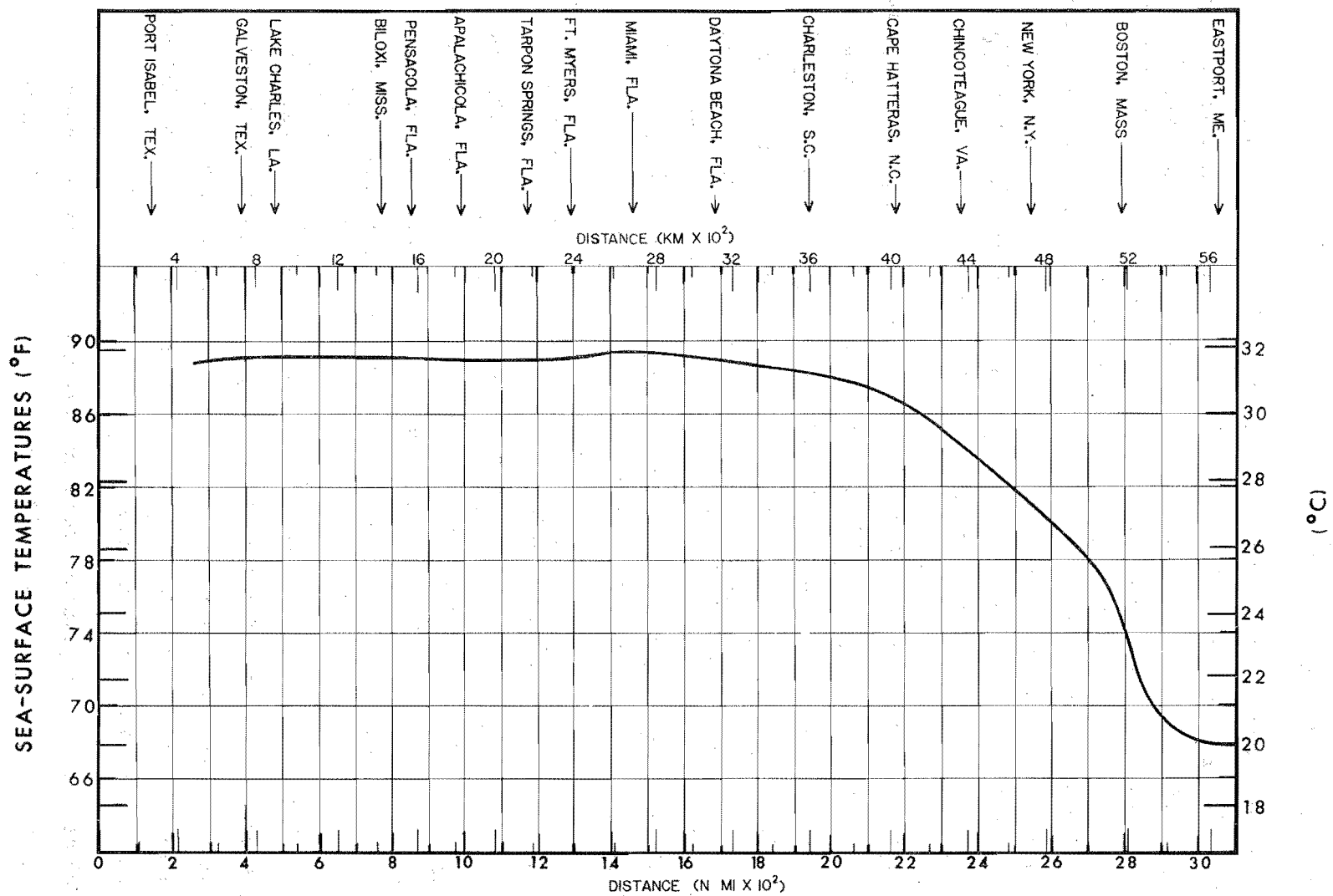
Figure 8.7.--99th percentile sea-surface temperatures along the gulf and east coasts.

figure 8.8. We did not accept a faster rate of increase because of the nearly east-west orientation of the coast in this region.

Figure 8.8 shows data for all storms with p_o <28.05 in. (95.0 kPa) [including estimated pressure readings from historical data prior to the turn of this century (table 8.3)]; the adopted p_o curve; and the curve from HUR 7-97 (U.S. Weather Bureau 1968). The p_o data are plotted using the same format as used in figures 8.2 to 8.4. PMH p_o tabular data for the east coast are presented in chapter 2.

8.3.7.2 GULF COAST. All the 10-kPa (2.95 in.) August mean heights along the gulf coast are lower than the height at Cape Hatteras, implying that PMH p_o along the gulf coast is less than that at Cape Hatteras. T_s (99th percentile) is also warmer everywhere in the Gulf of Mexico than at Cape Hatteras, also implying a lower PMH p_o along the gulf coast. This suggests a range of PMH p_o along the gulf coast somewhere between the 26.11 in. (88.4 kPa) p_o computed from the tropical sounding and the 26.40 in. (89.4 kPa) p_o computed at Cape Hatteras.

In contrast, the PMH p_o's for the Texas coast should be slightly higher than similar latitudes (26°-30°N) along the east coast because comparable 10 kPa (2.95 in.) heights are higher over the western gulf than along this portion of the east coast (see table 8.4).

Figure 8.7 also shows the 99% level of T_s for the gulf coast. From the middle Texas coast (milepost 300) to the Florida Keys (milepost 1400), T_s has a small range [between 89.0°F (31.7°C) and 89.5°F (31.9°C)].

8.3.7.2.1 NORTHEAST GULF COAST. Reasons for PMH p_o being higher along the northeastern gulf coast than anywhere else in the gulf are:

a. The influence of the Florida peninsula (see sec. 8.2.4). In order for the PMH to enter near normal to the coast at full intensity, it would have to be a recurved storm yielding a p_o higher than if the Florida peninsula did not exist and it had not recurved; (see sec. 8.3.7.2.1.2).

b. The difficulty of gaining entrance to the *concave* coast without weakening.

c. Observational data and analysis suggest a higher p_o; (see fig. 8.8).

PORT ISABEL, TEX.

GALVESTON, TEX.

LAKE CHARLES, LA.

BILOXI, MISS.

PENSACOLA, FLA.

APALACHICOLA, FLA.

TARPON SPRINGS, FLA.

FT. MYERS, FLA.

MIAMI, FLA.

DAYTONA BEACH, FLA.

CHARLESTON, S.C.

CAPE HATTERAS, N.C.

CHINCOTEAGUE, VA.

NEW YORK, N.Y.

BOSTON, MASS

EASTPORT, ME.

DISTANCE (KM X 10²)

CENTRAL PRESSURE (IN.)

(kPa)

U.S. WEATHER BUREAU, PMH (1968)

ADOPTED PMH CURVE

PRELIMINARY PMH CURVE

LEGEND

● YEAR OF HURRICANE (FOR EXAMPLE, 60 = 1960)
△ COMPLETE YEAR LISTED PRIOR TO 1900

DISTANCE (N MI X 10²)

Figure 8.8.—Plot showing the adopted PMH p_o, a preliminary p_o for the eastern Gulf of Mexico and the p_o from a study completed in 1968. The basic data set (1900-75) and observed or estimated historical p_o's prior to the 20th century are shown.

8.3.7.2.1.1 PRELIMINARY P_O. One would expect the PMH p_o near milepost 1100 to be higher than the PMH p_o of 26.21 in. (88.8 kPa) along the east coast at the same latitude (milepost 1700) because mean 10 kPa (2.95 in.) heights are higher over the Gulf of Mexico during the warmer part of the year. Yet, the milepost 1100 p_o should be lower than the PMH p_o at Cape Hatteras (26.40 in. or 89.4 kPa) because of higher heights at Cape Hatteras. The PMH p_o at Burrwood, La. (near milepost 700), based on 10 kPa height considerations (table 8.4) should be about 26.22 in. (88.8 kPa). A slightly higher PMH p_o farther east based on slightly cooler T_s yields a p_o of about 26.25 in. (88.9 kPa) which is 0.04 in. (0.1 kPa) higher than east coast PMH p_o near milepost 1700.

We set the PMH p_o near milepost 1100 at 26.25 in. (88.9 kPa) *before considering recurvature and subsequent filling considerations*. The dropoff in p_o southward from near milepost 1100 to the Florida Keys (see preliminary PMH curve fig. 8.8) is consistent with the dampening effect of the peninsula.

8.3.7.2.1.2. DETERMINATION OF FINAL P_O. The northeastern gulf coast near milepost 1100 will have higher PMH p_o than the 26.25 in. (88.9 kPa) indicated above. The Florida peninsula prevents an extreme steady state hurricane from entering a coastal area centered near milepost 1100 from the east through south. Also, intense storms moving from the north are not meteorologically realistic. Therefore, the PMH over this part of the northeastern gulf must be a recurved hurricane. We assume based on the discussion which follows that this recurved PMH will also be filling.

During a survey of 256 typhoons, which will follow, we found that 94 recurved with a p_o $\leq$29.00 in. (98.2 kPa). Eighty-nine of these storms either recurved while filling or deepened with a p_o >27.46 in. (93.0 kPa)-- the upper limit of PMH p_o for the east coast.

Riehl (1972) states "virtually all typhoons reached their peak intensity at or a little before the point of recurvature and subsequently decrease at some variable rate."

Point of recurvature is defined as the point where the θ of the storm just exceeds 180° (movement from just west of due south). For all practical

purposes point of recurvature may be considered to equal 180° for a recurving storm moving from 180° for less than a few hours.

The hurricane data show the trend for larger p_o's for recurving storms. Only two of them approach the severity of the PMH. One of these, the Labor Day hurricane of 1935, recurved west of Cedar Key after it had filled about 2 in. (~7 kPa) in 36 hours. Camille (1969), the other storm, did not recurve until after she made landfall along the Mississippi coast. Janet (1955), an extreme hurricane (27.00 in., 91.4 kPa) over the western Caribbean, did not recurve. Another extreme western Caribbean hurricane (Nov. 1932) did recurve after reaching a minimum p_o of 27.01 in. (91.5 kPa) but its filling rate is not known. Hattie (1961), still another extreme western Caribbean hurricane, followed an unusual track. After moving northward for a couple of days, she turned *westward* and devastated the country of Belize 1 day after attaining a minimum p_o of 27.17 in. (92.0 kPa).

To estimate the p_o along the coastal section under discussion (Florida panhandle to Cape Sable), we shall analyze the filling rates of recurved typhoons, and assume the results can be applied to hurricanes. There is no apparent reason why there would be a difference in filling rates in the western North Pacific and North Atlantic.

Chin (1972) evaluated reconnaissance eye-fix typhoon data gathered by aircraft of the U.S. Air Force and U.S. Navy for the period 1961-70. He summarized positions of all typhoons for this 10-year period by month, date and 6-hourly synoptic time, and gave values of sea-level p_o. The location and the p_o of the typhoons are often estimates. The positions are based on the best storm track produced by the Royal Observatory, Hong Kong. If available, the two fixes before and the two after each synoptic hour were used to interpolate coordinates for intermediate times. When data were not quite so abundant, Chin estimated positions only if there was at least one fix less than 12 hours from a synoptic hour. Weighting factors were also introduced by Chin to allow for time differences between the fixes and the reference hour. We made extensive use of Chin's data and raw data extracted from the *Annual Typhoon Reports* (U.S. Dept. of Defense 1971-74) in determining filling rates for typhoons.

We categorized all typhoons during the 14-yr period (1961-74), using 10 years of Chin's data and 4 years of typhoon reports, with the aim of identifying the filling rates of intense typhoons that had recurved. In order to do this, we started with all 256 typhoons during this period, not just those near the coasts of Japan, Taiwan, and the Philippines.

Figure 8.9 gives a schematic summary of these 256 typhoons. Sixteen were discarded because their p_o was >29.00 in. (98.2 kPa)--a p_o considered to be too high throughout this report for PMH guidance. Of the 240 remaining typhoons, 137 were discarded because they moved from an easterly direction for their entire lives prior to striking the Asian Mainland and, therefore, were not considered to have recurved. Another nine typhoons were rejected because they moved from the south or southwest from inception. The lowest p_o for these nine was 27.64 in. (93.6 kPa). After throwing out the last two groups of typhoons we were left with 94 that recurved before reaching the mainland. Of these 94, 76 had a p_o at the time of recurvature that was >27.76 in. (94.0 kPa)--a relatively high p_o about 1.65 in. (5.6 kPa) higher than the p_o for the PMH in tropical regions and not considered favorable for further study. This left 18 typhoons still under consideration. We determined that 15 of these 18 were affected appreciably by colder T_s, colder and drier air associated with extratropical weather systems, stalling, and/or filling interrupted by deepening within 24 hours of the point of recurvature. Only three typhoons [Nancy (1961), Violet (1961) and Trix (1971)], or about 1% of the original sample, remained to provide possible guidance to a PMH filling rate after recurvature. Data for these three typhoons are shown in table 8.11.

Violet had a relatively high p_o at the time of recurvature (compared to Nancy and Trix) but gave us some support. Trix had an incomplete p_o record following recurvature but helped substantiate pertinent findings. Nancy turns out to be the best typhoon to work with since it met all the following criteria:

a. extremely intense at the time of recurvature;

b. moved over a small sea-surface temperature gradient;
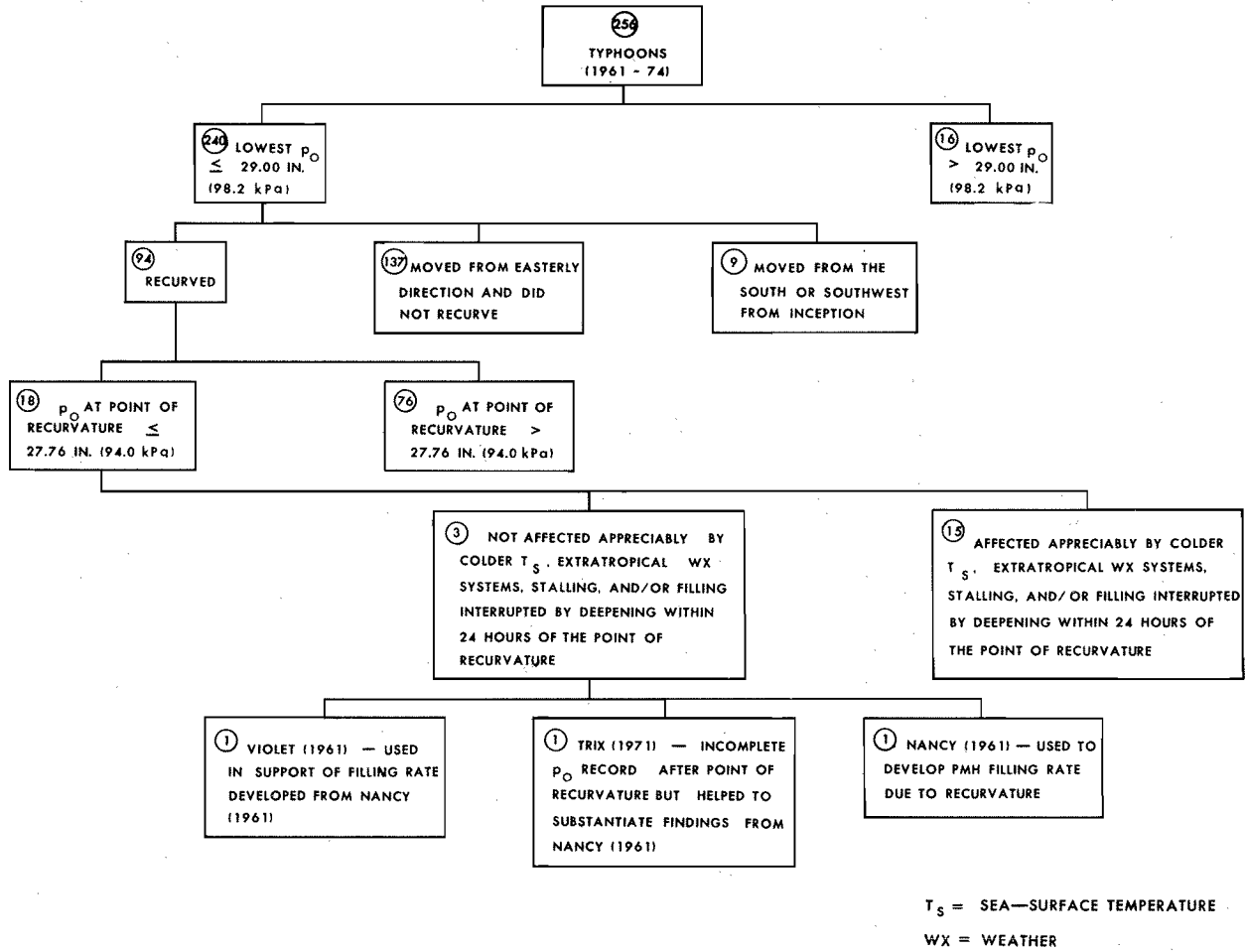
Figure 8.9.--Schematic summary of typhoons used for guidance on filling rate of PMH after recurvature over the northeast gulf coast.

Table 8.11.--Smoothed typhoon data used as guidance to recurvature filling [after Chin (1972) and U.S. Dept. of Defense 1961-74].

Date	Hour (GMT)	Lat. (°N)	Long. (°E)	P_0 (in.)	P_0 (kPa)
Typhoon Nancy (Sept. 1961)					
13	00	18.7	132.2	26.28	89.0
13	06	19.7	131.3	26.16	88.6
*13	08	20.0	131.1	26.05	88.2
13	12	20.7	130.7	26.13	88.5
13	18	21.9	129.8	26.40	89.4
13	22	22.7	129.7	26.64	90.2
14	00	23.1	129.2	26.67	90.3
14	06	24.8	128.9	26.70	90.4
14	12	26.2	128.8	26.78	90.7
**14	15	26.7	128.7	26.84	90.9
14	18	27.2	128.8	26.90	91.1
15	00	28.2	129.1	27.05	91.6
15	04	28.7	129.6	27.17	92.0
15	06	29.2	129.9	27.17	92.0
15	12	30.0	130.8	27.20	92.1
Typhoon Violet (Oct. 1961)					
7	06	20.1	140.8	26.10	88.4
* 7	07	20.3	140.7	26.04	88.2
7	12	21.2	140.0	26.10	88.6
7	18	22.0	139.2	26.49	89.7
8	00	22.8	138.7	26.90	91.1
8	04	23.4	138.3	27.05	91.6
8	06	23.8	138.0	27.08	91.7
8	12	25.0	137.3	27.20	92.1
8	18	26.3	136.9	27.34	92.6
** 8	22	27.3	136.7	27.46	93.0
9	00	27.8	136.8	27.58	93.4
9	06	29.4	137.0	27.94	94.6
9	12	31.3	137.7	28.23	95.6
9	18	33.7	138.8	28.56	96.7
10	00	35.8	140.0	28.73	97.3
10	06	38.5	142.0	28.85	97.7
Typhoon Trix (Aug. 1971)					
28	19	29.4	130.3	27.20	92.1
28	22	29.5	130.2	27.05	91.6
*29	00	29.6	130.1	26.99	91.4
29	04	29.8	130.0	27.02	91.5
29	07	30.2	130.0	27.05	91.6
**29	09	30.5	130.0	27.11	91.8
29	12	30.7	130.3	-	-

*Lowest central pressure
**Point of recurvature (movement from west of south begins)

c. moved through Gulf of Mexico latitudes;

d. remained tropical in character;

e. did not fill unevenly (sinusoidally);

f. traveled near the middle of the range of specified PMH forward speeds for the Gulf of Mexico (chapter 10).

The lowest p_o in typhoon Nancy was 26.05 in. (88.2 kPa), fig. 8.10a, near 20.0°N, 131.1°E, at about 0800 GMT September 13, 1961. At the time of recurvature, 31 hours later, her p_o was 26.84 in. (90.9 kPa). Nancy moved to 26.7°N over *mean monthly* T_s of 84° to 83°F [28.9° to 28.3°C (U.S. Navy 1969a)] during these 31 hours. During the succeeding 21 hours Nancy, still possessing tropical characteristics, moved 230 n.mi. (426 km) to 30°N [T_s = 82°F (27.8°C)] at an average speed of 11 kt (20 km/hr), while filling 0.36 in. (1.2 kPa) to 27.20 in. (92.1 kPa). The rate of filling after this is not known accurately, but we do know that about 36 hours after recurvature, Nancy's p_o stood at 27.68 in. (93.7 kPa) at Kyoto, Japan (35°N) where Nancy was becoming extratropical.

Figure 8.10a depicts the filling of Nancy from the time of lowest p_o. This figure clearly shows a 14-hr period ending about 2200 GMT September 13, 1961, when Nancy filled quite rapidly (section a of curve). We theorize that this rapid filling [0.60 in. (2.0 kPa) in 14 hours] was an "internal adjustment" to the slightly cooler T_s [falling below 84°F (28.9°C)] Nancy was passing over. We speculate [based not only on

Figure 8.10a.--*Variation of central pressure with time, typhoon Nancy (1961).*

Nancy but other typhoons including Dot and Violet (1961), Bess (1965), Irma (1971), and Ida (1972)] that a very intense steady state typhoon (hurricane) will begin to fill when the T_s drops below about 84°F (~29°C). Such an internal adjustment is shown for typhoon Violet in figure 8.10b.

Nancy's rate of filling following recurvature (0.36 in., 1.2 kPa/21 hours) shown by section c of figure 8.10a, is due partly to the fact that she was moving over a slight mean monthly T_s gradient of <2°F (~1°C). The additional filling evident in section c compared to section b (time between the internal adjustment termination and the point of recurvature) is most likely a result of recurvature. We assume that the overall filling rate indicated by section b of 0.20 in./17 hr (0.7 kPa/17 hr) between 2200 GMT September 13 and 1500 GMT September 14 would have continued if Nancy had not

Figure 8.10b.--Variation of central pressure with time, typhoon Violet (1961).

recurved. Such a filling rate would result in a 0.25 in. (0.8 kPa) increase in p_o during the next 21 hours ending at 1200 GMT September 15. In other words, we are saying that 0.11 in. (0.4 kPa) of the 0.36 in. (1.2 kPa) filling in 21 hours, or about one-third, results from recurvature.

We examined typhoon Violet (table 8.11). Violet's filling rate is shown in figure 8.10b. At the time of recurvature (about 2200 GMT October 8, 1961) her p_o was 27.46 in. (93.0 kPa). Violet's lowest p_o was 26.04 in. (88.2 kPa), 39 hours earlier. Her internal adjustment filling rate (sec. a of curve) was 0.86 in. (2.9 kPa) in 17 hours or, 0.71 in. (2.4 kPa) in 14 hours (compared to Nancy's 0.60 in., 2.0 kPa, in 14 hours). Thus, Violet's internal adjustment filling rate was greater than Nancy's. During the 22 hours between the end of the internal adjustment and the time of recurvature (sec. b of curve) Violet filled 0.56 in. (1.9 kPa). This is again a much faster rate than Nancy's comparable rate (section b, fig. 8.10a). Violet's p_o at 0600 GMT October 10 would have been about 28.26 in. (95.7 kPa) had the filling rate of 0.56 in./22 hours continued without

interruption. However, Violet filled at a much faster rate (sec. c of curve) than the above to 28.85 in. (97.7 kPa) at 0600 GMT October 10. Violet's assumed filling rate due to recurvature was 0.59 in. (2.0 kPa) in 32 hours or, comparing with Nancy, 0.39 in. (1.3 kPa) in 21 hours—over three times as fast. We would certainly not want to adopt such a fast filling rate after recurvature for the PMH in the northeastern Gulf of Mexico.

We mentioned earlier that Trix (1971), table 8.11 (the last of the three typhoons selected for guidance) had an incomplete p_o record following recurvature. Trix's filling rate prior to recurvature, however, of 0.12 in. (0.4 kPa) in 9 hours to 27.11 in. (91.8 kPa) is close to Nancy's 0.20 in. (0.7 kPa)/17 hr filling rate prior to recurvature. This correspondence lends support to the assumed filling rate for Nancy.

For the PMH in the Gulf of Mexico, we have adopted Nancy's filling rate (0.11 in./21 hours or about 0.4 kPa/21 hours) to adjust from a PMH p_o near 25°N with a track direction >190° to coastal p_o near milepost 1100.

This angle (190°) is 10° greater than the angle defining the point of recurvature and is the maximum value of track direction allowed a PMH over all areas except the northeast Gulf of Mexico; (see chapter 11).

Before we can determine the PMH p_o near milepost 1100, we need to delineate PMH tracks into the Florida west coast. We cannot pattern these tracks after the Labor Day hurricane of 1935 because it recurved too close to land and filled rapidly. Camille did not recurve and apparently was *not* too close to land (Florida peninsula) since she filled <0.15 in. (0.5 kPa) between 25° and 30°N. The problem is that we do not know how close "too close" is. We will blend two assumed PMH tracks into the Camille track (which extended across the gulf from extreme western Cuba to Bay St. Louis, Miss.) (fig. 8.11). These two tracks enter the northern portion of the west Florida coast after passing through the Yucatan Channel, thereby avoiding the west coast of Cuba. One track, labeled 8, is perpendicular to the coastline near milepost 1100 and the other track, labeled 9, is perpendicular to the Florida coastline between Cape Sable and Tampa Bay even though it is shown entering the coast near milepost 1170. The latter track is shorter than a track would be if drawn perpendicular to the coastline

at milepost 1170. Tracks 8 and 9 are
sample tracks shown to give the user
a feel for what a PMH track over the
northeastern Gulf of Mexico might
look like. We realize that a PMH
could follow tracks slightly dif-
ferent from those in figure 8.11.
The lengths of the two tracks to the
coast *from the time θ exceeds 190°*
are about 280 n.mi. (~520 km).

If we move the PMH at the same
speed as typhoon Nancy (11 kt,
20 km/hr) it would take about 25.5
hours to reach the coast after
recurvature and using Nancy's
filling rate would fill approxi-
mately 0.13 in. (0.4 kPa). This

Figure 8.11.--Likely paths of the PMH
into northeastern gulf coast. Also
shown is a portion of the Camille
(1969) storm track.

would yield a p_o of 26.38 in. (89.3 kPa) because the PMH p_o before consider-
ing recurvature has already been set at 26.25 in. or 88.9 kPa (sec.
8.3.7.2.1.1). If the PMH moved at its upper limit of 20 kt (37 km/hr) in
this region (chapter 10), it would fill about 0.07 in. (0.2 kPa) in the
14 hours required to travel the 280 n.mi. (~520 km). The p_o near milepost
1100 is then 26.32 in. (89.1 kPa).

8.3.7.2.1.3 FINAL P_o. Higher p_o in this concave portion of the Florida
coast means adjoining coastal reaches will be affected. Near milepost 700
at Burrwood, La., we have left the theoretically-derived p_o (26.22 in.,
88.8 kPa) unchanged. From there eastward, it is raised to a peak of
26.32 in. (89.1 kPa) northwest of milepost 1100. The increase in p_o is slow
at first, becoming steeper between mileposts 900 and 1000. The p_o near Cape
Sable, Fla. (fig. 8.8), remains unchanged (26.12 in., 88.5 kPa). North-
northwestward up to the coast, PMH p_o rises slowly to 26.16 in. (88.6 kPa)
at Fort Myers and then more rapidly to nearly 26.28 in. (89.0 kPa) at Tampa.

Figure 8.8 shows p_o data including values estimated from historical data readings prior to the turn of this century, the adopted PMH p_o curve and the curve from HUR 7-97 (U.S. Weather Bureau 1968). The PMH p_o tabular data are presented in chapter 2.

8.4   COMPARISON OF SPH AND PMH PRESSURE DROP

Now that we have SPH p_o and PMH p_o, it would pay to look at the pressure drop $(p_w - p_o)$ relation between the SPH and PMH. A comparison is particularly needed since the p_o's were derived using different methods.

Figure 8.12 shows Δp for the PMH (top curve) and the SPH (bottom curve). The curves are separated by as much as 1.80 in. (6.1 kPa) northwest of mile-post 1100 and as little as 1.15 in. (3.9 kPa) at milepost 3100. The difference between the curves from milepost 0 to 2700 ranges from 1.36 in. (4.6 kPa) near mileposts 0 and 1400 to 1.80 in. (6.1 kPa).

The rather rapid dropoff in the PMH Δp between mileposts 2700 and 2800 is attributed to the inability of the PMH north of Cape Cod to maintain itself over the colder water of that area. The SPH, being a weaker storm, has a higher p_o to begin with; it does not lose strength as rapidly in this area.

There is a relative minimum in Δp for the SPH between mileposts 1700 and 1900. The fact that the coast in this area does not intersect the tracks of severe hurricanes of record is the probable cause of this small minimum. This dip is not present on the PMH curve because there are no theoretical reasons for having a noticeably weaker PMH in this area. In other words, for the SPH, lower Δp in this area is reasonably characteristic of record storms whereas the potential for the most extreme event (the PMH) remains.

Along the gulf coast, the two Δp curves are similar with minimum values of Δp over the northeastern gulf coast. In other words, observations used in determining the SPH curve back up the more theoretical arguments employed in developing the PMH curve.
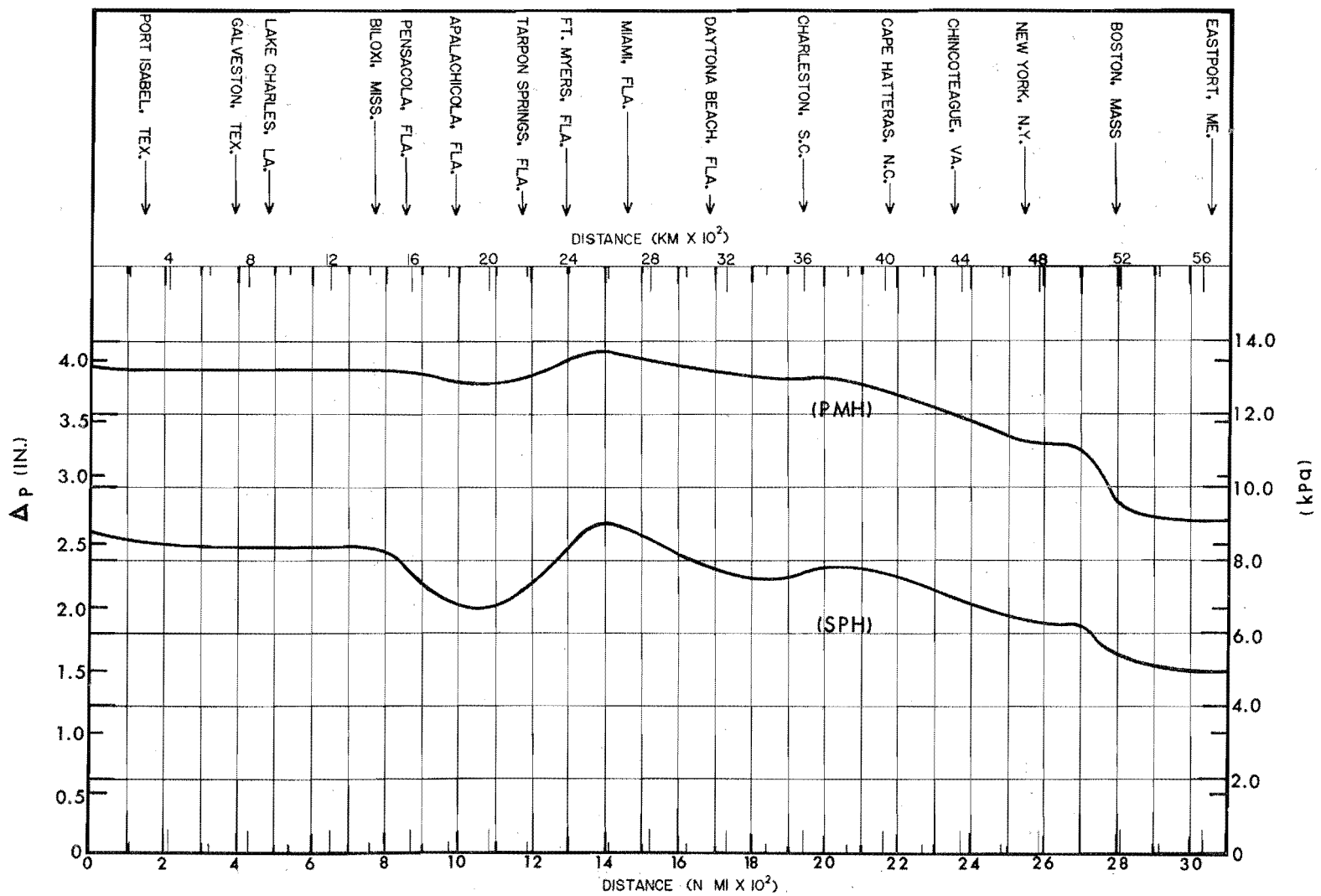
Figure 8.12.—Comparison of pressure drop (Δp) for the PMH and SPH.

9. RADIUS OF MAXIMUM WINDS

9.1 INTRODUCTION

The radius of maximum winds (R) is the radial distance from the hurricane center to the band of strongest winds within the hurricane wall cloud, just outside the hurricane eye. It is used as a measure of the lateral extent or size of hurricanes and is one important factor in the generation of storm surge. The peak surge that a hurricane can produce is dependent upon R, other factors being held constant. The larger the R the larger the surge until a critical value of R is reached; thereafter, the peak surge decreases with increasing R (Jelesnianski and Taylor 1973). This critical value of R (for peak surge generation) for a hurricane of given intensity is a function of the storm's forward speed (T) and track direction (θ) relative to the coast. It also varies with the width and steepness of the continental shelf and the curvature of the coast.

A hurricane that is both large and intense would have enormous destructive power. Myers (1954) applied a kinetic energy evaluation to coastal hurricanes and found an inverse relation between size (R) and intensity (p_o). An analysis of hurricane R vs p_o in NOAA *Technical Report* NWS 15 (Ho et al. 1975) also showed this inverse relation. The two hurricanes of record (Labor Day hurricane of 1935 and Camille) with central pressure below 26.87 in. (91.0 kPa) had well-formed vortices associated with small R's.

9.2 DATA

Values of R at or near the time of lowest p_o within 150 n.mi. (278 km) of the coast for record hurricanes are given in tables 4.1 to 4.4. In addition, data from western North Pacific typhoons were used in this study. These data are listed in tables 4.5 and 4.6. We also made use of studies on typhoon eye diameter by Ito (1962) and Bell (1974).

9.3 RANGE IN R FOR THE SPH

Figure 9.1 shows the R observed in hurricanes with p_o <28.35 in. (96.0 kPa) plotted along the gulf coast at the coastal location closest to the point
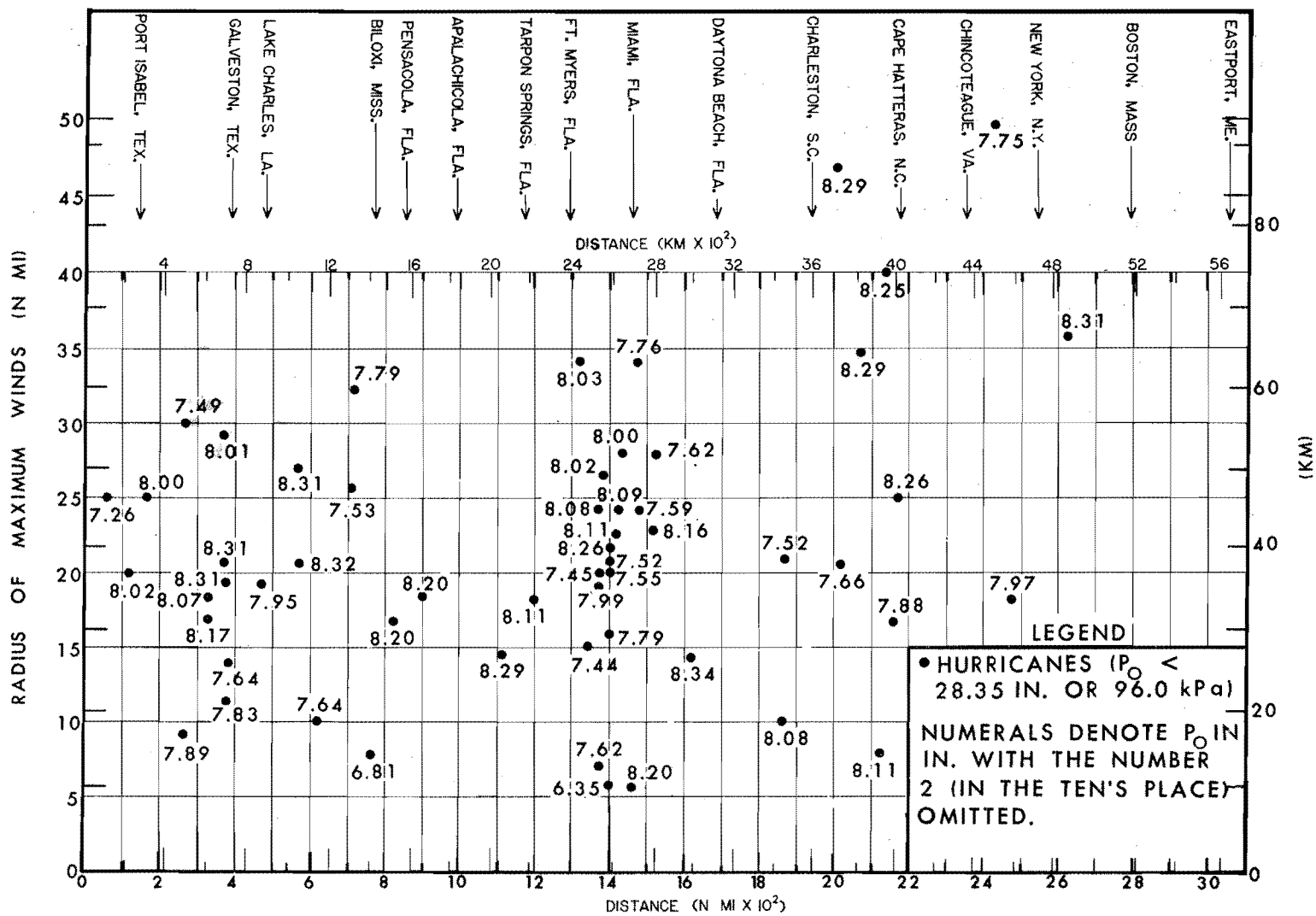
Figure 9.1.--Radius of maximum winds for hurricanes with central pressure <28.35 in. (96.0 kPa) listed beside each data point.
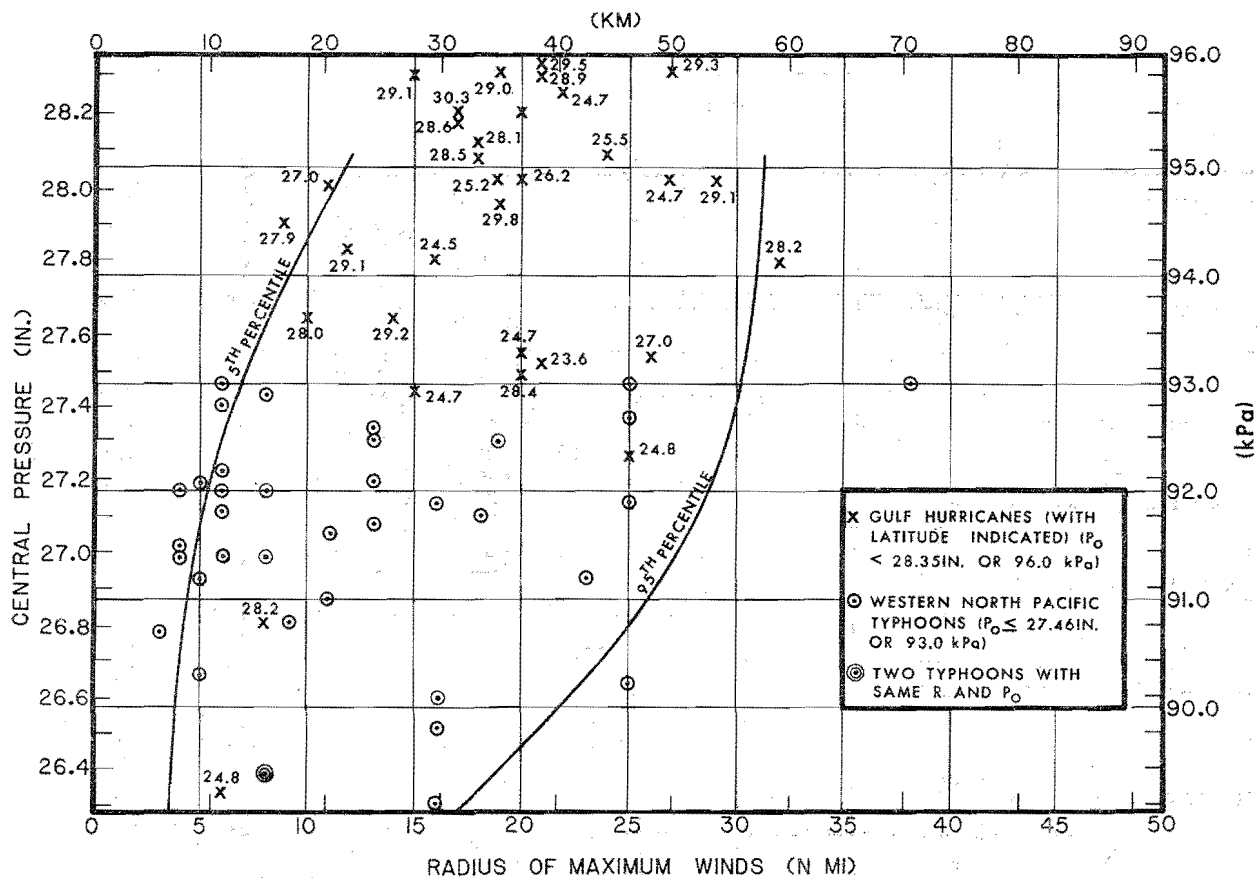
Figure 9.2a.--Variation of radius of maximum winds (R) with central pressure
for western North Pacific typhoons and gulf coast hurricanes. Solid lines
are smoothed curves joining the 5th and 95th percentiles of R. Latitude
of gulf coast hurricanes is also indicated.

where p_o was observed and along the east coast at the latitude where p_o was
observed. Data observed near the Florida Keys are plotted along milepost
1400.

Values of R for intense typhoons [$p_o \leq 27.46$ in. (93.0 kPa)] of the west-
ern North Pacific for the period 1960-74, and gulf coast hurricanes [p_o
<28.35 in. (96.0 kPa)] since 1900 are plotted against p_o in figure 9.2a.
Figure 9.2b is a similar plot of the same typhoon data and east coast hurri-
canes. In both of these figures the latitude of each hurricane location is
given. The diagrams reveal that for extreme storms [$p_o \leq 26.58$ in. (90.0
kPa)] the largest observed R is 16 n.mi. (30 km). An extreme R of 50 n.mi.
(93 km) was observed in the New England hurricane of 1938 [$p_o = 27.75$ in.
(94.0 kPa)].
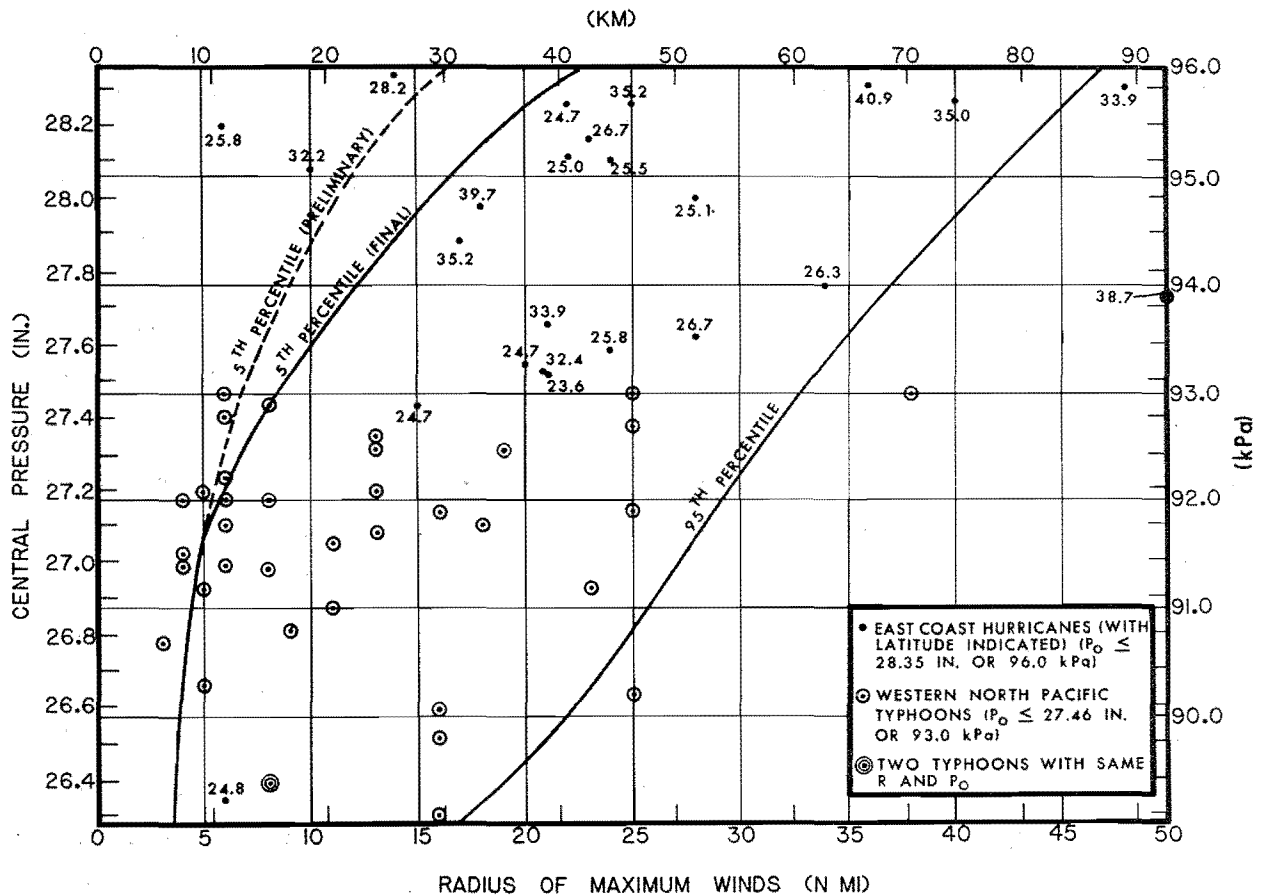
Figure 9.2b.--Variation of radius of maximum winds (R) with central pressure for western North Pacific typhoons and east coast hurricanes. Solid lines are smoothed curves joining the 5th and 95th percentiles of R. Dashed portion of the 5th percentile curve is a preliminary curve which does not reflect the increase in R with latitude shown by the solid curve.

Percentiles of R occurrences with hurricanes and typhoons were determined for selected p_o intervals. These selected intervals are: p_o <27.08 in. (91.7 kPa); <27.76 in. (94.0 kPa); p_o between 27.46 and 28.05 in. (93.0 to 95.0 kPa); and p_o between 27.76 and 28.35 in. (94.0 to 96.0 kPa).

Several small R values are reported in typhoons with p_o <27.08 in. (91.7 kPa). The R's in these typhoons were given less weight than that given gulf hurricanes when calculating the 5th percentile values in figure 9.2a because these p_o's are lower than that of the SPH. Gulf hurricanes and typhoons were given equal weight when we determined the 95th percentiles. The 5th and 95th percentile curves shown on figure 9.2a are drawn through the calculated values.

184

A nearly similar procedure was followed for the east coast hurricane and typhoon data. The outermost curves of fig. 9.2b, the 5th and 95th percentiles of east coast hurricanes and typhoons, do not reflect variations with latitude. Generally speaking, the R's observed in hurricanes in northerly latitudes are larger than those of southerly latitudes. The analysis discussed in chapter 5 supports this contention (see sec. 5.3.2.2). Therefore, the hurricanes north of 38°N were analyzed separately. Data for this region are scarce, so Carol (1954) and Donna (1960), table 4.2, with p_o's of 28.38 in. (96.1 kPa) were added to the sample. The solid portion of the 5th percentile curve above about 27.08 in. (91.7 kPa) includes hurricanes north of 38°N and takes into account the increase in R with latitude. The 95th percentile curve was unaltered by the separate analysis north of 38°N.

We have adopted the 95th percentile curves of figures 9.2a and 9.2b for the upper limit to values of R for the SPH for the gulf and east coasts. The lower limit of R comes from the 5th percentile curves of these figures. The 5th percentile curve used for the east coast is the one modified for latitude. The limited latitudinal range for the gulf coast suggested an adjustment for latitude was not required. This is supported by plots (not shown), of R vs. ψ for hurricanes in the Gulf of Mexico.

By entering figures 9.2a and 9.2b with SPH p_o (chapter 8), we obtain the range in R for the entire coast. The results are shown in figure 9.3. This figure also includes the hurricane R data from figure 9.1 plotted again along the gulf coast at the coastal location closest to the point where p_o was observed and along the east coast at the latitude where p_o was observed.

The upper and lower limits of R shown in figure 9.3 give the permissible range at all points of interest on the open coast. Any value within this range may be considered to be characteristic of an SPH at a given location. As indicated earlier, a critical R may vary with a combination of other factors.

Our results for larger R's may be compared with other studies that list the frequency of eye diameters of typhoons. Since the maximum winds of intense hurricanes are observed within the eye wall, we may approximate R from the eye diameter (Shea and Gray 1972). This distribution of eye
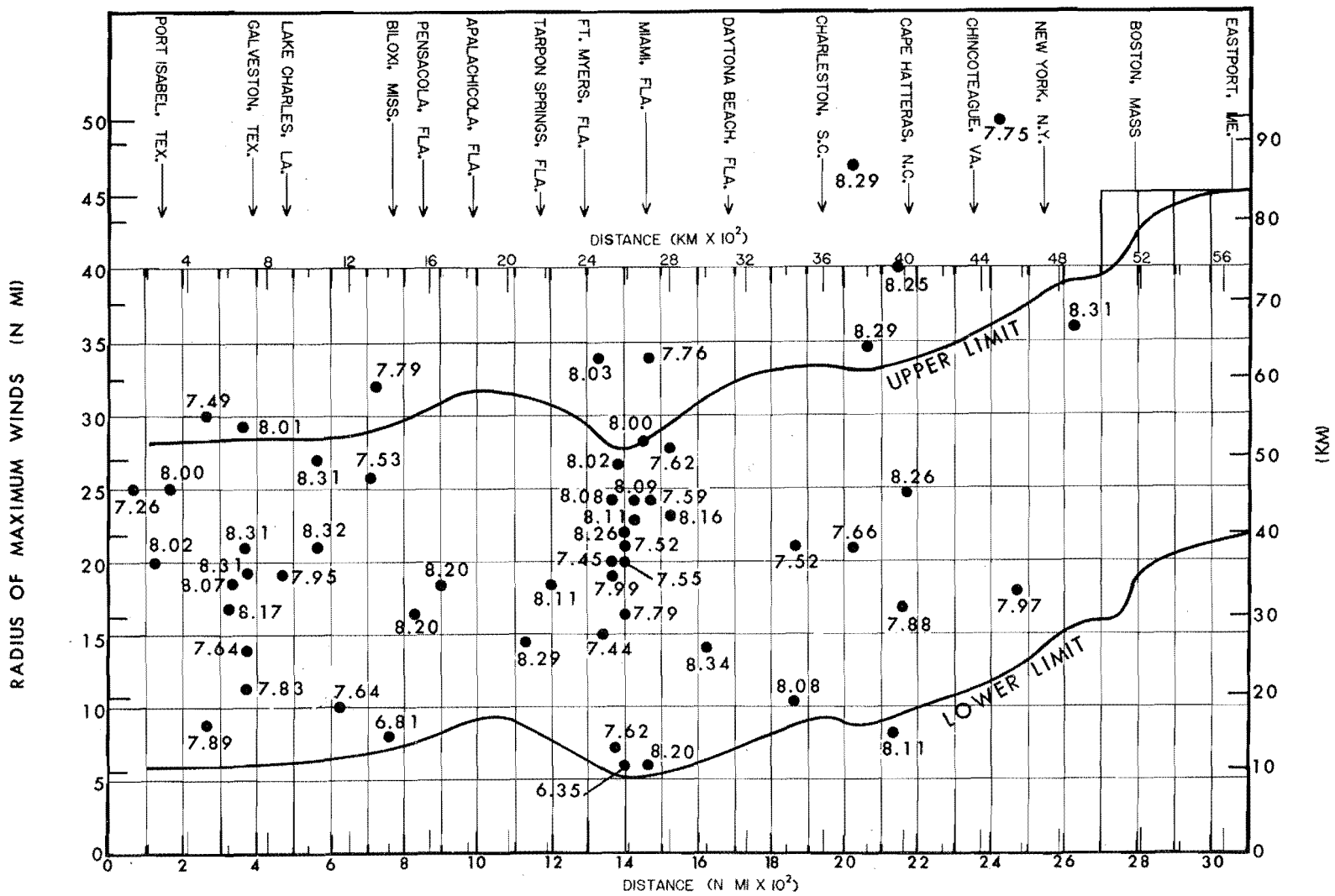
Figure 9.3.--Adopted upper and lower limits of radius of maximum winds for the SPH. Data are identical to that in figure 9.1.

diameters for the period 1958-68 (Bell 1974), gives a 95th percentile level of 38 n.mi. (70 km). Dividing by two and multiplying the result by 0.25 gives an approximate R of 24 n.mi. (44 km). This is for typhoons with p_o <27.76 in. (94.0 kPa). Another researcher (Ito 1962) gave the frequency distribution of eye diameters in typhoons for the period 1950-61. This 95th percentile R for typhoons having p_o ≤27.17 in. (92.0 kPa) is 34 n.mi. (63 km). Dividing by two and multiplying the result by 0.25 gives an approximate R value of 21 n.mi. (39 km). Our data show a 95th percentile R of 30 n.mi. (56 km) for hurricanes and typhoons having p_o <27.76 in. and 25 n.mi. (46 km) for hurricanes and typhoons having p_o ≤27.17 in.

9.4 RANGE IN R FOR THE PMH

The determination of the range in R for the PMH must use a different approach compared to the method just described for the SPH because of the limited number of storms with extreme values of p_o. The two hurricanes with p_o less than 26.87 in. (91.0 kPa) were observed along the northern gulf coast and over the Florida Keys. Both of these extreme hurricanes had small R's.

9.4.1 LOWER LIMIT OF R FOR THE PMH

The existence of a central core and spiral cloud bands associated with converging low-level inflow currents are well known phenomena in tropical cyclones. In a study of the dynamics of tropical cyclone eye formations, Kuo (1959) showed that there exists a limiting radius beyond which the converging current cannot penetrate. This agrees with the observations of a calm near the center and maximum winds some distance away at R. The converging current, which reaches its maximum speed at the limiting radius (R_{lim}), must therefore turn upward and then outward at upper levels. The surface defined by these innermost streamlines is identified as the eye wall.

Kuo has estimated R_{lim} as a function of other variables. His formula is:

$$R_{lim} = \left[\left(\frac{1-\beta}{2-\beta}^1 \; fr_o^{2-\beta} \right) \Big/ V_{max} \right]^{\frac{1}{1-\beta}} \qquad (9.1)$$

where, R_{lim} = limiting radius of maximum winds

   f   = coriolis parameter

r_o = an outer radius from which inflow air starts with negligible momentum relative to the earth.

V_{max} = maximum wind at R_{lim}.

β = fraction of tangential component of momentum generated in the inflow layer, between r_o and R_{lim}, that is dissipated by surface stress.

β^1 = a similar coefficient expressing stress opposition to coriolis force.

Kuo made computations to show the effects of various friction factors. A β of 0.5 and a β^1 of 0.4 give the smallest R_{lim}. The β value of 0.5 is comparable to the magnitude of frictional effects implicitly expressed in the Hydromet gradient wind equation 9.4. These small R_{lim} values are comparable to small R values observed in western North Pacific typhoons. We
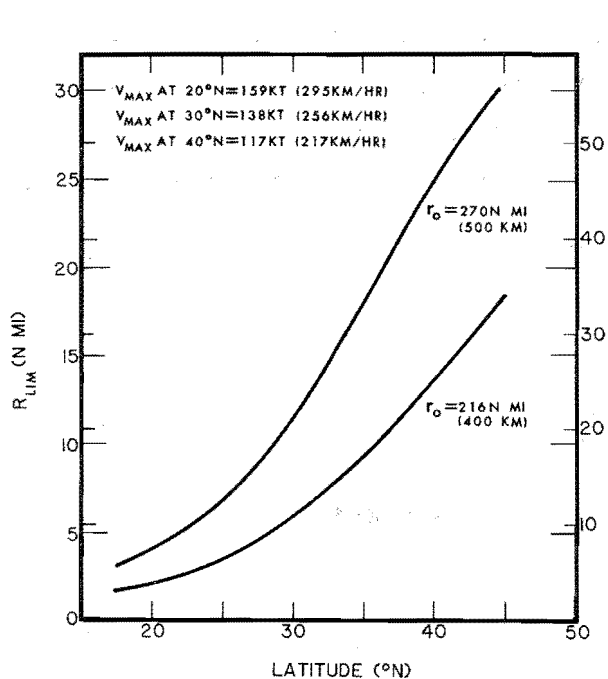
Figure 9.4.--Latitude vs. R_{lim}. The two curves are computed from equation 9.1 (after Kuo 1959).
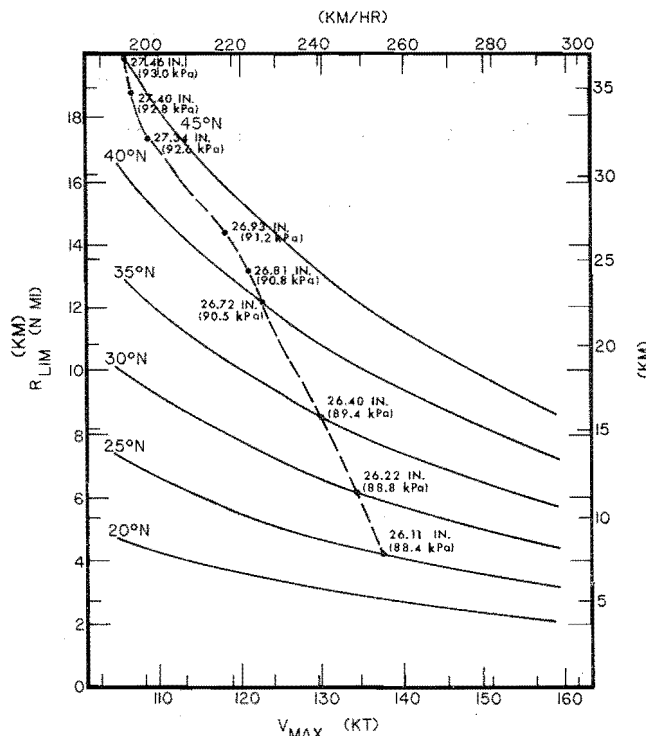
Figure 9.5.--V_{max} vs. R_{lim}. Dashed line determines R_{lim} computed from PMH p_o at selected latitudes using equations 9.1 and 9.4 and an r_o of 216 n.mi. (400 km).

assumed V_{max} values of 159, 138, and 117 kt (295, 256 and 217 km/hr) at latitudes 20°, 30° and 40°N, respectively, and then obtained the variation of R_{lim} with latitude for r_o's of 270 n.mi. (500 km) and 216 n.mi. (400 km). These variations are shown in figure 9.4. The two curves indicate the combined effects of V_{max} and latitude on R_{lim} for a storm of fixed r_o. The diagram also reveals the variation with r_o, i.e., a storm with a smaller r_o would have a smaller R_{lim} than one with a larger r_o. Hereafter, we will make use of an r_o of 216 n.mi. (400 km). In order to lend support to this choice, we approximated r_o for the Labor Day hurricane of 1935 and Camille (1969) by letting r_o be the closest distance p_w is to the center of each hurricane. For the Labor Day storm, r_o is slightly more than 300 n.mi. (556 km) and for Camille, r_o is about 180 n.mi. (334 km).

In estimating R_{lim} for the PMH, whose intensity is defined in terms of p_o, it is necessary to establish the variation of R with respect to p_o; (see sec. 9.1). This can be accomplished by applying a wind-pressure relation at various latitudes. Since the coriolis parameter (f) is a constant at a given latitude, and if we prescribe $\beta = 0.5$ and set r_o and β, to any arbitrary constant, R_{lim} in equation 9.1 can be expressed as a function of V_{max}:

$$R_{lim} = \frac{constant}{V_{max}^2} \qquad (9.2)$$

Since V_{max}^2 varies with Δp we have:

$$R_{lim} = \frac{constant}{\Delta p} \qquad (9.3)$$

The relation between Δp and V_{max} is obtained from the gradient wind equation:

$$V_{gx} = K (p_w - p_o)^{1/2} - \frac{Rf}{2} = V_{max}, \qquad (9.4)$$

$$where \quad K = \left(\frac{1}{\rho e}\right)^{1/2}; \quad e \approx 2.71828$$

A small R of 10 n.mi. (19 km) and p_w of 30.12 in. (102.0 kPa) for the PMH were used in the computations of V_{gx}. Values of K are derived in chapter 12.

On figure 9.5 we show computed points relating V_{max}, latitude, PMH p_o and R_{lim} that were computed from equations 9.1 and 9.4. The smoothed curve (dashed line), joining these points, gives the variation of R_{lim} with latitude for the PMH. This is adopted as the R_{lim} for the PMH.

9.4.2 UPPER LIMIT OF R FOR THE PMH

Figure 9.6 shows the variation of R with respect to p_o for the western North Pacific typhoons and gulf and east coast hurricanes with $p_o \leq 27.46$ in. (93.0 kPa) for the typhoons and 27.76 in. (94.0 kPa) for the hurricanes. The solid line envelops the largest observed or estimated R's of the typhoons and east coast hurricanes. Large R for gulf coast hurricanes were much smaller than those for east coast hurricanes and typhoons and had no effect in determining this line. The dashed line intersecting the lower
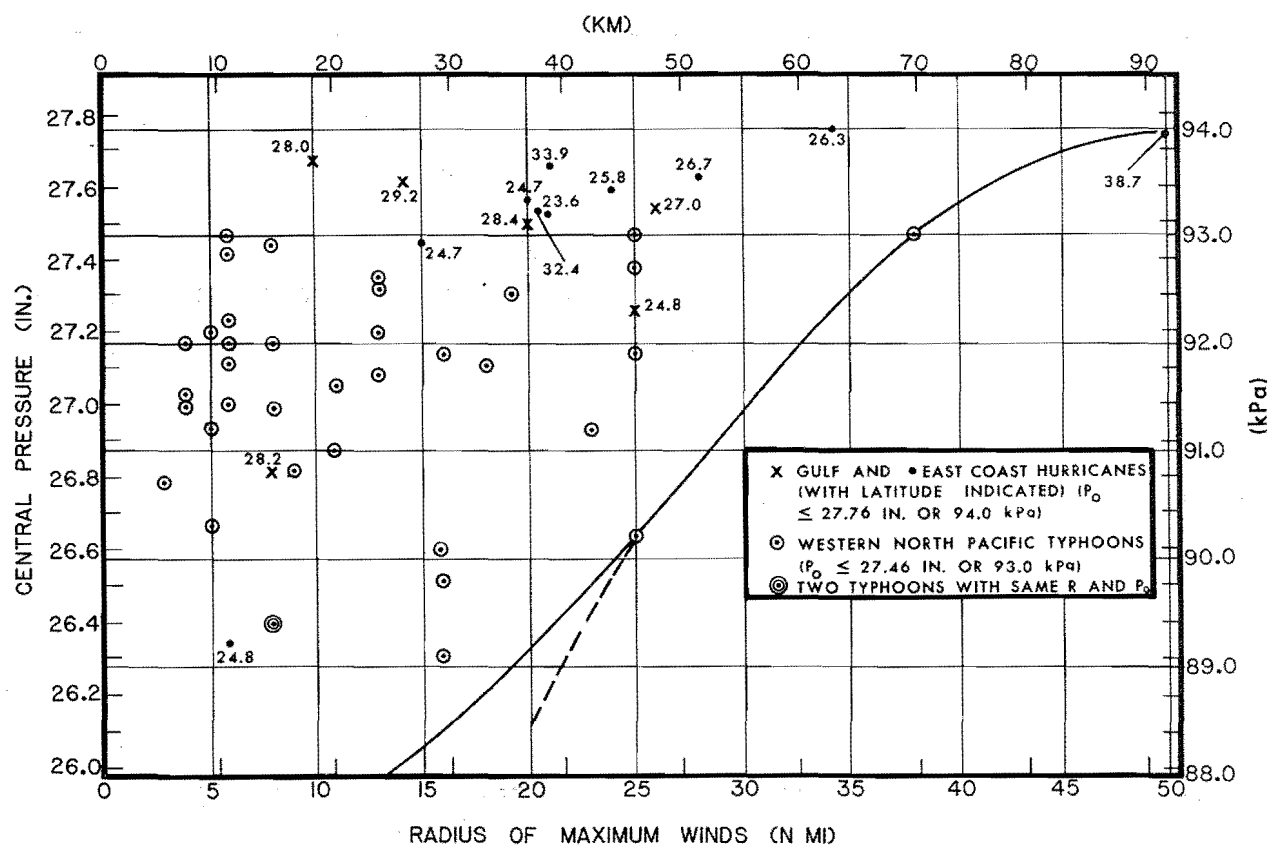
Figure 9.6.--Variation of radius of maximum winds (R) with central pressure for western North Pacific typhoons and hurricanes. Solid curve is an envelopment of the storm data. Dashed curve is a modification of the solid curve; it sets the upper limit of R at 20 n.mi. (37 km) for the PMH for the Florida Keys. Hurricane latitudes are also shown.

190

portion of the envelope sets the limit of large R at 20 n.mi. (37 km) for
the most intense hurricane at p_O = 26.11 in. (88.4 kPa). Ito (1962) shows
that an R of 20 n.mi. (37 km) has a frequency of occurrence of 1% for
typhoons with p_O ≤27.17 in. (92.0 kPa) while Bell (1974)shows this value of
R to be 3.1% for typhoons with p_O <27.17 in. (92.0 kPa). These values lend
support to our adopted value.

Figure 9.7 shows variations of R with latitude for the PMH. The dashed
curve is obtained by entering figure 9.6 with the PMH p_O (chapter 8) at
various latitudes along the east coast to obtain values of the upper limit
of R [e.g., p_O for the PMH is 26.11 in. (88.4 kPa) at 25°N, 26.38 in.
(89.3 kPa) at 35°N and 26.71 in. (90.4 kPa) at 40°N]. These R values are
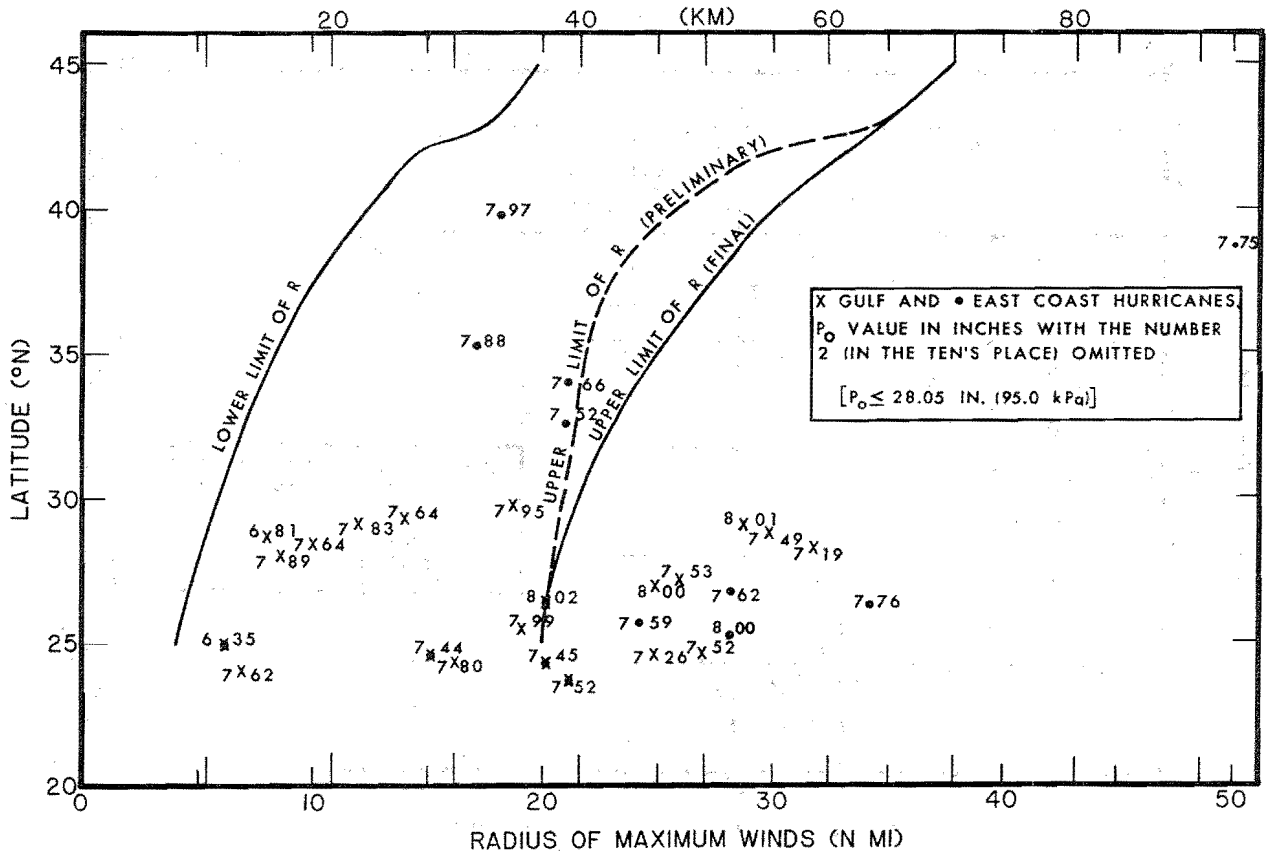
Figure 9.7.--Variation of the lower limit and upper limit of PMH radius of
maximum winds (R) with latitude. The lower limit of R curve is from
figure 9.5. Dashed curve is the upper limit of R using figures 9.6 and
8.8. The upper limit of R curve (final) is obtained after modifying the
dashed curve for latitude.

then plotted against latitude in figure 9.7 and a smoothed dashed line
fitted by eye. The lower limit of R curve is similarly obtained from
figure 9.5.

Figure 9.7 also shows data for east and gulf coast hurricanes with values
of p_o next to each point. A casual inspection of the plotted data clearly
indicates that some R values are greater than the envelope shown by the
dashed line. These R's [obtained from hurricanes with p_o $\leq$28.05 in.
(95.0 kPa)] should be larger than PMH R's because R decreases as the p_o of a
hurricane decreases (see fig. 5.1). That is, the R for the PMH would have
smaller values at each latitude than those observed in less severe hurri-
canes. At first glance, the dashed upper limit of R curve appears to be
drawn far away from the data point for the New England hurricane of 1938.
However, the PMH p_o is 1.09 in. (3.7 kPa) lower than the 1938 hurricane at
the latitude of the 1938 storm. The difference is slightly too large since
we have not yet considered the variation of R with ψ.

R values for intense western North Pacific typhoons were used to supple-
ment sparse hurricane data with low p_o. These R values for typhoons with p_o
<27.46 in. (93.0 kPa) were all observed south of 30°N at an average latitude
of 19.4°N, while the PMH of these intensities will occur at higher latitudes
(25°-45°N) along the east and gulf coasts. Therefore, the variation of R
with latitude has to be considered in assessing the upper limit of R for the
PMH. The variation of R with ψ of western North Pacific typhoons as well as
that of east coast hurricanes was used to obtain the solid curve to the
right of the dashed curve (preliminary upper limit of R) shown on figure
9.7. This variation of R with ψ was not used for the upper portion of the
curve (north of 43°N) where the solid line is superimposed on the dashed
line. Even larger R's at these northern latitudes would be more representa-
tive of hurricanes becoming extratropical, e.g., the New England hurricane
of 1938.

For the PMH, we therefore have increased the upper limit of R to the
values shown by the solid line of figure 9.7. This curve gives a maximum
increase of <5 n.mi. (~9 km) from the earlier enveloping curve (dashed line).

9.4.3 COASTAL ANALYSIS OF LOWER AND UPPER LIMITS OF R FOR THE PMH

The lower and upper limits of R curves shown in figure 9.8 give the range of R's for the PMH at points of interest on the open coast. The user should select any value of R within these limits that is critical for his application. Figure 9.8 also shows the hurricane R data from figure 9.1 plotted in the same manner.

The lower limit is from the curve on the left side of figure 9.7. Along the east coast, the upper limit is from the solid (final) curve on the right side of this figure. We could have used this same curve to show the upper limit of R along the gulf coast. If we had done this our range of the upper limit of R along the entire gulf coast would be <2 n.mi. (~3 km). Instead of using this curve from figure 9.7, we chose to vary the upper limit of R along the gulf coast with central pressure and indirectly with latitude. The reasons for making this choice are as follows:

a. The solid (final) upper limit curve was developed from *east coast* hurricanes and western North Pacific typhoons.

b. In chapter 5, we state that on the average the meteorological parameters for the gulf coast are better related to longitude than latitude. However, from table 5.1 we see that for gulf coast hurricanes the p_o vs. R correlation coefficient (.33) is significant at the 1 % level whereas the λ vs. R correlation coefficient (-.06) is much smaller and is not significant at the 5 % level.

Based on the above, we decided to relate the upper limit of R along the gulf coast to PMH p_o along the gulf coast (chapter 8, fig. 8.8) and then relate this p_o to the upper limit of R value for the same PMH p_o along the east coast. For example, the PMH p_o near milepost 1100 (n.mi.) is 26.32 in. (89.1 kPa). From figure 8.8, we see that along the east coast a PMH p_o of 26.32 in. lies near milepost 2000 (n.mi.). From figure 9.8, the upper limit of R at milepost 2000 is about 23 n.mi. (42.6 km). Therefore, the upper limit of R near milepost 1100 is also 23 n.mi.
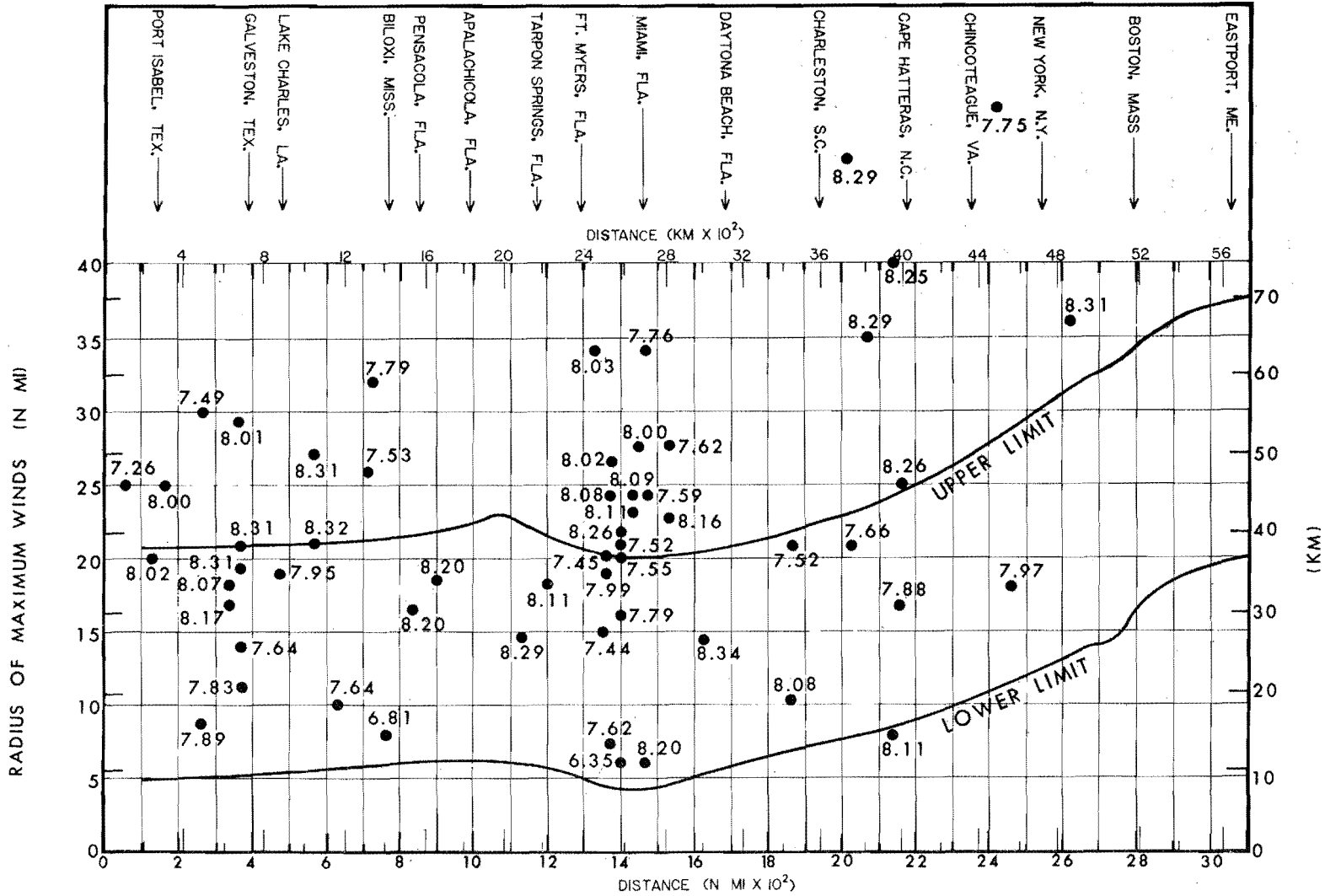
Figure 9.8.--Adopted upper and lower limits of radius of maximum winds for the PMH. Data are identical to that of figure 9.1.

9.4.4 APPLICATION OF R CRITERIA

As indicated earlier (sec. 9.1), the critical R for a PMH with a given forward speed that would produce the maximum peak surge on the coast is dependent upon geographical features of the coast (e.g., the configuration of the slope of the continental shelf and the curvature of the coast) and other factors. An example of such effects is given by hurricane Camille (1969) which struck the coast where the shelf topography becomes steeper with distance east of the storm center. Hurricane Camille (R = 8 n.mi., 15 km) gave a record surge in the Gulfport area. If the size of the storm had been larger with maximum winds farther from the storm center, the peak surge would have occurred in a steep shelf area where the surge would have a different potential. Thus, the critical R of a hurricane striking a particular location may be smaller than the R value given by the upper limit of R curve in figure 9.8. In applying R to a particular coastal location, the user should consider these and other more subtle effects of variations in R on the storm surge.

10. FORWARD SPEED

10.1 INTRODUCTION

10.1.1 USE OF FORWARD SPEED

The rate of translation, or forward speed (T), of the hurricane center is an important meteorological parameter. Taken together with track direction (θ) (chapter 11), it enables us to determine where a hurricane has been, is now, and may go. T makes up part of an asymmetry factor used in the determination of 10-m (32.8 ft) overwater winds. In simulating storm surge, the location of the hurricane can be determined at selected times if we know T and θ.

Depending on the specific coastal location for storm surge simulation or other wind field application, either a low or a high T could be most critical. Lower and upper limits of T will be set for the SPH and the PMH. Any value of T within these bounds may be used, and the user must evaluate the most critical T for a particular application.

10.1.2 FORWARD SPEEDS OF HISTORICAL HURRICANES

Forward speeds of hurricanes with p_o $\leq$29.00 in. (98.2 kPa) during the period 1900–78 are listed in tables 4.1 to 4.4.

10.1.3 RANGES OF T

Hurricane or typhoon data were used to develop portions of the PMH and SPH lower and upper coastal profiles of T. The profiles were completed by applying various meteorological concepts. PMH curves are developed first in section 10.2. The SPH curve development in section 10.3 makes use of the PMH results, particularly for the upper limit of T.

10.2 FORWARD SPEED FOR THE PMH

10.2.1 UPPER LIMIT OF T

10.2.1.1 RIO GRANDE TO MAYPORT, FLA. (LATITUDE 30.5°N). Figure 10.1 shows the T for hurricanes plotted against approximate coastal reference points. South of latitude 30.5°N (mileposts 0 to 1750 n.mi.), only six hurricanes moved faster than 18 kt (33 km/hr). These storms were weak
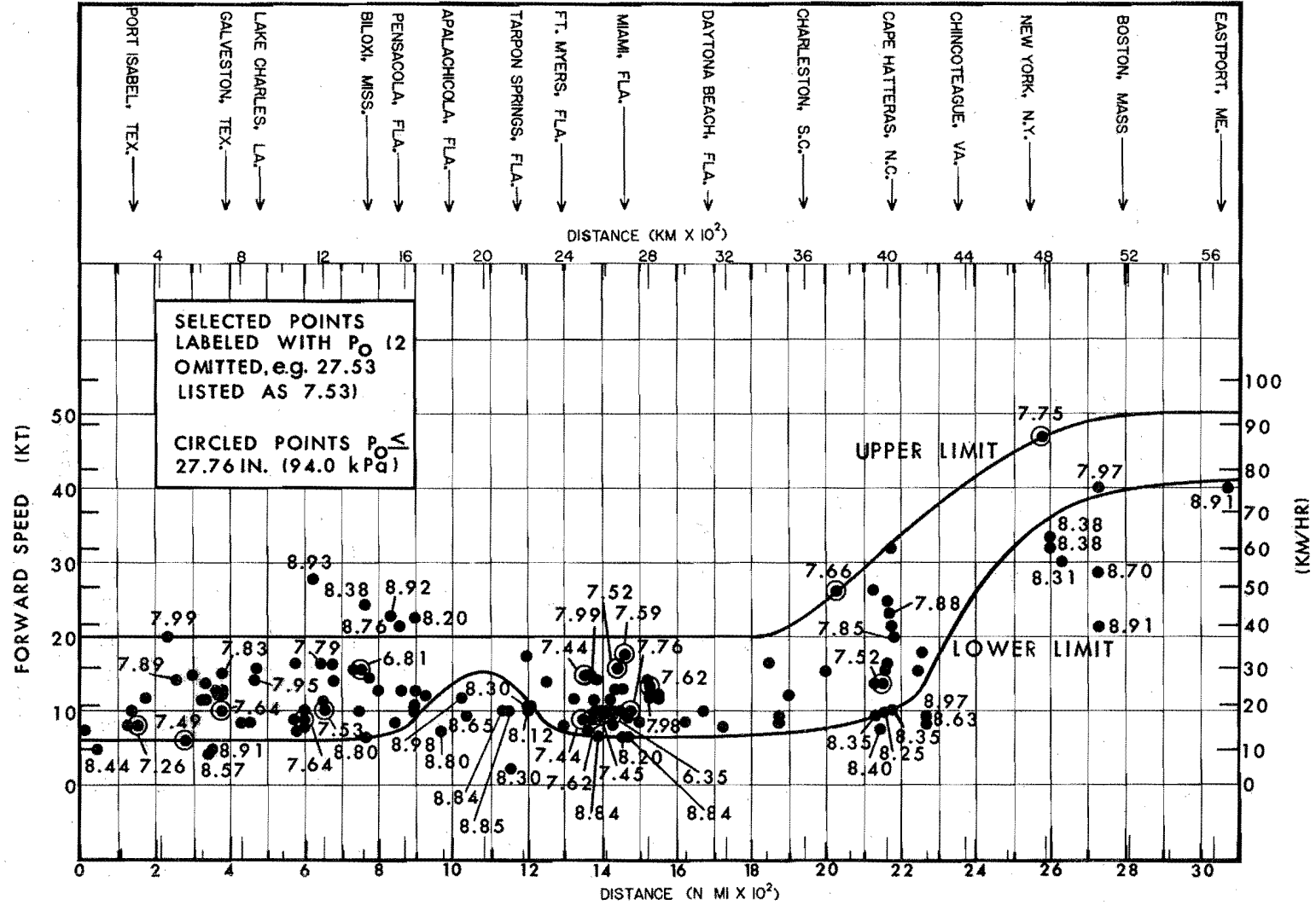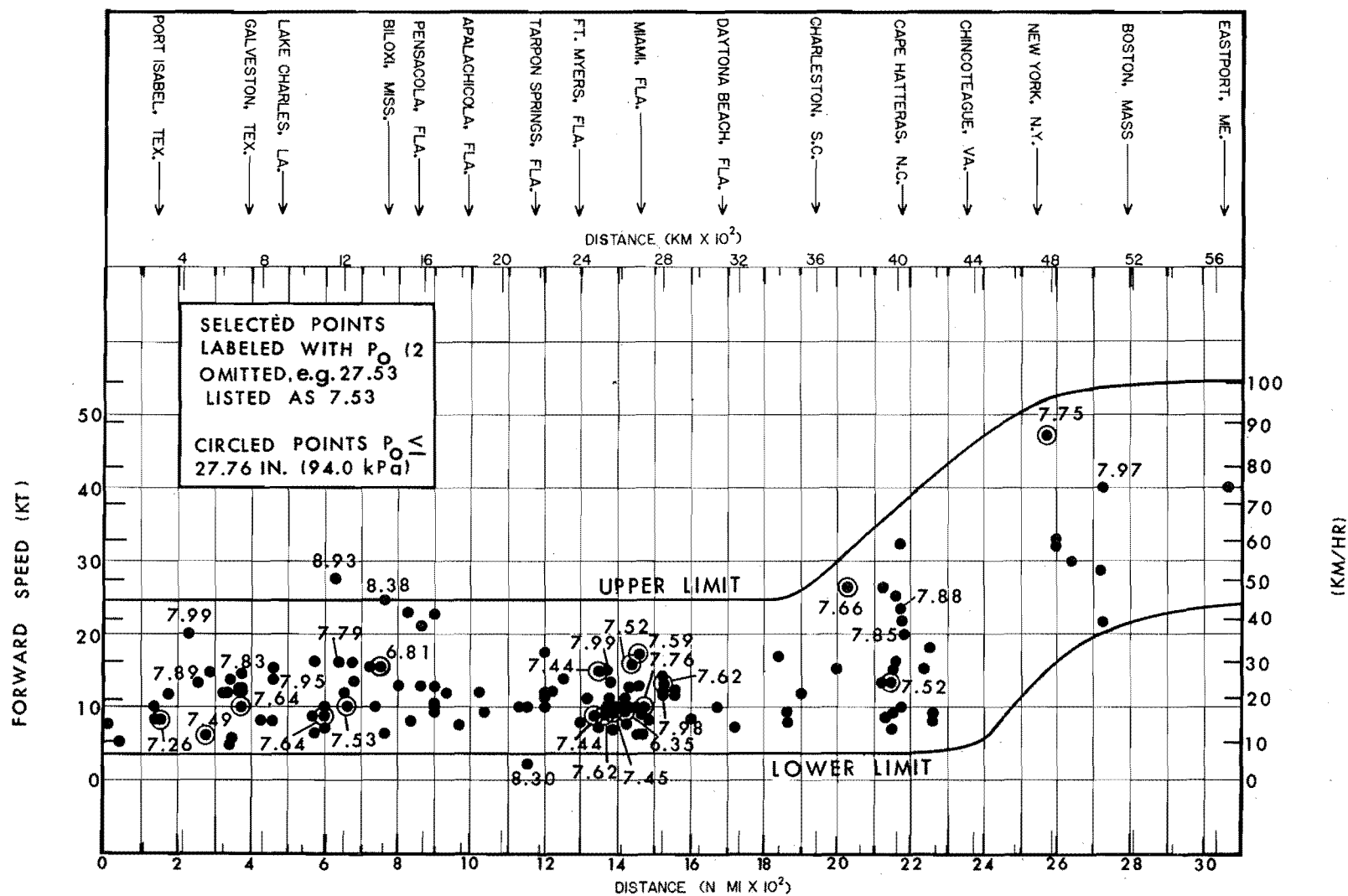
Figure 10.1.--Adopted PMH upper and lower limits of T. Data are from tables 4.1 to 4.4.
All data points falling outside the two curves are labeled with lowest central pressure
(p_o). All circled data points falling inside the two curves are labeled with lowest p_o.
Other data points (except those between mileposts 1300 and 1500) are labeled with lowest
p_o if this p_o is $\leq$ 28.00 in. (94.8 kPa).

compared to the PMH -- none had a p_0 lower than 27.99 in. (94.8 kPa). The remainder of the data (T $\leq$ 18 kt) up to about milepost 1800 does not exhibit any noticeable latitudinal variation. The east coast data plotted against latitude in figure 5.4 show no variation in T south of 30.5°N. We conclude that the fast T for the PMH is constant to milepost 1750.

Data from hurricanes in the central Gulf of Mexico, Caribbean Sea, and western North Atlantic were investigated in support of this conclusion. Three hurricanes were identified which had a p_0 <27.26 in. (92.3 kPa) -- p_0 of hurricane Beulah (1967), the third most intense hurricane in tables 4.1 to 4.4. These storms were over the western Caribbean Sea and are: the Nov. 5, 1932, hurricane (p_0 = 27.01 in., 91.5 kPa); Janet, 1955 (p_0 = 27.00 in., 91.4 kPa); and Hattie, 1961 (p_0 = 27.17 in., 92.0 kPa). Of these three, Janet had the highest T (20 kt, 37 km/hr) near 18°N, 86°W.

We also examined data for typhoons (table 10.1) having p_0's $\leq$ that of Camille, 1969 -- the second most intense hurricane (p_0 = 26.81 in., 90.8 kPa) in tables 4.1 to 4.4 -- in order to determine how fast extremely intense typhoons can move across the western North Pacific. Table 10.1 extends T data for extreme typhoons beyond the spatial limitations imposed in tables 4.5 and 4.6 which show nine typhoons with p_0 $\leq$26.81 in. The highest T for these nine typhoons is 15 kt (28 km/hr) associated with typhoon Emma of 1967 (p_0 = 26.81 in., 90.8 kPa). Figure 10.2 is a plot of T vs. p_0 at the time of lowest p_0 for the 31 typhoons of table 10.1. By increasing our sample of extreme typhoons, highest T's increase from 15 to 18 kt (28 to 33 km/hr). Typhoon Gilda (1967) is the storm traveling at 18 kt; it was moving west-northwestward with a p_0 of 26.28 in. (89.0 kPa). Gilda later filled to 27.14 in. (91.9 kPa) and its T decreased to 15 kt (28 km/hr) near 17.0°N, 131.8°E, as it drew closer to the Philippines (tables 4.5 and 4.6).

We have adopted 20 kt (37 km/hr) as the upper limit of T for the PMH for the entire coastal region south of 30.5°N. Looking at all extreme hurricane and typhoon data supported our selection of 20 kt rather than a higher value.

Table 10.1.--Forward speeds of western North Pacific typhoons (1961-75) with
$p_o \leq 26.81$ *in. (90.8 kPa) at time of lowest* p_o.

Typhoon	Year	T (kt)	(km/hr)	P_o (in.)	(kPa)
Nancy	1961	14	26	26.05	88.2
Violet	1961	10	19	26.05	88.2
Emma	1962	6	11	26.67	90.3
Karen	1962	15	28	26.48	89.7
Carmen	1963	10	19	26.52	89.8
Judy	1963	13	24	26.78	90.7
Sally	1964	13	24	26.40	89.4
Wilda	1964	9	17	26.73	90.5
Louise	1964	11	20	26.31	89.1
Opal	1964	14	26	26.67	90.3
Bess	1965	7	13	26.46	89.6
Kit	1966	15	28	26.49	89.7
Carla	1967	11	20	26.61	90.1
Emma	1967	14	26	26.81	90.8
Gilda	1967	18	33	26.28	89.0
Agnes	1968	9	17	26.70	90.4
Elaine	1968	8	15	26.81	90.8
Viola	1969	13	24	26.31	89.1
Elsie	1969	16	30	26.28	89.0
Olga	1970	13	24	26.70	90.4
Georgia	1970	11	20	26.70	90.4
Hope	1970	14	26	26.43	89.5
Joan	1970	11	20	26.61	90.1
Amy	1971	13	24	26.43	89.5
Nadine	1971	11	20	26.52	89.8
Irma	1971	16	30	26.11	88.4
Nora	1973	8	15	25.90	87.7
Patsy	1973	11	20	26.37	89.3
Nina	1975	15	28	26.70	90.4
Elsie	1975	12	22	26.58	90.0
June	1975	10	19	25.87	87.6
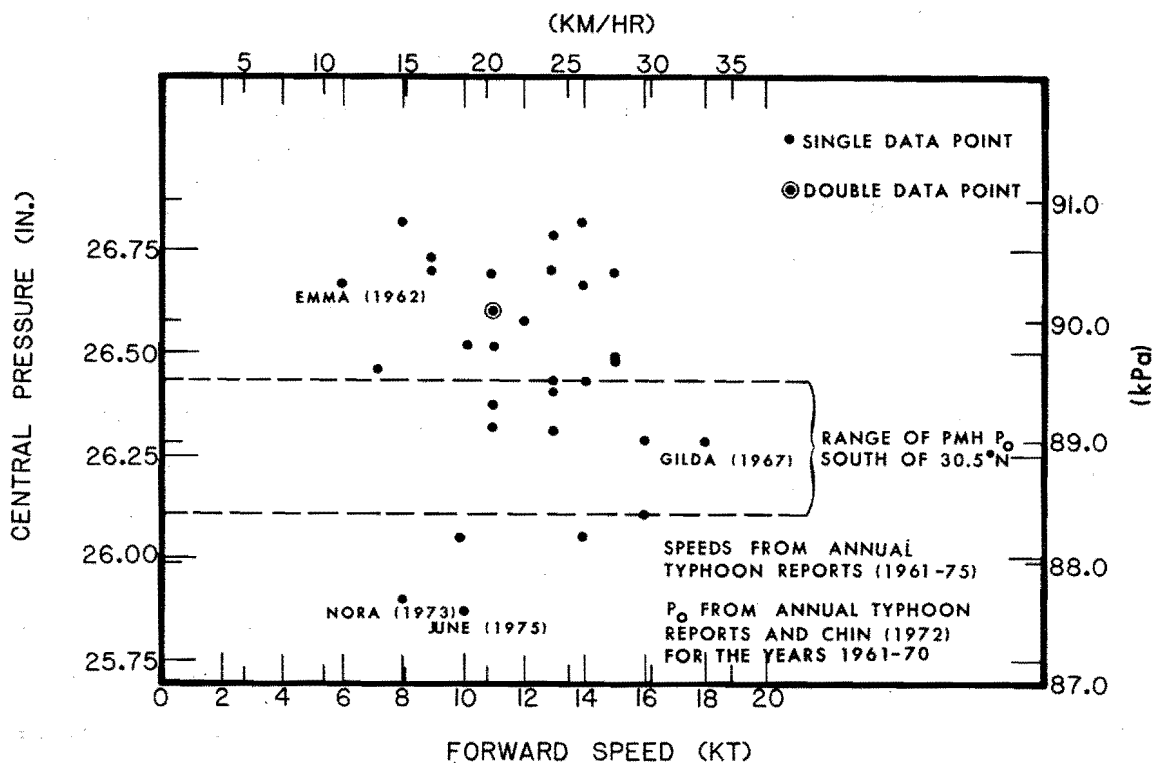
Figure 10.2.--Forward speed (T) vs. central pressure (p_o) for typhoons
listed in table 10.1.

10.2.1.2 MAYPORT, FLA. TO LATITUDE 45°N. A T envelope along the
east coast passes through the data point for the New England hurricane of
1938, which had a T of 47 kt (87 km/hr) near milepost 2600 (fig. 10.1). We
have adopted a T of 47 kt at this location as an upper limit for the PMH.
The PMH p_o is about an inch (3.4 kPa) lower than the 1938 hurricane at mile-
post 2600. Speeds faster than 47 kt near milepost 2600 would make the
storm increasingly asymmetrical leading to higher p_o. Therefore, such
speeds are reserved for points farther north. We have adopted an upper
limit for T of 50 kt (93 km/hr) at 45°N.

10.2.2 LOWER LIMIT OF T

10.2.2.1 RIO GRANDE TO SAVANNAH, GA. We recommend a lower limit of
T for the PMH of 6 kt (11 km/hr) over most of the Gulf of Mexico and the
east coast to near Savannah, Ga. (near milepost 1860, fig. 10.1). Of the
typhoons, Emma (1962) had the slowest T [6 kt (11 km/hr)] (fig. 10.2) at the
time of lowest p_o. In the next 24 hours, Emma slowed to 4 or 5 kt (~8 km/hr),

started to recurve and filled 0.56 in. (1.9 kPa). Environmental factors
were favorable for intensification. The filling was most probably the
result of both the slow movement and recurvature. Based on the typhoon
sample (fig. 10.2), 6 kt (11 km/hr) is considered the minimum stable speed
for the PMH in a tropical region. The Labor Day hurricane of 1935 had a T
of 9 kt (17 km/hr) and Camille the much higher T of 16 kt (30 km/hr). We
consider T below 6 kt to be a stalling speed for the PMH along the gulf
and east coasts.

Near milepost 1100 the minimum T is increased to 15 kt (28 km/hr) because
of particular characteristics of this area (described in chapter 8). Along
this area of the coast and extending west and south a PMH must recurve and
move quickly because it is a filling, nonsteady state hurricane.

10.2.2.2 SAVANNAH, GA. TO LATITUDE 45° N. The adopted lower limit
of T increases slowly from 6 kt (11 km/hr) to 10 kt (19 km/hr) at a point
near Cape Hatteras. North of there slow T's for the PMH are not considered
meteorologically reasonable because of lowering sea-surface temperatures.
Therefore, the lower limit curve (fig. 10.1) increases rapidly until it is
9 kt (17 km/hr) less than the PMH upper limit of T curve at 45°N. Slower-
moving hurricanes all have $p_o \geq 28.31$ in. (95.9 kPa). Faster T's are
necessary over the colder New England waters for the PMH to have the lowest
possible p_o. Over warmer waters farther south, a PMH can exist at slower T.

10.3 FORWARD SPEED FOR THE SPH

10.3.1 UPPER LIMIT OF T

10.3.1.1 GULF COAST. The SPH, although an intense hurricane, is
substantially weaker than the PMH. Weaker hurricanes in general are known
to travel within a broader range of T. Therefore, the SPH should have a
larger overall range in T than the PMH. Thus, we are justified in setting
the upper limit of T for the SPH higher than the upper limit of T for the
PMH. We recommend a value of 25 kt (46 km/hr) for the SPH upper limit of T
for the Gulf coast (fig. 10.3). This is 5 kt (9 km/hr) faster than the
upper limit of PMH T along the Gulf coast.

Figure 10.3.--Adopted SPH upper and lower limits of T. Data is from tables 4.1 to 4.4.
All data points falling outside the two curves are labeled with lowest central pressure
(p_o). All circled data points falling inside the two curves are labeled with lowest p_o.
Other data points (except those between mileposts 1300 and 1500) are labeled with lowest
p_o if this p_o is $\leq$ 28.00 in. (94.8 kPa).

10.3.1.2 EAST COAST. Along the east coast (fig. 10.3), we have adopted the 25-kt (46 km/hr) value from the Keys northward to Savannah. From there northward the upper limit of T curve exceeds an envelope of the data and is parallel to and 5 kt (9 km/hr) more than the PMH upper limit of T in figure 10.1.

10.3.2 LOWER LIMIT OF T

10.3.2.1 RIO GRANDE TO CAPE HATTERAS, N.C. Geisler (1970) has stated that there is a gradual transition from upwelling to no upwelling of cold subsurface sea water as hurricanes increase their T beyond 4 kt (7 km/hr). Upwelling weakens hurricanes. Others such as Black and Mallinger (1972) have spoken in support of Geisler's theory. We adopted 4 kt as the lower limit of T for the SPH over southern latitudes to a point just north of Cape Hatteras. This envelops the storm data except for the 28.30 in. (95.8 kPa) hurricane (fig. 10.3) moving at 3 kt (6 km/hr). This is reasonable because the storm was too weak to meet the SPH p_o criteria anywhere along the U.S. coast to latitude 45°N.

10.3.2.2 CAPE HATTERAS TO LATITUDE 45°N. The adopted SPH lower limit of T envelops the data of figure 10.3 over these northern latitudes and envelops the lower 5 percentile T north of milepost 2500 from Ho et al. (1975) for landfalling hurricanes.

11. TRACK DIRECTION

11.1 INTRODUCTION

Peripheral pressure (p_w), central pressure (p_o), radius of maximum winds (R) and forward speed (T), the subjects of chapters 7 to 10, are all used in computing 10-m (32.8-ft) overwater 10-min winds. Track direction (θ) is not used to compute wind speeds, but it is an important parameter because it is used to determine from what directions an SPH or a PMH may approach the coast. For example, a section of the coast that can be affected by an SPH from a wide range of directions is more likely to include a critical track to the coast than a coastal section accommodating only a narrow range of permissible directions.

11.2 DEFINITION OF TRACK DIRECTION (θ)

In this report, θ for the SPH and PMH is defined as the path of forward movement or track from which the hurricane is coming. θ is measured in degrees clockwise from north.

We must remember that the SPH and PMH are steady state hurricanes (see definition in sec. 1.2.3). As steady state hurricanes, we assume they do not change course during the last several hours before making landfall. Exiting hurricanes are not considered except along capes or the tip of peninsulas, e.g., Cape Hatteras, Cape Cod and the Mississippi Delta where the SPH and the PMH are permitted to exit after passing over a small land area.

11.3 VARIATIONS IN θ SHOWN BY HURRICANES OF RECORD

Figure 11.1 shows the track direction for hurricanes of record for the period 1900-75 for the gulf and east coasts. The direction was plotted at the point of landfall or the point at which bypassing hurricanes were nearest the coast (from tables 4.1 and 4.2). The scatter is large for the entire sample. New England hurricanes have not entered the coast from directions east of south.

In figure 11.2, the storm sample is restricted to hurricanes with p_o $\leq$ 28.05 in. (95.0 kPa) to milepost 2200 and to hurricanes with p_o
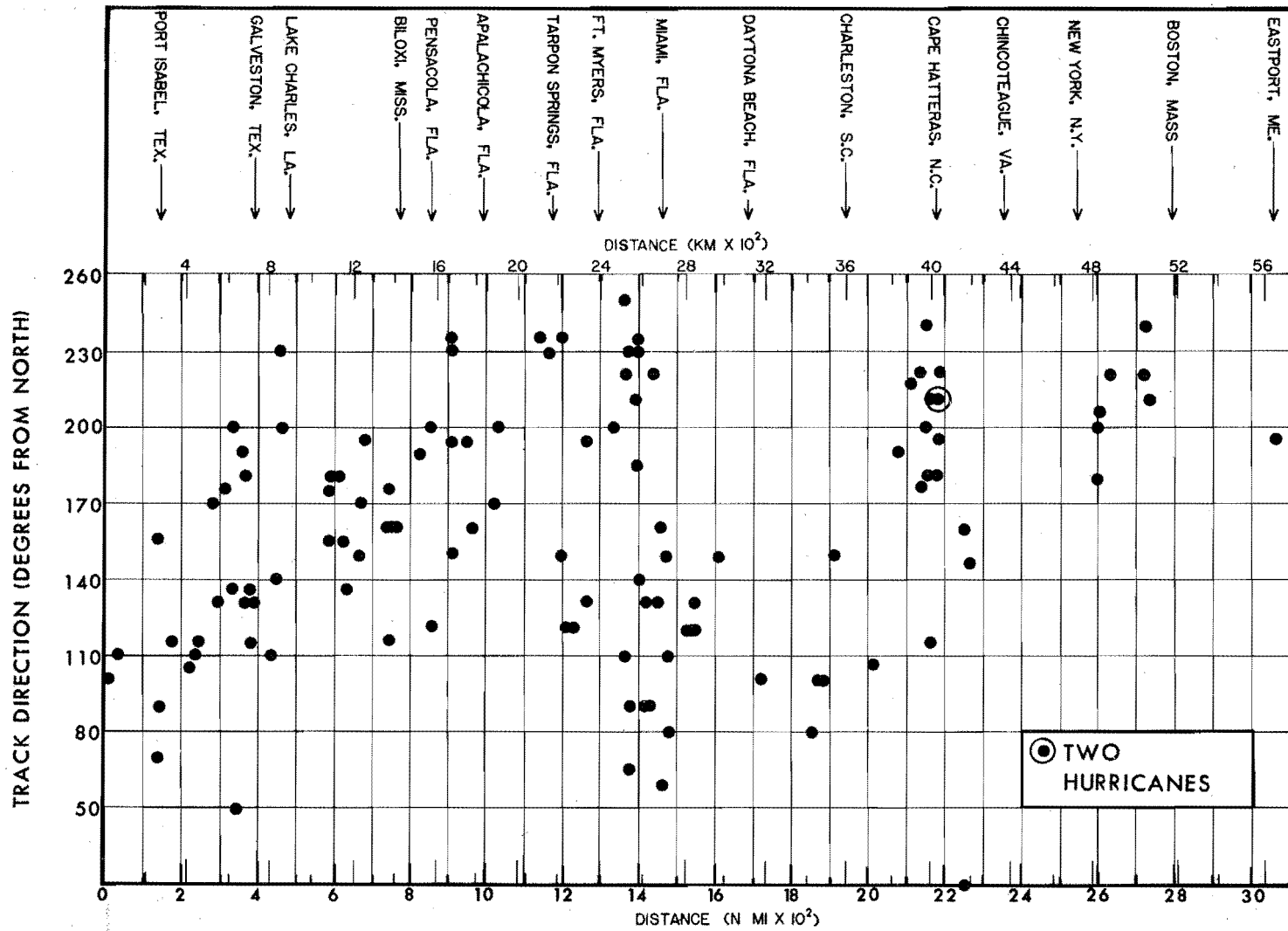
Figure 11.1.--Track direction for landfalling or bypassing hurricanes along the gulf and east coasts of the United States.
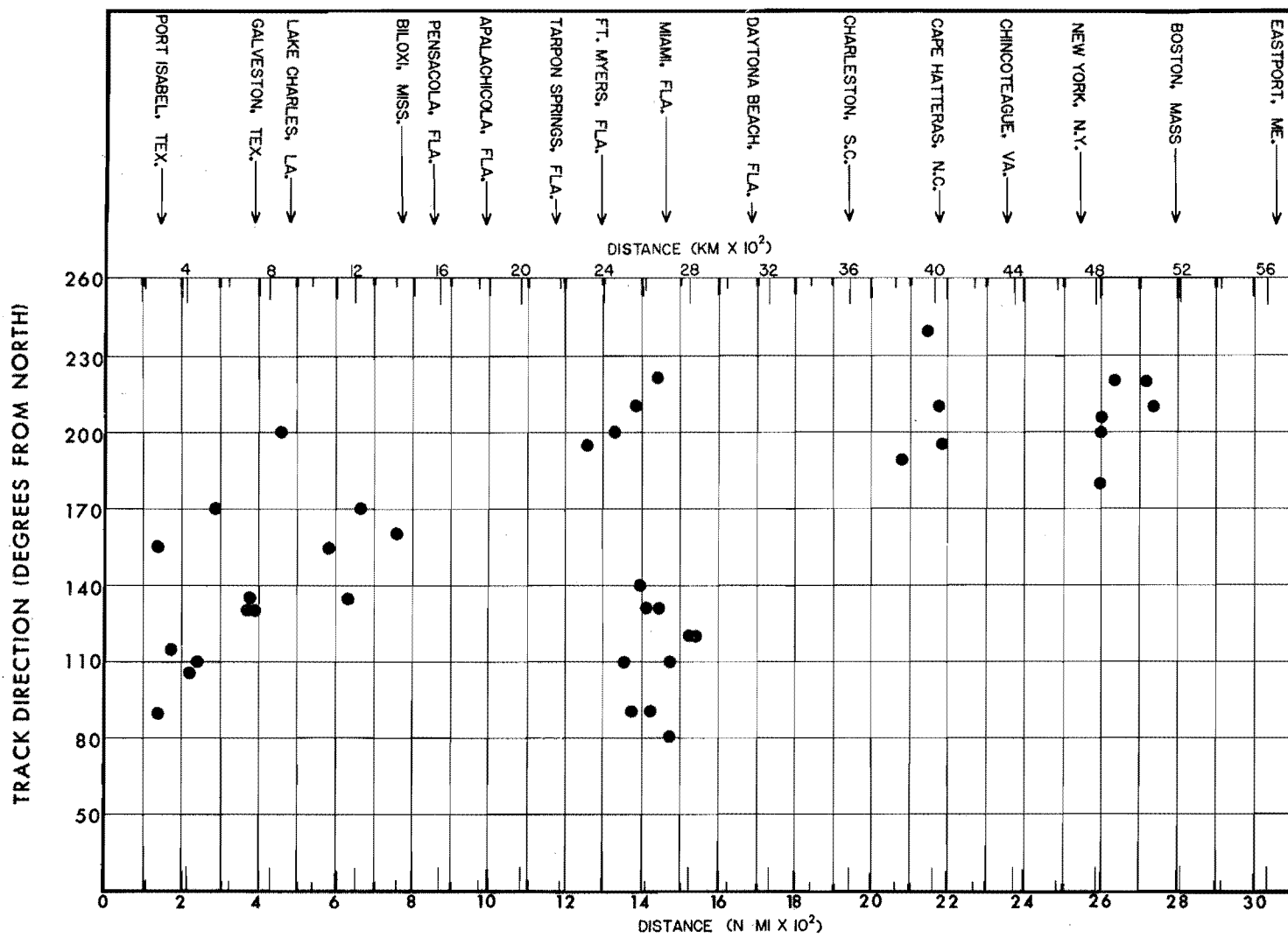
Figure 11.2.—Track direction for landfalling or bypassing hurricanes along the gulf and east coasts of the United States with p_O $\leq$28.05 in. (95.0 kPa) to milepost 2200 or with p_O $\leq$28.41 in. (96.2 kPa) north of milepost 2200.

$\leq$28.41 in. (96.2 kPa) north of milepost 2200. Three regions have several storms each: western gulf, south Florida, and the Carolinas to New England. The scatter in θ is quite large except from the Carolinas to New England where all severe hurricanes had θ between 180° and 240°.

11.4 GENERALIZED COASTAL ORIENTATIONS

We divided the gulf and east coasts into 21 straight line segments in order to study the variation of θ along the coast for the PMH and the SPH. These segments stretch from the Rio Grande, clockwise to Cape Sable, Fla. just west of milepost 1400. The other 11 extend from the vicinity of Cape Sable to the Canadian border ($\sim$45°N). The segments (fig. 11.3) range in length from about 45 n.mi. (83 km) to about 335 n.mi. (621 km). Table 11.1 contains geographical and meteorological data by segment. Track directions are listed for hurricanes (1900–75) entering or bypassing the coast with central pressure $\leq$ 28.05 in. (95.0 kPa) for segments 1 to 15, and with central pressure $\leq$ 28.41 in. (96.2 kPa) for segments 16 to 21 (from milepost 2200 to the Canadian border). The permissible PMH and SPH limits of θ defined in sections 11.5 and 11.6 and ranges of forward speed discussed in chapter 10 make up the right side of the table.

11.5 TRACK DIRECTION FOR THE PMH

11.5.1 RANGE OF θ OVER THE OPEN OCEAN

Initially, let us consider a PMH over the open ocean. From what directions can this PMH travel? Experience tells us that it will not be moving from the north. Should the range of θ be even more restricted? We know that hurricane Camille (1969) with a p_o of 26.81 in. (90.8 kPa) entered the Mississippi coast from θ = 160° without showing signs of weakening. If Camille had entered the coast from 180° instead of 160°, the typhoon data for storms moving from the south or southwest from inception (discussed in chapter 8, sec. 8.3.7.2.1.2) suggest to us that the p_o at landfall might have been higher. However, in this report we will not be quite so restrictive because this indication stemmed from typhoon data and not hurricane data. We assume that PMH θ over the open ocean will be limited to angles $\leq$ 190° but not to angles near 0°.
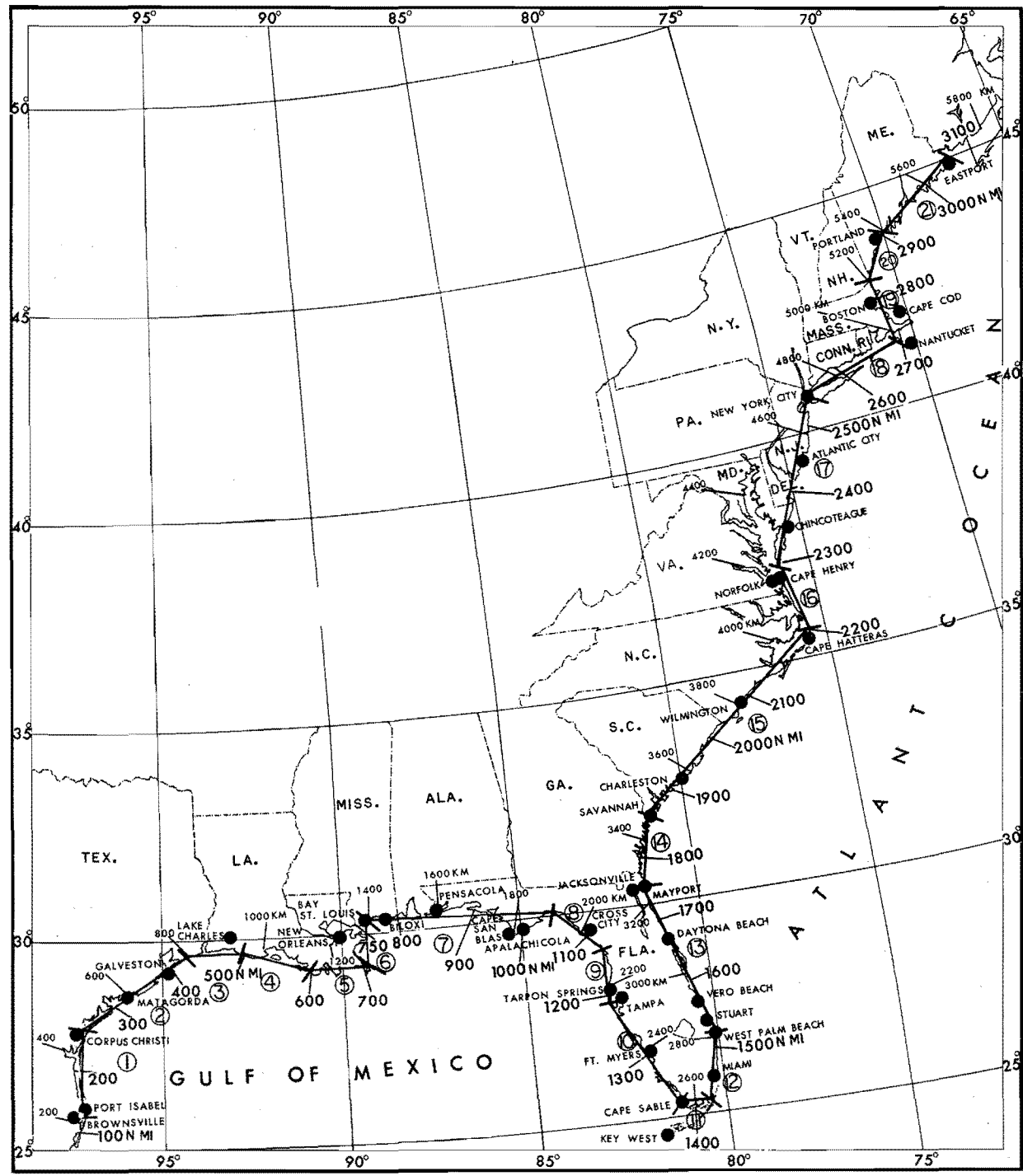
Figure 11.3.--Generalized straight line segments depicting orientation of gulf and east coasts of the United States.

Table 11.1.--Coastal segments, observed severe hurricane direction and permissible track direction limits before smoothing for the PMH and SPH.

Segment & length	Coastal orientation (from north)	Direction normal to coast	Cities or other landmarks	Severe hurricane (date) (name)	Severe hurricane direction (from north)	Severe hurricane central pres. within 150 n.mi. (278 km) of coast	Permissible ranges of forward speed (T) PMH	SPH	Permissible limits before smoothing † PMH	SPH
1 110 n.mi. (204 km)	(360°-180°)	(90°)	Mex.brder. to Corpus Christi,TX	18 Aug.1916	115°	28.00 in. (94.8 kPa)	slow 6 kt (11 km/hr)	slow 4 kt (7 km/hr)	A 70°-140°	A 50°-150°
				14 Sep.1919	105°	27.99 in. (94.8 kPa)				
				5 Sep.1933	090°	28.02 in. (94.9 kPa)	fast 20 kt (37 km/hr)	fast 25 kt (46 km/hr)	B 70°-150°	B 50°-160°
				20 Sep.1967 (Beulah)	155°	27.26 in. (92.3 kPa)				
Near intersection of segments 1-2				3 Aug.1970 (Celia)	115°	27.89 in. (94.4 kPa)				
2 195 n.mi. (361 km)	(55°-235°)	(145°)	Corpus Christi to vic. Sabine,TX	9 Sep.1900	130°	27.64 in. (93.6 kPa)	slow 6 kt (11 km/hr)	slow 4 kt (7 km/hr)	A 95°-190°	A 85°-195°
				17 Aug.1915	130°	28.01 in. (94.9 kPa)	fast 20 kt (37 km/hr)	fast 25 kt (46 km/hr)	B 85°-190°	B 75°-200°
				14 Aug.1932	135°	27.83 in. (94.2 kPa)				
				11 Sep.1961 (Carla)	170°	27.49 in. (93.1 kPa)				
3 75 n.mi. (139 km)	(85°-265°)	(175°)	Vic.Sabine to vic. Tigre Pt., LA.	27 Jun.1957 (Audrey)	200°	27.95 in. (94.7 kPa)	slow 6 kt (11 km/hr)	slow 4 kt (7 km/hr)	A 150°-190°	A 140°-205°
							fast 20 kt (37 km/hr)	fast 25 kt (46 km/hr)	B 140°-190°	B 130°-215°
4 115 n.mi. (213 km)	(110°-290°)	(200°)*	Vic. Tigre Pt. to Isle Derniere	8 Sep.1974 (Carmen)	155°	27.64 in. (93.6 kPa)	slow 6 kt (11 km/hr)	slow 4 kt (7 km/hr)	A 150°-190°	A 140°-250°
							fast 20 kt (37 km/hr)	fast 25 kt (46 km/hr)	B 140°-190°	B 130°-250°
5 75 n.mi. (139 km)	(90°-270°)	(180°)	Isle Derniere to Port Eads, LA.	29 Sep.1915	170°	27.53 in. (93.2 kPa)	slow 6 kt (11 km/hr)	slow 4 kt (7 km/hr)	A 130°-190°	A 120°-240°
				10 Sep.1965 (Betsy)	135°	27.79 in. (94.1 kPa)	fast 20 kt (37 km/hr)	fast 25 kt (46 km/hr)	B 120°-190°	B 110°-250°
6 75 n.mi. (139 km)	(360°-180°)	(90°)*#	Port Eads, LA., to vic. Long Beach, MS.	18 Aug.1969 (Camille)	160°	26.81 in. (90.8 kPa)	slow 6 kt (11 km/hr)	slow 4 kt (7 km/hr)	A 135°-140°	A 125°-150°
							fast 20 kt (37 km/hr)	fast 25 kt (46 km/hr)	B 125°-150°	B 115°-160°

Table 11.1.—*Coastal segments, observed severe hurricane direction and permissible track direction limits before smoothing for the PMH and SPH - continued.*

Segment & length	Coastal orientation (from north)	Direction normal to coast	Cities or other landmarks	Severe hurricane (date) (name)	Severe hurricane direction (from north)	Severe hurricane central pres. within 150 n.mi. (278 km) of coast	Permissible ranges of forward speed (T)		Permissible limits before smoothing †	
							PMH	SPH	PMH	SPH
7 265 n.mi. (491 km)	(95°–275°)	(185°)	Vic. Long Beach to mouth of Aucilla R., FL	No severe hurricanes			slow 6–14 kt (11–26 km/hr) fast 20 kt (37 km/hr)	slow 4 kt (7 km/hr) fast 25 kt (46 km/hr)	A 135°–190° B 125°–190°	A 125°–245° B 115°–250°
8 90 n.mi. (167 km)	(130°–310°)	(220°)	Mouth of Aucilla R. to Homosassa, FL	No severe hurricanes			slow 14–15 kt (26–28 km/hr) fast 20 kt (37 km/hr)	slow 4 kt (7 km/hr) fast 25 kt (46 km/hr)	A B 215°–245°	A 215°–245° B 205°–250°
9 75 n.mi. (139 km)	(185°–5°)	(275°)*#	Homosassa to Indian Rocks Beach, FL	No severe hurricanes			slow 13–14 kt (24–26 km/hr) fast 20 kt (37 km/hr)	slow 4 kt (7 km/hr) fast 25 kt (46 km/hr)	A B 215°–245°	A 215°–250° B 205°–250°
10 190 n.mi. (352 km)	(150°–330°)	(240°)*	Indian Rocks Beach to Cape Sable (East Cape), FL	18 Oct.1910 21 Sep.1948	200° 210°	27.80 in. (94.1 kPa) 27.62 in. (93.5 kPa)	slow 6–13 kt (11–24 km/hr) fast 20 kt (37 km/hr)	slow 4 kt (7 km/hr) fast 25 kt (46 km/hr)	A 180°–190° B 180°–190°	A 180°–250° B 170°–250°
Near intersection of segments 10-11				3 Sep.1935 10 Sep.1960 (Donna)	130° 140°	26.35 in. (89.2 kPa) 27.45 in. (93.0 kPa)				
11 45 n.mi. (83 km)	(80°–260°)	(170°)	Cape Sable (East Cape) to Key Largo, FL	28 Sep.1929	090°	28.00 in. (94.8 kPa)	slow 6 kt (11 km/hr) fast 20 kt (37 km/hr)	slow 4 kt (7 km/hr) fast 25 kt (46 km/hr)	A 120°–190° B 110°–190°	A 110°–230° B 100°–240°
			Severe hurricanes whose P_0 values were applied to the Florida Keys	10 Sep.1919 21 Oct.1926 19 Oct.1944 8 Sep.1965 (Betsy)	110° 220° 195° 090°	27.44 in. (92.9 kPa) 27.52 in. (93.2 kPa) 28.02 in. (94.9 kPa) 27.99 in. (94.8 kPa)				

Table 11.1.--*Coastal segments, observed severe hurricane direction and permissible track direction limits before smoothing for the PMH and SPH - continued.*

Segment & length	Coastal orientation (from north)	Direction normal to coast	Cities or other landmarks	Severe hurricane (date) (name)	Severe hurricane direction (from north)	Severe hurricane central pres. within 150 n.mi. (278 km) of coast	Permissible ranges of forward speed (T) PMH	SPH	Permissible limits before smoothing † PMH	SPH
12 90 n.mi. (167 km)	(10°-190°)	(100°)	Key Largo to Palm Beach Harbor,FL.	18 Sep.1926	110°	27.59 in. (93.4 kPa)	slow 6 kt (11 km/hr)	slow 4 kt (7 km/hr)	A 70°-150°	A 50°-160°
				17 Sep.1947	080°	27.76 in. (94.0 kPa)	fast 20 kt (37 km/hr)	fast 25 kt (46 km/hr)	B 70°-160°	B 50°-170°
Near intersection of segments 12-13				17 Sep.1928	120°	27.62 in. (93.5 kPa)				
13 250 n.mi. (463 km)	(340°-160°)	(70°)	Palm Beach Harbor to Amelia Is., FL	4 Sep.1933	120°	27.98 in. (94.8 kPa)	slow 6 kt (11 km/hr) fast 20 kt (37 km/hr)	slow 4 kt (7 km/hr) fast 25 kt (46 km/hr)	A 70°-120° B 70°-130°	A 50°-130° B 50°-140°
14 90 n.mi. (167 km)	(20°-200°)	(110°)	Amelia Is., FL to GA - SC line	No severe hurricanes			slow 6 kt (11 km/hr) fast 20-21 kt (37-39 km/hr)	slow 4 kt (7 km/hr) fast 25-26 kt (46-48 km/hr)	A 90°-120° B 80°-130°	A 80°-130° B 70°-140°
15 335 n.mi. (621 km)	(50°-230°)	(140°)	GA-SC line to Cape Hatteras,NC Severe hurricanes whose ctr. bypassed NC Outer Banks	15 Oct.1954 (Hazel) 10 Sep.1954 (Edna) 28 Aug.1958 (Daisy) 27 Sep.1958 (Helene)	190° 210° 180° 240°	27.66 in. (93.7 kPa) 27.85 in. (94.3 kPa) 28.26 in. (95.7 kPa) 27.52 in. (93.2 kPa)	slow 6-10 kt (11-18 km/hr) fast 21-36 kt (39-67 km/hr)	slow 4 kt (7 km/hr) fast 26-41 kt (48-76 km/hr)	A 90°-190° B 80°-190°	A 80°-200° B 70°-210° C 60°-220°
Near intersection of segments 15-16				14 Sep.1944	195°	27.88 in. (94.4 kPa)				
16 110 n.mi. (204 km)	(350°-170°)	(80°)	Cape Hatteras to Cape Charles, VA	No severe hurricanes			slow 10-17 kt (18-32 km/hr) fast 36-43 kt (67-80 km/hr)	slow 4-5 kt (7-9 km/hr) fast 41-48 kt (76-89 km/hr)	B 70°- 140° C 70°-150°	A 50°-140° B 50°-150° C 50°-160°

Table 11.1.--Coastal segments, observed severe hurricane direction and permissible track direction limits before smoothing for the PMH and SPH - continued.

Segment & length	Coastal orientation (from north)	Direction normal to coast	Cities or other landmarks	Severe hurricane (date) (name)	Severe hurricane direction (from north)	Severe hurricane central pres. within 150 n.mi. (278 km) of coast	Permissible ranges of forward speed (T) PMH	SPH	Permissible limits before smoothing † PMH	SPH
17 225 n.mi. (417 km)	(25°–205°)	(115°)	Cape Charles,VA to Brooklyn, NY	No severe hurricanes			slow 17–33 kt (32–61 km/hr) fast 43–48 kt) (80–89 km/hr)	slow 5–15 kt (9–28 km/hr) fast 48–53 kt (89–98 km/hr)	B 80°–175° C 80°–185°	A 70°– 175° B 70°–185° C 70°–195°
18 140 n.mi. (260 km)	(70°–250°)	(160°)	Brooklyn to vic. Martha's Vineyard,MA	21 Sep.1938 15 Sep.1944 31 Aug.1954(Carol) 12 Sep.1960(Donna)	180° 220° 200° 205°	27.75 in. (94.0 kPa) 28.31 in. (95.9 kPa) 28.38 in. 96.1 kPa) 28.38 in. (96.1 kPa)	slow 33–38 kt (61–70 km/hr) fast 48–49 kt (89–91 km/hr)	slow 15–19 kt (28–35 km/hr) fast 53–54 kt (98–100 km/hr)	B 90°–190° C 90°–190°	B 80°–190° C 80°–200°
Near intersection of segments 18-19				11 Sep.1954(Edna)	210°	27.97 in. (94.7 kPa)				
19 90 n.mi. (167 km)	(350°–170°)	(80°)*#	Vic. Martha's Vineyard to MA–NH line	No severe hurricanes			slow 38–40 kt (70–74 km/hr) fast 49 kt (91 km/hr)	slow 19–22 kt (35–41 km/hr) fast 54 kt (100 km/hr)	C 100°–150°	B 90°–150° C 90°–160°
20 60 n.mi. (111 km)	(30°–210°)	(120°)	MA–NH line to Casco Bay, ME	No severe hurricanes			slow 40–41 kt (74–76 km/hr) fast 49–50 kt (91–93 km/hr)	slow 22–23 kt (41–43 km/hr) fast 54–55 kt (100–102 km/hr)	C 120°–170°	B 110°–170° C 110°–180°
21 165 n.mi. (306 km)	(60°–240°)	(150°)	Casco Bay, ME to Vic. 45°N	No severe hurricanes			slow 41 kt (76 km/hr) fast 50 kt (93 km/hr)	slow 23–24 kt (43–44 km/hr) fast 55 kt (102 km/hr)	C 140°–190°	B 130°–200° C 130°–210°

* Segments where PMH cannot enter normal to coast (before smoothing).
# Segments where SPH cannot enter normal to coast (before smoothing).
† For definitions of categories A, B, and C see tables 11.2 and 11.3.

211

We also need to know if a PMH can travel from the east-northeast or even northeast. During the time period between their lowest p_o's and 12 hours before their lowest p_o's, all typhoons (1960-75) with $p_o \leq$ Camille's were moving from $\theta \geq 90°$. Typhoon Nora (1973), one of the three most severe typhoons on record in terms of p_o, moved from the east ($\theta = 90°$) at latitude 14.8°N for more than 3 hours while its p_o varied between 25.90 in. (87.7 kPa) and 25.93 in. (87.8 kPa). None of this sample of great typhoons moved from north of due east around the time of minimum p_o. The question now is can a PMH do so?

In the Northern Hemisphere a direction of movement from <90° is not common for a hurricane (typhoon). Riehl (1954) states, "motion toward the southwest occurs under a deep northeasterly flow. Preferred regions are the western parts of the Gulf of Mexico and the China Sea, where such upper (air) currents are common, especially in August."

Only the hurricanes of August 5, 1933 ($\theta = 70°$) and Fern of 1971 ($\theta = 50°$) followed a course from between the north and east over the western Gulf of Mexico during our period of record (1900-78). These two hurricanes had $p_o \geq 28.79$ in.(97.5 kPa). However, on Sept. 2, 1977, extreme hurricane Anita (not included on figs. 11.1 and 11.2 or table 11.1) entered a sparsely populated region of Mexico about 145 n.mi. south of Brownsville, Tex., from a $\theta = 60°$. A p_o of 27.34 in. (92.6 kPa) was measured by aircraft reconnaisance just prior to landfall. This p_o is within 0.15 in. (0.5 kPa) of SPH p_o for this portion of the coast.

Over the eastern gulf, the only hurricane traveling from between north and east that did not cross the Florida Peninsula was Inez of 1966 ($\theta = 65°$). This storm's p_o was 28.85 in. (97.7 kPa). In the Atlantic, the strongest hurricane following a course from between north and east was the storm of September 17, 1947 ($\theta = 80°$), which entered the Florida east coast near Fort Lauderdale with $p_o = 27.76$ in. (94.0 kPa).

The number of typhoons moving from the northeasterly quadrant over the South China Sea is also small (Crutcher and Quayle 1974). A typhoon of hurricane Camille intensity (26.81 in. [90.8 kPa]) or stronger has never intensified or developed over the China Sea as far as we can ascertain.

Typhoons such as Viola (1969) have passed through the Formosa Strait between Taiwan and Luzon, moving generally from the east or east-southeast, with p_o < Camille's, but have then filled. The only way a typhoon can enter the China Sea without crossing land is through the Formosa Strait. In addition, typhoons will weaken over the China Sea since sea-surface temperatures are cooler than over the Philippine Sea where the world's tropical cyclones have achieved maximum intensity. Only weak typhoons have moved from the northeast over the Philippine Sea.

Thus, we have learned not only that movement from <90° is uncommon for a hurricane, and occurs under a deep northeasterly flow, but also that none of the typhoons or hurricanes of near PMH intensity have followed tracks from the northeast. We conclude initially that hurricane movement from $\leq$45° will not lead to PMH intensity. Since movement from the east is possible (the extreme typhoon Nora), it also seems likely that a PMH could move from a direction slightly north of east, while maintaining its PMH p_o. Probably, Nora could have moved from slightly north of east. We therefore assume that a PMH can travel from a direction between east and east-northeast, limiting θ to $\geq$ 70°.

We have thus set the limits of θ for the PMH over the open ocean to between 70° and 190° (measured clockwise). We must now determine how the orientation of the 21 coastal segments affect this generalization.

Throughout much of the rest of this chapter we will refer to maximum θ and minimum θ (or maximum permissible θ and minimum permissible θ). Maximum θ is simply the largest numerical value of θ considered, and minimum θ is the smallest numerical value. For example, in discussing the open ocean criterion for the PMH, minimum θ = 70°.

11.5.2   RANGE IN θ ALONG THE COAST BEFORE SMOOTHING

11.5.2.1   DEPENDENCY ON FORWARD SPEED AND ANGLE OF APPROACH.

At this point, we wish to make two basic assumptions:

a. A PMH cannot travel close and parallel to a coast without weakening.

b. If a PMH is traveling close and parallel to a coast, the faster it moves the less it weakens.

214

The following discussion is meant to convey to the reader our concept for the minimum track angle permissible between the PMH and a random stretch of coast without filling. Figure 11.4 is a schematic that shows the percentage of the storm over the coast when the hurricane tracks have various entrance angles to the same location. A line labeled 90° is perpendicular to the coast. Three other lines are drawn at angles of 20°, 30° and 45°. Let the four circles represent the same PMH moving toward the coast. When the PMH, following the track perpendicular to the coast, is a distance equal to the radius of the circle from the coast (r) the land is not affecting the PMH winds. If, however, the PMH follows the 45° track, about 10% of the circle will be overland when the distance along the track is equal to r; similarly, if it follows the 30° track about 20% will be overland, and if it follows the 20° track, about 30% (nearly one-third of its circulation) will be overland. (Of course, if tracks were drawn

FIGURE 11.4 SCHEMATIC REPRESENTATION OF PMH NEAR THE COAST

Figure 11.4.--Schematic representation of PMH near the coast.

at 135°, 150°, and 160°, the results would be identical, except that the effect would be on the other half of the PMH).

From the discussion of the percent of the storm's circulation overland for selected angles to the coast, we have adopted allowable angles between the coast and θ related to the minimum speed a hurricane can have without weakening (table 11.2). We make the additional assumption that a PMH following a track with an angle <20° to the coast will weaken regardless of its forward speed.

In table 11.2 our three speed categories range from slowest (category A) to fastest (category C). The speeds within these categories were decided arbitrarily. In category A, 6 kt (11 km/hr) is the lowest limit of PMH forward speed criteria. The 10-kt (18 km/hr) speed is an arbitrary 5 kt (9 km/hr) greater than the allowable speed of a stalling hurricane ($\leq$ 5 kt).

Table 11.2.--Relation between forward speed (T) and the allowable angles between the coast and track direction (θ) for the PMH.

Speed category	Forward speeds (T)	Allowable angles between the coast and θ
A	6 kt ≤ T ≤ 10 kt (11 km/hr ≤ T ≤ 18 km/hr)	40° - 140°
B	10 kt < T ≤ 36 kt (18 km/hr < T ≤ 67 km/hr)	30° - 150°
C	T > 36 kt (T > 67 km/hr)	20° - 160°

Thus, for any coastal location, the allowable range in angles between the coast and θ for the PMH are determined by the forward speeds specified in chapter 10. We are assuming the size (R) of the hurricane (see sec. 11.7) will not be a major factor in limiting θ.

11.5.2.2 RANGE IN θ FOR INDIVIDUAL COASTAL SEGMENTS. We have given an open ocean criterion in section 11.5.1 and a general coastal criterion dependent on forward speed in section 11.5.2.1. Some of the 21 coastal segments (fig. 11.3 and table 11.1) use only these two criteria in setting the permissible PMH limits before smoothing. Other segments have additional criteria, e.g., cool sea-surface temperatures and their effect on θ. We will first look at the segments using only the open ocean and general coastal criteria.

Permissible θ limits for segments 1, 2, 4, 5, 7, 11-13, 15 and 16 are based on our open ocean criterion and the criterion indicated in table 11.2. For example, segment 16 has a coastal orientation (from north) of 350°-170°. The open ocean criterion gives PMH θ limits of 70° to 190°. Table 11.1, however, gives θ limits of 70° to 140° for category B and 70° to 150° for category C. The minimum θ of 70° in each category is from the open ocean criterion. The maximum θ for each category comes from the allowable angles given in table 11.2. For example, for category B, we may move 150° clockwise from 350° (350° + 150° = 500° or 140°) or 30° counterclockwise from 170° (170° - 30° = 140°) and obtain 140°. A similar method is used for category C, which is associated with higher forward speeds.

Additional criteria were imposed on the remaining segments. We will discuss segments 3, 14, 6, 8-10, and finally segments 17-21.

Segment 3 is short and recessed or indented away from adjoining segments 2 and 4. We have set θ between 150°-190° for category A and 140°-190° for category B. Segments 2, 3, and 4 all have a maximum permissible θ of 190° from the open ocean criterion. According to our coastal criterion (table 11.2) the minimum θ for segment 3 should be 125° (85°+40°) for speed category A and 115° (85°+30°) for category B because its coastal orientation is 85°-265°. The range of θ, however, is restricted further because the longer segment 4 controls access of the PMH to segment 3. A slow moving PMH entering from 125° would be only 15° off the coast of segment 4, which is too close to maintain PMH intensity. We solve this problem by assigning segment 3 the identical permissible PMH limits given segment 4.

Essentially the same procedure is followed when dealing with segment 14, also a short segment and recessed between segments 13 and 15. However, in this case, access to the coast is controlled by both segments 13 and 15.

Segment 6 is the most unorthodox of all 21 segments. Not only is it a short segment but its orientation is perpendicular to segment 5 and nearly perpendicular to segment 7. Its maximum θ (speed categories A and B) meet the general criteria of table 11.2. Its minimum permissible θ's for the PMH are controlled by the much longer segment 7.

Now we will consider limits on θ for segments 8 and 9. We explained in section 8.3.7.2.1.2 that a PMH would be a recurving hurricane over the northeastern Gulf of Mexico. Figure 8.11 shows two approximate PMH tracks, one entering segment 8 and the other entering segment 9.

Both tracks have an orientation of 230°. We have adopted a 30° range and set the permissible limits for segments 8 and 9 between 215° and 245°. Only speed category B applies to these two segments (see sec. 10.2.2.1).

Category A for segment 10 is assigned permissible limits (before smoothing) of 180° to 190° rather than a single angle of 190° (minimum coastal

orientation 150° + 40° coastal criterion = 190°). We give a range of 10° because we do not know enough about PMH θ to assign a single angle to this 190 n.mi. (352 km) stretch of coast.

Maximum θ for the northernmost five segments (17-21) were determined by the procedures used for the other segments. For segments 17 and 19, the coastal criterion (table 11.2) was controlling. For segments 18 and 21, the controlling factor was the open ocean criterion (θ = 190°). Along segment 20, the maximum θ of 170° was a slight modification of the coastal criterion to keep the PMH center from passing over a large portion of Massachusetts. Hurricanes passing over large land areas will fill (chapter 15) and, hence, will not be steady state; (see chapter 1).

Minimum θ for the northernmost five segments (17-21) was determined using an extension of the previous criteria and considering as additional factors a) the trend shown in the data toward gradually increasing minimum θ as we proceed northward, and b) the colder sea-surface temperatures, even in anomalously warm situations, from Virginia northward at the time of the PMH.

Hurricanes traveling at progressively faster forward speeds are not likely to be moving from the east quadrant because the fastest forward speeds are generally associated with hurricane recurvature and certainly pertain to θ ≥ 135° (movement from the southeast). Therefore, we set minimum θ = 140° for segment 21, the segment containing the fastest forward speeds. We assign segment 17 a minimum of θ = 80° in order to: a) avoid having a PMH enter this segment at an angle parallel to the coastal orientation of adjacent segment 18, and b) acknowledge the limiting effect of colder sea surface temperatures to the north. In a progressively more restrictive fashion, we set minimum θ = 90° for segment 18 (based on the coastal criterion); 100° for segment 19; 120° for segment 20; and as already stated 140° for segment 21. A hurricane entering the middle of segment 21 at a θ less than 110° would pass over southern Nova Scotia, whereas a hurricane entering the coast near 45° would have to travel from θ > 150° without crossing land.

This increase in the value of minimum θ (from 80° for segment 17 to 140° for segment 21), although somewhat arbitrary, is considered reasonable when compared with available data. A glance at east coast hurricanes (tables 4.2 and 4.4) indicates that of the eight hurricanes traveling at speeds ≥ 25 kt or 46 km/hr (median slow speed for segment 17) the minimum θ was 180°. Also, maximum sea-surface temperature data during late summer and early autumn lend support to our minimum θ's for segments 17-21 before smoothing (U.S. Navy 1975).

11.5.3 RANGE IN θ ALONG THE COAST AFTER SMOOTHING.

The curves of figure 11.5 show the permissible limits of θ for the PMH *after* smoothing across coastal segments. The maximum allowable range of θ within the segments *before* smoothing is shown by hatching. Figure 11.6 shows these curves plotted with these data of figure 11.1. Points falling outside the curves are labeled with central pressure.

Smoothing in figure 11.5 was accomplished by connecting limits for the 21 individual coastal segments with smooth curves, making sure that the curves show realistic θ near segment intersections and also within portions of the segments where there are large departures in actual coastal orientation from the generalized segment orientation. The smooth outer curves represent the maximum allowable range of θ *after* smoothing. The smooth inner curves represent the decrease of the allowable range for the lower speed category A (≤ 10 kt [≤ 18 km/hr]) for segments 1-7 and 10-15 and category B (10 kt < T ≤ 36 kt or 18 km/hr < T ≤ km/hr) for segments 16-18. Only category C (T > 36 kt or 67 km/hr) applies to segments 19-21 and only category B applies to segments 8-9. A single minimum θ curve is analyzed for segments 16-21 even though two forward speed categories apply in segments 16, 17 and a portion of 18.

Milepost 1800 (3336 km) provides an example of a point along the coast crossed by two inner and two outer curves. The two outer curves indicate that for forward speeds >10 kt or 18.5 km/hr (speed category B), the allowable range of θ is 75° to 130°. The two inner curves tell us that for forward speeds ≤ 10 kt or 18.5 km/hr (category A), the allowable range of θ decreases to 85° to 125°. Along some stretches of the coast such as near
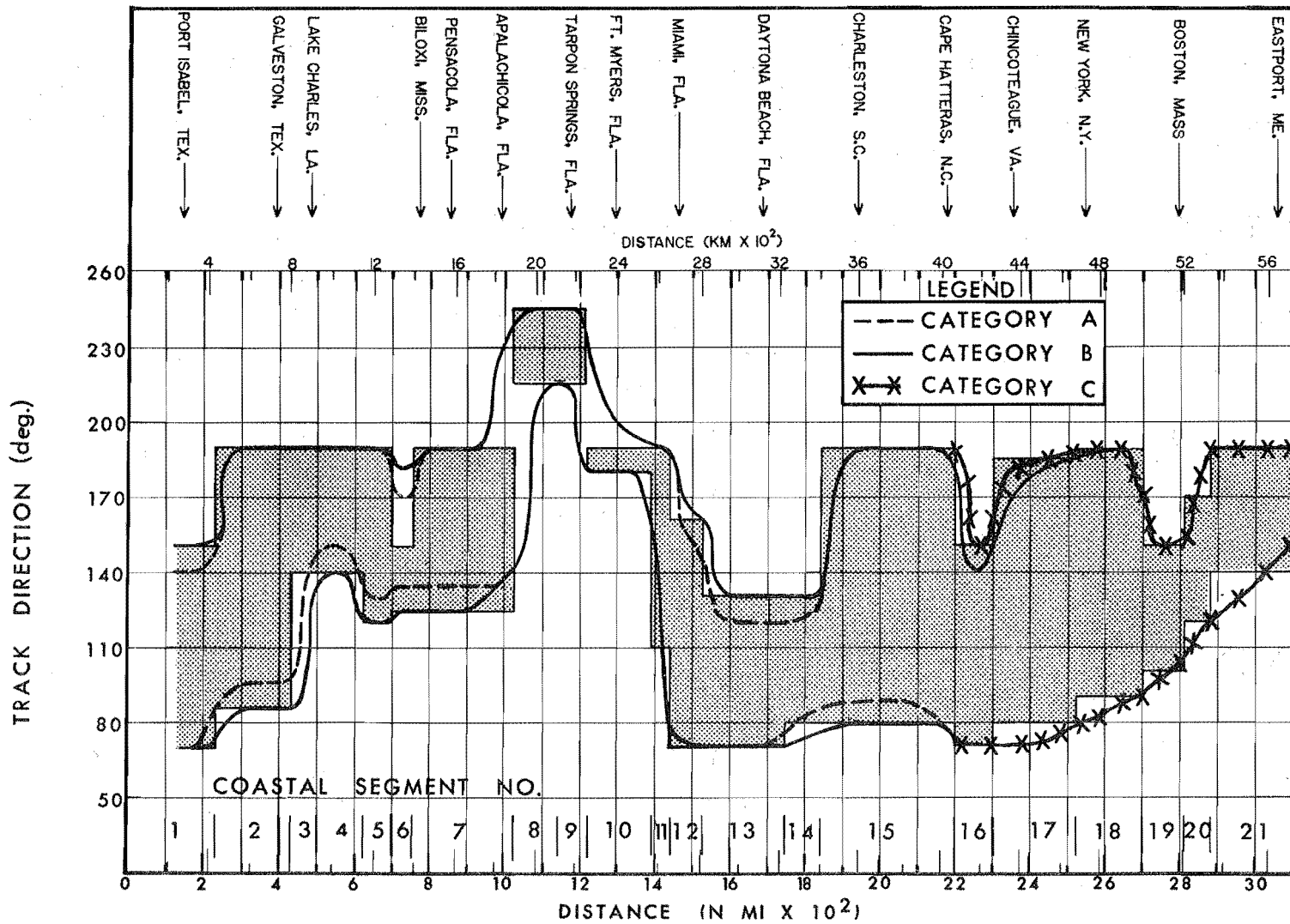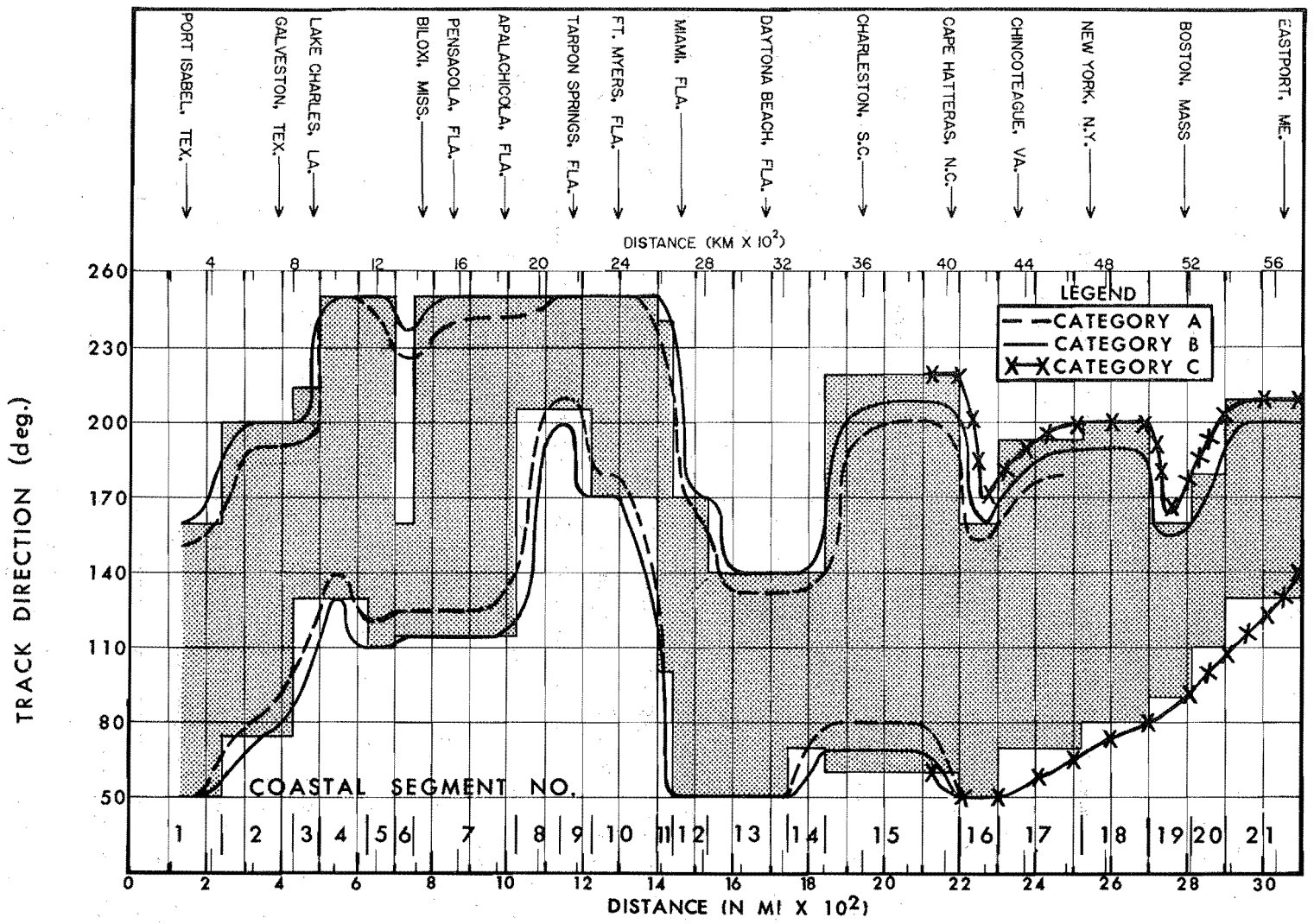
Figure 11.5.--*Permissible limits of θ for the PMH. The maximum limits before smoothing are shown by hatching. Allowable limits after smoothing for forward speed categories A, B, and C (see table 11.2) are shown by smooth curves.*
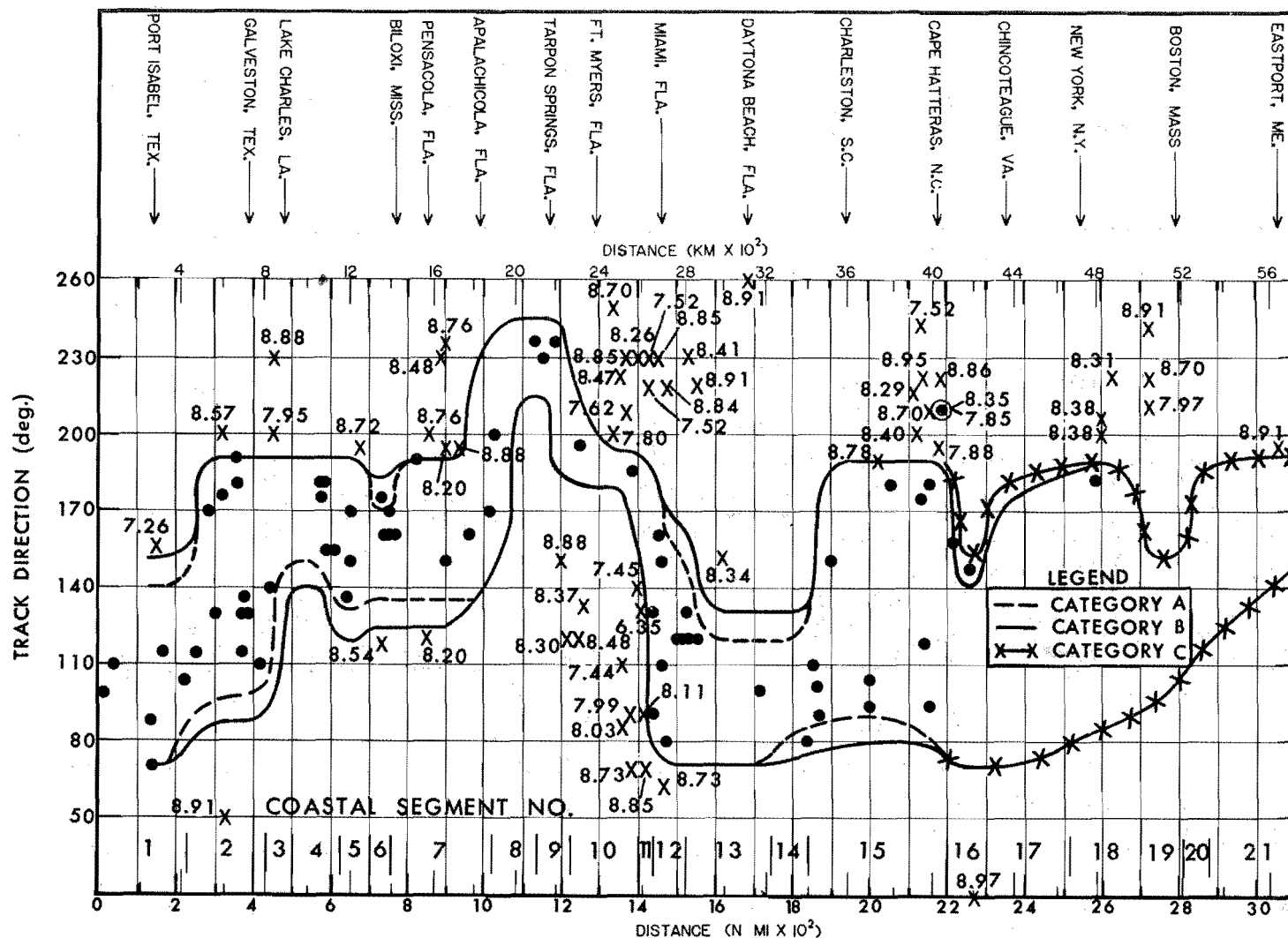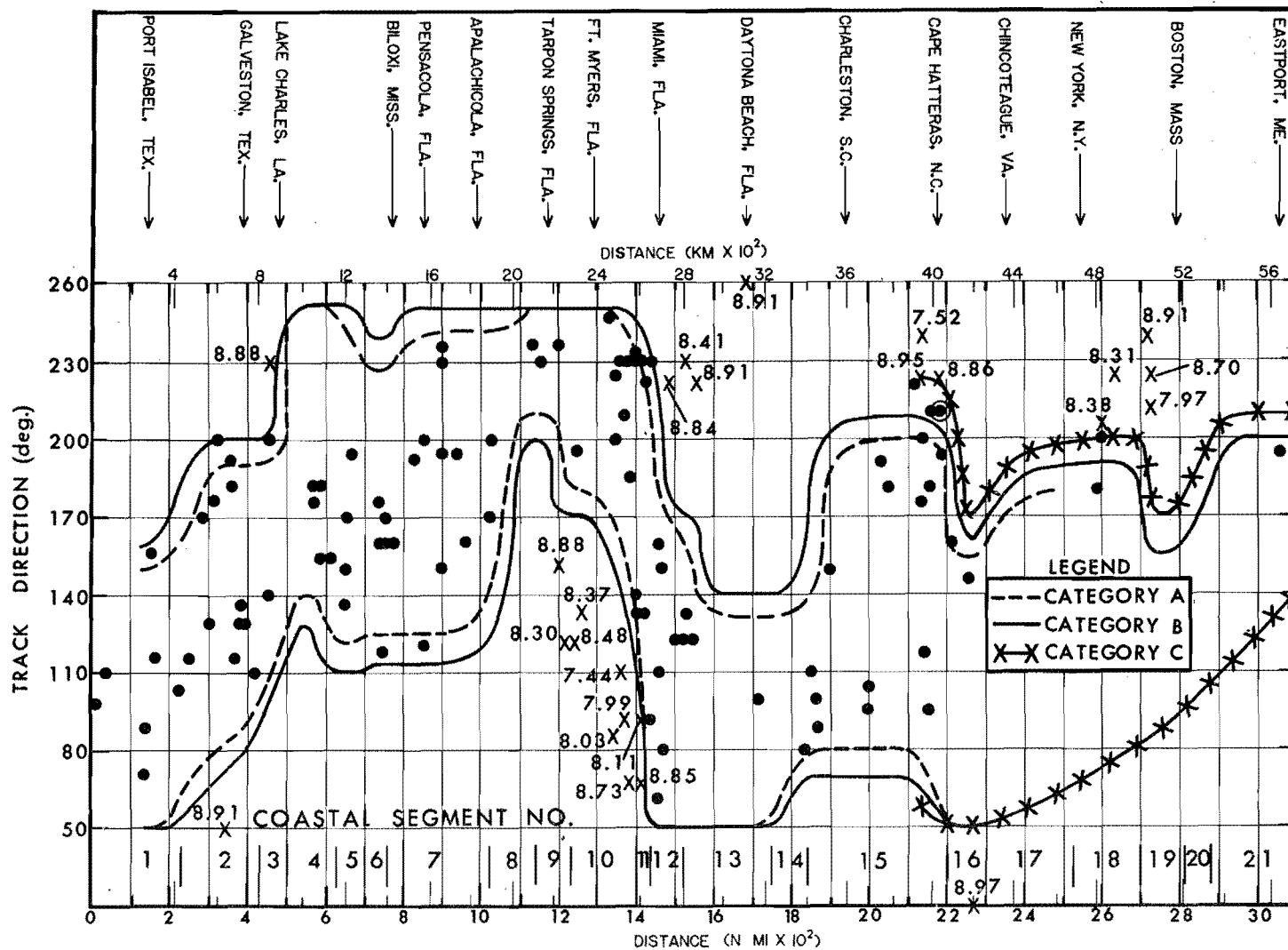
Figure 11.6.—*Maximum allowable range of PMH θ after smoothing is represented by the area between the outermost curves. Data points are the same as those in figure 11.1. Those inside the outermost curves are indicated by a dot and those outside these curves by an X. Two hurricanes plotted at the same position are indicated by a* ⊙ . *Plotted values (shown for data falling outside the curves) are central pressure in inches of Hg (example: 8.72 = 28.72 in.)*

milepost 250 (463 km), an outermost and an innermost curve merge into a
single curve. Here, the permissible maximum limits of θ are the same (160°)
for the entire range of forward speeds.

11.6   TRACK DIRECTION FOR THE SPH

Track directions(θ) for the SPH given in this section are considered to be
"reasonably characteristic." The data show that storms weaker than the SPH
have a wider range of θ.

11.6.1 RANGE IN θ OVER THE OPEN OCEAN

In section 11.5.1, we set the limits of θ for the PMH over the open ocean
between 70° and 190° (measured clockwise from north). The limits of θ for
the SPH should cover a wider range of angles.

We have adopted limits between 50° and 250° (measured clockwise from
north) for the SPH over the open ocean. We believe that movement from θ
< 50° of a hurricane will not lead to SPH intensity. Hurricane Anita of
September 1977, (see sec. 11.5.1) entered the coast of Mexico from a θ = 60°
Its 27.34 in. (92.6 kPa) p_o was near SPH intensity. Therefore, we need to
include θ = 60° in our SPH range . An angle of 50° is therefore a reasonable
minimum permissible θ for the SPH. Recurved hurricanes (≅225°)are a rather
common phenomenon (figs. 11.1 and 11.2), especially in more northerly lati-
tudes. In fact, these storms will often move at θ>225°, although only one
hurricane with $p_o \leq 28.05$ in. (95.0 kPa) has exceeded this value (fig. 11.2).
This is bypassing hurricane Helene with p_o of 27.52 in. (93.2 kPa) and θ of
240° near Cape Hatteras. We wish to exceed the θ of Helene and also be
able to bring an SPH normally into most of the west Florida coast. For the
maximum SPH θ over the open ocean θ = 250° meets these requirements .

11.6.2   RANGE IN θ ALONG THE COAST BEFORE SMOOTHING

11.6.2.1   DEPENDENCY ON FORWARD SPEED AND ANGLE OF APPROACH.

Our constraints in θ for the SPH are not as restrictive as they are for the
PMH. For each of our speed categories (category A now includes speeds as
low as 4 kt or 7 km/hr), we have increased our range of allowable angles
between the coast and θ by 20°. These angles are shown in table 11.3.

Table 11.3.--Relation between forward speed (T) and the allowable angles between the coast and track direction (θ) for the SPH.

Speed category	Forward speeds (T)	Allowable angles between the coast and θ
A	4 kt ≤ T ≤ 10 kt (7 km/hr ≤ T ≤ 18 km/hr)	30° - 150°
B	10 kt < T ≤ 36 kt (18 km/hr< T ≤ 67 km/hr)	20° - 160°
C	T > 36 kt (T > 67 km/hr)	10° - 170°

11.6.2.2 RANGE IN θ FOR INDIVIDUAL COASTAL SEGMENTS. The permissible SPH limits of segments 1, 4, 5, 7, 9-13, 15 and 16 agree with our open ocean criterion and the criterion listed in table 11.3.

Additional criteria were imposed on the remaining segments (2, 3, 6, 8, 14, and 17-21) before permissible SPH limits were set (table 11.1). The reasons for additional criteria for segments 3, 6, and 14 are identical to the reasons given for the PMH in section 11.5.2.2. Reasons for imposing additional criteria on segments 2, 8, and 17-21 follow.

In segment 2, SPH category A has a maximum θ of 195° and category B has a maximum θ of 200°. These θ's keep the SPH from traveling over southern Texas and northeastern Mexico.

Because of the coastal orientation, only an SPH that has recurved may enter segment 8. Segment 8 takes its minimum θ from segment 9 and its maximum from segment 7.

Maximum θ is determined by the coastal criterion (table 11.3) for segments 17 and 19. For the PMH, we gave a range of 90° to 190° for segment 18 even though segment 17 would tend to limit θ to angles less than 185° over Long Island and Connecticut. We did this because 18 is relatively long, juts out from the coast, and is not concave like segment 14, for example. For the SPH, we increase the range from 190° to 200° for category C and leave θ at 190° for category B. Along segment 20, we increase the range for category C from 170° for the PMH to 180° for the SPH to allow the SPH a larger range. An SPH with θ = 180° will pass over

the western portion of the Cape Cod peninsula. In segment 21, the SPH maximum θ is 210°. Angles >210° are not permissible because the hurricane would pass over southern New England.

Minimum θ for the northernmost five segments (17-21) is determined by subtracting 10° from the PMH minimum θ for these segments.

11.6.3 RANGE IN θ ALONG THE COAST AFTER SMOOTHING

The curves of figure 11.7 show the permissible limits of θ for the SPH *after* smoothing across coastal segments. Figure 11.8 shows these curves plotted with the data of figure 11.1. Points falling outside the curves are labeled with central pressure.

Smoothing in figure 11.7 was accomplished in the same way as the smoothing for the PMH (see sec. 11.5.3). The SPH curves in figure 11.7 always envelop the corresponding PMH curves; i.e., an SPH being a weaker hurricane than the PMH has a wider range of allowable θ at any coastal point. The smooth outer curves represent the maximum allowable range of θ after smoothing. The smooth inner curves represent the decrease of the allowable range for the lower speed category A ($\leq$ 10 kt or $\leq$ 18 km/hr) for segments 1-17 and category B (10 kt < T $\leq$ 36 kt or 18 km/hr < T < 67 km/hr) for segments 17-21. A single minimum θ curve is analyzed for segments 16-21. This is done even though three forward speed categories apply to an SPH entering segment 16 and portions of segments 15 and 17, and segments 18-21 are represented by two forward speed categories.

11.7 INTERPRETATION OF RESULTS OF SECTIONS 11.5 AND 11.6

Some readers may find it paradoxical for the SPH, the weaker storm, to have a larger range in direction than the PMH, the stronger storm. After all, the PMH is what probably can happen, while the SPH is what is likely to happen within some undefined but long period of time. However, the truth is that the rarer the hurricane, the more ideal or favorable the ambient conditions must be which lead to a narrower range of θ. To put it another way, PMH θ's are more limited than the SPH because the lower central pressure of the PMH can only be accommodated by a smaller range of θ.

Figure 11.7.--Permissible limits of θ for the SPH. The maximum limits before smoothing are shown by hatching. Allowable limits after smoothing for forward speed categories A, B, and C (see table 11.3) are shown by smooth curves.

Figure 11.8.—Maximum allowable range of SPH θ after smoothing is shown by the area between the outermost curves. Data points are the same as those in figure 11.1. Those inside the outermost curves are indicated by a dot and those outside these curves by an X. Two hurricanes plotted at the same position are indicated by a ⊙. Plotted values(shown for data falling outside the curves) are central pressure in inches of Hg (example: 8.88 = 28.88 in.).

The developed ranges of θ are dependent on forward speed (T). Radius of maximum winds (R) is not employed in developing the θ ranges. One reason R was not used is because it shows little correlation (0.19) with θ for gulf coast storms. East coast recurved hurricanes ($\theta \geq 180°$) have larger R, which could indicate that these storms may require a smaller range of θ with respect to the coast to remain steady state, but not enough is known about the interrelation between θ and R under nonrecurvature conditions to have R dependent on θ in this report.

12. OVERWATER WINDS

12.1 THE MAXIMUM GRADIENT WIND SPEED EQUATION

12.1.1 INTRODUCTION

The meteorological parameters p_W, p_O and R, discussed in chapters 7, 8, and 9, respectively, are used in determining maximum theoretical gradient wind speed (V_{gx}). Gradient wind is defined as a wind blowing under conditions of circular motion, parallel to the isobars, in which the centripetal and coriolis accelerations together exactly balance the horizontal pressure-gradient force per unit mass. Gradient wind is independent of duration. The maximum gradient wind speed in a hurricane is the maximum gradient wind at the radius of maximum winds. The larger the pressure drop ($\Delta p = p_W - p_O$), the larger the gradient wind speed (everything else being equal).

The maximum gradient wind speed in this study is computed from the equation:

$$V_{gx} = K (p_W - p_O)^{1/2} - \frac{Rf}{2} \qquad (12.1)$$

where

p_W = peripheral pressure from weather maps

p_O = central pressure

R = radius of maximum winds

f = coriolis parameter*

$K = \left(\frac{1}{\rho e}\right)^{1/2}$ = density of the air (ρ) computed from sea-surface temperatures; $e \cong 2.71828$

12.1.2 DERIVATION

In order to derive the maximum gradient wind speed equation, we should first define the cyclostrophic wind. Cyclostrophic wind is that horizontal wind for which the centripetal acceleration exactly balances the horizontal

---

*Twice the component of the Earth's angular velocity about the local vertical, $2\Omega \sin \psi$, where Ω is the angular speed of the earth and ψ is the latitude. Since the earth is in rigid rotation, the coriolis parameter is equal to the component of the Earth's vorticity about the local vertical.

228

pressure-gradient force per unit mass. Cyclostrophic wind approximates gradient wind best in hurricanes under conditions when R and f are small, i.e., small-size hurricanes at low latitudes. Maximum winds occur at R when winds are cyclostrophic. The maximum winds for the SPH and PMH are nearly in cyclostrophic balance since the second term on the right side of eq. 12.1 is much smaller than the first term.

We will show that:

$$V_{cx} = K \ (p_w - p_o)^{1/2} \tag{12.2}$$

where V_{cx} = maximum cyclostrophic wind speed.

A standard formula for the cyclostrophic wind speed is:

$$\frac{V_c^{\ 2}}{r} = \frac{1}{\rho} \frac{dp}{dr} \tag{12.3}$$

where V_c = cyclostrophic wind speed

     p = the pressure at radius r

     ρ = air density

A standard formula for the gradient wind speed is:

$$\frac{V_g^{\ 2}}{2} + fV_g = \frac{1}{\rho} \frac{dp}{dr} \tag{12.4}$$

where

       V_g = gradient wind speed.

Equating the left hand members of eq. 12.3 and 12.4 we obtain:

$$\frac{V_g^{\ 2}}{r} + fV_g = \frac{V_c^{\ 2}}{r} \tag{12.5}$$

which may be solved for $V_c - V_g$:

$$V_c^2 - V_g^2 = rfV_g$$

$$(V_c + V_g)(V_c - V_g) = rfV_g$$

$$V_c - V_g = \frac{rfV_g}{V_c + V_g} \tag{12.6}$$

Over the range of hurricane wind speeds of interest to this study, the difference between the quantities V_c and V_g is small compared with the quantities themselves. The approximation is made in the right hand member of eq. 12.6 that V_c and V_g are equal.
This yields:

$$V_c - V_g \cong \frac{rf}{2} \tag{12.7}$$

and

$$V_{cx} - V_{gx} \cong \frac{Rf}{2}$$

Neglecting the approximation, we have

$$V_{gx} = V_{cx} - \frac{Rf}{2} \tag{12.8}$$

From chapter 6, the Hydromet Pressure Profile Formula is:

$$\frac{p - P_o}{P_w - P_o} = e^{-R/r}$$

or

$$p - P_o = (P_w - P_o) e^{-R/r} \tag{12.9}$$

Equation 12.9 may be solved for the pressure gradient $(p - P_o)$ by taking derivatives:

$$\frac{dp}{dr} = \frac{(P_w - P_o) Re^{-R/r}}{r^2} \tag{12.10}$$

230

From eq. 12.3

$$\frac{dp}{dr} = \frac{\rho V_c^2}{r}$$

So

$$\frac{\rho V_c^2}{r} = \frac{(p_w - p_o) \, Re^{-R/r}}{r^2}$$

and

$$V_c^2 = \frac{(p_w - p_o) \, Re^{-R/r}}{\rho r} \qquad (12.11)$$

For V_{cx}, $r = R$;

then

$$V_{cx}^2 = \frac{(p_w - p_o)}{\rho e} \qquad (12.12)$$

and

$$V_{cx} = \left[\frac{(p_w - p_o)}{\rho e}\right]^{1/2} \qquad (12.13)$$

Since $K = \left(\frac{1}{\rho e}\right)^{1/2}$, we have derived eq. 12.2:

$$V_{cx} = K \, (p_w - p_o)^{1/2}$$

Substituting equation 12.2 into eq. 12.8, we obtain eq. 12.1:

$$V_{gx} = K \, (p_w - p_o)^{1/2} - \frac{Rf}{2}$$

Eq. 12.1, the maximum gradient wind speed equation, has now been rigorously derived.

The next task is to determine suitable values of the K coefficient for the SPH and the PMH.

12.1.3 DETERMINATION OF THE K COEFFICIENT

12.1.3.1 BACKGROUND. Eq. 12.13 shows that the magnitude of the maximum gradient wind is dependent not only on the pressure difference, but also on the air density at R, which has been included in K.

We should not overlook a significant fact. The kinetic energy of the hurricane wind, proportional to ρV^2, is responsible both for exerting stress on a water surface (thereby producing surges and waves) and wind damage. In comparing thin air (large value of K) with dense air (small value of K), both experiencing the same travel from high to low pressure, the thin air will be moving faster but the kinetic energy will be identical.

From the above discussion, it appears that we have two options. We can assume a standard ρ, hence a standard value of K, because the kinetic energy will be identical anyway, or we can justify a latitudinal variation of density as a matter of convenience and realism.

In NHRP 33 (Graham and Nunn 1959) a standard value of 73 was used for K along both coasts for the SPH. This is based on the air density at 68°F (20°C) and a pressure of 29.53 in. (100.0 kPa). The numerical value of K depends on the units used; in this case the wind speed is in miles per hour and the pressure is in inches of mercury. Given K in the above units, we can convert it for use with either knots and inches of mercury or kilo-meters/hour and kilopascals by multiplying by 0.868 or 0.8805. HUR 7-97 used a latitudinal variation of K (in the same units as in NHRP 33) ranging from 76.8 at latitude 24°N to 72.8 at latitude 42°N. This variation was based on the variation in maximum sea-surface temperatures along the east coast, using what is now out of date data. The draft revision of NHRP 33 (HUR 7-120) used the same values of K for computation of maximum gradient winds as those used in HUR 7-97.

12.1.3.2 ADOPTED VARIATION IN K. In this report, we recommend that K be varied with latitude. We base the latitudinal variation of K on the variation of the 0.99 probability level sea-surface temperature (a rare event) for the PMH and the 0.75 probability level (above average but not rare) for the SPH, making the assumption that the air temperature is the

same as the sea-surface temperature. This assumption is less likely in northern latitudes where the hurricane transports warmer tropical air over colder water.

A recent publication (U.S. Navy 1975) gives sea-surface temperature (T_s) frequencies by blocks over coastal waters of the North Atlantic Ocean and Gulf of Mexico (fig. 12.1). Figure 12.2 is a plot of the 99% and 75% frequency levels of T_s for August, the month of highest temperatures, against coastal reference points from tables 4.1 to 4.4. For the gulf coast, the variation is very slight, the 99% frequency level varying between 89.0° and 89.5°F (31.7° and 31.9°C). For the east coast, the variation is large, the 99% level is about 89.5°F (31.9°C) near milepost 1400 and about 68.0°F (20.0°C) at milepost 3100.

Figures 12.3 and 12.4 show smoothed values of the K factor for three units of measurement for the SPH and the PMH, respectively. These values were computed for a number of locations along the east coast using the central pressure (p_o) determined in chapter 8. Values of K between 24° and 30°N may also be applied to the gulf coast with little loss of

Figure 12.1.--Blocks used to calculate sea-surface temperatures in determining latitudinal variation of K coefficient (after U.S. Navy 1975).

accuracy. Temperatures were taken from the 75% frequency level values of figure 12.2 for the SPH and the 99% frequency level values for the PMH. These temperatures are adjusted to virtual temperature (assuming saturation) in order to determine air density.
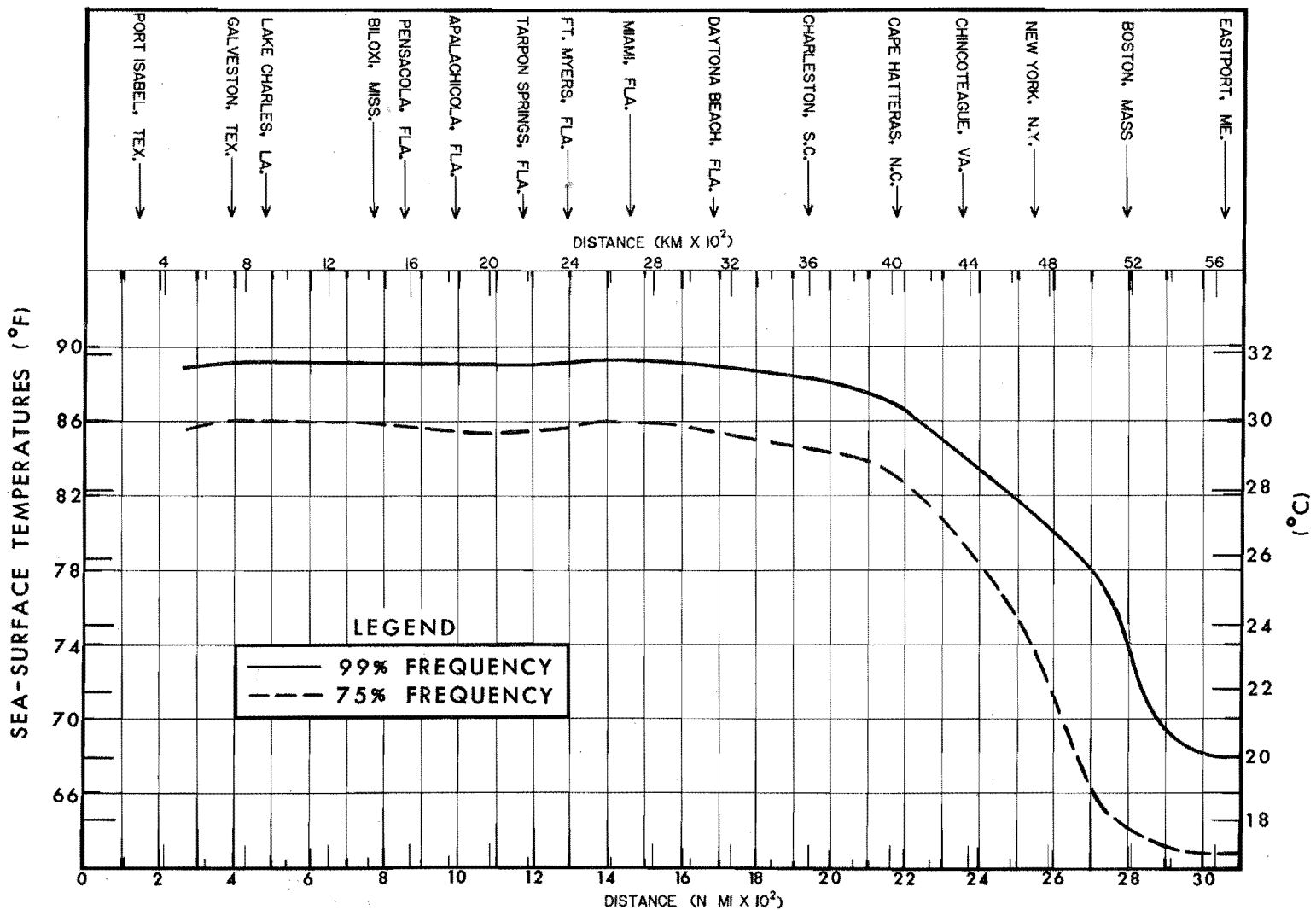
Figure 12.2.--Sea-surface temperatures, 99th percentile and 75th percentile, along the gulf and east coasts during August.
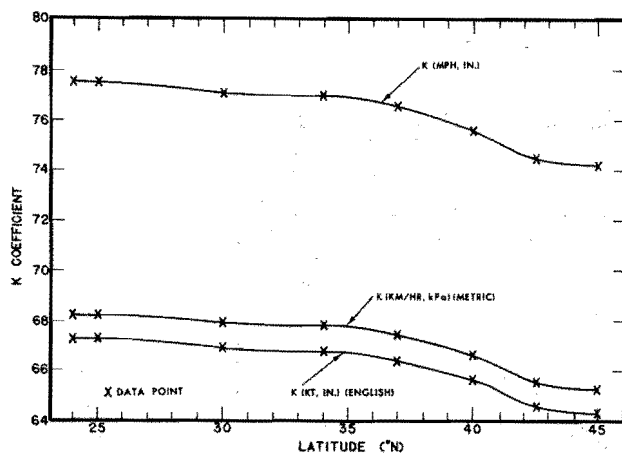
Figure 12.3.--Values of latitude-
dependent K coefficient for three
units of measurement for the SPH.
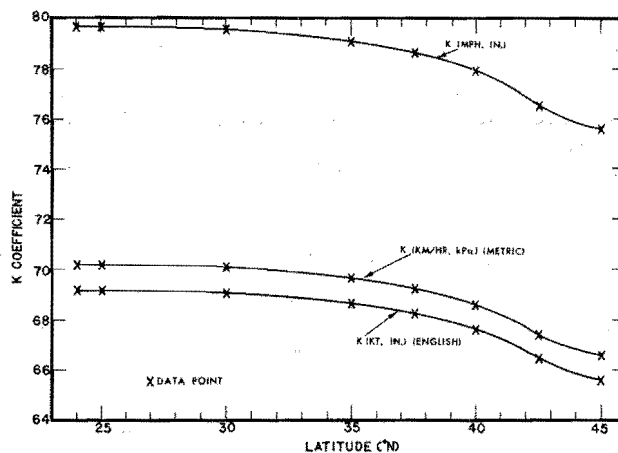
Figure 12.4.--Values of latitude-
dependent K coefficient for three
units of measurement for the PMH.

The difference in the numerical values of K at 24°N and 45°N is about 4%
for the SPH and 5% for the PMH. If the user does not wish to vary K with
latitude, a constant could be applied. Maximum wind speeds would differ by
a few percent by employing such a constant.

12.2 TEN-METER, 10-MINUTE OVERWATER WINDS

12.2.1 INTRODUCTION

Observed maximum 10-m (32.8-ft), 10-min winds (V_x) over open water in hur-
ricanes of above average intensity have been found to vary from about 75 to
100% of V_{gx} (Myers 1954). Occasionally, however, V_x over open water in
hurricanes of above average intensity exceeds V_{gx}. When this happens,
supergradient winds result. These winds are especially prevalent in the
right semicircle of a hurricane (Shea and Gray 1972).

We see from the above that the V_{gx} can be equal or even less than V_x in
some cases. The value of V_x will exceed V_{gx} in fast-moving hurricanes. The
applicable asymmetry factor will be discussed in section 12.2.3.1.

Empirical equations have been used in previous reports to estimate the
maximum 10-m, 10-min overwater wind speed. This maximum wind will occur at

some point around the circle defined by R. These equations take the form:

$$V_x = F (V_{gx}) + A \qquad (12.14)$$

where

V_x = maximum 10-m, 10-min overwater wind speed.

F = reduction factor to convert from maximum gradient wind speed to 10-m, 10-min overwater wind speed.

V_{gx} = maximum gradient wind speed defined by eq. 12.1.

A = asymmetry factor resulting from the forward speed (T) of the hurricane.

12.2.1.1 RECOMMENDED REDUCTION FACTORS (F) FOR SPH AND PMH. A factor, F, of 0.865 (to convert from V_{gx} to V_x) was developed from data observed in the 1949 hurricane that crossed Lake Okeechobee, Fla. It was used as the standard in previous reports because it not only was from this well-documented hurricane, but also because it lay about half way between the 0.75 to 1.00 ratios cited in section 12.2.1 (Myers 1954). Supergradient winds (F factor >1.00) were not considered in these reports. Since supergradient winds in intense hurricanes (Shea and Gray 1972) now appear to be more prevalent than earlier reports indicated, some slight increase in the 0.865 value would be appropriate. Additionally, because of the accuracy implied by this value (which is not justified by the data), it should be rounded. For these reasons, we have adopted 0.9 for the SPH. We have adopted 0.95 for the PMH on the grounds of representing a more extreme condition.

12.2.2 WINDS IN A STATIONARY HURRICANE

For a stationary hurricane, equation 12.14 reduces to:

$$V_x = 0.9 \ V_{gx}, \text{ for the SPH} \qquad (12.15)$$

$$V_x = 0.95 \ V_{gx}, \text{ for the PMH,} \qquad (12.16)$$

since A, the asymmetry factor, equals zero. V_x for a stationary hurricane we shall call V_{xs}.

Knowing V_{xs}, we can use relative wind profile information in chapter 13 to determine 10-m, 10-min overwater winds at any distance from the hurricane center.

12.2.3 WINDS IN A MOVING HURRICANE

12.2.3.1 THE ASYMMETRY FACTOR.

Equation 12.14 includes an asymmetry factor A, which is added on the right of the storm track and subtracted on the left, which when combined with F (V_{gx}) gives V_x—the maximum 10-m, 10-min overwater wind in a moving hurricane.

The general equation for A is:

$$A = yT^x \cos \beta \qquad (12.17)$$

where y and x are two empirical constants, T is the forward speed of the hurricane, and β is the angle between track direction (θ) and the surface wind direction (θ_a), measured counterclockwise from θ.

12.2.3.1.1 CONSTANTS Y AND X.

In previous studies (Graham and Nunn 1959, U.S. Weather Bureau 1968), y was assumed to be 0.5 and x to be 1.0.

In the present study, we have reviewed this assumption. It appears to yield results that are unreasonable with T. Consideration of the energy imparted to the storm's circulation by a factor of 0.5 when T is large, suggests a lesser adjustment. Also, when T is small, there is not enough asymmetry across the hurricane.

These concepts were tested with several values of both y and x. When T is expressed in knots, a value of y = 1.5 and x = 0.63 yielded satisfactory results. At T = 6 kt, the asymmetry factor would add a maximum of 4.6 kt to speeds in the right semicircle; at T = 50 kt, the maximum additive value would be 17.6 kt. At approximately 20 kt, the maximum additive value would be 10 kt.

The value of y is independent of the units of measure, while x depends on the forward speed units of the storm. Similar factors of x and y could have been developed for other units. We chose instead to expand eq. 12.17 as follows:

$$A = yT^x T_o^{(1-x)} \cos \beta \qquad (12.18)$$

where T_o is a parameter in speed units and the other factors are as previously defined. We have already chosen to use $y = 1.5$, $x = 0.63$ when T is in knots. In this case, eq. 12.18 reduces to eq. 12.17 by definition, i.e., $T_o = 1$ kt. T_o equals 0.514791 when units are in m s^{-1}, 1.853248 when in km hr^{-1} and 1.151556 when in mi hr^{-1}.

12.2.3.1.2 THE ANGLE β. The angle β varies:

a. Around the hurricane at any constant radial distance (r), and

b. Along a radial at varying distances from the hurricane center.

12.2.3.2 ADOPTED SPH AND PMH MAXIMUM 10-M, 10-MIN OVERWATER WIND EQUATIONS. Equation 12.14 has provided a general form for these equations. Values of F are defined in section 12.2.1.1 and the asymmetry factor is evaluated in section 12.2.3.1. Using this information, V_x for the SPH can be determined from:

$$V_x = 0.9 \ V_{gx} + 1.5 \ (T^{0.63}) \ (T_o^{0.37}) \cos \beta \qquad (12.19)$$

and for the PMH from:

$$V_x = 0.95 \ V_{gx} + 1.5 \ (T^{0.63}) \ (T_o^{0.37}) \cos \beta \qquad (12.20)$$

V_x is defined as occurring at the point along the circumference of maximum winds where the actual wind direction is parallel to the track direction (θ). Here, $\beta = 0$ and $\cos \beta = 1$. The inherent relation between β and inflow angle (ϕ) requires the point at which V_x occurs to fall in the right-rear quadrant of a hurricane. Chapter 13 will set allowable limits of rotation for this point.

12.2.3.3 SPH AND PMH 10-M, 10-MIN OVERWATER WIND EQUATION AT ANY r. The equation for 10-m, 10-min overwater winds at any distance (r) from the hurricane center is:

$$V = V_s + 1.5 \ (T^{0.63}) \ (T_o^{0.37}) \cos \beta \qquad (12.21)$$

where V is the wind speed at radius r and V_s is the wind speed in a stationary hurricane at radius r. Relative wind profiles for computing V_s are developed in chapter 13.

12.2.3.3.1 ALONG A RADIAL THROUGH V_x (RADIAL M). The procedure for computing V along any radial is most easily understood by first computing V along the radial M through the point of maximum wind. The variation of β with r along this radial is illustrated schematically in figure 12.5.

For better understanding we are letting R = 15 n.mi. (28 km). Since the inflow angle (ϕ) (see chapter 14) varies with r, β must also vary with r. The tangential wind direction (θ_t) is normal to the radial as shown in the diagram. θ_t at any point along this radial is a constant. Since the track direction (θ) is a constant, the angle between θ and θ_t at any point along this radial is a constant. At r = R, β = 0 by definition because radial M passes through V_x. Thus, cos β = 1.

Figure 12.5.--Illustration of the relation between track direction (θ), tangential wind direction (θ_t), and actual surface wind direction (θ_a) along the radial through point of maximum wind (radial M) β is given for r = 10, 15, and 25 n.mi. (19, 28 and 46 km) for this example of a PMH with R = 15 n.mi. (28 km).

The right side of figure 12.5 illustrates that at some point where r >R, β is the difference between ϕ at this point and ϕ at r = R, where $\beta = \phi_R - \phi_R = 0$. Therefore:

$$\beta = (\phi_r - \phi_R) \qquad (12.22)$$

For example, from figure 14.7 (PMH) for an R of 15 n.mi. (28 km), ϕ = 7.2° at r = 15 n.mi. and 20.6° for r = 25 n.mi. (46 km). Then:

$$\beta = (\phi_{25} - \phi_{15})$$

$$\beta = 20.6° - 7.2° = 13.4°$$

The left side of figure 12.5 indicates how at some point where r <R, β is the difference between ϕ at this point and ϕ at r = R. Therefore, we may again make use of eq. 12.22:

$$\beta = (\phi_r - \phi_R)$$

From figure 14.7, $\phi = 3.0°$ if we let r = 10 n.mi. (19 km). Therefore:

$$\beta = (\phi_{10} - \phi_{15})$$

$$\beta = 3.0° - 7.2° = -4.2° = 355.8°$$

12.2.3.3.2 ALONG ANY OTHER DESIRED RADIAL. The β's along any other radial are determined by modifying the β_M's computed along radial M. The angles β along other profiles are computed by adding the number of degrees counterclockwise between radial M and the desired radial to the computed β_M's. For example, at r = 25 n.mi. (46 km) in sec. 12.2.3.3.1, β would equal 103.4° not 13.4° if our desired radial lay 90° counterclockwise from radial M. At r = 10 n.mi. (19 km), β would equal 85.8°, not 355.8°.

12.3 VALUES OF V_{gx} AND V_x FOR RECORD HURRICANES

Tables 4.1 and 4.2 list values of V_{gx} and V_x in kilometers/hour and tables 4.3 and 4.4 in knots for the gulf and east coasts of the United States for hurricanes with central pressure $\le$ 29.00 in. (98.2 kPa) during the period 1900-78. Values of K and the coriolis parameter (f) are evaluated at the latitude of the minimum p_o. K values were taken from figure 12.3 for all but two hurricanes, the Labor Day hurricane of 1935 and hurricane Camille (1969), whose p_o's are much lower than the SPH. For these two, the K of figure 12.4 was used. The values of V_{gx} and V_x were computed using equations 12.1 and 12.19 for all hurricanes except the Labor Day hurricane of 1935 and Camille (1969). Equations 12.1 and 12.20 were used for these two storms. For V_x, cos β = 1.

V_x, the maximum 10-m, 10-min sustained overwater wind speed, is not the wind normally reported as the maximum sustained wind in a hurricane by reconnaissance aircraft. They normally report sustained 1-min winds, not 10-min winds. Sometimes, sustained winds of shorter duration are reported. Therefore, these reconnaissance winds have the tendency to be 15% or more higher than V_x. Also, the winds are measured at flight level and only estimated near the surface. In addition, many wind reports in the literature are gusts or sustained winds of short duration.

Hurricane Camille's (1969) V_x is 121 kt or 224 km/hr (tables 4.3 and 4.1).
This compares with highest SPH V_x of about 106 kt (196 km/hr) near milepost
700 (tables 2.3 and 2.4) and a highest PMH V_x of 139 kt (258 km/hr) found in
tables 2.5 and 2.6). The Labor Day hurricane of 1935 had a V_x of 130 kt
(241 km/hr), or the highest V_x of any record hurricane. The highest SPH V_x
at milepost 1400 is 110 kt (204 km/hr) while the highest PMH V_x is 141 kt
(261 km/hr). Camille and the Labor Day hurricane are therefore stronger
than the SPH and weaker than the PMH. In contrast, the less intense New
Orleans hurricane of 1915 has a V_x of 95 kt (176 km/hr) which is less than
the SPH V_x of about 106 kt (196 km/hr) near milepost 700. The results
presented above are true even if we had used SPH K and F for Camille and
the Labor Day hurricane and PMH K and F for the 1915 hurricane.

12.4 V_{gx} AND V_x FOR THE SPH AND PMH

Maximum computed values of V_{gx} and V_x for the SPH and the PMH are listed
by 100-n.mi. (185-km) intervals in both metric and English units (tables 2.3
to 2.6). Figures 2.22 to 2.27 show a comparison of these winds with maximum
computed winds for hurricanes of record using observed or estimated values of
meteorological parameters or factors for each hurricane. All wind computa-
tions are based on equations 12.1, 12.19 and 12.20.

12.5   COMPARISON WITH OTHER RESEARCH

Comparisons between this report and other research are not overly benefi-
cial because other studies have not tried to define upper limits in the
same way we have. Nevertheless, a comparison with another recent study
should indicate whether or not our winds are very much "out of line."

A recent study by Atkinson and Holliday (1977) using actual measurements
of peak gusts in western North Pacific tropical cyclones with a wide range
of p_o between 27.11 and 29.35 in. (91.8 and 99.4 kPa), yielded a central
pressure-maximum 1-min sustained wind speed relation. The authors state
this relation has "proved suitable for both high and low wind speeds, a
feature not found in previous relationships." The authors state, "Hope-
fully, this wind pressure relationship can be refined and improved in
future years as more cases are added to this sample and more accurate
techniques for measuring surface winds in tropical cyclones are developed."

Atkinson and Holliday's sample of 76 storms over a 28-year period was restricted to cases where they were reasonably certain that a coastal or island station experienced the cyclone's maximum winds during its passage. Extrapolation of their mean relation (between p_o and wind speed from these 76 storms) beyond the data allows a comparison of their winds with the winds from this report. p_o's corresponding to the range of PMH p_o along the east coast were selected to compare the Atkinson and Holliday winds to the PMH VLU and VUL level winds. These are the strongest and weakest PMH winds (tables 2.5 and 2.6). To make this comparison, our PMH 10-min winds were converted to 1-min winds using the formula given by Thom (1973). Table 12.1 lists these converted winds and those from Atkinson and Holliday's extrapolated relation.

We see from table 12.1 that our estimated PMH winds are everywhere higher than Atkinson and Holliday's for the same p_o. At the least, we feel comfortable that the PMH winds exceed those of Atkinson and Holliday's. Any evaluation must be tempered by the assumptions that:

a. Atkinson and Holliday's procedure for estimating 1-min sustained winds from peak gusts and our use of Thom's relation for adjusting 10-min sustained winds to 1-min sustained winds are both reasonable.

b. Atkinson and Holliday's choice of p_w (29.83 in., 101.0 kPa) permits a direct comparison of winds for the same p_o; (sec. 8.3.3.4).

c. The mean curve fitted to the 76 data points, expressed by the non-linear equation (Atkinson and Holliday 1977),

$$V_m = 6.7 \ (1010 - p_c)^{0.644} \tag{12.23}$$

where V_m is the maximum sustained surface wind speed (kt) and p_c is the mean sea-level pressure (mb), can be extrapolated to 26.11 in. (88.4 kPa) extending the relation 1.00 in. (3.4 kPa) beyond their most intense storm.

d. East coast PMH winds should be larger than winds developed from eq. 12.23 because extrapolation using this equation requires average rather than upper limit winds. [An envelopment of their data (not shown) gives wind values closer to but not exceeding PMH VLU and VUL winds].

Table 12.1.--*Comparison of maximum sustained 1-min, 10-m winds (Atkinson and Holliday 1977) 10-min, 10-m PMH winds adjusted to 1-min, 10-m winds for selected common p_o levels. Use caution in interpreting this table; see text.*

PMH p_o (east coast)		Estimated PMH maximum sustained 1-min*, 10-m winds from VLU column, tables 2.5 and 2.6 (east coast)		Estimated PMH maximum sustained 1-min*, 10-m winds from VUL column, tables 2.5 and 2.6 (east coast)		Atkinson and Holliday's maximum sustained 1-min 10-m winds	
(in.)	(kPa)	(kt)	(km/hr)	(kt)	(km/hr)	(kt)	(km/hr)
27.46	93.0	134	248	128	237	113	209
27.17	92.0	143	265	137	254	122	226
26.87	91.0	150	278	143	265	130	241
26.58	90.0	157	291	149	276	138	256
26.28	89.0	160	296	151	280	146	271
26.11	88.4	164	304	156	289	151	280

*Obtained from tables 2.5 and 2.6 by dividing the 10-min values by 0.863 (see notes for tables 4.1 to 4.4).

e.   Other less recognizable differences between our winds and those of Atkinson and Holliday would have a negligible effect on values in table 12.1.

13. RELATIVE WIND PROFILES

13.1 INTRODUCTION

In the last chapter we developed equations for computing 10-m (32.8-ft), 10-min overwater winds at any point around the circumference of maximum winds. We also need to determine how the winds should decrease with distance both inward and outward from R so that we may define the entire hurricane wind field for the SPH and the PMH.

We have already mentioned in the last chapter that wind profiles both inward and outward from R could have been determined from the adopted pressure profile (eq. 6.1). We chose instead to shape the profile after wind observations from hurricanes of record. Profiles were derived that relate the relative wind (V/V_x) to distance (r) outward from the hurricane center and the radius of maximum wind (R). These profiles were then adjusted to remove the effect of forward speed (T). The results, termed "standardized" profiles, insure continuity in wind fields outward and inward from R.

13.2 DEVELOPMENT OF STANDARDIZED PROFILES FOR WINDS OUTWARD FROM R

13.2.1 DATA

Wind fields constructed for severe hurricanes of record were the primary source of data for developing standardized profiles for relative winds outward from R. These wind fields are representative of average 10-m, 10-min overwater values for nonstationary hurricanes. A wind profile was constructed through the region of maximum winds. A secondary data source was wind profiles constructed for severe hurricanes for which no analyzed wind fields were available. Wind records at stations or ships in or near the path of the storm were used in constructing partial wind fields that were then used in constructing wind profiles through the region of maximum winds.

Table 13.1 lists the hurricanes used for determining the standardized profiles along with other pertinent information. Analyzed wind fields were not available for storms identified with a plus (+). The central pressure (p_o) listed in most cases is the minimum occurring within 150 n.mi. (278 km) of

Table 13.1.—Available hurricane wind profile data

Hurricane	No.	Date of wind profile	Central pressure[1] (p_0) (in.)	(kPa)	Radius of Max. winds (R) (n.mi.)	(km)	Forward speed (kt)	(km/hr)	Max. wind speed (V_x)[2] (kt)	(km/hr)	Stationary storm rel. wind speed (V_s/V_{xs}) @ rel. distances (r/R) of: .2	4	8	12	Wind speed (kt) and stationary storm rel. wind speed (V_s/V_{xs}) @ 60 n.mi. (111 km)		200 n.mi. (371 km) from storm center	
Donna (nr. S. Carolina)	1a	9/11/60	28.67	97.1	34	63	20	37	85	158	0.65	0.43	0.28	(0.11)	63	0.71	35	0.33
Donna (nr. New Eng.)	1b	9/12/60	28.38	96.1	48	89	33	61	85	158	.68	.45	--	--	81	.94	44	.43
Carla (central gulf)	2a	9/10/61	27.61	93.5	20	37	8	15	104	193	.93	.79	.49	.39	90	.86	48	.43
Carla (nr. land)	2b	9/11/61	27.49	93.1	30	56	5	9	102	189	.81	.56	.33	.19	84	.82	43	.40
Gracie	3	9/29/59	28.08	95.1	10	19	10	18	105	195	.91	.63	.36	.28	44	.38	26	.20
Ione	4	9/18/55	28.35	96.0	20	37	16	30	93	172	.89	.71	.42	.27	76	.80	37	.33
Camille	5	8/17/69	26.81	90.8	12	23	13	24	120	222	.89	.66	.45	.36	75	.60	39	.28
Florida Keys (+)	6	9/03/35	26.34	89.2	6	11	7	13	122	226	.90	.67	.45	.31	34	.25	--	--
New England	7	9/14/44	28.32	95.9	23	43	30	56	82	152	.68	.35	.15	--	50	.54	--	--
Pensacola (+)	8	10/19/16	28.76	97.4	19	35	15	28	69	128	.62	.50	.12	--	48	.65	--	--
Celia (+)	9	8/03/70	27.88	94.4	9	17	13	24	95	176	.67	.44	.23	.15	33	.29	--	--
Florida (+)	10	8/27/49	28.17	95.4	20	37	13	24	81	150	.68	.39	--	--	41	.46	--	--
Helene	11	9/27/58	27.52	93.2	20	37	14	26	95	176	.83	.55	.28	.17	67	.68	27	.22
Audrey	12	6/27/57	27.94	94.6	19	35	18	33	110	204	.68	.44	.25	.13	60	.50	--	--
Galveston	13	9/09/00	27.64	93.6	14	26	10	18	77	143	.78	.47	.26	--	37	.43	--	--
New Orleans (+)	14	9/19/47	28.53	96.6	18	33	20	37	97	180	.78	.43	(.22)	--	54	.51	--	--
Central gulf	15	9/13/19	27.99	94.8	32	59	10	18	91	167	.80	.55	.29	--	76	.82	--	--
New England	16	9/21/38	27.76	94.0	50	93	40	74	85	158	.49	.27	--	--	78	.90	--	--
Hilda	17	10/01/64	28.23	95.6	21	39	5	9	96	178	.77	.56	.39	.27	64	.65	36	.35
Carol	18	8/31/54	28.38	96.1	22	41	33	61	84	156	.77	.58	.31	.14	62	.69	30	.23
Debra	19	7/24/59	29.06	98.4	14	26	5	9	72	133	.76	.58	.39	(.18)	42	.56	--	--
New Orleans	20	9/29/15	27.52	93.2	23	43	11	20	92	171	.73	.46	--	--	61	.64	--	--
Betsy	21	9/10/65	27.79	94.1	32	59	14	26	101	187	.74	.46	.18	--	80	.77	32	.26
Texas	22	10/03/49	28.44	96.3	20	37	12	22	75	139	.77	(.64)	--	--	62	.81	--	--
Flossy	23	9/24/56	28.76	97.4	22	41	10	18	73	135	.75	.59	.45	.32	60	.80	--	--
Hazel	24	10/15/54	27.67	93.7	18	33	23	43	84	156	.71	.57	.46	.37	55	.60	39	.39
S. Carolina coast (+)	25	8/11/40	28.79	97.5	20	37	10	18	85	158	.91	.54	.25	.19	60	.68	23	.21

Note: [1]Underlined central pressures are at time of wind field analysis; otherwise, they are minimum central pressures as listed in tables 4.1 - 4.4.
[2]V_x from wind field or wind profile analysis.
( ) = extrapolated; -- = beyond extent of wind field or wind profile analysis.
(+) = wind profile determined from a partial analysis based on nearby wind records; otherwise from a detailed wind field analysis.

the coast as found in tables 4.1 to 4.4. Exceptions are the underlined central pressures, which were observed at the time of each wind field analysis.

Examples of wind profiles are shown in figure 13.1 for Donna (1960) when she was off the South Carolina and the New England coasts. Similar wind profiles were constructed for all hurricanes listed in table 13.1.

13.2.2 ANALYSIS

Hurricane wind profiles for nonstationary storms, e.g., those in table 13.1 and figure 13.1, contain asymmetry. This asymmetry is dependent on forward speed (T) and yields stronger winds in the right semicircle of a storm than would be observed in a stationary hurricane; (see sec. 12.2.3.1).

We wish to develop standardized profiles for stationary hurricanes and then in application add the asymmetry due to the selected T. The value of V_x for each hurricane in table 13.1 is often an approximation, being most correct when
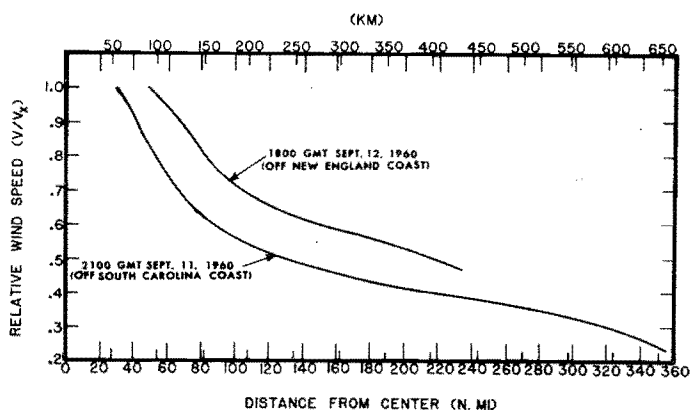
Figure 13.1.--Relative wind speed profiles outward from R vs. distance from center for Donna (1960).

the wind field analysis fits the true wind field of the hurricane. We will treat V_x as a known quantity located at a point at a distance R from the hurricane center in the right semicircle of each nonstationary hurricane. From chapter 12 (eq. 12.14, 12.19 and 12.20), we recall

$$V_x = F (V_{gx}) + 1.5 (T^{0.63}) \cos \beta \qquad (13.1)$$

when T is expressed in knots and cos β = 1.

Knowing the forward speed (T) for each hurricane at the given analysis time, we can subtract the effects of T from the wind profiles at distances outward from R by making use of the asymmetry term $[1.5 (T^{0.63})]$ in eq. 13.1. This exercise results in stationary hurricane relative wind profiles for the hurricanes in table 13.1. Removing the asymmetry, eq. 13.1 then becomes

$$V_{xs} = F (V_{gx}) \qquad\qquad (13.2)$$

where V_{xs} = maximum 10-m, 10-min overwater wind speed for a stationary hurricane. Values of V_s/V_{xs} (where V_s is the overwater wind speed at distance r in a stationary storm) were extracted from the storm profiles at discrete values of r. Examples are shown in table 13.1 at r = 60 n.mi. (111 km) and 200 n.mi. (371 km).

Plots were made of V_s/V_{xs} for various relative distances (r/R) vs. R. Four such plots are shown in figures 13.2 to 13.5. These plots were obtained from the final standardized profiles. Preliminary curves (not shown) were drawn to provide a best "eye fit" to the storm data by weighting the extreme
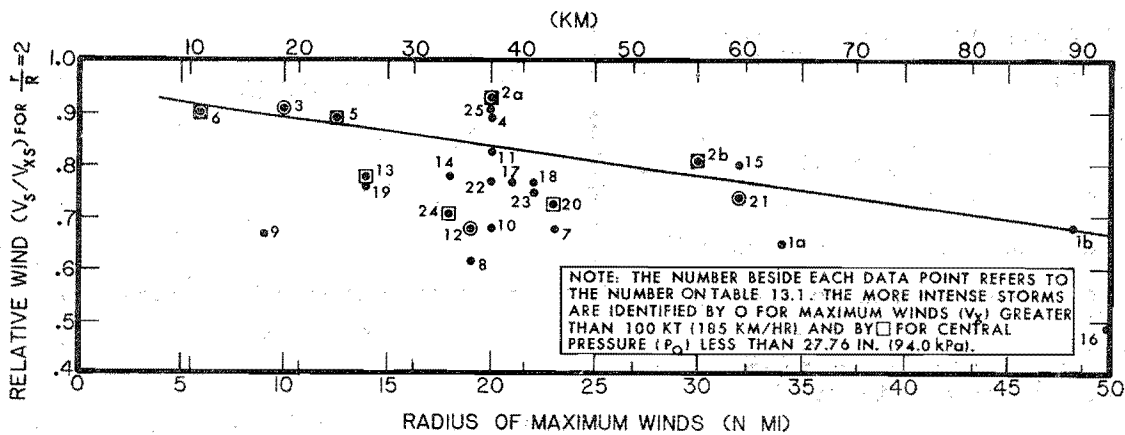
Figure 13.2.--V_s/V_{xs} for r/R of 2 vs. radius of maximum winds.
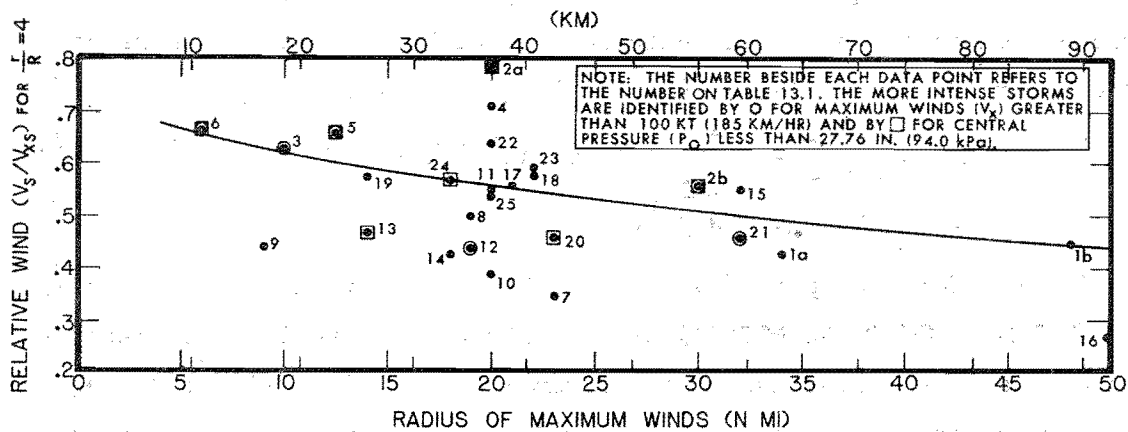
Figure 13.3.--V_s/V_{xs} for r/R of 4 vs. radius of maximum winds.

storms more heavily. These curves were used to determine a first approximation family of curves (standardized profiles) of V_s/V_{xs} versus r for a set of R's.

This first approximation set was then checked and adjusted when necessary by numerous cross plots and by comparing the results with individual hurricane wind profiles. The objective was to determine a consistent set of standardized profiles that best fit the data.

13.2.3 RESULTS

After checking numerous cross plots and making use of hand smoothing techniques, a set of standardized profiles was adopted. This is shown in
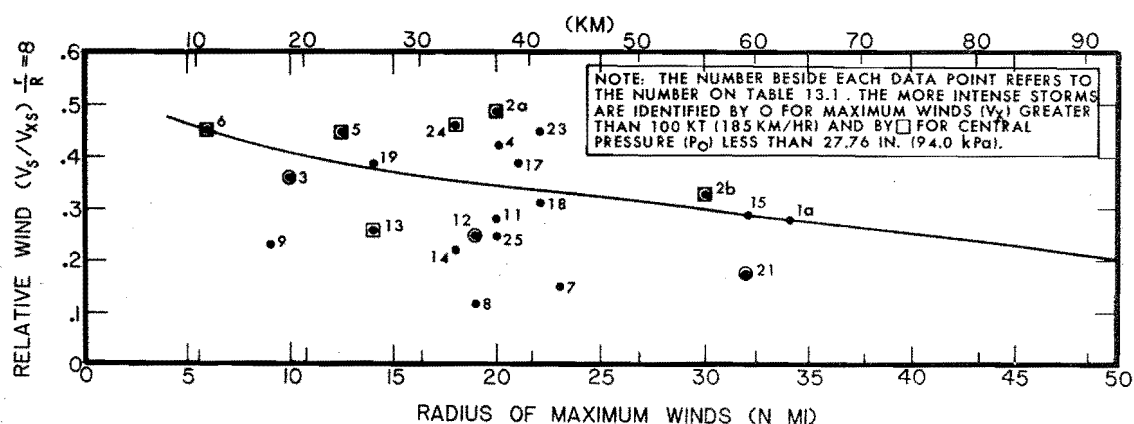
Figure 13.4.--V_s/V_{xs} for r/R of 8 vs. radius of maximum winds.
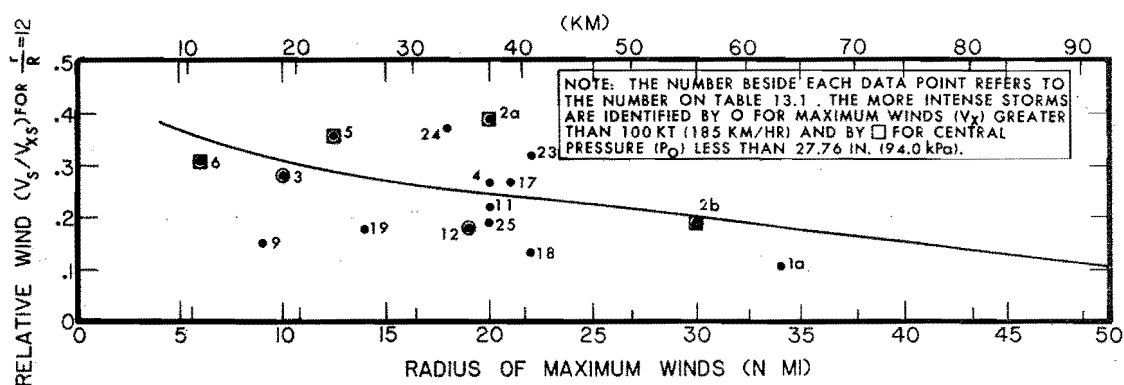
Figure 13.5.--V_s/V_{xs} for r/R of 12 vs. radius of maximum winds.

figure 13.6 where V_s/V_{xs} is plotted against r. The curves shown on figures 13.2 to 13.5 were obtained from figure 13.6. They indicate that the standardized profiles are a reasonable fit to the hurricane data.
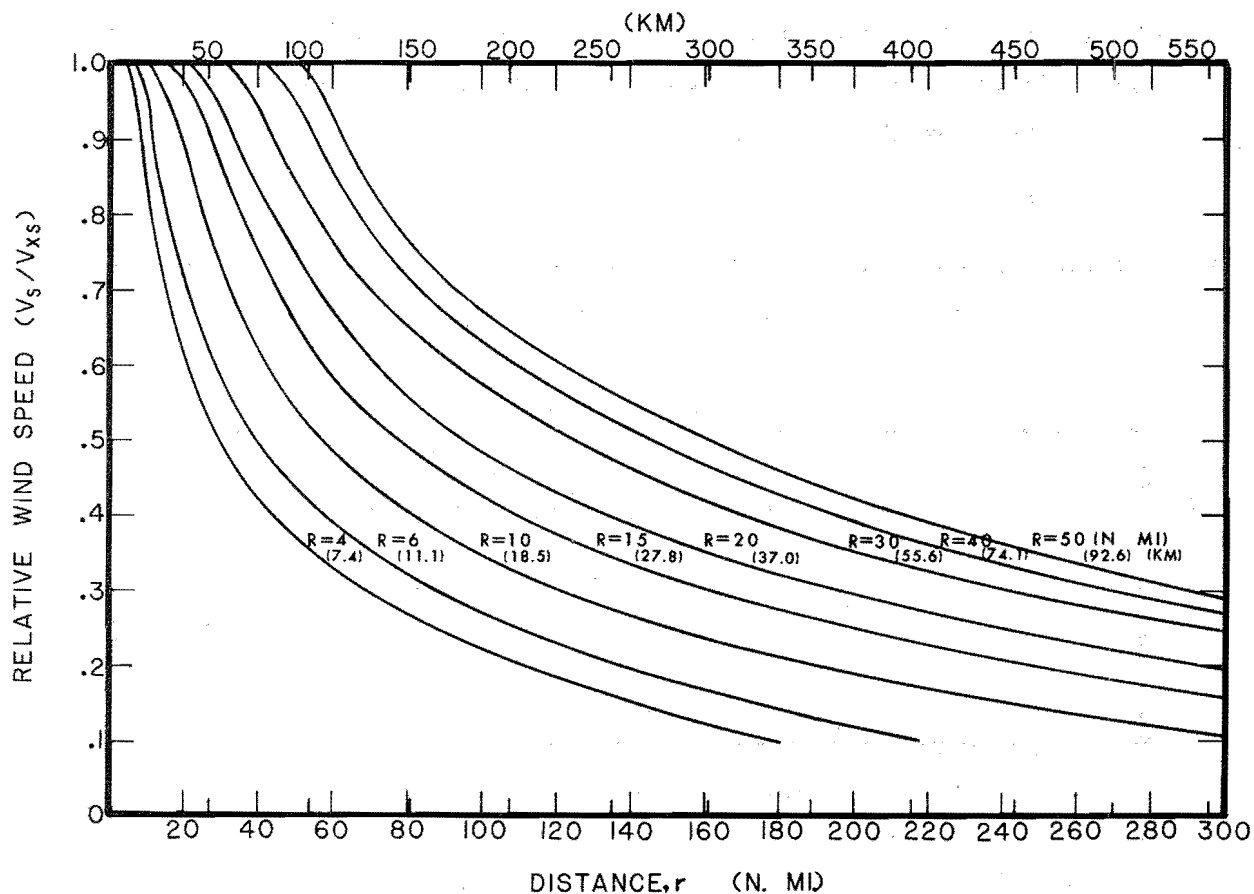
Figure 13.6.--Adopted standardized wind profiles outward from R.

Whether or not the standardized profiles of figure 13.6 may be used for both the SPH and the PMH can be assessed by referring to figures 13.7 and 13.8. Here, the relative wind (V_s/V_{xs}) for relative distances (r/R) of 4 and 8, respectively, are plotted against hurricane central pressures. While there appears to be a small trend to higher values of V_s/V_{xs} for lower central pressures, there is insufficient data to judge whether the trend is significant. We will use the relative wind profiles of figure 13.6 for both the SPH and the PMH wind fields.
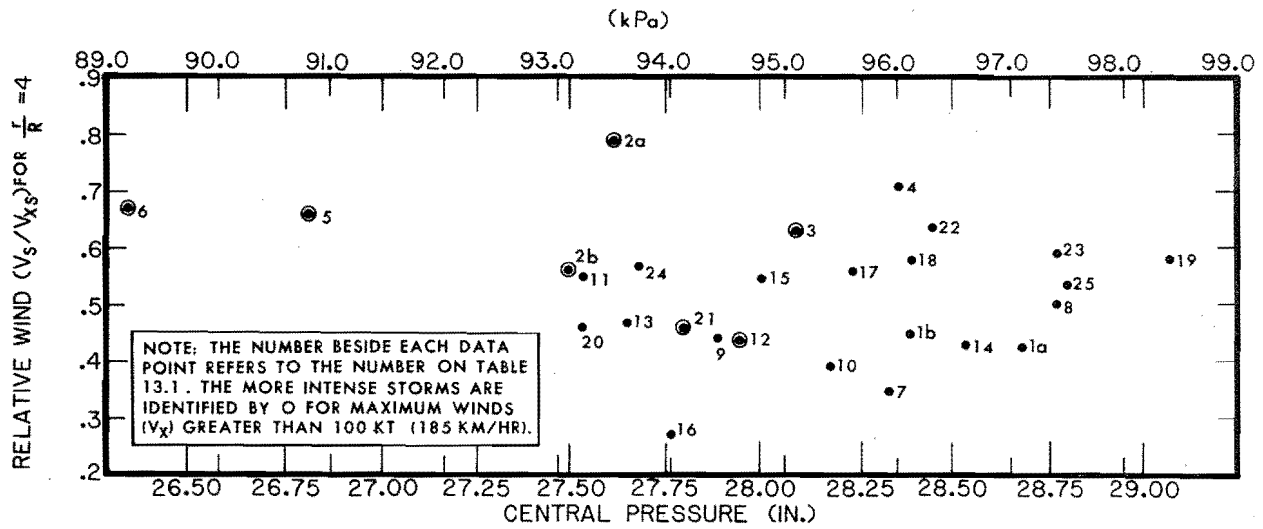
Figure 13.7.--V_s/V_{xs} for r/R = 4 vs. central pressure
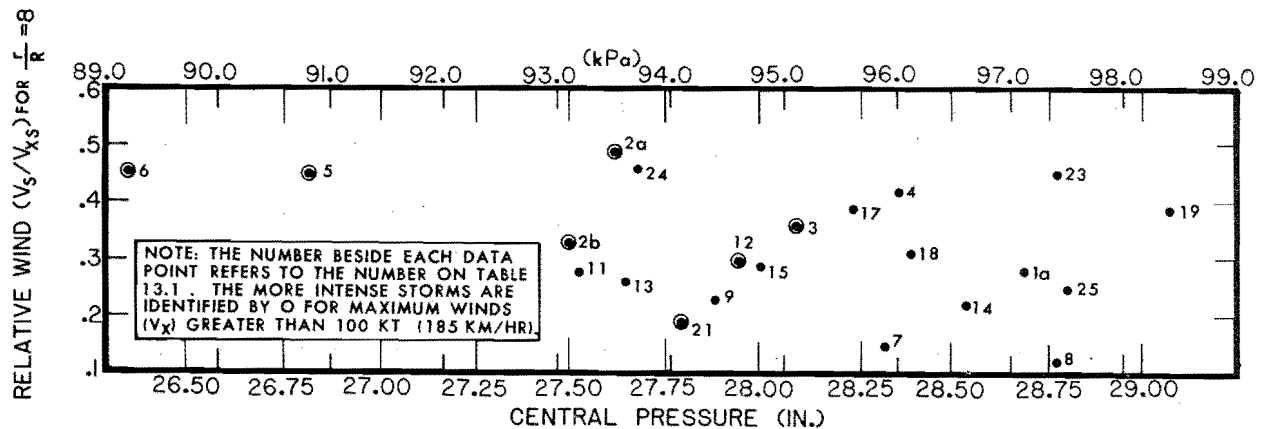
Figure 13.8.--V_s/V_{xs} for r/R = 8 vs. central pressure

13.3 DEVELOPMENT OF A STANDARDIZED PROFILE FOR WINDS WITHIN R

13.3.1 DATA

Wind profiles were constructed from wind records of Weather Bureau (now National Weather Service) reconnaissance aircraft by Colon (1963) in his study on the evolution of wind fields during the life cycle of tropical cyclones. This same data source extended through 1969 was used by Shea and Gray (1972) in their study on the structure and dynamics of the hurricane's inner core region. Shea and Gray subtracted the forward speed from the data. Using these data, we selected the most severe hurricanes from the cited

references for analysis. The p_o and R for these severe hurricanes of record
are listed in table 13.2.

*Table 13.2.--Selected severe hurricane data for development of a wind
profile within the radius of maximum winds (R)*

Hurricane	Date	Latitude	Central pressure (p_o) (in.)	(kPa)	Radius of maximum winds (R) (n.mi.)	(km)
Helene	Sept. 26, 1958	30°N	27.82	94.2	15	27.8
Donna	Sept. 9, 1960	23°N	27.46	93.0	15	27.8
Carla	Sept. 10, 1961	27°N	27.61	93.5	20	37.1
Esther	Sept. 16, 1961	23°N	27.61	93.5	12	22.2
Flora	Oct. 3, 1963	17°N	27.64	93.6	8	14.8

13.3.2 ANALYSIS

Figure 13.9 shows the variation of stationary hurricane relative wind
speed (V_s/V_{xs}) within R for the storms in table 13.2. The wind profiles
were constructed from winds obtained at flight levels [between the 80- and
56-kPa or 23.62-and the 16.54-in. levels.] Because of the similarity of
the wind profiles in the lower half of the troposphere (Shea and Gray 1972),
no attempt has been made to normalize the observed values to a standard
height. Figure 13.9 shows that,in general, in intense storms the wind drops
off rapidly inward from R. Esther is an exception to this generalization.

Figure 13.10 shows mean wind profiles constructed from hurricane wind data
compiled by Shea and Gray (1972) for the 900- to 700-mb (26.58-to 20.67-in.)
level for intense hurricanes ($p_o \leq 27.91$ in. or 94.5 kPa), weaker hurricanes
($p_o \geq 28.50$ in. or 96.5 kPa), and hurricanes centered north of 30°N, regard-
less of intensity. The mean profile constructed by the same authors from
all data considered (22 hurricanes) is also shown. In general, hurricane
wind profiles inside R indicate a gradual decrease in magnitude for weak
storms and a much sharper drop in wind speed for intense storms.
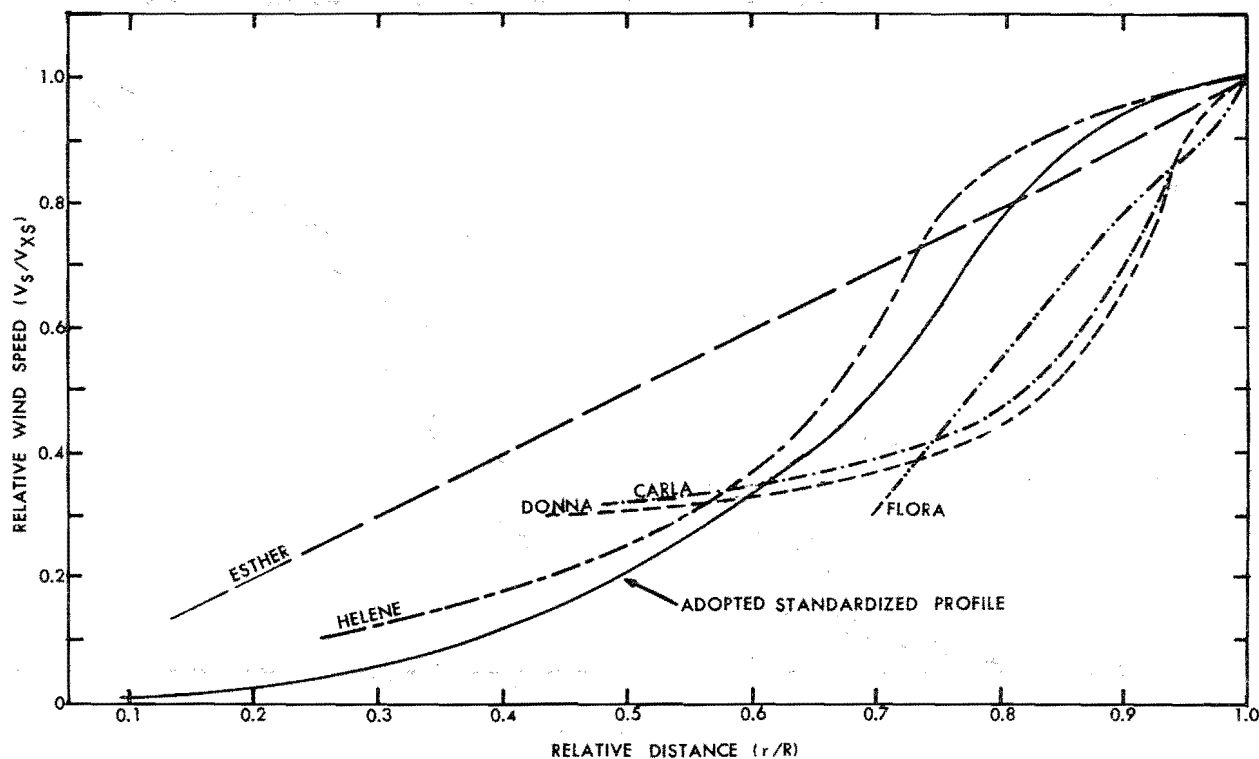
Figure 13.9.--Relative wind speed profiles within the radius of maximum winds for stationary hurricanes [after Shea and Gray (1972)]. The solid curve is the adopted standardized profile from figure 13.11.

13.3.3 RESULTS

For the SPH and the PMH, we have adopted the relative wind profile within R given in figure 13.11. This profile is a slight envelopment of the intense hurricanes of figure 13.10. The upper portion of the adopted profile was modified to avoid being discontinuous with the adopted standardized profile from R outward. Figures 13.9 and 13.10 compare the adopted standardized profile with the other wind profiles.

13.4 CONCLUDING REMARKS ON RELATIVE WIND PROFILES

The relative wind profiles shown in figures 13.6 and 13.11 enable us to determine values of V_s at various r's given V_{xs} [$V_{xs} = F(V_{gx})$; see sec. 13.2.2]. Once we have determined V_s, we can compute actual winds (V) in a moving hurricane by using the following equation:
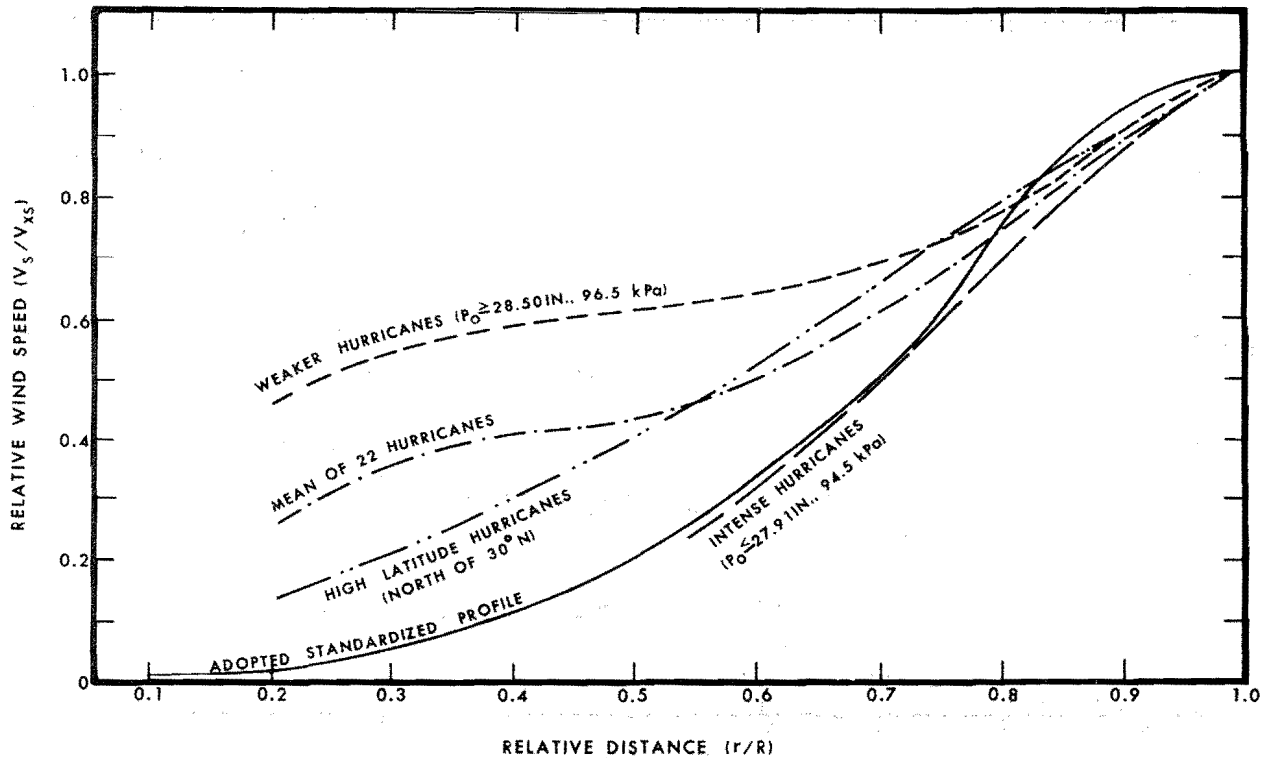
Figure 13.10.--Relative wind speed profiles within the radius of maximum winds. The solid curve is the adopted standardized profile from figure 13.11. The other four curves were constructed from data compiled by Shea and Gray (1972) for stationary hurricanes.

$$V = V_s + A$$

since, from chapter 12,

$$A = 1.5 \ (T^{0.63}) \ (T_o^{0.37}) \ \cos \beta$$

$$V = V_s + 1.5 \ (T^{0.63}) \ (T_o^{0.37}) \ \cos \beta \qquad (13.3)$$

Note: $T_o = 1$ when T, V and V_s are in knots.

$T_o = 0.514791$ when T, V and V_s are in ms^{-1}

$T_o = 1.151556$ when T, V and V_s are in $mi \ hr^{-1}$

$T_o = 1.853248$ when T, V and V_s are in $km \ hr^{-1}$
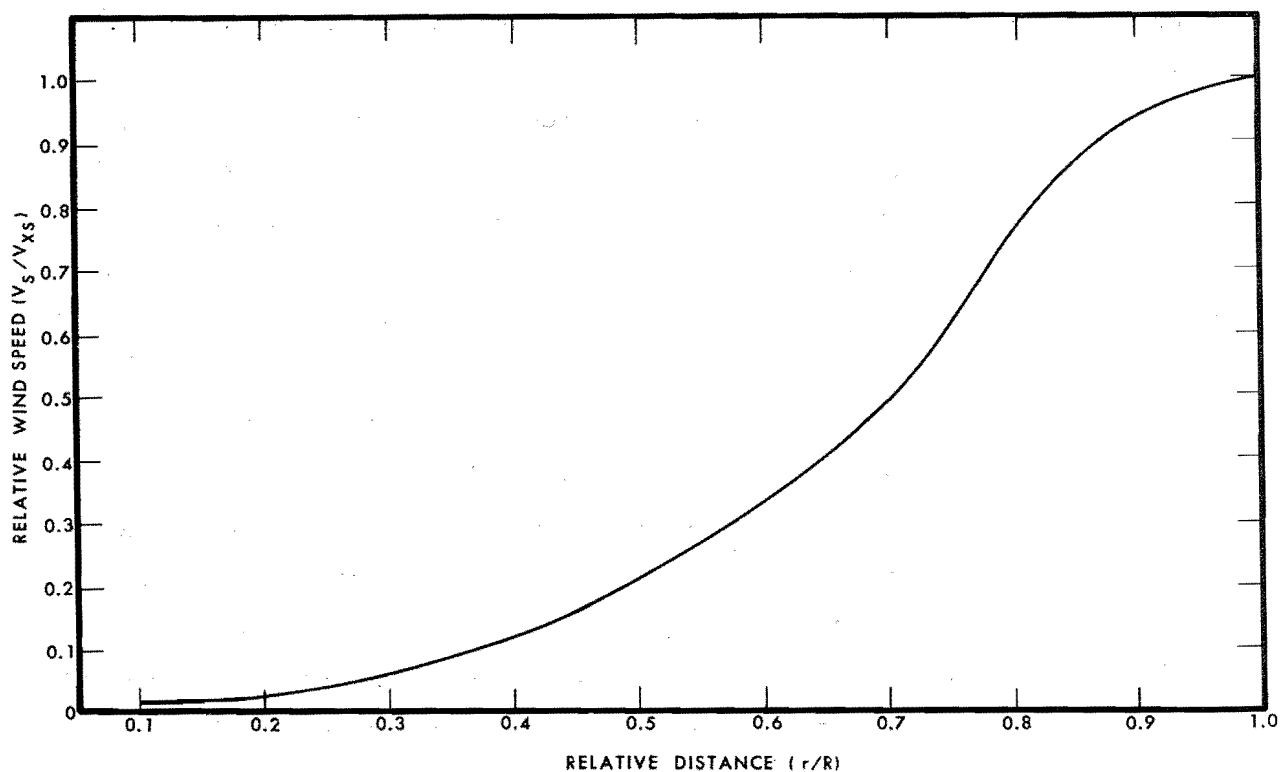
Figure 13.11. Variation of relative wind speed with relative distance (r/R) within the radius of maximum winds for the stationary SPH and PMH.

13.5   LIMITS OF ROTATION OF WIND FIELDS

13.5.1   INTRODUCTION

The orientation of the isotach pattern (lines of equal wind speed) with respect to track direction (chapter 11) needs to be determined in order to construct reasonable wind fields. Are there constraints to the angle between the direction (θ) and the location of the region of maximum winds? The computational scheme developed in section 12.2.3 will result in the region of maximum winds falling in the right rear quadrant (as related to the storm motion). We have reviewed observational data to ascertain if this restriction is realistic.

13.5.2 LOCATION OF REGION OF MAXIMUM WINDS IN SEVERE HURRICANES

Hawkins (1971) states, "It is a well-known fact that wind speeds on the right-hand side of the storm (looking in the direction toward which the storm is heading) are stronger than the winds on the left. This phenomenon can be associated with greater radius of trajectory curvature associated with parcels moving cyclonically on the right of the storm than on the left." Myers and Malkin (1961) have also discussed this. They attributed greater speeds on the right-hand side mostly to the smaller effects of asymmetry in the horizontal pressure gradient rather than to differences in the radius of trajectory curvature between the right and left-hand side of the hurricane.

Simpson and Pelissier (1971) relate, however, "Sometimes when a hurricane is intensifying and its circulation is not in a quasi-steady state, the isotach maximum ... apparently tends to migrate ... around the vortex center .... The maximum convection in the eyewall rotates with the isotach maximum, and the eyewall sometimes breaks open in those quadrants that are normally the strongest in steady-state hurricanes." This was the case with Celia (1970) as she moved from 115° and underwent rapid deepening 1.27 in. (4.3 kPa) during the 15-hr period before landfall near Corpus Christi, Texas. Lowest central pressure was 27.89 in. (94.4 kPa). Figure 13.12 shows the track of Celia across southern Texas and wind reports (fastest mile and peak gusts) from stations to the north and south of the track. The figure shows that at the Corpus Christi Weather Service Office (CRPWSO) the fastest mile, SW 109 kt (202 km/hr) and peak gusts, SW 140 kt (260 km/hr), occurred at 2228 GMT on August 3. These gusts were the highest of any observed near Corpus Christi Bay. From the storm track, this means that the location of maximum winds was over 200° from the direction the storm was moving. This agrees with reconnaissance reports which located the maximum winds at a point 215° clockwise from the direction Celia was going at 1856 GMT, August 3 and 250° from that direction at 2228 GMT, August 3.

Hawkins and Imbembo (1976) studied hurricane Inez (1966) over the north-eastern Caribbean Sea during the 24-hr period when she was intensifying from 28.41 in. (96.2 kPa) to 27.37 in. (92.7 kPa). At the end of the deepening period, "Streamlines at 28.05 in. (95.0 kPa) indicated the strongest winds, in excess of 130 kt (241 km/hr) were located anomalously in an area to the
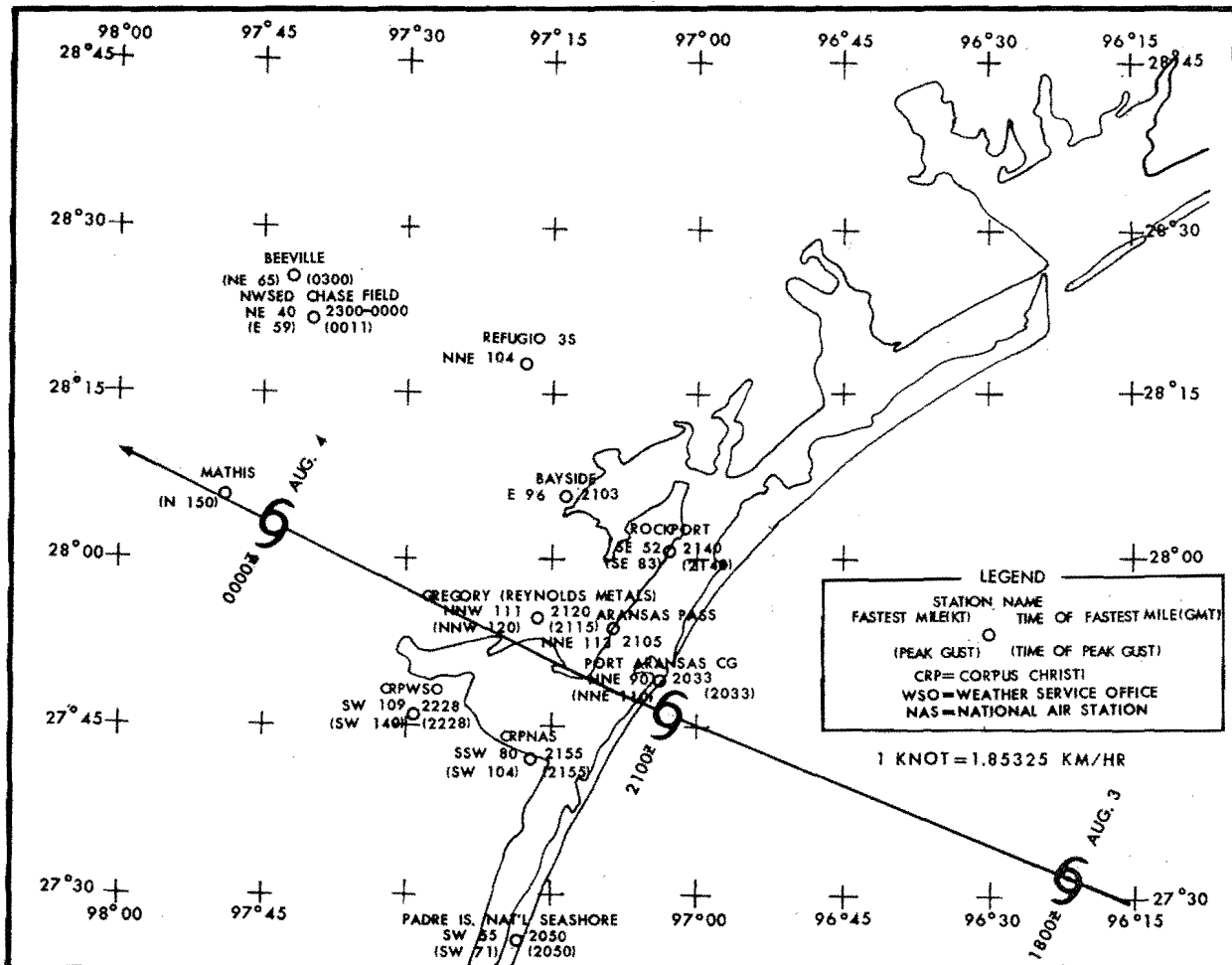
Figure 13.12.--Track of hurricane Celia (Aug. 1970) and wind reports near point of landfall. Time in GMT. Wind speed in knots.

rear of the moving storm. Except for an open section in the front portion, winds in excess of 120 kt (222 km/hr) were recorded in all quadrants."

The isotach maximum migrated slightly with time in Inez too, increasing from a 200° angle (clockwise from the track direction) measured from 8090 ft (2466 m) at the beginning of the 24-hr period to 210° measured at 1770 ft (540 m) at the end of the period. The difference in the angle may have been > 10° since the isotach maximum in Inez was observed to rotate clockwise with increasing height at both times.

13.5.3 ADOPTED LIMITS OF ROTATION FOR THE SPH AND THE PMH

In this report and in previous SPH and PMH studies, the SPH and the PMH are considered to be in a steady state; (see definition in sec. 1.2.3). A PMH deepening as it approaches the coast conflicts with the definition of the PMH. Our assumption of steady state is somewhat more arbitrary for the SPH, since SPH p_o can theoretically become lower. We recognize from the discussion in section 13.5.2 that a deepening SPH would have wider limits of rotation of its wind field. Celia and Inez were rapidly deepening nonsteady state hurricanes.

We propose to allow the region of maximum winds for a PMH or an SPH to have limits of rotation between 0° and 180° clockwise from track direction as defined in chapter 11. These limits are an expansion of the limits allowed in previous studies and the theoretical constraints mentioned in section 13.5.1 to acknowledge a broader range of possibilities than were previously thought to be reasonable. The steady state SPH and PMH will be barred from having their isotach maximum in the left semicircle with respect to track direction.

Sometimes the isotach maximum will remain over water after landfall. The location of the isotach maximum is then set by the position of the SPH or PMH with respect to the water. It may fall outside of the 0°-through-180° limits imposed on the SPH and PMH prior to landfall.

14. WIND INFLOW ANGLE

14.1 INTRODUCTION

Hurricane winds blow spirally inward and not along circles of equal wind speed concentric with the hurricane center. The angles between the true wind direction and tangents to these circles have been known by many names. Deflection angle, angle of incurvature, crossing angle, and inflow angle have all been used. We will use the term inflow angle (ϕ). In this chapter, we will determine a range of reasonable ϕ's that can be used for the SPH and the PMH.

14.2 RESULTS OF OTHER STUDIES

The earliest SPH study (Graham and Nunn 1959) specified a value of ϕ of 20° from the hurricane center to the radius of maximum winds (R), a transition from 20° to 25° between R and 1.2 R, and 25° beyond 1.2R. Later studies for the PMH (U.S. Weather Bureau 1968) and for the SPH (National Weather Service 1972) varied this somewhat. Although 25° continued to be used from 1.2 R outward, angles from 0° at the hurricane center increasing to 10° at R were specified. A transition from 10° to 25° was used between R and 1.2 R. These criteria are shown graphically in figure 14.1.

Hughes (1952) used a median ϕ of 10° to 15° to construct a "mean hurricane" from weather reconnaissance missions at low levels. Ausman (1959) found a mean surface ϕ ranging from 30° to -5° with the median near 16° based on ship reports around six hurricanes (a minus sign means the true wind blows outward from the hurricane center). Malkus and Riehl (1960) assumed ϕ constant for distances >54 n.mi. (100 km)
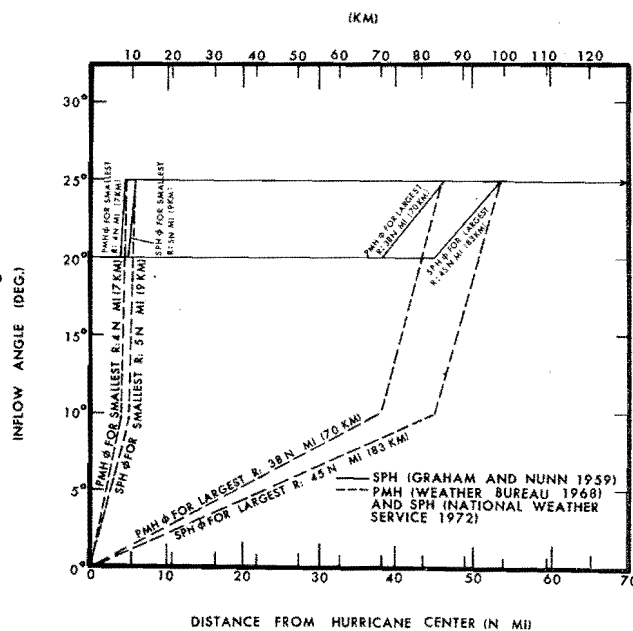
Figure 14.1.--Inflow angles from earlier SPH and PMH studies applied to smallest and largest R values (figs. 9.3 and 9.8) of the present study.

from the center, decreasing inward linearly to 0° at the eyewall. For moderate hurricanes ($p_0 \simeq$ 28.53 in., 96.6 kPa), ϕ reached a maximum value of 20°. For intense and extreme hurricanes ($p_0 \leq$ 26.87 in., 91.0 kPa), ϕ had a maximum value of 25°. Figure 14.2 shows the ϕ's of Malkus and Riehl for intense and extreme hurricanes applied to the R's of this study.

Jelesnianski (1967) related inflow angle to maximum surface winds, R and pressure drop ($p_w - p_0$). Nomograms can be constructed at a given latitude at prescribed distances from the hurricane center. He gives an example at 30°N of the range of ϕ at 87 n.mi. (161 km) from the center of a hypothetical stationary hurricane (figure 14.3).

Frank (1976) shows mean ϕ for three distances of 120 to 360 n.mi. (222 to 667 km), or 2° to 6° of latitude, from the typhoon center (fig. 14.4a). Mean ϕ is not shown any closer to the center. The basis for his study is a composite of 10 years (1961-70) of western North Pacific rawinsonde data (~18,000 soundings) from 30 stations most of which are near sea level. The
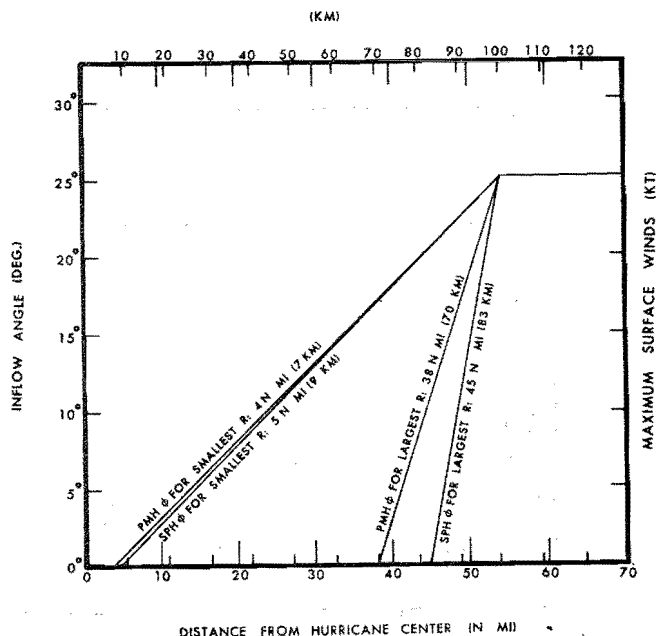
Figure 14.2.--Inflow angles from Malkus and Riehl (1960) applied to smallest and largest R values (figs. 9.3 and 9.8) of the present study.
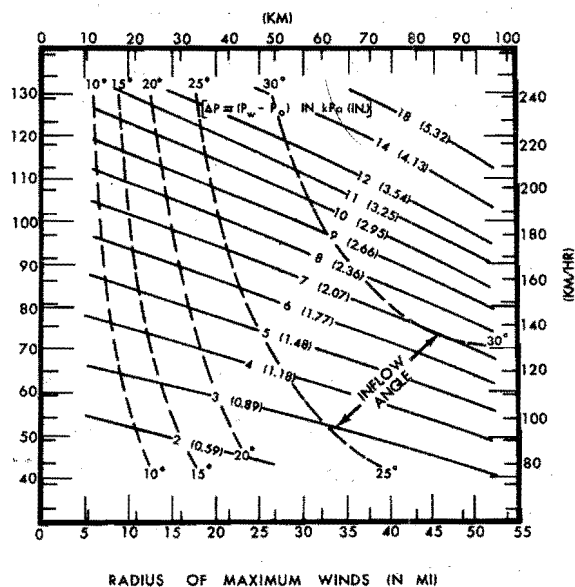
Figure 14.3.--Nomogram for determining inflow angles (given radius of maximum winds, pressure drop, and maximum surface winds) at a distance of 87 n.mi. (161 km) from the hurricane center (after Jelesnianski 1967).
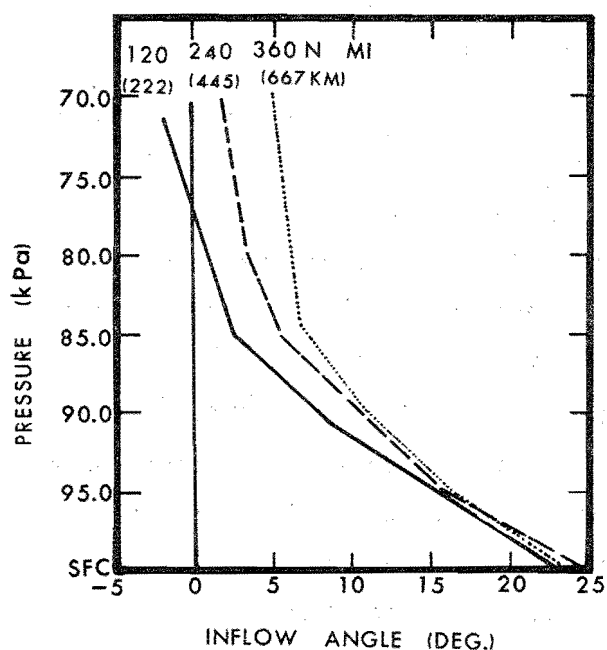
Figure 14.4a.--Inflow angles at 120, 240, and 360 n.mi. (222, 445 and 667 km) from the typhoon center (after Frank 1976).
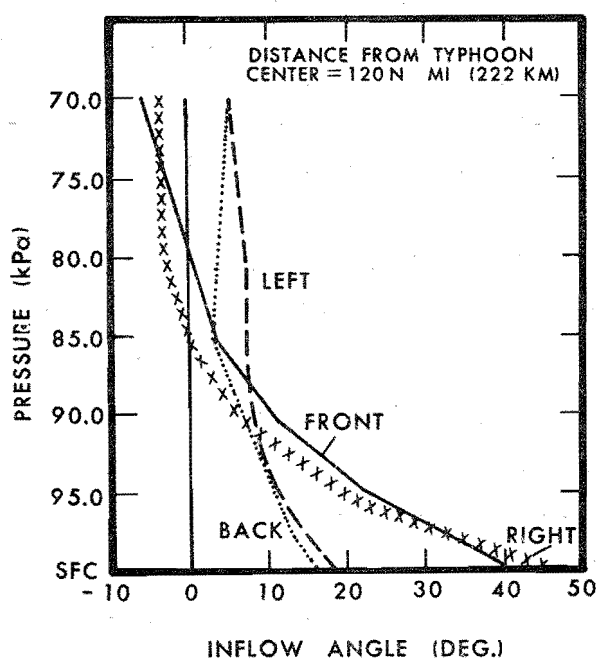
Figure 14.4b.--Inflow angles at 120 n. mi. (222 km) from the typhoon center for four storm quadrants (after Núñez and Gray 1978).
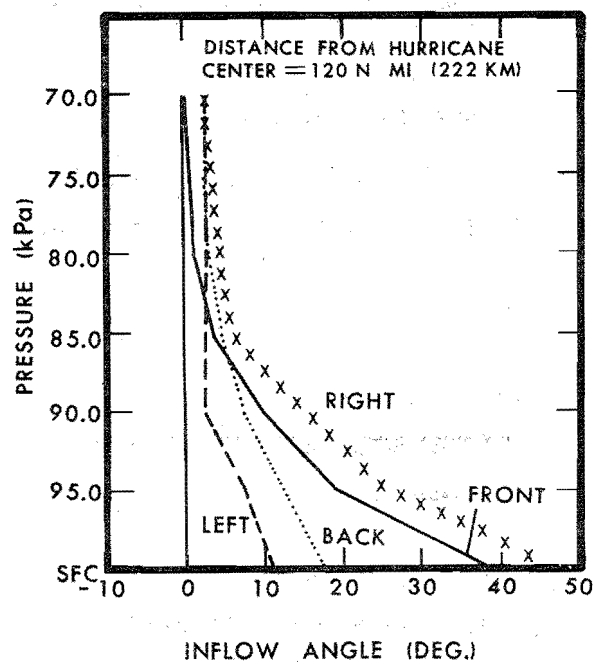
Figure 14.4c.--Inflow angles at 120 n.mi. (222 km) from the hurricane center for four storm quadrants (after Núñez and Gray 1978).

mean ϕ at the surface was almost identical for the three distances and averaged about 24°. His value at 95.0 kPa (28.05 in.) agreed with the 16° reported by Ausman (1959) at the ocean's surface.

Núñez and Gray (1978) have utilized Frank's compositing technique and typhoon data set and also studied 14 years (1961-74) of hurricane data (4650 soundings). Figure 14.4b shows mean ϕ for four quadrants of a mean typhoon at a distance of 120 n.mi. (222 km) from the eye center. Figure 14.4c is for a mean hurricane and follows the same format as 14.4b. The

quadrants are labeled front, left, back and right. The front quadrant is defined as being centered around track direction (θ).

Núñez and Gray state, "In the boundary layer the front and right quadrants have a greater inflow angle than the left and back. The relationship is true at 4° and 6° also (not shown). For the hurricane, at all three radii, the boundary layer's inflow angle magnitude decreases from quadrant to quadrant in the following order: right, front, back, left. For the typhoon the order is different: front, right, left, back."

At the surface, mean ϕ in figure 14.4b (typhoons) is about 30°, or about 6° larger than what Frank calculated over three distances while averaging around a belt of octants. Mean ϕ at the surface in figure 14.4c (hurricanes) is about 27°.

14.3 ESTIMATION OF INFLOW ANGLES USING SHIP DATA

We attempted to use ship data* as guidance for the SPH/PMH ϕ's. Using ship reports, plots were made for ϕ vs. distance from the hurricane center for hurricanes Carla (September 9–11, 1961) and Celia (August 3, 1970). As expected, the data for both storms exhibited high scatter. Figure 14.5 shows the plot for Celia. We concluded that data from ship reports would not be very helpful in setting ϕ's for this study.

14.4 RECOMMENDED INFLOW ANGLES FOR THE SPH AND THE PMH

Jelesnianski (1967, 1972) and Chow (1971) varied ϕ with R. Jelesnianski and Taylor (1973) have given dynamic justification for such a variation based on the equations of motion.

14.4.1 ASSUMPTIONS OR CONSTRAINTS

In our analysis, we have decided to rely heavily on the results of Jelesnianski but we simplify them based on the following additional assumptions or constraints.

---

* Data from operational reconnaissance flights into hurricanes were not used to calculate ϕ near sea level because such flights do not obtain wind reports precise enough to use for ϕ studies. Doppler winds are measured under the assumption that the reference plane below, in this case the ocean, is stationary (Hawkins 1975). It is unlikely that any such condition prevails during an SPH/PMH.

a. The SPH is modeled after Jelesnianski's nomogram (fig. 14.3) for a Δp of 2.08 in. (7.0 kPa). This Δp is a mean between that at the Florida Keys and at 45°N.

b. For the PMH we used the same model but with a Δp of 3.34 in. (11.3 kPa). This Δp is halfway between the PMH Δp for the Florida Keys and the PMH Δp for 45°N [(13.6 kPa + 9.0 kPa)/2 = 11.3 kPa].

c. Maximum ϕ will occur at a distance of 3R.

d. ϕ will decrease outward but remain positive from 3R to the outer periphery of the hurricane circulation, i.e., r_o where p_w is found.

e. ϕ will have a constant value for a given R at a given distance in any horizontal direction from the hurricane center.

f. ϕ does not vary with forward speed (T).

g. ϕ does not vary with latitude (24° to 45°N.)

These simplifying assumptions or constraints may occasionally lead to over-simplified results. However, we think that in the mean sizable errors will not occur.

14.4.2 ANALYSIS

Jelesnianski's nomogram (fig. 14.3) gives values of ϕ for a distance of 87 n.mi. (161 km) from the hurricane center. For other distances out to 130 n.mi. (241 km), comparable ϕ values were obtained indirectly from computations of storm surge heights. Using these values and the nomogram, SPH ϕ's (fig. 14.6) and PMH ϕ's (fig. 14.7) were determined for selected values of R for a continuum of distances from the hurricane center out to 130 n.mi.

Although the two figures were derived using median Δp's for the SPH
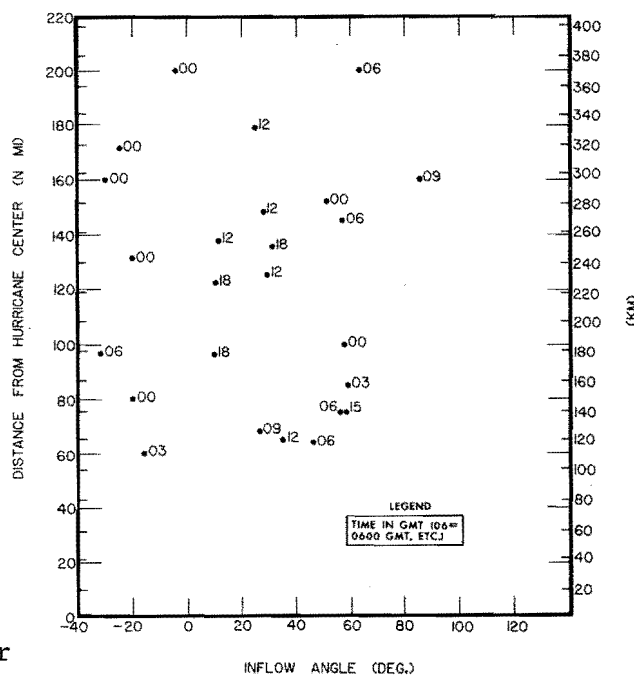
Figure 14.5.--Inflow angles based on ship reports from the vicinity of hurricane Celia (R = 9 n.mi., 17 km) on August 3, 1970.
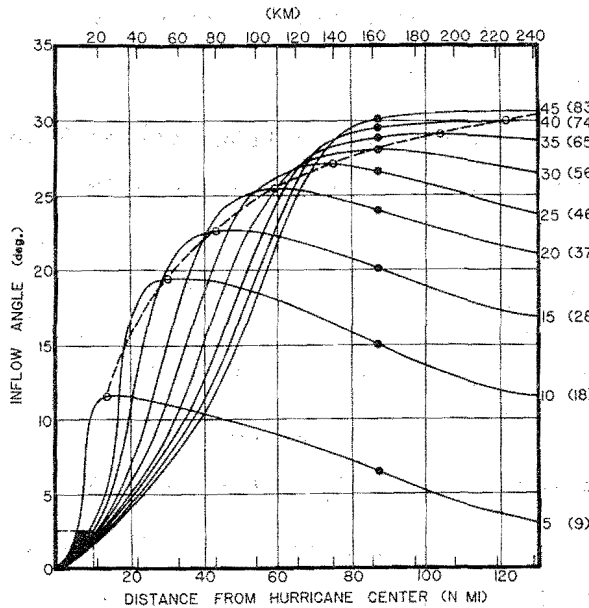
Figure 14.6.—Adopted SPH inflow angles vs. distance from the hurricane center at selected R values. Open circles denote maximum inflow angle at each R. Closed circles are points taken from the nomogram on figure 14.3.

Figure 14.7.—Same as figure 14.6 except for the PMH.

and PMH, they may be used at all coastal locations with little loss of accuracy. The points plotted on the two figures at 87 n.mi. (161 km) are taken from the nomogram and can be used to interpolate ϕ between 5-n.mi. (9-km) intervals. The dashed line on each figure connecting the other points delineates a line of maximum ϕ which is also helpful in interpolating for intermediate R values.

Figure 14.8 is a replot of figure 14.5 with SPH/PMH curves, obtained from figures 14.6 and 14.7,

Figure 14.8.—Same as figure 14.5 with SPH/PMH curves (obtained from figures 14.6 and 14.7) superimposed.

superimposed. The R in Celia (1970) was 9 n.mi. (17 km). Our theoretical approach is a reasonable fit to this highly scattered data.

14.5   COMPARISON OF RESULTS WITH OTHER RESEARCH

We believe that from the standpoint of dynamics, ϕ values from figures 14.6 and 14.7 are an improvement over previous inflow angle criteria given in NHRP 33, HUR 7-97, and HUR 7-120 (fig. 14.1). Curves of R are continuous and do not have sharp breaks as before. Maximum ϕ is no longer a constant numerical value for all R's. Our results agree with the work of Jelesnianski and Taylor (1973) which indicates increasing ϕ as hurricanes become more intense. Lastly, maximum ϕ does not extend out to the outer periphery of the hurricane, which is in agreement with Chow (1971).

SPH ϕ ranges from 0° to a maximum of 30.5° and PMH ϕ from 0° to 32°. Chow gives a maximum ϕ of 34° at a distance of 3R from the hurricane center. Thus, a median ϕ is in good agreement with both Hughes (1952) and Ausman (1959). Figure 14.2, from Malkus and Riehl (1960), is much like figure 14.1 except that ϕ reaches 0° at R. Although ϕ's in some hurricanes reach 0° at R, other hurricanes would have inflow extending inward beyond R. However, most hurricanes have slight outflow rather than inflow very near their centers (Malkus 1958). Nevertheless, we contend that a continuous decrease of ϕ from maximum ϕ to 0° at the hurricane center is a justifiable simplifying assumption for the SPH and the PMH.

At and near the surface, the mean ϕ's (fig. 14.4a) of Frank (1976) are within 2° of each other between 120 and 360 n.mi. (222 and 667 km) from the storm center. Thus, we have support for assuming a nearly constant (but slightly decreasing) ϕ beyond 130 n.mi. (241 km). Frank (1976) and Núñez and Gray (1978) give mean ϕ between 24° and 30° at the surface. One would expect their data to show larger mean ϕ than our results because they used a number of elevated land stations, resulting in greater surface friction and more inflow.

15. ADJUSTMENTS OF WIND SPEED FOR FRICTIONAL EFFECTS AND FOR FILLING OVERLAND

15.1 INTRODUCTION

When a hurricane moves toward the coast eventually to make landfall, more and more of its wind field moves overland. The rougher character of the land compared to the water results in a reduction of wind speed. When the eye of the storm later moves ashore, further weakening takes place because of a reduction in energy since the surface air is no longer warmed by the ocean. This leads to a cooling of the eye and eventual loss of tropical character-istics (Dunn and Miller 1964). In this chapter, we will develop criteria for adjusting wind speeds when the SPH and PMH approach shore and for filling when overland.

15.2 ADJUSTMENT OF WIND SPEED FOR FRICTIONAL EFFECTS

15.2.1 BACKGROUND

Winds near the surface of the earth depend on a number of factors, includ-ing the winds above the surface boundary layer, the thickness of the boundary layer, the surface roughness, the surface stress, and the elevation of measurement. We seldom know all these factors.

The effect of an abrupt change in surface roughness on the airflow close to the ground has been studied, both theoretically and experimentally, in recent years (e.g., Peterson 1971). In studies of dynamic processes near the coast, the modification in surface boundary layer wind structure with onshore winds was discussed by Echols (1970) and Echols and Wagner (1972) and the shear stress on a beach and on an awash zone by Hsu (1970a and 1970b). Panofsky and Peterson (1972) point out that measured wind profiles on a narrow cape varied with the wind direction in a manner consistent with effects of upwind terrain features. Reiso and Vincent (1976) reported on the estimation of winds over the Great Lakes and proposed a ratio of over-lake wind speed to overland wind speed approaching 1.2 for moderate overland wind speeds of 30-42 kt (56-78 km/hr) under conditions of neutral stability.

Since a portion of the hurricane circulation will be overland as it ap-proaches the coast, a conversion from overwater to overland wind speeds is required in order to describe the hurricane winds. In earlier studies by the

National Weather Service (e.g., Graham and Nunn 1959), the adjustment
factors for wind speed near shore were derived from limited observations on
Lake Okeechobee (Myers 1954) during the hurricanes of August 1949 and
October 1950. By studying wind observations on and near Lake Ontario, we
attempted to improve on the Lake Okeechobee adjustment factors.

15.2.2 LAKE ONTARIO DATA FROM IFYGL

During the International Field Year for the Great Lakes (IFYGL), detailed
wind observations were made on and around Lake Ontario. Towers were used
for near shore observations and buoys served as observation platforms on the
lake (Foreman 1976). The period of observations from buoys was from May 1
to October 15, 1972. We selected winds that were greater than 20 kt (37 km/
hr) for 6 hours or longer. The daily (24-hr) resultant and average winds
obtained in this manner tended to cancel out diurnal land and sea breeze
effects. Eleven cases were selected for further analysis and led to the
following results:

a. Onshore winds show a sharp decrease upwind within 1 n.mi. (1-2 km) of
shore.

b. Offshore winds increased with distance up to about 22 n.mi. (40 km)
from shore; wind speeds seemed to remain steady at distances greater than
22 n.mi. from shore.

Results from both the Lake Ontario data and the Lake Okeechobee data
indicate that onshore winds should reduce sharply at or very close to the
coast and offshore winds should increase more gradually out to some distance
offshore and then remain steady. Two important differences exist, however.
First, the Lake Ontario wind speeds are much lower than those observed
over Lake Okeechobee. Second, the terrain near Lake Ontario is rough as
compared to the marshy lowlands near Lake Okeechobee. These differences
make the Lake Ontario data less desirable for application along most of the
U.S. east and gulf coasts than the Lake Okeechobee data. Therefore, we used
the Lake Okeechobee results.

15.2.3 DEFINITION OF FRICTION CATEGORIES

The effect of friction on winds is complex. The varied physical form of the Earth's surface requires involved studies just to determine relations over a specified area. For this generalized study, we identified four categories of friction surfaces: a) water, b) awash, c) land, and d) rough terrain.

Definitions of the four categories are: Water—an open water surface with no significant obstructions to surface winds, e.g., oceans (including all tidewater to the indicated coastline) and large inland water bodies. Awash—normally dry ground with tree or shrub growth, hills, or dunes, which are inundated during a storm surge. Land—flat or rolling terrain and buildings, not inundated. Rough terrain—major urban areas, dense forest areas and mountains or ridges with abrupt changes in elevation over short distances.

15.2.4 ADOPTED ADJUSTMENT OF WIND SPEED FOR FRICTIONAL EFFECTS

15.2.4.1 ONSHORE WINDS. Figure 15.1 shows the adopted variation of the onshore to overwater wind speed ratio (k_c) at the coast for awash, land, and rough terrain. We also show data (scattered large black dots) from Lake Okeechobee which suggest an average ratio for land of 0.89 (fig. 27 of Myers 1954). The 0.95 for awash areas is approximately half-way between the value for land and 1.0. The adopted ratio of 0.83 for rough terrain was based on observations of high winds in severe hurricanes. The above three ratios,

Figure 15.1.—Onshore to overwater winds ratio (k_c).

which do not vary with wind speed and apply at the immediate coast or boundary from water to some other friction category, are shown in table 15.1.
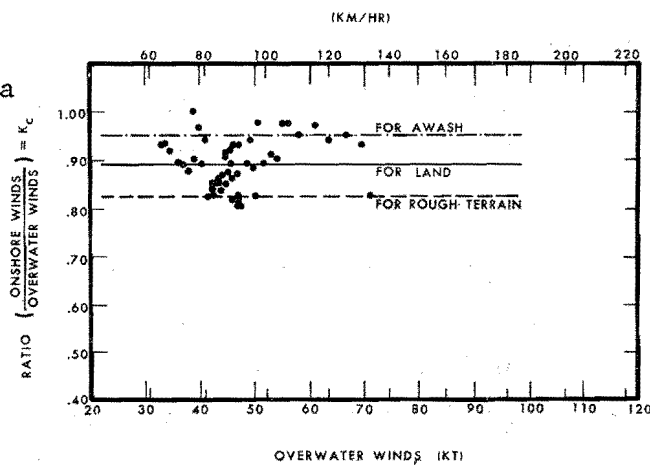
Table 15.1.--Onshore to overwater winds ratio (k_c)

Water to land	:	0.89
Water to awash	:	0.95
Water to rough terrain	:	0.83

15.2.4.2 OFFSHORE WINDS. Figure 15.2 shows the adopted variation of the offshore to overwater wind speed ratio (k_e) for awash, land, and rough terrain areas. In addition, a curve and data are shown (fig. 30 of Myers 1954) for Lake Okeechobee which indicate that the reduction of wind speed due to friction is larger for lower wind speeds.
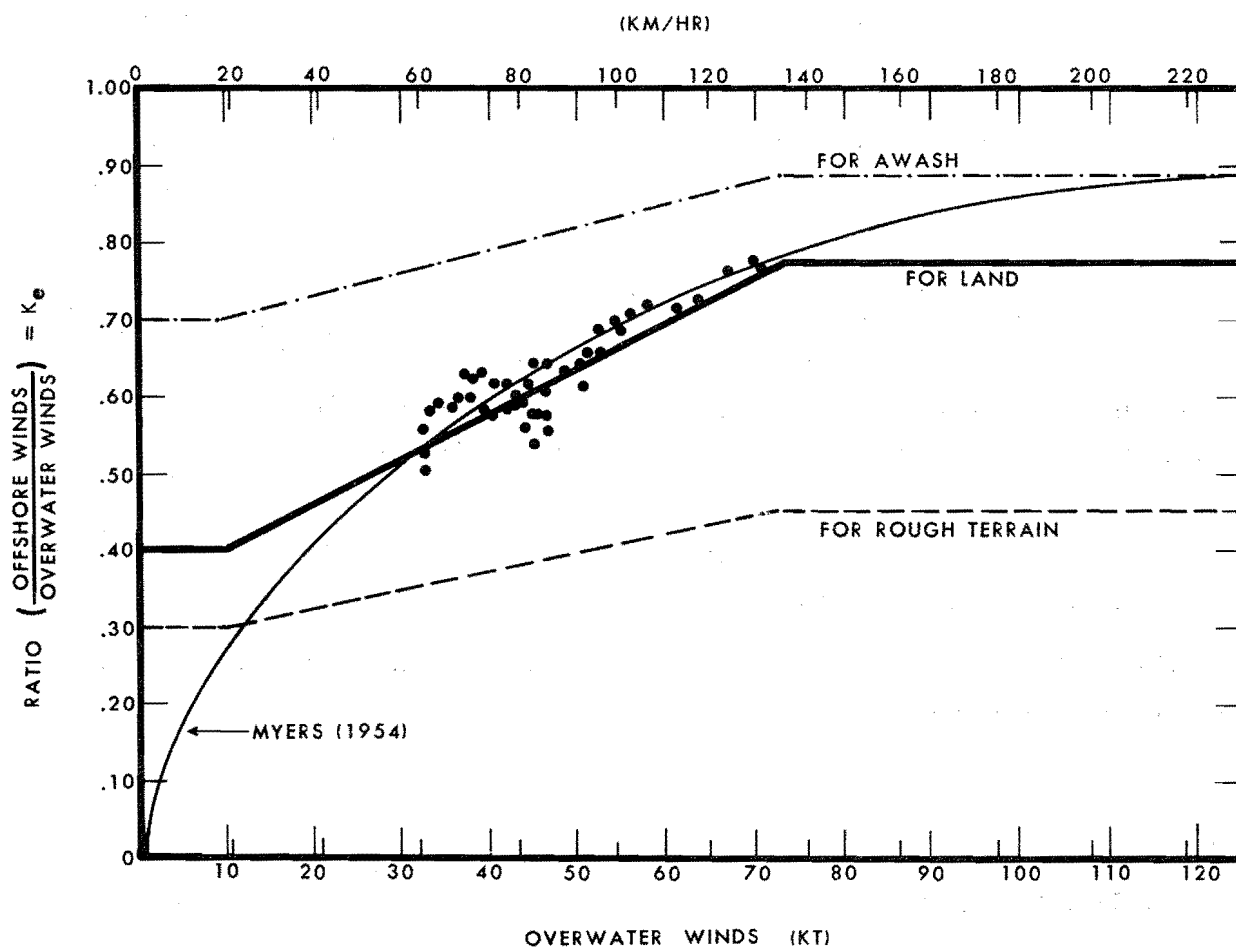
Figure 15.2.--Offshore to overwater winds ratio (k_e)

We recommend using adjustments from the solid heavy curve (land) of figure
15.2 for a comparatively smooth shoreline (see definition of land in sec.
15.2.3). For awash areas, we recommend the dashed-dotted curve, which lies
halfway between the land curve and 1.0. For rough terrain, we recommend the
dashed curve. This is based on a 0.4 factor observed at Brookhaven National
Laboratory (Myers and Jordan 1956), considered a rough site.

In previous studies, the offshore to overwater wind ratio was allowed to
increase to unity 10 n.mi. (19 km) offshore based on the Lake Okeechobee data.
Although Lake Ontario data indicate that lower wind speeds would require a
longer distance to reach equilibrium, we feel this is a refinement we are not
able to justify. We therefore assume the ratio reaches unity 10 n.mi. (19 km)
offshore for all wind speeds.

The adjustments given in this chapter are not applicable at places where
the surface friction category changes at inland locations far from the coast.
For example, our methods are applicable over the coastal plain of Virginia,
but not over the Blue Ridge Mountains farther inland.

15.2.4.3 THE SURFACE FRICTION COEFFICIENT. In prescribing the wind
field of a hurricane approaching the coast, the wind path crosses the coast
from the sea at a point (see sec. 15.2.4.1), traverses land for some
distance, and then exits the coast at another point downstream (see sec.
15.2.4.2). We know that the ratios in table 15.1 must be further reduced to
the ratios given in figure 15.2 as the wind traces this path. The process by
which we make this computational reduction is described below.

In a general sense, the 10-m (32.8-ft), 10-min frictionally reduced wind
speed near shore is:

$$V_k = kV \qquad (15.1)$$

where,

V = the 10-m (32.8-ft), 10-min overwater wind speed for a given
location.

V_k = the 10-m (32.8-ft), 10-min wind speed adjusted for underlying
terrain.

k = the surface friction coefficient at a given location.

We assume that the surface friction coefficient (k) will reach equilibrium after the wind has been over a specific friction category for 10 n.mi. (19 km). That is k will vary for the first 10 n.mi. downwind from a boundary between two surface friction categories, after which it reaches equilibrium. This criterion holds for onshore and offshore winds.

The surface friction coefficient (k) can be computed from:

$$k = k_e + Q (k_i - k_e)$$ (15.2)

where,

k_e = the equilibrium surface friction coefficient at a point. This is dependent on wind speed as well as the surface friction category (see sec. 15.2.4.2)

k_i = the previous surface friction coefficient at the last upwind boundary between surface friction categories. $k_i = k_c$ at the boundary between water and other surfaces.

Q = a coefficient ranging in value from 1.0 to 0.

Q is simply an interpolation device and is computed from:

$$Q = 1 - 0.195s + 0.0095s^2$$ (15.3)

where s is the distance from surface friction category boundaries. Q is defined as 0 when s $\geq$ 10 n.mi. (19 km). At the initial boundary of any surface friction category, Q is 1.0. The solution of equation 15.3 is shown graphically in figure 15.3. Similar equations could be developed for a faster or slower approach to equilibrium.
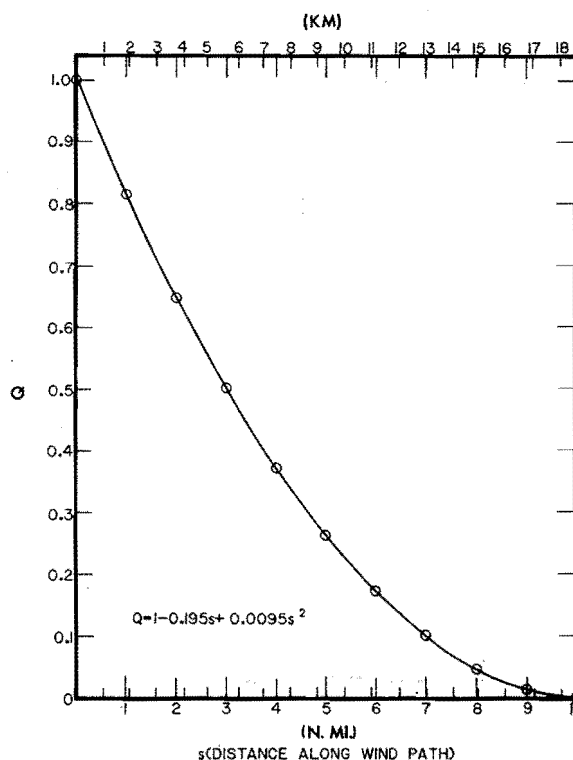
Figure 15.3.--Graphical solution for Q (eq. 15.3).

A schematic portrayal of adjustments is shown in figure 15.4. The k_e values shown are for overwater wind speeds $\geq$ 73 kt (135 km/hr). Figure 15.2 shows that k_e varies with wind speed < 73 kt.
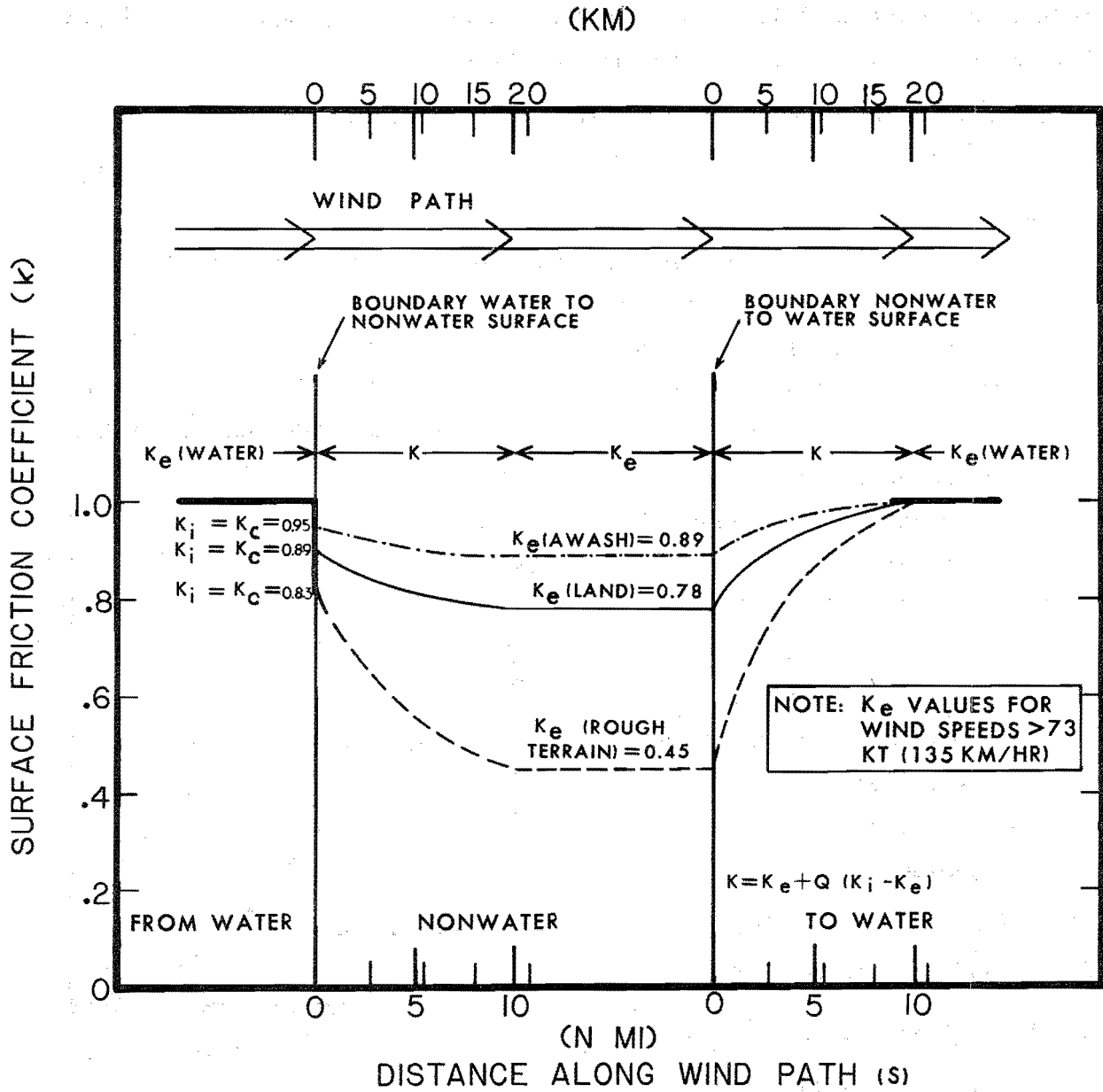
Figure 15.4. *Schematic of nearshore frictional adjustments.*

15.3 ADJUSTMENT OF WIND SPEED FOR FILLING OVERLAND

15.3.1 INTRODUCTION

It is a well-known fact that hurricanes begin to fill after their center crosses from sea to land. Central pressure (p_o) rises and winds start dropping off. Hubert (1955) was one of the first to note that filling is most pronounced in the innermost portion of the hurricane, with less pronounced effects farther from the center.

15.3.2 REASONS FOR AND EFFECTS OF FILLING OF HURRICANES OVERLAND

Palmén and Newton (1969) state "Filling results because the heat flux from the Earth's surface becomes negligibly small when a storm moves inland, resulting in a reduction of the temperature excess of the core." This decrease of heat leads to a decrease in the production of kinetic energy. Miller (1963) confirmed the earlier work of Bergeron (1954) in stating that filling stems principally from the reduction of equivalent potential tempeture (θ_e) of the rising air around the hurricane core. Miller also noted that filling due to surface friction was of minor importance compared to the removal of the oceanic heat source.

Palmén and Newton (1969) have summarized the effects of filling overland. "Owing to the removal of the oceanic heat source in the inner region, the baroclinity is reduced since the air ascending in the inner cloud wall now has somewhat lower θ_e. As a result, the outward radial wind component in upper levels is reduced. The previous balance between the mass inflow in low levels and mass outflow in upper levels is thus temporarily disturbed, leading to an integrated net mass convergence and pressure rise. During this phase, the cyclone tends to approach a depth around 1000 mb, according to Malkus and Riehl (1960), determined only by the release of latent heat intrinsic to the moist surface layer in its outer parts."

15.3.3 DATA

We selected 16 extreme hurricane events (table 15.2). Eight of these events from the period 1928-55 with p_o <28.41 in. (96.2 kPa) were analyzed by Malkin (1959). The other eight were extreme hurricanes since 1957. The

criterion for choosing these latter eight was that they made landfall with $p_o \leq 27.99$ in. (94.8 kPa) along the Gulf of Mexico coast and $p_o \leq 28.38$ in. (96.1 kPa) along the east coast. We accepted Malkin's data and analysis after checking for consistency by constructing a central pressure-time profile (graph showing the increase of central pressure with time) after landfall for the 1938 hurricane and comparing this profile with Malkin's profile for this storm. Figures 15.5 and 15.6 show tracks of all 16 hurricanes.
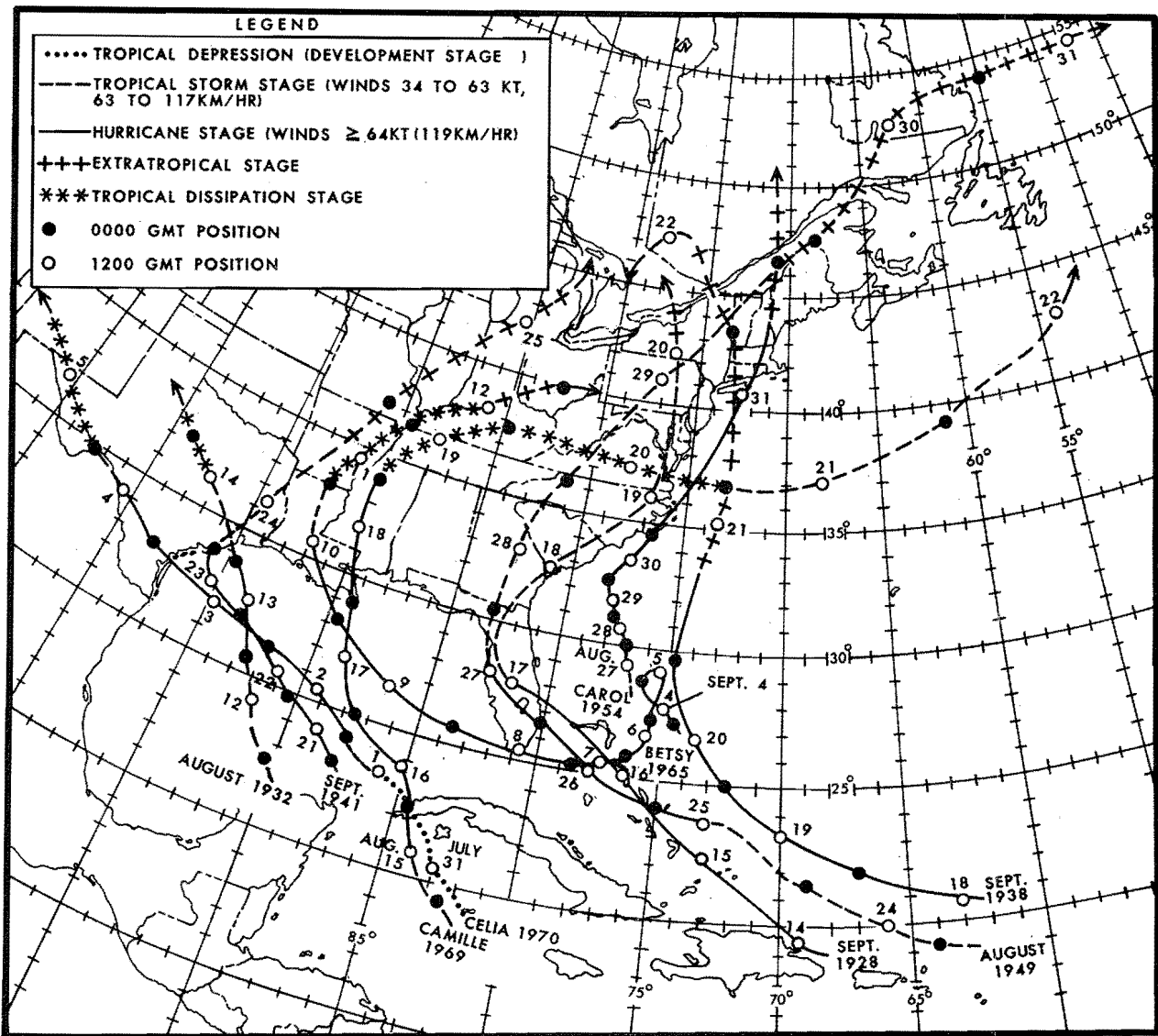
Figure 15.5.--Partial tracks of hurricanes of September 1928, August 1932, September 1938, September 1941, August 1949, Carol (1954), Betsy (1965) Camille (1969), and Celia (1970).
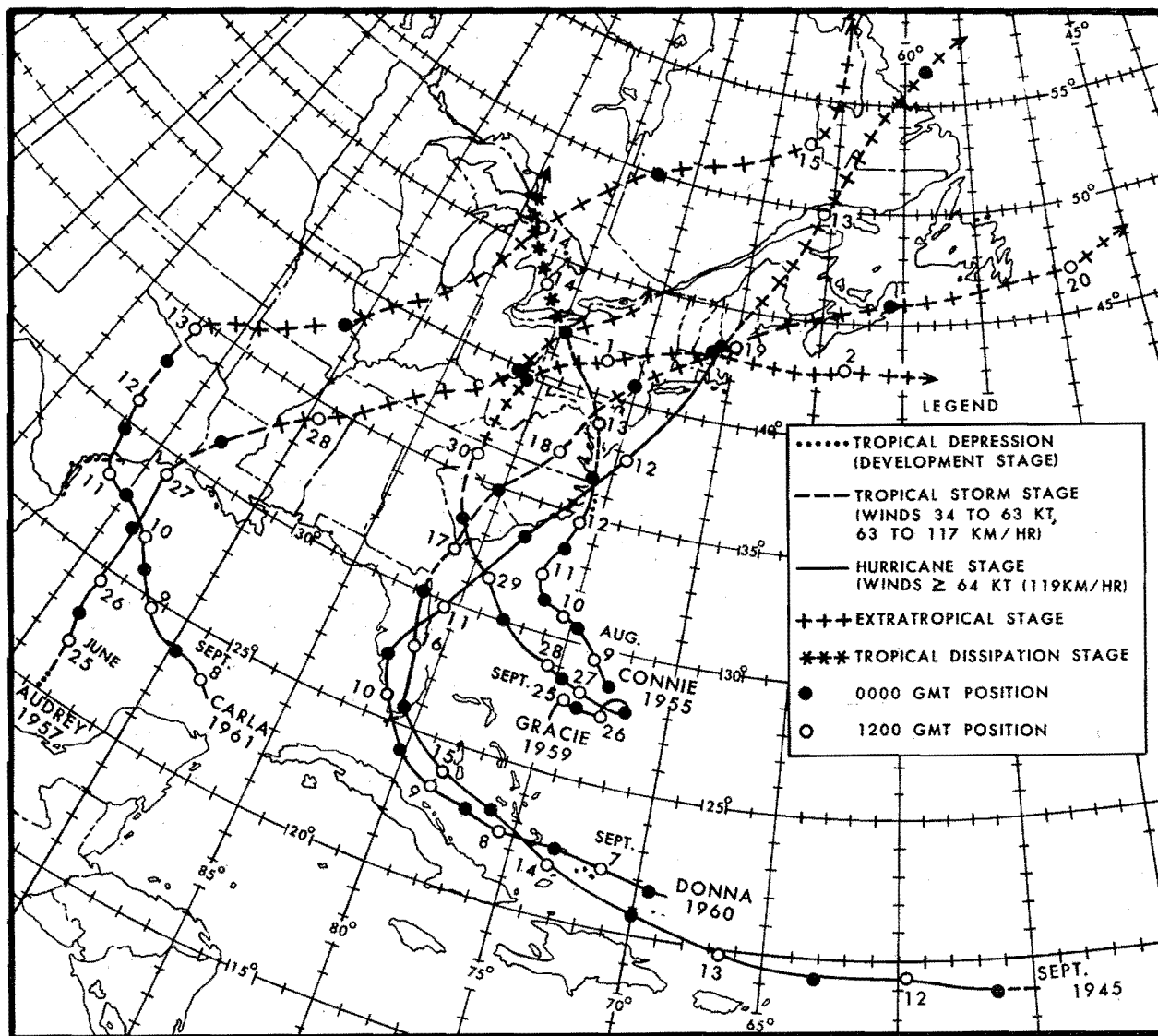
Figure 15.6.--Partial tracks of hurricanes of September 1945, Connie (1955), Audrey (1957), Gracie (1959), Donna (1960) and Carla (1961).

15.3.4 ANALYSIS

Adjustment factors (ff) for estimating the decrease of the overwater wind speeds after landfall may be computed using the classical assumption that the speeds are directly proportional to the square root of the pressure drop $(\Delta p = p_w - p_o)$. ff is defined here as the square root of Δp at some specified time after landfall divided by the square root of Δp at landfall (Δp_t), or $(\Delta p/\Delta p_t)^{1/2}$. Therefore, we first need to analyze the change in Δp with time after landfall for the 16 hurricanes.

Table 15.2.--Classification of hurricanes

Geograph-ical region	Number of hurricanes	Hurricane	Forward speed (kt)	(km/hr)	State of landfall	Description of region
A	7	Aug. 14, 1932	15	28	Texas	Gulf coast
		Sep. 23, 1941	13	24	Texas	from Missis-
		Audrey (1957)	14	26	Louisiana	sippi west-
		Carla (1961)	6	11	Texas	ward
		Betsy (1965)	17	32	Louisiana	
		Camille (1969)	16	30	Mississippi	
		Celia (1970)	14	26	Texas	
B	4	Sep. 17, 1928	13	24	Florida	Florida south
		Sep. 15, 1945	10	19	Florida	of 27°N
		Aug. 27, 1949	14	26	Florida	
		Donna (1960)	9	17	Florida	
C	5	Sep. 21, 1938	47	87	New York	East coast
		Carol (1954)	33	61	New York	from S. Caro-
		Connie (1955)	7	13	N. Carolina	lina northward
		Gracie (1959)	12	22	S. Carolina	
		Donna (1960)	32	59	New York	

Graphs were constructed showing sea-level pressure readings from stations with available continuous pressure records during the time period when a hurricane passed by that station after landfall vs. distance of the stations from the hurricane center for seven of the eight hurricanes not previously considered and the New England hurricane of 1938. [For hurricane Donna over Florida, we dispensed with these graphs and used the pressure-time profile given by Miller (1964)]. The data on each graph were for different times, varying in the extreme by 3 or 4 hours. Composite pressure-distance profiles were then analyzed at 3- or 4-hour intervals from a few hours after landfall (t) out to t + 24 hours. These profiles were then extrapolated to distance = 0 to give estimated p_o. In drawing these pressure-distance profiles, data from some stations were given less weight because it didn't appear to fit well into the overall data mass.

The next step was to construct central pressure-time profiles. These were constructed using:

a.   The estimated p_o values from the pressure-distance profiles.

b.   Single point lowest pressure-time after landfall data from other stations and some of those in a. that were close to the hurricane center.

c. National Meteorological Center weather map analyses of p_o.

d. Estimates of p_o at landfall from other studies e.g., Ho et al. (1975).

These profiles were subjectively weighted to the data and eye-fitted.
Figures 15.7a and 15.7b are examples of these central pressure-time profiles.
The letters next to each data point correspond to the lettered items in this
paragraph. Gracie hit the east coast and Camille the gulf coast.
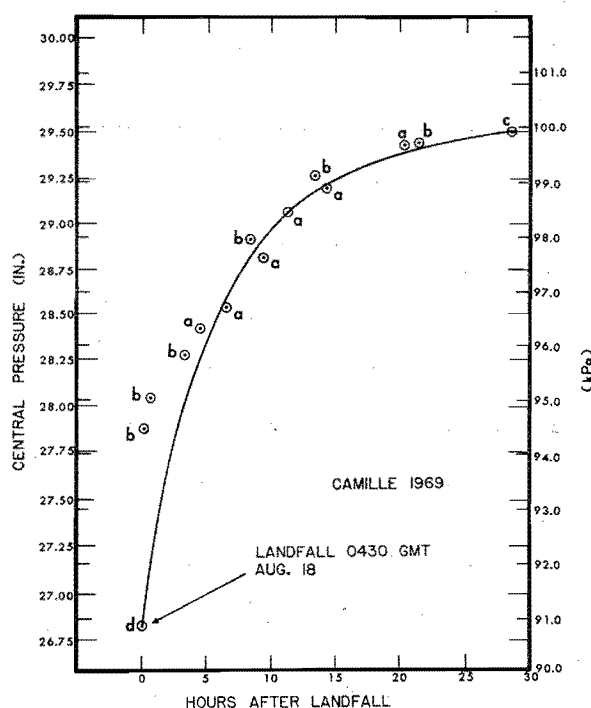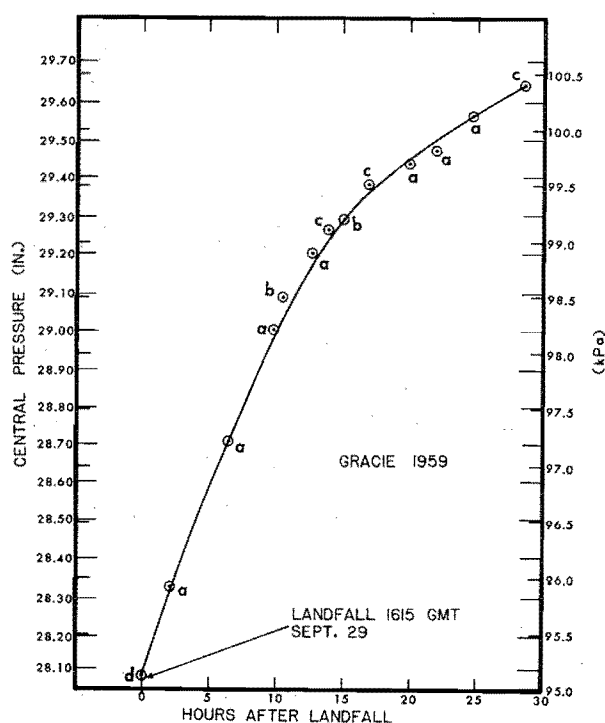
Figure 15.7a.--Increase of central
    pressure (p_o) with time for hurri-
    cane Gracie (1959) after she crossed
    the South Carolina coast. Data
    marked with an "a" are from pres-
    sure-distance profiles; "b" data
    are lowest pressure data at a
    station close to the hurricane
    center; "c" data are from weather
    maps; "d" data are estimates of p_o
    at landfall from other studies.

Figure 15.7b.--Increase of central
    pressure (p_o) with time for hurricane
    Camille (1969) after she crossed the
    Mississippi coast. Data marked with
    an "a" are from pressure-distance
    profiles; "b" data are lowest pres-
    sure data at a station close to the
    hurricane center; "c" data are from
    weather maps; "d" data are estimates
    of p_o at landfall from other studies.

An analysis of p_w with time after landfall was also needed for the nine
hurricanes. Values of p_w were taken from 3-hourly weather maps. Figures

15.8a and 15.8b show eye-fitted curves of the change of p_w with time after landfall for Gracie and Camille.

HOURS AFTER LANDFALL
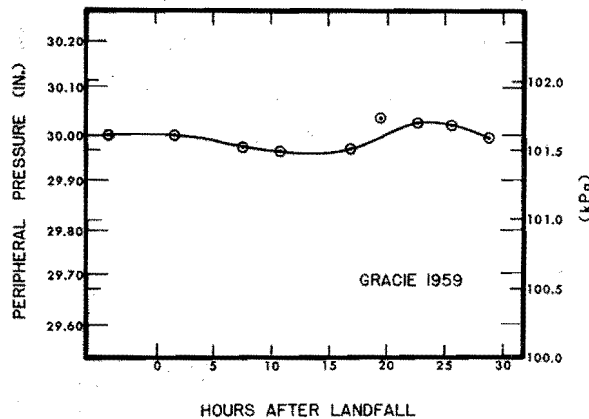
Figure 15.8a.--Variation of peripheral pressure (p_w) with time for hurricane Gracie (1959) after she crossed the South Carolina coast.
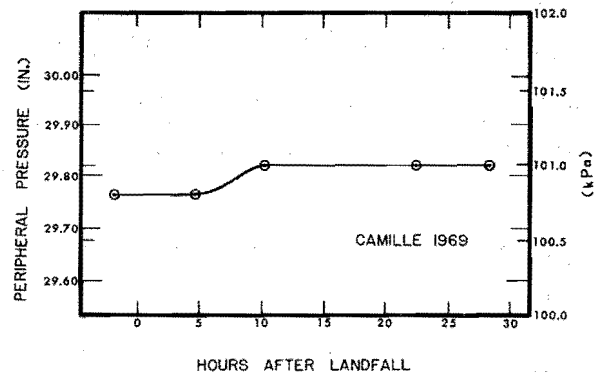
Figure 15.8b.--Variation of peripheral pressure (p_w) with time for hurricane Camille (1969) after she crossed the Mississippi coast.

We broke our sample of 16 hurricanes into three groups based on the coastal region where each entered land. These regions are shown in figure 15.9. Region A is the coast between Corpus Christi, Tex., and Mississippi; region B, the coast of Florida south of 27°N; and region C, the coast from South Carolina to Long Island, N.Y. Storms in these regions are in table 15.2.

We did not attempt to incorporate forward speed (T) into our determination of ff because we did not have a full range of T in our sample (table 15.2). Thirteen of the 16 hurricanes had forward speeds between 6 and 17 kt (11 and 32 km/hr), while the other three storms (all affecting New England) had speeds of 32, 33 and 47 kt (59, 61 and 87 km/hr).

Figure 15.10 is a graph of average ff vs. time after landfall for hurricanes in regions A, B and C. Rather large regional differences are seen in the adjustment factors. We calculated the region B adjustment curve for the four hurricanes (table 15.2) using the mainland (between Marco and Everglades City) as Donna's landfall point rather than Conch Key in the Florida Keys. The difference in Donna's filling rate following landfall at either of these
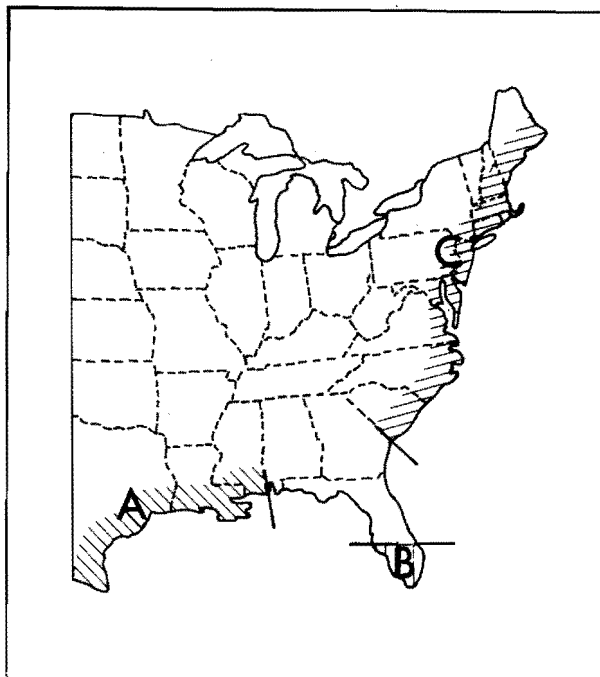
Figure 15.9.--Map showing extended boundaries of regions A, B, and C.

Figure 15.10.--Variation in adjustment factors with time for three geographic regions. Region A (o———o) includes the gulf coast states of Texas, Louisiana, and Mississippi. Region B (•———•) is Florida south of 27°N. Region C (x———x) represents the east coast from South Carolina northward.

two points was small enough not to have an effect on the mean curve for region B.

15.3.5 DISCUSSION OF ANALYSIS

We need to assess the adjustment curves (fig. 15.10) for meteorological reasonableness. First, we would expect the adjustment for the Florida peninsula (region B) to be the least, i.e., slowest filling, of the three regions because more of a storm's circulation can be over water while the center is inland. We find this is so. Next, we might expect hurricanes to fill the fastest along the middle and northern east coast (region C) because hurricanes there travel the fastest away from the oceanic heat source. However, our results show that the Gulf coast storms (region A) fill the fastest. This is probably because they do not take on extratropical characteristics as often as east coast (region C) hurricanes. Our data sample bears this out. Fifty-seven percent of the region A hurricanes became extratropical before dissipating whereas 80 percent of the region C hurricanes dissipated as

278

extratropical cyclones. We would expect this to be true because region C storms often penetrate to more northerly latitudes where the air is cooler and drier.

15.3.6 RESULTS

Figure 15.11 shows smoothed curves from figure 15.10. These are to be used for the designated areas only. Region A has been extended to the Mexican border and region C to the Canadian border in order to include the entire coastline.

Figure 15.12 illustrates the coastal boundaries of the three curves and, by way of the dashed lines, coastal sections where linear interpolation should be used to develop intermediate curves.

Curves A and C (fig. 15.11) can be expressed by the following equation:

$$W_I = W_C \, e^{(\alpha t + \beta t^2)} \quad (15.4)$$

where,

W_I = the overland wind speed at some specified time after landfall (friction effects not considered).

W_C = the overwater wind speed at landfall.

t = time

α and β are coefficients.

For the gulf coast from Mississippi westward (curve A) $\alpha = -0.035$ and $\beta = 0.00013$ and for the east coast north of Savannah, Georgia (curve C) $\alpha = -0.026$ and $\beta = 0.00018$.
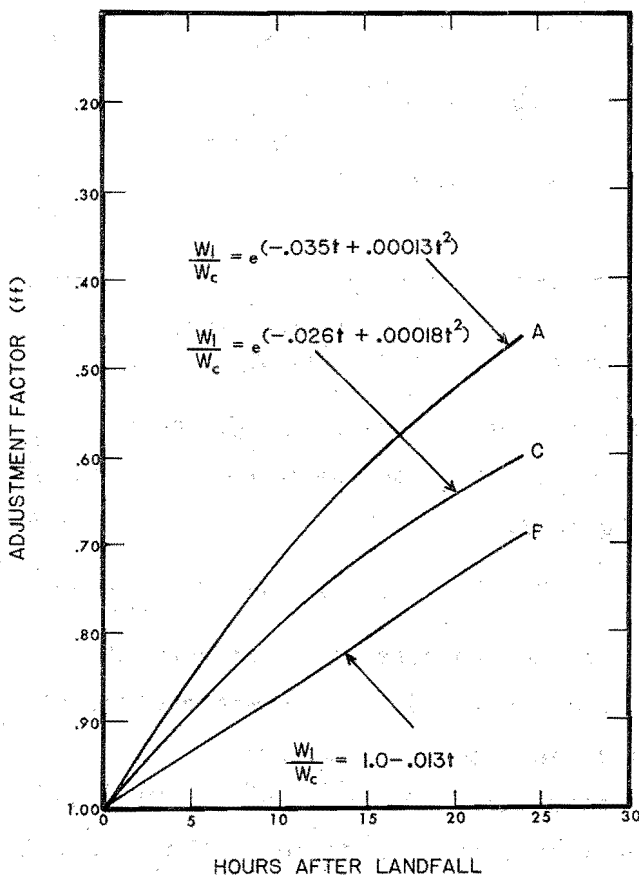
Figure 15.11.—Smoothed adjustment factor curves for reducing hurricane wind speeds when center is overland for three geographic regions defined in figure 15.9.
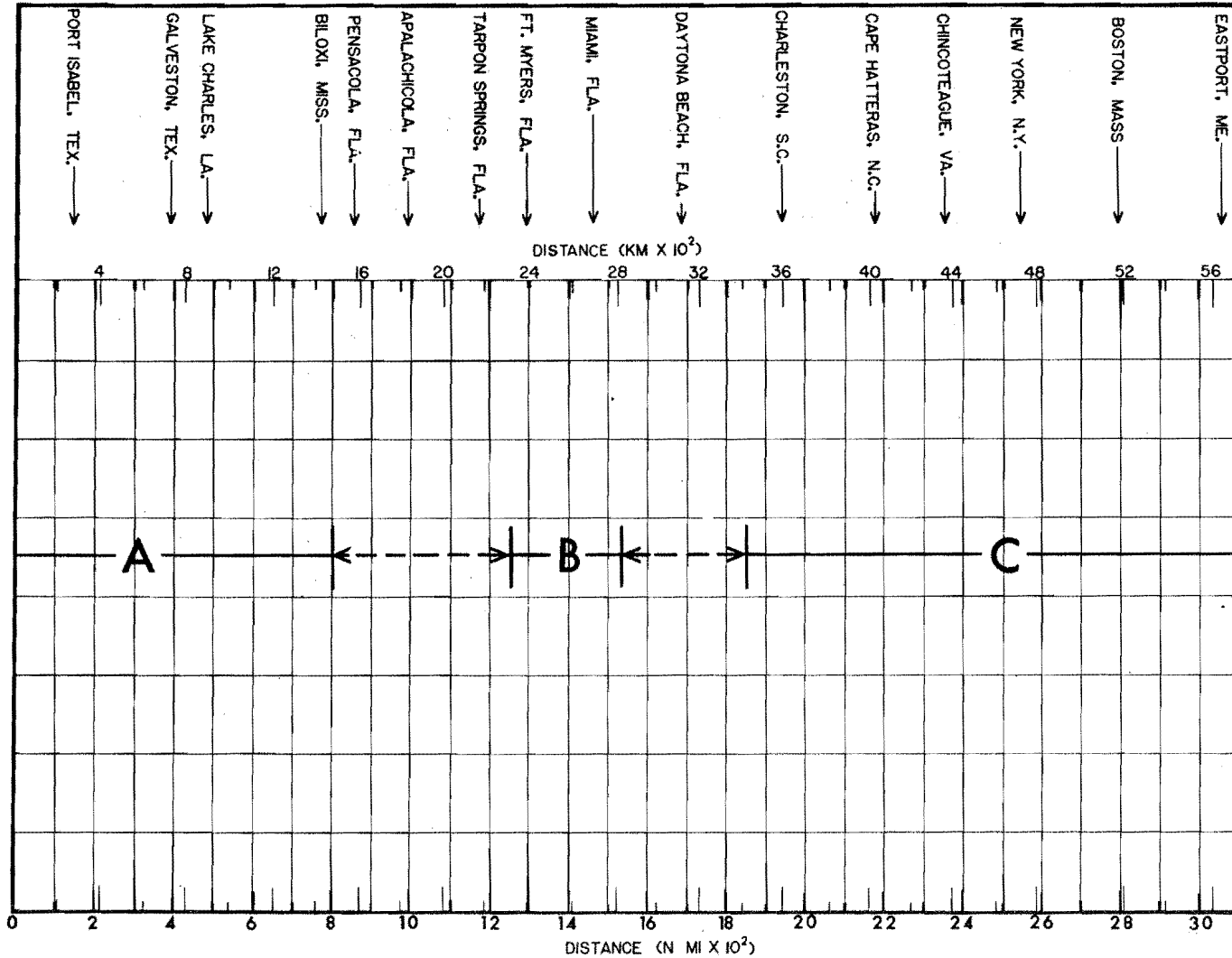
Figure 15.12.—Limits of the three geographic regions (A, B, and C). The dashed lines delineate where linear interpolation should be used to develop intermediate curves in figure 15.11.

Curve B (fig. 15.11) for the Florida coast south of 27°N can be expressed by a linear regression line in terms of t:

$$W_I = W_C \ (1.0 \ -0.013t) \tag{15.5}$$

15.3.7 Discussion of Results

15.3.7.1 Comparison of SPH and PMH Adjustment Factors.

The adjustments in figure 15.11 are to be applied directly as a percent of the overwater wind field isotachs. They provide an estimate of the reduction in wind speed *due to filling* anywhere in the hurricane, if we assume only slight variations in the shape of the overwater and overland wind speed profiles with time.

Our hurricane sample indicates that there is a trend for the more intense hurricanes to fill faster except over the Florida peninsula where there is a slight tendency for the more intense to fill more slowly. These trends are seen in table 15.3. In this table the Δp_t's of hurricanes within each region are ranked (rank 1, the largest). We also have ranked the adjustment for each storm for t + 6, t + 14 and t + 22 hours (rank 1, the lowest number, or greatest filling).

Correlation coefficients were computed for various times, t, between Δp_t at the coast and the adjustments of table 15.3. The results (significant at the 5-percent level) support the idea that the more intense hurricanes fill faster. Correlation coefficients of -0.79, -0.75 and -0.60 were computed for 6 hours after landfall for: 1) gulf coast hurricanes (region A), 2) hurricanes north of 27° (regions A and C), and 3) all hurricanes (regions A, B, and C), respectively. Correlation coefficients for the other time periods (t + 14 and t + 22) were nearly of the same order of magnitude. From table 15.3 we see that the somewhat lower correlation for group 3) probably results because intense Florida peninsula hurricanes tend to fill more slowly than less intense storms and because there is more scatter in the larger sample.

Table 15.3.--*Hurricane pressure drop at landfall and computed wind speed adjustments*

Geographic region	Hurricane	Δp_t (in.)	(kPa)	Δp_t Rank	Adjustment factor (ff) at t + 6*	ff Rank	Adjustment factor (ff) at t + 14*	ff Rank	Adjustment factor (ff) at t + 22*	ff Rank
	Aug.14,1932	2.10	7.1	3	.77	2	.55	2	.37	1
	Sep.23,1941	1.54	5.2	7	.94	7	.81	7	.62	7
	Audrey	1.79	6.05	6	.85	4	.60	4	.43	4
A	Carla	2.27	7.7	2	.88	5	.68	5	.61	6
	Betsy	1.86	6.3	5	.93	6	.73	6	.52	5
	Camille	2.92	9.9	1	.67	1	.46	1	.37	1
	Celia	1.93	6.55	4	.79	3	.56	3	.41	3
	Sep.17,1928	2.27	7.7	1	.92	3	.86	4	.76	–
	Sep.15,1945	1.86	6.3	3	.95	4	.83	3	.70	–
B	Aug.27,1949	1.80	6.1	4	.89	1	.80	1	.68	–
	Donna	2.02	6.85	2	.91	2	.80	1	–	–
	Sep.21,1938	2.13	7.2	1	.77	1	.65	3	.51	1
	Carol	1.68	5.7	3	.80	2	.64	2	.55	3
C	Connie	1.45	4.9	4	.98	5	.90	5	.81	5
	Gracie	1.92	6.5	2	.83	3	.62	1	.53	2
	Donna	1.45	4.9	4	.87	4	.83	4	.75	4

*t + 6 = 6 hours after landfall, etc.

282

Another set of correlation coefficients was computed for the same three storm groups, leaving out the most severe storm, Camille. These correlation coefficients for t + 6 hours are -0.46, -0.55 and -0.30 for groups 1), 2) and 3), respectively. The new coefficients are not significant at the 5-percent level.

The significance of the correlation coefficients using Camille are clearly a result of the effect of one hurricane on a small sample. The addition of more storms over the next few decades could result in a loss of significance. Therefore, we have decided to use the same adjustment factors for both the SPH and PMH wind fields.

15.3.7.2 OTHER RESEARCH INVOLVING OVERLAND FILLING. Malkin (1959) also showed that the square root of the average pressure gradient $(\Delta p/D_W *)$ when used in a similar procedure to ours gave wind speeds that were reasonably consistent with some observations. This procedure results in a faster drop-off of wind speed with time than is indicated by using only Δp.

Goldman and Ushijima (1974) determined decreases in wind speed inland for hurricanes Carla, Camille and Celia. They studied the extent of damaging winds at landfall and inland up to 78 n.mi. (145 km) and compared observed peak gusts (not Δp) at the coast when the storm entered with peak gusts inland at some later time. Near the strongest portion of the eyewall 6 hours after landfall, Goldman and Ushijima calculated the percentage reduction from peak gusts at 0.66 for Carla and 0.70 for Camille and Celia. By contrast, the adjustment factor (ff) at t + 6 (6 hours after landfall), listed in table 15.3, gives a percentage reduction from 10-m, 10-min winds of 0.88 for Carla, 0.67 for Camille, and 0.79 for Celia. In making this comparison, we note that 1) Goldman and Ushijima are considering frictional effects in addition to filling effects while we are not and 2) they are using peak gusts while we deal with sustained winds.

---

*D_W is the average distance from the pressure center to the points where p_W is calculated.

15.3.7.3 PMH OR SPH CROSSING FLORIDA PENINSULA FROM EAST TO WEST.

A hurricane approaching from the sea produces a much higher surge than a hurricane of equal intensity exiting the coast. However, of possible importance is whether a PMH or SPH can enter the Florida peninsula from the east, cross the peninsula, and be stronger than a PMH or SPH entering the peninsula from the west. Such a question would be most critical for the area just north of the 29th parallel where the distance from the east coast to the west coast is only about 100 n.mi. (185 km) and where the central pressure difference between the two coasts is the largest.

We have made computations based on filling rates while overland which show that the winds on the west coast of Florida from an east coast PMH or SPH striking milepost 1700 (fig. 1.1) and crossing the peninsula cannot be stronger than the winds from a gulf coast PMH or SPH striking milepost 1100 directly from the sea. This would also be the case at points along the central and southern portions of the peninsula because the difference in p_o between the two coasts increases with latitude.

16. THE STALLED PMH

16.1 INTRODUCTION

For some problems it is necessary to evaluate the degree of scouring or erosion of beaches from intense hurricanes. Naturally, the slower the storm moves, the greater the beach damage. In this chapter we estimate the properties of a slow moving PMH.

We assume that a PMH moving at 5 kt or less for a period of at least 24 hours is particularly critical to the beaches. We classify storms meeting this criteria as *stalling*. A study by the Florida Power and Light Company (1975) using data between 1901 and 1973 for the Gulf of Mexico and the Atlantic south of 35°N classified 2 hurricanes as stalling. In that study, a hurricane was so classified if its average forward speed (T) was $\leq$ 5 kt (9 km/hr) for a period of 2 days or longer.

North of the Virginia-North Carolina border (milepost 2260), where the lower limit of forward speed begins to significantly exceed stalling speed, we need to consider how much a PMH will weaken before it reaches stalling speed. For this region, numerous assumptions must be made concerning the transition from a slow speed PMH storm to the storm just before it reaches stalling speed. Discussion of these assumptions and resulting procedures begin with section 16.5.

16.2 BACKGROUND

Stalled hurricanes weaken because in an environment of slight steering winds, warm air cannot be transported away from the hurricane core quickly enough (Beebe and Simpson 1976). Thus, the mechanism of lower-level inflow combined with upper-level outflow which is essential to a mature hurricane, begins to break down. In addition, cooling of surface water due to upwelling in the wake of a hurricane leads to weakening of a stalled hurricane (Geisler 1970). Leipper (1967) reported that, in hurricane Hilda (1964), stalling and an outbreak of cold air behind the storm caused the sea-surface temperature (T_s) to fall 10.8°F (6°C). Hilda then filled 0.61 in. (2.1 kPa) and, after striking the coast, became extratropical. Using airborne infrared thermometers and airborne expendable bathythermographs, Black and Mallinger

(1972) documented the presence of cold surface water beneath slow-moving weakening hurricane Ginger in 1971. Smith (1975) reported that the movement of hurricane Celia (1970) over colder T_s's and shallower mixed-layer* depths probably contributed to its filling. The storm initially deepened to 28.50 in. (96.5 kPa), then filled to 29.12 in. (98.6 kPa).

When air and sea-surface temperatures are about the same, evaporation and conduction of heat are minimized and little energy is extracted from the sea by the hurricane. Leipper and Volgenau (1972) computed the hurricane heat potential of the Gulf of Mexico for four summers and identified areas of low-heat potential where a storm could be supported for only one or two days. The sea-surface temperature in the gulf is normally about 81°F (27-28°C) in summer. We conclude that a hurricane stalled for longer than 2 days over waters a few degrees colder than this would weaken and would not extract enough heat energy from the ocean to reintensify.

16.2.1 EFFECTS OF SEA-SURFACE TEMPERATURE ON "CROSSOVER" TYPHOONS

The influence of cool sea-surface temperatures on the intensity of hurricanes may be studied statistically by examining the intensities of tropical cyclones crossing the wake of a recent tropical cyclone. Brand (1971) extracted 57 "crossover" typhoons from 12 years of typhoon data in the western North Pacific Ocean (1958-69). He defined crossover typhoons as those that crossed the track of a previous typhoon within 30 days. He concluded that both the movement and the intensity of a tropical cyclone may be affected by the cooler water left in the wake of an earlier storm. Thirty-eight of the 57 cases he studied indicated an intensity decrease in the later storm. He also pointed out that a larger percentage of storms showed a decrease of intensity at high latitudes than at low latitudes. This could be related to the latitudinal variation of mixed-layer depth.

---

*The mixed layer extends downward from the ocean surface, is virtually iso-thermal, and frequently exists above the thermocline. The thermocline is a vertical temperature gradient which is appreciably steeper than the gradient above it. Below the thermocline, temperatures continue to decrease but at a slower rate.

16.2.2 Geographic Variation in Sea-Surface Temperature Drops

Table 16.1 lists some hurricanes for which T_s dropped following the passage of the storm. The storm tracks and approximate locations of these events are shown in figure 16.1. The average change in T_s for 7 gulf hurricanes was -4.0°F (2.2°C) and for 5 Atlantic hurricanes -3.7°F (2.1°C). (-6.3°F or -3.5°C was used for Carla in the gulf, while -5.4°F or -3.0°C was used for Betsy and -5.9°F or -3.3°C for Ginger in the Atlantic. Betsy is included in the counts of both gulf and Atlantic hurricanes.) The difference between the two regions is negligible. Most of the T_s drops on figure 16.1 fall between 25° and 30°N; therefore, no conclusions can be made on the latitudinal variation of T_s drops. However, the mixed layer depth decreases to the north, enhancing the ability of a hurricane to produce a colder wake at higher than at lower latitudes.

16.3 DATA

We studied Atlantic hurricanes that occurred west of 40°W for 1955-75* and western North Pacific typhoons for 1961-75. The criterion used for selection of cases was $p_o \leq 29.00$ in. (98.2 kPa) for hurricanes and $p_o \leq 28.20$ in. (95.5 kPa) for typhoons at the time stalling began. Also, a storm could not have its eye over land during a stall and could not have reached its maximum intensity more than 24 hours prior to the time stalling began. The storm sample is listed in table 16.2. Central pressure and other data were obtained from aircraft reconnaissance reports. The reports for typhoons are published in the *Annual Typhoon Reports* by the Joint Typhoon Warning Center, Guam (U.S. Department of Defense 1961-72). The data for hurricanes came from the unpublished records of NOAA. The storm tracks are shown in figures 16.2a and 16.2b.

All storms meeting our criteria began their stall at or south of 36.5°N. We shall cover characteristics of stalling storms for this region first. For the region north of 36.5°N, our results are more subjective and are discussed separately.

---

*Reconnaissance data prior to 1955 are not considered to be as reliable as subsequent data.

Table 16.1.--Sea-surface temperature (T$_s$) changes associated with the passage of various hurricanes

Hurricane	Maximum ΔT$_s$ (°F)	(°C)	Source
Donna, Sept. 1960 (off Carolinas)	-2.7	-1.5	Hazelworth, 1968
Ethel, Sept. 1960 (mid-Gulf)	-4.5	-2.5	Hazelworth 1968
Carla, Sept. 9, 1961 (western Gulf)	-9	-5	Hazelworth, 1968
Carla, Sept. 10, 1961 (off Texas coast)	-3.6	-2	Stevenson and Armstrong, 1965
Arlene, Aug. 1963 (near Bermuda)	-1.8	-1	Hazelworth, 1968
Cleo, Aug. 1964 (near south Florida)	-2.7	-1.5	Hazelworth, 1968
Hilda, Oct. 1964 (mid-Gulf)	-10.8	-6	Leipper, 1967
Betsy, Sept. 1, 1965 (north of Puerto Rico)	-4.5	-2.5	Landis and Leipper, 1968
Betsy, Sept. 4, 1965 (NE of Bahamas)	-6.3	-3.5	Landis, 1966
Betsy, Sept. 9, 1965 (Gulf)	-1.8	-1	McFadden, 1967; Taylor, 1966
Camille, Aug. 1969 (northern Gulf)	-1.8	-1	Jensen, 1970
Celia, Aug. 1970 (mid-Gulf)	0	0	Molinari and Franceschini, 1971
Ginger, Sept. 27, 1971 (NE of Bahamas)	-7.2	-4	Black and Mallinger, 1972
Ginger, Sept. 28, 1971 (NE of Bahamas)	-4.5	-2.5	Black and Mallinger, 1972
Eloise, Sept. 1975 (northern Gulf)	-2.7	-1.5	Price, 1976
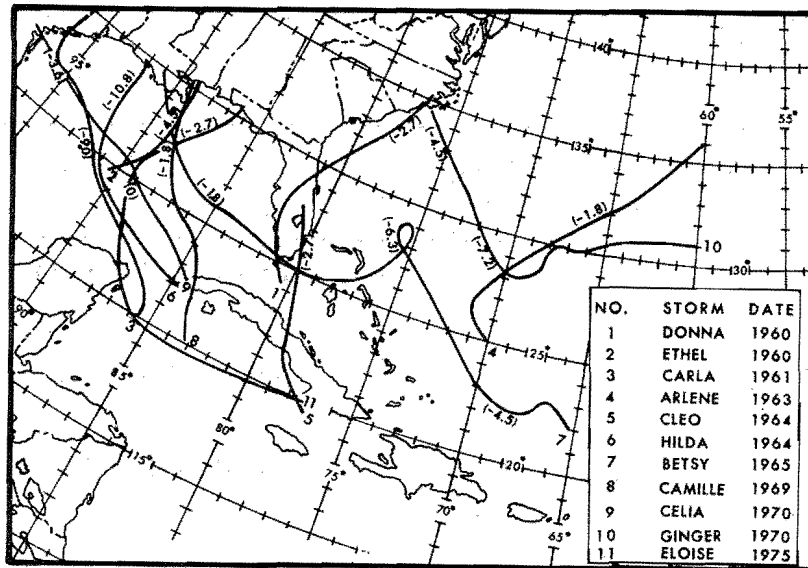
Figure 16.1.--Partial hurricane tracks and approximate locations of reported sea-surface temperature drops (°F). See table 16.1.

Table 16.2.--Most intense stalled hurricanes and typhoons selected for analysis.

	Lowest p_0 near the time stalling began*		Duration of stalling
	(in.)	(kPa)	(hr)
Hurricanes			
Betsy, Sept. 1961	27.91	94.5	54
Hilda, Oct. 1964	27.99	94.8	36
Betsy, Sept. 1965	27.85	94.3	24
Faith, Aug. 1966	28.26	95.7	36
Heidi, Oct. 1967	28.97	98.1	72
Typhoons			
Ellen, Dec. 1961	27.91	94.5	36
Emma, Oct. 1962	26.61	90.1	60
Trix, Sept. 1965	27.46	93.0	24
Harriet, Nov. 1967	28.11	95.2	36
Agnes, Sept. 1968	26.67	90.3	30
Faye, Oct. 1968	26.90	91.1	30
June, Nov. 1969	27.61	93.5	24
Wendy, Sept. 1971	27.02	91.5	30
Rita, July 1972	26.84	90.9	60

*These p_0's occurred between 18 hours before stalling began to 8 hours after for hurricanes and between 21 hours before stalling began to 6 hours after for typhoons.
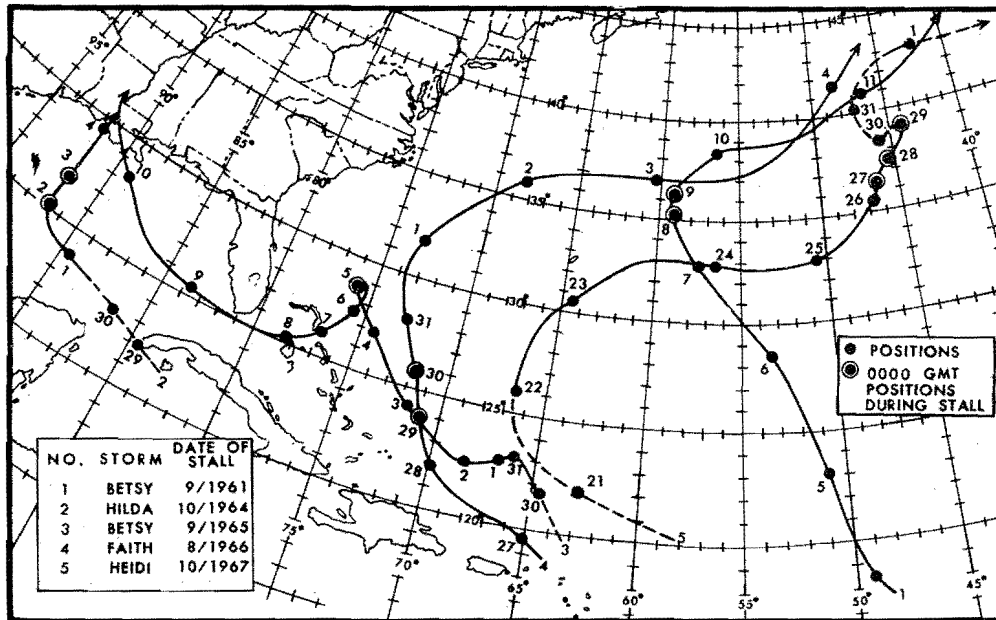
Figure 16.2a.--Partial tracks of selected hurricanes (table 16.2). Dots denote storm positions at 0000 GMT; circled dots are approximate positions where the storm stalled.
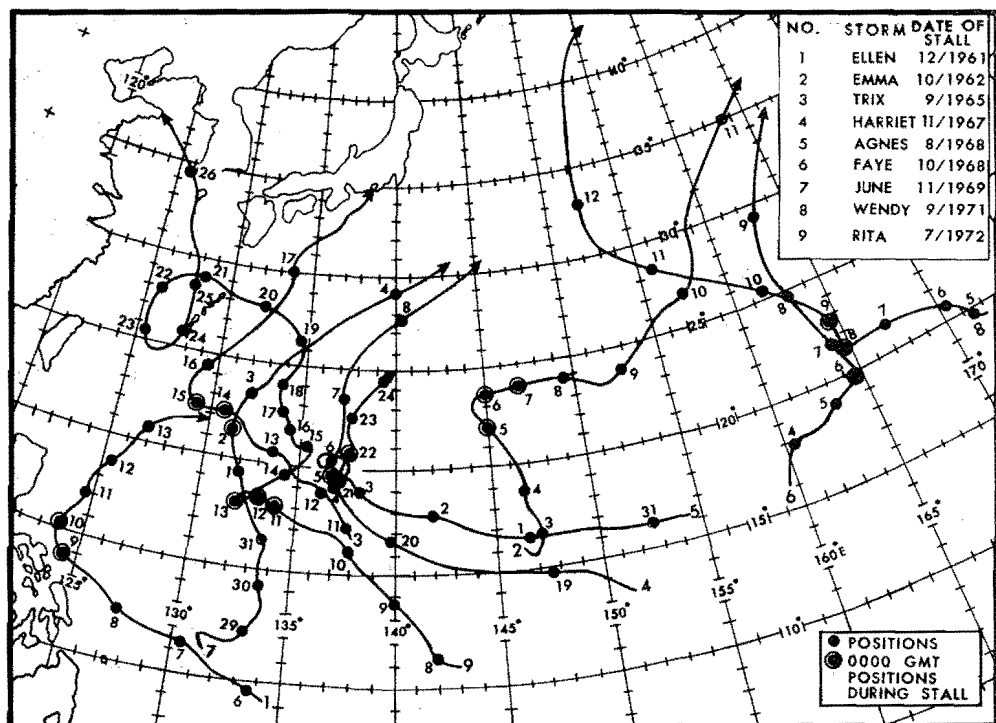
Figure 16.2b.--Same as figure 16.2a except for selected typhoons.

16.4 STALLED PMH SOUTH OF 36.5°N

16.4.1 VARIATION IN INTENSITY

16.4.1.1 ΔP BEFORE AND AFTER TIME OF STALL. The variation of intensity, Δp, $(p_w - p_o)$, before and after stalling for the selected storms (table 16.2) is shown in figures 16.3a and 16.3b. Central pressure values (p_o) are from aircraft reconnaissance reports and peripheral pressure values (p_w) are from daily weather maps from the Northern Hemisphere map series (Environmental Data Service 1961-72). Time zero in figures 16.3a and 16.3b indicates the time at which the storm begins a stall (moves at a forward speed $\leq$ 5 kt or 9 km/hr). Arrows indicate the end of the stalling period. The storms reached their maximum intensity preceding stalling, with three exceptions. Two hurricanes (Faith and Heidi) and one typhoon (Trix) were at their maximum intensity 6 to 8 hours after stalling commenced. Since maximum intensity is reached at different times relative to the beginning of a stall, we will use as reference the time of maximum intensity rather than the time of the beginning of the stall.

16.4.1.2 VARIATION OF ΔP OVER ΔP$_{MAX}$ WITH TIME AFTER ΔP$_{MAX}$

Figures 16.4a and 16.4b show the variation in intensity with time from maximum intensity (t = 0) for the selected stalled hurricanes and typhoons, respectively. The variation is in terms of the ratio of the intensity to the maximum intensity. Arrows indicate the end of the stalling period. In general, during the first 30 to 40 hours after reaching maximum intensity, the more intense storms weaken at a faster rate. After stalling for 30 hours, typhoon Wendy (fig. 16.4b) reintensified to near her original strength as her forward speed picked up to 13 kt (24 km/hr). Wendy's intensity decreased by about 40 percent in 36 hours* while she moved at a T of about 4 kt (7 km/hr). Stalling in this case can be traced to the light steering currents associated with a breakdown of the subtropical high to the northwest. The subsequent deepening of the typhoon was linked to a strengthening of these currents after a rebuilding of the high to the northeast.

---

*Wendy began her stall at the time of maximum intensity.
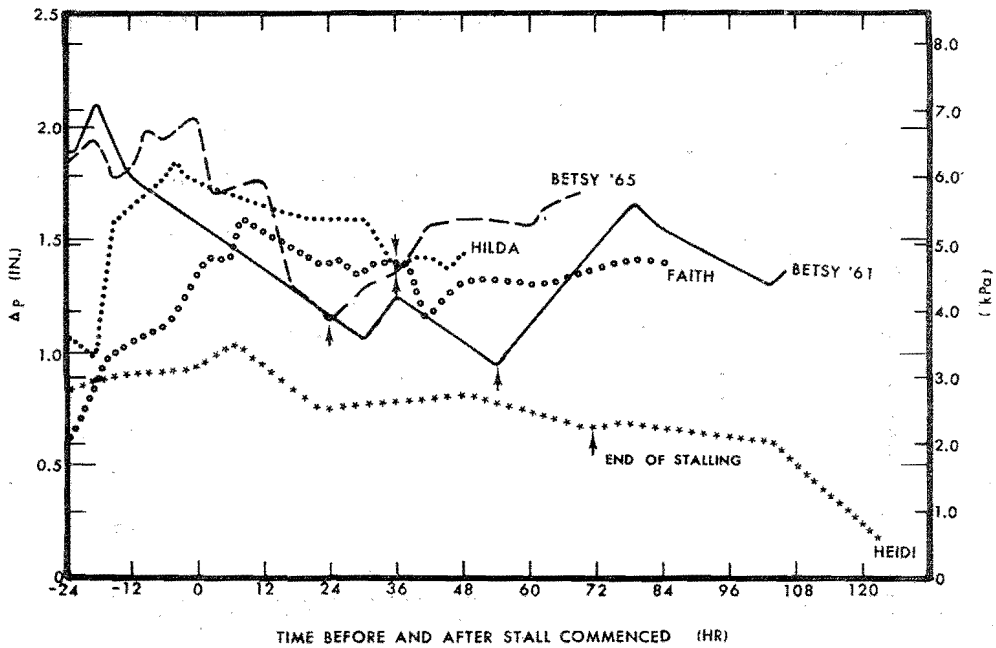
Figure 16.3a.--Variation in pressure drop $(p_w - p_o)$ for selected stalling hurricanes. Arrows indicate the end of the stalling period. Time = 0 marks the beginning of the stalling period.
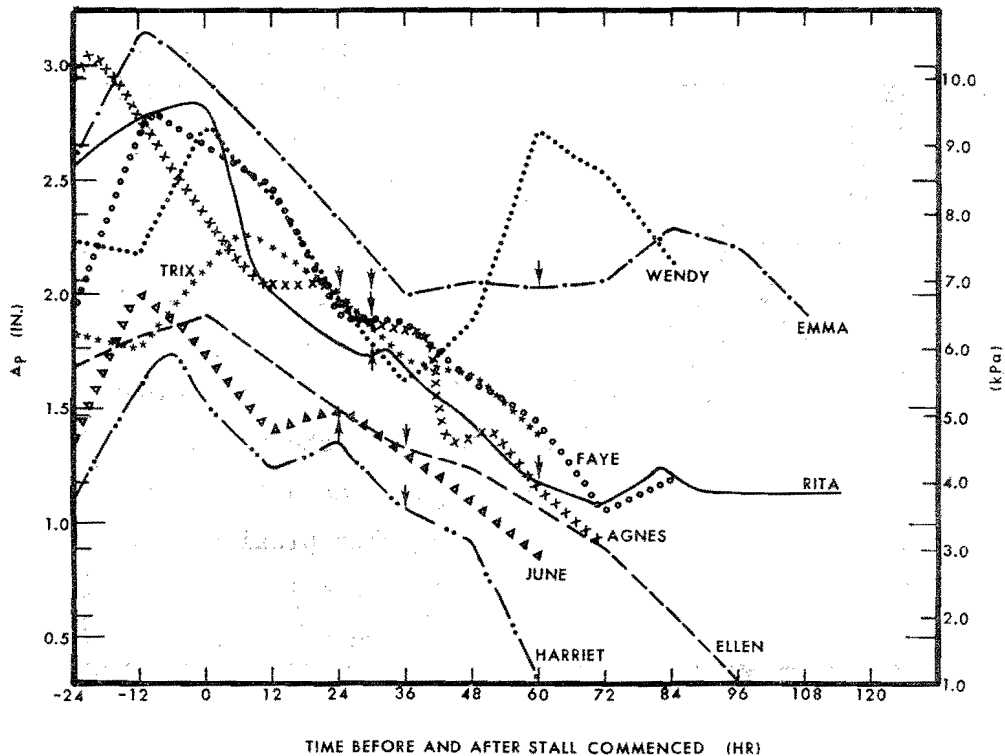
Figure 16.3b.--Same as figure 16.3a except for selected stalling typhoons.
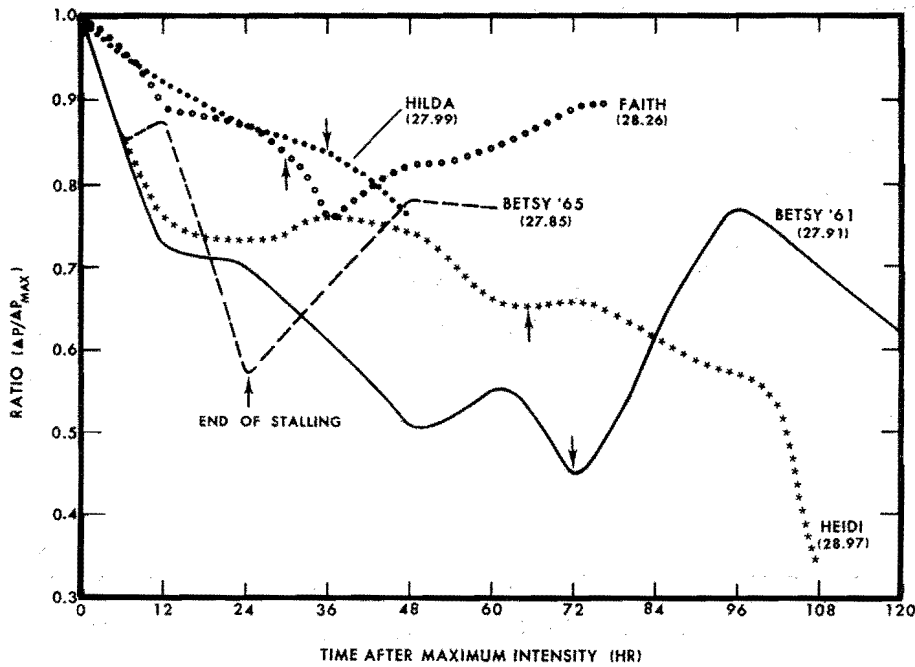
Figure 16.4a.--Variation in pressure drop $(p_w - p_o)$ from the maximum pressure drop reached in selected stalling hurricanes. Arrows indicate the end of the stalling period. Time = 0 marks the time of maximum intensity. The data next to each storm lists the central pressure at time = 0 in inches (Hg).
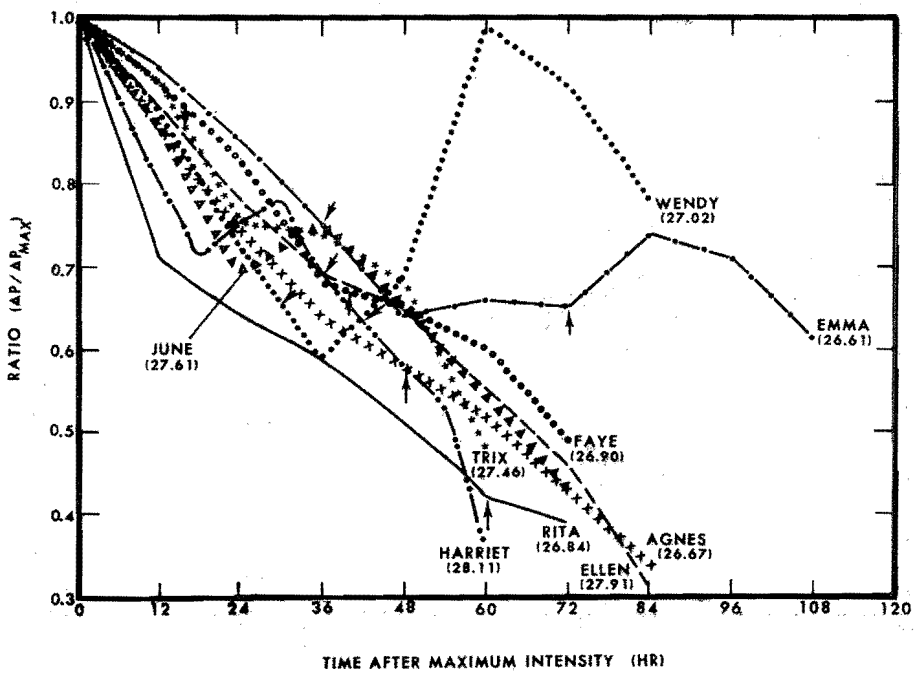
Figure 16.4b.--Same as figure 16.4a except for selected stalling typhoons.

16.4.1.3 VARIATION OF Δp_{MAX} WITH Δp AFTER MAXIMUM INTENSITY

Figures 16.5a, 16.5b, and 16.5c show the maximum storm intensity (Δp_{max}) plotted against the intensity (Δp) 24, 36, and 48 hours, respectively, after the maximum intensity is reached. A line of best fit is drawn by eye on each of the diagrams. The deviation of each line of best fit from the 45° line indicates that the decrease in Δp from the maximum Δp is greatest at the upper end of the curve corresponding to storms with the greatest intensities. We note that the three plots show good agreement between stalled hurricanes and typhoons.

16.4.1.4 VARIATION IN PMH WIND SPEED WITH TIME AFTER STALL.

Two curves of figure 16.6 show the average rates of weakening for the stalled hurricanes and typhoons of table 16.2. An average of the two (solid curve) indicates a 23% and 33% decrease in pressure drop 24 hours and 48 hours, respectively, after the storms began to stall. The top and bottom curves give the full range in intensity variation of the storms studied.

Figures 16.5 a, b, and c indicate that the decrease in Δp after stalling begins is greatest for the more intense storms. Since the PMH has a greater intensity than any recorded hurricane, we may expect an even greater decrease in intensity when it stalls. However, in view of the uncertainties inherent in a study of this kind, we have adopted the average decrease in storm intensity given by the solid curve in figure 16.6 for the rate of decrease for the PMH south of latitude 36.5°N (Virginia – North Carolina border).

This curve has been expressed in terms of the decrease in wind speed for the PMH through the classical pressure-wind relation:

$$\frac{\Delta p}{\Delta p_{max}} = \left(\frac{v}{v_{max}}\right)^2 \tag{16.1}$$

The resulting stalling adjustment factor (sf) is shown in figure 16.7 by a solid curve out to 60 hours after the time of stall, and by a dashed curve to 120 hours. The dashed curve is based partially on hurricane Heidi. Hurricane Carol (1965) stalled for 120 hours over the open North Atlantic but diminished to tropical storm strength for about 12 hours during that period. We think a former PMH can stall for 120 hours south of Virginia and maintain hurricane strength.
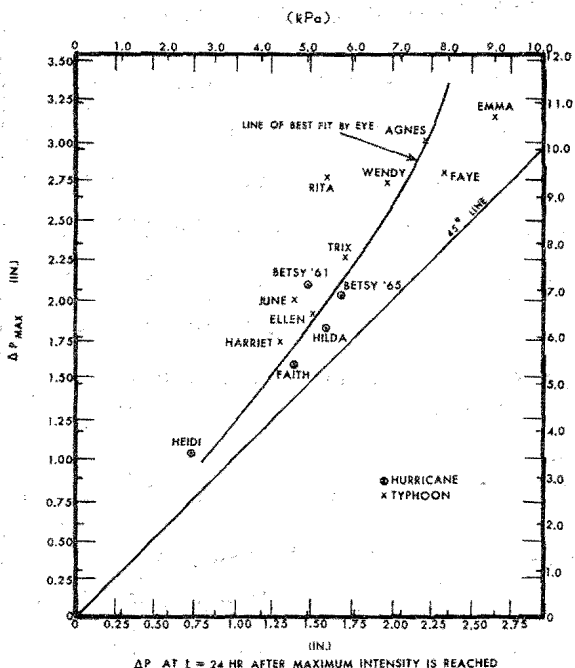
Figure 16.5a.--Variation of maximum pressure drop with pressure drop 24 hours later for selected stalling hurricanes and typhoons. Note the line of best fit by eye.
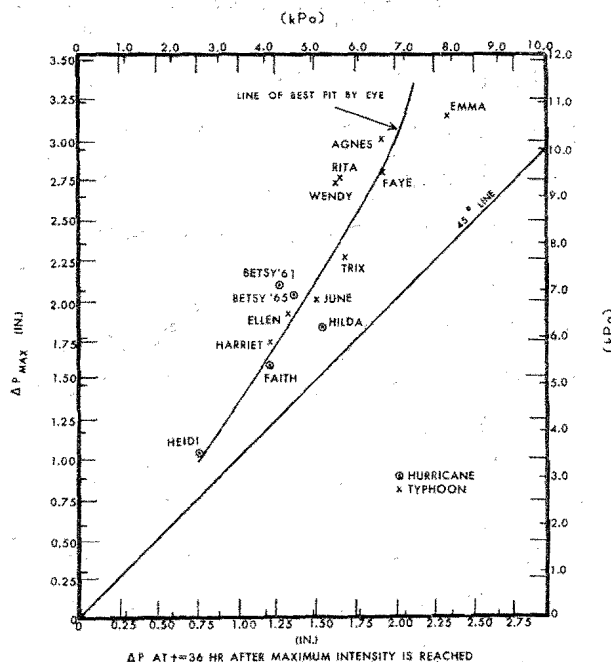
Figure 16.5b.--Same as figure 16.5a except abscissa refers to time 36 hours later.

16.4.2 VARIATION IN FORWARD SPEED

Figures 16.8a and 16.8b show the variation with time of the forward speed (T) of selected stalled storms. These T's are 6-hr averages. All T's <5 kt (9 km/hr) are shown as 5 kt. The hurricanes and typhoons generally moved at speeds between 6 and 16 kt (11 to 30 km/hr) during the 24 hours prior to stalling. This does not exclude the possible stalling of faster moving storms. The diagrams also show that the storms moved at T's ranging from 6 to 30 kt (11 to 56 km/hr) 36 hours after the end of their last stall. On the average, the T increased to about 10 kt (19 km/hr) 24 hours
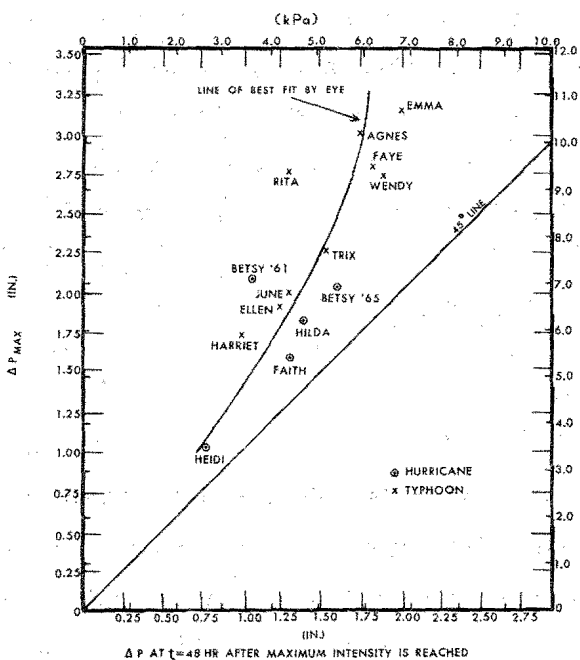
Figure 16.5c.--Same as figure 16.5a except abscissa refers to time 48 hours later.
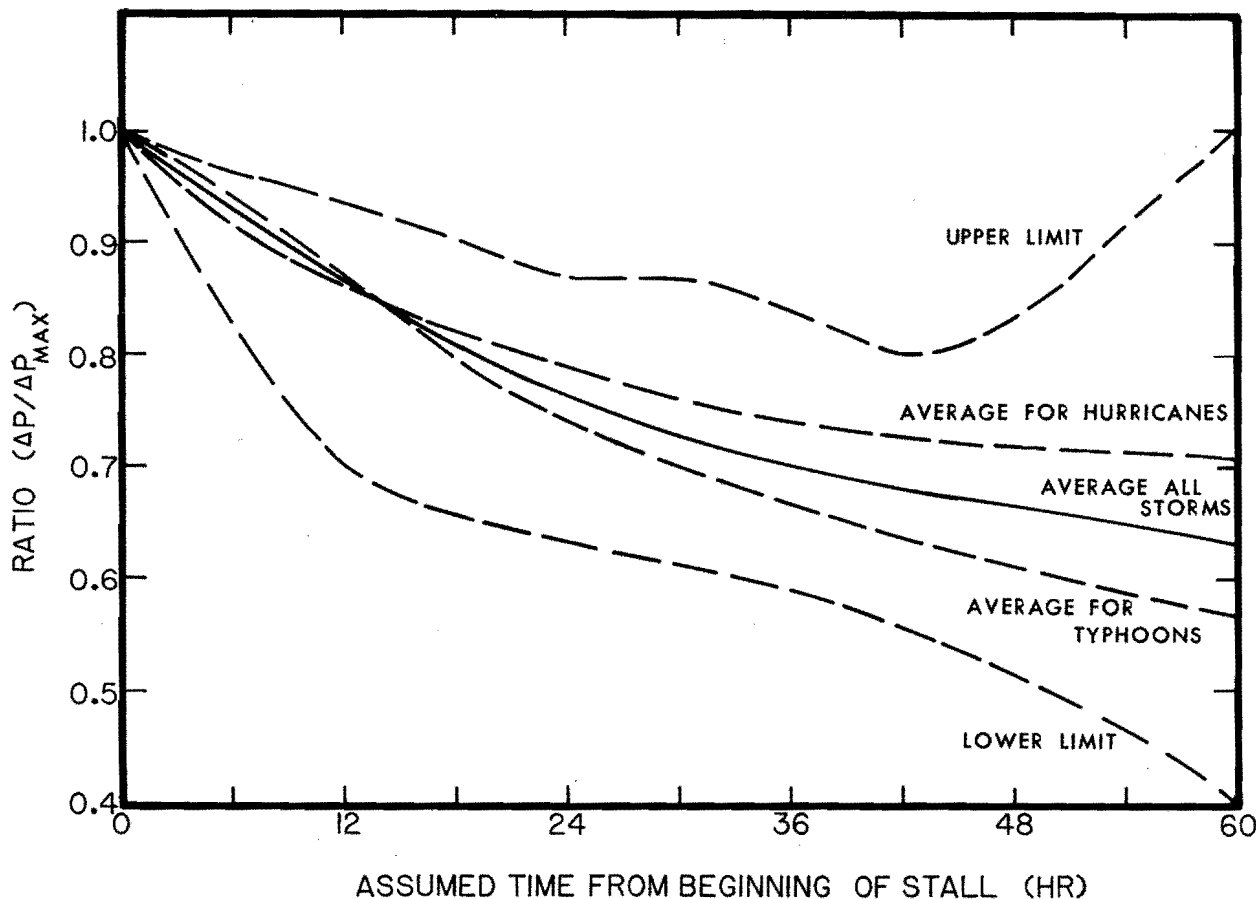
Figure 16.6.--Ratio of pressure drop $(p_w - p_o)$ to the maximum pressure drop.
Time = 0 represents the assumed time stalling begins corresponding to the
time of maximum pressure drop. The upper and lower limit curves are enve-
lopes of observed data for the selected stalling hurricanes and typhoons.
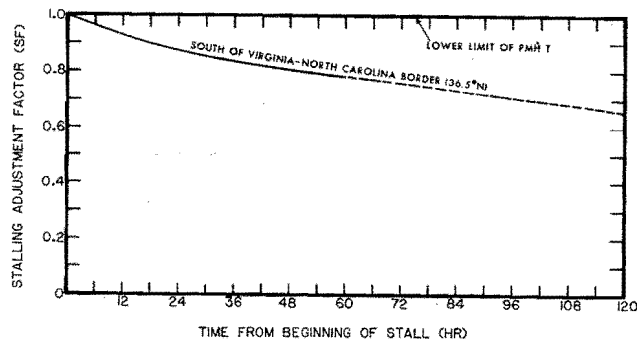
Figure 16.7.--Stalling adjustment
factor (sf) curve for the PMH to be
used south of the Virginia - North
Carolina border (36.5°N).

after stalling ceased, and to 14 kt
(26 km/hr) 48 hours after. The T after
stalling seems to be independent of
the storm's initial intensity. Two
typhoons which moved slowly after
stalling (Harriet and Ellen) continued
to weaken to tropical storm strength.
Other slow-moving storms (Betsy of
1965, Agnes, and Rita) maintained
hurricane or typhoon intensity (figs.
16.3a and 16.3b).

296
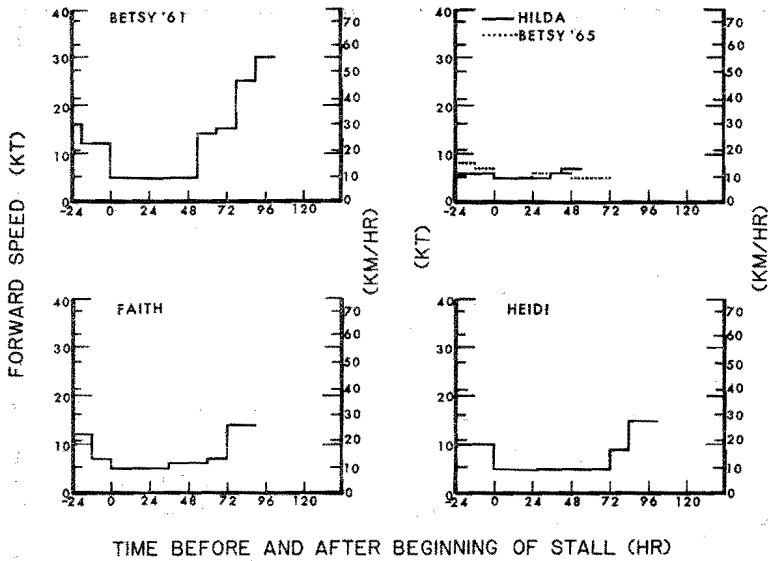
Figure 16.8a.—Variation of forward speed (T)
with time for selected stalling hurricanes.
Time = 0 indicates the beginning of stall
(T ≤ 5 kt, 9 km/hr)
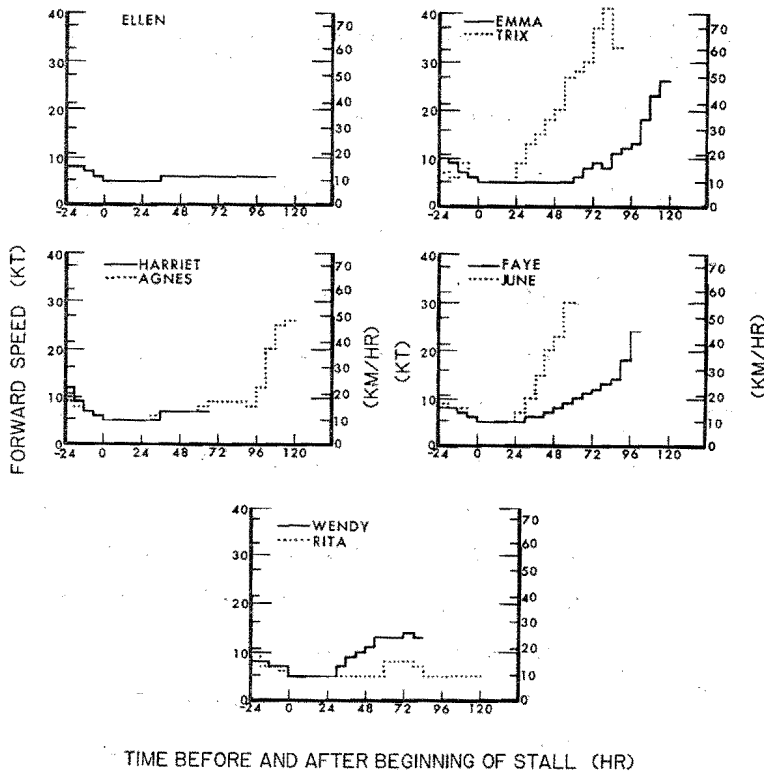
Figure 16.8b.—Same as figure 16.8a except for
selected stalling typhoons.

T for a stalled hurricane is given by definition, i.e., ≤ 5 kt (9 km/hr). Prior to stalling a PMH can have the range of T given in chapter 10. The rate of increasing T after stalling for a former PMH has been left unanswered.

16.4.3   TRACK DIRECTION

Since looping and other erratic storm motions may accompany a stalled hurricane, no limiting values are assigned to θ for a stalled PMH.

16.4.4   RADIUS OF MAXIMUM WINDS AND INFLOW ANGLE

The increase in p_o because of stalling would indicate larger R's for the stalled case, but because this increase is often small south of the Virginia – North Carolina border, we recommend no change, i.e., use figure 9.8. From Virginia northward we recommend a variation in R prior to and after stalling; (see sec. 16.5.7).

We recommend that figure 14.7 continue to be used to compute inflow angle (ϕ) for the former PMH after it stalls.

16.4.5 LENGTH OF STALL

The length of stall (figs. 16.8a and 16.8b, table 16.2) for the selected hurricanes and typhoons varies from 24 hours (3 storms) to 72 hours for hurricane Heidi, which was weak when it stalled (fig. 16.3a). The length of stall for the selected hurricanes and typhoons (omitting Heidi) varies from 24 to 60 hours (typhoons Emma and Rita.)* We think a former PMH can stall and maintain hurricane strength for 120 hours south of Virginia.

16.4.6 REINTENSIFICATION WHEN THE STALL IS OVER

The reintensification of a storm after stalling ceases is restrained by sea-surface temperatures. Thirty years ago, Palmén (1948) postulated that a tropical storm cannot develop into hurricane intensity over waters with surface temperatures of 78.8°F (26°C) or less. This critical limit is still accepted today. The mean August sea-surface temperature, lowering with increasing latitude, drops to about 64.4°F (18°C) off the New England coast near 43°N (U.S. Navy 1969b).

After stalling is over and T again exceeds 5 kt (9 km/hr), a former PMH south of 36.5°N may reintensify to the maximum intensity it had before stalling. The time required for a storm to regain PMH intensity and the rate of this reintensification has not been studied extensively but is linked to the length of the stall and also, therefore, to the degree of weakening. In our storm sample, the only storm to regain its maximum intensity was typhoon Wendy. It regained this intensity 30 hours after stalling ended (fig. 16.3b). The length of Wendy's stall was also 30 hours. A PMH as a stronger storm would probably require a reintensification period longer than its stall period.

---

*Intense hurricanes have stalled for longer periods near land. Hurricane Flora stalled over eastern Cuba for 4 days in October 1963.

16.5   STALLED PMH NORTH OF 36.5°N

16.5.1   INTRODUCTION

Examination of our sample of stalled hurricanes and typhoons shows only one north of 36°N and none north of 39°N. Nevertheless, this does not preclude a hurricane stalling or looping from Delaware Bay (39°N) northward. Since this report is developed to provide comprehensive guidelines for the PMH along the gulf and east coasts of the United States, it is necessary to develop criteria for a stalled PMH for the entire region. The criteria are extensions of those prepared for south of Virginia (36.5°N) and are based on meteorological reasoning which includes indications from more southerly hurricanes.

16.5.2   RATE OF DECREASE OF WIND SPEED

The rate of decrease of the wind speed south of 36.5°N (fig. 16.7) was developed from storms over sea-surface temperatures at or above 79°F (26°C). From southern Florida to Cape Hatteras, the sea-surface temperature decreases slowly.   North of about 36.5°N the decrease becomes more rapid (see fig. 12.2) with considerably less potential energy from the sea-surface. It is reasonable for a stalled hurricane to have a more rapid rate of decrease in wind speed over cold water. Since some energy is still available from the water surface, the rate of decrease should be less than that for decreasing winds for overland filling along the east coast (curve C, fig. 15.11). For the region north of Cape Cod (42°N), a curve was interpolated one-fourth the distance between the warmer water curve (fig. 16.7) and the overland filling curve. Figure 16.9 shows these three curves and several interpolated curves. All curves are dashed beyond 60 hours. For the coast between 36.5°N and Cape Cod, the rate of decrease in wind speed may be obtained by using the curves on figure 16.9 and, if necessary, linearly interpolating between them.

16.5.3   DECREASE IN T FOR A PMH NORTH OF THE VIRGINIA-NORTH CAROLINA BORDER

North of 36.5° the lower limits of T for a PMH are too fast (13 kt, 24 km/hr) for a storm to reach stall speed($\leq$ 5 kt, 9 km/hr) in a few hours or less. Some intermediate limits must be set on the rate of decrease of T for a PMH in order to approach stalling speed at a logical rate. During this
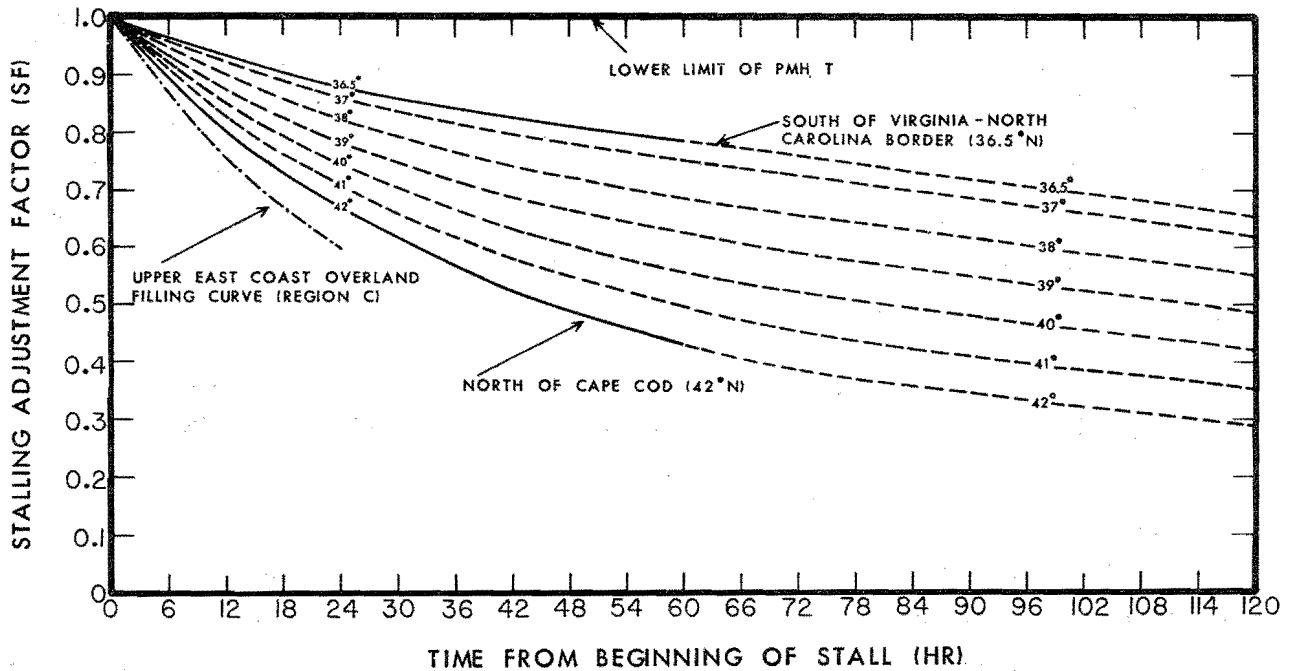
Figure 16.9.--Stalling adjustment factor (sf) curves for the PMH to be used north of the Virginia - North Carolina border. The upper straight line shows the lower limit of PMH T (no weakening).

period, the storm must weaken, but at a lesser rate than during a stalled condition.

16.5.3.1 MAXIMUM AND MINIMUM RATES OF DECREASING FORWARD SPEED (T). We need to set maximum and minimum rates of decrease of T for the former PMH. Figure 16.8a shows that Betsy's (1961) T dropped 7 kt (13 km/hr) in 6 hours prior to stalling. This is the greatest decrease in T of the storms examined, but our data sample is very small. We have decided to allow a former PMH to decrease at a maximum rate of 15 kt (28 km/hr) during the first 6 hours after its T falls below the lower limits, and to decrease an additional 10 kt (19 km/hr) during each additional 6-hr period until the stalled T of 5 kt (9 km/hr) is achieved. We set a minimum rate of decrease of T for the storm at 10 kt (19 km/hr) during the first 6 hours and at 8 kt (15 km/hr) for each additional 6-hr period.

16.5.3.2 CHOOSING θ. Once a PMH drops below the limiting T and begins to weaken, it is no longer bound by the permissible limits of θ given in figure 11.6. However, we will require that the θ chosen be within the permissible limits for the SPH (fig. 11.8) over the distance between the LT point [where T first falls below the minimum T (T_L)], and the stall point. This is reasonable since, though weaker than a PMH, the hurricane is still of greater than SPH intensity. The user should select a θ at the latitude of the LT point and then determine if this direction remains within permissible limits between the LT point and the stall point.

16.5.3.3 DEFINITION OF THE POINT WHERE T DECREASES BELOW THE MINIMUM LIMIT. The LT point pertains to the point where the PMH first falls below the minimum speed (T_L) permissible for maintaining PMH intensity. It does not pertain to the point where the former PMH reaches the 5 kt (9 km/hr) stall speed. The distance between these two points is dependent on a) the magnitude of T_L, i.e., the larger the T_L, the larger the distance traveled between these two points, and b) the rate of speed decrease selected between the maximum and minimum rates of decreasing T given in section 16.5.3.1. We will see in section 16.5.4.2 that former PMH's moving from the south or near south must start dropping off from PMH T_L south of New England or the hurricane will cross the coast before reaching stall speed (5 kt or 9 km/hr).

16.5.3.4 DETERMINATION OF LT POINT KNOWING POINT OF STALL. In order to determine the point where the PMH first drops below the T_L, we must choose a θ (sec. 16.5.3.2) that a former PMH will follow to the stall point. We must also choose the rate of decreasing forward speed (sec. 16.5.3.1). This will not present much of a problem for a hurricane moving toward the stall point from the east (possible south of milepost 2800) because the latitude for the stall and the LT points is the same. In that unique case, we would arrive at the LT point by taking an average T $[T_L + 5$ kt (9 km/hr) $\div$ 2] and multiply the result by the time it takes to decrease from the T_L to 5 kt (depends on chosen rate of decreasing speed). This will give a distance eastward of the stall point where the LT point is located.

In all other cases, the LT point is located with more difficulty. A helpful first guess at the location of the LT point may be made by taking average T

(as explained earlier), using the T_L for the stall point, and then multiplying that average T by the time it takes to decrease to 5 kt. This distance measured along the chosen θ will be greater than the distance to the LT point for θ >90° because T_L decreases with decreasing latitude. (For θ between 50° and 90° the reverse is true.) The user can then choose LT at an arbitrary point closer to (farther from) the stall point and compute a shorter (longer) distance to the stall point using an average T (using the T_L at this arbitrary point) and the chosen rate of decrease in T. If required, additional LT points should be selected until a point is found that permits the storm to reach a stall point at or very near the selected stall point. If the stall point selected is some distance offshore, this distance must be considered in selecting the LT point.

16.5.4 DECREASE OF INTENSITY FOR A NONSTALLED FORMER PMH MOVING SLOWER THAN THE LOWER LIMITS OF T (T_L)

Once a PMH begins to move at a speed less than the lower limits of T (T_L) it will begin to decrease in intensity. As the storm continues to slow, it will continue to weaken until it reaches its stalled speed (5 kt or 9 km/hr) where further weakening will occur as described in section 16.5.2. The rate of weakening prior to stall should be less than the rate of weakening after the hurricane stalls. This is so because a stalled storm will be affected more by upwelling of cold water than will a nonstalled storm, even one approaching stall speed (Geisler 1970).

16.5.4.1 GENERAL CONSIDERATIONS INVOLVING P_O. In developing quantitative loss of intensity with time for a former PMH after T has dropped below T_L, we must weaken the storm fast enough so that its p_O at the stall point is less than that of the PMH at that point. The former PMH should not weaken at such a rapid rate that the decrease in intensity before reaching stall speed is greater than the weakening rate of a stalled PMH.

16.5.4.2 PROCEDURE FOR DECREASING WIND SPEED AT LT POINT TO WIND SPEED AT STALL POINT. Once the LT point has been located, the milepost or latitude of this point is determined and then an overwater wind field for that milepost is reduced using the following procedure and the curves of figure 16.9:

a. Enter the abscissa of figure 16.9 with the time from when the T of the hurricane fell below LT to when it reached the stall T. Draw a vertical line up to the curve marked with the latitude of the stall point.

b. Read off the percentage adjustment at that point on the y-axis. This would be the percentage by which the whole wind field would be multiplied if a former PMH had actually stalled for this period of time.

c. Since our storm has not stalled it would weaken at a lesser but unknown rate. We have elected to assume that the storm would decrease at a rate only 70 percent of a stalled PMH. Thus, we increase the value of (b) by 30 percent of 1.0 - the value of (b) to give a lesser reduction.

d. Multiply the entire wind field by the percentage in (c) to obtain a reduced wind field. After stalling, this wind field will be further reduced by using the method given in section 16.5.2 with the curves of figure 16.9.

e. If a portion of the wind field is over land, it will need to be reduced further on account of friction; (see chapter 15).

The average rate of decrease of wind speed from the PMH wind speed computed for a slowing PMH should be used with caution. For example, a former PMH traveling from the south or near south and stalling just north of Cape Cod may have originally dropped below T_L south of the Virginia - North Carolina border if its T is decreasing at the minimum rate or a slightly faster rate. During the early part of its passage from North Carolina to Massachusetts, therefore, the hurricane would probably be weakening at a lesser rate than the given average rate of weakening to the stall point north of Cape Cod. Such differences in rates would become smaller as we rotate θ toward 90°. If the user wishes to approximate a decrease in intensity not too long after T drops below PMH T_L it is probably appropriate to use a rate of decrease less than an average curve would indicate.

16.5.5 FORWARD SPEED

T for a stalled hurricane is given by definition, i.e. $\leq$ 5 kt (9 km/hr). Prior to stalling, a PMH can have the range of T given in chapter 10. The rate of increasing T after stalling for a former PMH has been left unanswered

16.5.6 TRACK DIRECTION

Since looping and other erratic storm motions may accompany a stalled hurricane, no limiting values are assigned to θ for a stalled PMH.

16.5.7 RADIUS OF MAXIMUM WINDS AND INFLOW ANGLE

North of the Virginia – North Carolina border, we recommend that R be increased as a former PMH weakens while slowing down and stalling. This increase should relate to the variation in p_o. The initial R should be from within the limits of R (fig. 9.8) at the milepost corresponding to the LT point. The R after T falls below T_L and during the stall should be determined by increasing the R in proportion to the upper and lower limits of figure 9.8. Enter that figure at the milepost corresponding to a higher p_o associated with the amount of decrease of wind speed obtained from figure 16.9. This higher p_o is determined using equation 16.1. Knowing the original Δp_{max}, V_{max} and the maximum wind speed at the end of the stall period, we compute a new Δp at the stall point. Seeing that p_w is constant with latitude*, a higher p_o can be determined ($\Delta p = p_w - p_o$). This p_o will correspond to an east coast milepost in figure 8.8. R is then read at that milepost. If the higher p_o exceeds 27.46 in. (93 kPa), R may be increased at the rate of 1 n.mi. (1.9 km) for every 0.12 in. (0.4 kPa) increase in p_o at the upper limit of R and 1 n.mi. (1.9 km) for every 0.42 in. (1.4 kPa) increase in p_o at the lower limit of R. For R's between these limits, interpolate.

As R varies, so will inflow angle (ϕ). Continue to use figure 14.7 to compute ϕ north of 36.5°N. If R exceeds 38 n.mi. (70 km) use figure 14.6 [for R >45 n.mi. (83 km), use the R = 45 n.mi. curve].

16.5.8 REINTENSIFICATION WHEN THE STALL IS OVER

North of the Virginia – North Carolina border a former PMH cannot reintensify to the maximum intensity it had before stalling. The colder water at these latitudes would prevent the full regeneration of the storm to its initial PMH intensity at the LT point. We believe this would be the case

---

*We consider p_w to be constant with latitude for the PMH. As a former PMH weakens, especially during a stall, p_w would probably decrease toward SPH p_w. We will neglect this.

everywhere, even for a former PMH which moved at $\theta = 50°$ to a stall point off the Virginia capes where the water is the warmest and PMH p_o is lower than the PMH p_o at the LT point. The actual rate of reintensification of a former PMH to an intensity less than its PMH p_o at the LT point was not addressed in this report.

16.5.9 LIMITATIONS

These procedures are approximate and are based on several assumptions. Curves and procedures were developed to maintain maximum intensity for the stalled storm within a logical framework. Only additional knowledge and data can support our conclusions. The procedures developed in this section are subject to the following limitations:

a. An LT point cannot be located north of 45°N.

b. An LT point may not be more than 300 n.mi. (556 km) from any point on the U.S. east coast, including capes.

c. The procedure is undefined if a former PMH crosses land between the LT point and the stall point.

Limitation (a) is called for because we have defined the PMH to only 45°N. Limitation (b) is adopted because our east coast data sample extended outward 150 n.mi. (278 km) from the coast. We will assume that additional data between 150 and 300 n.mi. (278 and 556 km) from the coast would be of the same family as the "closer in" data. We are unwilling to make this assumption beyond 300 n.mi. (556 km). Limitation (c) is given because a former PMH would also be filling and, therefore, weakening more rapidly if it crossed land between the LT and stall points.

16.5.10 ADDITIONAL REMARKS

The problem of p_o at the stall point being lower than the stall point PMH p_o will not occur. Tests made with p_o and wind speeds given in tables 2.3 to 2.6, for several stall points along the east coast, showed this to be so. The manner in which the slopes of the wind curves (fig. 16.9, then increased by 30 percent; see sec. 16.5.4.2), used from the Virginia-North Carolina border northward, roughly vary with cooler sea-surface temperatures, prevent this problem.

By employing a percentage of the weakening rate for stalling as the storm moves from the LT point to the stall point (sec. 16.5.4), we are assured by definition of lesser weakening prior to stalling than after stalling.

16.5.11 EXAMPLE OF CALCULATION OF DECREASE IN PMH WINDS NORTH OF 36.5°N

The following is an example of how to decrease PMH winds for stalling north of 36.5°N. We will assume:

   a. A former PMH stalls just south of the Rhode Island coast near 41.3°N.

   b. The hurricane moves from $\theta = 180°$.

   c. The hurricane decreases its T at the maximum rate (sec. 16.5.3.1).

The initial T_L would be taken at the Rhode Island coast near milepost 2650 and would equal 37 kt (69 km/hr). Using this T_L as a first guess (sec. 16.5.3.4) we obtain an average T of 21 kt (39 km/hr), or 37 kt + 5 kt ÷ 2. It takes 16.2 hours for a PMH to slow down from 37 kt to 5 kt (69 km/hr to 9 km/hr) at the assumed maximum rate of decrease in T. Multiplication of 21 kt by 16.2 hours gives a distance of 340 n.mi. (630 km) or 5.7° due south of 41.3°N. This gives an LT point at 35.6°N, or about 200 n.mi. (370 km) east of Cape Hatteras. Here T_L is only 10 kt (19 km/hr). This is not our final LT point because a former PMH would slow down to 5 kt (9 km/hr) from 10 kt (19 km/hr) in just 2 hours using the maximum rate. This would obviously not be enough time to travel 340 n.mi. (630 km).

As a second guess, we will arbitrarily put an LT point east of the New Jersey coast near milepost 2460 (39.5°N) where $T_L = 30$ kt (56 km/hr). In this case, we obtain an average T of 17.5 kt (32.5 km/hr), or 30 kt + 5 kt ÷ 2. Twelve hours will pass before a PMH with a T_L of 30 kt (56 km/hr) slows down to 5 kt (9 km/hr) at the maximum rate. Multiplication of 17.5 kt by 12 hours gives a distance of 210 n.mi. (389 km) due north of 39.5°N, or 3.5° north of 39.5°N, giving a stall point at 43.0°N in southern New Hampshire, or 1.7° north of the required stall point. Our guess of 39.5°N for the LT point was too far north. We know that 35.6°N is too far south (first guess) and 39.5°N is too far north (second guess) for the LT point.

As a third guess, we will select a point east of Delaware Bay near milepost 2400 (38.8°N) where $T_L = 26$ kt (48 km/hr). Here, we obtain an average T of

15.5 kt (28.8 km/hr), or 26 kt + 5 kt ÷ 2. It takes 9.6 hours for a PMH to slow down from 26 kt to 5 kt (48 km/hr to 9 km/hr) at the maximum rate. Multiplication of 15.5 kt by 9.6 hours gives a distance of 149 n.mi. (276 km) due north of 38.8°N or 2.5° north of 38.8°N, giving a stall point at 41.3°N. This is the required stall point. The LT point is therefore 38.8°N.

The wind speed of the PMH at the LT point is decreased to the wind speed at the stall point by using the procedure given in section 16.5.4.2 and refer- ring to figure 16.9. Interpolate a curve for 41.3° (between the 41° and 42°N curves). Draw a vertical line up from 9.6 hours on the abscissa (the time from when the T of the hurricane fell below T_L to when it reached 5 kt, or 9 km/hr) to the interpolated curve. Read 0.851 on the y-axis; this is the adjustment to the winds due to stalling for 9.6 hours. The designated stalling factor (sf) is 0.851. The percentage reduction over the whole wind field if a former PMH had actually stalled for 9.6 hours would be 14.9%; or (1 -0.851) x 100. Since, in this example, the hurricane was slowing down to 5 kt (9 km/hr) during the 9.6 hours it took to travel from the LT point to the stall point, its winds would decrease at only 70 percent of 14.9% or 10.4%. Subtracting 10.4% from 100% gives 89.6%, the percentage to be applied over the entire PMH wind field corresponding to the LT point at 38.8°N (due south of milepost 2650) after the hurricane has moved to 41.3°N, just south of the Rhode Island coast. This adjusted wind field will be further reduced after stalling by using the procedures given in section 16.5.2 with the curves of figures 16.9. For example, if the former PMH stalls near 41.3°N for 12 hours, this *new wind field* will be reduced by 18% by employing an sf of 0.82.

Since the storm stalled just south of the Rhode Island coast, most of its northern semicircle will be over land and a portion of its wind field will have to be reduced further to account for friction (see chapter 15).

16.6 EFFECT OF LAND ON STORM WEAKENING

One would expect stalled hurricanes with a part of their circulation over land to weaken more rapidly than those whose circulation is entirely over water, all other things being equal. We are unable to find an adequate number of hurricanes which stalled close to land or whose eyes drifted over land during a stall to verify this idea. A larger sample of typhoons was available. However, western North Pacific land masses (Philippines, Taiwan, and Japan) would not be representative of the U.S. east and gulf coasts.

Lacking data, we recommend the use of a constant weakening rate for a stalled hurricane over the western North Atlantic or Gulf of Mexico, whether or not it is close to land.

16.7 OTHER RESEARCH

Beebe and Simpson (1976) have studied the hydrometeorological aspects of stalling and meandering hurricanes. Their investigation indicated that after stalling to a forward speed of ≤ 4 kt (7 km/hr), a hurricane with the strength of Camille (1969) would be able to maintain its intensity for only a very short period. Such a storm would have potential for causing much greater coastal erosion than has been observed historically.

We allow an SPH (weaker than Camille) to travel at 4 kt whereas a PMH (stronger than Camille along the gulf coast and most of the east coast) is allowed to move at speeds of 6 kt (11 km/hr) or more.

308

ACKNOWLEDGMENTS

REFERENCES

American Meteorological Society, 1974-78: *Monthly Weather Review*, Boston, Mass.

Atkinson, G.D. and C. R. Holliday, 1977: Tropical cyclone minimum sea-level pressure/maximum sustained wind relationship for the western North Pacific. *Monthly Weather Review*, Vol. 105, No. 4, pp. 421-27.

Ausman, M., 1959: Some Computations of the Inflow Angle in Hurricanes near the Ocean Surface. *Department of Meteorology Report on Research*, University of Chicago, Chicago, Ill., 19 pp.

Beebe, R. C. and R. H. Simpson, 1976: Hydrometeorological aspects of stalling and meandering hurricanes. *Conference on Hydrometeorology*, 20-22 April 1976, American Meteorological Society, Boston, Mass., 138 pp.

Bell, G., 1974: Observations on the size of the typhoon eye. *Proceedings of the WMO Technical Conference on Typhoon Modification, Manila*, 15-18 October 1974, WMO No. 408.

Bergeron, T., 1954: The problem of tropical hurricanes. *Quarterly Journal Royal Meteorological Society*, Vol. 80, No. 344, pp. 131-164.

Black, P. G. and W. D. Mallinger, 1972: The mutual interaction of hurricane Ginger and the upper mixed layer of the ocean. *Project Stormfury Annual Report* 1971, Appendix D, U.S. Department of Defense and U.S. Department of Commerce, Miami, Fla., pp. 63-87.

Brand, S., 1971: The effects on a tropical cyclone of cooler surface waters due to upwelling and mixing produced by a prior tropical cyclone. *J. of Appl. Meteor.*, Vol. 10, No. 5, pp. 865-874.

Chin, P. C., 1972: *Tropical Cyclone Climatology for the China Seas and Western Pacific from 1884 to 1970, Vol. I: Basic Data*. Royal Observatory, Hong Kong, 207 pp.

Chow, Shu-hsien, 1971: A Study of the Wind Field in the Planetary Boundary Layer of a Moving Tropical Cyclone, *Masters Thesis*, New York University, Department of Meteorology, New York, N.Y., 58 pp.

Cline, I. M., 1926: *Tropical Cyclones*. McMillan Company, New York, N.Y., 301 pp.

Colon, J. A., 1963: On the Evolution of the Wind Field During the Life Cycle of Tropical Cyclones. *National Hurricane Research Project Report* No. 65, U.S. Weather Bureau, Department of Commerce, Washington, D.C., 36 pp.

Craddock, J.M., 1969: *Statistics in the Computer Age*. American Elsevier Pb. Co., New York, N.Y., 214 pp.

Crutcher, H. L. and R. G. Quayle, 1974: Mariners Worldwide Climatic Guide to Tropical Storms at Sea *(NAVAIR 50-1C-61)*. U.S. Department of Defense, Asheville, N.C., 426 pp. (312 charts).

Cry, G. W., 1965: Tropical Cyclones of the North Atlantic Ocean, *U.S. Weather Bureau Technical Paper* No. 55, U.S. Weather Bureau, Department of Commerce, Washington, D.C., 148 pp.

Dixon, W. J. and F. J. Massey, Jr., 1957: *Introduction to Statistical Analysis*. McGraw-Hill Book Co., Inc., New York, N.Y., 488 p. (Table A-30a).

Dunn, G. E. and B. I. Miller, 1964: *Atlantic Hurricanes*. Louisiana State University Press, Baton Rouge, La., 377 pp.

Echols, W. T., 1970: Modification in Surface Boundary Layer Wind Structure with Onshore Flow, *Atmospheric Science Group Report 23*, University of Texas, Austin, Tex., 59 pp.

Echols, W. T. and N. K. Wagner, 1972: Surface roughness and internal boundary layer near a coastline, *J. of Appl. Meteor.*, Vol. 11, No. 4, pp. 658-662.

Environmental Data Service, 1899-1972: *Daily Series, Synoptic Weather Maps Part 1, Northern Hemisphere*. National Oceanic and Atmospheric Administration, U.S. Department of Commerce, Asheville, N.C.

Environmental Data Service, 1900-75: *Climatological Data*. National Oceanic and Atmospheric Administration, U.S. Department of Commerce, Asheville, N.C.

Florida Power and Light Co., 1975: *St. Lucie Plant No. 2, Preliminary Safety Analysis Report*. Docket No. 50-389 and Docket File.

Foreman, J., 1976: IFYGL Physical Data Collection System: Description of Archived Data. *NOAA Technical Report* EDS 15, National Oceanic and Atmospheric Administration, U.S. Department of Commerce, Washington, D.C., 175 pp.

Frank, W. M., 1976: The Structure and Energetics of the Tropical Cyclone. *Atmospheric Science Paper No. 258*, Department of Atmospheric Science, Colorado State University, Ft. Collins, Colo., 180 pp.

Geisler, J. E., 1970: Linear theory of the response of a two layer ocean to a moving hurricane. *Geophysical Fluid Dynamics*, Gordon and Breach Science Publishers, United Kingdom, pp. 249-272.

Gentry, R. C., 1967: Structure of the upper troposphere and lower stratosphere in the vicinity of hurricane Isbell, 1964. *Papers in Meteorology and Geophysics*, Vol. 8, No. 4, December, pp. 293-310.

Goldman, J. L. and T. Ushijima, 1974: Decrease in hurricane winds after landfall. *Journal of the Structural Division*, Vol. 100, No. ST 1, pp. 129-141.

Goodyear, H.V., 1968: Frequency and Areal Distributions of Tropical Storm Rainfall in the United States Coastal Region on the Gulf of Mexico. *ESSA Technical Report* WB-7, Environmental Science Services Administration, U.S. Department of Commerce, Silver Spring, Md., 33 pp.

Graham, H. E. and D. E. Nunn, 1959: Meteorological Considerations Pertinent to Standard Project Hurricane, Atlantic and Gulf Coasts of the United States. *National Hurricane Research Project* Report No. 33, U.S. Weather Bureau, Department of Commerce, Washington, D.C., 76 pp.

Graham, H. E. and G. N. Hudson, 1960: Surface Winds Near the Center of Hurricanes (and Other Cyclones). *National Hurricane Research Project* Report No. 39, U.S. Weather Bureau, Department of Commerce, Washington, D.C., 200 pp.

Harris, D. L., 1959: An Interim Hurricane Storm Surge Guide. *National Hurricane Research Project* Report No. 32, U.S. Weather Bureau, Department of Commerce, Washington, D.C., 24 pp.

Haurwitz, B., 1935: The height of tropical cyclones and of the "eye" of the storm. *Monthly Weather Review*, Vol. 63, No. 2, February, pp. 45-49.

Hawkins, H. F., 1971: Comparison of results of the hurricane Debbie (1969) modification experiments with those from Rosenthal's numerical model simulation experiments. *Monthly Weather Review*, Vol. 99, No. 5, pp. 427-434.

Hawkins, H.F., 1975: National Hurricane and Experimental Meteorology Laboratory, Environmental Research Laboratories, National Oceanic and Atmospheric Administration, U.S. Department of Commerce, Coral Gables, Fla. (personal communication).

Hawkins, H. F. and S. M. Imbembo, 1976: The structure of a small intense hurricane - Inez 1966. *Monthly Weather Review*, Vol. 104, No. 4, pp. 418-442.

Hazelworth, J. B., 1968: Water temperature variations resulting from hurricanes. *J. Geophys*. Res., Vol. 73, pp. 5105-5123.

Ho, F. P., R. W. Schwerdt, and H. V. Goodyear, 1975: Some climatological characteristics of hurricanes and tropical storms, gulf and east coasts of the United States. *NOAA Technical Report* NWS 15, National Weather Service, National Oceanic and Atmospheric Administration, U.S. Department of Commerce, Washington, D.C., 87 pp.

Hsu, S. A., 1970a: The shear stress of sea breeze on a swash zone. *Proceedings, Twelfth Conference on Coastal Engineering,* Council on Wave Research.

Hsu, S. A., 1970b: Measurement of shear stress and roughness length on a beach. *J. of Geophys. Res.,* Vol. 76, No. 12, pp. 2880-2885.

Hubert, L. F., 1955: Frictional filling of hurricanes. *Bulletin of the American Meteorological Society,* Vol. 36, No. 9, pp. 440-445.

Hughes, L. A., 1952: On the low-level wind structure of tropical storms. *J. of Meteor.,* Vol. 9, pp. 422-428.

Huschke, R. E., ed., 1959: *Glossary of Meteorology.* American Meteorological Society, Boston, Mass., 638 pp.

Ito, H., 1962: Aspects of typhoon development. *Proceedings, WMO Inter-Regional Seminar on Tropical Cyclones,* Japan Meteorological Agency, Tokyo, Japan.

Japan Meteorological Agency, 1972: *Climatic Table of Japan, Part 3, Extremes and Rankings of Primary Meteorological Elements for the Whole Period of Observation up to 1970.* Tokyo, 465 pp.

Jelesnianski, C. P., 1967: Numerical computations of storm surges with bottom stress. *Monthly Weather Review,* Vol. 95, No. 11, pp. 740-756.

Jelesnianski, C. P., 1972: SPLASH (Special Program to List Amplitudes of Surges from Hurricanes) I. Landfall Storms. *NOAA Technical Memorandum NWS TDL-46,* National Weather Service, National Oceanic and Atmospheric Administration, U. S. Department of Commerce, Silver Spring, Md., 52 pp.

Jelesnianski, C. P. and A. D. Taylor, 1973: A Preliminary View of Storm Surges Before and After Storm Modifications. *NOAA Technical Memorandum ERL WMPO-3* (NHRL 102), Environmental Research Laboratories, National Oceanic and Atmospheric Administration, U.S. Department of Commerce, Boulder, Colo., 33 pp.

Jensen, J. J., 1970: Calculated and Observed Changes in Sea-surface Temperature Associated with Hurricane Passage. U.S. Naval Postgraduate School, *Masters Thesis,* Monterey, Calif., 55 pp.

Kuo, H. L., 1959: Dynamics of convective vortices and eye formation. *The Atmosphere and the Sea in Motion,* Rockefeller Institute Press, New York, N.Y., pp. 413-424.

Landis, R. C., 1966: *Synoptic Analysis of Near Surface and Sub-surface Temperatures in the Atlantic Ocean Following Hurricane Betsy.* Texas A & M University, Dept. of Oceanography, College Station, Tex., 37 pp.

Landis, R. C. and D. F. Leipper, 1968: Effects of hurricane Betsy upon Atlantic Ocean temperature based on radio-transmitted data. *J. of Appl. Meteor.*, Vol. 7, pp. 554-562.

Leipper, D. F., 1967: Observed ocean conditions and hurricane Hilda, 1964. *J. Atmos. Sci.*, Vol. 24, pp. 182-196.

Leipper, D. F. and D. Volgenau, 1972: Hurricane heat potential of the Gulf of Mexico. *J. Phys. Oceano.*, Vol. 2, pp. 218-224.

List, R. J., ed., 1951: Smithsonian Meteorological Tables. *Smithsonian Miscellaneous Collections*, Vol. 114, Sixth Revised Edition, Smithsonian Institution, Washington, D. C., 527 pp.

Ludlam, D. M., 1963: *Early American Hurricanes, 1492-1870.* American Meteorological Society, Boston, Mass., 198 pp.

McFadden, J. D., 1967: Sea-surface temperatures in the wake of hurricane Betsy (1965). *Monthly Weather Review*, Vol. 95, No. 5, pp. 299-302.

Malkin, W., 1959: Filling and Intensity Changes in Hurricanes Over Land. *National Hurricane Research Project* Report No. 34, U.S. Weather Bureau, Department of Commerce, Washington, D.C., 18 pp.

Malkus, J. S., 1958: On the structure and maintenance of the mature hurricane eye. *J. of Meteor.*, Vol. 15, pp. 337-349.

Malkus, J. S. and H. Riehl, 1960: On the dynamics and energy transformations in steady-state hurricanes. *Tellus*, Vol. 12, No. 1, pp. 1-20.

Miller, B. I., 1963: On the Filling of Tropical Cyclones Over Land. *National Hurricane Research Project* Report No. 66, U.S. Weather Bureau, Department of Commerce, Washington, D.C., 82 pp.

Miller, B. I., 1964: A study of the filling of hurricane Donna (1960) over land. *Monthly Weather Review*, Vol. 92, No. 9, pp. 389-406.

Mills, F. C., 1955: *Statistical Methods*. 3rd ed. Holt, Rinehart and Winston, New York, N.Y., 842 p. (Table VII).

Molinari, R. L. and G. O. Franceschini, 1971: *Bathythermograph Sections Across the Path of Hurricane Celia.* Texas A & M University, College Station, Tex. (unpublished).

Myers, V.A., 1954: Characteristics of United States Hurricanes Pertinent to Levee Design for Lake Okeechobee, Florida. *Hydrometeorological Report* No. 32, U.S. Weather Bureau, Department of Commerce and U.S. Army Corps of Engineers, Washington, D.C., 106 pp.

Myers, V. A. and E. S. Jordan, 1956: Winds and pressure over the sea in the hurricane of September 1938. *Monthly Weather Review*, Vol. 84, No. 7, pp. 261-270.

314

Myers, V. A. and W. Malkin, 1961: Some Properties of Hurricane Wind Fields as Deduced from Trajectories. *National Hurricane Research Project* Report No. 49, U.S. Weather Bureau, Department of Commerce, Washington, D.C., 45 pp.

National Oceanic and Atmospheric Administration, 1900-73: *Monthly Weather Review*, U.S. Department of Commerce, Rockville, Md.

National Weather Service, 1972: Revised Standard Project Hurricane Criteria for the Atlantic and Gulf Coasts of the United States, *Memorandum* HUR 7-120, National Oceanic and Atmospheric Administration, U.S. Department of Commerce, Silver Spring, Md. (unpublished).

Núñez, E. and W. M. Gray, 1978: A comparison between West Indies hurricanes and Pacific typhoons. Conference papers, *11th Technical Conference on Hurricanes and Tropical Meteorology*, American Meteorological Society, Boston, Mass., pp. 528-534

Palmén, E., 1948: On the formation and structure of tropical hurricanes, *Geophysica*, Vol. 3, pp. 26-38.

Palmén, E. and C. Newton, 1969: *Atmospheric circulation systems, their structure and physical interpretation.* Academic Press, New York, N.Y. and London, pp. 515-522.

Panofsky, H. A. and E. L. Petersen, 1972: Wind profiles and change of terrain roughness at Riso. Quart. J. Royal Met. Soc. Vol. 98, pp. 845-854.

Peterson, E. W., 1971: Predictions of the momentum exchange coefficient for flow over heterogeneous terrain. *J. of Appl. Met.*, Vol. 10, No. 5, pp. 958-961.

Price, J. F., 1976: Sea-surface temperature response to hurricane Eloise. Abstracts, the 1976 AGU Spring Annual Meeting, *Transactions of AGU*, Vol. 57, p. 260.

Ratner, B., 1957: Upper Air Climatology of the United States. *U.S. Weather Bureau Technical Paper* No. 32, Parts 1 and 2, Department of Commerce, Washington, D.C., 339 pp. (total for both parts).

Reid, R. O. and B. W. Wilson, 1954: Compendium of Results of Storm Tide and Wave Analysis for Full Hurricane Conditions at Freeport, Texas. *A & M Project Report* 91 (Reference 54-64F), Department of Oceanography, Texas A & M Research Foundation, College Station, Tex., 45 pp.

Reiso, D. T. and C. L. Vincent, 1976: Estimation of Winds Over the Great Lakes. *Miscellaneous Paper* H-76-2, Hydraulic Laboratory, U.S. Army Engineer Waterways Experiment Station, Vicksburg, Miss., 61 pp.

Riehl, H., 1954: *Tropical Meteorology.* McGraw-Hill Book Co., Inc., New York, N.Y., 392 pp.

Riehl, H., 1972: Intensity of recurved typhoons. *J. of Appl. Meteor.*, Vol. 11, No. 4, pp. 613-615.

Schloemer, R. W., 1954: Analysis and Synthesis of Hurricane Wind Patterns over Lake Okeechobee, Florida. *Hydrometeorological Report* No. 31, U.S. Weather Bureau, Department of Commerce and U.S. Army Corps of Engineers, Washington, D.C., 49 pp.

Shea, D. J. and W. M. Gray, 1972: The Structure and Dynamics of the Hurricane's Inner Core Region. *Atmospheric Science Paper* No. 182, NOAA Grant N22-65-72(G), NSF Grant GA 19937, Department of Atmospheric Science, Colorado State University, Fort Collins, Colo., 134 pp.

Sheets, R. C., 1967: On the Structure of Hurricane Janice (1958). *ESSA Technical Memorandum* IERTM-NHRL 76, U.S. Department of Commerce, Miami, Fla., 37 pp.

Sheets, R. C., 1969: Some mean hurricane soundings. *J. of Applied Meteor.*, Vol. 8, No. 1, February, pp. 134-146.

Simpson, R. H., 1952: Exploring eye of typhoon "Marge," 1951. *Bulletin of the American Meteorological Society*, Vol. 33, No. 7, pp. 286-298.

Simpson, R. H. and J. M. Pelissier, 1971: Atlantic hurricane season of 1970. *Monthly Weather Review*, Vol. 99, No. 4, April, pp. 269-277.

Smith, C. L., 1975: On the intensification of hurricane Celia (1970). *Monthly Weather Review*, Vol. 103, No. 2, pp. 131-148.

Stevenson, R. E. and R. S. Armstrong, 1965: Heat loss from the waters of the northwest Gulf of Mexico during hurricane Carla. *Geo. quis. Intern.*, Vol. 5, pp. 49-57.

Sugg, A. L., L. G. Pardue, and R. L. Carrodus, 1971: Memorable Hurricanes of the United States Since 1873. *NOAA Technical Memorandum* NWS SR-56, National Weather Service, National Oceanic and Atmospheric Administration, U.S. Department of Commerce, Fort Worth, Tex., 52 pp.

Taylor, J. G., 1966: *An Approach to the Analysis of Sea-surface Temperature Data for Utilization in Hurricane Forecasting in the Gulf of Mexico.* Texas A & M University, College Station, Tex., 107 pp.

Thom, H. C. S., 1973: Distribution of extreme winds over oceans. *Journal of the Waterways, Harbors and Coastal Engineering Division*, Proceedings of the American Society of Civil Engineers, Vol. 99, No. WWI, pp .1-17.

U.S. Department of Defense, 1960-75: *Annual Typhoon Reports.* Fleet Weather Central Joint Typhoon Warning Center, Guam, Mariana Islands.

U.S. Navy, 1969a: *Monthly Charts of Mean, Minimum, and Maximum Sea-surface Temperature of the North Pacific Ocean.* Naval Oceanographic Office, Washington, D. C., 58 pp.

U.S. Navy, 1969b: Historical mean surface temperature data, Western North Atlantic. *The Gulf Stream* (Supplement), Naval Oceanographic Office, Washington, D.C., 8 pp.

U.S. Navy, 1975: *Summary of Synoptic Meteorological Observations North American Coastal Marine Areas - Revised.* Vol. 1-4, Naval Weather Service Command, Asheville, N.C., 2291 pp.

U.S. Weather Bureau, 1957: Survey of Meteorological Factors Pertinent to Reduction of Loss of Life and Property in Hurricane Situations. *National Hurricane Research Project* Report No. 5, Department of Commerce, Washington, D.C., 87 pp.

U.S. Weather Bureau, 1959a: Relations Between SPH Isovel Patterns and Probable Maximum Events for Lower New England Area. *Memorandum HUR 7-59* Department of Commerce, Washington, D.C. (unpublished).

U.S. Weather Bureau, 1959b: Relations Between SPH Isovel Patterns and Probable Maximum Events for the New Orleans Area. *Memorandum HUR 7-61* Department of Commerce, Washington, D.C. (unpublished).

U.S. Weather Bureau, 1968: Meteorological Characteristics of the Probable Maximum Hurricane, Atlantic and Gulf Coasts of the United States. *Memorandum HUR 7-97,* and Peripheral Pressures for Probable Maximum Hurricanes. *Memorandum HUR 7-97A,* Department of Commerce, Silver Spring, Md. (unpublished).

Willett, H. C., 1955: *A Study of the Tropical Hurricane Along the Atlantic and Gulf Coasts of the United States.* Inter-Regional Insurance Conference, New York, N.Y., 63 pp.

CONVERSIONS

TO CONVERT FROM	TO	USE THE FOLLOWING EQUATION

TEMPERATURE

degrees, Fahrenheit	degrees, Celsius	$t_c = (t_f - 32)/1.8$
degrees, Fahrenheit	degrees, Kelvin	$t_k = (t_f - 32)/1.8 + 273.16$
degrees, Celsius	degrees, Kelvin	$t_k = t_c + 273.16$

TO CONVERT FROM	TO	MULTIPLY BY

DISTANCE

feet	meters	0.305
miles (nautical)	kilometers	1.853
miles (statute)	kilometers	1.609
miles (statute)	miles (nautical)	0.868

PRESSURE

inches (Hg)	kilopascals	3.386
millibars	inches (Hg)	0.030
millibars	kilopascals	0.100

SPEED

knots	kilometers/hour	1.853
knots	miles/hour	1.152
miles/hour	kilometers/hour	1.609

NWS 16 Storm Tide Frequencies on the South Carolina Coast. Vance A. Myers, June 1975, 79 p. (COM-75-11335)

NWS 17 Estimation of Hurricane Storm Surge in Apalachicola Bay, Florida. James E. Overland, June 1975. 66 p. (COM-75-11332)

NWS 18 Joint Probability Method of Tide Frequency Analysis Applied to Apalachicola Bay and St. George Sound, Florida. Francis P. Ho and Vance A. Myers, November 1975, 43 p. (PB-251123)

NWS 19 A Point Energy and Mass Balance Model of a Snow Cover. Eric A. Anderson, February 1976, 150 p. (PB-254653)

NWS 20 Precipitable Water Over the United States, Volume 1: Monthly Means. George A. Lott, November 1976, 173 p. (PB-264219)

NWS 20 Precipitable Water Over the United States, Volume II: Semimonthly Maxima. Francis P. Ho and John T. Riedel, July 1979, 359 p.

NWS 21 Interduration Precipitation Relations for Storms - Southeast States. Ralph H. Frederick, March 1979, 66 p. (PB-297192)

NWS 22 The Nested Grid Model. Norman A. Phillips, March 1979, 85 p.

NOAA SCIENTIFIC AND TECHNICAL PUBLICATIONS

The National Oceanic and Atmospheric Administration was established as part of the Department of Commerce on October 3, 1970. The mission responsibilities of NOAA are to assess the socioeconomic impact of natural and technological changes in the environment and to monitor and predict the state of the solid Earth, the oceans and their living resources, the atmosphere, and the space environment of the Earth.

The major components of NOAA regularly produce various types of scientific and technical information in the following kinds of publications:

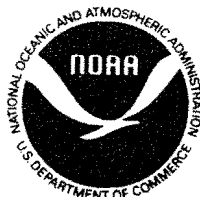PROFESSIONAL PAPERS — Important definitive research results, major techniques, and special investigations.

CONTRACT AND GRANT REPORTS — Reports prepared by contractors or grantees under NOAA sponsorship.

ATLAS — Presentation of analyzed data generally in the form of maps showing distribution of rainfall, chemical and physical conditions of oceans and atmosphere, distribution of fishes and marine mammals, ionospheric conditions, etc.

TECHNICAL SERVICE PUBLICATIONS — Reports containing data, observations, instructions, etc. A partial listing includes data serials; prediction and outlook periodicals; technical manuals, training papers, planning reports, and information serials; and miscellaneous technical publications.

TECHNICAL REPORTS — Journal quality with extensive details, mathematical developments, or data listings.

TECHNICAL MEMORANDUMS — Reports of preliminary, partial, or negative research or technology results, interim instructions, and the like.